frontiers | Research Topics

Efficacy and mechanism of herbal medicines and their functional compounds in preventing and treating cardiovascular diseases and cardiovascular disease risk factors

Edited by
Qing Yong He, Yu-Qing Zhang, Jie Wang, Jian Zhang, Kuo Gao, Chen Huei Leo and Zhongfeng Li

Coordinated by
Tiantian Meng

Published in
Frontiers in Pharmacology

FRONTIERS EBOOK COPYRIGHT STATEMENT

The copyright in the text of individual articles in this ebook is the property of their respective authors or their respective institutions or funders. The copyright in graphics and images within each article may be subject to copyright of other parties. In both cases this is subject to a license granted to Frontiers.

The compilation of articles constituting this ebook is the property of Frontiers.

Each article within this ebook, and the ebook itself, are published under the most recent version of the Creative Commons CC-BY licence. The version current at the date of publication of this ebook is CC-BY 4.0. If the CC-BY licence is updated, the licence granted by Frontiers is automatically updated to the new version.

When exercising any right under the CC-BY licence, Frontiers must be attributed as the original publisher of the article or ebook, as applicable.

Authors have the responsibility of ensuring that any graphics or other materials which are the property of others may be included in the CC-BY licence, but this should be checked before relying on the CC-BY licence to reproduce those materials. Any copyright notices relating to those materials must be complied with.

Copyright and source acknowledgement notices may not be removed and must be displayed in any copy, derivative work or partial copy which includes the elements in question.

All copyright, and all rights therein, are protected by national and international copyright laws. The above represents a summary only. For further information please read Frontiers' Conditions for Website Use and Copyright Statement, and the applicable CC-BY licence.

ISSN 1664-8714
ISBN 978-2-8325-3021-4
DOI 10.3389/978-2-8325-3021-4

About Frontiers

Frontiers is more than just an open access publisher of scholarly articles: it is a pioneering approach to the world of academia, radically improving the way scholarly research is managed. The grand vision of Frontiers is a world where all people have an equal opportunity to seek, share and generate knowledge. Frontiers provides immediate and permanent online open access to all its publications, but this alone is not enough to realize our grand goals.

Frontiers journal series

The Frontiers journal series is a multi-tier and interdisciplinary set of open-access, online journals, promising a paradigm shift from the current review, selection and dissemination processes in academic publishing. All Frontiers journals are driven by researchers for researchers; therefore, they constitute a service to the scholarly community. At the same time, the *Frontiers journal series* operates on a revolutionary invention, the tiered publishing system, initially addressing specific communities of scholars, and gradually climbing up to broader public understanding, thus serving the interests of the lay society, too.

Dedication to quality

Each Frontiers article is a landmark of the highest quality, thanks to genuinely collaborative interactions between authors and review editors, who include some of the world's best academicians. Research must be certified by peers before entering a stream of knowledge that may eventually reach the public - and shape society; therefore, Frontiers only applies the most rigorous and unbiased reviews. Frontiers revolutionizes research publishing by freely delivering the most outstanding research, evaluated with no bias from both the academic and social point of view. By applying the most advanced information technologies, Frontiers is catapulting scholarly publishing into a new generation.

What are Frontiers Research Topics?

Frontiers Research Topics are very popular trademarks of the *Frontiers journals series*: they are collections of at least ten articles, all centered on a particular subject. With their unique mix of varied contributions from Original Research to Review Articles, Frontiers Research Topics unify the most influential researchers, the latest key findings and historical advances in a hot research area.

Find out more on how to host your own Frontiers Research Topic or contribute to one as an author by contacting the Frontiers editorial office: frontiersin.org/about/contact

Efficacy and mechanism of herbal medicines and their functional compounds in preventing and treating cardiovascular diseases and cardiovascular disease risk factors

Topic editors

Qing Yong He — Guang'anmen Hospital, China Academy of Chinese Medical Sciences, China

Yu-Qing Zhang — McMaster University, Canada

Jie Wang — Guang'anmen Hospital, China Academy of Chinese Medical Sciences, China

Jian Zhang — Tianjin Medical University, China

Kuo Gao — Beijing University of Chinese Medicine, China

Chen Huei Leo — Singapore University of Technology and Design, Singapore

Zhongfeng Li — Capital Normal University, China

Topic Coordinator

Tiantian Meng — Guang'anmen Hospital, China Academy of Chinese Medical Sciences, China

Citation

He, Q. Y., Zhang, Y.-Q., Wang, J., Zhang, J., Gao, K., Leo, C. H., Li, Z., Meng, T., eds. (2023). *Efficacy and mechanism of herbal medicines and their functional compounds in preventing and treating cardiovascular diseases and cardiovascular disease risk factors*. Lausanne: Frontiers Media SA. doi: 10.3389/978-2-8325-3021-4

Table of contents

frontiers | Frontiers in Pharmacology

TYPE Editorial
PUBLISHED 03 July 2023
DOI 10.3389/fphar.2023.1236821

Check for updates

OPEN ACCESS

EDITED BY
Javier Echeverria,
University of Santiago, Chile

REVIEWED BY
Adolfo Andrade-Cetto,
National Autonomous University of Mexico, Mexico

*CORRESPONDENCE
Jian Zhang,
zhangjian_tina@163.com
Kuo Gao,
515123134@qq.com
Qingyong He,
heqingyongg@163.com

RECEIVED 08 June 2023
ACCEPTED 27 June 2023
PUBLISHED 03 July 2023

CITATION
Meng T, Zhang Y, Wang J, Leo CH, Li Z, Zhang J, Gao K and He Q (2023), Editorial: Efficacy and mechanism of herbal medicines and their functional compounds in preventing and treating cardiovascular diseases and cardiovascular disease risk factors. *Front. Pharmacol.* 14:1236821. doi: 10.3389/fphar.2023.1236821

COPYRIGHT
© 2023 Meng, Zhang, Wang, Leo, Li, Zhang, Gao and He. This is an open-access article distributed under the terms of the Creative Commons Attribution License (CC BY). The use, distribution or reproduction in other forums is permitted, provided the original author(s) and the copyright owner(s) are credited and that the original publication in this journal is cited, in accordance with accepted academic practice. No use, distribution or reproduction is permitted which does not comply with these terms.

Editorial: Efficacy and mechanism of herbal medicines and their functional compounds in preventing and treating cardiovascular diseases and cardiovascular disease risk factors

Tiantian Meng[1], Yuqing Zhang[2], Jie Wang[1], Chen Huei Leo[3], Zhongfeng Li[4], Jian Zhang[5]*, Kuo Gao[6]* and Qingyong He[1]*

[1]Department of Cardiology, Guang'anmen Hospital, China Academy of Chinese Medical Sciences, Beijing, China, [2]Department of Health Research Methods, Evidence, and Impact, McMaster University, Hamilton, ON, Canada, [3]Department of Science, Mathematics and Technology, Singapore University of Technology and Design, Singapore, Singapore, [4]Department of Chemistry, Capital Normal University, Beijing, China, [5]Shanghai Key Laboratory of New Drug Design, School of Pharmacy, East China University of Science and Technology, Shanghai, China, [6]Beijing University of Chinese Medicine, Beijing, China

KEYWORDS

cardiovascular disease, cardiovascular disease risk factors, herbal medicine, efficacy, mechanism

Editorial on the Research Topic
Efficacy and mechanism of herbal medicines and their functional compounds in preventing and treating cardiovascular diseases and cardiovascular disease risk factors

Introduction

Cardiovascular disease (CVD) ranks among the leading causes of mortality worldwide, posing a substantial global public health challenge (Roth et al., 2020). Prevalent CVDs, such as coronary heart disease (CHD), atherosclerosis (AS), and heart failure (HF), afflict hundreds of millions of individuals across the globe. Prevalent cases of CVD nearly doubled from 271 million in 1990 to 523 million in 2019 (Roth et al., 2020). In addition, risk factors for CVD, including dyslipidemia, diabetes, and hypertension, are recognized as critical contributors to the onset of CVDs. The persistently rising incidence of CVD underscores the limitations of current therapeutic approaches, necessitating the identification of novel alternative treatments.

In recent years, herbal medicines have increasingly demonstrated their potential as alternative therapies for cardiovascular-related diseases (Chen et al., 2022; Lai et al., 2022; Meng et al., 2022). However, given the scarcity of clinical evidence, further investigation is warranted to elucidate the efficacy and underlying mechanisms of herbal medicine in treating CVDs.

The purpose of this Research Topic was to probe the effectiveness and mechanistic basis of herbal medicines in treating CVDs. A total of 15 papers were included in our Research Topic, including 6 original articles and 9 reviews.

Atherosclerosis

AS is a chronic inflammatory disease of the vasculature, characterized by the formation of fibrous and fatty lesions on arterial walls, with a complex pathogenesis (Tall and Bornfeldt, 2023).

In this Research Topic, a mini review by Guo et al. showed that emodin exerted antiatherogenic effects through its anti-inflammatory effects, regulation of lipid metabolism, and protection of endothelial cells. Furthermore, Liu et al. suggested that ginseng could also delay AS progression by antioxidant activity, modulation of autophagy, and inhibition of apoptosis. Moreover, the influence of gut microbiota on AS has garnered increasing interest in recent years. Herbal medicine demonstrates significant therapeutic effects in modulating gut microbiota and ameliorating AS. Xie et al. demonstrated that ginsenoside Rc (GRc) could play an antiatherogenic role by regulating gut microbiota and fecal metabolites *in vivo*. Li et al. further reviewed the mechanism of gut microbiota in AS, concluding that gut microbiota played an essential role in the occurrence and aggravation of AS by modulating immunity and metabolism, which indicated that vascular mitochondria might be the key medium for gut microflora disorder. Certain herbal medicines and their components, including berberine, resveratrol, allicin, quercetin, and curcumin, could regulate both the gut microbiota and vascular mitochondria to exert therapeutic effects on AS plaques. In addition, AS encompasses various cellular processes and signaling pathways, with the mTOR signaling pathway emerging as a crucial regulatory route. Wu et al. summarized the influence of the mTOR signaling pathway on AS plaques, with a focus on lipid metabolism, autophagy, immune response, and antiaging. Their findings indicated that targeting the inhibition of the mTOR signaling pathway might represent a promising avenue for the treatment of AS. Botanical drugs containing natural compounds, such as quercetin and resveratrol, could modulate autophagy, attenuate immune responses, and delay AS progression by inhibiting the mTOR signaling pathway.

Hypertension

Hypertension is characterized by a systemic elevation in arterial blood pressure, defined as office systolic blood pressure ≥ 130 mmHg and diastolic blood pressure ≥ 80 mmHg (Tschanz et al., 2020). Despite considerable advancements in pharmacological interventions, the treatment and control of hypertension continue to be suboptimal. In recent years, emerging evidence has highlighted the potential of herbal medicine as an alternative therapeutic approach for hypertension (Lai et al., 2022; Meng et al., 2022).

In this Research Topic, a meta-analysis by Lin et al. demonstrated that Banxia Baizhu Tianma decoction (BXD) combined with conventional therapy (CT) significantly reduced blood pressure compared to CT alone. Additionally, in terms of blood lipids, inflammation, homocysteine, and endothelial function, the combination of BXD and CT was superior to CT alone. Network pharmacology suggested that the drug targets might be ACE, AKT1, NOS3, and PPARG. Guo et al. summarized the regulatory mechanism of emodin on blood pressure and found that emodin played an antihypertensive role by inhibiting deendothelialized aortic vasoconstriction induced by phenylephrine. The combination of emodin and irbesartan was found to alleviate myocardial fibrosis in hypertensive rats.

Platelet aggregation and thrombus

Platelet aggregation and thrombosis can result in partial or complete occlusion of blood vessels (Li et al., 2022). Although certain antithrombotic agents have demonstrated efficacy, maintaining the balance between embolism prevention and bleeding risk remains challenging (Kwaan and Bennett, 2012).

Qin et al. provided a comprehensive summary of the antithrombotic potential of Astragali Radix and its active metabolites, revealing their ability to protect against vascular endothelial cell damage, decrease coagulation factor levels, and inhibit the fibrinolytic system. Additionally, the combination of Astragali Radix and anti-platelet drugs such as aspirin or clopidogrel could significantly enhance the antiplatelet effect and reduce the risk of bleeding. Liu et al. reviewed the antithrombotic mechanism of ginseng. This review showed that ginsenosides played an antithrombotic role by improving platelet aggregation, suppressing thrombin, and inhibiting fibrin binding with IIb/β3 on platelets. Furthermore, synergistic interactions among various ginsenosides could amplify the overall antithrombotic effect.

Cornary heart disease

CHD is characterized by coronary artery stenosis or occlusion caused by atherosclerotic lesions. Common manifestations of CHD encompass stable angina pectoris (SAP), unstable angina pectoris (UAP), and myocardial infarction (MI). As clinical evidence accumulates, herbal medicine is emerging as an alternative approach for primary and secondary prevention in patients with CHD (Lv et al., 2022; Ma et al., 2023).

In this Research Topic, a meta-analysis by Wei et al. showed that the combination of Shexiang Baoxin pill and CT is superior to CT alone in reducing cardiovascular adverse events, improving cardiac function, and alleviating angina. In another meta-analysis, Xi et al. evaluated the efficacy of Xueshuantong (lyophilized) injection (XST) for UAP. The results showed that patients received XST combined with CT experienced fewer angina episodes and exhibited reduced levels of cholesterol, triglycerides, whole blood viscosity and plasma viscosity. Tan et al. adopted improved network pharmacology combined with metabolomics to investigate the molecular mechanism of Huoxue Qingre decoction (HXQR) for CHD. It was found that puerarin, kaempferol, luteolin, baicalein, and

TABLE 1 Plant names in traditional Chinese medicine preparations.

Preparations	Plant names in the preparations	Source
Shexiang Baoxin pill	Moschus berezovskii, M. sifanicus or M. moschiferus (Shexiang), Panax ginseng C.A.Mey. (Renshen), *Bos taurus* domesticus Gmelin (Niuhuang), Cinnamomum cassia Presl (Rougui), Liquidambar orientalis Mill. (Suhexiang), *Bufo gargarizans* Cantor (Chansu), and Borneolum Syntheticum (Bingpian)	Wei et al.
Xueshuantong injection	Panax notoginseng saponins	Xi et al.
Huoxue Qingre decoction	Salvia miltiorrhiza Bunge (Danshen), Panax ginseng C.A.Mey. (Renshen), Coptis chinensis Franch. (Huanglian), Pinellia ternata (Thunb.) Makino (Fabanxia), Paeonia lactiflflora Pall. (Chishao), Panax notoginseng (Burk) F. H. Chen (Sanqi), Pueraria lobata (Willd.) Maesen and S.M. Almeida ex Sanjappa and Predeep (Gegen), and Cistanche deserticola Ma (Roucongrong)	Tan et al.
Suxiao Jiuxin pill	Ligusticum chuanxiong Hort. (Chuanxiong) and Borneolum syntheticum (Bingpian)	Li et al.
Qishen granule	Astragalus mongholicus Bunge (Huangqi), Salvia miltiorrhiza Bunge (Danshen), Aconitum carmichaeli Debeaux (Wutou), Scrophularia ningpoensis Hemsl. (Xuanshen), *Lonicera japonica* Thunb. (Rendong), and Glycyrrhiza glabra L. (Gancao)	Du et al.
Yiqi Fumai injection	Panax ginseng C.A. Mey. (Renshen), Ophiopogon ja ponicus (Thunb.) Ker Gawl (Maidong), and Schisandra chinensis (Turcz.) Baill (Wuweizi)	Lv et al.
Linggui Zhugan decoction	Poria cocos (Schw.) Wolf (Fuling), Neolitsea cassia (L.) Kosterm. (Guizhi), Atractylodes macrocephala Koidz. (Baizhu), and Glycyrrhiza glabra L. (Gaocao)	Yu et al.
Banxia Baizhu Tianma decoction	Pinellia ternata (Thunb.) Makino (Banxia), Atractylodes macrocephala Koidz. (Baizhu), Citrus × aurantium L. (Chenpi), Glycyrrhiza uralensis Fisch. ex DC. (Gancao), Gastrodia elata Blume (Tianma), and Poria cocos (Schw.) Wolf (Fuling)	Lin et al.

tanshinone iia might be the predominant active ingredients of HXQR for CHD.

MI arises from acute and sustained ischemia and hypoxia in the coronary artery, leading to subsequent myocardial cell death. Li et al. demonstrated that Suxiao Jiuxin pill (SJP) could relax the coronary artery by the Akt-eNOS-NO pathway and thereby protect against acute MI in rats. A mini review by Guo et al. summarized the therapeutic effect of emodin in MI, suggesting that this compound might prevent myocardial cell damage by inhibiting apoptosis and inflammatory responses.

Myocardial ischemia-reperfusion injury

Myocardial ischemia–reperfusion (I/R) injury refers to the damage inflicted on myocardial cells during the reperfusion of coronary arteries. Its pathogenesis is primarily associated with oxidative stress, inflammation, calcium overload, energy metabolism disorder, apoptosis, and ferroptosis (Li et al., 2018; Fan et al., 2021; Wang et al., 2022; Xia et al., 2022). The results of single-aspect treatment are unsatisfactory. Due to its multicomponent and multitarget nature, herbal medicine may provide new insights into myocardial I/R injury.

Li et al. conducted a meta-analysis to assess the clinical and preclinical evidence supporting the efficacy of curcumin in treating myocardial I/R injury. The meta-analysis of clinical studies showed that curcumin could decrease the incidence of cardiac insufficiency and major adverse cardiovascular events. The meta-analysis of preclinical studies showed that curcumin exerted cardioprotective effects mainly by antioxidant, anti-inflammatory, antifibrotic and antiapoptotic effects. Liu et al. showed that ginsenosides could protect the heart from myocardial I/R injury through antioxidant effects, potentially linked to the reduction in intracellular calcium overload and the inhibition of the JNK signaling pathway. Another review by Guo et al. showed that emodin could confer protection against myocardial I/R injury by modulating inflammation, oxidative stress, and apoptosis in MI models.

Heart failure

HF represents the end stage of various CVDs and constitutes a complex clinical syndrome (Groenewegen et al., 2020). Current standard treatment for HF remains unsatisfactory.

Du et al. conducted a randomized controlled trial, demonstrating that Qishen granule (QSG), when added to standard treatment, improved N-terminal pro-B-type natriuretic peptide levels, six-min walking distance, New York Heart Association class, and quality of life in patients with chronic HF compared to placebo. Lv et al. provided a comprehensive overview of the clinical evidence and mechanism of Yiqi Fumai injection (YQFM) for HF. This study indicated that YQFM could improve heart function, inhibit ventricular remodeling, and enhance quality of life in patients with HF through multiple mechanisms, including anti-inflammation, anti-apoptosis, antioxidation, regulating miRNA expression, improving mitochondrial function, and maintaining the balance of matrix metalloproteinase and tissue inhibitor of metalloproteinase. In an animal experiment, Yu et al. demonstrated that Linggui Zhugan decoction (LGZG) improved myocardial antioxidant capacity and mitochondrial function by activating the SIRT1/AMPK/PGC-1a signaling pathway, thereby enhancing cardiac function in rats with HF. Liu et al. indicated that ginsenosides could improve ventricular remodeling and alleviate failure by scavenging free radicals, improving antioxidant enzyme function and enhancing metabolic capacity. Moreover, ginsenosides were found to exert protective effects

against HF resulting from cardiotoxicity. Guo et al. summarized the mechanism of emodin in treating HF, concluding that emodin could potentially delay HF progression by improving mitochondrial energy metabolism, reducing histone deacetylase activity in cardiomyocytes, inhibiting myocardial fibrosis and regulating calcium homeostasis.

Conclusion

This Research Topic encompasses 15 articles covering a wide range of studies on herbal medicines, including traditional Chinese medicine preparations and their functional compounds for CVDs and relevant risk factors. Table 1 presents the plant names in the traditional Chinese medicine preparations. These findings significantly enhance our comprehension of the therapeutic effects and mechanisms of herbal medicines for cardiovascular-related diseases. In addition, several potential therapeutic targets for CVDs were identified. Some of these studies have also identified several active ingredients in herbal medicines, providing promising candidates for new drug development. In summary, our Research Topic furnishes scientific evidence supporting the efficacy of herbal medicine in the treatment of CVDs and their risk factors, bolstering the prospects of herbal medicine as an alternative therapeutic approach for CVDs.

Author contributions

All authors listed have made a substantial, direct, and intellectual contribution to the work and approved it for publication.

Funding

This work is supported by the Traditional Chinese Medicine Ancient Book Documents and Characteristic Technology Inheritance Project of the National Administration of Traditional Chinese Medicine (GZY-KJS-2020-079), Research and Transformation Application of Clinical Characteristic Diagnosis and Treatment Techniques in the Capital (Z221100007422081), Beijing-Tianjin-Hebei Basic Research Cooperation Project (No. J200020), National Natural Science Foundation of China (81903950), and Scientific Launching Research Foundation of Beijing University of Chinese Medicine (2022-JYB-XJSJJ008).

Conflict of interest

The authors declare that the research was conducted in the absence of any commercial or financial relationships that could be construed as a potential conflict of interest.

Publisher's note

All claims expressed in this article are solely those of the authors and do not necessarily represent those of their affiliated organizations, or those of the publisher, the editors and the reviewers. Any product that may be evaluated in this article, or claim that may be made by its manufacturer, is not guaranteed or endorsed by the publisher.

References

Chen, L., Fu, G., Hua, Q., Zhu, H. Y., Deng, Y., Wu, W., et al. (2022). Efficacy of add-on danhong injection in patients with unstable angina pectoris: A double-blind, randomized, placebo-controlled, multicenter clinical trial. *J. Ethnopharmacol.* 284, 114794. doi:10.1016/j.jep.2021.114794

Fan, Z., Cai, L., Wang, S., Wang, J., and Chen, B. (2021). Baicalin prevents myocardial ischemia/reperfusion injury through inhibiting ACSL4 mediated ferroptosis. *Front. Pharmacol.* 12, 628988. doi:10.3389/fphar.2021.628988

Groenewegen, A., Rutten, F. H., Mosterd, A., and Hoes, A. W. (2020). Epidemiology of heart failure. *Eur. J. Heart Fail.* 22, 1342–1356. doi:10.1002/ejhf.1858

Kwaan, H. C., and Bennett, C. L. (2012). Adverse effects of drugs on hemostasis and thrombosis. *Semin. Thromb. Hemost.* 38, 755–758. doi:10.1055/s-0032-1329596

Lai, X., Dong, Z., Wu, S., Zhou, X., Zhang, G., Xiong, S., et al. (2022). Efficacy and safety of Chinese herbal medicine compared with losartan for mild essential hypertension: A randomized, multicenter, double-blind, noninferiority trial. *Circ. Cardiovasc. Qual. Outcomes* 15, e007923. doi:10.1161/CIRCOUTCOMES.121.007923

Li, L., Pan, C. S., Yan, L., Cui, Y. C., Liu, Y. Y., Mu, H. N., et al. (2018). Ginsenoside Rg1 ameliorates rat myocardial ischemia-reperfusion injury by modulating energy metabolism pathways. *Front. Physiol.* 9, 78. doi:10.3389/fphys.2018.00078

Li, X., Guo, T., Feng, Q., Bai, T., Wu, L., Liu, Y., et al. (2022). Progress of thrombus formation and research on the structure-activity relationship for antithrombotic drugs. *Eur. J. Med. Chem.* 228, 114035. doi:10.1016/j.ejmech.2021.114035

Lv, J., Liu, S., Guo, S., Gao, J., Song, Q., and Cui, X. (2022). Tongxinluo capsule as supplementation and cardiovascular endpoint events in patients with coronary heart disease: A systematic review and meta-analysis of randomized, double-blind, placebo-controlled trials. *J. Ethnopharmacol.* 289, 115033. doi:10.1016/j.jep.2022.115033

Ma, X., Wang, Q., Liu, C., Liu, J., Luo, G., He, L., et al. (2023). Regulation of phospholipid peroxidation signaling by a traditional Chinese medicine formula for coronary heart disease. *Phytomedicine* 114, 154749. doi:10.1016/j.phymed.2023.154749

Meng, T., Wang, P., Xie, X., Li, T., Kong, L., Xu, Y., et al. (2022). Efficacy and safety of songling xuemaikang capsule for essential hypertension: A systematic review and meta-analysis of randomized controlled trials. *Phytomedicine* 107, 154459. doi:10.1016/j.phymed.2022.154459

Roth, G. A., Mensah, G. A., Johnson, C. O., Addolorato, G., Ammirati, E., Baddour, L. M., et al. (2020). Global burden of cardiovascular diseases and risk factors, 1990-2019: Update from the GBD 2019 study. *J. Am. Coll. Cardiol.* 76, 2982–3021. doi:10.1016/j.jacc.2020.11.010

Tall, A. R., and Bornfeldt, K. E. (2023). Inflammasomes and atherosclerosis: A mixed picture. *Circ. Res.* 132, 1505–1520. doi:10.1161/CIRCRESAHA.123.321637

Tschanz, C. M. P., Cushman, W. C., Harrell, C. T. E., Berlowitz, D. R., and Sall, J. L. (2020). Synopsis of the 2020 U.S. Department of veterans affairs/U.S. Department of defense clinical practice guideline: The Diagnosis and management of hypertension in the primary care setting. *Ann. Intern. Med.* 173, 904–913. doi:10.7326/M20-3798

Wang, R., Wang, M., Liu, B., Xu, H., Ye, J., Sun, X., et al. (2022). Calenduloside E protects against myocardial ischemia-reperfusion injury induced calcium overload by enhancing autophagy and inhibiting L-type Ca(2+) channels through BAG3. *Biomed. Pharmacother.* 145, 112432. doi:10.1016/j.biopha.2021.112432

Xia, B., Li, Q., Wu, J., Yuan, X., Wang, F., Lu, X., et al. (2022). Sinomenine confers protection against myocardial ischemia reperfusion injury by preventing oxidative stress, cellular apoptosis, and inflammation. *Front. Pharmacol.* 13, 922484. doi:10.3389/fphar.2022.922484

frontiers | Frontiers in Pharmacology

TYPE Original Research
PUBLISHED 15 September 2022
DOI 10.3389/fphar.2022.990476

Check for updates

OPEN ACCESS

EDITED BY
Kuo Gao,
Beijing University of Chinese Medicine, China

REVIEWED BY
Wenkai Li,
Shanghai University of Traditional Chinese Medicine, China
Stanislav Kotlyarov,
Ryazan State Medical University , Russia
Helda Tutunchi,
Tabriz University of Medical Sciences, Iran

*CORRESPONDENCE
Guoping Liu,
lgp2680@sina.com
Runhui Liu,
lyliurh@126.com

†These authors have contributed equally to this work and share first authorship

SPECIALTY SECTION
This article was submitted to Ethnopharmacology, a section of the journal Frontiers in Pharmacology

RECEIVED 10 July 2022
ACCEPTED 17 August 2022
PUBLISHED 15 September 2022

CITATION
Xie B, Zu X, Wang Z, Xu X, Liu G and Liu R (2022), Ginsenoside Rc ameliorated atherosclerosis via regulating gut microbiota and fecal metabolites. *Front. Pharmacol.* 13:990476. doi: 10.3389/fphar.2022.990476

COPYRIGHT
© 2022 Xie, Zu, Wang, Xu, Liu and Liu. This is an open-access article distributed under the terms of the Creative Commons Attribution License (CC BY). The use, distribution or reproduction in other forums is permitted, provided the original author(s) and the copyright owner(s) are credited and that the original publication in this journal is cited, in accordance with accepted academic practice. No use, distribution or reproduction is permitted which does not comply with these terms.

Ginsenoside Rc ameliorated atherosclerosis *via* regulating gut microbiota and fecal metabolites

Bin Xie[1†], Xianpeng Zu[1†], Zhicong Wang[1], Xike Xu[1], Guoping Liu[2*] and Runhui Liu[1*]

[1]School of Pharmacy, Naval Medical University, Shanghai, China, [2]Department of General Surgery, Xin Hua Hospital Affiliated to Shanghai Jiao Tong University School of Medicine, Shanghai, China

Atherosclerosis (AS) and the accompanied cardiovascular diseases (CVDs) were the leading cause of death worldwide. Recently, the association between CVDs, gut microbiota, and metabolites had aroused increasing attention. In the study, we headed our investigation into the underlying mechanism of ginsenoside Rc (GRc), an active ingredient of ginsenosides used for the treatment of CVDs, in apolipoprotein E-deficient (ApoE$^{-/-}$) mice with high-fat diet (HFD). Seven-week-old male ApoE$^{-/-}$ mice were randomly divided into four groups: the normal control (NC) group, the HFD group, the GRc group (40 mg/kg/d), and the atorvastatin (Ato) group (10 mg/kg/d). Atherosclerotic injury was evaluated by aortic lesions, serum lipid levels, and inflammatory factors. The composition of gut microbiota and fecal metabolite profile were analyzed using 16S rRNA sequence and untargeted metabolomics, respectively. The results showed that GRc significantly alleviated HFD-induced aortic lesions, reduced serum levels of total cholesterol (TC), triglyceride (TG), low-density lipoprotein cholesterol (LDL-C), tumor necrosis factor-α (TNF-α), and interleukin (IL)-6 and IL-1β, and increased high-density lipoprotein cholesterol (HFD-C) level, as well as the alteration of gut microbiota composition, function, and metabolite profile. GRc also reversed HFD change of Bacteroidetes and Firmicutes at the phylum level, Muribaculaceae, *Lactobacillus*, *Ileibacterium*, *Bifidobacterium*, *Faecalibaculum*, *Oscillibacter*, *Blautia*, and *Eubacterium_coprostanoligenes_group* at the genus level, and 23 key metabolites involved in taurine and hypotaurine metabolism, arginine biosynthesis, ATP-binding cassette (ABC) transporters, primary bile acid biosynthesis, purine metabolism, tricarboxylic acid (TCA) cycle, and glucagon signaling pathways. Additionally, eight differential intestinal floras at the genus level were associated with 23 key differential metabolites involving atherosclerotic injury. In conclusion, our results demonstrated that GRc ameliorated atherosclerotic injury, regulated microbial and metabolomic changes in HFD-induced ApoE$^{-/-}$ mice, and suggested a potential correlation among gut microbiota, metabolites, and atherosclerotic injury regarding the mechanisms of GRc against AS.

KEYWORDS

atherosclerosis, gut microbiota, fecal metabolites, ginsenoside Rc, correlation

Introduction

Cardiovascular diseases (CVDs) are a group of disorders of the heart and blood vessels and the leading cause of death worldwide. Almost 17 million people died from CVDs in 2019, occupying 32% of global deaths (World Health Organization, 2021, https://www.who.int/news-room/fact-sheets/detail/cardiovascular-diseases-(cvds)). Atherosclerosis (AS), a systemic chronic inflammatory disease resulting in CVDs, is characterized by the formation of fibrofatty lesions in the artery wall (Genkel et al., 2020). The risk factors for AS and its thrombotic complications include low-density lipoprotein cholesterol (LDL-C), hypertension, cigarette smoking, obesity, and diabetes mellitus (Libby et al., 2019). Although the pathogenesis of AS is not totally clear, numerous investigations consider it a disorder of lipid metabolism, inflammation, and vascular endothelial damage (Libby et al., 2019). Despite the advanced treatment applied to clinic, such as lipid-lowering, anti-platelet, and anti-inflammatory drugs, there are therapeutic challenges including side effects and nonadherence to pharmacological therapy, which lead to most patients not meeting their desirable therapeutic goal (Libby et al., 2019). Therefore, the mortality resulting from AS and its complications is still high, and more advanced treatments for AS are urgent.

Accumulating studies indicate the role of gut microbiota and its metabolites on human diseases. Alterations in the composition of intestinal floras have been observed in a growing body of disorders including CVDs (Witkowski et al., 2020). Some microbial species from the intestine were found in the plaque of atherosclerotic patients, suggesting that gut microbiota might have a direct impact on AS (Fak et al., 2015). Recently studies showed that there was much more difference in the gut microbiota composition of patients with AS than healthy controls (Chen et al., 2021). In addition, the gut microbiota and its metabolites regulated inflammation, immunity, cholesterol, and lipid metabolism, which underlined the initiation and progression of AS (Jonsson and Backhed, 2017; Ma and Li, 2018). Various technologies for investigation of microbiota and its effects on host metabolism, such as bacterial 16S rRNA gene sequencing and metabolomics, allow further study of the relationship between gut metabolism and AS, as well as potential novel therapeutic targets.

Panax ginseng C.A. Meyer, a well-known medicinal herb, has been used for preventive and therapeutic purposes for thousands of years in Asian countries. Increasing studies reported the pharmacological activities and chemical components of *P. ginseng* (Mancuso and Santangelo, 2017; Wu et al., 2018). Ginsenosides, generally classified into protopanaxadiol and propanaxatriol due to the difference in C-6 chiral carbon substitution sites, are the main active components of *P. ginseng* used for the treatment of metabolic syndrome and CVDs (Fan et al., 2020; Im, 2020). Most Chinese patent medicines containing ginsenosides had been applied for AS, such as Shexiang Baoxin Pill, Yixingtongmai decoction, Tongxinluo, Xin-Ji-Er-Kang, and Tiaopi Huxin recipe (Zhang et al., 2022). Previous studies showed that protopanaxadiol-type ginsenoside Rd, Rb1, and Rg3 exhibited anti-atherosclerotic effects (Xue et al., 2021), and ginsenoside Rb1 could regulate gut microbiota and amino acid metabolism to improve HFD-induced insulin resistance in mice (Yang et al., 2021). A protopanaxadiol ginsenoside Rc (GRc) is an active ingredient of ginsenosides. Although it was poorly absorbed after oral administration in the host (Sun et al., 2014), it exhibited multiple pharmacological functions, including neuroprotective (Huang et al., 2021), anti-tumor (Zhu et al., 2021), anti-adipogenic (Yang and Kim, 2015), anti-inflammatory, and anti-oxidant (Shi et al., 2022) effects. However, the role of GRc against AS has not been investigated yet. Considering its poor bioavailability and chemical structure similar to Rd, Rb1, and Rg3, we hypothesized that GRc might have protective effects against AS and if so, the underlying mechanisms of anti-atherosclerotic effects could be probably associated with the regulation of gut microbiota and fecal metabolites. In this study, the role and potential mechanism of GRc against AS in HFD-induced ApoE$^{-/-}$ mice were investigated for the first time using 16S rRNA sequence and untargeted fecal metabolomics methods (Figure 1). Based on the fact that GRc had a similar chemical structure to ginsenoside Rb1 which had anti-atherosclerotic effect and regulated gut microbiota composition, the study aimed to examine the anti-atherosclerotic effects and potential mechanisms of GRc against AS and provide a candidate small molecule for the prevention and treatment of CVDs.

Materials and methods

Reagents and materials

GRc (molecular weight = 1079.27, Lot: 20210419, CAS: 11021-14-0, and purity ≥98.0%) was purchased from Shanghai Sunny Biotech Co., Ltd. (Shanghai, China). Atorvastatin (Ato, Approval No. H20051408) was obtained from Pfizer Pharmaceuticals Ltd. (NY, United States). The kits for determining total cholesterol (TC), triglyceride (TG), LDL-C, and high-density lipoprotein cholesterol (HDL-C) were products of Nanjing Jiancheng Institute of Biological Engineering (Nanjing, China). The ELISA kits for mouse tumor necrosis factor-α (TNF-α), interleukin-6 (IL-6), and interleukin-1β (IL-1β) were provided by Neobioscience (Shenzhen, China).

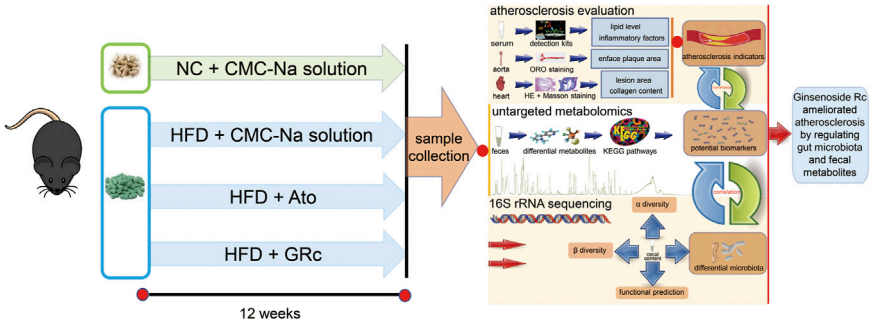

FIGURE 1
Workflow for examining the anti-atherosclerotic effects and potential mechanisms of GRc against AS in ApoE$^{-/-}$ mice. Differential gut microbiota, fecal metabolites, and AS indexes were conjointly analyzed in the study.

Animals and treatment

Seven-week-old male C57/BL6 ApoE$^{-/-}$ mice of weight 23.7 ± 4 g (License Number: SCXK (Su) 2018-0008) were purchased from Jiangsu GemPharmatech Co., Ltd. (Jiangsu, China). All mice were maintained under a suitable environmental condition (22 ± 1°C, relative humidity of 60%, and 12 h/12 h light/dark cycle). All animal procedures were conducted according to the Guideline for the Care and Use of Laboratory Animals from Naval Medical University and approved by the Ethics Committee of Naval Medical University.

Mice were acclimated for 1 week and randomly assigned to four groups (n = 6): (1) the normal control (NC) group with a normal chow diet; (2) the high-fat diet (HFD) group containing 21% fat and 1.25% cholesterol (same volume of 0.5% sodium carboxymethyl cellulose solution by gavage); (3) the GRc group fed with HFD containing GRc (40 mg/kg /d GRc by gavage), and (4) the Ato group fed with HFD containing Ato (10 mg/kg/d Ato by gavage). GRc and Ato were dissolved in 0.5% sodium carboxymethyl cellulose solution, and all mice were fed once daily for 12 weeks consecutively. Body weight was monitored and recorded each week during the study.

At the end of the experiment, all animals were fasted overnight and anesthetized. Whole blood was drawn from the eyeball. Serum samples were isolated from whole blood through centrifugation at 2,500 g for 15 min at 4 °C and then immediately stored at −80 °C. Other organs or tissues were collected separately for further study.

Assessment of atherosclerotic lesions

Atherosclerotic lesions were assessed with a protocol previously described (Lu et al., 2019), and the whole aorta from the arch to the iliac bifurcation was carefully removed and fixed in 4% paraformaldehyde solution overnight. Then, the aorta was washed three times with phosphate-buffered saline and stained with 0.5% Oil Red O (ORO) working solution. The extent of aortic AS was evaluated as the percentage of ORO-positive stained red area in relation to the area of the entire aorta luminal surface. Then, the hearts of mice were embedded in optimal cutting temperature compound and cut into 10-μm sections for histological analysis of atherosclerotic lesions in the aortic sinus. Measurement and quantification of the lesion area and the collagen content were carried out based on hematoxylin and eosin (H&E) and Masson's trichrome staining, respectively. Representative images were analyzed using Image-Pro Plus 6.0 software (Media Cybernetics).

Determination of serum biochemical parameters

Serum TC, TG, LDL-C, and HDL-C were measured using kits from Nanjing Jiancheng Bioengineering Institute following the manufacturer's protocols. Serum systemic inflammatory cytokine levels of TNF-α, IL-6, and IL-1β were evaluated using ELISA kits according to the manufacturer's instructions. The absorbance was measured at the corresponding wavelength using a Bio-Tek microplate reader (Winooski, VT, United States).

16S rRNA sequencing and analysis

Cecal contents were snap-frozen and stored at −80°C after collection. Genomic DNA was extracted from cecal contents using the MagPure Soil DNA LQ Kit (Magen) according to the manufacturer's instructions. Concentration and quality of DNA were verified using a NanoDrop 2000 spectrophotometer

(Thermo Fisher) and agarose gel electrophoresis, respectively. A thermocycler polymerase chain reaction (PCR) system (Bio-Rad) was applied for the amplification of the V3–V4 hypervariable parts of the bacterial 16S rRNA gene via primers 343F (5′-TACGGRAGGCAGCAG-3′) and 798R (5′- AGGGTATCT AAT-CCT-3′). The reverse primer contained a sample barcode, and both primers were connected with an Illumina sequencing adapter. The amplicon quality was visualized using gel electrophoresis. PCR products were purified with AMPure XP beads (Agencourt) and then quantified using a Qubit dsDNA assay kit (Life Technologies). Equal amounts of purified amplicon were pooled for subsequent sequencing.

Quality-filtration of raw FASTQ files was achieved via Trimmomatic (v0.35) followed by their merging through FLASH (v1.2.11). Reads with 75% of bases above Q20 were retained using QIIME software (v1.8.0). Then, reads with chimera were detected and removed using VSEARCH software (v2.4.2). Operational taxonomic units (OTUs) were grouped with a similarity cutoff of 97% utilizing VSEARCH, and the representative read of each OTU was selected using the QIIME (v1.8.0) package. All representative reads were annotated and blasted against the SILVA database (v132) using the RDP classifier with a confidence threshold of 70%. Microbial alpha (α) diversity in cecal contents was accessed by the indexes of Chao1 and Shannon. Beta (β) diversity was evaluated by principal coordinate analysis (PCoA) on an unweighted unifrac distance matrix. Linear discriminant analysis (LDA) coupled with effect size (LEfSe) measurements based on the non-parametric factorial Kruskal–Wallis sum-rank test and the Wilcoxon rank-sum test was used to identify taxa significantly different biomarkers between groups, with $p < 0.05$ and an LDA score threshold of 4. The phylogenetic investigation of communities by reconstruction of unobserved states (PICRUSt2) was applied to predict functional genes of the classified members of the microbiome through closed-reference-based OTU mapping against the Greengenes database (Langille et al., 2013). The 16S rRNA gene amplicon sequencing and analysis were conducted by OE Biotech Co., Ltd. (Shanghai, China).

LC-MS-based untargeted metabolomics analysis

A volume of 60 mg fecal sample was transferred to a 1.5-ml Eppendorf tube. Two small steel balls were added to the tube. A volume of 24 μL internal standard (2-chloro-l-phenylalanine in methanol, 0.3 mg/ml) and extraction solvent with methanol/water (4/1, *v/v*) were added to each sample. QC samples were prepared by mixing aliquots of all samples to be a pooled sample. Samples were stored at −20°C for 5 min and then ground at 60 Hz for 2 min, ultrasonicated in cold water for 10 min, and stored at −20°C for 5 h. The extract was centrifuged at 13,000 g and 4°C for 10 min. A measure of 150 μl of supernatant from each tube was collected using crystal syringes, filtered through 0.22-μm microfilters, transferred to LC vials, and analyzed using a Dionex Ultimate 3000 RS UHPLC (Thermo Fisher Scientific) fitted with a Q-Exactive Plus Quadrupole-Orbitrap mass spectrometer equipped with a heated electrospray ionization (ESI) source. An ACQUITY UPLC HSS T3 (1.8 μm, 2.1 × 100 mm) was used, and the mobile phase consisted of acetonitrile and water containing 0.1% formic acid. Additionally, the following parameters were set: flow rate, 0.35 ml/min; column temperature, 45°C; and injection volume, 2 μl. The mass range was from *m/z* 100 to 1,000. The resolution was set at 70,000 for the full MS scans and 17,500 for HCD MS/MS scans. The collision energy was set at 10, 20, and 40 eV.

The original LC/MS data were processed using Progenesis QI (v2.3) software for baseline filtering, peak identification, integral, retention time correction, peak alignment, and normalization. Compound identification was based on the precise mass-to-charge ratio (*m/z*), secondary fragments, and isotopic distribution using the Human Metabolome Database (HMDB), LIPIDMAPS (v2.3), METLIN, EMDB, PMDB, and self-built databases to perform qualitative analysis. The matrix was imported in R to carry out principal component analysis (PCA) to observe the overall distribution among the samples and the stability of the whole analysis process. Partial least squares discriminant analysis (PLS-DA) was utilized to distinguish the metabolites that differ between groups. To prevent overfitting, 7-fold cross-validation and 200 response permutation testing were applied to evaluate the quality of the model. Variable importance in projection (VIP) scores was used to select differential metabolites between groups. Candidate metabolites having VIP > 1 and $p < 0.05$ were selected as potential biomarkers. Kyoto Encyclopedia of Genes and Genomes (KEGG) was applied for pathway annotation of differential metabolites.

GC-MS-based untargeted metabolomics analysis

Metabolic profiling of the derivative sample was analyzed using an Agilent 7890B gas chromatography system (Agilent Technologies Inc., CA, United States) equipped with a DB-5MS fused silica capillary column (30 m × 0.25 mm × 0.25 μm). Helium (> 99.999%) was used as the carrier gas at a constant flow rate of 1 ml / min through the column. Then, parameter conditions were set as follows: injector temperature, 260°C; injection volume, 1 μl; MS quadrupole temperature, 150°C; ion source temperature, 230°C; collision energy, 70 eV; and mass range, 50–500 m/z. The QC samples were injected every 10 runs for data quality control.

The obtained GC/MS raw data were converted to an ABF format via Analysis Base File Converter software, followed by

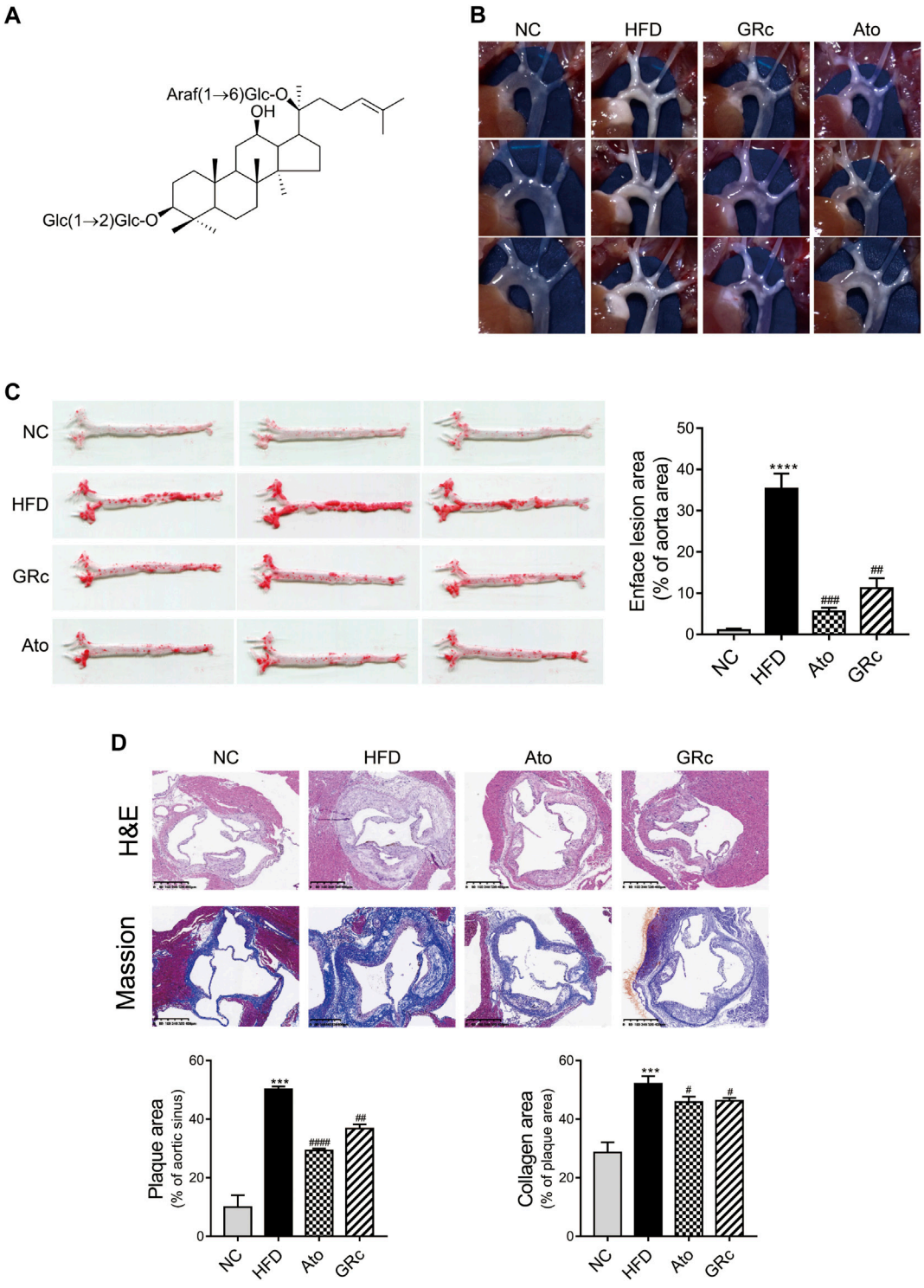

FIGURE 2
GRc alleviated atherosclerotic lesions in HFD-induced ApoE$^{-/-}$ mice (n = 6). **(A)** Chemical structure of GRc. **(B)** Photographs of the aortic arch captured using the microscope. **(C)** Representative photographs of the whole aorta by Oil Red O staining, and the plaque area of the whole aorta was quantitated. **(D)** Representative images of aortic sinus sections by H&E staining and Masson's staining; bar = 400 μm. The lesion and collagen area in the aortic sinus were quantitated. The data are expressed as means ± SEM. *p < 0.05, **p < 0.01, and ***p < 0.001 vs. NC; #p < 0.05, ##p < 0.01, and ###p < 0.001 vs. HFD. NC, normal control; HFD, high-fat diet; Ato, atorvastatin; GRc, ginsenoside Rc.

importing into MS-DIAL software for peak detection, deconvolution, alignment, and filtering. Metabolite characterization was based on the LUG database (untargeted database of GC-MS from Luming-bio). All internal standards and pseudo-positive peaks were removed. Then, the data matrix with three-dimensional datasets including sample information, peak names, and intensities was acquired for further analysis.

Statistical analysis

Variability of serum biochemical parameters, plaque lesion area, the relative abundance of gut microbiota, and the segmented integration of metabolites were analyzed using GraphPad Prism 7 (GraphPad Software, Inc. United States). A part of the 16S rRNA analysis was carried out in R software. Metabolite cluster and Spearman correlation were analyzed using a cloud platform (https://cloud.oebiotech.cn/task/detail/correlation-multiomics-oehw/). The data were expressed as mean ± S.E.M. One-way ANOVA, *t*-test, Welch's ANOVA, and Welch-corrected *t*-test were used according to data features. A p-value < 0.05 was considered statistically significant.

Results

Ginsenoside Rc reduced atherosclerotic lesions in high-fat diet-induced ApoE$^{-/-}$ mice

The chemical structure of GRc is shown in Figure 2A. During the period of the animal experiment, the body weight of mice was monitored to investigate the effects of GRc on the physiological characteristics. As shown in Supplementary Figure S1, the weight gain showed no significant difference in NC, HFD, Ato, and GRc groups during treatment periods, implying that the dose of GRc in the study was safe for HFD-induced ApoE$^{-/-}$ mice.

HFD-induced ApoE$^{-/-}$ mice have been widely used to construct the animal model of AS (Zhang et al., 2021). The effect of GRc on AS was determined by the size of plaque lesions in the entire aorta of HFD-induced ApoE$^{-/-}$ mice. The atherosclerotic plaque area in the aorta of the HFD group had a significant increase compared with that of the NC group. Compared with the HFD group, GRc or Ato significantly reduced the aortic plaque area in HFD-induced ApoE$^{-/-}$ mice (Figures 2B,C). Then, the atherosclerotic lesions and collagen content in the aortic sinus were measured and quantified using H&E and Masson's trichrome staining. The size of atherosclerotic lesions and collagen content in the aortic sinus were much larger in the HFD group than the NC group. Compared with the HFD group, GRc or Ato treatment apparently reduced the size of the atherosclerotic lesion area and collagen content in the aortic sinus (Figure 2D), demonstrating that GRc treatment was similar to Ato regarding the reduction of HFD-induced atherosclerotic injury.

Ginsenoside Rc improved lipid levels and systemic inflammation in ApoE$^{-/-}$ mice fed with high-fat diet

Given that lipid levels and systemic inflammatory cytokines play an important role in the progress of AS, we further determined the levels of serum TC, TG, LDL-C, HDL-C, TNF-α, IL-6, and IL-1β. Compared with the NC group, serum TC, TG, and LDL-C in the HFD group significantly increased, while serum HDL-C was significantly decreased. Treatment with GRc or Ato significantly decreased TC, TG, and LDL-C levels and increased HDL-C levels (Figures 3A–D). As shown in Figures 3E–G, serum TNF-α, IL-6, and IL-1β were much higher in ApoE$^{-/-}$ mice fed with HFD than the NC group. Both GRc and Ato groups markedly reduced inflammatory cytokines TNF-α, IL-6, and IL-1β. These results indicated that GRc improved lipid levels and systemic inflammation in HFD-fed ApoE$^{-/-}$ mice.

Effects of ginsenoside Rc on the composition of gut microbiota in ApoE$^{-/-}$ mice

Sequencing of 16S rRNA was conducted to determine the effect of GRc treatment on gut microbiota composition. Overall, a total of 1,741,378 clean reads were obtained from 24 cecal samples (72,557.42 ± 281.66 clean reads per sample), and 1,506,396 valid tags with average lengths ranging from 415.83 to 419.56 were observed. After data processing, a total of 9,802 OTUs (2,414.13 ±75.93 OTUs per sample) were obtained. To further observe community richness and diversity, intestinal microbial richness was accessed by the Chao1 index and intestinal microbial diversity by the Shannon index. The curves within each sample were flat in the Shannon rarefaction map (Supplementary Figure S2), implying that the range of sequencing was able to determine the biodiversity of bacterial communities. As shown in Figures 4A,B, Chao1 and Shannon indexes in the HFD group significantly decreased compared with those in the NC group, indicating that there were markedly decreased intestinal microbial richness and diversity after HFD intake in ApoE$^{-/-}$ mice. PCoA based on unweighted unifrac metrics was used to demonstrate the difference in the composition of the bacterial communities. PCoA spots in the same group were well clustered, implying that there was a similar composition of the bacterial communities among samples from the same group. The distance of PCoA spots in NC, HFD, and GRc groups was apparently

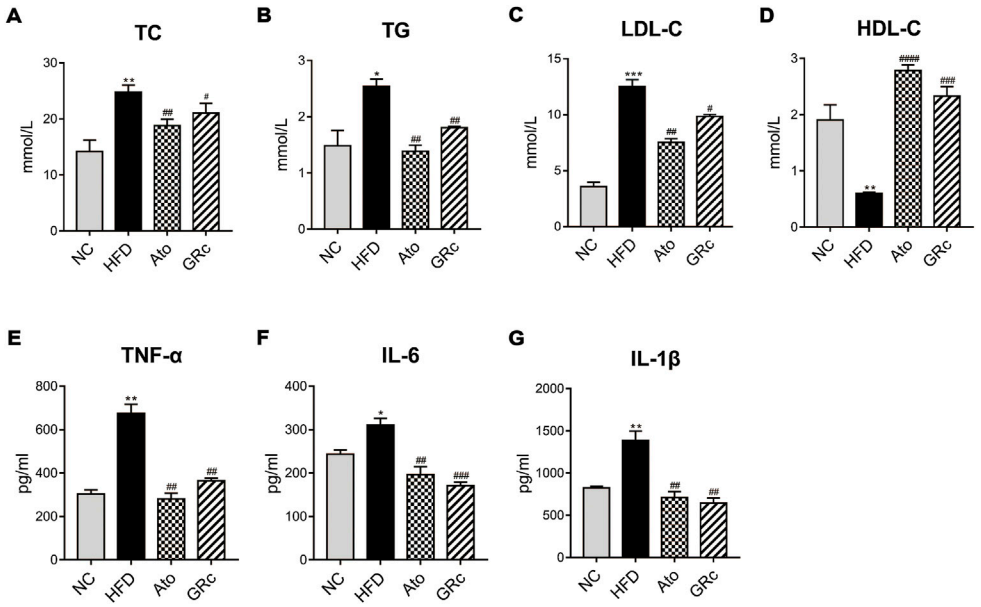

FIGURE 3
GRc regulated lipid and systemic inflammatory cytokines in HFD-induced ApoE$^{-/-}$ mice. **(A–D)** Levels of serum lipids (TC, TG, LDL-C, and HDL-C) per group. **(E–G)** Levels of inflammatory cytokines (TNF-α, IL-6, and IL-1β) per group. The data are expressed as means ± SEM. *p < 0.05, **p < 0.01, and ***p < 0.001 vs. NC; #p < 0.05, ##p < 0.01, and ###p < 0.001 vs. HFD. NC, normal control; HFD, high-fat diet; Ato, atorvastatin; GRc, ginsenoside Rc.

separated, which suggested different constructures of the bacterial communities among the groups. The GRc-related difference was represented by PC1, which explained 26.25% of the total variation in the microbial composition. The HFD-related difference was represented by PC2, which explained 18.38% of the total variation (Figure 4C). The PCoA results showed that GRc treatment contributed more to gut microbiota structure than HFD feeding alone.

The gut microbiota significantly changed at different taxonomic levels among the groups as shown in Supplementary Figure S3. The differential intestinal floras related to CVDs were listed. At the phylum level, the top six microflora of mice were Bacteroidetes, Firmicutes, Desulfobacterota, Proteobacteria, Campilobacterota, and Actinobacteriota, the composition of which differed apparently among NC, HFD, and GRc groups. The abundance of Bacteroidetes in the HFD group was much lower than that in the NC group, while GRc or Ato treatment reversed the change. Compared with the NC group, the HFD group had a markedly increased abundance of Firmicutes, which was significantly decreased in the GRc or Ato group. The aforementioned results lead to a higher ratio of Firmicutes to Bacteroidetes in the HFD group than that in the NC group, and a lower ratio in the GRc or Ato group than that in the HFD group (Figure 4D). At the genus level, the relative abundance of *Faecalibaculum*, *Oscillibacter*, *Eubacterium_coprostanoligenes_group*, and *Blautia* was much higher, while the relative abundance of Muribaculaceae, *Lactobacillus*, *Ileibacterium*, and *Bifidobacterium* markedly reduced after HFD feeding. The imbalance of intestinal floras was recovered to some extent by GRc treatment which reversed the effects of HFD at the genus level of microbiota composition. The Ato group exhibited no significant effects on *Ileibacterium*, *Bifidobacterium*, and *Lactobacillus* (Figure 4E). Overall, GRc treatment could regulate specific intestinal flora at different taxonomic levels.

In addition, the LEfSe analysis was used for highlighting the core bacterial phenotypes from the phylum to genus contributing to the variations in the microbiota composition. As shown in Figures 5A,B, the NC group was enriched with the phylum Bacteroidetes, the class Bacteroidia, the order Bacteroidales and Lachnospiraceae, and the family Muribaculaceae (from family to genus), Rikenellaceae, and Lachnospiraceae, as well as the genus *Alistipes*, Rikenellaceae_*RC9_gut_group*, and Lachnospiraceae_*NK4A136_group* , while the HFD group was enriched with the phylum Firmicutes and Proteobacteria, the class Clostridia, Bacilli, and Gammaproteobacteria, the order Oscillospirales, Erysipelotrichales and Enterobacterales, the family Tannerellaceae, Bacteroidaceae, Eubacterium_coprostanoligenes_group (from family to genus), Oscillospiraceae, Erysipelatoclostridiaceae, and Enterobacteriaceae, and the genus *Parabacteroides*, *Bacteroides*, *Colidextribacter*, *Erysipelatoclostridium*, and

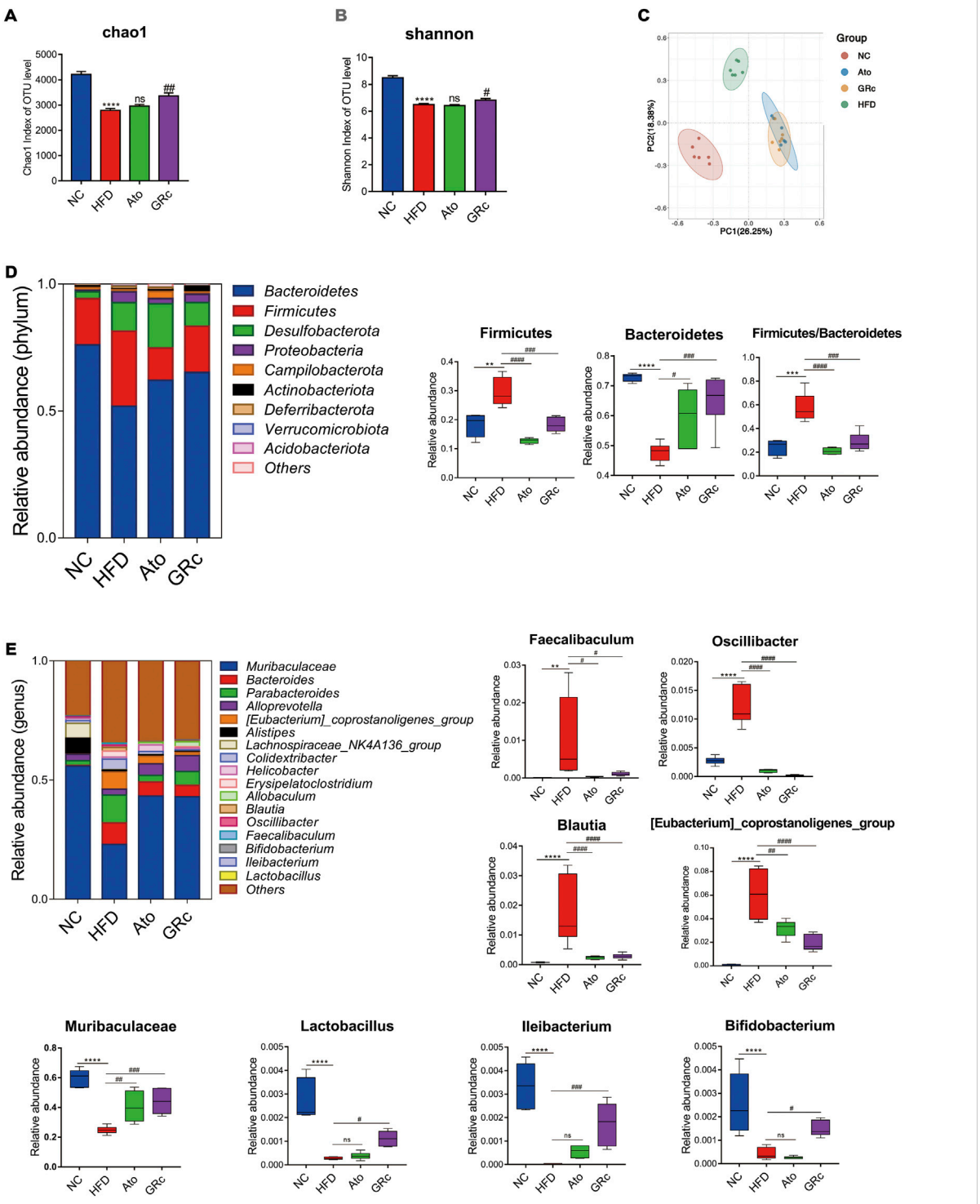

FIGURE 4
Effects of GRc on the composition of gut microbiota in HFD-induced ApoE$^{-/-}$ mice (n = 6). **(A–B)** Richness and diversity of the gut microbiome were assessed by Chao1 and Shannon indexes, respectively. **(C)** PCoA analysis based on unweighted unifrac metrics for all samples at the OUT level. **(D)** Structure and relative abundance of Firmicutes and Bacteroidetes at the phylum level and the ratio of Firmicutes/Bacteroidetes. **(E)** Structure and relative abundance of Muribaculaceae, *Eubacterium_coprostanoligenes_group*, *Faecalibaculum*, *Oscillibacter*, *Blautia*, *Ileibacterium*, *Lactobacillus*, and *Bifidobacterium* at the genus level. The data are expressed as means ± SEM. *p < 0.05, **p < 0.01, and ***p < 0.001 vs. NC; #p < 0.05, ##p < 0.01, and ###p < 0.001 vs. HFD; ns, not significant; NC, normal control; HFD, high-fat diet; Ato, atorvastatin; GRc, ginsenoside Rc.

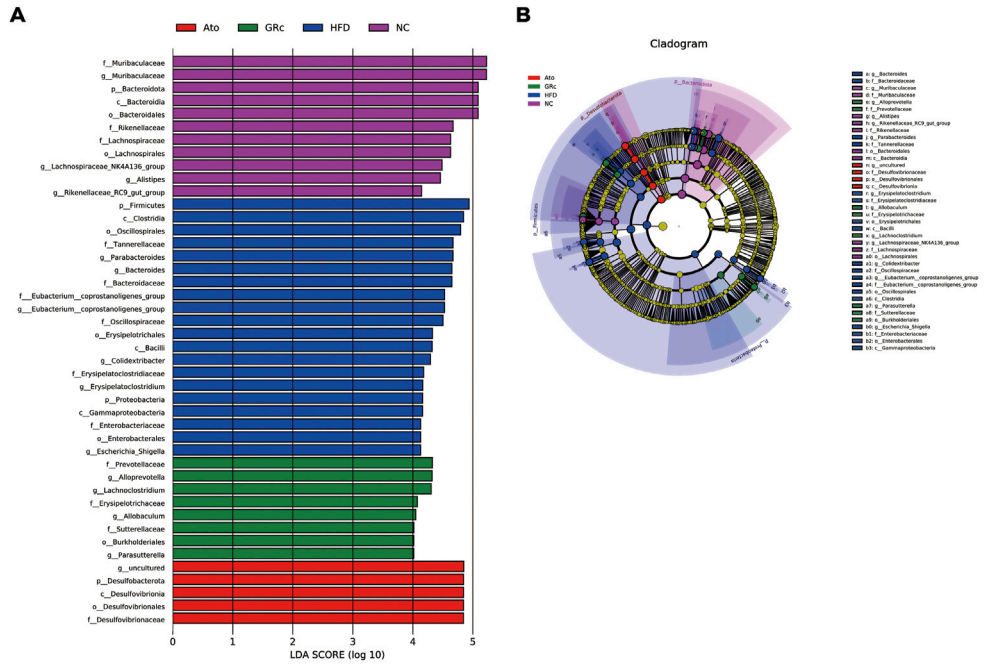

FIGURE 5
Core bacterial phenotype analysis in HFD-induced ApoE$^{-/-}$ mice (n = 6). **(A)** LDA scores of taxa enriched at different taxonomy levels (LDA significant threshold = 4). **(B)** Taxonomic cladogram generated by LEfSe analysis showing taxa significantly enriched in the NC group (purple), HFD group (blue), GRc group (green), and Ato group (red), respectively. Each ring represents a taxonomic level from phylum to genus. The diameter of each dot on the ring represents the relative abundance of the taxon. NC, normal control; HFD, high-fat diet; Ato, atorvastatin; GRc, ginsenoside Rc.

Escherichia_Shigella. The aforementioned results indicated that HFD feeding reduced the gut microbiota enriched in the NC group. The gut microbiota enriched in the GRc group were the order Burkholderiales, the family Prevotellaceae, Erysipelotrichaceae, and Sutterellaceae, and the genus *Alloprevotella*, *Lachnoclostridium*, *Allobaculum*, and *Parasutterella*, while intestinal flora in the Ato group was enriched at the lowest level.

Predictive functional profiling of microbial communities by PICRUSt2

Functional profiling of microbial communities in level 2 of KEGG pathways was predicted by PICRUSt2. When fed with HFD, the microbiome in mice had significantly more functional genes for CVDs, biosynthesis of other secondary metabolites, cell growth and death, carbohydrate metabolism, amino acid metabolism, endocrine system, digestive system, energy metabolism, cancers, cellular processes, and signaling (Figure 6A). Compared with the HFD group, the GRc group contained significantly less functional genes for CVDs, implying that microbial communities in the GRc group might have a protective role in CVDs (Figure 6B). After Ato treatment, the microbiome in mice had significantly less functional genes for immune system diseases, nervous system, carbohydrate metabolism, enzyme families, endocrine system, lipid metabolism, cellular processes and signaling, transcription, and membrane transport, while microbiome genes for CVDs tended to increase (Figure 6C).

Ginsenoside Rc modulated the fecal metabolites in ApoE$^{-/-}$ mice

The PLS-DA and OPLS-DA models were used to confirm the differences in fecal metabolites in groups. Seven-fold cross-validation and 200 response permutation testing were applied to prevent overfitting, and the results showed good quality of the models (Supplementary Figure S4). The PLS-DA plots showed an excellent separation among the NC, HFD, and GRc groups, while there was no obvious separation between Ato and HFD groups (Figures 7A,B). In addition, the OPLS-DA plots between HFD and NC groups also exhibited apparent differences (Figure 7C), implying that there was a significant difference in fecal metabolites between HFD and NC groups. Then, differential

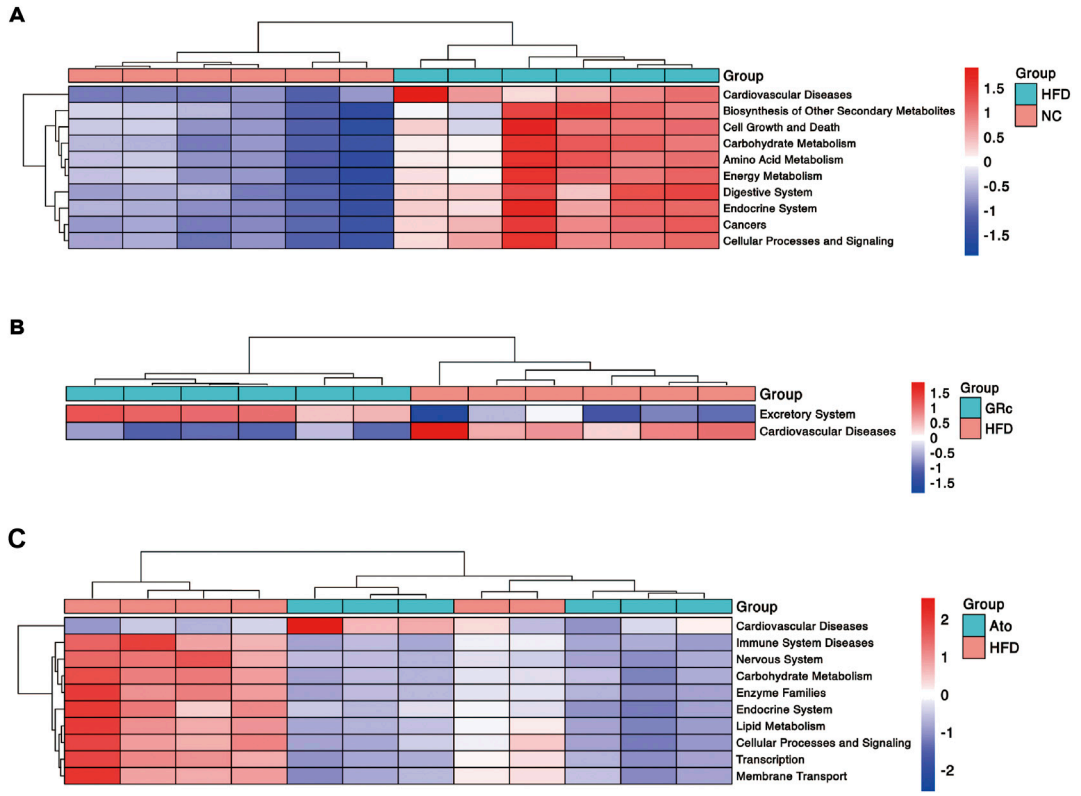

FIGURE 6
Predictive functional profiling of microbial communities by PICRUSt2 (n = 6). **(A)** Differences in intestinal microbiome functional profiling between HFD and NC groups. **(B)** Differences in intestinal microbiome functional profiling between GRc and HFD groups. **(C)** Differences in intestinal microbiome functional profiling between Ato and HFD groups. NC, normal control; HFD, high-fat diet; Ato, atorvastatin; GRc, ginsenoside Rc.

metabolites between HFD and NC groups were selected with the criteria of VIP > 1 and $p < 0.05$. Compared with the NC group, there were 510 significantly upregulated and 605 downregulated metabolites in the HFD group (Figure 7D). Expectedly, the OPLS-DA plots between GRc and HFD groups showed clear separation (Figure 7E). In the GRc group, 307 metabolites were significantly upregulated and 339 metabolites were downregulated in HFD-induced ApoE$^{-/-}$ mice (Figure 7F). These results implied that GRc could modulate fecal metabolic profiles in ApoE$^{-/-}$ mice fed with HFD.

Ginsenoside Rc regulated the metabolic pathways related to atherosclerosis

To display the differences in the fecal profile clearly, top 50 differential metabolites between HFD/NC and GRc/HFD were clustered and are shown in Figures 8A,B. Then, KEGG pathway enrichment analysis was performed based on the whole differentially expressed metabolites. Notably, the significantly different metabolites between NC and HFD groups were enriched in 53 significant pathways ($p < 0.05$) (Figure 8C), and the differential metabolites between HFD and GRc groups were enriched in 28 significant pathways ($p < 0.05$) (Figure 8D). There were 23 overlapped pathways between NC/HFD and HFD/GRc, including purine metabolism, tricarboxylic acid (TCA) cycle, taurine and hypotaurine metabolism, arginine biosynthesis, glucagon signaling pathway, ATP-binding cassette (ABC) transporters, and primary bile acid biosynthesis, which were related to AS. These pathways might be potential pathogenesis mechanisms and therapeutic targets (Table 1), and the differential metabolites from the aforementioned seven pathways were investigated. In the purine metabolism pathway, adenine and uric acid were apparently increased in the HFD group and significantly decreased in the GRc group, and the same trend appeared in the levels of malic acid, fumaric acid, oxoglutaric acid, citric acid in the TCA cycle, and glucagon signaling pathways. In the taurine and hypotaurine metabolism pathway, taurine and L-glutamate in the HFD group were lower than those in the NC group, and these metabolites were

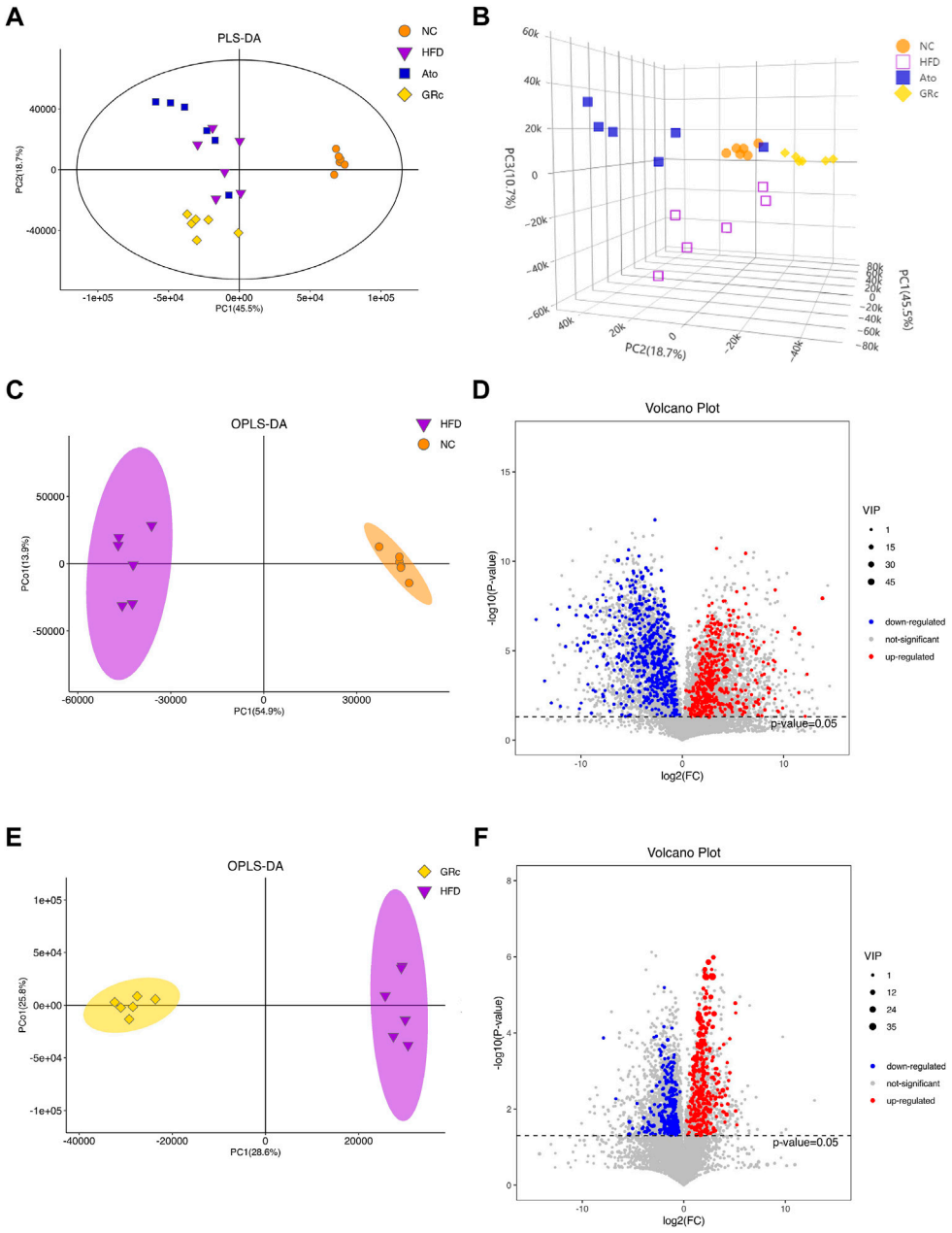

FIGURE 7
GRc modulated the fecal metabolites in ApoE$^{-/-}$ mice (n = 6). **(A)** Two-dimensional PLS-DA score plots per group. **(B)** Three-dimensional PLS-DA score plots per group. **(C)** OPLS-DA score plot in NC and HFD groups. **(D)** Relative volcano plot in NC and HFD groups. **(E)** OPLS-DA score plot in GRc and HFD groups. **(F)** Relative volcano plot in GRc and HFD groups. NC, normal control; HFD, high-fat diet; Ato, atorvastatin; GRc, ginsenoside Rc.

apparently increased after GRc treatment; the same trend was detected in citrulline, ornithine, L-glutamate, and L-glutamine in the arginine biosynthesis pathway and sorbitol, allose, lysine, and hydroxyproline in the ABC transporter pathway. In the primary bile acid biosynthesis pathway, cholesterol and glycochenodeoxycholic acid (GCDCA) were higher, while the levels of cholic acid (CA), chenodeoxycholic acid (CDCA), glycine, isolithocholic acid (isoLCA), taurochenodeoxycholic acid (TCDCA), and taurocholic acid (TCA) were lower in the HFD group than those in the NC group. These metabolites were significantly reversed in the GRc group (Supplementary Tables S1, S2).

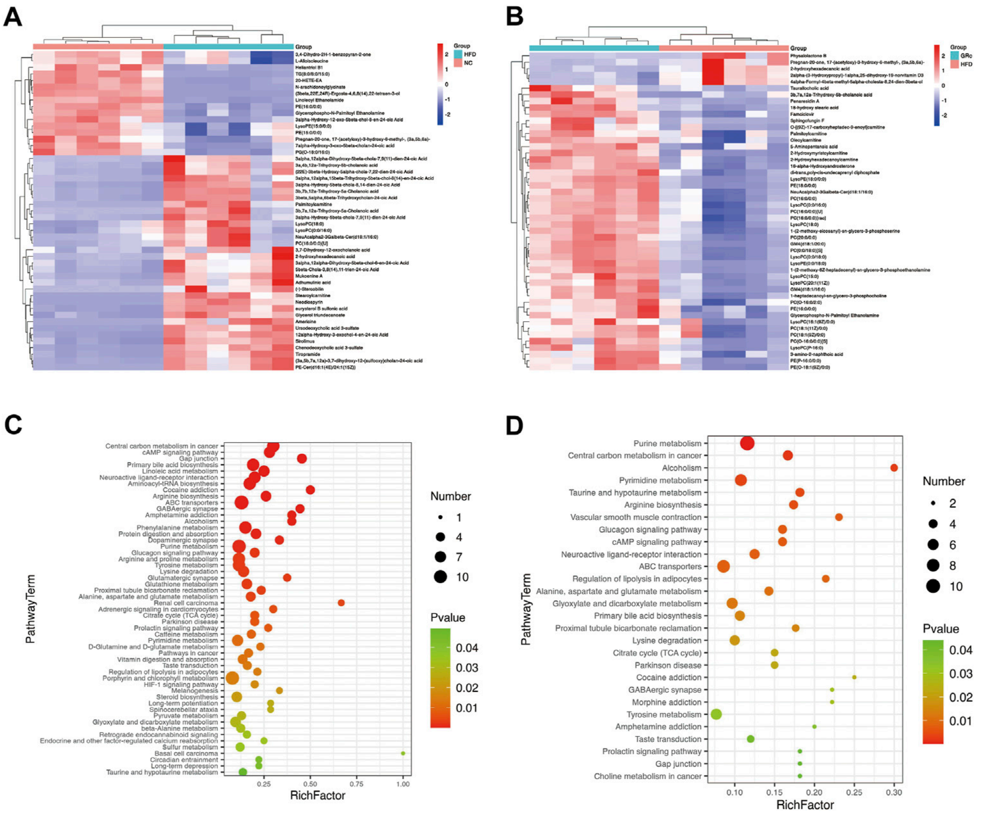

FIGURE 8
GRc regulated the metabolic pathways in ApoE$^{-/-}$ mice (n = 6). **(A)** Clustering heatmap of differential metabolites in feces between HFD and NC groups. **(B)** Clustering heatmap of differential metabolites in feces between GRc and HFD groups. **(C)** KEGG pathway enrichment scatterplot between HFD and NC groups. **(D)** KEGG pathway enrichment scatterplot between GRc and HFD groups. Rich factor indicates the number of differentially expressed metabolites located in the KEGG/the total number of metabolites located in the KEGG (NC, normal control; HFD, high-fat diet; GRc, ginsenoside Rc).

TABLE 1 Potential metabolite pathway regulated by GRc in the AS model.

No.	KEGG pathway	HFD/NC		GRc/HFD	
		Rich factor	*p*-value	Rich factor	*p*-value
1	Purine metabolism	0.1158	0.000829	0.1158	0.000136
2	TCA cycle	0.2000	0.006123	0.1500	0.022725
3	Taurine and hypotaurine metabolism	0.1364	0.049406	0.1818	0.004204
4	Arginine biosynthesis	0.2608	0.000163	0.1739	0.004969
5	Glucagon signaling pathway	0.2000	0.002161	0.1600	0.006768
6	ABC transporters	0.1290	0.000170	0.0860	0.007640
7	Primary bile acid biosynthesis	0.1915	0.000005	0.1064	0.014404

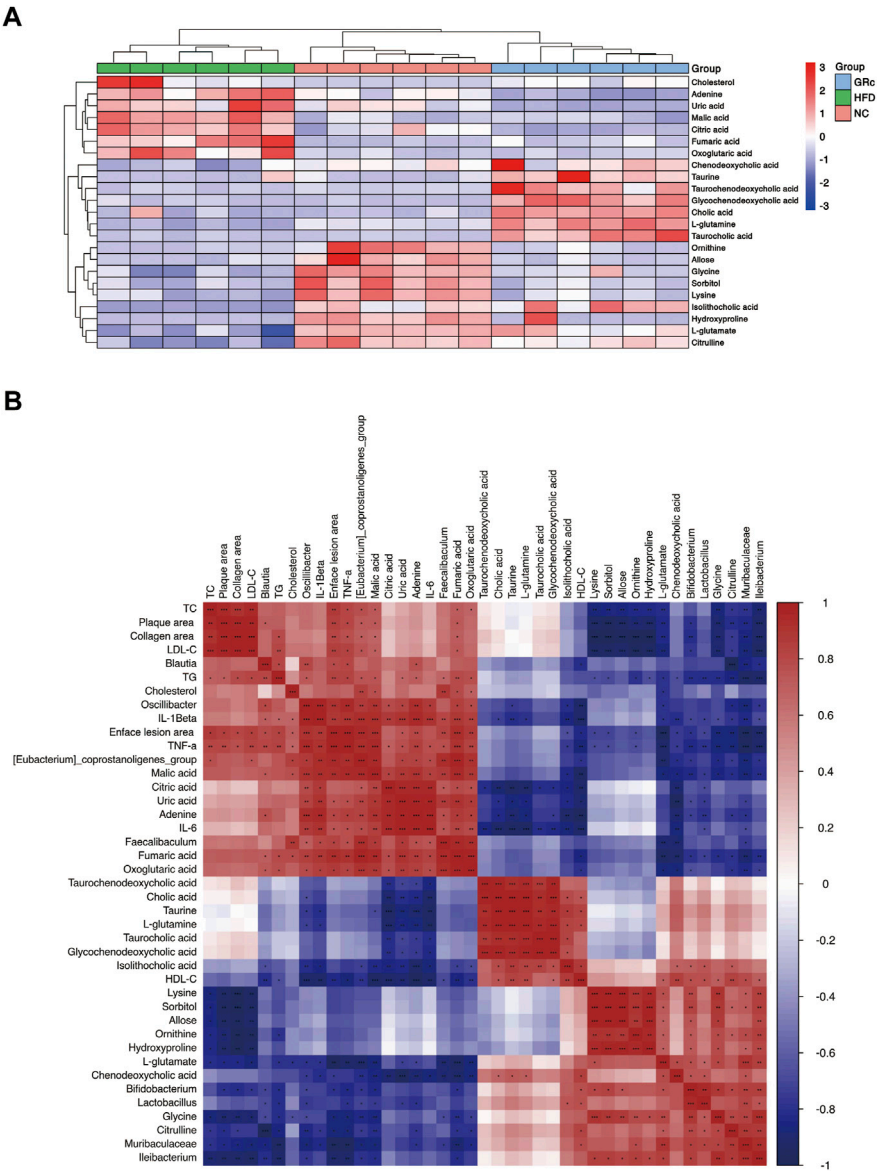

FIGURE 9
Correlation between gut metabolism and atherosclerosis. **(A)** Clustering heatmap of potential biomarkers in feces. **(B)** Spearman correlation analysis among gut microbiota, differentially expressed fecal metabolites, and atherosclerotic parameters. The correlation analysis value is represented by the colors of grinds. Red represents positive correlation, and blue represents negative correlation. *$p < 0.05$, **$p < 0.01$, and ***$p < 0.001$ (NC, normal control; HFD, high-fat diet; GRc, ginsenoside Rc).

Correlation between gut metabolism and atherosclerosis

To further understand the metabolic difference, we clustered the heatmap of potential biomarkers in purine metabolism, TCA cycle, taurine and hypotaurine metabolism, arginine biosynthesis, glucagon signaling pathway, ABC transporters, and primary bile acid biosynthesis pathways. As shown in Figure 9A, potential biomarkers in feces were well clustered in different groups. Compared with the HFD group, differentially expressed fecal metabolites in the GRc group were generally closer to the NC group, implying that gut metabolism was more similar to the GRc group than the NC group. Spearman correlation was examined for the possible connection among gut microbiota, potential biomarkers in feces, and atherosclerotic indexes.

We first investigated the relationship between gut microbiota and fecal potential biomarkers. *Blautia* was positively correlated

with adenine and negatively correlated with citrulline. The *Eubacterium_coprostanoligenes_group* had a positive correlation with fumaric acid, malic acid, citric acid, oxoglutaric acid, adenine, uric acid, and cholesterol, with a negative correlation with L-glutamate, citrulline, glycine, and CDCA. *Faecalibaculum* was positively correlated with malic acid, citric acid, adenine, uric acid, and cholesterol while negatively correlated with L-glutamate and CDCA. *Oscillibacter* was positively correlated with fumaric acid, malic acid, citric acid, oxoglutaric acid, adenine, and uric acid, with a negative correlation with taurine, L-glutamate, citrulline, and isoLCA. Then, *Bifidobacterium* was positively correlated with L-glutamate, ornithine, isoLCA, and glycine while negatively correlated with fumaric acid, malic acid, oxoglutaric acid, adenine, uric acid, and cholesterol. *Lactobacillus* was positively correlated with L-glutamate, sorbitol, allose, lysine, hydroxyproline, and isoLCA and negatively correlated with fumaric acid, malic acid, citric acid, adenine, and uric acid. Muribaculaceae had a positive correlation with L-glutamate, citrulline, ornithine, sorbitol, lysine, hydroxyproline, and glycine, with a negative correlation with fumaric acid, malic acid, oxoglutaric acid, adenine, and uric acid. Finally, *Ileibacterium* was positively correlated with L-glutamate, citrulline, ornithine, L-glutamine, sorbitol, lysine, hydroxyproline, and glycine while negatively correlated with fumaric acid, malic acid, and oxoglutaric acid. Above all, *Blautia*, *(Eubacterium)_coprostanoligenes_group*, *Faecalibaculum*, and *Oscillibacter* seemed to have a positive correlation with metabolites in the glucagon signaling pathway, TCA cycle pathway (fumaric acid, malic acid, citric acid, and oxoglutaric acid), and purine metabolism (adenine and uric acid) and a negative correlation with metabolites in taurine and hypotaurine metabolism (taurine and L-glutamate), arginine biosynthesis (citrulline, ornithine, and L-glutamine), ABC transporter pathway (sorbitol, allose, lysine, and hydroxyproline), and primary bile acid biosynthesis (CDCA, isoLCA, and glycine), while *Bifidobacterium*, *Lactobacillus*, Muribaculaceae, and *Ileibacterium* showed opposite changes.

Regarding the relationship between fecal potential biomarkers and atherosclerotic indexes, almost metabolites in the glucagon signaling pathway and TCA cycle pathway (fumaric acid, malic acid, citric acid, and oxoglutaric acid) were positively correlated with atherosclerotic indexes except the HDL-C level, and uric acid and adenine in the purine metabolism pathway were positively correlated with enface lesion area and serum levels of TG, IL-6, IL-1β, and TNF-α. Metabolites in taurine and hypotaurine metabolism (L-glutamate) and arginine biosynthesis (citrulline and ornithine) were negatively correlated with atherosclerotic parameters except the HDL-C level, and metabolites in ABC transporters (sorbitol, allose, lysine, and hydroxyproline) negatively correlated with atherosclerotic parameters except serum levels of HDL-C, IL-6, and IL-1β. Furthermore, fecal potential biomarkers in the primary bile acid biosynthesis (CA, CDCA, TCA, TCDCA, GCDCA, isoLCA, and glycine) pathway had a negative correlation mainly with inflammatory factors (Figure 9B). These results implied that metabolites in purine metabolism, TCA cycle, and glucagon signaling pathways positively correlated with atherosclerotic injury, while those in taurine and hypotaurine metabolism, arginine biosynthesis, ABC transporters, and primary bile acid biosynthesis pathways were negatively correlated with atherosclerotic injury. In general, there was an intensive connection among gut microbiota, differentially expressed fecal metabolites, and AS.

Discussion

In the present study, we investigated the impact and potential mechanism of GRc against AS in HFD-induced ApoE$^{-/-}$ mice. The changes in serum lipid and inflammatory cytokines, compositional structure of gut microbiota, fecal metabolites, and KEGG enrichment pathways were observed after treatment with GRc. In addition, the correlation between gut metabolism and AS was determined. We found that GRc markedly alleviated atherosclerotic plaque in ApoE$^{-/-}$ mice. Meanwhile, GRc treatment not only improved serum lipid disorder and systematic inflammation but also increased the diversity and richness of gut microbiota.In addition, GRc treatment regulated specific gut microbiota, fecal metabolites, and relative metabolic pathways related to CVDs. Moreover, differential fecal metabolites between groups also showed a strong correlation with differential gut microbiota and atherosclerotic injury.

The elevated plasma LDL-C concentration is a major risk factor for atherosclerotic CVDs. Lowering serum lipid permitted the initiation and the progression of AS (Khatana et al., 2020). In contrast, plasma HDL-C concentrations exert a protective influence on inflammation, oxidation, angiogenesis, and glucose homeostasis and have favorable effects on AS (Nicholls and Nelson, 2019). The current study demonstrated that GRc treatment significantly reduced the plasma levels of TC, TG, and LDL-C and increased HDL-C levels in HFD-induced ApoE$^{-/-}$ mice, which has been frequently used as the predominant animal model of AS. Apart from lipid disorders, the convincing evidence indicated that AS is a chronic inflammatory disease, characterized by elevated inflammatory cytokines such as TNF-α, IL-1β, and IL-6 in serum or atherosclerotic plaque (Libby et al., 2018). Our results indicated that serum levels of TNF-α, IL-1β, and IL-6 were

markedly decreased after GRc treatment. Moreover, atherosclerotic plaque in the aorta, atherosclerotic lesions, and collagen content in the aortic sinus were significantly ameliorated in the GRc group. Similar results were found in the Ato group, implying that both GRc and Ato had anti-atherosclerotic effect.

In recent years, remarkable attention has been attracted toward the gut and its accompanying microbial communities due to their important roles in physiological and pathological events in the host (Andoh, 2016). Increasing studies indicated that gut microbiota changes are associated with numerous disease states including CVDs (Witkowski et al., 2020). It has been reported that reduced diversity and richness of gut microbial species increased the risk of developing AS (Menni et al., 2018). Our study was consistent with previous results that the HFD decreased the diversity of gut microbiota (Han et al., 2020), and GRc treatment significantly increased the diversity and richness of microbial species in ApoE$^{-/-}$ mice. Consistent with a previous study (Kim et al., 2019; SudunLiu et al., 2019), Ato treatment had no obvious effects on diversity and richness of microbial species. In addition, the altered composition of the bacterial communities in different specific microbial species at different taxonomic levels also had an intensive connection with CVDs. Firmicutes and Bacteroidetes are two dominant phyla in the composition of human gut microbiota. An increased Firmicutes to Bacteroidetes ratio was reported to be positively associated with CVDs (De Filippis et al., 2016; Emoto et al., 2016). Firmicutes deteriorated metabolic endotoxins and inflammation and increased the risk of obesity and AS, while Bacteroidetes had an opposite impact (Abdallah Ismail et al., 2011; Dong et al., 2019). PCoA analysis in our results showed that there was much more significance in the composition of gut microbiota in NC, HFD, and GRc groups, in which relative abundances of gut microbiota at phylum and genus levels also showed a marked difference. GRc treatment markedly increased the abundance of Bacteroidetes and decreased that of Firmicutes and then contributed to a decrease in the Firmicutes to Bacteroidetes ratio which was higher in the HFD group. In accordance with previous studies (Kim et al., 2019; Zimmermann et al., 2020), Ato treatment significantly increased the abundance of Bacteroidetes and decreased Firmicutes in HFD-induced mice. Emerging evidence suggested that bacteria of Deferribacteraceae and *Eubacterium_coprostanoligenes_group* are correlated with trimethylamine/trimethylamine N-oxide production, which was considered a risk marker for the development of AS into CVDs (Koeth et al., 2013; Rath et al., 2017), while Lachnospiraceae was associated with the lower trimethylamine N-oxide level and anti-thrombotic phenotype (Zhu et al., 2016). On the other hand, a high level of *Eubacterium_coprostanoligenes_group* was linked with obesity, which is a risk factor for AS (Gomes et al., 2018). Furthermore, both *Lactobacillus* and *Bifidobacterium* are widely reported beneficial to human health. *Lactobacillus acidophilus* modulated oxidative stress, inflammatory process (Chen et al., 2013), and lipid metabolism via regulating reverse cholesterol transport in HFD-induced ApoE$^{-/-}$ mice (Huang et al., 2014; Zhao et al., 2019), while *Bifidobacterium* displayed an effect of decreasing visceral fat mass in people (Rath et al., 2017), subsequently ameliorated the progression of AS, and mitigating effects on HFD-induced obesity was accompanied with an increased Muribaculaceae level (Ohue-Kitano et al., 2019). The 16S rRNA analysis in our experiment showed that the family of Deferribacteraceae and *Eubacterium_coprostanoligenes*_group were significantly increased and Muribaculaceae, Lachnospiraceae, Bifidobacteriaceae, and Lactobacillaceae were markedly decreased in the HFD group. GRc treatment reversed the effect on gut microbiota at the family level induced by HFD, while Ato treatment only reversed the levels of Muribaculaceae and *Eubacterium_coprostanoligenes*_group induced by HFD. At the genus level, the studies showed that elevated abundance of *Oscillibacter* was closely related to gut permeability and inflammation in obese mice (Lam et al., 2012), while *Ileibacterium* protected mice from adiposity (Den Hartigh et al., 2018). Our investigation showed that GRc significantly increased the relative abundance of *Lactobacillus*, *Bifidobacterium*, *Ileibacterium*, and Muribaculaceae, with a decreased relative abundance of *Oscillibacter*, *Eubacterium_coprostanoligenes_group*, *Blautia*, and *Faecalibacterium*, while Ato treatment had a similar effect to GRc without significantly reversing levels of *Lactobacillus*, *Bifidobacterium*, and *Ileibacterium* induced by HFD. The results of *Blautia* and *Faecalibacterium* in our study were inconsistent with previous studies that showed *Blautia* was reduced in HFD-induced mice (Wu et al., 2020) and *Faecalibacterium* exhibited cardio-protective effects (Gerdes et al., 2020), while some other intestinal floras including *Bacteriodes* and *Parabacteriodes* were reduced by GRc treatment in our study, which might potentially influence the AS progression and would worth further study. In addition to the composition of the intestinal flora, the whole function of microbial communities receives increasing attention (Whidbey and Wright, 2019). Predictive functional profiling of microbial communities by PICRUSt2 showed that GRc significantly reduced functional genes for CVDs, while Ato tended to enhance functional genes for CVDs. Above all, GRc might exhibit anti-atherosclerotic effects by regulating the gut microbiota related to AS.

Metabolomics has been routinely applied as a tool for the discovery of biomarkers, system-level effects of metabolites, and subtle alterations in biological pathways, which might provide insights into the mechanisms underlying various diseases (Johnson et al., 2016). PLS-DA and OPLS-DA analyses in our study showed significantly different fecal metabolic phenotypes between NC/HFD and GRc/HFD. Then, fecal differential metabolites between groups were clustered and annotated in

KEGG pathways. Accumulating evidence showed an intensive connection between metabolites of gut microbiota and CVDs. Uric acid and adenine are end products of purine metabolism in humans. An intensive connection has been shown between elevated uric acid and CVDs, and the mechanisms underlying deleterious effects of elevated uric acid on cardiovascular health included increased oxidative stress, reduced availability of nitric oxide and endothelial dysfunction, promotion of local and systemic inflammation, vasoconstriction and proliferation of vascular smooth muscle cells, insulin resistance, and metabolic dysregulation (Ndrepepa, 2018). Our results showed that high levels of uric acid and adenine were induced by HFD, while GRc markedly reduced uric acid and adenine in the purine metabolism pathway. Recent studies have shown that mitochondrial metabolites in the TCA cycle were not only considered mere intermediate substrates for energy generation but also acted as key signaling molecules regulating gene transcription and translation. Succinate has emerged as a circulating biomarker for several metabolic and CVDs (Pell et al., 2016; Serena et al., 2018; Ceperuelo-Mallafre et al., 2019). On the other hand, elevated malic acid and citric acid were associated with a higher risk of CVDs (Bullo et al., 2021), and fumaric acid accumulation activated gene transcription for TNF-α and IL6 cytokines and increased ROS signaling via binding to glutathione (Blatnik et al., 2008; Zheng et al., 2015). In our study, we found that HFD significantly increased the metabolites in the TCA cycle or glucagon signaling pathways, such as malic acid, fumaric acid, oxoglutaric acid, and citric acid. GRc markedly decreased aforementioned metabolites. Recently, a strong relationship between alterations in amino acid metabolism and the development of AS had been observed, in which L-arginine and its metabolism improved NO-dependent vasodilator function and reduced atherosclerotic plaques with reversed endothelial dysfunction (Zaric et al., 2020). In our study, GRc did not significantly influence the L-arginine level but increased the intermediate substrates for arginine biosynthesis, including citrulline, ornithine, L-glutamate, and L-glutamine, which might accelerate the biosynthesis and utilization of L-arginine. In addition, GRc increased sorbitol, allose, lysine, and hydroxyproline in the composition of ABC transporters which were widely considered receptors of reverse cholesterol transport with an important role in the prevention and treatment of AS (Kotlyarov and Kotlyarova, 2021). Taurine was considered to improve antioxidant effects and lipid profile and reduce atherosclerotic lesion formation. The hypocholesterolemic effects of taurine are mediated by enhanced cholesterol degradation and the excretion of bile acid (Zaric et al., 2020). Bile acid is an important signaling molecule and metabolic regulator of lipid, glucose, and energy metabolism in AS (Chiang et al., 2020). Fecal excretion of bile acid is a major rink for cholesterol, and bile acids lost in the process need to be replaced by *de novo* synthesis from cholesterol. Furthermore, bile acids have also been shown to influence host lipid metabolism through the farnesoid X receptor (FXR) and the Takeda G-protein-coupled bile acid receptor (TGR) in the intestine and liver. Primary bile acids such as CA and CDCA and the secondary bile acids such as lithocholic acid (LCA) and deoxycholic acid (DCA) are FXR agonists, while LCA and DCA act as agonists to TGR5 (Schoeler and Caesar, 2019). Activation of FXR and TGR5 promoted energy metabolism and significantly reduced atherosclerotic formation (Miyazaki-Anzai et al., 2018). Our results showed that cholesterol was reduced, and the levels of taurine, CA, CDCA, glycine, isoLCA, TCDCA, and TCA were increased upon GRc treatment. An increase in primary bile acids and secondary bile acids might accelerate the enterohepatic circulation and fecal excretion of bile acids and activation of FXR and/or TGR5 and then hasten cholesterol metabolism, given that most isoLCA is excreted into feces and small amounts reabsorbed to the liver. Consequently, GRc treatment markedly regulated fecal metabolites in HFD-induced ApoE$^{-/-}$ mice. The underlying mechanism of GRc relieving AS might result from improving CVD-related metabolic pathways, in which differential metabolites were annotated. These results to some extent proved the predictive functional profiling of microbial communities by PICRUSt2. Taken together, fecal differential metabolites mentioned previously might be potential biomarkers of GRc treatment against AS in ApoE$^{-/-}$ mice.

Previous studies reported that *Eubacterium_coprostanoligenes_group* (Gomes et al., 2018) and *Oscillibacter* (Lam et al., 2012) could aggravate CVDs, while *Lactobacillus*, *Bifidobacterium*, Muribaculaceae, and *Ileibacterium* exerted protective effects (Huang et al., 2014; Rath et al., 2017; Den Hartigh et al., 2018; Ohue-Kitano et al., 2019; Zhao et al., 2019), implying that *Lactobacillus*, *Bifidobacterium*, Muribaculaceae, and *Ileibacterium* were beneficial intestinal floras to cardiovascular health, while *Eubacterium_coprostanoligenes_group* and *Oscillibacter* played the opposite roles. After GRc treatment, atherosclerotic injury in HFD-induce mice was alleviated.In addition, beneficial intestinal floras to cardiovascular health were increased and harmful ones were decreased, accompanied by increased fecal differential metabolites in taurine and hypotaurine metabolism (taurine and L-glutamate), arginine biosynthesis (citrulline, ornithine, and L-glutamine), ABC transporters (sorbitol, allose, lysine, and hydroxyproline), primary bile acid biosynthesis (CA, CDCA, TCA, TCDCA, GCDCA, isoLCA, and glycine), and decreased metabolites in purine metabolism (adenine and uric acid), TCA cycle, and glucagon signaling pathway (fumaric acid, malic acid, citric acid, and oxoglutaric acid). A correlation between gut metabolism and AS was investigated. Adenine and uric acid in the purine metabolism pathway had a positive correlation with intestinal floras, namely, *Eubacterium_coprostanoligenes_group*, *Faecalibaculum*, and

Oscillibacter, and AS indexes (enface lesion area, TG, and inflammatory factors) while negatively correlated with intestinal floras, namely, *Lactobacillus*, *Bifidobacterium*, and Muribaculaceae, which were consistent with previous studies that uric acid and adenine aggravate AS (Ndrepepa, 2018).

Of note, previous reports indicated that fumaric acid accumulation could accelerate inflammation (Zheng et al., 2015). Malic acid and citric acid might be risk factors for AS (Bullo et al., 2021). Our study showed that fumaric acid, citric acid, and malic acid in the TCA cycle were positively correlated with gut microbiota (*Eubacterium_coprostanoligenes_group*, *Faecalibacterium*, and *Oscillibacter*) and AS indexes and negatively correlated with intestinal floras (*Lactobacillus*, *Bifidobacterium*, Muribaculaceae, and *Ileibacterium*). Metabolites in the ABC transporter pathway were positively correlated with intestinal floras (*Lactobacillus*, Muribaculaceae, and *Ileibacterium*) and negatively connected with AS indexes (enface lesion area, plaque area, collagen area, TC, TG, LDL-C, and TNF-α). Moreover, citrulline in arginine biosynthesis was negatively correlated with gut microbiota (*Eubacterium_coprostanoligenes_group* and *Oscillibacter*) and AS indexes, while it was positively connected with Muribaculaceae and *Ileibacterium*. Ornithine was negatively correlated with AS indexes (enface lesion area, plaque area, collagen area, TC, TG, LDL-C, and TNF-α) while positively correlated with intestinal floras (*Bifidobacterium*, Muribaculaceae, and *Ileibacterium*) in our study, supporting that L-arginine and its metabolism could improve AS (Zaric et al., 2020). Furthermore, increased bile acids might accelerate the enterohepatic circulation and fecal excretion of bile acids and activation of FXR and/or TGR5 and then hasten cholesterol metabolism and improve AS (Miyazaki-Anzai et al., 2018; Schoeler and Caesar, 2019; Chiang et al., 2020). A correlation among gut microbiota, bile acids, and AS indexes was in good agreement with the studies mentioned previously, and CDCA was negatively correlated with gut microbiota (*Eubacterium_coprostanoligenes_group* and *Faecalibacterium*) and AS indexes (enface lesion area, TG, and inflammatory factors), while it was positively connected with HDL-C. Glycine showed a negative correlation with *Eubacterium_coprostanoligenes_group* and AS indexes, with a positive correlation with intestinal floras (*Bifidobacterium*, Muribaculaceae, and *Ileibacterium*). Notably, isoLCA was negatively correlated with *Oscillibacter* and AS indexes (enface lesion area and inflammatory factors) while positively correlated with *Lactobacillus*, *Bifidobacterium*, and HDL-C levels. The altered intestinal floras, fecal differential metabolites mentioned previously, and atherosclerotic injury showed an intensive correlation. *Eubacterium_coprostanoligenes_group*, *Faecalibaculum*, *Oscillibacter*, and *Blautia* enriched in the HFD group, indicating a positive correlation with the differential metabolites that were positively correlated with atherosclerotic injury and negatively correlated with a negative regulator of atherosclerotic injury. *Ileibacterium*, *Lactobacillus*, *Bifidobacterium*, and Muribaculaceae enriched in NC, GRc, and Ato groups with a reverse correlation. We hypothesized that GRc treatment regulated the composition of gut microbiota related to CVDs, followed by a change in fecal metabolic profiles from harmful to beneficial to cardiovascular health and finally alleviated AS. In the study, we reported the anti-atherosclerotic role of GRc in HFD-induced ApoE$^{-/-}$ mice for the first time and applied the method of integrated analysis of 16S rRNA sequence and untargeted fecal metabolomics, which might provide a strategy for investigating other medicines. We also explored the mechanisms of GRc against AS from a novel perspective of gut metabolism. The validation of the results was absent in the study, and we will continue further experiments such as fecal transplantation in germ-free mice.

Conclusion

In this study, GRc reduced atherosclerotic lesions, improved lipid levels, and systemic inflammation in HFD-induced ApoE$^{-/-}$ mice without significant change in body weight. Considering the poor bioavailability of GRc in oral administration, GRc exerted an anti-atherosclerotic role probably through comprehensive effects of regulating gut microbiota and differentially expressed fecal metabolites closely related to CVDs. Our study for the first time reported the anti-atherosclerotic effect of GRc in ApoE$^{-/-}$ mice induced with HFD. However, metabolites in serum and the role of some other intestinal floras regulated by GRc are still to be clarified.

Data availability statement

The datasets presented in this study can be found in online repositories. The names of the repository/repositories and accession number(s) can be found below: National Center for Biotechnology Information (NCBI) BioProject, http://www.ncbi.nlm.nih.gov/bioproject/874848, PRJNA874848.

Ethics statement

The animal study was reviewed and approved by the Animal Care and Use Committee of Naval Medical University.

Author contributions

RL and GL designed the study and reviewed the manuscript. BX, XZ, and ZW performed the experiments. BX, XZ, and GL analyzed and interpreted the data. XX directed the design of animal experiments. BX and XZ wrote the manuscript. All the authors approved the submitted manuscript for publication and other aspects of the work.

Funding

This work was funded by the National Natural Science Foundation of China (Nos. 82073981 and 82004215), the Key Research and Development Program of China (2019YFC1711000), the Shanghai Municipal Health Commission Project (20204Y0326), the Three-year Action Plan for Shanghai TCM Development and Inheritance Program ZY(2021-2023)-0401, and the Sailing Program of Naval Medical University.

Conflict of interest

The authors declare that the research was conducted in the absence of any commercial or financial relationships that could be construed as a potential conflict of interest.

Publisher's note

All claims expressed in this article are solely those of the authors and do not necessarily represent those of their affiliated organizations, or those of the publisher, the editors, and the reviewers. Any product that may be evaluated in this article, or claim that may be made by its manufacturer, is not guaranteed or endorsed by the publisher.

Supplementary material

The Supplementary Material for this article can be found online at: https://www.frontiersin.org/articles/10.3389/fphar.2022.990476/full#supplementary-material

References

Abdallah Ismail, N., Ragab, S. H., Abd Elbaky, A., Shoeib, A. R., Alhosary, Y., and Fekry, D. (2011). Frequency of Firmicutes and Bacteroidetes in gut microbiota in obese and normal weight Egyptian children and adults. *Arch. Med. Sci.* 7, 501–507. doi:10.5114/aoms.2011.23418

Andoh, A. (2016). Physiological role of gut microbiota for maintaining human health. *Digestion* 93, 176–181. doi:10.1159/000444066

Blatnik, M., Thorpe, S. R., and Baynes, J. W. (2008). Succination of proteins by fumarate: mechanism of inactivation of glyceraldehyde-3-phosphate dehydrogenase in diabetes. *Ann. N. Y. Acad. Sci.* 1126, 272–275. doi:10.1196/annals.1433.047

Bullo, M., Papandreou, C., Garcia-Gavilan, J., Ruiz-Canela, M., Li, J., Guasch-Ferre, M., et al. (2021). Tricarboxylic acid cycle related-metabolites and risk of atrial fibrillation and heart failure. *Metabolism.* 125, 154915. doi:10.1016/j.metabol.2021.154915

Ceperuelo-Mallafre, V., Llaurado, G., Keiran, N., Benaiges, E., Astiarraga, B., Martinez, L., et al. (2019). Preoperative circulating succinate levels as a biomarker for diabetes remission after bariatric surgery. *Diabetes Care* 42, 1956–1965. doi:10.2337/dc19-0114

Chen, J., Qin, Q., Yan, S., Yang, Y., Yan, H., Li, T., et al. (2021). Gut microbiome alterations in patients with carotid atherosclerosis. *Front. Cardiovasc. Med.* 8, 739093. doi:10.3389/fcvm.2021.739093

Chen, L., Liu, W., Li, Y., Luo, S., Liu, Q., Zhong, Y., et al. (2013). Lactobacillus acidophilus ATCC 4356 attenuates the atherosclerotic progression through modulation of oxidative stress and inflammatory process. *Int. Immunopharmacol.* 17, 108–115. doi:10.1016/j.intimp.2013.05.018

Chiang, J. Y. L., Ferrell, J. M., Wu, Y., and Boehme, S. (2020). Bile acid and cholesterol metabolism in atherosclerotic cardiovascular disease and therapy. *Cardiol. Plus* 5, 159–170. doi:10.4103/2470-7511.305419

De Filippis, F., Pellegrini, N., Vannini, L., Jeffery, I. B., La Storia, A., Laghi, L., et al. (2016). High-level adherence to a Mediterranean diet beneficially impacts the gut microbiota and associated metabolome. *Gut* 65, 1812–1821. doi:10.1136/gutjnl-2015-309957

Den Hartigh, L. J., Gao, Z., Goodspeed, L., Wang, S., Das, A. K., Burant, C. F., et al. (2018). Obese mice losing weight due to trans-10, cis-12 conjugated linoleic acid supplementation or food restriction harbor distinct gut microbiota. *J. Nutr.* 148, 562–572. doi:10.1093/jn/nxy011

Dong, Y., Cheng, H., Liu, Y., Xue, M., and Liang, H. (2019). Red yeast rice ameliorates high-fat diet-induced atherosclerosis in Apoe(-/-) mice in association with improved inflammation and altered gut microbiota composition. *Food Funct.* 10, 3880–3889. doi:10.1039/c9fo00583h

Emoto, T., Yamashita, T., Sasaki, N., Hirota, Y., Hayashi, T., So, A., et al. (2016). Analysis of gut microbiota in coronary artery disease patients: a possible link between gut microbiota and coronary artery disease. *J. Atheroscler. Thromb.* 23, 908–921. doi:10.5551/jat.32672

Fak, F., Tremaroli, V., Bergstrom, G., and Backhed, F. (2015). Oral microbiota in patients with atherosclerosis. *Atherosclerosis* 243, 573–578. doi:10.1016/j.atherosclerosis.2015.10.097

Fan, W., Huang, Y., Zheng, H., Li, S., Li, Z., Yuan, L., et al. (2020). Ginsenosides for the treatment of metabolic syndrome and cardiovascular diseases: Pharmacology and mechanisms. *Biomed. Pharmacother.* 132, 110915. doi:10.1016/j.biopha.2020.110915

Genkel, V. V., Kuznetcova, A. S., and Shaposhnik, I. (2020). Biomechanical forces and atherosclerosis: From mechanism to diagnosis and treatment. *Curr. Cardiol. Rev.* 16, 187–197. doi:10.2174/1573403X15666190730095153

Gerdes, V., Gueimonde, M., Pajunen, L., Nieuwdorp, M., and Laitinen, K. (2020). How strong is the evidence that gut microbiota composition can be influenced by lifestyle interventions in a cardio-protective way? *Atherosclerosis* 311, 124–142. doi:10.1016/j.atherosclerosis.2020.08.028

Gomes, A. C., Hoffmann, C., and Mota, J. F. (2018). The human gut microbiota: Metabolism and perspective in obesity. *Gut Microbes* 9, 308–325. doi:10.1080/19490976.2018.1465157

Han, Y., Park, H., Choi, B. R., Ji, Y., Kwon, E. Y., and Choi, M. S. (2020). Alteration of microbiome profile by D-allulose in amelioration of high-fat-diet-induced obesity in mice. *Nutrients* 12, E352. doi:10.3390/nu12020352

Huang, Q., Su, H., Qi, B., Wang, Y., Yan, K., Wang, X., et al. (2021). A SIRT1 activator, ginsenoside Rc, promotes energy metabolism in cardiomyocytes and neurons. *J. Am. Chem. Soc.* 143, 1416–1427. doi:10.1021/jacs.0c10836

Huang, Y., Wang, J., Quan, G., Wang, X., Yang, L., and Zhong, L. (2014). Lactobacillus acidophilus ATCC 4356 prevents atherosclerosis via inhibition of intestinal cholesterol absorption in apolipoprotein E-knockout mice. *Appl. Environ. Microbiol.* 80, 7496–7504. doi:10.1128/AEM.02926-14

Im, D. S. (2020). Pro-resolving effect of ginsenosides as an anti-inflammatory mechanism of panax ginseng. *Biomolecules* 10, E444. doi:10.3390/biom10030444

Johnson, C. H., Ivanisevic, J., and Siuzdak, G. (2016). Metabolomics: beyond biomarkers and towards mechanisms. *Nat. Rev. Mol. Cell Biol.* 17, 451–459. doi:10.1038/nrm.2016.25

Jonsson, A. L., and Backhed, F. (2017). Role of gut microbiota in atherosclerosis. *Nat. Rev. Cardiol.* 14, 79–87. doi:10.1038/nrcardio.2016.183

Khatana, C., Saini, N. K., Chakrabarti, S., Saini, V., Sharma, A., Saini, R. V., et al. (2020). Mechanistic insights into the oxidized low-density lipoprotein-induced atherosclerosis. *Oxid. Med. Cell. Longev.* 2020, 5245308. doi:10.1155/2020/5245308

Kim, J., Lee, H., An, J., Song, Y., Lee, C. K., Kim, K., et al. (2019). Alterations in gut microbiota by statin therapy and possible intermediate effects on hyperglycemia and hyperlipidemia. *Front. Microbiol.* 10, 1947. doi:10.3389/fmicb.2019.01947

Koeth, R. A., Wang, Z., Levison, B. S., Buffa, J. A., Org, E., Sheehy, B. T., et al. (2013). Intestinal microbiota metabolism of L-carnitine, a nutrient in red meat, promotes atherosclerosis. *Nat. Med.* 19, 576–585. doi:10.1038/nm.3145

Kotlyarov, S., and Kotlyarova, A. (2021). The role of ABC transporters in lipid metabolism and the comorbid course of chronic obstructive pulmonary disease and atherosclerosis. *Int. J. Mol. Sci.* 22, 6711. doi:10.3390/ijms22136711

Lam, Y. Y., Ha, C. W., Campbell, C. R., Mitchell, A. J., Dinudom, A., Oscarsson, J., et al. (2012). Increased gut permeability and microbiota change associate with mesenteric fat inflammation and metabolic dysfunction in diet-induced obese mice. *PLoS One* 7, e34233. doi:10.1371/journal.pone.0034233

Langille, M. G., Zaneveld, J., Caporaso, J. G., Mcdonald, D., Knights, D., Reyes, J. A., et al. (2013). Predictive functional profiling of microbial communities using 16S rRNA marker gene sequences. *Nat. Biotechnol.* 31, 814–821. doi:10.1038/nbt.2676

Libby, P., Buring, J. E., Badimon, L., Hansson, G. K., Deanfield, J., Bittencourt, M. S., et al. (2019). Atherosclerosis. *Nat. Rev. Dis. Prim.* 5, 56. doi:10.1038/s41572-019-0106-z

Libby, P., Loscalzo, J., Ridker, P. M., Farkouh, M. E., Hsue, P. Y., Fuster, V., et al. (2018). Inflammation, immunity, and infection in atherothrombosis: JACC review topic of the week. *J. Am. Coll. Cardiol.* 72, 2071–2081. doi:10.1016/j.jacc.2018.08.1043

Lu, L., Qin, Y., Zhang, X., Chen, C., Xu, X., Yu, C., et al. (2019). Shexiang Baoxin Pill alleviates the atherosclerotic lesions in mice via improving inflammation response and inhibiting lipid accumulation in the arterial wall. *Mediat. Inflamm.* 2019, 6710759. doi:10.1155/2019/6710759

Ma, J., and Li, H. (2018). The role of gut microbiota in atherosclerosis and hypertension. *Front. Pharmacol.* 9, 1082. doi:10.3389/fphar.2018.01082

Mancuso, C., and Santangelo, R. (2017). Panax ginseng and Panax quinquefolius: From pharmacology to toxicology. *Food Chem. Toxicol.* 107, 362–372. doi:10.1016/j.fct.2017.07.019

Menni, C., Lin, C., Cecelja, M., Mangino, M., Matey-Hernandez, M. L., Keehn, L., et al. (2018). Gut microbial diversity is associated with lower arterial stiffness in women. *Eur. Heart J.* 39, 2390–2397. doi:10.1093/eurheartj/ehy226

Miyazaki-Anzai, S., Masuda, M., Kohno, S., Levi, M., Shiozaki, Y., Keenan, A. L., et al. (2018). Simultaneous inhibition of FXR and TGR5 exacerbates atherosclerotic formation. *J. Lipid Res.* 59, 1709–1713. doi:10.1194/jlr.M087239

Ndrepepa, G. (2018). Uric acid and cardiovascular disease. *Clin. Chim. Acta.* 484, 150–163. doi:10.1016/j.cca.2018.05.046

Nicholls, S. J., and Nelson, A. J. (2019). HDL and cardiovascular disease. *Pathology* 51, 142–147. doi:10.1016/j.pathol.2018.10.017

Ohue-Kitano, R., Taira, S., Watanabe, K., Masujima, Y., Kuboshima, T., Miyamoto, J., et al. (2019). 3-(4-Hydroxy-3-methoxyphenyl)propionic acid produced from 4-Hydroxy-3-methoxycinnamic acid by gut microbiota improves host metabolic condition in diet-induced obese mice. *Nutrients* 11, E1036. doi:10.3390/nu11051036

Pell, V. R., Chouchani, E. T., Frezza, C., Murphy, M. P., and Krieg, T. (2016). Succinate metabolism: a new therapeutic target for myocardial reperfusion injury. *Cardiovasc. Res.* 111, 134–141. doi:10.1093/cvr/cvw100

Rath, S., Heidrich, B., Pieper, D. H., and Vital, M. (2017). Uncovering the trimethylamine-producing bacteria of the human gut microbiota. *Microbiome* 5, 54. doi:10.1186/s40168-017-0271-9

Schoeler, M., and Caesar, R. (2019). Dietary lipids, gut microbiota and lipid metabolism. *Rev. Endocr. Metab. Disord.* 20, 461–472. doi:10.1007/s11154-019-09512-0

Serena, C., Ceperuelo-Mallafre, V., Keiran, N., Queipo-Ortuno, M. I., Bernal, R., Gomez-Huelgas, R., et al. (2018). Elevated circulating levels of succinate in human obesity are linked to specific gut microbiota. *ISME J.* 12, 1642–1657. doi:10.1038/s41396-018-0068-2

Shi, L., Fu, W., Xu, H., Li, S., Yang, X., Yang, W., et al. (2022). Ginsenoside Rc attenuates myocardial ischaemic injury through antioxidative and anti-inflammatory effects. *Pharm. Biol.* 60, 1038–1046. doi:10.1080/13880209.2022.2072518

SudunLiu, S., Xiao, C., Peng, C., Liang, L., He, X., Zhao, S., et al. (2019). Probiotic strains improve high-fat diet-induced hypercholesterolemia through modulating gut microbiota in ways different from atorvastatin. *Food Funct.* 10, 6098–6109. doi:10.1039/c9fo00444k

Sun, J., Wu, W., Guo, Y., Qin, Q., and Liu, S. (2014). Pharmacokinetic study of ginsenoside Rc and simultaneous determination of its metabolites in rats using RRLC-Q-TOF-MS. *J. Pharm. Biomed. Anal.* 88, 16–21. doi:10.1016/j.jpba.2013.08.015

Whidbey, C., and Wright, A. T. (2019). Activity-based protein profiling-enabling multimodal functional studies of microbial communities. *Curr. Top. Microbiol. Immunol.* 420, 1–21. doi:10.1007/82_2018_128

Witkowski, M., Weeks, T. L., and Hazen, S. L. (2020). Gut microbiota and cardiovascular disease. *Circ. Res.* 127, 553–570. doi:10.1161/CIRCRESAHA.120.316242

World Health Organization (2021). *Cardiovascular diseases (CVDs)*. Available at: https://www.who.int/news-room/fact-sheets/detail/cardiovascular-diseases-(cvds (accessed May 3, 2022).

Wu, M., Yang, S., Wang, S., Cao, Y., Zhao, R., Li, X., et al. (2020). Effect of berberine on atherosclerosis and gut microbiota modulation and their correlation in high-fat diet-fed ApoE-/- mice. *Front. Pharmacol.* 11, 223. doi:10.3389/fphar.2020.00223

Wu, W., Jiao, C., Li, H., Ma, Y., Jiao, L., and Liu, S. (2018). LC-MS based metabolic and metabonomic studies of Panax ginseng. *Phytochem. Anal.* 29, 331–340. doi:10.1002/pca.2752

Xue, Q., He, N., Wang, Z., Fu, X., Aung, L. H. H., Liu, Y., et al. (2021). Functional roles and mechanisms of ginsenosides from Panax ginseng in atherosclerosis. *J. Ginseng Res.* 45, 22–31. doi:10.1016/j.jgr.2020.07.002

Yang, J. W., and Kim, S. S. (2015). Ginsenoside Rc promotes anti-adipogenic activity on 3T3-L1 adipocytes by down-regulating C/EBPα and PPARγ. *Molecules* 20, 1293–1303. doi:10.3390/molecules20011293

Yang, X., Dong, B., An, L., Zhang, Q., Chen, Y., Wang, H., et al. (2021). Ginsenoside Rb1 ameliorates glycemic disorder in mice with high fat diet-induced obesity via regulating gut microbiota and amino acid metabolism. *Front. Pharmacol.* 12, 756491. doi:10.3389/fphar.2021.756491

Zaric, B. L., Radovanovic, J. N., Gluvic, Z., Stewart, A. J., Essack, M., Motwalli, O., et al. (2020). Atherosclerosis linked to aberrant amino acid metabolism and immunosuppressive amino acid catabolizing enzymes. *Front. Immunol.* 11, 551758. doi:10.3389/fimmu.2020.551758

Zhang, L., Huang, J., Zhang, D., Lei, X., Ma, Y., Cao, Y., et al. (2022). Targeting reactive oxygen species in atherosclerosis via Chinese herbal medicines. *Oxid. Med. Cell. Longev.* 2022, 1852330. doi:10.1155/2022/1852330

Zhang, Y., Fatima, M., Hou, S., Bai, L., Zhao, S., and Liu, E. (2021). Research methods for animal models of atherosclerosis (Review). *Mol. Med. Rep.* 24, 871. doi:10.3892/mmr.2021.12511

Zhao, Z., Wang, C., Zhang, L., Zhao, Y., Duan, C., Zhang, X., et al. (2019). Lactobacillus plantarum NA136 improves the non-alcoholic fatty liver disease by modulating the AMPK/Nrf2 pathway. *Appl. Microbiol. Biotechnol.* 103, 5843–5850. doi:10.1007/s00253-019-09703-4

Zheng, L., Cardaci, S., Jerby, L., Mackenzie, E. D., Sciacovelli, M., Johnson, T. I., et al. (2015). Fumarate induces redox-dependent senescence by modifying glutathione metabolism. *Nat. Commun.* 6, 6001. doi:10.1038/ncomms7001

Zhu, H., He, Y. S., Ma, J., Zhou, J., Kong, M., Wu, C. Y., et al. (2021). The dual roles of ginsenosides in improving the anti-tumor efficiency of cyclophosphamide in mammary carcinoma mice. *J. Ethnopharmacol.* 265, 113271. doi:10.1016/j.jep.2020.113271

Zhu, W., Gregory, J. C., Org, E., Buffa, J. A., Gupta, N., Wang, Z., et al. (2016). Gut microbial metabolite TMAO enhances platelet hyperreactivity and thrombosis risk. *Cell* 165, 111–124. doi:10.1016/j.cell.2016.02.011

Zimmermann, F., Roessler, J., Schmidt, D., Jasina, A., Schumann, P., Gast, M., et al. (2020). Impact of the gut microbiota on atorvastatin mediated effects on blood lipids. *J. Clin. Med.* 9, E1596. doi:10.3390/jcm9051596

Glossary

AS atherosclerosis

CVDs cardiovascular diseases

GRc ginsenoside Rc

ApoE apolipoprotein E-deficient

NC normal control

HFD high-fat diet

Ato atorvastatin

TC total cholesterol

TG triglyceride

LDL-C low-density lipoprotein cholesterol

HDL-C high-density lipoprotein cholesterol

TNF-α tumor necrosis factor-α

IL-6 interleukin-6

IL-1β interleukin-1β

ABC ATP-binding cassette

TCA (cycle) tricarboxylic acid (cycle)

ORO Oil Red O

H&E hematoxylin and eosin

OTU operational taxonomic unit

PCoA principal coordinate analysis

LDA linear discriminant analysis

LEfSe linear discriminant analysis coupled with effect size

PICRUSt phylogenetic investigation of communities by reconstruction of unobserved states

PCA principal component analysis

PLS-DA partial least-squares-discriminant analysis

VIP variable importance in projection

KEGG Kyoto Encyclopedia of Genes and Genomes

CA cholic acid

CDCA chenodeoxycholic acid

isoLCA isolithocholic acid

TCDCA taurochenodeoxycholic acid

TCA tricarboxylic acid

GCDCA glycochenodeoxycholic acid

FXR farnesoid X receptor

TGR Takeda G-protein-coupled bile acid receptor

LCA lithocholic acid

DCA deoxycholic acid

frontiers | Frontiers in Pharmacology

TYPE Original Research
PUBLISHED 20 October 2022
DOI 10.3389/fphar.2022.1025540

Check for updates

OPEN ACCESS

EDITED BY
Kuo Gao,
Beijing University of Chinese Medicine, China

REVIEWED BY
Yong Wang,
Beijing University of Chinese Medicine, China
Hongwei Wu,
China Academy of Chinese Medical Sciences, China
Fei Lin,
The First Affiliated Hospital of Xinxiang Medical University, China

*CORRESPONDENCE
Xuan-Hui He,
hexuanzi1646@sina.com
Heng-Wen Chen,
chenhengwen@163.com

†These authors have contributed equally to this work

SPECIALTY SECTION
This article was submitted to Ethnopharmacology, a section of the journal Frontiers in Pharmacology

RECEIVED 23 August 2022
ACCEPTED 11 October 2022
PUBLISHED 20 October 2022

CITATION
Tan Y-Q, Jin M, He X-H and Chen H-W (2022), Huoxue Qingre decoction used for treatment of coronary heart disease network analysis and metabolomic evaluation. *Front. Pharmacol.* 13:1025540. doi: 10.3389/fphar.2022.1025540

COPYRIGHT
© 2022 Tan, Jin, He and Chen. This is an open-access article distributed under the terms of the Creative Commons Attribution License (CC BY). The use, distribution or reproduction in other forums is permitted, provided the original author(s) and the copyright owner(s) are credited and that the original publication in this journal is cited, in accordance with accepted academic practice. No use, distribution or reproduction is permitted which does not comply with these terms.

Huoxue Qingre decoction used for treatment of coronary heart disease network analysis and metabolomic evaluation

Yu-Qing Tan†, Min Jin†, Xuan-Hui He* and Heng-Wen Chen*

Department of Pharmacy, Guang'anmen Hospital, China Academy of Chinese Medical Sciences, Beijing, China

Objective: Network pharmacology provides new methods and references for the research of traditional Chinese medicine, but some problems remain, such as single evaluation components and index methods, imperfect relevant databases, unscientific prediction results, and lack of verification of results. Herein, we used a modified network pharmacology research method to explore the potential network analysis mechanism of Huoxue Qingre decoction in the treatment of coronary heart disease and utilized clinical trials for assessment.

Methods: Based on literature research, the targets corresponding to the drug were obtained with the assistance of the TCMSP database and Swiss Target Prediction, and the target proteins were corrected using the UniProt database. The targets related to coronary heart disease was obtained through the GeneCards database. A protein-protein interaction network diagram was constructed, and a "component-intersection target" network diagram was drawn based on Cytoscape 3.6.2 software. The mapped targets were imported into the DAVID bioinformatics platform, which underwent Gene Ontology (GO) function and Kyoto Encyclopedia of Genes and Genomes (KEGG) pathway enrichment analysis, and the network pharmacology prediction results were evaluated through clinical trials.

Results: We obtained 151 compounds related to Huoxue Qingre decoction, 286 genes after evaluation and deduplication, and 426 genes related to coronary heart disease. Finally, 81 common target genes were obtained with 32 pathways according to the KEGG pathway enrichment analysis. The validation results of the clinical trials showed that a total of 98 differential metabolites were found in the treatment of coronary heart disease with Huoxue

Abbreviations: ADRB2, β-2 adrenergic receptor; AR, androgen receptor; BP, biological process; CC, cellular component; CDase, ceramidase; Cer, ceramide; CHD, Coronary heart disease; DL, drug-like; ESR1, estrogen receptor; GO, Gene Ontology; HXQR, Huoxue Qingre decoction; KCNH2, potassium voltage-gated channel subfamily H member 2; KEGG, Kyoto Encyclopedia of Genes and Genomes; MF, molecular function; NOS2, inducible nitric oxide lyase; NOS3, endothelial nitric oxide synthase; OB, oral bioavailability; PPARG, peroxisome proliferator-activated receptor γ; PPI, protein-protein interaction; PTGS2, prostaglandin G/H synthase 2; S1P, sphingosine-1-phosphate; SCN5A, sodium channel protein type 5 subunit α; SLC6A4, sodium-dependent serotonin transporter; SM, N-oleoyl-D-sphingomyelin; SMase, sphingomyelinase; Sph, sphingosine; SphK, sphingosine kinase; TCM, traditional Chinese medicine; TCMSP, Traditional Chinese Medicine Systems Pharmacology Database.

Qingre decoction, involving a total of 16 metabolic pathways. Compared with the network pharmacology prediction results, it was found that only the pathways in cancer (hsa05200) were the common pathways in the top 32 signaling pathways predicted by network pharmacology. The expanded network pharmacology prediction results revealed that the sphingolipid signaling pathway (hsa04071) and prostate cancer pathway (hsa05215) matched the predicted metabolic pathways, with differential metabolites of N-oleoyl-D-sphingomyelin and 1-methyl-6-phenyl-1h-imidazole[4,5-b] pyridine-2-amine.

Conclusion: Through the network analysis and metabolomic evaluation, there may be three signaling pathways that involve the Huoxue Qingre decoction in the treatment of coronary heart disease: pathways in cancer (hsa05200), sphingolipid signaling pathway (hsa04071), and prostate cancer pathway (hsa05215).

KEYWORDS

network pharmacology, traditional Chinese medicine (TCM), Huoxue Qingre decoction, coronary heart disease (CHD), metabolomics

Introduction

Network pharmacology is an emerging, cross and cutting-edge discipline in the systematic study of drugs in the era of artificial intelligence and big data. It emphasizes that the molecular associations between drugs and therapeutic objects can be obtained from the perspective of the system level and the whole of the biological network. It has been widely used in the interpretation of the overall mechanism of action of traditional Chinese medicine (TCM) compounds, and in the analysis of drug combinations and formula compatibility law, providing new ideas for the study of complex systems of TCM (Zhang et al., 2019). In recent years, the number of articles on network pharmacology has rapidly increased every year, with hundreds of articles being published. According to a search with the subject term "network pharmacology," more than 2,800 Chinese knowledge network studies were conducted in 2021.

Coronary heart disease (CHD), also known as coronary atherosclerotic heart disease, is caused by narrowing or obstruction of the vascular lumen due to atherosclerotic lesions in the coronary vessels, resulting in myocardial ischemia, hypoxia, or necrosis. Coronary atherosclerosis is a factor involved in the pathogenesis of CHD. It has been reported that the current number of patients with cardiovascular diseases in China is 290 million, of which the number of patients with CHD is as high as 11 million, and this has become a major public health problem in China (Benjamin et al., 2017; Hu et al., 2019).

At present, there have been satisfactory results in the use of TCM for the treatment of CHD. The combination of western medicine disease identification and TCM syndrome differentiation has become an important form of clinical diagnosis, treatment, and rehabilitation of CHD. In TCM, blood stasis is considered to be a factor leading to the dystrophy of the heart vessels, which leads to pain when the heart vessels are abnormal, thus causing "chest obstruction" and "heartache." Its characteristics are basically consistent with the symptoms of modern CHD. Qi is the commander of the blood, and the normal operation of blood depends on the normal promotion of Qi. If the vitality is deficient and unable to circulate the blood, the blood flow will be slow and there will be blood stasis. Therefore, the treatment of CHD should focus on promoting blood circulation and invigorating Qi (China Association of Chinese Medicine Cardiovascular Disease Branch, 2019).

Huoxue Qingre (HXQR) decoction is the clinical experience of Guang'anmen Hospital in the treatment of CHD with significant therapeutic effect. HXQR consists of eight herbs, including *Salvia miltiorrhiza* Bunge (Danshen, DS), *Panax ginseng* C.A.Mey. (Renshen, RS), *Coptis chinensis* Franch. (Huanglian, HL), *Pinellia ternata* (Thunb.) Makino (Fabanxia, BX), *Paeonia lactiflora* Pall. (Chishao, CS), *Panax notoginseng* (Burk) F. H. Chen (Sanqi, SQ), *Pueraria lobata* (Willd.) Maesen & S.M. Almeida ex Sanjappa & Predeep (Gegen, GG), and *Cistanche deserticola* Ma (Roucongrong, RCR). It has the effects of invigorating Qi and activating blood circulation, clearing heat, and removing phlegm. In this formula, *Salvia miltiorrhiza* is the monarch drug. *Panax ginseng*, *Coptis chinensis*, and *Pinellia ternata* are the minister drugs. *Paeonia lactiflora*, *Panax notoginseng*, *Puerariae Lobatae*, and *Cistanche deserticola* are adjuvant drugs. Previously, our group found that HXQR improves the mitochondrial structure and function of cardiomyocytes, inhibits inflammatory factors and myocardial apoptosis, and thus improves ventricular remodeling after myocardial

TABLE 1 The composition of traditional Chinese medicine (TCM) in HXQR.

Composed of TCM	Composed of TCM (Chinese)	Medicinal parts	Percentage (%)	Active ingredient content of TCM (%)
Salvia miltiorrhiza Bunge	Danshen	Dry roots and rhizomes	20.8	tanshinone IIA 0.25, salvianolic acid B 5.3
Panax ginseng C.A.Mey	Renshen	Dry roots and rhizomes	8.3	ginsenoside Rg1 and Re 0.48, ginsenoside Rb1 0.28
Coptis chinensis Franch	Huanglian	Dry roots and rhizomes	6.9	berberine 7.6, epiberberine 1.30, coptisine 2.1, palmatine 2.1
Pinellia ternata (Thunb.) Makino	Fabanxia	Dry tuber	8.3	—
Paeonia lactiflora Pall	Chishao	Dry roots and rhizomes	16.7	Paeoniflorin 3.3
Panax notoginseng (Burkill) F.H.Chen	Sanqi	Dry roots and rhizomes	17.4	ginsenoside Rg1, ginsenoside Rb1, and notoginsenoside R1 6.2
Pueraria lobata (Willd.) Maesen & S.M. Almeida ex Sanjappa & Predeep	Gegen	Dry tuber	20.8	Puerarin 3.1
Cistanche deserticola Ma	Roucongrong	Dry fleshy stem	13.9	Echinacoside and acteoside 0.43

infarction (Chen et al., 2017; Chen et al., 2018; Wang et al., 2019).

Network pharmacology provides new methods and references for TCM research, but problems still remain such as single evaluation components and index methods, imperfect relevant databases, unscientific prediction results, and insufficient validation of results. Therefore, in the current study, we intend to adopt and improve the network pharmacology research method (Zhang and Li, 2015; Xie et al., 2019), explore the potential mechanism of HXQR in the treatment of critical coronary strain, and verify results through clinical trials. This study will provide a demonstration for the in-depth study of network pharmacology, promote the further development and application of network pharmacology, and provide a reference for the clinical application and mechanism research of HXQR decoction and other TCM compounds.

Materials and methods

Preparation of HXQR decoction

HXQR was provided by the Department of Pharmacy, Guang'anmen Hospital, China Academy of Chinese Medical Science. It consists of *Salvia miltiorrhiza* Bunge (Danshen, 20.8%, Collection bar code PE02053963, product batch number 15102502), *Panax ginseng* C.A.Mey. (Renshen, 8.3%, Collection bar code PE 01471910, product batch number 15102902), *Coptis chinensis* Franch. (Huanglian, 6.9%, Collection bar code PE01268317, product batch number 15111102), *Pinellia ternata* (Thunb.) Makino (Fabanxia, 8.3%, Collection bar code PE02240636, product batch number SAA171), *Paeonia lactiflora* Pall. (Chishao, 16.7%, Collection bar code PE02247249, product batch number 16011601), *Panax notoginseng* (Burk) F. H. Chen (Sanqi, 4.2%, Collection bar code PE 01976963, product batch number 15041601), *Pueraria lobata* (Willd.) Maesen & S.M. Almeida ex Sanjappa & Predeep (Gegen, 20.8%, Collection bar code PE02015760, product batch number 15121701), and *Cistanche deserticola* Ma (Roucongrong, 13.9%, Collection bar code PE 01542425, product batch number 160260541) (Table 1). All medicinal names have been unified using the Kew Medicinal plant names service. All specimens are deposited in Chinese National Herbarium, Institute of Botany, Chinese Academy of Sciences (20 Nanxincun, Xiangshan, Beijing, China). All medicinal materials are provided by Beijing Kangmei Pharmaceutical Co., Ltd. (Beijing, China).

The medicinal herbs of HXQR were extracted by 10 times of water through heating reflux for twice, each time for 1.0 h. The extracts were mixed and concentrated under reduced pressure. The relative density was about 1.12 (measured at 20°C). Ethanol was added to bring the ethanol content to 70%. After 24 h, the extracts were concentrated (density 1.20 at 50°C), and dried in vacuum at 60°C. Finally, all the extracts were crushed and mixed to get an extract of HXQR.

The dry extract yielding rate of HXQR was 26.00%. The contents of active ingredients in HXQR extract were 3.58% for salvianolic acid B, 0.76% for *Coptis chinensis* total alkaloids (berberine, epiberberine, coptisine and palmatine), 0.33% for ginsenoside Rb1, 1.60% for paeoniflorin, 1.95% for puerarin, 0.24% for echinacoside (Chen et al., 2016). All components are tested by HPLC (Aglient 1100, Agilent Technologies, Inc., CA, United States).

Prediction of the main active ingredients and targets of HXQR decoction

Based on the systematic database of TCM pharmacology and the analysis platform (Traditional Chinese Medicine Systems Pharmacology Database (TCMSP)), the components of the main chemicals in HXQR decoction were retrieved. *S. miltiorrhiza*, *P. ginseng*, *C. chinensis*, *P. ternata*, *P. veitchii*, *P. notoginseng*, *P. lobata*, and *C. deserticola* were searched to establish a chemical database for HXQR with oral bioavailability (OB) ≥30% and drug-like (DL) ≥0.18, combined with the TCM pharmacopoeia and published literature to supplement active ingredients. According to the TCMSP database and Swiss Target Prediction, the targets corresponding to the drug were queried, and the obtained target proteins were evaluated and corrected using the UniProt database, converted into the corresponding standard gene names, and saved in the drug target database for HXQR.

Obtaining CHD targets

In the GeneCards database, with "coronary heart disease" as the keyword, a search was performed for CHD-related genes. These genes were exported to the Excel program, and gene evaluation was performed with the median, and the median was taken for four times to evaluate the genes with a relevance score greater than the median, and a CHD target database was then established.

Construction of a target protein-protein interaction (PPI) network for HXQR

Mapping targets of diseases and drugs were obtained. Cytoscape 3.6.2 software was used to associate each compound with the corresponding targets to construct an "active ingredients-common targets" network. The STRING database was used to select the "homo sapiens" identification, construct the PPI network, analyze its network topological parameters, and find the key targets with node degree as an important parameter.

GO functional enrichment and KEGG biological pathway enrichment analysis

HXQR and CHD mapping targets were imported into the DAVID bioinformatics platform for Gene Ontology (GO) function and Kyoto Encyclopedia of Genes and Genomes (KEGG) pathway enrichment analysis. The p value was used as the condition to analyze the pathway of target regulation biology. The main signaling pathways and biological processes of HXQR exerting pharmacological effects were analyzed to explore the possible mechanism of HXQR in the treatment of CHD.

Molecular docking of the main active components of HXQR with target proteins

The Uniprot database and RCSB PDB protein structure database (https://www.rcsb.org/) were used to find the PDB ID (Protein Data Bank Identification) of key targets, and obtain protein information, and utilized Pymol software to process molecules and saved them as pdb format. The active ingredient information of the drug corresponding to the target in the TCMSP database was downloaded and saved in mol2 format. Molecular docking was performed using SYBYL-X 2.0 software, and the results were analyzed by the obtained total score.

Assessment of network pharmacology prediction results by metabolomics in clinical trials

There is a comprehensive understanding of the purpose, methods, benefits, and possible risks of this study, which has been registered in the TCM Clinical Trials Registry (http://www.chictr.org.cn/index.aspx; Chi CTR-IOR-17013189). This trial has been approved by the ethics committee (Guang'anmen Hospital, China Academy of Chinese Medical Sciences, No. 2017-083-KY-01).

The clinical trial of HXQR for CHD was conducted by our group according to the registered trial protocol. Only the serum of patients in the control group and experimental group (9:11) was used for metabolomics analysis in the current study, and the metabolomics analysis method was performed according to the Fujisaka method (Fujisaka et al., 2018). The analytical instrument used for this experiment was a liquid chromatography-mass spectrometry system composed of a Waters ACQUITY UPLC ultra-high performance liquid chromatography-tandem AB Triple TOF 5600 high-resolution mass spectrometer.

Chromatographic conditions: chromatographic column ACQUITY UPLC BEH C18 (100 mm × 2.1 mm, 1.7 μm); column temperature 45°C; mobile phase: (A) water (containing 0.1% formic acid), (B) acetonitrile/methanol (2/3) (v/v) (containing 0.1% formic acid); flow rate: 0.4 ml/min; injection volume: 5 μl; elution conditions: A% (95%–0) gradient elution. Mass spectrometric conditions: electrospray ionization (ESI) ion source, the positive and negative ion scanning modes were used for sample mass spectrometric signal acquisition.

TABLE 2 Basic information of chemical constituents of HXQR.

HXQR ingredients	Molecule name	MOL ID	OB/%	DL
Salvia miltiorrhiza Bunge	Cryptotanshinone	MOL007088	52.34	0.4
Salvia miltiorrhiza Bunge	tanshinone iia	MOL007154	49.89	0.4
Salvia miltiorrhiza Bunge	tanshinone i	MOL007157	29.27	0.36
Salvia miltiorrhiza Bunge	salvianolic acid b	MOL007074	3.01	0.41
Salvia miltiorrhiza Bunge	przewalskin b	MOL007064	110.32	0.44
Salvia miltiorrhiza Bunge	(2R)-3-(3,4-dihydroxyphenyl)-2-[(Z)-3-(3,4-dihydroxyphenyl) acryloyl]oxy-propionic acid	MOL007132	109.38	0.35
Salvia miltiorrhiza Bunge	(Z)-3-[2-[(E)-2-(3,4-dihydroxyphenyl)vinyl]-3,4-dihydroxy-phenyl]acrylic acid	MOL007140	88.54	0.26
Salvia miltiorrhiza Bunge	(6S)-6-hydroxy-1-methyl-6-methylol-8,9-dihydro-7H-naphtho [8,7-g]benzofuran-10,11-quinone	MOL007150	75.39	0.46
Salvia miltiorrhiza Bunge	formyltanshinone	MOL007058	73.44	0.42
Salvia miltiorrhiza Bunge	miltionone II	MOL007120	71.03	0.44
Salvia miltiorrhiza Bunge	epidanshenspiroketallactone	MOL007105	68.27	0.31
Salvia miltiorrhiza Bunge	(6S)-6-(hydroxymethyl)-1,6-dimethyl-8,9-dihydro-7H-naphtho [8,7-g]benzofuran-10,11-dione	MOL007155	65.26	0.45
Salvia miltiorrhiza Bunge	prolithospermic acid	MOL007130	64.37	0.31
Salvia miltiorrhiza Bunge	2-(4-hydroxy-3-methoxyphenyl)-5-(3-hydroxypropyl)-7-methoxy-3-benzofurancarboxaldehyde	MOL007050	62.78	0.4
Salvia miltiorrhiza Bunge	Przewaquinone B	MOL007068	62.24	0.41
Salvia miltiorrhiza Bunge	digallate	MOL000569	61.85	0.26
Salvia miltiorrhiza Bunge	Danshenol B	MOL007081	57.95	0.56
Salvia miltiorrhiza Bunge	Danshenol A	MOL007082	56.97	0.52
Salvia miltiorrhiza Bunge	przewaquinone c	MOL007069	55.74	0.4
Salvia miltiorrhiza Bunge	isocryptotanshi-none	MOL007108	54.98	0.39
Salvia miltiorrhiza Bunge	neocryptotanshinone	MOL007125	52.49	0.32
Salvia miltiorrhiza Bunge	tanshinaldehyde	MOL007079	52.47	0.45
Salvia miltiorrhiza Bunge	danshenspiroketallactone	MOL007094	50.43	0.31
Salvia miltiorrhiza Bunge	Isotanshinone II	MOL007111	49.92	0.4
Salvia miltiorrhiza Bunge	miltionone I	MOL007119	49.68	0.32
Salvia miltiorrhiza Bunge	deoxyneocryptotanshinone	MOL007098	49.4	0.29
Salvia miltiorrhiza Bunge	(E)-3-[2-(3,4-dihydroxyphenyl)-7-hydroxy-benzofuran-4-yl] acrylic acid	MOL007048	48.24	0.31
Salvia miltiorrhiza Bunge	6-o-syringyl-8-o-acetyl shanzhiside methyl ester	MOL007051	46.69	0.71
Salvia miltiorrhiza Bunge	tanshinone VI	MOL007156	45.64	0.3
Salvia miltiorrhiza Bunge	salvianolic acid g	MOL007141	45.56	0.61
Salvia miltiorrhiza Bunge	isoimperatorin	MOL001942	45.46	0.23
Salvia miltiorrhiza Bunge	dihydrotanshinonel	MOL007101	45.04	0.36
Salvia miltiorrhiza Bunge	manool	MOL007115	45.04	0.2
Salvia miltiorrhiza Bunge	miltirone II	MOL007123	44.95	0.24
Salvia miltiorrhiza Bunge	3α-hydroxytanshinonella	MOL007045	44.93	0.44
Salvia miltiorrhiza Bunge	Poriferasterol	MOL001659	43.83	0.76
Salvia miltiorrhiza Bunge	Dehydrotanshinone II A	MOL002651	43.76	0.4
Salvia miltiorrhiza Bunge	sclareol	MOL007077	43.67	0.21
Salvia miltiorrhiza Bunge	salvianolic acid j	MOL007142	43.38	0.72
Salvia miltiorrhiza Bunge	Przewaquinone E	MOL007152	42.85	0.45
Salvia miltiorrhiza Bunge	Tanshindiol B	MOL007151	42.67	0.45
Salvia miltiorrhiza Bunge	(6S,7R)-6,7-dihydroxy-1,6-dimethyl-8,9-dihydro-7H-naphtho [8,7-g]benzofuran-10,11-dione	MOL007070	41.31	0.45

(Continued on following page)

TABLE 2 (*Continued*) Basic information of chemical constituents of HXQR.

HXQR ingredients	Molecule name	MOL ID	OB/%	DL
Salvia miltiorrhiza Bunge	2-isopropyl-8-methylphenanthrene-3,4-dione	MOL007041	40.86	0.23
Salvia miltiorrhiza Bunge	przewaquinone f	MOL007071	40.31	0.46
Salvia miltiorrhiza Bunge	microstegiol	MOL007118	39.61	0.28
Salvia miltiorrhiza Bunge	α-amyrin	MOL006824	39.51	0.76
Salvia miltiorrhiza Bunge	neocryptotanshinone ii	MOL007124	39.46	0.23
Salvia miltiorrhiza Bunge	dan-shexinkum d	MOL007093	38.88	0.55
Salvia miltiorrhiza Bunge	Miltirone	MOL007122	38.76	0.25
Salvia miltiorrhiza Bunge	1,2,5,6-tetrahydrotanshinone	MOL001601	38.75	0.36
Salvia miltiorrhiza Bunge	dihydrotanshinlactone	MOL007100	38.68	0.32
Salvia miltiorrhiza Bunge	przewalskin a	MOL007063	37.11	0.65
Salvia miltiorrhiza Bunge	Methylenetanshinquinone	MOL007061	37.07	0.36
Salvia miltiorrhiza Bunge	poriferast-5-en-3beta-ol	MOL001771	36.91	0.75
Salvia miltiorrhiza Bunge	miltipolone	MOL007121	36.56	0.37
Salvia miltiorrhiza Bunge	luteolin	MOL000006	36.16	0.25
Salvia miltiorrhiza Bunge	sugiol	MOL002222	36.11	0.28
Salvia miltiorrhiza Bunge	C09092	MOL007107	36.07	0.25
Salvia miltiorrhiza Bunge	1-methyl-8,9-dihydro-7H-naphtho[5,6-g]benzofuran-6,10,11-trione	MOL007127	34.72	0.37
Salvia miltiorrhiza Bunge	NSC 122421	MOL007149	34.49	0.28
Salvia miltiorrhiza Bunge	4-methylenemiltirone	MOL007049	34.35	0.23
Salvia miltiorrhiza Bunge	5,6-dihydroxy-7-isopropyl-1,1-dimethyl-2,3-dihydrophenanthren-4-one	MOL007036	33.77	0.29
Salvia miltiorrhiza Bunge	salvilenone l	MOL007143	32.43	0.23
Salvia miltiorrhiza Bunge	3-beta-Hydroxymethyllenetanshiquinone	MOL007059	32.16	0.41
Salvia miltiorrhiza Bunge	salviolone	MOL007145	31.72	0.24
Salvia miltiorrhiza Bunge	Salvilenone	MOL007085	30.38	0.38
Coptis chinensis Franch	palmatine	MOL000785	64.6	0.65
Coptis chinensis Franch	berberine	MOL001454	36.86	0.78
Coptis chinensis Franch	coptisine	MOL001458	30.67	0.86
Coptis chinensis Franch	epiberberine	MOL002897	43.09	0.78
Coptis chinensis Franch	Corchoroside A_qt	MOL002907	104.95	0.78
Coptis chinensis Franch	Moupinamide	MOL008647	86.71	0.26
Coptis chinensis Franch	Magnograndiolide	MOL000622	63.71	0.19
Coptis chinensis Franch	(R)-Canadine	MOL002903	55.37	0.77
Coptis chinensis Franch	Worenine	MOL002668	45.83	0.87
Coptis chinensis Franch	Obacunone	MOL013352	43.29	0.77
Coptis chinensis Franch	Berlambine	MOL002904	36.68	0.82
Coptis chinensis Franch	berberrubine	MOL002894	35.74	0.73
Coptis chinensis Franch	Palmidin A	MOL000762	35.36	0.65
Panax ginseng C.A.Mey	Ginsenoside Re	MOL005338	4.27	0.12
Panax ginseng C.A.Mey	Celabenzine	MOL005314	101.88	0.49
Panax ginseng C.A.Mey	Aposiopolamine	MOL005308	66.65	0.22
Panax ginseng C.A.Mey	Frutinone A	MOL005321	65.9	0.34
Panax ginseng C.A.Mey	Inermin	MOL003648	65.83	0.54
Panax ginseng C.A.Mey	Girinimbin	MOL005356	61.22	0.31
Panax ginseng C.A.Mey	Fumarine	MOL000787	59.26	0.83
Panax ginseng C.A.Mey	malkangunin	MOL005360	57.71	0.63
Panax ginseng C.A.Mey	kaempferol	MOL000422	41.88	0.24

(Continued on following page)

TABLE 2 (*Continued*) Basic information of chemical constituents of HXQR.

HXQR ingredients	Molecule name	MOL ID	OB/%	DL
Panax ginseng C.A.Mey	Dianthramine	MOL005318	40.45	0.2
Panax ginseng C.A.Mey	ginsenoside Rg5_qt	MOL005401	39.56	0.79
Panax ginseng C.A.Mey	Deoxyharringtonine	MOL005317	39.27	0.81
Panax ginseng C.A.Mey	Chrysanthemaxanthin	MOL004492	38.72	0.58
Panax ginseng C.A.Mey	alexandrin_qt	MOL005399	36.91	0.75
Panax ginseng C.A.Mey	Panaxadiol	MOL005376	33.09	0.79
Panax ginseng C.A.Mey	Gomisin B	MOL005357	31.99	0.83
Panax ginseng C.A.Mey	Ginsenoside-Rh4_qt	MOL005348	31.11	0.78
Pinellia ternata (Thunb.) Makino	(3S,6S)-3-(benzyl)-6-(4-hydroxybenzyl)piperazine-2,5-quinone	MOL006957	46.89	0.27
Pinellia ternata (Thunb.) Makino	beta-D-Ribofuranoside, xanthine-9	MOL006967	44.72	0.21
Pinellia ternata (Thunb.) Makino	12,13-epoxy-9-hydroxynonadeca-7,10-dienoic acid	MOL006937	42.15	0.24
Pinellia ternata (Thunb.) Makino	10,13-eicosadienoic	MOL006936	39.99	0.2
Pinellia ternata (Thunb.) Makino	Cycloartenol	MOL003578	38.69	0.78
Pinellia ternata (Thunb.) Makino	24-Ethylcholest-4-en-3-one	MOL001755	36.08	0.76
Pinellia ternata (Thunb.) Makino	Cavidine	MOL002670	35.64	0.81
Pinellia ternata (Thunb.) Makino	coniferin	MOL000519	31.11	0.32
Pinellia ternata (Thunb.) Makino	gondoic acid	MOL005030	30.7	0.2
Paeonia lactiflora Pall	paeoniflorin	MOL001924	53.87	0.79
Paeonia lactiflora Pall	paeoniflorgenone	MOL001918	87.59	0.37
Paeonia lactiflora Pall	paeoniflorin_qt	MOL001925	68.18	0.4
Paeonia lactiflora Pall	1-o-beta-d-glucopyranosylpaeonisuffrone_qt	MOL006996	65.08	0.35
Paeonia lactiflora Pall	evofolinB	MOL007022	64.74	0.22
Paeonia lactiflora Pall	9-ethyl-neo-paeoniaflorin A_qt	MOL007018	64.42	0.3
Paeonia lactiflora Pall	(2R,3R)-4-methoxyl-distylin	MOL006992	59.98	0.3
Paeonia lactiflora Pall	4-ethyl-paeoniflorin_qt	MOL007008	56.87	0.44
Paeonia lactiflora Pall	4-o-methyl-paeoniflorin_qt	MOL007012	56.7	0.43
Paeonia lactiflora Pall	(+)-catechin	MOL000492	54.83	0.24
Paeonia lactiflora Pall	Lactiflorin	MOL001921	49.12	0.8
Paeonia lactiflora Pall	Albiflorin_qt	MOL007005	48.7	0.33
Paeonia lactiflora Pall	ellagic acid	MOL001002	43.06	0.43
Paeonia lactiflora Pall	Spinasterol	MOL004355	42.98	0.76
Paeonia lactiflora Pall	campest-5-en-3beta-ol	MOL005043	37.58	0.71
Paeonia lactiflora Pall	stigmast-7-en-3-ol	MOL006999	37.42	0.75
Paeonia lactiflora Pall	1-o-beta-d-glucopyranosyl-8-o-benzoylpaeonisuffrone_qt	MOL006994	36.01	0.3
Paeonia lactiflora Pall	Ethyl oleate (NF)	MOL002883	32.4	0.19
Paeonia lactiflora Pall	8-debenzoylpaeonidanin	MOL007014	31.74	0.45
Paeonia lactiflora Pall	benzoyl paeoniflorin	MOL007003	31.14	0.54
Paeonia lactiflora Pall	isobenzoylpaeoniflorin	MOL007025	31.14	0.54
Paeonia lactiflora Pall	(1S,2S,4R)-trans-2-hydroxy-1,8-cineole-B-D-glucopyranoside	MOL006990	30.25	0.27
Paeonia lactiflora Pall	Albiflorin	MOL007004	30.25	0.77
Panax notoginseng (Burk) F. H. Chen	notoginsenoside r1	MOL007487	5.43	0.13
Panax notoginseng (Burk) F. H. Chen	Mandenol	MOL001494	42	0.19
Panax notoginseng (Burk) F. H. Chen	ginsenoside f2	MOL007475	36.43	0.25
Panax notoginseng (Burk) F. H. Chen	DFV	MOL001792	32.76	0.18
Pueraria lobata (Willd.) Maesen & S.M. Almeida ex Sanjappa & Predeep	puerarin	MOL012297	24.03	0.69
Pueraria lobata (Willd.) Maesen & S.M. Almeida ex Sanjappa & Predeep	formononetin	MOL000392	69.67	0.21
Pueraria lobata (Willd.) Maesen & S.M. Almeida ex Sanjappa & Predeep	3′-Methoxydaidzein	MOL002959	48.57	0.24

(Continued on following page)

TABLE 2 (*Continued*) Basic information of chemical constituents of HXQR.

HXQR ingredients	Molecule name	MOL ID	OB/%	DL
Pueraria lobata (Willd.) Maesen & S.M. Almeida ex Sanjappa & Predeep	Daidzein-4,7-diglucoside	MOL003629	47.27	0.67
Cistanche deserticola Ma	acteoside	MOL003333	2.94	0.62
Cistanche deserticola Ma	echinacoside	MOL008875	3.14	0.38
Cistanche deserticola Ma	Yangambin	MOL007563	57.53	0.81
Cistanche deserticola Ma	Marckine	MOL008871	37.05	0.69
Pinellia ternata (Thunb.) Makino, *Paeonia lactiflora* Pall	baicalein	MOL002714	33.52	0.21
Panax ginseng C.A.Mey., *Panax notoginseng* (Burk) F. H. Chen	Diop	MOL002879	43.59	0.39
Panax ginseng C.A.Mey., *Panax notoginseng* (Burk) F. H. Chen	Sanchinoside C1	MOL005341	10.04	0.28
Panax ginseng C.A.Mey., *Panax notoginseng* (Burk) F. H. Chen	ginsenoside rh2	MOL005344	36.32	0.56
Panax ginseng C.A.Mey., *Panax notoginseng* (Burk) F. H. Chen	ginsenoside Rb1	MOL007476	6.24	0.04
Panax ginseng C.A.Mey., *Cistanche deserticola* Ma	arachidonate	MOL005320	45.57	0.2
Panax ginseng C.A.Mey., *Cistanche deserticola* Ma	suchilactone	MOL005384	57.52	0.56
Coptis chinensis Franch, *Panax notoginseng* (Burk) F. H. Chen, *Cistanche deserticola* Ma	quercetin	MOL000098	46.43	0.28
Salvia miltiorrhiza Bunge, *Pinellia ternata* (Thunb.) Makino, *Paeonia lactiflora* Pall	Baicalin	MOL002776	40.12	0.75
Panax ginseng C.A.Mey., *Pinellia ternata* (Thunb.) Makino, *Paeonia lactiflora* Pall., *Panax notoginseng* (Burk) F. H. Chen	Stigmasterol	MOL000449	43.83	0.76
Panax ginseng C.A.Mey., *Pinellia ternata* (Thunb.) Makino, *Paeonia lactiflora* Pall., *Panax notoginseng* (Burk) F. H. Chen, *Pueraria lobata* (Willd.) Maesen & S.M. Almeida ex Sanjappa & Predeep, *Cistanche deserticola* Ma	beta-sitosterol	MOL000358	36.91	0.75

Results

Main potential active ingredients in HXQR

The chemical constituents of each drug in HXQR were searched by TCMSP, including 67 chemical constituents related to *S. miltiorrhiza*, 14 chemical constituents related to *C. chinensis*, 25 chemical constituents related to *P. ginseng*, 13 chemical constituents related to *P. ternata*, 27 chemical constituents related to *P. veitchii*, 11 chemical constituents related to *P. notoginseng*, five chemical constituents related to *P. lobata*, and eight chemical constituents related to *C. deserticola*. Combined with the results of the pharmacopoeia and literature analysis, nine components, salvianolic acid B, tanshinone I, ginsenoside Rg1, ginsenoside Re, ginsenoside Rb1, notoginsenoside R1, puerarin, echinacoside, and acteoside, were added to obtain a total of 172 active ingredients, and 151 compounds were obtained after deleting the duplicates.

Among them, MOL002714 is a common component of *P. ternata* and *P. veitchii*; MOL002879, MOL005341, MOL005344, and MOL007476 are common components of *P. ginseng* and *P. notoginseng*; MOL005320 and MOL005384 are common components of *P. ginseng* and *C. deserticola*; MOL000098 is a common component of *C. chinensis*, *P. notoginseng*, and *C. deserticola*; MOL002776 is a common component of *S. miltiorrhiza*, *P. ternata*, and *P. ternata*; MOL000449 is a common component of *P. ginseng*, *P. veitchii*, *P. veitchii*, and *P. notoginseng*; and MOL000358 is a common component of *P. ginseng*, *P. ternata*, *P. veitchii*, *P. notoginseng*, *P. lobata*, and *C. deserticola*. The four components with the highest OB were: MOL007064 przewalskin b, MOL007132 (2R)-3-(3,4-dihydroxyphenyl)-2-[(Z)-3-(3,4-dihydroxyphenyl)acryl]oxy-propionic acid, MOL002907 corchoroside aqt, and MOL005314 celabenzine. The four components with the highest DL were: MOL013352 obacunone, MOL012297 puerarin, MOL008875 echinacoside, and MOL008871 marckine. The results are shown in Table 2.

Main active ingredient-target network for HXQR

A total of 2166 constituent targets were retrieved through the TCMSP database and the UniProt website (https://www.uniprot.org/). Human genes corresponding to TCM drug targets were searched to remove duplicates, and finally, 286 genes were obtained. A network diagram of "HXQRs-active ingredient-drug targets" was drawn. The active ingredients in the figure are expressed according to the last five digits of the MOD ID. TCM drugs are represented by initials. There are a total of 445 nodes and 1734 edges, as shown in Figure 1.

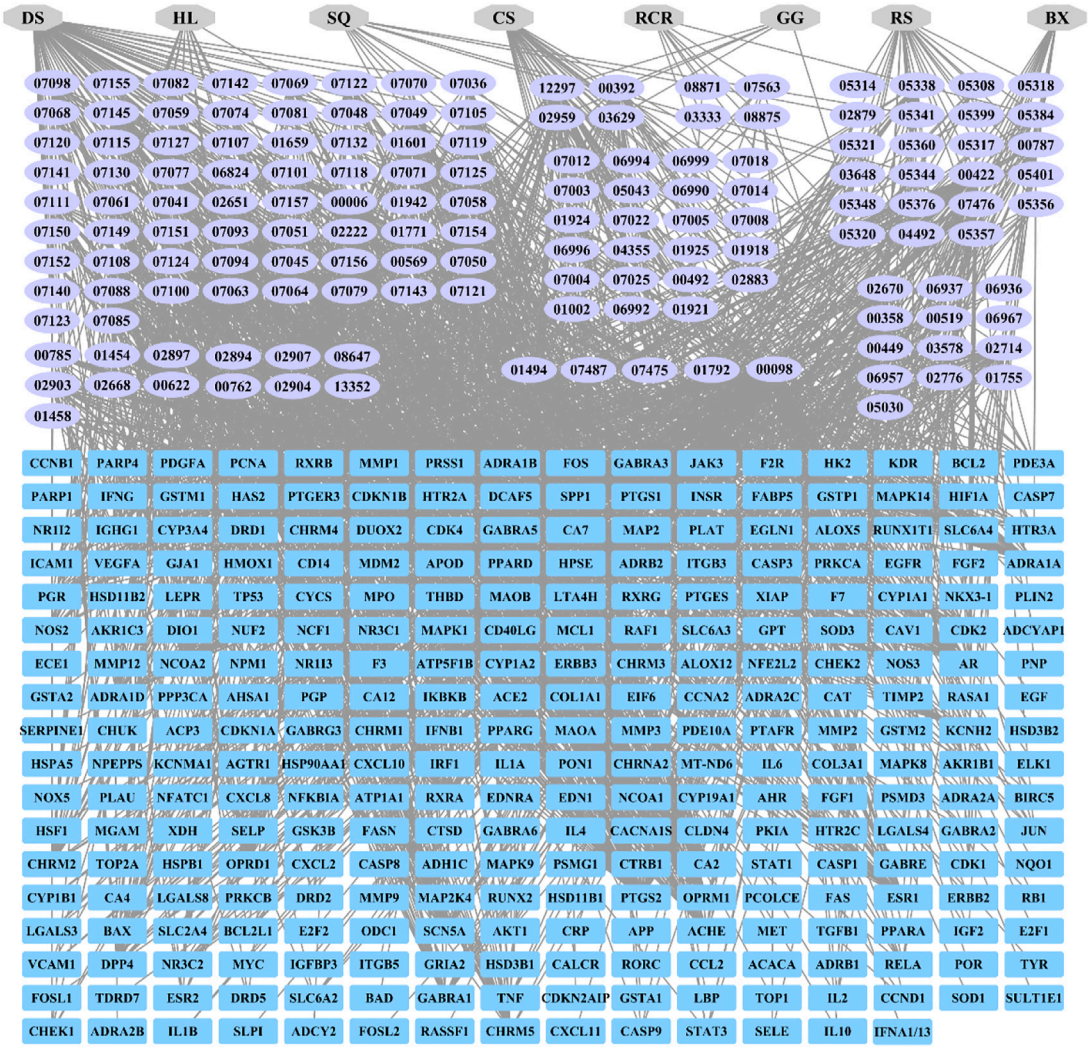

FIGURE 1
HXQR-active ingredients-drug targets.

Prediction of potential targets of HXQR in the treatment of CHD

A search was performed in the GeneCards database to find the median genes related to coronary heart disease, and the genes with a relevance score greater than the median were further analyzed. Subsequently, 426 targets were obtained that intersected with the targets of the main active components of HXQR, which yielded 81 common target genes, as shown in Figure 2. Cytoscape 3.7.2 was used to visualize the relationship between the targets of the active ingredients of HXQR in the treatment of CHD. The analysis showed that HXQR involved 110 active components in the treatment of CHD, with 190 nodes and 523 edges in the network diagram. The node degree reflects the importance of nodes in the network. The area of the network diagram was directly proportional to the area ratio using the degree reaction.

The results showed that prostaglandin G/H synthase 2 (PTGS2), β-2 adrenergic receptor (ADRB2), sodium channel protein type 5 subunit α (SCN5A), androgen receptor (AR), estrogen receptor (ESR1), inducible nitric oxide lyase (NOS2), sodium-dependent serotonin transporter (SLC6A4), endothelial nitric oxide synthase (NOS3), potassium voltage-gated channel subfamily H member 2 (KCNH2), peroxisome proliferator-activated receptor γ (PPARG), and other targets were the core nodes of the network, as shown in Figure 3. In terms of compounds, quercetin (MOL000098), puerarin (MOL012297), luteolin (MOL000006), kaempferol (MOL000422), tanshinone iia (MOL007154), and baicalein (MOL002714) were associated with multiple targets and may

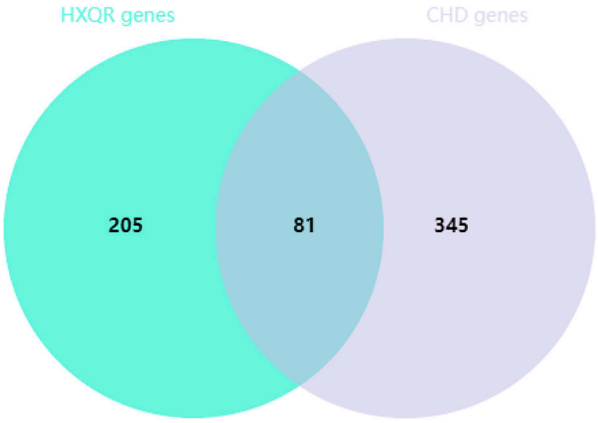

FIGURE 2
Intersection of active ingredients of HXQR and CHD targets.

be the main active components of HXQR decoction in the treatment of CHD.

HXQR-targets-CHD PPI network construction

The drug and disease intersection targets from 81 mappings were analyzed by the STRING database to construct the potential target PPI network, and the results were shown in Figure 4. There were 81 targets in the PPI network that had the ability to interact with proteins, and 1514 edges represented the interactions between proteins. The average degree value was 37.383. There were 45 target proteins with a degree value greater than that of the average. The top 20 were IL6, AKT1, VEGFA, TNF, CCL2, IL1B, EGF, CASP3, CXCL8, MAPK1, MMP9, EDN1, PTGS2, NOS3, SERPINE1, IL10, TP53, EGFR, ICAM1, and MMP2,

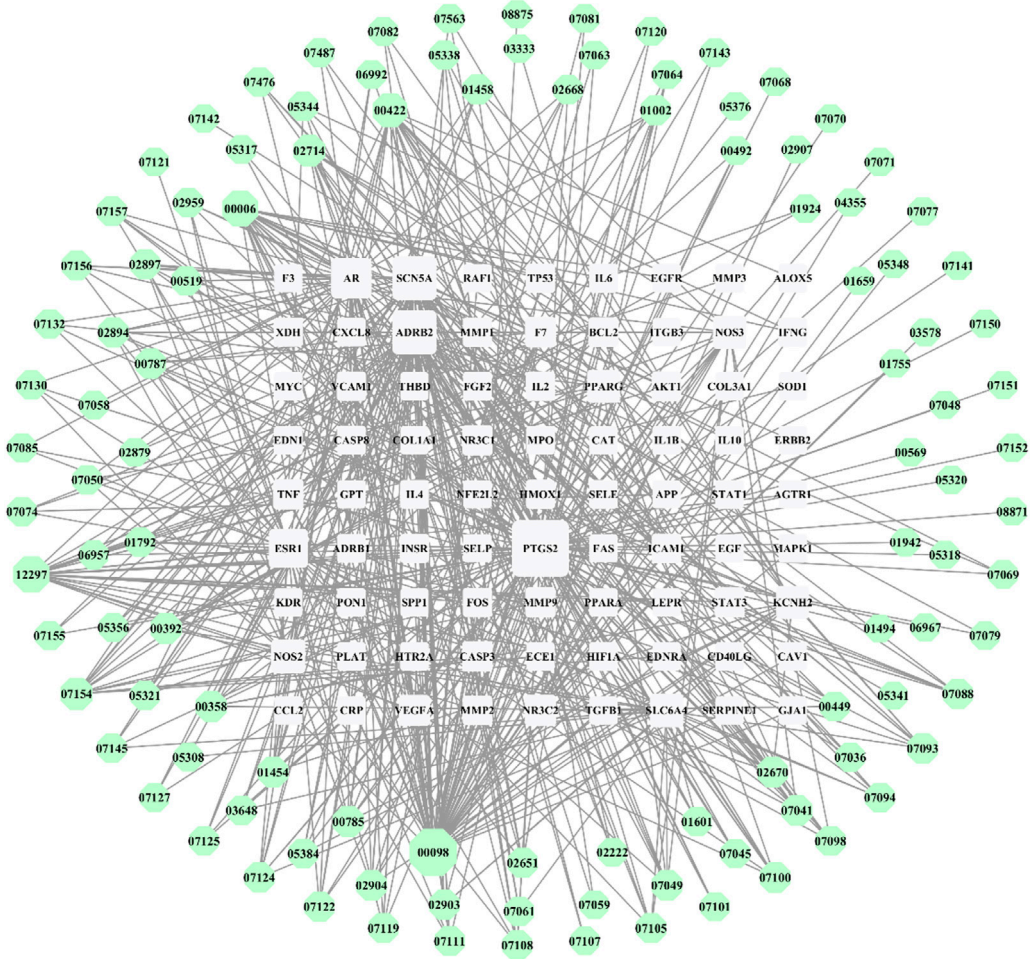

FIGURE 3
Active ingredients–targets of HXQR.

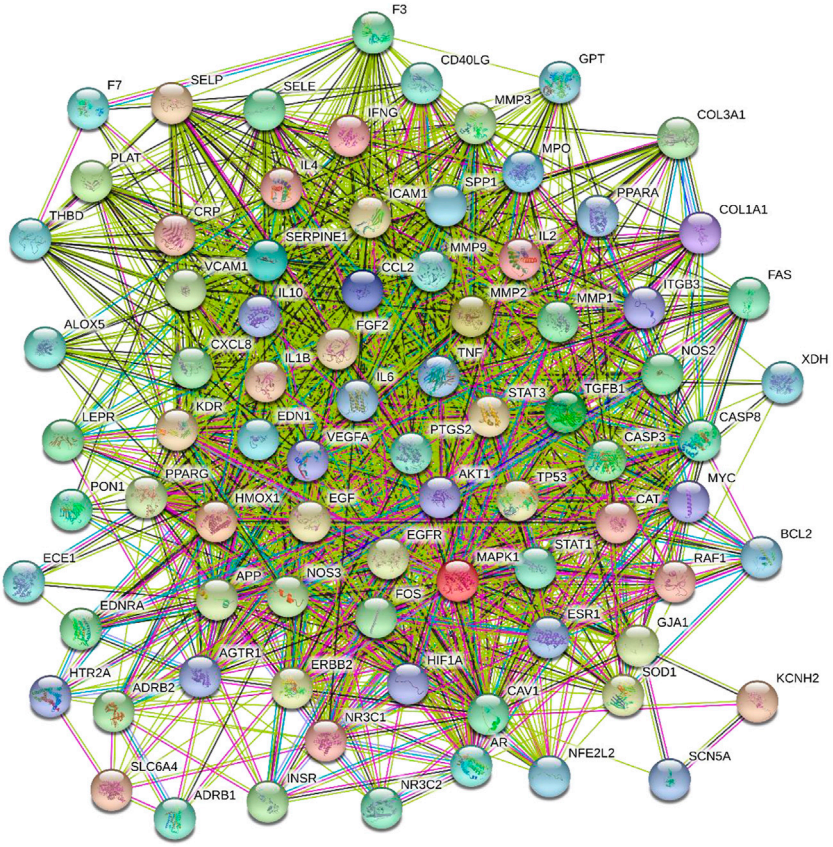

FIGURE 4
PPI network diagram of the targets of CHD treated by HXQR.

which suggested that these proteins might play a key role in the treatment of CHD with HXQR.

GO functional enrichment of HXQR

The common targets of HXQR and CHD were subjected to GO enrichment analysis and included three aspects: biological process (BP), cellular component (CC), and molecular function (MF), and at $p < 0.01$, 254 items were obtained for BP, 26 items for CC, and 41 items for MF. BPs mainly involve positive regulation of transcription by the RNA polymerase II promoter, positive regulation of transcription, DNA template, gene expression, signal transduction, inflammatory response, cell proliferation, aging, drug response, negative regulation of apoptotic process, and response to hypoxia; CCs mainly involve the plasma membrane, extracellular space, extracellular region, cytosol, and extracellular exosome; MFs mainly involve protein binding, identical protein binding, enzyme binding, protein homodimerization activity, and cytokine activity. Among them, three aspects are in the descending order of enrichment number, and the first 20 items were plotted. The p value is taken as the negative logarithm in the figure, and the significance is expressed by the depth of color. The number of enriched genes is expressed by the size of the bubbles, and the greater the number, the larger the bubble, as shown in Figures 5A–C.

KEGG pathway enrichment analysis

KEGG pathway enrichment analysis was performed on the common targets of HXQR and CHD, and it was determined that 105 pathways were associated with them. Evaluating with $p < 0.05$ and number of genes greater than or equal to 10 resulted in 32 pathways. Among them, the enrichment number is arranged in descending order, and the bubble is plotted as shown in Figure 6, in which the p value is taken as the negative logarithm, the color indicates the size, and the gene number is expressed as the bubble size.

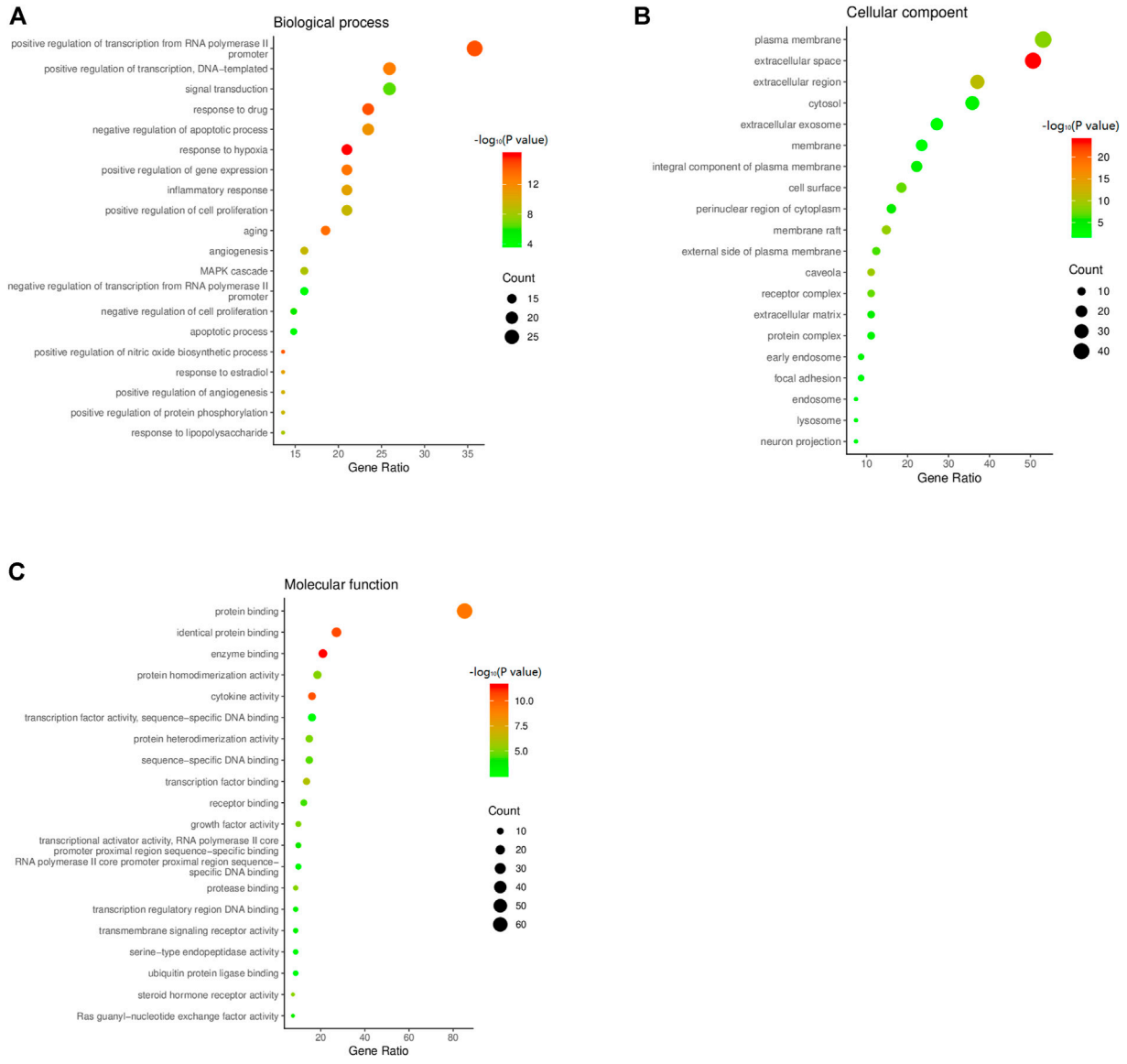

FIGURE 5
(A) Biological process of GO function bubble chart of the targets of CHD treated by HXQR. **(B)** Cellular compoent of GO function bubble chart of the targets of CHD treated by HXQR. **(C)** Molecular function of GO function bubble chart of the targets of CHD treated by HXQR.

Molecular docking analysis

Five key targets with high relevance in the PPI network: IL6, AKT1, VEGFA, TNF, and CCL2 were selected to obtain PDB IDs and target structures, and the five targets were docked to their corresponding active ingredients, respectively, and when the target was combined with the compound structure, the higher the docking score, the more stable the binding of the target with the chemical (Table 3). The average docking score was 4.9 points, which showed good binding strength, and 12 of them ≥5 points, suggesting that the core target has good binding ability with HXQR decoction active ingredients. Most of the compounds were linked to the core target in hydrogen-hydrogen bonds and arranged in descending order of docking score, and the docking structure diagram with a docking score greater than six is shown below (Figures 7A–E).

Analysis of metabolomics assessment results in clinical trials

The research group carried out a small sample randomized double-blind study in the early stage. 32 patients with borderline

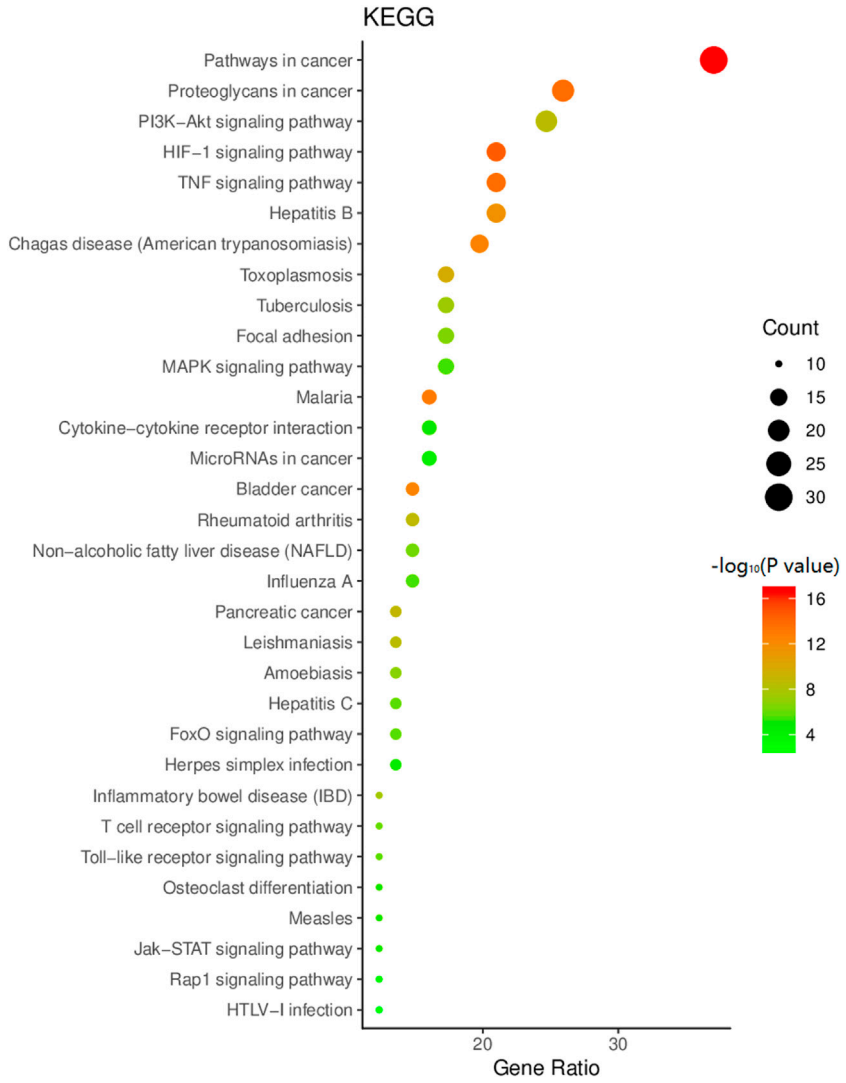

FIGURE 6
KEGG enrichment analysis bubble diagram.

coronary artery disease were included and randomly divided into the experimental group and the control group according to the ratio of 1:1. Both groups received conventional western medicine treatment. On this basis, the test group was given HXQR, while the control group was given HXQR placebo. After 6 months of treatment, the study found that compared with the control group, the degree of stenosis of the target plaque area in the experimental group was significantly reduced after treatment (p = 0.033) (Figure 8).

The ratios were (38.42 ± 20.68)% and (52.00 ± 13.15)%, respectively, while there was no statistical difference between the average CT value of the target plaque and the calcification score of the target plaque (Figures 9, 10).

The TCM symptom score of angina pectoris of CHD showed a significantly higher decrease of the treatment score than that of the control group (p = 0.028) (Figure 11), and the symptoms of chest tightness and palpitations were significantly improved. Before and after the treatment, there was no significant difference in total cholesterol, triglyceride, high density lipoprotein, low density lipoprotein and very low-density lipoprotein between the two groups. The blood and urine routine, liver and kidney function and electrocardiogram were within the normal range before and after treatment in the two groups, with no significant difference. The study showed that HXQR for patients with borderline coronary artery disease could significantly improve chest tightness and palpitations, and had a good effect in stabilizing plaques and improving the degree of coronary stenosis (Huang, 2019).

Metabolomic analysis by clinical serum resulted in 2490 metabolites that were obtained, with 1180 in the negative

TABLE 3 Docking scores between key targets and drug components.

Target	MOL ID		PDB ID	Total score
IL6	MOL000006	luteolin	4o9h	5.89
IL6	MOL000098	quercetin	4o9h	4.57
IL6	MOL001924	paeoniflorin	4o9h	6.13
AKT1	MOL000006	luteolin	3o96	5.24
AKT1	MOL000098	quercetin	3o96	5.27
AKT1	MOL000422	kaempferol	3o96	4.4
AKT1	MOL002714	baicalein	3o96	3.97
AKT1	MOL012297	puerarin	3o96	5.86
VEGFA	MOL000006	luteolin	3v2a	6.37
VEGFA	MOL000098	quercetin	3v2a	6.2
VEGFA	MOL001002	ellagic acid	3v2a	4.41
VEGFA	MOL002714	baicalein	3v2a	4.5
VEGFA	MOL005338	Ginsenoside Re	3v2a	5.48
VEGFA	MOL007157	tanshinone i	3v2a	3.45
VEGFA	MOL007476	ginsenoside Rb1	3v2a	4.48
VEGFA	MOL007487	notoginsenoside r1	3v2a	2.5
VEGFA	MOL012297	puerarin	3v2a	5.64
TNF	MOL000006	luteolin	3wd5	4.46
TNF	MOL000098	quercetin	3wd5	4.07
TNF	MOL000422	kaempferol	3wd5	6.47
TNF	MOL001924	paeoniflorin	3wd5	5.7
TNF	MOL005344	ginsenoside rh2	3wd5	6.44
TNF	MOL007088	cryptotanshinone	3wd5	2.57
TNF	MOL012297	puerarin	3wd5	3.94
CCL2	MOL000098	quercetin	1dok	4.63

mode and 1310 in the positive mode. The VIP value of the first principal component of the OPLS-DA model was >0.1, and the *p*-value of the *t*-test was <0.05 for differential metabolite identification, and a total of 98 differential metabolites were found (Figure 12). Metabolic pathway enrichment analysis of the differential metabolites based on the KEGG database revealed a total of 16 metabolic pathways (Figure 13). By comparing the metabolomics results of this clinical trial with the prediction results of network pharmacology, only the cancer pathway (hsa05200) was found to be its common pathway among the top 32 signaling pathways predicted by network pharmacology.

The results of extended network pharmacology prediction indicated that the sphingolipid signaling pathway (hsa04071) and prostate cancer pathway (hsa05215) matched the predicted metabolic pathway, indicating that HXQR may be involved in the treatment of CHD through three signaling pathways, including the cancer pathway (hsa05200), sphingolipid signaling pathway (hsa04071), and prostate cancer pathway (hsa05215). The differential metabolites may be N-oleoyl-D-sphingomyelin (d18:1/22:0) (SM, upregulated), 1-methyl-6-phenyl-1h-imidazole[4,5-b]

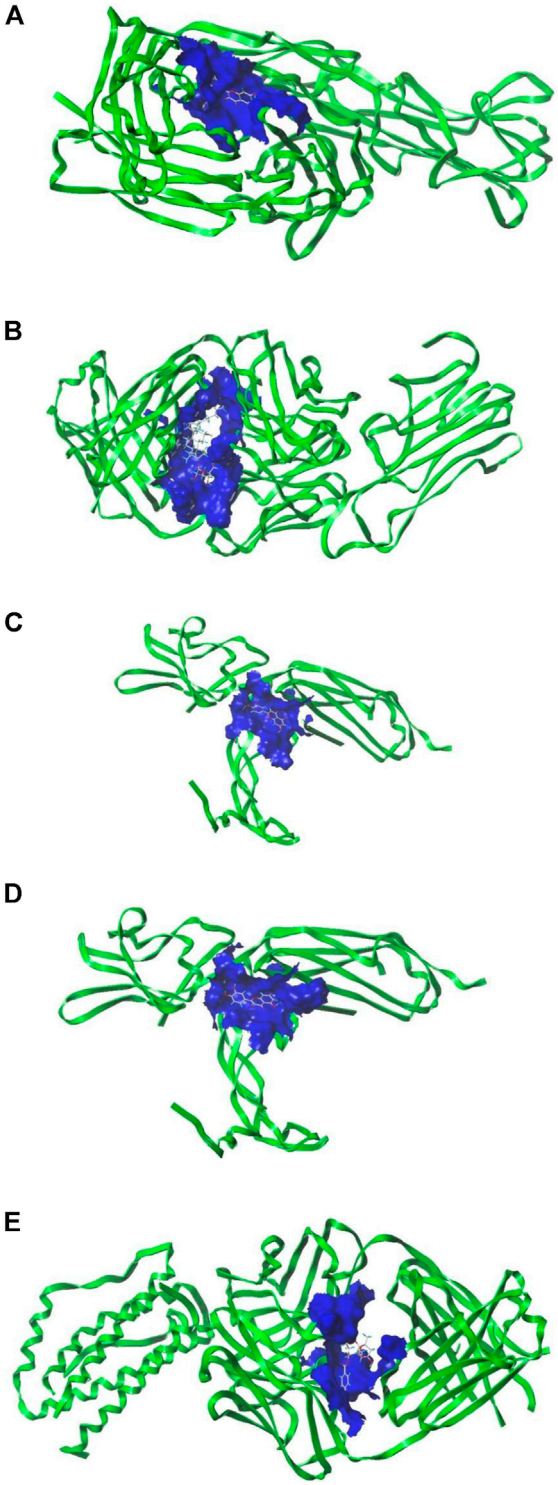

FIGURE 7
(A) Docking diagram of TNF- kaempferol. **(B)** Docking diagram of TNF- ginsenoside rh2. **(C)** Docking diagram of VEGFA-luteolin. **(D)** Docking diagram of VEGFA-quercetin. **(E)** Docking diagram of IL6-paeoniflorin.

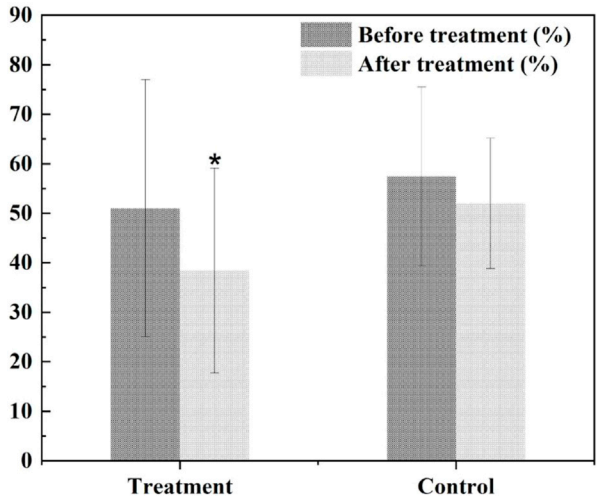

FIGURE 8
The degree of stenosis of the target plaque area. *p < 0.05 compared with the control.

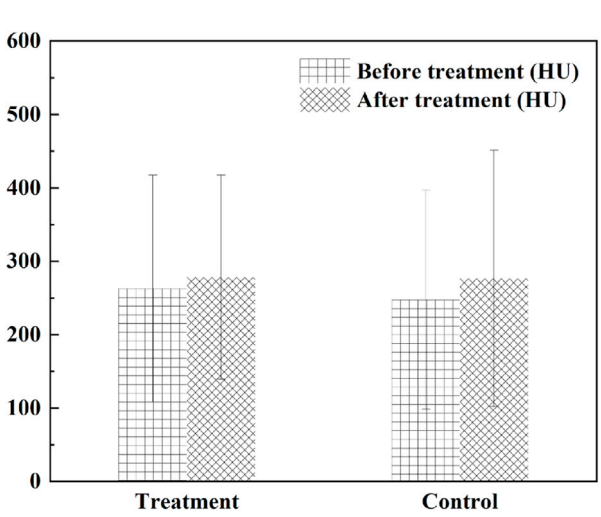

FIGURE 9
The average CT value of the target plaque.

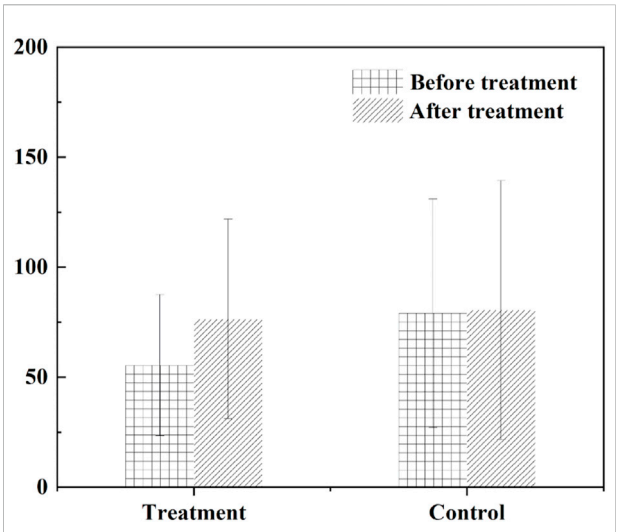

FIGURE 10
The calcification score of the target plaque.

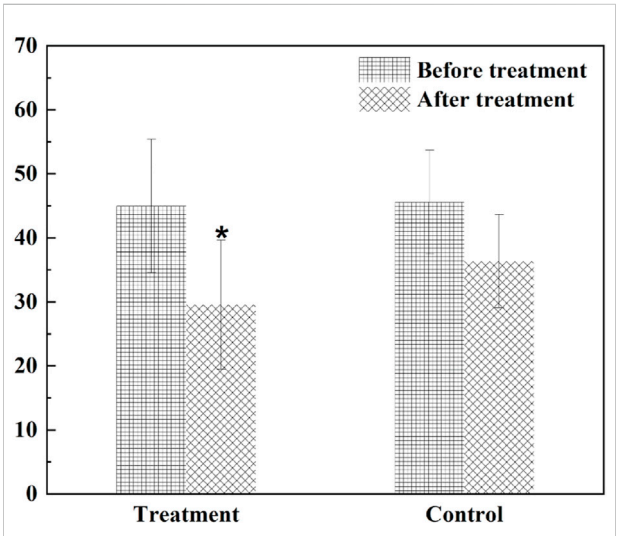

FIGURE 11
The TCM symptom score of angina pectoris of CHD. *p < 0.05 compared with the control.

pyridine-2-amine and 1-phenyl-6-phenyl-1H-imidazo[4,5-b] pyridine-2-amine (downregulated).

The metabolomics results showed that after treatment with HXQR, the key metabolites of the sphingolipid signaling pathway (hsa04071), Cer (d18:2/23:0), and Cer (t18:0/20:0 (2OH)), SM (d18:1/22:0), and SM (d18:1/24:1 (15Z)), were significantly increased (p < 0.01), and the level of S1P in serum was decreased (p = 0.08) (Figure 14). 1-Methyl-6-phenyl-1H-imidazo[4,5-b]pyridin-2-amine is a key differential metabolite of prostate cancer (hsa05200) and pathways in cancer (hsa05215), which may lead to DNA damage, but the specific cause is not clear and requires in-depth study.

The level of Cer (d18:2/23:0), Cer (t18:0/20:0 (2OH), SM (d18:1/22:0), and SM (d18:1/24:1 (15Z)), were significantly increased after treatment with HXQR (p < 0.01), and the level of S1P in serum was decreased after treatment with HXQR (p = 0.08).

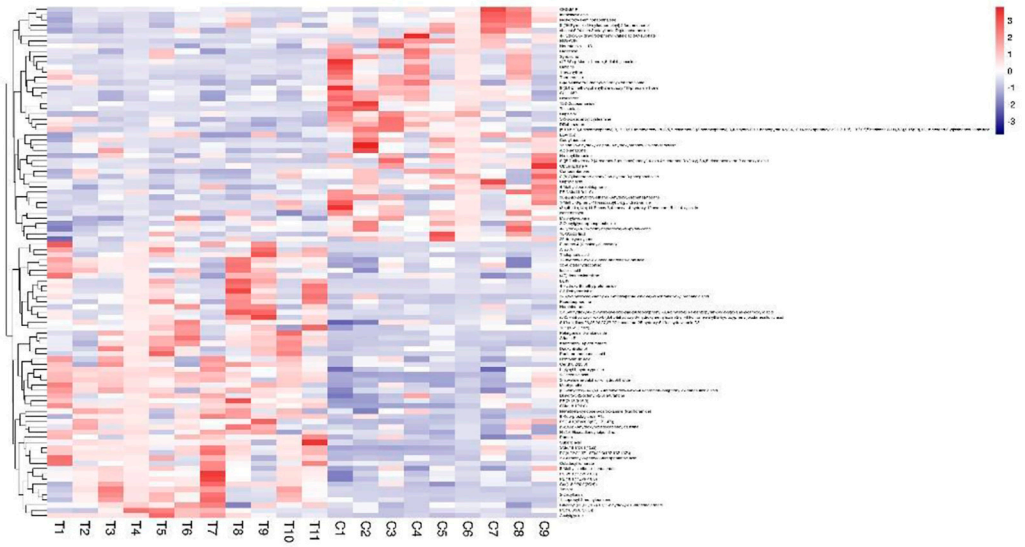

FIGURE 12
Hotspot chart of metabolomics differential metabolites in clinical trials.

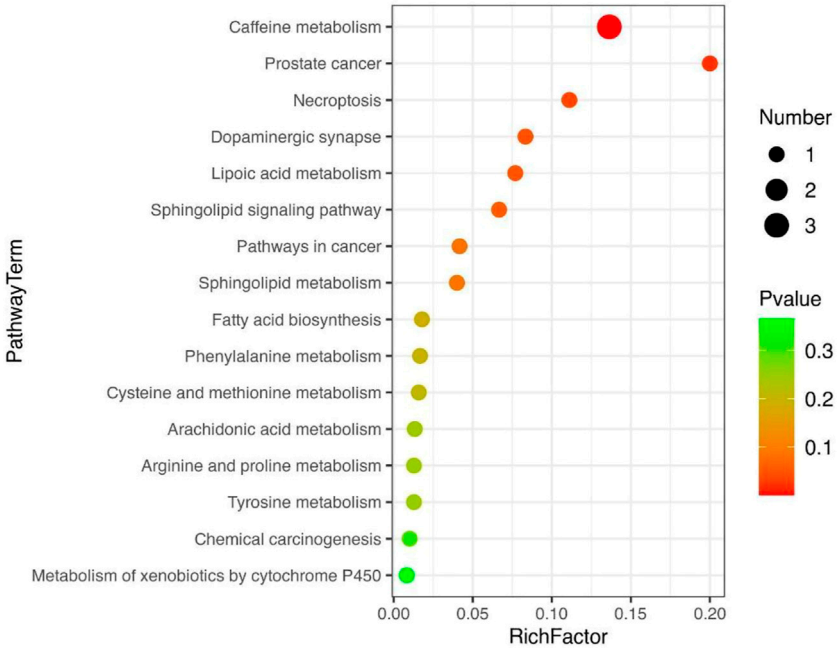

FIGURE 13
Bubble diagram of KEGG enrichment analysis for metabolomics of clinical trials.

Discussion

Modern medical research indicates that the human body is an organism with a complex network. Cardiovascular and cerebrovascular diseases, cancer, tumors and other chronic diseases are not driven by a single cause. Only by analyzing a variety of signal transduction pathways of diseases can achieve a final ideal therapeutic effect. TCM compound preparations are

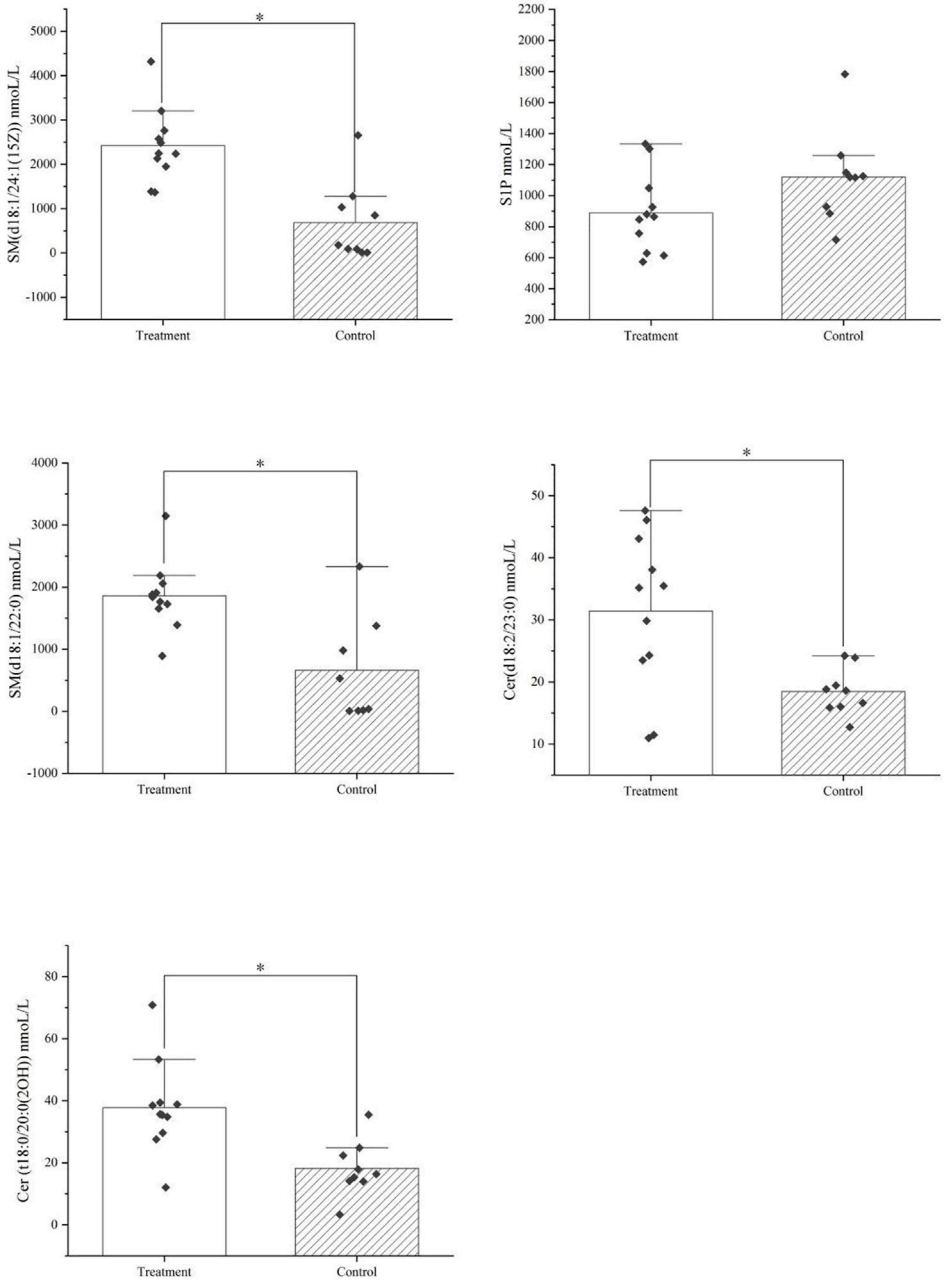

FIGURE 14
The key metabolites of the sphingolipid signaling pathway (hsa04071) after treatment with HXQR.

widely used in clinical practice, with significant effect, and play an important role in disease prevention and treatment. However, how to deeply elucidate the complex chemical system and mechanism of action of TCM from the molecular level and establish a complete system including active ingredients and targets has become the focus and difficulty of modernization research of TCM. Network pharmacology provides a new method and reference for the study of TCM, which is consistent with the overall mechanism of action of TCM "multiple components and multiple targets" and has received the attention and favor of the majority of researchers. However, from our group's analysis of numerous studies related to network pharmacology, we can conclude that the following problems may need to be solved in current network pharmacology research.

It is unreasonable to evaluate chemical compositions with only DL and OB values, and sometimes the conclusions drawn

are unscientific or even incorrect. Network pharmacology generally uses OB ≥30% and DL ≥0.18 as conditions to evaluate active ingredients, ignoring some components with unqualified OB values or/and DL values such as tanshinones, ginsenosides, notoginsenosides, puerarin, verbascoside, and echinacoside that play a major role. Therefore, it would be helpful to perform a comprehensive analysis that fully considers the possible active ingredients recorded in the Chinese Pharmacopoeia and authoritative studies while using DL and OB values. In the current study, the project team adopted OB ≥30% and DL ≥0.18, and evaluated the active ingredients in HXQR in combination with the active ingredients indicated in the Chinese Pharmacopoeia.

There is still a space for improvement in the TCMSP and analysis platform. At present, the active ingredients and targets of some commonly used TCMs are missing, resulting in serious biases in the results and conclusions. For example, it is debatable that most of the network pharmacology literature will now conclude that β-sitosterol is the active ingredient. β-Sitosterol is widely presented in nature, and confers a variety of pharmacological effects, but the network pharmacological research literature that has used β-sitosterol as an active ingredient is worth pondering. The TCMSP database currently lacks commonly used active ingredients, and contains information errors and other circumstances that require continuous improvement by researchers for optimal and rational use.

Network pharmacological results need to undergo a series of validations to draw scientific conclusions. In this study, 151 active ingredients and 286 targets of HXQR in the treatment of CHD were obtained by network pharmacology research technology, and 81 common targets were obtained by mapping the active ingredient targets of HXQR with CHD targets. KEGG pathway enrichment analysis showed that 105 pathways were related to them, 32 pathways were obtained by analyzing with $p < 0.05$, and the number of genes was greater than or equal to 10. In terms of compounds, quercetin (MOL000098), puerarin (MOL012297), luteolin (MOL000006), kaempferol (MOL000422), tanshinone iia (MOL007154), and baicalein (MOL002714) were associated with multiple targets and may be the main active components of HXQR decoction in the treatment of CHD. *In vitro* and *in vivo* experiments have also confirmed that quercetin has the effects of antihypertensive, regulating blood lipid, lowering blood pressure, anti-atherosclerosis and inhibiting cardiotoxicity (Papakyriakopoulou et al., 2022). Kaempferol flavonoid compounds have antioxidant and antiplatelet potential and can improve cardiovascular disease by improving oxidative stress (Olas, 2020). Puerarin, as a natural isoflavone, has been developed into a variety of injectable dosage forms for widespread use. It can be used for a variety of diseases such as atherosclerosis, cardiac hypertrophy, heart failure, myocardial infarction and hypertension and other diseases (Zhou et al., 2021). Luteolin has antioxidant and anti-inflammatory effects, and has protective effects in various diseases such as ischemia/reperfusion (I/R) injury, heart failure (HF) and atherosclerosis (AS) and can inhibit apoptosis (Xu et al., 2012; Luo et al., 2017). Tanshinone iia is well studied, also has dosage forms such as injections, has anti-inflammatory and antioxidant activities, and can induce significant cardioprotection by enhancing angiogenesis (Guo et al., 2020). Baicalein can intervene signaling molecules and protect cardiomyocytes from ischemia/hypoxia injury by acting on PI3K/Akt, MAPKs, and NF-κB/p65 signaling pathways (He et al., 2015). The data from the above studies also indicate the intervention effect of the main active ingredients on cardiovascular disease and also provide support for docking.

Metabolomics of clinical trials of HXQR for the treatment of CHD showed that the differential metabolites were identified by VIP value of the first principal component of the OPLS-DA model >0.1 and p-value value of t-test < 0.05, with only 98 differential metabolites, which were enriched for metabolic pathways and could correspond to 16 pathways. In comparing these 16 clinically proven effective pathways with the network pharmacology prediction results, only three pathways were found to be identical, which may be related to the small sample size in this study. This result demonstrated that HXQR played a role in the treatment of CHD through three signaling pathways: the cancer pathway (hsa05200), the sphingolipid signaling pathway (hsa04071), and the prostate cancer pathway (hsa05215). However, we found that these three signaling pathways only had cancer pathway (hsa05200) in the top 32 predicted pathways, and prostate cancer pathway (hsa05215) and sphingolipid signaling pathway (hsa04071) in the 36th and 60th of the KEGG prediction results of network pharmacology, respectively, which also indicated that the unvalidated network pharmacology results may be severely biased and must be subject to the large sample size and strict scientific validation before arriving at any scientific conclusions.

SM is mainly located on the cell membrane, lipoproteins (especially LDL), and other lipid-rich tissue structures, which is very important for maintaining the micro-control function of the cell membrane structure so that it can regulate the activity of growth factor receptors and extracellular matrix proteins. Its degradation and anabolic intermediates are known as sphingomyelins, which have the effect of regulating cell biological functions (Cirillo et al., 2021). The metabolites of SM include ceramide (Cer) and sphingosine-1-phosphate (S1P), of which Cer is a central molecule in sphingomyelin metabolism, and its biological functions mainly include inducing apoptosis, and the regulation of cell differentiation, cellular immunity, and inflammatory responses. In this process, sphingomyelinase (SMase) is the key enzyme regulating SM

metabolism, which can decompose SM to produce Cer and phosphorylcholine. Cer is cleaved to sphingosine (Sph) by ceramidase (CDase), and phosphatidylcholine generates S1P by sphingosine kinase (SphK), which then activates the downstream MAPK, BAX/BCL-2, and PI3K/AKT signaling pathways involved in the regulation of cell proliferation and apoptosis (Nishino et al., 2019; Cirillo et al., 2021; Green et al., 2021). The current study showed that higher plasma levels of Cer-16 and SM-16 were associated with increased risk of heart failure, and higher levels of Cer-22, SM-20, SM-22, and SM-24 with decreased risk of heart failure (Lemaitre et al., 2019; Fretts et al., 2021). Plasma S1P and sphingomyelin levels were significantly negatively correlated with the left ventricular ejection fraction and the severity of dyspnea (Polzin et al., 2017; Deshpande et al., 2018). This also demonstrates the consistency of the clinical trial evaluation with the network pharmacological analysis.

Conclusion

Through network analysis and metabolomic evaluation, there may be three signaling pathways that involve the Huoxue Qingre decoction in the treatment of CHD: pathways in cancer (hsa05200), sphingolipid signaling pathway (hsa04071), and prostate cancer pathway (hsa05215). Network pharmacology provides a method reference for the study of modernization of TCM. However, it is necessary to recognize the existing problems of network pharmacology and adopt a reasonable method to solve these problems in order to draw possible and correct conclusions.

Data availability statement

The datasets presented in this study can be found in online repositories. The names of the repository/repositories and accession number(s) can be found in the article/ Supplementary Material.

Ethics statement

The studies involving human participants were reviewed and approved by Guang'anmen Hospital, China Academy of Chinese Medical Sciences. The patients/participants provided their written informed consent to participate in this study.

Author contributions

Y-QT: Methodology, Investigation, Formal analysis, Writing – original draft, Writing – review and editing. MJ: Conceptualization. X-HH: Methodology, Investigation. H-WC: Conceptualization, Supervision, Writing, Funding acquisition. All of the authors read and approved the submitted version.

Funding

This study was supported by the China Academy of Chinese Medical Sciences Innovation Fund-Major research project (CI 2021A05011; CI 2021A04619; CI 2021B017-05); and the National Natural Science Foundation of China (No. 82074396).

Acknowledgments

We thank LetPub (www.letpub.com) for its linguistic assistance during the preparation of this manuscript.

Conflict of interest

The reviewer HW declared a shared parent affiliation with the authors to the handling editor at the time of the review. The authors declare that the research was conducted in the absence of any commercial or financial relationships that could be construed as a potential conflict of interest.

Publisher's note

All claims expressed in this article are solely those of the authors and do not necessarily represent those of their affiliated organizations, or those of the publisher, the editors and the reviewers. Any product that may be evaluated in this article, or claim that may be made by its manufacturer, is not guaranteed or endorsed by the publisher.

Supplementary material

The Supplementary Material for this article can be found online at: https://www.frontiersin.org/articles/10.3389/fphar.2022.1025540/full#supplementary-material

References

Benjamin, E. J., Blaha, M. J., Chiuve, S. E., Cushman, M., Das, S. R., Deo, R., et al. (2017). Heart disease and stroke statistics-2017 update: A report from the American heart association. *Circulation* 135 (10), e146–e603. doi:10.1161/CIR.0000000000000485

Chen, H. W., Dong, Y., He, X., Li, J., and Wang, J. (2018). Paeoniflorin improves cardiac function and decreases adverse postinfarction left ventricular remodeling in a rat model of acute myocardial infarction. *Drug Des. Dev. Ther.* 12, 823–836. doi:10.2147/DDDT.S163405

Chen, H. W., Li, J., Lin, F., Li, J. P., and Wang, J. (2017). Effect of xuanbi antong formula in improving ventricular remodeling in myocardial infarction rats and its mechanism. *Chin. J. Exp. Tradit. Med. Form.* 23 (23), 71–78. doi:10.13422/j.cnki.syfjx.2017230071

Chen, H. W., Zhang, C. Y., Ren, W. G., Wang, J., and Wei, B. J. (2016). Multi-index integrated evaluation method optimizes water-extraction and ethanol precipitation of Xuanbi'antong formula (XBF). *Chin. J. Chin. Mat. Med.* 41, 70–74. doi:10.4268/cjcmm20160114

China Association of Chinese Medicine Cardiovascular Disease Branch (CACMDB) (2019). Guideline for diagnosis and treatment of Chinese medicine in stable angina coronary artery disease. *J. Tradit. Chin. Med.* 60 (21), 1880–1890. doi:10.13288/j.11-2166/r.2019.21.015

Cirillo, F., Piccoli, M., Ghiroldi, A., Monasky, M. M., Rota, P., La Rocca, P., et al. (2021). The antithetic role of ceramide and sphingosine-1-phosphate in cardiac dysfunction. *J. Cell. Physiol.* 236 (7), 4857–4873. doi:10.1002/jcp.30235

Deshpande, G. P., Imamdin, A., Lecour, S., and Opie, L. H. (2018). Sphingosine-1-phosphate (s1p) activates stat3 to protect against de novo acute heart failure (ahf). *Life Sci.* 196, 127–132. doi:10.1016/j.lfs.2018.01.023

Fretts, A. M., Jensen, P. N., Hoofnagle, A. N., McKnight, B., Sitlani, C. M., Siscovick, D. S., et al. (2021). Circulating ceramides and sphingomyelins and risk of mortality: The cardiovascular health study. *Clin. Chem.* 67 (12), 1650–1659. doi:10.1093/clinchem/hvab182

Fujisaka, S., Avila-Pacheco, J., Soto, M., Kostic, A., Dreyfuss, J. M., Pan, H., et al. (2018). Diet, genetics, and the gut microbiome drive dynamic changes in plasma metabolites. *Cell Rep.* 22 (11), 3072–3086. doi:10.1016/j.celrep.2018.02.060

Green, C. D., Maceyka, M., Cowart, L. A., and Spiegel, S. (2021). Sphingolipids in metabolic disease: The good, the bad, and the unknown. *Cell Metab.* 33 (7), 1293–1306. doi:10.1016/j.cmet.2021.06.006

Guo, R., Li, L., Su, J., Li, S., Duncan, S. E., Liu, Z., et al. (2020). Pharmacological activity and mechanism of tanshinone IIA in related diseases. *Drug Des. devel. Ther.* 14, 4735–4748. doi:10.2147/DDDT.S266911

He, X., Hao, C., and Li, Z. (2015). Advances in study on baicalein for regulation of signaling pathways in myocardial ischemia/hypoxia. *Chin. Tradit. Herb. Drugs.* 46 (11), 1685–1691. doi:10.7501/j.issn.0253-2670.2015.11.024

Hu, S. S., Gao, R. L., Liu, L. S., Zhu, M. L., Wang, W., and Wang, Y. J. (2019). Summary of the 2018 report on cardiovascular diseases in China. *Chin. Circ. J.* 34 (03), 209–220. doi:10.3969/j.issn.1000-3614.2019.03.001

Huang, M. Y. (2019). Clinical study on xuanbi antong formula in treatment of coronary borderline lesions with phlegm, blood stasis and heat syndrome. *Chin. Acad. Chin. Med. Sci.*, 1–73. Master's thesis.

Lemaitre, R. N., Jensen, P. N., Hoofnagle, A., Mcknight, B., Fretts, A. M., King, I. B., et al. (2019). Plasma ceramides and sphingomyelins in relation to heart failure risk: The cardiovascular health study. *Circ. Heart Fail.* 12 (7), e005708. doi:10.1161/CIRCHEARTFAILURE.118.005708

Luo, Y., Shang, P., and Li, D. (2017). Luteolin: A flavonoid that has multiple cardio-protective effects and its molecular mechanisms. *Front. Pharmacol.* 8, 692. doi:10.3389/fphar.2017.00692

Nishino, S., Yamashita, H., Tamori, M., Mashimo, M., Yamagata, K., Nakamura, H., et al. (2019). Translocation and activation of sphingosine kinase 1 by ceramide-1-phosphate. *J. Cell. Biochem.* 120 (4), 5396–5408. doi:10.1002/jcb.27818

Olas, B. (2020). Honey and its phenolic compounds as an effective natural medicine for cardiovascular diseases in humans? *Nutrients* 12 (2), 283. doi:10.3390/nu12020283

Papakyriakopoulou, P., Velidakis, N., Khattab, E., Valsami, G., Korakianitis, I., and Kadoglou, N. P. (2022). Potential pharmaceutical applications of quercetin in cardiovascular diseases. *Pharm. (Basel, Switz.* 15 (8), 1019. doi:10.3390/ph15081019

Polzin, A., Piayda, K., Keul, P., Dannenberg, L., Mohring, A., Gräler, M., et al. (2017). Plasma sphingosine-1-phosphate concentrations are associated with systolic heart failure in patients with ischemic heart disease. *J. Mol. Cell. Cardiol.* 110, 35–37. doi:10.1016/j.yjmcc.2017.07.004

Wang, L. H., He, X. H., Ma, T., Tian, P. P., Li, J., and Chen, H. W. (2019). Optimization of water extraction and alcohol precipitation process and improvement of cardiac function in rats with myocardial infarction (stasis-heat syndrome) for GCRF formula. *Chin. J. New Drug.* 28 (07), 862–870.

Xie, J., Gao, S., Li, L., Xu, Y. L., Gao, S. M., and Yu, C. Q. (2019). Research progress and application strategy on network pharmacology in Chinese materia medica. *Chin. Tradit. Herb. Drug.* 50 (10), 2257–2265. doi:10.7501/j.issn.0253-2670.2019.10.001

Xu, T., Li, D., and Jiang, D. (2012). Targeting cell signaling and apoptotic pathways by luteolin: Cardioprotective role in rat cardiomyocytes following ischemia/reperfusion. *Nutrients* 4 (12), 2008–2019. doi:10.3390/nu4122008

Zhang, R., Zhu, X., Bai, H., and Ning, K. (2019). Network pharmacology databases for traditional Chinese medicine: Review and assessment. *Front. Pharmacol.* 10, 123. doi:10.3389/fphar.2019.00123

Zhang, Y. Q., and Li, S. (2015). Progress in network pharmacology for modern research of traditional Chinese medicine. *Chin. J. Pharmacol. Toxicol.* 29 (06), 883–892. doi:10.3867/j.issn.1000-3002.2015.06.002

Zhou, Y. X., Zhang, H., and Peng, C. (2021). Effects of puerarin on the prevention and treatment of cardiovascular diseases. *Front. Pharmacol.* 12, 771793. doi:10.3389/fphar.2021.771793

frontiers | Frontiers in Pharmacology

TYPE Systematic Review
PUBLISHED 14 November 2022
DOI 10.3389/fphar.2022.1002713

Check for updates

OPEN ACCESS

EDITED BY
Qing Yong He,
Guang'anmen Hospital, China Academy of Chinese Medical Sciences, China

REVIEWED BY
Jianbo Guo,
The University of Hong Kong, Hong Kong SAR, China
Yu-Qing Zhang,
McMaster University, Canada
Tiantian Meng,
Guang'anmen Hospital, China Academy of Chinese Medical Sciences, China

*CORRESPONDENCE
Mingjun Zhu,
zhumingjun317@163.com
Yongxia Wang,
wyxchzhq@163.com

†These authors have contributed equally to this work

SPECIALTY SECTION
This article was submitted to Ethnopharmacology, a section of the journal Frontiers in Pharmacology

RECEIVED 25 July 2022
ACCEPTED 31 October 2022
PUBLISHED 14 November 2022

CITATION
Wei J, Ma T, Zhou C, Hao P, Li B, Wang X, Yu R, Zhu M and Wang Y (2022), Efficacy and safety of Shexiang Baoxin Pill for stable coronary artery disease: A systematic review and meta-analysis of 42 randomized controlled trials. *Front. Pharmacol.* 13:1002713. doi: 10.3389/fphar.2022.1002713

COPYRIGHT
© 2022 Wei, Ma, Zhou, Hao, Li, Wang, Yu, Zhu and Wang. This is an open-access article distributed under the terms of the Creative Commons Attribution License (CC BY). The use, distribution or reproduction in other forums is permitted, provided the original author(s) and the copyright owner(s) are credited and that the original publication in this journal is cited, in accordance with accepted academic practice. No use, distribution or reproduction is permitted which does not comply with these terms.

Efficacy and safety of Shexiang Baoxin Pill for stable coronary artery disease: A systematic review and meta-analysis of 42 randomized controlled trials

Jingjing Wei[1,2†], Teng Ma[3†], Cheng Zhou[1†], Pengle Hao[1], Bin Li[2], Xinlu Wang[2], Rui Yu[2], Mingjun Zhu[2*] and Yongxia Wang[2*]

[1]The First Affiliated Hospital of Henan University of Chinese Medicine, Zhengzhou, Henan, China, [2]Department of Cardiovascular Diseases, The First Affiliated Hospital of Henan University of Chinese Medicine, Zhengzhou, Henan, China, [3]Second Teaching Hospital of Tianjin University of Traditional Chinese Medicine, Tianjin, China

Objective: Patients with stable coronary artery disease (SCAD) still have a higher risk of adverse cardiovascular events. Shexiang Baoxin Pill (SBP) is widely used as a complementary and alternative treatment for SCAD. This study aimed to further verify the therapeutic effect and safety of SBP on SCAD.

Methods: Seven databases were involved in this meta-analysis as of 1 June 2022. Data was collected from all the randomized controlled trials (RCTs) of the combination of SBP and conventional western medicine (CWM) in treating SCAD which was conducted by two independent authors. Risk of bias was assessed using the Cochrane risk-of-bias 2.0 (RoB2.0) tool, and the meta-analysis was accomplished with Review Manager 5.3. Furthermore, the Grading of Recommendations Assessment, Development and Evaluation (GRADE) profiler 3.2.2 software was selected to grade the current evidence in our findings.

Results: 42 articles, involving 6,694 patients were screened among all the 1,374 records in the analysis. The results demonstrated that the combination therapy was more efficient than CWM alone in lowering the incidence of major adverse cardiovascular events (MACE, RR = 0.50, 95% CI: 0.37 to 0.68, $p < 0.00001$) and ameliorating the total effective rate of angina symptom improvement (RR = 1.23, 95% CI: 1.19 to 1.28, $p < 0.00001$), the effective rate of electrocardiogram improvement (RR = 1.34, 95% CI: 1.26 to 1.43, $p < 0.00001$), the frequency of angina pectoris (MD = −2.83, 95% CI: −3.62 to −2.05, $p < 0.00001$), and the duration of angina pectoris (MD = −1.32, 95% CI: −2.04 to −0.61, $p = 0.0003$). We also found that, after SBP treatment, a more positive blood lipid level and left ventricular ejection fraction without the increase in adverse cases were calculated in our meta-analysis. What's more, Subgroup analysis indicated that treatment duration may be the source of heterogeneity. The certainty of the evidence for MACE, and electrocardiogram improvement exhibited moderate certainty, and the certainty of the evidence for the remaining outcomes was judged as low certainty. The trial sequential analysis further affirmed the clinical efficacy of SBP.

Conclusion: The available evidence indicates that SBP may be an effective therapeutic option in patients with SCAD. However, considering the inferior quality and inconsistent results in the included trials, further rigorous RCTs are required.

Systematic Review Registration: https://www.crd.york.ac.uk/prospero, identifier [CRD42022334529].

KEYWORDS

Shexiang Baoxin Pill, stable coronary artery disease, randomized controlled trials, meta-analysis, grade

1 Introduction

Stable coronary artery disease (SCAD) is the most common type of coronary heart disease (CHD), mainly including stable angina pectoris, stable phase after acute coronary syndrome, and ischemic cardiomyopathy (Montalescot et al., 2013). A report from the American Heart Association (AHA) in 2016 showed that the incidence of SCAD is much higher than that of myocardial infarction, which is twice as high as that of myocardial infarction and is expected to reach 18% of the adult population by 2030 (Mozaffarian et al., 2016). Notably, SCAD can remain stable for a long time or can become unstable at any time due to plaque rupture or erosion leading to acute coronary events. Currently, aspirin and statins are the standard secondary prevention approach in reducing the risk of cardiovascular events in patients with SCAD. However, patients who receive secondary prevention still have a 4%–12% risk of major adverse cardiovascular events (MACE), and there is still a considerable residual cardiovascular risk (Bhatt et al., 2010; Feres et al., 2013). How to further reduce the risk of recurrent cardiovascular events in SCAD remains a hot spot and a challenge for current research.

In recent years, with the increasing clinical evidence of traditional Chinese medicine (TCM) for the treatment of CHD, TCM may become a supplementary and alternative medicine for the primary and secondary prevention of patients with SCAD (Liang and Gu, 2021). Shexiang Baoxin Pill (SBP) is currently one of the most commonly used aromatic medicines for the treatment of cardiovascular diseases in China, which has been widely used to relieve and prevent angina-related symptoms since its marketing in 1981 (Guo et al., 2021; Wei et al., 2021). SBP is a Chinese medicine compound prescription composed of Moschus (the dried preputial secretion of *Moschus berezovskii, M. sifanicus or M. moschiferus*), Radix Ginseng (*Panax ginseng C.A.Mey.*), Bovis Calculus Artifactus (the dried gall-stone of *Bos taurus domesticus Gmelin*), Cinnamomi Cortex (*Cinnamomum cassia*), Styrax (*Liquidambar orientalis Mill.*), Bufonis Venenum (*Bufo gargarizans*), and Borneolum Syntheticum (*Dryobalanops aromatica C.F.Gaertn.*) (Supplementary Material S1). It has been recommended for the treatment of CHD by the "Guidelines for TCM diagnosis and treatment of stable angina pectoris of coronary heart disease" (China Association of Chinese Medicine Cardiovascular Disease Branch, 2019). Network pharmacology analysis found that SBP and its plasma absorption compounds can dilate blood vessels by upregulating cyclooxygenase-2 and downregulating intercellular adhesion molecule-1 (Fang et al., 2017). Pharmacological studies have shown that SBP has a protective effect on damaged vascular endothelial cells, and can inhibit inflammation of the vascular wall and stabilize atherosclerotic plaques during the atherosclerotic process (Lu et al., 2019; Zhang et al., 2020). Recent studies have found that SBP can affect the endothelial cell signaling pathway to promote the expression of therapeutic angiogenesis-related genes, and it is speculated that this mechanism may be related to the compounds such as ginsenosides and cinnamaldehyde contained in it (Hu et al., 2021). A previous review evaluated the relevant randomized Controlled Trials (RCTs) before December 2017 and showed the efficacy and safety of SBP in the treatment of stable angina (Pan et al., 2019). A subsequent review reported that SBP combined with conventional therapy can improve coronary microvascular function (Wang et al., 2021). In recent years, several research trials have focused on the clinical efficacy and safety of SBP as an additional treatment for SCAD (Wang, 2016; Peng et al., 2017). In particular, a multicenter, double-blind, placebo-controlled phase IV randomized clinical trial in 2021 reaffirmed the clinical value of SBP in patients with SCAD (Ge et al., 2020). Regrettably, there are no relevant systematic reviews to summarize the efficacy and safety of SBP in the treatment of SCAD in terms of both methodological quality and quality of evidence.

Therefore, we conducted a systematic review and meta-analysis based on the available evidence to strictly evaluate the efficacy and safety of SBP for SCAD, and to clarify the strength of the evidence for SBP, to better guide clinical application.

2 Methods

2.1 Program and registration

This report adhered to the Preferred Reporting Items for Systematic Reviews and Meta-Analyses 2020 statement (Page et al., 2021) (Supplementary Material S2). We have already

registered our protocol on the PROSPERO (number: CRD42022334529).

2.2 Search strategy

Two investigators independently searched the databases including PubMed, The Cochrane Library, Web of Science, China National Knowledge Infrastructure (CNKI), China Science and Technology Journal Database (VIP), WanFang Database, and SinoMed from inception until 1 June 2022. The method for searching was based on subject headings combined with free words. In addition, we also manually retrieved the reference lists of published literature to search for other relevant studies. Unpublished literature was identified by searching the websites of national and international medical specialty societies, clinical trial registration platforms, and clinical practice guideline collections. The search strategies were formulated by physicians (MZ and YW), and statisticians (BL and XW). We have provided detailed search strategies in Supplementary Material S3.

2.3 Inclusion and exclusion criteria

2.3.1 Types of research

Only RCTs of SBP for patients with SCAD were included and not restricted by language or publication type.

2.3.2 Types of participants

All subjects (age ≥18 years) of the included study meet the diagnostic criteria for SCAD established by the AHA, the European Society of Cardiology, or the Chinese Medical Association (Fihn et al., 2012; Montalescot et al., 2013; Interventional Cardiology Group of Cardiovascular Branch of Chinese Medical Association., 2018). No restrictions were made regarding gender, country, or race.

2.3.3 Types of interventions

The experimental group and control group were both treated with antiplatelet drugs, lipid-lowering drugs, vasodilators of nitrate, and other conventional western medicine (CWM) recommended by the guideline (Interventional Cardiology Group of Cardiovascular Branch of Chinese Medical Association., 2018). The experimental group was added with SBP (produced by Shanghai Hutchison Pharmaceuticals Co., Ltd.) for adjuvant therapy.

2.3.4 Types of outcomes

The primary outcomes are as follows: 1) MACE including cardiovascular death, nonfatal myocardial infarction, and nonfatal stroke; 2) the total effective rate of angina symptom improvement (significant effectiveness: symptom basically disappeared, and the number of angina attacks decreased by at least 80%; effective: symptom improved significantly, and the number of angina attacks decreased by 50%–80%; inefficacy: no significant improvement in symptom, less than 50% reduction in the number of angina attacks) (according to "Guiding Principles for Clinical Research of New Chinese Medicines") (Ministry of health of the people's republic of China, 2002); 3) electrocardiogram (ECG) improvement (significant effectiveness: ECG returned to the normal range; effective: ST segment was reduced, and after treatment, it rose above 0.05 mV but did not reach the normal level, or the T wave changed from a flat state to an upright state; inefficacy: the ECG had no significant changes compared to before treatment; worsening of disease: the ST segment was reduced by more than 0.05 mV after treatment; the T wave state was completely changed, and ectopic heart rate occurred); 4) adverse events (AEs) including clinical symptoms, signs, laboratory abnormalities.

The secondary outcomes are as follows: 1) angina pectoris frequency: in the unit of times/week; 2) angina pectoris duration: in the unit of min/time; 3) left ventricular ejection fraction (LVEF); 4) blood lipid level including total cholesterol (TC), triglyceride (TG), low-density lipoprotein cholesterol (LDL-C), and high-density lipoprotein cholesterol (HDL-C).

2.3.5 Exclusion criteria

The exclusion criteria were as follows: 1) duplicate published literature; 2) the included studies did not report the outcomes of interest of this systematic review; 3) the baseline information of patients was inconsistent; 4) intervention measures combined with other TCM.

2.4 Literature screening and data extraction

The literature retrieved from each database is imported into Endnote software for deduplication, and two researchers screen the literature according to the inclusion and exclusion criteria, extract the information, and recheck each other's work. If there is any disagreement, the third researcher will be invited to discuss and make a decision. Data were extracted using a standardized data extraction form to extract information including first author, year of publication, sample size, gender, age, disease condition, intervention measures, treatment duration, and outcome indicators.

2.5 Risk of bias assessment

Two reviewers independently assessed the risk of bias in the RCTs using the Cochrane risk-of-bias 2.0 (RoB2.0) tool (Liu et al., 2019). The assessment of ROB includes the following five domains: 1) bias arising from the randomization process; 2) bias due to deviations from intended interventions; 3) bias due to

missing outcome data; 4) bias in the measurement of the outcome; 5) bias in the selection of the reported result. Finally, a judgment of the overall risk of bias is generated. The ROB was judged as "low", "high", or "some concerns". Disagreements between the two researchers were resolved through consultation with a third researcher.

2.6 Data analysis

The software Review Manager 5.3 is used for statistical analysis. Cochran's Q and I^2 are chosen to test for heterogeneity, and if there is statistical heterogeneity among the findings ($I^2 \geq 50\%$, $p < 0.10$), a random-effects model will be selected, and conversely, a fixed-effects model will be used. Binary variables were analyzed using relative risk (RR) as the pooled statistic, and continuous variables were analyzed using weighted mean difference (MD) as the pooled statistic, both of which describe the 95% confidence interval (CI). Meta-regression will be performed to find the reasons for heterogeneity, such as publication year, age, course of treatment, and sample size. Further, the statistically significant factors obtained by meta-regression will be used as grouping indicators for subgroup analysis. Sensitivity analyses were performed by omitting each study at a time to assess the consistency and stability of the pooled results. In addition, we examined potential publication bias using Egger's test method. Finally, the TSA 0.9.5.10 Beta software was used to perform TSA analysis on the associated results.

2.7 Assessing the certainty of evidence

The Grading Recommendations Assessment, Development, and Evaluation (GRADE) technique was used to assess the certainty of the evidence (Goldet and Howick, 2013) following the instructions of the website (https://training.cochrane.org/handbook/current/chapter-14/). RCT evidence is initially classified as high quality, but it can be downgraded due to the risk of bias, inconsistency, indirectness, imprecision, and publication bias. The level of evidence is classified into four categories: "high," "moderate," "low," and "very low".

3 Results

3.1 Literature search results

The flowchart of search results is shown in Figure 1 according to the PRISMA study. We included 1,374 records from seven electronic databases. After duplicate studies were removed, we screened 528 titles and abstracts and finally obtained 65 full-text articles. Among them, 23 studies were excluded, of which 12 studies were not RCTs, two studies were inconsistent interventions, five studies did not match the research purpose and outcomes, and four studies were published repeatedly. Supplementary Material S4 contains a list of studies that were excluded by reading the full text. Eventually, 42 eligible studies are included (Sun, 2010; Xu et al., 2010; Shi and Hang, 2011; Guo and Tan, 2012; Jiang, 2012; Wu et al., 2012; Sun, 2013; Yang et al., 2013; Zou et al., 2013; Chen, 2014; Huang et al., 2014; Liu, 2014; Wang, 2014; Zhao, 2014; Hou, 2015; Ji, 2015; Tan, 2015; Wang et al., 2015; Ding, 2016; Miao et al., 2016; Pan, 2016; Wang, 2016; Xia, 2016; Peng et al., 2017; Liu, 2018; Lv, 2018; Wang, 2018; Wang et al., 2018; Zhao, 2018; Zhao et al., 2018; Liao and Huang, 2019; Chen and Chen, 2020; Ge et al., 2020; Wang ang Zhu, 2020; Gao and Chen, 2021; Xia et al., 2021; Xie and Huang, 2021; Zhao and Xie, 2021; Zhou, 2021; Pan et al., 2022; Yang, 2022; Zhao et al., 2022).

3.2 Basic features of literature research

Table 1 shows the basic information of the included studies. All of the trials were double-arm RCTs. All of the studies were operated in China. One study was published in English (Ge et al., 2020), and the others were written in Chinese. A total of 6,694 patients were randomly divided into an SBP group and a control group, including 4,256 men. The mean age of the participants ranged from 51.6 to 81.7 years, who can be defined as middle-aged and elderly patients. Sample sizes range from 30 participants per arm to 1,335 people per arm. In all included studies, the standard type, and dose of CWM in the SBP treatment group were the same as those in the control group. The ingredients of SBP in all studies were the same, and the dosage of SBP in the experimental group was 22.5–67.5 mg three times a day. The shortest intervention period was 2 weeks while the longest was 24 months, and 3 months were the main ones (11/42, 26.19%). Three trials provided specific follow-up after treatment, with a maximum follow-up of 24 months (Peng et al., 2017; Ge et al., 2020) and a minimum follow-up of 6 months (Gao and Chen, 2021). A total of three studies received funding support (Tan, 2015; Ge et al., 2020; Ge et al., 2020; Zhao et al.). All the studies examined the effect of SBP combined with CWM on SCAD, six studies (Yang et al., 2013; Ding, 2016; Peng et al., 2017; Ge et al., 2020; Gao and Chen, 2021; Zhao and Xie, 2021) for MACE, twenty-seven studies (Sun, 2010; Xu et al., 2010; Shi and Hang, 2011; Guo and Tan, 2012; Sun, 2013; Chen, 2014; Huang et al., 2014; Liu, 2014; Wang, 2014; Hou, 2015; Ji, 2015; Tan, 2015; Wang et al., 2015; Ding, 2016; Wang, 2016; Xia, 2016; Liu, 2018; Lv, 2018; Wang et al., 2018; Zhao, 2018; Zhao et al., 2018; Chen and Chen, 2020; Zhu, 2020; Gao and Chen, 2021; Wang ang; Xia et al., 2021; Pan et al., 2022; Zhao et al., 2022) for the total effective rate of angina symptom improvement, sixteen studies (Sun, 2010; Xu et al., 2010;

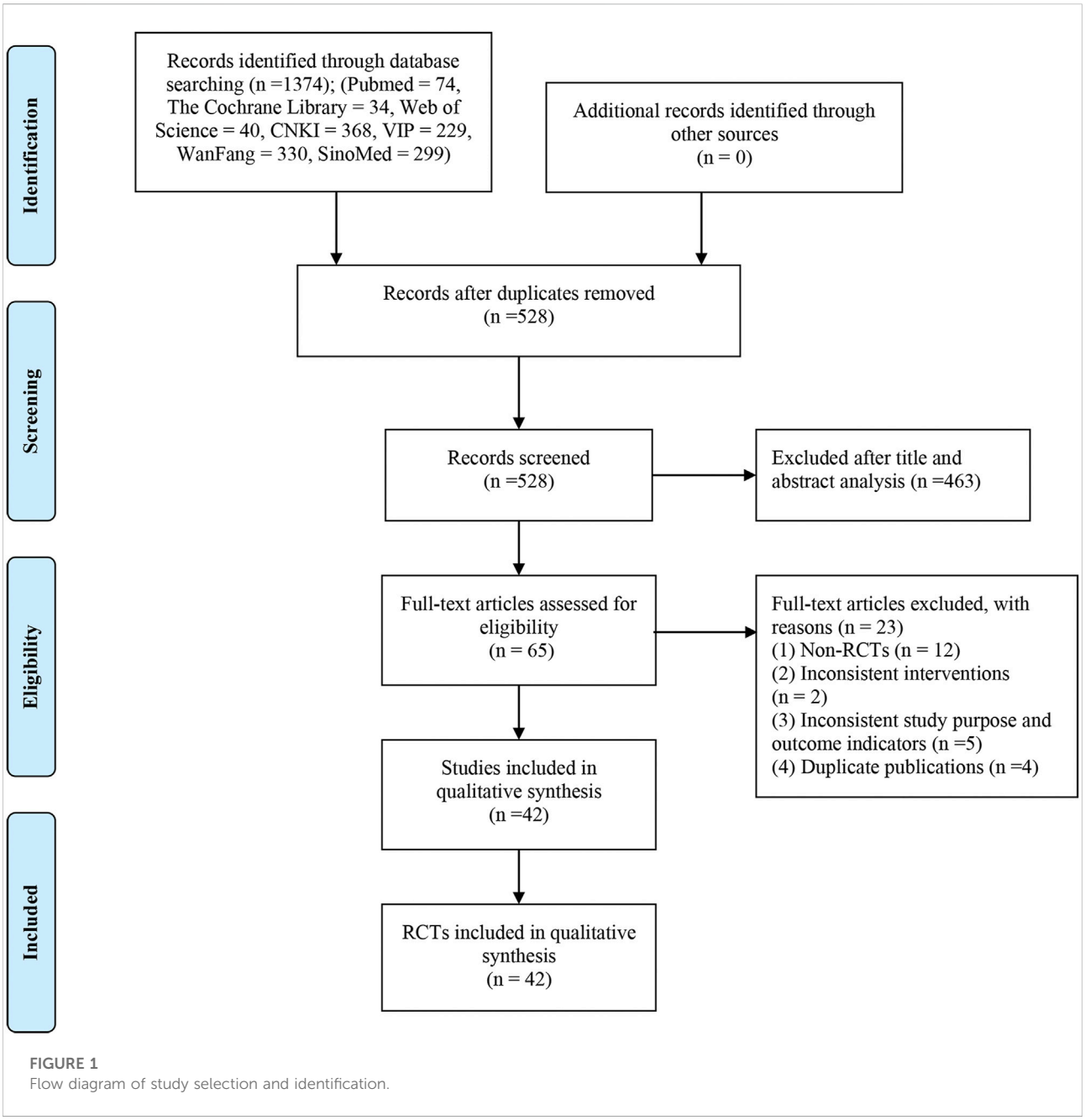

FIGURE 1
Flow diagram of study selection and identification.

Guo and Tan, 2012; Sun, 2013; Liu, 2014; Wang, 2014; Zhao, 2014; Hou, 2015; Ji, 2015; Xia, 2016; Lv, 2018; Wang et al., 2018; Zhao et al., 2018; Wang ang Zhu, 2020; Gao and Chen, 2021; Pan et al., 2022) for ECG improvement, eighteen studies (Xu et al., 2010; Guo and Tan, 2012; Sun, 2013; Zou et al., 2013; Wang, 2014; Chen, 2014; Zhao, 2014; Hou, 2015; Ji, 2015; Pan, 2016; Xia, 2016; Peng et al., 2017; Lv, 2018; Ge et al., 2020; Wang ang Zhu, 2020; Liu, 2018; Gao and Chen, 2021; Zhao and Xie, 2021) for AEs. Supplementary Material S5 provided follow-up times for all outcome measures.

3.3 Literature quality assessment

Supplementary Material S6 shows the risk of bias of the included studies for each outcome from low to high risk. All 42 studies referred to randomization, of which 12 used the random number table (Wang, 2016; Peng et al., 2017; Liu, 2018; Wang, 2018; Liao and Huang, 2019; Chen and Chen, 2020; Wang and Zhu, 2020; Gao and Chen, 2021; Ge, 2021; Xia et al., 2021; Xie and Huang, 2021; Pan et al., 2022), and the remaining 30 studies did not specifically report randomization method.

TABLE 1 Characteristics of the included trials.

Study ID	Sample size	Gender	Age (year)		Angina classification(CCS)	Duration	Interventions		SBP dosage	Outcomes
	(T/C)	(M/F)	T	C			T	C		
Ge et al., 2020	1,335/1,327	1886/776	63.9 ± 9.8	63.7 ± 9.9	I~III	24 months	SBP + CWM	CWM + placebo	45mg, t.i.d	①④
Yang, (2022)	40/40	50/30	71.53 ± 5.06	73.38 ± 5.47	I~IV	3 months	SBP + CWM	CWM	67.5mg, t.i.d	⑤⑥⑦
Zhao et al., 2022	54/54	59/49	62.1 ± 10.4	62.5 ± 10.8	I~III	1 month	SBP + CWM	CWM	45mg, t.i.d	②⑤⑥⑧
Pan et al., 2022	68/65	70/63	74.23 ± 8.47	76.87 ± 7.69	I~IV	1 month	SBP + CWM	CWM	45mg, t.i.d	②③⑤⑧
Zhou, (2021)	35/35	41/29	71.33 ± 11.20	71.23 ± 11.12	NR	2 weeks	SBP + CWM	CWM	67.5mg, t.i.d	⑤⑥
Zhao and Xie, (2021)	75/75	79/71	72.3 ± 11.5	72.4 ± 11.9	I~IV	6 months	SBP + CWM	CWM	45mg, t.i.d	①④
Xie and Huang, (2021)	39/39	43/35	61.38 ± 5.74	61.19 ± 5.62	I~IV	2 months	SBP + CWM	CWM	67.5mg, t.i.d	⑤⑥
Xia et al., 2021	61/61	74/48	65.53 ± 8.67	65.53 ± 8.67	I~III	3 months	SBP + CWM	CWM	67.5mg, t.i.d	②⑤⑥⑧
Gao and Chen, (2021)	78/78	83/73	63 ± 12	63 ± 12	I~IV	3 months	SBP + CWM	CWM	45mg, t.i.d	①②③④
Wang and Zhu, (2020)	40/40	52/28	70.5 ± 9.5	71.2 ± 9.8	I~III	2 weeks	SBP + CWM	CWM	67.5mg, t.i.d	②③④
Chen and Chen, (2020)	44/44	56/32	65.09 ± 7.52	65.33 ± 7.40	I~III	3 months	SBP + CWM	CWM	22.5–45mg, t.i.d	②⑤⑥
Zhao et al., 2018	40/40	41/39	58.80 ± 8.38	56.53 ± 8.93	I~IV	2 months	SBP + CWM	CWM	45mg, t.i.d	②③
Zhao, (2018)	45/45	50/40	55.16 ± 5.83	54.92 ± 5.08	I~III	6 months	SBP + CWM	CWM	45mg, t.i.d	②
Wang et al., 2018	30/30	24/36	55.00 ± 7.53	60.00 ± 4.88	I~IV	6 months	SBP + CWM	CWM	45mg, t.i.d	②③
Liu, (2018)	79/79	85/73	56.4 ± 2.3	56.9 ± 2.4	I~IV	2 months	SBP + CWM	CWM	67.5mg, t.i.d	②④
Peng et al., 2017	60/54	65/49	60.56 ± 3.53	61.65 ± 4.75	I~III	24 months	SBP + CWM	CWM + placebo	45mg, t.i.d	①④⑤
Xia, (2016)	40/40	52/28	61.0 ± 7.5	60.2 ± 8.7	NR	6 months	SBP + CWM	CWM	45mg, t.i.d	②③④
Wang, (2016)	45/45	62/28	65.46 ± 5.53	66.35 ± 6.57	I~IV	12 months	SBP + CWM	CWM	45mg, t.i.d	②⑧
Ding, (2016)	42/42	50/34	59 ± 2.3	60 ± 2.2	I~III	6 months	SBP + CWM	CWM	45mg, t.i.d	①②
Wang et al., 2015	40/40	47/33	68.3 ± 5.2	68.3 ± 5.2	NR	1 month	SBP + CWM	CWM	45mg, t.i.d	②⑤
Tang, (2015)	84/82	92/74	67.54 ± 4.27	67.09 ± 4.45	NR	3 months	SBP + CWM	CWM	45mg, t.i.d	②⑤
Ji, (2015)	34/34	33/35	61.21 ± 9.17	62.23 ± 8.87	I~III	2 months	SBP + CWM	CWM	45mg, t.i.d	②③④⑤⑥
Hou, (2015)	34/34	49/19	71 ± 1.6	72 ± 1.2	I~III	2 months	SBP + CWM	CWM	45mg, t.i.d	②③④
Zhao, (2014)	60/60	66/54	63 ± 8.5	64 ± 4.5	I~IV	6 months	SBP + CWM	CWM	45mg, t.i.d	③④⑧
Wang, (2014)	55/50	61/44	81.7 ± 6.03 (total)		I~IV	3 months	SBP + CWM	CWM	45mg, t.i.d	②③④
Liu, (2014)	30/30	35/25	60.5 (total)		I~IV	3 months	SBP + CWM	CWM	45mg, t.i.d	②③

(Continued on following page)

TABLE 1 (*Continued*) Characteristics of the included trials.

Study ID	Sample size	Gender	Age (year)		Angina classification(CCS)	Duration	Interventions		SBP dosage	Outcomes
	(T/C)	(M/F)	T	C			T	C		
Huang et al., 2014	60/60	71/49	66.31 ± 5.25	66.75 ± 6.25	II~III	1 month	SBP + CWM	CWM	45mg, t.i.d	②
Chen, 2014	45/45	52/38	57.3 ± 2.1	58.1 ± 1.8	I~IV	2 months	SBP + CWM	CWM	45–67.5mg, t.i.d	②④
Zou et al., 2013	54/54	60/48	64.5 ± 9.6 (total)		I~IV	3 months	SBP + CWM	CWM	45mg, t.i.d	④
Yang et al., 2013	45/45	46/44	62.7 ± 10.4	61.4 ± 10.3	I~IV	1 month	SBP + CWM	CWM	45mg, t.i.d	①
Sun, (2013)	56/56	65/57	51.6	51.7	I~IV	2 months	SBP + CWM	CWM	22.5–45mg, t.i.d	②③④
Lv, (2018)	32/32	38/26	56.3 ± 4.9 (total)		I~IV	2 months	SBP + CWM	CWM	45mg, t.i.d	②③④⑧
Guo and Tan, (2012)	58/56	99/15	76.3	74.6	NR	6 weeks	SBP + CWM	CWM	45mg, t.i.d	②③④⑤⑥
Shi and Hang, (2011)	65/62	79/48	56.83 ± 11.89	55.26 ± 11.00	II~III	2 weeks	SBP + CWM	CWM	45mg, t.i.d	②
Xu et al., 2010	42/41	46/37	67.54 ± 4.27	67.09 ± 4.45	I~IV	3 months	SBP + CWM	CWM	45mg, t.i.d	②③④⑤⑦⑧
Sun, (2010)	50/50	73/27	58.5	57.2	NR	3 months	SBP + CWM	CWM	45–67.5mg, t.i.d	②③
Wang, (2018)	51/51	65/37	65.0 ± 6.0	65.3 ± 6.2	NR	2 months	SBP + CWM	CWM	45mg, t.i.d	⑦
Miao et al., 2016	40/38	42/36	67 ± 9	65 ± 12	NR	2 months	SBP + CWM	CWM	45mg, t.i.d	⑦⑧
Liao and Huang (2019)	47/47	61/33	70.67 ± 7.95	71.24 ± 8.13	NR	6 months	SBP + CWM	CWM	45mg, t.i.d	⑦
Pan, (2016)	45/45	50/40	46.4 ± 5.2	43.7 ± 4.5	NR	1 month	SBP + CWM	CWM	45mg, t.i.d	⑦④
Wu et al., 2012	44/44	49/39	64	63	NR	3 months	SBP + CWM	CWM	45mg, t.i.d	⑦
Jiang, (2012)	42/42	55/29	72.6	73.5	NR	6 months	SBP + CWM	CWM	45mg, t.i.d	⑦

T, trial group; C, control group; NR, not report; SBP, shexiang baoxin pill; CWM, the conventional western medicine (antiplatelet drugs, lipid-lowering drugs, vasodilators of nitrate, and other conventional western medicine recommended by the guideline); t. i.d., three times a day; CCS, canadian cardiovascular society; Outcomes: ①major adverse cardiovascular events, ②the total effective rate of angina symptom improvement, ③electrocardiogram improvement, ④adverse events,⑤angina pectoris frequency, ⑥angina pectoris duration, ⑦left ventricular ejection fraction, ⑧blood lipid index.

Only one trial (Ge, 2021) adequately reported allocation concealment details. Three studies (Wang, 2016; Peng et al., 2017; Ge, 2021) reported the use of double-blinding, which was considered a low risk of "bias due to deviations from intended interventions". For the total effective rate of angina symptom improvement, one study (Zhao, 2018) included 90 subjects, but only 88 subjects had outcome data, and no reason was explained, with a high risk of "bias due to miss outcome data". Due to the objectivity of the outcome indicators, some results have no or little room for judgment, and "bias in the selection of the reported result" of LVEF and blood lipid level should be considered "low risk". In addition, we found that one of the studies included in this review (Ge, 2021) had a low risk of "bias in the selection of the reported result" because the methods of outcome measurement and analysis were consistent with the prespecified protocol, whereas the remaining 41 studies did not find pre-specified study protocols and were assessed as "some concerns" of "bias in the selection of the reported result".

3.4 Primary outcome measures

3.4.1 MACE

Six trials with 3,272 patients reported the occurrence of MACE. There was little statistical heterogeneity among the

TABLE 2 Results of subgroup analysis.

Outcome or subgroup	Studies	Participants	MD/RR (95%CI)	*Z*	*P*	Heterogeneity	
						I^2	*P*
1. Adverse Events	18	4,422	0.75 (0.44, 1.25)	1.11	0.27	51%	0.007
Treatment duration							
≤2 months	9	844	0.99 (0.35, 2.83)	0.02	0.98	57%	0.02
3 months	4	452	0.95 (0.41, 2.21)	0.12	0.91	0%	0.48
6 months	3	350	0.26 (0.12, 0.55)	3.54	0.0004	0%	0.53
12 months	2	2,776	1.02 (0.87, 1.20)	0.24	0.81	0%	0.33
2. Angina Pectoris Frequency	13	1,304	−2.83 (−3.62, −2.05)	7.07	<0.00001	99%	<0.00001
Treatment duration							
<2 months	5	505	−2.74 (−2.89, −2.58)	34.84	<0.00001	39%	0.16
2 months	2	146	−0.65 (−0.90, −0.39)	5.00	<0.00001	76%	0.04
3 months	5	539	−1.62 (−2.02, −1.22)	7.95	<0.00001	42%	0.14
24 months	1	114	−20.12 (−21.95, −18.29)	21.49	<0.00001	—	—
3. Angina Pectoris Duration	8	728	−1.32 (−2.04, −0.61)	3.63	0.0003	100%	<0.00001
Treatment duration							
<2 months	3	292	−2.17 (−2.34, −2.00)	24.56	<0.00001	81%	0.005
2 months	2	146	−0.60 (−1.17, −0.03)	2.06	0.04	98%	<0.00001
3 months	3	290	−1.04 (−1.34, −0.73)	6.68	<0.00001	71%	0.03
4. LVEF	8	699	4.88 (3.19, 6.57)	5.66	<0.00001	65%	0.005
Treatment duration							
≤2 months	3	270	5.65 (3.58, 7.72)	5.34	<0.00001	33%	0.22
3 months	3	251	5.59 (3.41, 7.77)	5.03	<0.00001	26%	0.26
6 months	2	178	3.50 (−1.47, 8.47)	1.38	0.17	87%	0.005
5. TC	7	734	−0.59 (−0.78, −0.40)	6.03	<0.00001	82%	<0.00001
Treatment duration							
≤2 months	3	319	−0.63 (−0.98, −0.27)	3.44	0.0006	83%	0.003
3 months	2	205	−0.36 (−0.65, −0.07)	2.40	0.02	52%	0.15
≥6 months	2	210	−0.75 (−0.93, −0.58)	8.56	<0.00001	0%	0.36
6. TG	8	798	−0.36 (−0.53, −0.19)	4.17	<0.0001	87%	<0.00001
Treatment duration							
1 month	2	241	−0.55 (−0.91, −0.20)	3.07	0.002	92%	0.0006
2 months	2	142	−0.26 (−0.36, −0.17)	5.46	<0.00001	0%	0.44
3 months	2	205	−0.18 (−0.69, 0.34)	0.66	0.51	93%	<0.0001
≥6 months	2	210	−0.55 (−1.13, 0.03)	1.87	0.06	79%	0.03
7. LDL-C	8	798	−0.35 (−0.44, −0.25)	7.01	<0.00001	77%	<0.0001
Treatment duration							
1 month	2	241	−0.45 (−0.59, −0.31)	6.22	<0.00001	61%	0.11
2 months	2	142	−0.32 (−0.58, −0.06)	2.38	0.02	65%	0.09
3 months	2	205	−0.32 (−0.39, −0.24)	8.18	<0.00001	0%	0.89
≥6 months	2	210	−0.33 (−0.45, −0.21)	5.37	<0.00001	0%	0.37
8. HDL-C	4	446	0.31 (0.08, 0.54)	2.61	0.009	96%	<0.0001
Treatment duration							
1 month	2	241	0.40 (−0.02, 0.82)	1.86	0.06	97%	<0.00001
3 months	2	205	0.22 (−0.05, 0.50)	1.59	0.11	94%	<0.00001

CI, confidence interval; MD, mean difference; RR, risk ratio; LVEF, left ventricular ejection fraction; TC, total cholesterol; TG, triglyceride; LDL-C, low-density lipoprotein cholesterol; HDL-C, high-density lipoprotein cholesterol.

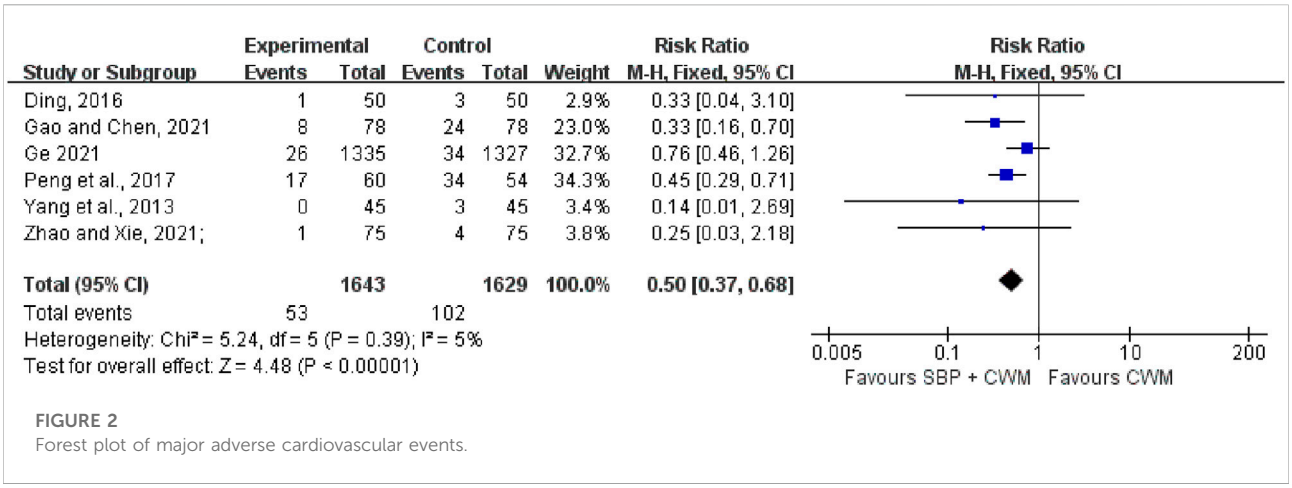

FIGURE 2
Forest plot of major adverse cardiovascular events.

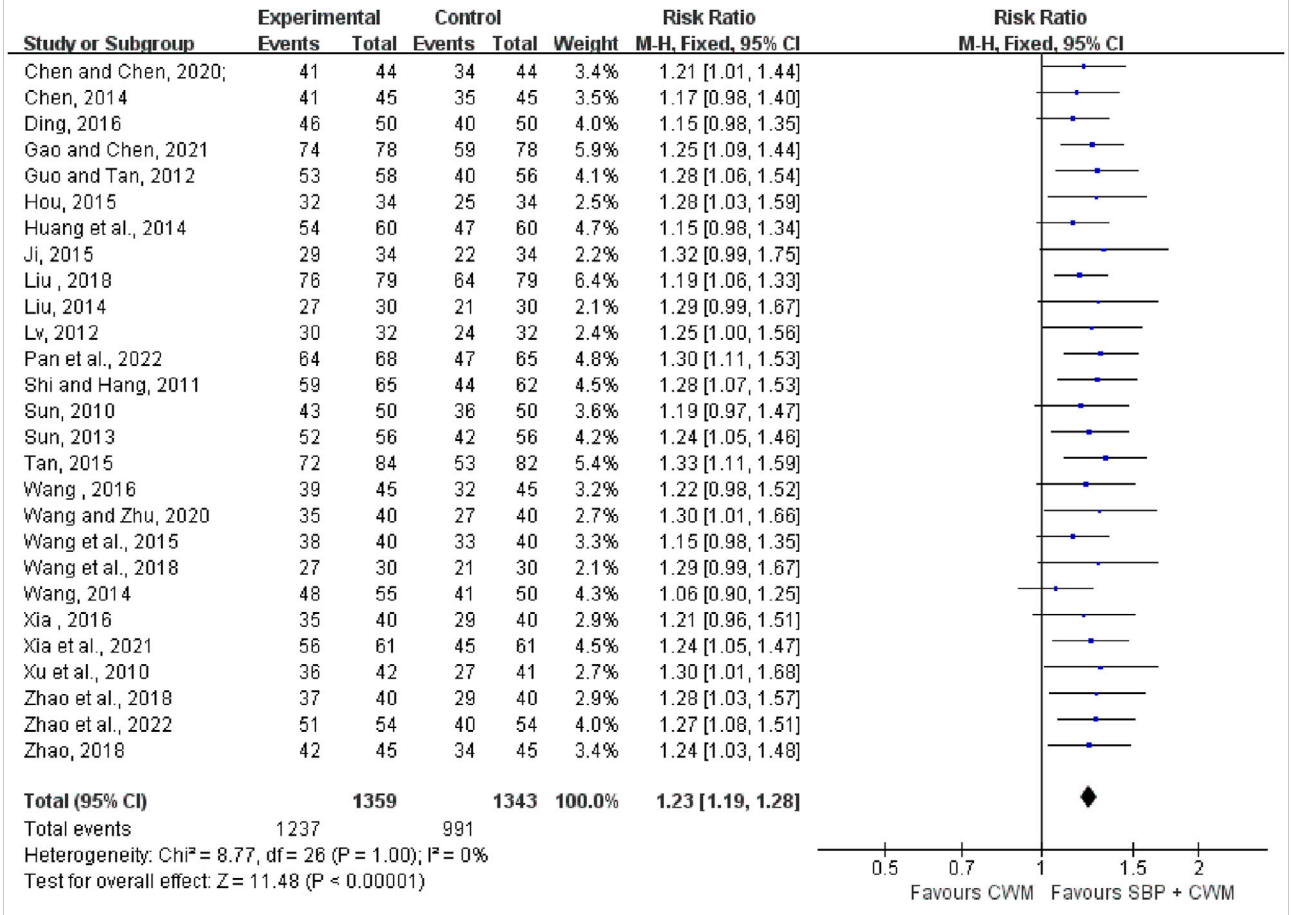

FIGURE 3
Forest plot of the total effective rate of angina symptom improvement.

studies (I^2 = 5%, p = 0.39), and a fixed-effect model was used for meta-analysis. The results indicated that the experimental group (SBP plus CWM) had better efficacy in lowering the incidence of MACE compared with the control group (RR = 0.50, 95% CI: 0.37 to 0.68, p < 0.00001; Figure 2).

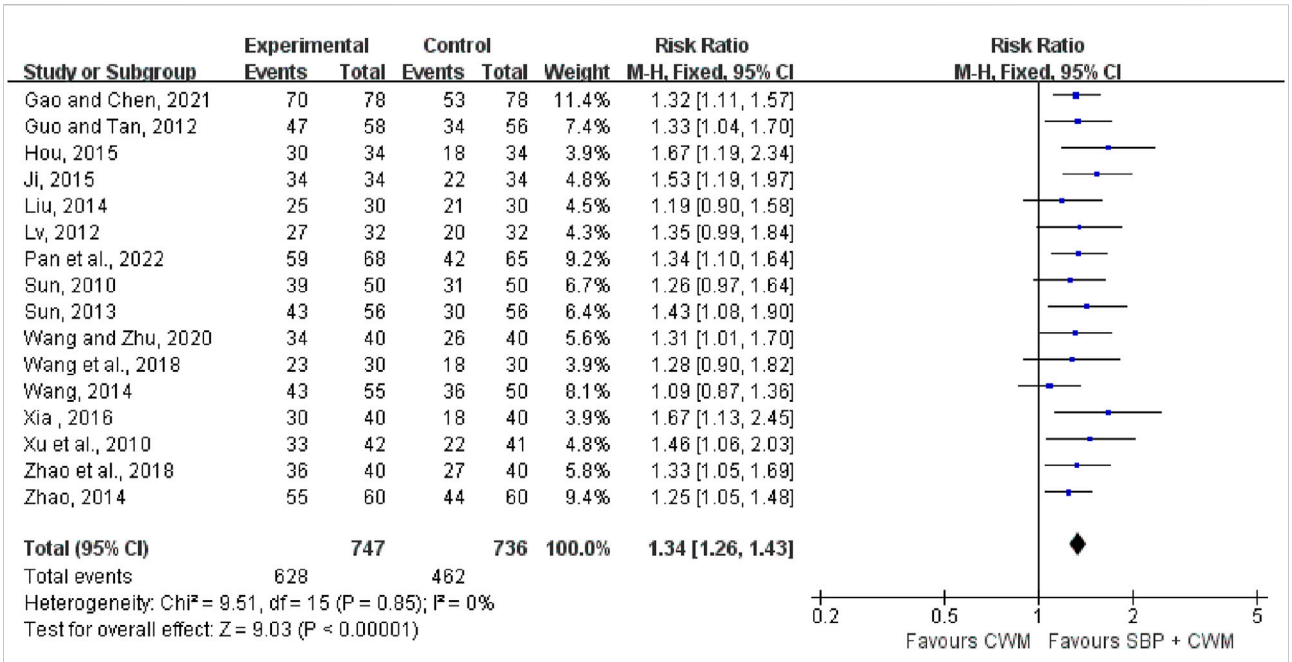

FIGURE 4
Forest plot of electrocardiogram improvement.

3.4.2 Angina symptom improvement

Twenty-seven trials with 2,702 patients reported the total effective rate of angina symptom improvement. The meta-analysis indicated that SBP therapy significantly improved the total effective rate of angina symptom improvement showing a compelling homogeneity (RR = 1.23, 95% CI: 1.19 to 1.28, $p < 0.00001$; $I^2 = 0\%$; Figure 3).

3.4.3 ECG improvement

Sixteen trials with 1,483 cases reported the effective rate of ECG improvement. The results showed that compared with the control group, the experimental group could significantly increase the effective rate of ECG improvement (RR = 1.34, 95% CI: 1.26 to 1.43, $p < 0.00001$; $I^2 = 0\%$), see Figure 4 for details.

3.4.4 AEs

Eighteen studies documented AEs in a total of 4,422 patients. Compared with CWM, the SBP group did not increase the risk of AEs (RR = 0.75, 95% CI: 0.44 to 1.25, $p = 0.27$; $I^2 = 51\%$; Figure 5) suggesting SBP therapy was safe. Our results revealed that gastrointestinal discomfort, tongue numbness, headache, and rash constitute the most frequently occurring AEs. Remarkable adverse reactions were modest, with no severe adverse impacts, detailed information is shown in Supplementary Material S7.

3.5 Secondary outcome measures

3.5.1 Angina pectoris frequency

Thirteen studies covering 1,304 patients included angina pectoris frequency as the outcome. The merged data indicated that the combination of SBP was more effective than CWM alone in reducing the frequency of angina pectoris (MD = −2.83, 95% CI: −3.62 to −2.05, $p < 0.00001$; $I^2 = 99\%$; Figure 6).

3.5.2 Angina pectoris duration

As shown in Figure 7, eight studies (728 patients) were included to compare the differences between the experimental group and the control group for the duration of angina pectoris. The results of the heterogeneity test showed that $I^2 = 100\%$, $p < 0.00001$, indicating a high degree of heterogeneity among the studies, so a random-effects model was used for the analysis. The results of the Meta-analysis indicated that compared with the control group, the experimental group could effectively shorten the duration of angina pectoris in patients with SCAD (MD = −1.32, 95% CI: −2.04 to −0.61, $p = 0.0003$).

3.5.3 Left ventricular ejection fraction

Eight studies covering 699 patients included LVEF (Figure 8) as the outcome. Compared with CWM, the combination of SBP showed a higher increase in LVEF (MD = 4.88, 95% CI: 3.19 to 6.57, $p < 0.00001$; $I^2 = 65\%$).

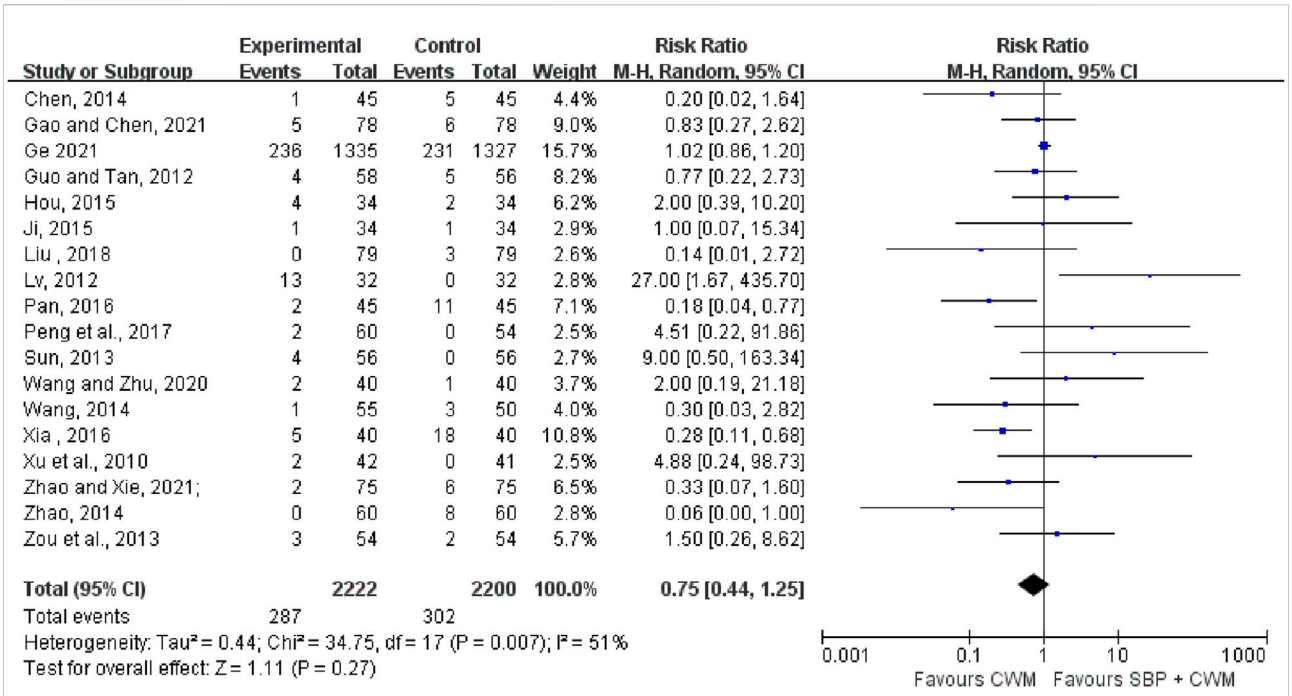

FIGURE 5
Forest plot of adverse events.

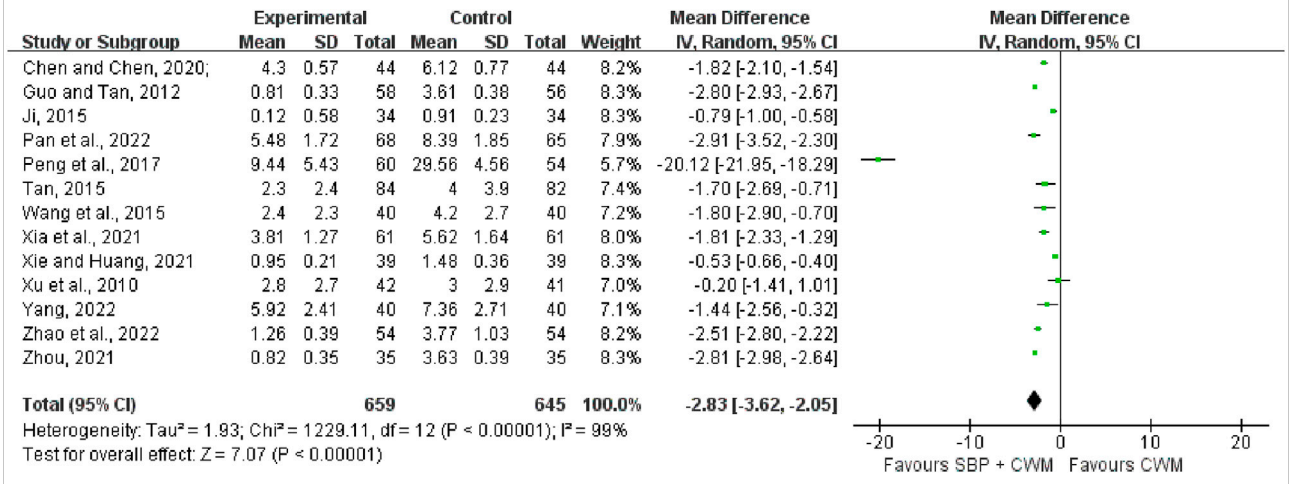

FIGURE 6
Forest plot of angina pectoris frequency.

3.5.4 Blood lipid level

Blood lipid level was measured with TC, TG, LDL-C, and HDL-C. Seven studies covering 734 patients reported SBP therapy reduced TC (MD = −0.59, 95% CI: −0.78 to −0.40, $p < 0.00001$; $I^2 = 82\%$; Figure 9). Eight studies reported TG, containing 798 patients. Compared with CWM, SBP treatment showed a decrease in TG (MD = −0.36, 95% CI: −0.53 to −0.19, $p < 0.00001$; $I^2 = 87\%$; Figure 9). LDL-C was reported in eight studies (MD = −0.35, 95% CI: −0.44 to −0.25, $p < 0.00001$; $I^2 = 77\%$; Figure 9) indicating SBP treatment substantially lowered LDL-C. HDL-C was recorded in four trials with the improvement in the experimental group (MD = 0.31, 95% CI: 0.08 to 0.54, $p = 0.009$; $I^2 = 96\%$; Figure 10).

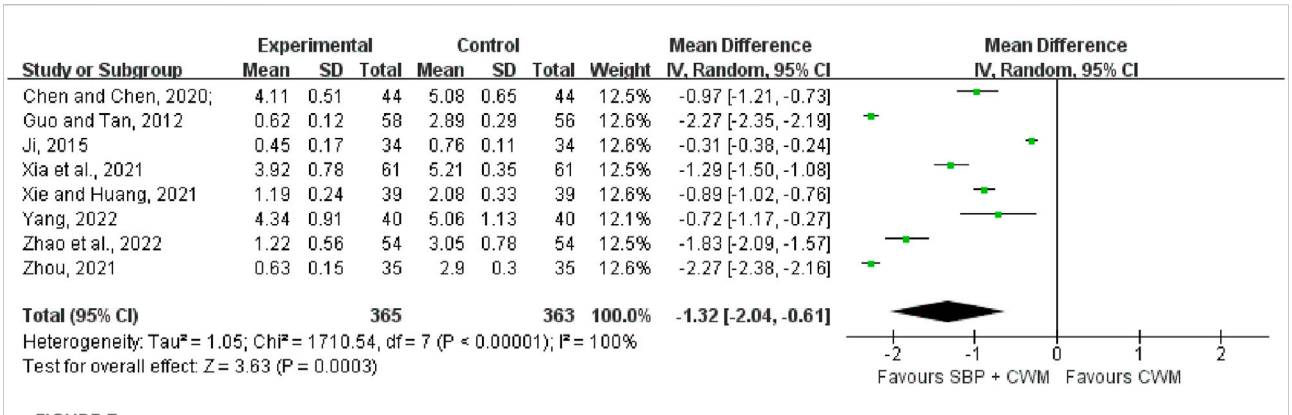

FIGURE 7
Forest plot of angina pectoris duration.

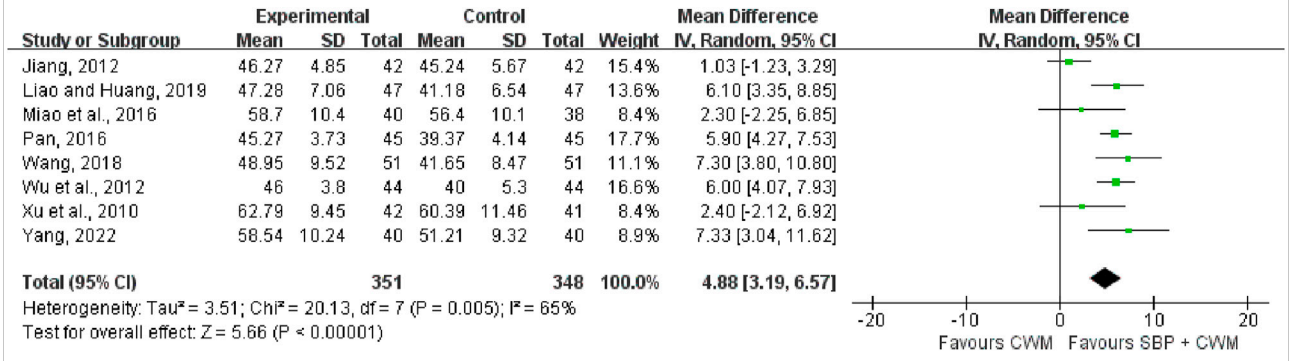

FIGURE 8
Forest plot of left ventricular ejection fraction.

3.6 Meta-regression and subgroup analysis

As results of angina pectoris frequency, angina pectoris duration, LVEF, TC, TG, LDL-C, and HDL-C showed high heterogeneity in our study, we performed a meta-regression analysis based on publication year, mean age, duration of treatment, and sample size. The results of meta-regression analysis showed that the duration of treatment and sample size were significant sources of heterogeneity for angina pectoris duration, and TG, respectively ($p < 0.05$). In addition, the results revealed that publication year, mean age, treatment duration, and sample size were not remarkable sources of heterogeneity for angina pectoris frequency, LVEF, TC, LDL-C, and HDL-C (all $p > 0.05$; Supplementary Material S8).

The intervention course of the drug was crucial to the clinical efficacy. We used subgroup analyses to determine whether treatment effects differed by treatment duration. As shown in Table 2 and Supplementary Material S9, the results of subgroup analysis were consistent with the overall study results. Regardless of the length of the course of treatment, SBP combined with CWM could significantly improve the incidence of angina pectoris frequency, angina pectoris duration, LVEF, and blood lipid level. We also found that with the prolongation of the course of treatment, the benefit of some indicators was more obvious, and the combined effect size was larger, such as TC, TG, and LDL-C. In addition, for some outcomes, heterogeneity was reduced after the subgroup analysis, such as angina pectoris frequency, angina pectoris duration, LVEF, TC, and LDL-C, suggesting that treatment duration may be the source of heterogeneity. However, it should be noted that there is still considerable heterogeneity in the remaining subgroups, suggesting that heterogeneity may come from other sources. We believed that the differences in detection equipment and techniques used in different studies may be one of the main sources.

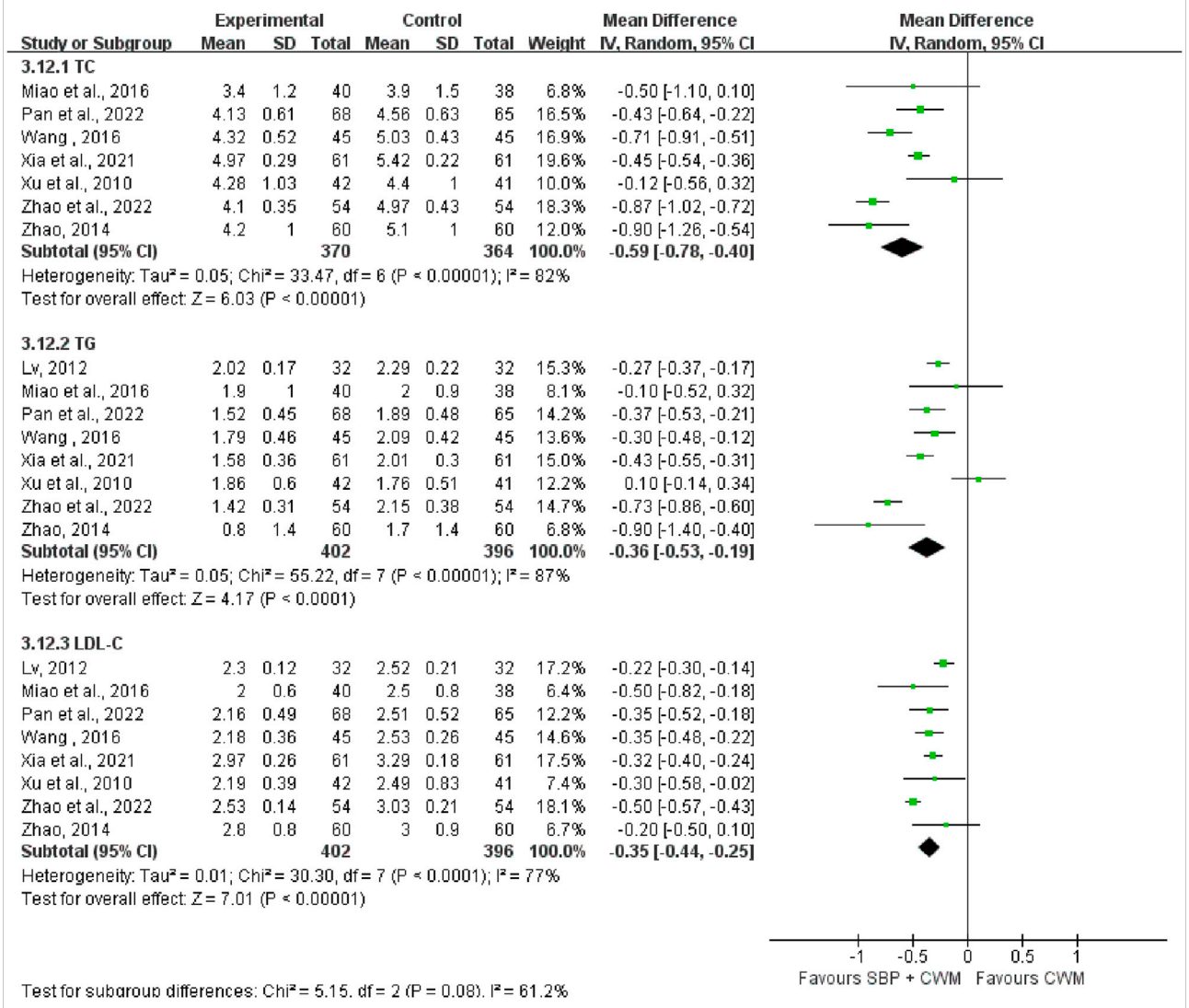

FIGURE 9
Forest plots of total cholesterol, triglyceride, and low-density lipoprotein cholesterol.

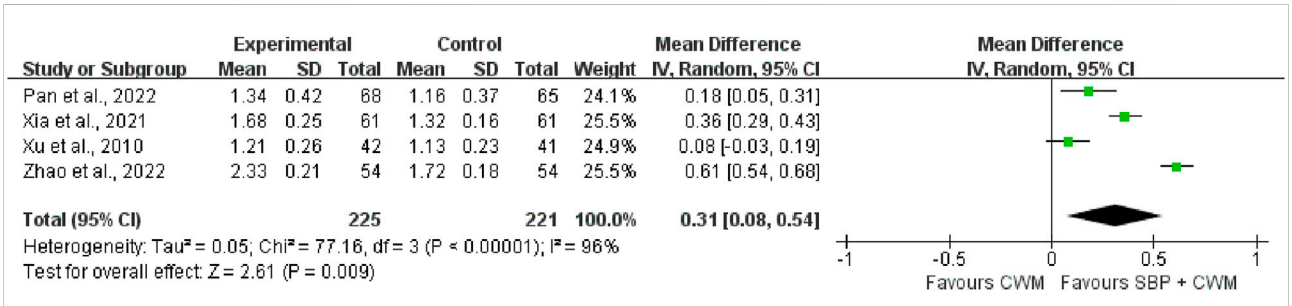

FIGURE 10
Forest plot of high-density lipoprotein cholesterol.

3.7 Sensitivity analysis and publication bias

The main outcomes, encompassing MACE, the total effective rate of angina symptom improvement, ECG improvement, and AEs were tested by the sensitivity analysis, which involved removing each trial in turn to assess the robustness of the main outcome. The pooled RR values of MACE, the total effective rate of angina symptom improvement, and ECG improvement were relatively stable and reliable, according to Supplementary Material S10. However, one study (Ge, 2021) had a certain impact on the stability of the results of adverse events, which may be related to the study's high quality, multiple centers, wide population, and long follow-up.

Publication bias was conducted on the outcomes in which trials were over ten. Egger's test was conducted to confirm the publication bias. As shown in Supplementary Material S11, the results showed ECG improvement ($p = 0.073$), AEs ($p = 0.585$), and angina pectoris frequency ($p = 0.438$) were reliable. Egger's test of the total effective rate of angina symptom improvement demonstrated that the p-value was less than 0.05 ($p = 0.035$), which indicated that there is publication bias.

3.8 GRADE assessment

Using GRADE (Table 3), we judged the certainty in our estimates to be low across primary outcomes. For MACE, and ECG improvement, we downgraded the evidence by one level for serious risk of bias, and the evidence was judged as moderate certainty. For the total effective rate of angina symptom improvement, we downgraded the evidence by two levels owing to the serious risk of bias and publication bias, and the evidence was judged as low certainty. For AEs, angina pectoris frequency, angina pectoris duration, LVEF, and blood lipid indicators, we downgraded the evidence by two levels owing to the serious risk of bias and heterogeneity, and the evidence was judged as low certainty.

3.9 Trial sequential analysis

We performed the trial sequential analysis of six trials reporting MACE. The parameters of this study were set as follows: type I error probability $\alpha = 5\%$, statistical power $1\text{-}\beta = 80\%$, and RR reduced by 20%. The sample size was used as the required information size (RIS) for the two-sided test. The results show that the cumulative Z value after the fifth study (Ge et al., 2020) has crossed the traditional boundary value and the TSA boundary value. Although the cumulative amount of information has not reached the required information size (RIS = 7,719), more experiments are not needed, and a positive conclusion can be obtained in advance, as shown in Figure 11.

4 Discussion

Generally, SCAD progresses more slowly and is milder than acute coronary syndrome. Notably, there is a common misunderstanding that the management and treatment of SCAD are mature. The reality is that the rate of misdiagnosis and underdiagnosis of SCAD is high, the quality of life of patients is reduced due to angina pectoris, the application of secondary preventive measures is insufficient, pharmacological treatment is inadequate, the patient benefit is not evident and medical costs increase, resulting in a significant number of patients converting to ACS and there is still a considerable residual cardiovascular risk (De Luca et al., 2019). In the treatment of coronary artery disease, Chinese medicine has played an important role (Liang and Gu, 2021). As a modern Chinese patent medicine, SBP has become the main supplementary drug for secondary prevention of SCAD patients in China, but there has been a lack of high-quality clinical evidence on the effect of SBP on adverse cardiovascular events in patients with SCAD and the safety of long-term use of SBP. In 2018, the "Chinese Expert Consensus on Shexiang Baoxin Pills for the Treatment of Coronary Heart Disease and Angina Pectoris" was officially published (Cardiovascular Diseases Professional Committee of Chinese Association of Integrated Traditional and Western Medicine, 2018), which systematically reviewed and summarized the pharmacological effects, clinical efficacy and safety of SBP, and strongly promoted the clinical application of SBP. With the deepening of clinical practice and research, more and more high-quality research evidence of SBP has been published. Therefore, it is necessary to conduct a systematic review and meta-analysis on the efficacy and safety of SBP in the treatment of SCAD, incorporate more strong evidence, and further clarify the applicable population and the strength of the evidence, to better guide the clinical application of SBP.

4.1 Summary of evidence

Our meta-analysis evaluated the clinical efficacy and safety of SBP in patients with SCAD through the 42 included studies with a total of 6,694 patients, which is the first study focusing on SBP treatment for SCAD patients. The results indicated that SBP combined with CWM could improve the incidence of MACE, the total effective rate of angina symptom improvement and ECG improvement, angina pectoris frequency, angina pectoris duration, and LVEF suggesting the experimental group was superior in clinical efficacy. The ultimate goal of drug therapy for SCAD is to reduce mortality, improve long-term survival, decrease the incidence of important cardiovascular events, and ensure the quality of life. MACE, as the hard endpoint of clinical observation, can objectively and directly reflect drug efficacy and disease prognosis. This study showed that the incidence of MACE was 3.23% (53/1,643) in the experimental group

TABLE 3 GRADE evidence profile.

Quality assessment						No of patients		RR/MD (95% CI)	Quality	Importance
No. Of studies	Risk of bias	Inconsistency	Indirectness	Imprecision	Publication bias	SBP combined with CWM	CWM			
MACE										
6	serious[a]	no serious	no serious	no serious	none	53/1,643 (3.23%)	102/1,629 (6.26%)	RR = 0.50 (0.37, 0.68)	⊕⊕⊕O moderate	CRITICAL
Angina Symptom Improvement										
27	serious[a]	no serious	no serious	no serious	Presence[b]	1,237/1,359 (91.02%)	991/1,343 (73.79%)	RR = 1.23 (1.19, 1.28)	⊕⊕OO low	CRITICAL
ECG Improvement										
16	serious[a]	no serious	no serious	no serious	none	628/747 (84.07%)	462/736 (62.77%)	RR = 1.34 (1.26, 1.43)	⊕⊕⊕O moderate	CRITICAL
Adverse Events										
18	serious[a]	serious[c]	no serious	no serious	none	287/2,222 (12.92%)	302/2,200 (13.73%)	RR = 0.75 (0.44, 1.25)	⊕⊕OO low	CRITICAL
Angina Pectoris Frequency										
13	serious[a]	serious[c]	no serious	no serious	none	659	645	MD = −2.83 (−3.62, −2.05)	⊕⊕OO low	CRITICAL
Angina Pectoris Duration										
8	serious[a]	serious[c]	no serious	no serious	none	365	363	MD = −1.32 (−2.04, −0.61)	⊕⊕OO low	IMPORTANT
LVEF										
8	serious[a]	serious[c]	no serious	no serious	none	351	348	MD = 4.88 (3.19, 6.57)	⊕⊕OO low	IMPORTANT
TC										
7	serious[a]	serious[c]	no serious	no serious	none	370	364	MD = −0.59 (−0.78, −0.40)	⊕⊕OO low	IMPORTANT
TG										
8	serious[a]	serious[c]	no serious	no serious	none	402	396	MD = −0.36 (−0.53, −0.19)	⊕⊕OO low	IMPORTANT
LDL-C										
8	serious[a]	serious[c]	no serious	no serious	none	402	396	MD = −0.35 (−0.44, −0.25)	⊕⊕OO low	IMPORTANT
HDL-C										
4	serious[a]	serious[c]	no serious	no serious	none	225	221	MD = 0.31 (0.08, 0.54)	⊕⊕OO low	IMPORTANT

SBP, shexiang baoxin pill; CWM, the conventional western medicine; CI, confidence interval; MD, mean difference; RR, risk ratio;
[a]Random protocol, blinding, and allocation concealment of some studies were not clear;
[b]Quantitative evaluation of the included data indicated publication bias;
[c]Heterogeneity ($I^2 > 50\%$, $p < 0.05$) was found.

10.3389/fphar.2022.1002713

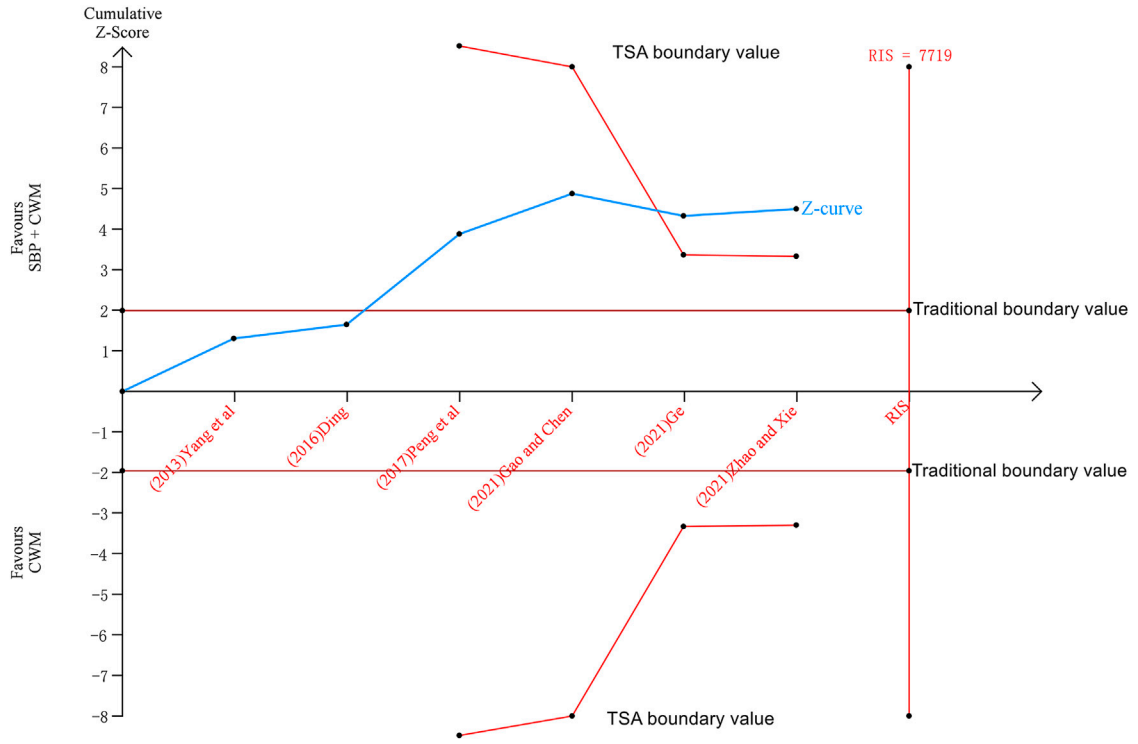

FIGURE 11
Trial sequential analysis of major adverse cardiovascular events.

compared with 6.26% (102/1,629) in the control group. The incidence of MACE in the SBP treatment group after treatment was 48.4% lower than that in the control group. The total effective rate of angina symptom improvement and ECG improvement, angina pectoris frequency, and angina pectoris duration can directly assess the severity of the disease and the degree of symptom relief in patients with angina pectoris. LVEF can reflect left ventricular function and provide a certain reference value for the diagnosis and prognosis. Our study found that SBP combined with CWM in the treatment of SCAD has the advantages of improving the total effective rate of angina symptom improvement and ECG improvement, angina pectoris frequency, angina pectoris duration, and LVEF. Dyslipidemia, especially elevated LDL-C, is an important risk factor for cardiovascular morbidity and mortality (Kopin and Lowenstein, 2017). Meta-analysis in this study demonstrated that SBP could remarkably improve the levels of TC, TG, LDL-C, and HDL-C in SCAD patients.

According to the SBP adverse reaction/event report of the National Adverse Drug Reaction Monitoring System (https://www.adrs.org.cn/), the adverse reactions of SBP collected from 2017 to 2021 were 346 cases (about 0.027%), 419 cases (about 0.029%), 479 cases (about 0.035%), 581 cases (about 0.040%), and 775 cases (about 0.048%), belonging to the rare range. Our study also listed AEs in trials to observe the safety of SBP in SCAD patients. Eighteen studies documented AEs in a total of 4,422 patients. According to the report, gastrointestinal discomfort, tongue numbness, headache, and rash are the highest four adverse symptoms. Other adverse cases including red face, liver and kidney damage, arrhythmia, and hypotension were also recorded. Altogether, compared with conventional treatment, SBP therapy did not increase the risk of AEs. What's more, the results of subgroup analyses according to treatment duration are consistent with the overall study results. Our results also found that treatment duration may be the source of heterogeneity in angina pectoris frequency, angina pectoris duration, LVEF, TC, and LDL-C. Moreover, we determined that the outcomes of MACE, the total effective rate of angina symptom improvement, and ECG improvement were stable and reliable by sensitivity analysis. GRADE is a common method for assessing the certainty of clinical evidence and is widely used in the preparation and revision of guidelines and expert consensus. The overall certainty of the evidence of the outcomes exhibited moderate or low certainty with heterogeneity and methodological problems. Hence, we provide supporting evidence that, to a remarkable extent, SBP can potentially be recommended for planned use for SCAD patients.

4.2 Comparison with previous studies

Multiple systematic reviews and meta-analyses have demonstrated the efficacy and safety of TCM in treating stable coronary artery disease. A meta-analysis constituting high-quality articles involving 824 patients revealed that the application of TCM in the treatment of angina pectoris can improve the therapeutic effect, shorten the attack time, reduce the frequency of angina pectoris, and improve the quality of life (Chen et al., 2021), which was consistent with our results. Nevertheless, their study had no obvious reducing effect on blood lipids. The reason may be the numerous varieties of formulations and ingredients of TCM and insufficient clinical samples. A previous meta-analysis found that corn silk decoction, a Chinese medicine prescription, may improve the levels of TC, TG, and LDL-C (Shi et al., 2019). However, this study did not pay much attention to the clinical endpoints of TCM and could not provide direct evidence of prognosis. The findings of two other meta-analyses indicated that the combination of TCM significantly improved performance compared with CWM solely for the treatment of angina pectoris (Liu et al., 2016; Huiping et al., 2019). Regrettably, they both suffered from methodological quality deficiencies. A prior systematic review demonstrated that in patients with SCAD, revascularization combined with conventional therapy did not lead to an overall survival advantage over medical therapy alone (Laukkanen and Kunutsor, 2021). However, revascularization plus medical therapy may reduce the overall risk of the composite outcome of all-cause death, myocardial infarction, readmission, revascularization, or stroke. This contemporary meta-analysis highlights more effective symptomatic relief of angina pectoris with appropriate adjustment of medical therapy and invasive strategies.

4.3 Limitations

This review is the first attempt to focus on the efficacy and safety of SBP in the treatment of SCAD and has the strength to follow the rigorous review process of Cochrane methodology, reporting standards such as PRISMA, and addressing quality of evidence using the GRADE system. Although we tried to identify all the available evidence, this study has several limitations. Firstly, a high risk of bias existed owing to the lack of blinding and the unclear randomization methods. Secondly, substantial heterogeneity was observed in most outcomes except MACE, the total effective rate of angina symptom improvement, and ECG improvement. Subgroup analysis showed reduced heterogeneity according to treatment duration. Since SCAD was complex, etiology, disease history, nursing treatment, and western treatment strategies may all contribute to the presence of heterogeneity. More research in specific areas is needed to fully assess how these factors play a role in heterogeneity. Thirdly, GRADE evidence quality ratings are mostly low or moderate, and relevant results should be treated with caution.

4.4 Implications for research

We herein reveal important ideas that may advance research in this field. Firstly, it is evident that strategies that improve the methodological quality of RCTs are urgently needed. Going forward, we recommend that more high-quality RCTs should be conducted to improve the strength of the evidence, especially focusing on the implementation of subject-centered randomization, allocation concealment, and blinding. Secondly, RCTs should be reported completely and comprehensively by the CONSORT statement (Cheng, et al., 2017), with particular attention to the reporting of etiology, medical history, nursing treatment, western treatment strategies, and follow-up to find sources of heterogeneity and clarify the prognosis of SCAD patients. Thirdly, despite the revelation that SBP therapy in the analyzed studies was somewhat safe for patients with SCAD, further investigations are needed to confirm the safety of SBP for SCAD. A standard reporting format for adverse drug reactions has been developed (Bian, et al., 2010), and we propose that close attention should be paid to improving the reporting of adverse reactions of SBP. To conclusively understand the long-term safety profile of SBP in patients with SBP, clinical studies incorporating longer follow-up periods are recommended. Our results suggest that SBP combined with CWM can be an alternative treatment for SCAD patients, nonetheless, further large clinical studies should be conducted to explore the long-term safety, efficacy, and optimized dosages of SBP for treating SCAD.

5 Conclusion

In summary, the available evidence indicates that SBP combined with CWM may be effective in the treatment of SCAD to improve the incidence of MACE, the total effective rate of angina symptom improvement and ECG improvement, angina pectoris frequency, angina pectoris duration, LVEF, blood lipid level. However, the risk of bias in the included studies was generally low to high, and the credibility of some results was reduced by heterogeneity. Moreover, the safety of Shexiang Baoxin Pill remains uncertain, more carefully designed large-sample, long-term follow-up RCT should be carried out in the future to provide reliable evidence for SBP in treating SCAD.

Data availability statement

The original contributions presented in the study are included in the article/Supplementary Materials, further inquiries can be directed to the corresponding authors.

Author contributions

MZ and YW conceived and designed this study. JW wrote the paper and analyzed the data. TM and CZ performed the literature search, selection, the risk of bias, and data extraction. BL and XW assessed the quality of the study. RY and PH revised the manuscript. All authors contributed to the article and approved the submitted version.

Funding

The Ministry of Science and Technology of the People's Republic of China's Key Projects during the 13th Five-Year Plan Period (2019YFC1710003), the National Natural Science Foundation of China (82074226; 82030120), the Chinese Medicine Evidence-Based Capacity Building Project of State Administration of Traditional Chinese Medicine (2019XZZX-XXG003) supported the study.

Conflict of interest

The authors declare that the research was conducted in the absence of any commercial or financial relationships that could be construed as a potential conflict of interest.

Publisher's note

All claims expressed in this article are solely those of the authors and do not necessarily represent those of their affiliated organizations, or those of the publisher, the editors and the reviewers. Any product that may be evaluated in this article, or claim that may be made by its manufacturer, is not guaranteed or endorsed by the publisher.

Supplementary material

The Supplementary Material for this article can be found online at: https://www.frontiersin.org/articles/10.3389/fphar.2022.1002713/full#supplementary-material

References

Bhatt, D. L., Eagle, K. A., Ohman, E. M., Hirsch, A. T., Goto, S., Mahoney, E. M., et al. (2010). Comparative determinants of 4-year cardiovascular event rates in stable outpatients at risk of or with atherothrombosis. *JAMA* 304 (12), 1350–1357. doi:10.1001/jama.2010.1322

Bian, Z. X., Tian, H. Y., Gao, L., Shang, H. C., Wu, T. X., Li, Y. P., et al. (2010). Improving reporting of adverse events and adverse drug reactions following injections of Chinese materia medica. *J. Evid. Based. Med.* 3 (1), 5–10. doi:10.1111/j.1756-5391.2010.01055.x

Cardiovascular Diseases Professional Committee of Chinese Association of Integrated Traditional and Western Medicine (2018). Chinese expert Consensus on shexiang baoxin pills for the treatment of coronary heart disease and angina pectoris. *Chin. J. Integr. Med.* 38 (02), 145–153. doi:10.7661/j.cjim.20170801.307

Chen, W., Wang, B., Ge, Y., Xu, H., Jiang, C., Yu, P., et al. (2021). A systematic review and meta-analysis of clinical research on treating angina pectoris of coronary heart disease with traditional Chinese medicine to promote blood circulation and remove blood stasis. *Ann. Palliat. Med.* 10 (10), 10506–10514. doi:10.21037/apm-21-2233

Chen, X. Z., and Chen, C. (2020). Observation of shexiang baoxin pills for stable Angina pectoris of coronary heart disease and its regulating effect on ROS and CT-1 in serum. *Chin. J. New Chin. Med.* 51 (10), 87–89. doi:10.13457/j.cnki.jncm.2019.10.025

Cheng, C. W., Wu, T. X., Shang, H. C., Li, Y. P., Altman, D. G., Moher, D., et al. (2017). CONSORT extension for Chinese herbal medicine formulas 2017: Recommendations, explanation, and elaboration (traditional Chinese version). *Ann. Intern. Med.* 167 (2), W7-W20. W7–W20. doi:10.7326/IsTranslatedFrom_M17-2977_1

Cheng, Z. J. (2014). Shexiang Baoxin Pill combined with Xiaoxintong in the treatment of 45 cases of stable angina pectoris. *Chin. Med. Mod. Distance Educ. China* 2014 (21), 60–61. doi:10.3969/j.issn.1672-2779.2014.21.035

China Association of Chinese Medicine Cardiovascular Disease Branch (2019). Guidelines for TCM diagnosis and treatment of stable angina pectoris of coronary heart disease. *J. Tradit. Chin. Med.* 60 (21), 1880–1890. doi:10.13288/j.11-2166/r.2019.21.015

De Luca, L., Temporelli, P. L., Riccio, C., Gonzini, L., Marinacci, L., Tartaglione, S., et al. (2019). Clinical outcomes, pharmacological treatment, and quality of life of patients with stable coronary artery diseases managed by cardiologists: 1-year results of the START study. *Eur. Heart J. Qual. Care Clin. Outcomes* 5 (4), 334–342. doi:10.1093/ehjqcco/qcz002

Ding, H. (2016). Observation on the curative effect of Shexiang Baoxin Pill in the treatment of stable angina pectoris. *China Heal Care Nutr.* 26 (21), 249–250.

Fang, H. Y., Zeng, H. W., Lin, L. M., Chen, X., Shen, X. N., Fu, P., et al. (2017). A network-based method for mechanistic investigation of Shexiang Baoxin Pill's treatment of cardiovascular diseases. *Sci. Rep.* 7, 43632. doi:10.1038/srep43632

Feres, F., Costa, R. A., Abizaid, A., Leon, M. B., Marin-Neto, J. A., Botelho, R. V., et al. (2013). Three vs twelve months of dual antiplatelet therapy after zotarolimus-eluting stents: The OPTIMIZE randomized trial. *JAMA* 310 (23), 2510–2522. doi:10.1001/jama.2013.282183

Fihn, S. D., Gardin, J. M., Abrams, J., Berra, K., Blankenship, J. C., Dallas, A. P., et al. (2012). 2012 ACCF/AHA/ACP/AATS/PCNA/SCAI/STS guideline for the diagnosis and management of patients with stable ischemic heart disease: A report of the American college of Cardiology foundation/American heart association task force on practice guidelines, and the American college of physicians, American association for thoracic surgery, preventive cardiovascular nurses association, society for cardiovascular angiography and interventions, and society of thoracic surgeons. *J. Am. Coll. Cardiol.* 60 (24), e44–e164. doi:10.1016/j.jacc.2012.07.013

Gao, T. H., and Chen, Z. H. (2021). Observation on the curative effect of Shexiang Baoxin Pill in the adjuvant treatment of stable coronary heart disease. *Chin. J. Integr. Med. Cardio-/Cerebrovascuiar Dis.* 19 (21), 3807–3808. doi:10.12102/ji.ssn.1672-1349.2021.21.040

Ge, J. B., Fan, W. H., Zhou, J. M., Shi, H. M., Ji, F. S., Wu, Y., et al. (2020). Efficacy and safety of shexiang baoxin pill (MUSKARDIA) in patients with stable coronary artery disease: A multicenter, double-blind, placebo-controlled phase IV randomized clinical trial. *Chin. Med. J.* 134 (2), 185–192. doi:10.1097/CM9.0000000000001257

Goldet, G., and Howick, J. (2013). Understanding GRADE: An introduction. *J. Evid. Based. Med.* 6 (1), 50–54. doi:10.1111/jebm.12018

Guo, J., Qin, Z., He, Q., Fong, T. L., Lau, N. C., Cho, W., et al. (2021). Shexiang baoxin pill for acute myocardial infarction: Clinical evidence and molecular mechanism of antioxidative stress. *Oxid. Med. Cell. Longev.* 2021, 7644648. doi:10.1155/2021/7644648

Guo, M., and Tan, B. (2012). Observation of curative effect of shexiang baoxin pill in treating stable Angina pectoris of senile coronary heart disease. *Mod. J. Integr. Traditional Chin. West. Med.* 21 (22), 2433–2434. doi:10.3969/j.issn.1008-8849.2012.22.018

Hou, J. F. (2015). Observation on the effect of Shexiang Baoxin Pill combined with Xiaoxintong in the treatment of senile stable angina pectoris. *Chin. J. Rural Med. Pharm.* 2015 (15), 28–29. doi:10.3969/j.issn.1006-5180.2015.15.018

Hu, J., Zhao, Y., Wu, Y., Yang, K., Hu, K., Sun, A., et al. (2021). Shexiang baoxin pill attenuates ischemic injury by promoting angiogenesis by activation of aldehyde dehydrogenase 2. *J. Cardiovasc. Pharmacol.* 77 (3), 408–417. doi:10.1097/FJC.0000000000000967

Huang, L., Zhang, L., and Li, G. L. (2014). Shexiang Baoxin Pill combined with aspirin in the treatment of 60 cases of senile blood stasis type stable angina pectoris. *Chin. J. Integr. Med. Cardio-/Cerebrovascuiar Dis.* 12 (02), 177–178. doi:10.3969/j.issn.1672-1349.2014.02.025

Huiping, W., Yu, W., Pei, J., Jiao, L., Shian, Z., Hugang, J., et al. (2019). Compound salvia pellet might be more effective and safer for chronic stable angina pectoris compared with nitrates: A systematic review and meta-analysis of randomized controlled trials. *Med. Baltim.* 98 (9), e14638. doi:10.1097/MD.0000000000014638

Ji, J. H. (2015). Clinical observation of Shexiang Baoxin pills combined with Western medicine in the treatment of 68 cases of stable angina pectoris. *China's Naturop.* 23 (11), 47–48.

Jiang, X. D. (2012). Observation of curative effect of shexiang baoxin pill on ischemic cardiomyopathy. *Chin. Med. Mod. Distance Educ. China* 10 (13), 50–51. doi:10.3969/j.issn.1672-2779.2012.13.033

Kopin, L., and Lowenstein, C. (2017). Dyslipidemia. *Ann. Intern. Med.* 167 (11), ITC81-ITC96–ITC96. doi:10.7326/AITC201712050

Laukkanen, J. A., and Kunutsor, S. K. (2021). Revascularization versus medical therapy for the treatment of stable coronary artery disease: A meta-analysis of contemporary randomized controlled trials. *Int. J. Cardiol.* 324, 13–21. doi:10.1016/j.ijcard.2020.10.016

Liang, B., and Gu, N. (2021). Traditional Chinese medicine for coronary artery disease treatment: Clinical evidence from randomized controlled trials. *Front. Cardiovasc. Med.* 8, 702110. doi:10.3389/fcvm.2021.702110

Liao, J. Y., and Huang, E. (2019). Observation of curative effect of shexiang baoxin pill on ischemic cardiomyopathy. *Chin. J. Mod. Drug Appl.* 13 (08), 131–132. doi:10.14164/j.cnki.cn11-5581/r.2019.08.076

Liu, G. P. (2014). Clinical observation of Shexiang Baoxin Pill combined with Xiaoxintong in the treatment of stable angina pectoris. *Inn. Mong. J. Traditional Chin. Med.* 33 (23), 6–7. doi:10.16040/j.cnki.cn15-1101.2014.23.036

Liu, H. M. (2018). Therapeutic effect and safety of oral musk Baoxin pill in patients with stable angina pectoris of coronary heart disease. *Chin. J. Cardiovasc Rehabil. Med.* 27 (06), 684–687. doi:10.3969/j.issn.1008-0074.2018.06.17

Liu, K., Sun, D. Q., Liao, X., and Zhang, L. (2019). Interpretation of the risk of bias assessment tool for randomized controlled trials, rev. 2.0. 2016:8565907. *Chin. J. Evid. Based Cardiovasc Med.* 11 (03), 284–291. doi:10.3969/j.issn.1674-4055.2019.03.05

Liu, W., Xiong, X., Yang, X., Chu, F., and Liu, H. (2016). The effect of Chinese herbal medicine gualouxiebaibanxia decoction for the treatment of angina pectoris: A systematic review. *Evid. Based. Complement. Altern. Med.* 2016, 8565907. doi:10.1155/2016/8565907

Lu, L., Qin, Y., Zhang, X., Chen, C., Xu, X., Yu, C., et al. (2019). Shexiang baoxin pill alleviates the atherosclerotic lesions in mice via improving inflammation response and inhibiting lipid accumulation in the arterial wall. *Mediat. Inflamm.* 2019, 6710759. doi:10.1155/2019/6710759

Lv, H. (2018). Clinical observation of shexiang baoxin pill in treating 64 cases of coronary heart disease with stable Angina pectoris. *China Mod. Med.* 19 (32), 116–117. doi:10.3969/j.issn.1674-4721.2012.32.058

Miao, H. X., Zhu, Y. Z., Ye, C. X., and Zeng, J. (2016). Effects of shexiang baoxin pill on ultrasound, inflammatory index and blood lipid in old myocardial infarction. *Chin. Foreign Med. Res.* 14 (27), 25–27. doi:10.14033/j.cnki.cfmr.2016.27.012

Montalescot, G., Sechtem, U., Achenbach, S., Andreotti, F., Arden, C., Budaj, A., et al. (2013). 2013 ESC guidelines on the management of stable coronary artery disease: The task force on the management of stable coronary artery disease of the European society of Cardiology. *Eur. Heart J.* 34 (38), 2949–3003. doi:10.1093/eurheartj/eht296

Mozaffarian, D., Benjamin, E. J., Go, A. S., Arnett, D. K., Blaha, M. J., Cushman, M., et al. (2016). Executive summary: Heart disease and stroke statistics-2016 update: A report from the American heart association. *Circulation* 133 (4), 447–454. doi:10.1161/CIR.0000000000000366

Page, M. J., McKenzie, J. E., Bossuyt, P. M., Boutron, I., Hoffmann, T. C., Mulrow, C. D., et al. (2021). The PRISMA 2020 statement: An updated guideline for reporting systematic reviews. *Int. J. Surg.* 88, 105906. doi:10.1016/jijsu/2021/105906

Pan, F. Q., Xi, Y. T., Huang, T. F., Cao, Y. H., and Wu, W. (2019). Meta analysis of shexiang baoxin pills in treatment of stable Angina pectoris. *Lishizhen Med. Materia Medica Res.* 30 (12), 3041–3045. doi:10.3969/jissn.1008-0805.2019.12.077.012

Pan, F. Y., Fan, X. T., and Huang, B. Y. (2022). Clinical study on shexiang baoxin pills combined with metoprolol for stable Angina pectoris of coronary heart disease in senile patients. *J. New Chin. Med.* 54 (04), 43–46. doi:10.13457/j.cnki.jncm.2022.04.012

Pan, M. Y. (2016). Effect of shexiang baoxin pill on cardiac function of patients with ischemic heart disease. *J. North Pharm.* 13 (5), 112–113.

Peng, B. B., Han, Y., and Han, Q. H. (2017). Observation on the curative effect of Shexiang Baoxin Pill in the treatment of stable angina pectoris. *Chin. J. Integr. Med. Cardio-/Cerebrovascuiar Dis.* 15 (04), 460–462. doi:10.3969/j.issn.1672-1349.2017.04.020

Shi, B., and Hang, Y. (2011). Heart pill of musk combined with western medicine treatment of stable Angina pectoris 65 cases of blood stasis. *J. Pract. Traditional Chin. Intern. Med.* 25 (12), 34–35. doi:10.3969/j.issn.1671-7813.2011.12.19

Shi, S., Yu, B., Li, W., Shan, J., and Ma, T. (2019). Corn silk decoction for blood lipid in patients with angina pectoris: A systematic review and meta-analysis. *Phytother. Res.* 33 (11), 2862–2869. doi:10.1002/ptr.6474

Sun, J. H. (2010). Clinical observation of shexiang baoxin pill in treating stable Angina pectoris. *Hebei Med. J.* 32 (9), 1182. doi:10.3969/j.issn.1002-7386.2010.09.091

Sun, X. L. (2013). Clinical observation of shexiang baoxin pill in treating stable Angina pectoris. *Henan Med. Res.* 22 (4), 583–584. doi:10.3969/j.issn.1004-437X2013.04.056

Tan, Y. L. (2015). Effect of shexiang baoxin pill on clinical symptoms of elderly patients with stable Angina pectoris. *Henan Tradit. Chin. Med.* 35 (2), 257–259. doi:10.16367/j.issn.1003-5028.2015.02.0108

Wang, G. Z., Wang, H. P., and Zhu, A. P. (2015). Observation on the curative effect of Shexiang Baoxin Pill in the treatment of stable angina pectoris. *Cardiovasc. Dis. J. Integr. traditional Chin. West. Med.* 3 (23), 90–91. doi:10.16282/j.cnki.cn11-9336/r.2015.23.053

Wang, H. C. (2014). Clinical observation of Shexiang Baoxin Pill in the treatment of senile stable exertional angina pectoris. *Med. Inf.* 2014 (21), 278. doi:10.3969/j.issn.1006-1959.2014.21.327

Wang, L. F., Yie, J., and Yang, W. L. (2018). Observation of curative effect of oral administration of Shexiang Baoxin pills in patients with stable angina pectoris. *Prev. Treat. Cardio-Cerebral-Vascular Dis.* 18 (01), 67–68. doi:10.3969/jissn.1009_816x.2018.01.022

Wang, M., Shan, Y., Sun, W., Han, J., Tong, H., Fan, M., et al. (2021). Effects of shexiang baoxin pill for coronary microvascular function: A systematic review and meta-analysis. *Front. Pharmacol.* 12, 751050. doi:10.3389/fphar.2021.751050

Wang, X. Y. (2016). Long-term curative effect of heart-protecting musk pill on stable Angina pectoris accompanied by hyperlipemia. *China Licens. Pharm.* 13 (9), 3–6. doi:10.3969/j.issn.1672-5433.2016.09.001

Wang, Y. X., and Zhu, B. (2020). Clinical efficacy of Shexiang Baoxin Pill combined with diltiazem in the treatment of elderly patients with stable angina pectoris of coronary heart disease. *J. Chengdu Med. Coll.* 15 (03), 373–375. doi:10.3969/j.issn.1674-2257.2020.03.022

Wang, Z. C. (2018). Clinical therapeutic effects on old myocardial infarction treated with shexiang baoxin pills and trimetazidine hydrochloride tablets in the patients. *World J. Integr. Traditional West. Med.* 13 (01), 128–130+134. doi:10.13935/j.cnki.sjzx.180135

Wei, J., Liu, S., Wang, X., Li, B., Qiao, L., Wang, Y., et al. (2021). Efficacy and safety of shexiang baoxin pill for coronary heart disease after percutaneous coronary intervention: A systematic review and meta-analysis. *Evid. Based. Complement. Altern. Med.* 2021, 2672516. doi:10.1155/2021/2672516

Wu, R., Jia, X. F., and He, X. L. (2012). Observation and analysis of curative effect of shexiang baoxin pill in treating 88 cases of ischemic cardiomyopathy. *Chin. Community Dr.* 14 (14), 230–231. doi:10.3969/j.issn.1007-614x.2012.14.216

Xia, X. L. (2016). Influence of oral administration of Shexiang Baoxin Pill for at least 6 months on clinical events in patients with stable angina pectoris. *China Prac. Med.* 2016 (1), 165–166. doi:10.14163/j.cnki.11-5547/r.2016.01.124

Xia, Z. L., Zhang, X., Jin, L. T., and Chen, H. Y. (2021). Clinical effects of Shexiang Baoxin Pills combined with conventional treatment on stable angina pectoris in patients with coronary artery diseases. *Chin. Tradit. Pat. Med.* 43 (07), 1772–1774. doi:10.3969/j.issn.1001-1528.2021.07.017

Xie, H., and Huang, R. J. (2021). Effects of Shexiang Baoxin Pill combined with nitroglycerin on angina attack and inflammatory factor levels in patients with stable angina pectoris of coronary heart disease. *Prev. Treat. Cardiovasc. Dis.* 11 (28), 21–23.

Xu, M., Sun, N. L., Li, J. H., Zhang, J., Wei, B. Q., et al. (2010). Clinical observation on the efficacy of Shexiang Baoxin pills in the treatment of SAP in the elderly patients. *Chin. J. Geriatr. Heart Brain Vessel Dis.* 12 (8), 695–698. doi:10.3969/j.issn.1009-0126.2010.08.008

Yang, G. L., Wang, S. P., Zhou, H. X., and Jiang, Y. R. (2013). Effect of Shexiang Baoxin Pill on platelet aggregation in patients with stable angina pectoris. *Chin. J. Integr. Med. Cardio-/Cerebrovascuiar Dis.* 11 (3), 288–289. doi:10.3969/j.issn.1672-1349.2013.03.018

Yang, J., Shi, L., Chen, H., Wang, X., Jiao, J., Yang, M., et al. (2022). Strategies comparison in response to the two waves of COVID-19 in the United States and India. *Int. J. Equity Health* 29 (02), 57–59. doi:10.1186/s12939-022-01666-9

Zhang, J., Cui, Q., Zhao, Y., Guo, R., Zhan, C., Jiang, P., et al. (2020). Mechanism of angiogenesis promotion with Shexiang Baoxin Pills by regulating function and signaling pathway of endothelial cells through macrophages. *Atherosclerosis* 292, 99–111. doi:10.1016/j.atherosclerosis.2019.11.005

Zhao, J. C., Yang, Y. J., and Tian, Y. J. (2022). Efficacy evaluation of Shexiangbaoxin pills in treatment of stable angina pectoris with syndrome of yang deficiency and cold congelation and its effects on inflammatory factors CD31 and CD62P. *Hebei Med. J.* 44 (04), 516–519. doi:10.3969/j.issn.1002-7386.2022.04.008

Zhao, L. (2018). Efficacy of Shexiang Baoxin Pill in the treatment of elderly patients with stable angina pectoris. *Chin. Community Dr.* 34 (03), 74+76. doi:10.3969/j.issn.1007-614x.2018.3.45

Zhao, Q., Zhong, M., Tang, B., and Jin, Q. S. (2018). Clinical observation of shexiang baoxin pill in adjuvant treatment of chronic stable Angina pectoris. *Health Horiz.* 2018 (14), 101. doi:10.3969/j.issn.1005-0019.2018.14.127

Zhao, W. X. (2014). Clinical analysis of Shexiang Baoxin Pill in the treatment of stable angina pectoris complicated with carotid atherosclerosis. *Hebei Med. J.* 2014 (7), 1023–1024. doi:10.3969/j.issn.1002-7386.2014.07.025

Zhao, Y., and Xie, L. (2021). Clinical efficacy and safety observation of Shexiang Baoxin Pill combined with diltiazem in the treatment of stable angina pectoris in elderly patients with coronary heart disease. *Guizhou Med. J.* 45 (12), 1934–1935.

Zhou, S. Y. (2021). Efficacy of Shexiang Baoxin Pill combined with diltiazem in the treatment of senile coronary heart disease with stable angina pectoris. *Health Horiz.* 2021 (8), 100.

Zou, H. L., Guo, H. W., Tang, J., and Zhang, A. J. (2013). Effect of shexiang baoxin pill combined with aspirin on serum adiponectin, endothelin-1, nitric oxide in stable Angina pectoris. *Chin. J. Integr. Med. Cardio-/Cerebrovascuiar Dis.* 11 (2), 143–144. doi:10.3969/j.issn.1672-1349.2013.02.008

frontiers | Frontiers in Pharmacology

TYPE Review
PUBLISHED 24 November 2022
DOI 10.3389/fphar.2022.1040235

Check for updates

OPEN ACCESS

EDITED BY
Qing Yong He,
Guang'anmen Hospital, China Academy of Chinese Medical Sciences, China

REVIEWED BY
Hua Yang,
China Pharmaceutical University, China
Kunming Qin,
Jiangsu Ocean Universiity, China
Yan Liu,
Heilongjiang University of Chinese Medicine, China

*CORRESPONDENCE
Hongcai Shang,
shanghongcai@foxmail.com

SPECIALTY SECTION
This article was submitted to Ethnopharmacology, a section of the journal Frontiers in Pharmacology

RECEIVED 09 September 2022
ACCEPTED 14 November 2022
PUBLISHED 24 November 2022

CITATION
Lv S, Wang Y, Zhang W and Shang H (2022), The chemical components, action mechanisms, and clinical evidences of YiQiFuMai injection in the treatment of heart failure. *Front. Pharmacol.* 13:1040235. doi: 10.3389/fphar.2022.1040235

COPYRIGHT
© 2022 Lv, Wang, Zhang and Shang. This is an open-access article distributed under the terms of the Creative Commons Attribution License (CC BY). The use, distribution or reproduction in other forums is permitted, provided the original author(s) and the copyright owner(s) are credited and that the original publication in this journal is cited, in accordance with accepted academic practice. No use, distribution or reproduction is permitted which does not comply with these terms.

The chemical components, action mechanisms, and clinical evidences of YiQiFuMai injection in the treatment of heart failure

Shichao Lv[1,2], Yunjiao Wang[2], Wanqin Zhang[2] and Hongcai Shang[1]*

[1]Key Laboratory of Chinese Internal Medicine of MOE, Dongzhimen Hospital, Beijing, China, [2]Department of Geriatrics, First Teaching Hospital of Tianjin University of Traditional Chinese Medicine, Tianjin, China

YiQiFuMai injection (YQFM), derived from Shengmai Powder, is wildly applied in the treatment of cardiovascular diseases, such as coronary heart disease and chronic cardiac insufficiency. YiQiFuMai injection is mainly composed of Radix of *Panax ginseng* C.A. Mey. (Araliaceae), Radix of *Ophiopogon japonicus* (Thunb.) Ker Gawl (Liliaceae), and Fructus of *Schisandra chinensis* (Turcz.) Baill (Schisandraceae), and Triterpene saponins, steroidal saponins, lignans, and flavonoids play the vital role in the potency and efficacy. Long-term clinical practice has confirmed the positive effect of YiQiFuMai injection in the treatment of heart failure, and few adverse events have been reported. In addition, the protective effect of YiQiFuMai injection is related to the regulation of mitochondrial function, anti-apoptosis, amelioration of oxidant stress, inhibiting the expression of inflammatory mediators, regulating the expression of miRNAs, maintaining the balance of matrix metalloproteinases/tissue inhibitor of metalloproteinases (MMP/TIMP) and anti-hypoxia.

KEYWORDS

heart failure, YiQiFuMai injection, chemical components, clinical evidences, mechanisms

1 Introduction

Heart failure whose incidence rate rises year by year, is the late stage of cardiovascular disease with high mortality and rehospitalization rates. The latest epidemiological survey showed that the prevalence of heart failure in China was 1.3% (an estimated 13.7 million patients), which had increased by 44% in the past 15 years (Hao et al., 2019). And the mortality rates of heart failure within 30 days, 1 year and 5 years after hospitalization were 10.4%, 22% and 42.3% respectively. The rehospitalization rates within 1 year among patients with acute and chronic heart failure were 43.9% and 31.9% respectively (Loehr et al., 2008; Maggioni et al., 2013). As the last battlefield for the prevention and treatment of cardiovascular diseases, heart failure has caused the heavy economic burden to society and joined the rank of grievous public health problems. So far, pharmacotherapy aiming at blocking the renin angiotensin aldosterone system and sympathetic nervous system is

the cornerstone in the treatment of heart failure. And new drugs have earned a place, such as angiotensin receptor neprilysin inhibitor (ARNI) and sodium glucose cotransporter two inhibitor (SGLT2i) (McDonagh et al., 2021). Although great progress has realized in the prevention and treatment of heart failure, the overall prognosis is still poor, and the 5-year survival rate is equivalent to that of some malignant tumors (Stewart et al., 2001). Exploring effective and thorough strategy for the treatment of heart failure remains to be done.

Traditional Chinese Medicine, based on the concept of holism, differentiates syndromes and gives treatment in a Multi-target and individualized way, and its advantages lie in increasing exercise tolerance, improving the quality of life, elevating cardiac function, delaying myocardial remodeling, reducing mortality and rehospitalization rates (Zhang and Li, 2014; Sun et al., 2016). Shengmai Powder, first described in a classic named '*Yi Xue Qi Yuan*', is composed of Radix of *Panax ginseng* C.A. Mey. (Araliaceae), Radix of *Ophiopogon japonicus* (Thunb.) Ker Gawl (Liliaceae), and Fructus of *Schisandra chinensis* (Turcz.) Baill (Schisandraceae), which has effects of replenishing qi, recovering pulse, nourishing yin, and promoting body fluid production (Zhang, 1978). It is commonly applied in the treatment of heart failure, coronary heart disease, hypertension, and viral myocarditis (Wu, 1997). Chinese patent medicines derived from Shengmai Powder include YiQiFuMai injection (YQFM), Shengmai injection, Shenmai injection, Shengmai San, Shengmai Yin, Shengmai capsule, *etc.* Studies have demonstrated the cardioprotective effects of Shengmai-related formulas, inccluding improving cardiac function, ameliorating ventricular remodeling, suppressing inflammation, reducing collagen deposition, and inhibiting apoptosis (Cao Z. H. et al., 2019; Yin et al., 2020).

YQFM, the product of Traditional Chinese Medicine combined with modern pharmaceutical technology, not only retains the effecy of Shengmai Powder, but also takes effect more quicky (Du et al., 2021). It is the only powder injection traditional Chinese medicine cardiotonic approved for listing by the state at present (Fu et al., 2020). YQFM is mainly comprised of Radix of *Panax ginseng* C.A. Mey. (Araliaceae), Radix of *Ophiopogon japonicus* (Thunb.) Ker Gawl (Liliaceae), and Fructus of *Schisandra chinensis* (Turcz.) Baill (Schisandraceae). Modern pharmacological studies have shown that, as the main active substance of Radix of *Panax ginseng* C.A. Mey. (Araliaceae), ginsenosides effectively inhibited myocardial hypertrophy, improved myocardial ischemia, promoted vascular regeneration and inhibited apoptosis (Wang W. et al., 2016). Research has found that Radix of *Ophiopogon japonicus* (Thunb.) Ker Gawl (Liliaceae) guarded cardiovascular system by resisting myocardial ischemia, arrhythmia, thrombosis and improving microcirculation (Fan et al., 2020). The study showed that Fructus of *Schisandra chinensis* (Turcz.) Baill (Schisandraceae) acted on various signal pathways to protect myocardial cells from inflammation, apoptosis, oxidative stress, atherosclerosis and other advert effects (Xing et al., 2021). Therefore, YQFM can improve heart function and alleviate heart failure by reducing myocardial ischemia-reperfusion injury, antioxidant stress, regulating ventricular remodeling, and reducing the release of inflammatory factors (Ju et al., 2018). In clinical practice, it is mainly used for the treatment of heart failure, coronary heart disease, angina pectoris and other cardiovascular diseases (Zhang et al., 2021). In 2007, China Food and Drug Administration approved YQFM for the treatment of cardiovascular diseases, including coronary heart disease, exertional angina pectoris and chronic cardiac insufficiency. And YQFM is recommended for acute exacerbation of heart failure in the 'expert consensus on diagnosis and treatment of chronic heart failure with integrated traditional Chinese and Western medicine' (Chinese Association of Integrative Medicine, 2016). Research has showed that YQFM significantly reduced the level of N-terminal pro-B-type natriuretic peptide (NT-proBNP), improved cardiac function, and relieved symptoms and signs in patients with acute heart failure (Wang et al., 2021). This review summarized the components, mechanisms and clinical evidences of YQFM in the treatment of heart failure in order to provide a theoretical basis for clinical practice.

1.1 Chemical components of YiQiFuMai injection in the treatment of heart failure

YQFM is mainly comprised of Radix of *Panax ginseng* C.A. Mey. (Araliaceae), Radix of *Ophiopogon japonicus* (Thunb.) Ker Gawl (Liliaceae), and Fructus of *Schisandra chinensis* (Turcz.) Baill (Schisandraceae). Triterpene saponins are the main components of Radix of *Panax ginseng* C.A. Mey. (Araliaceae). In addition, steroidal saponins, flavonoids, and carbohydrates are the main components of Radix of *Ophiopogon japonicus* (Thunb.) Ker Gawl (Liliaceae) while lignans compounds are the main components of Fructus of *Schisandra chinensis* (Turcz.) Baill (Schisandraceae) (Table 1). With the development of analytical methods such as high-performance liquid chromatography (HPLC), liquid-mass spectrometry (LMS) and metabolomics, these new technologies have been applied to explore the chemical components of YQFM. For instance, Zhou et al. have identified the components of QYFM with the help of liquid chromatography electrospray ionization mass spectrometry (LC-ESI-MS), including ginsenoside Rf, Rb1, Rb2, Rb3, Rd, Rg3, 20 (S), ginsenoside F2, and Schisandrin B (Zhou et al., 2009). Liu et al. have identified 21 saponins in YQFM by HPLC coupled with quadrupole time-of-flight tandem mass spectrometry (HPLC-Q-TOF-MS), and among them, 13 saponins were reported for the first time (Liu et al., 2018). Furthermore, Wang et al. have determined the contents of fructose, glucose, sucrose, and maltose in YQFM by HPLC-evaporative light scattering and electrospray (Wang Y. et al., 2020). Liu et al. not only identified 65 compounds of YQFM by ultrafast liquid

TABLE 1 Chemical components of YiQiFuMai injection.

Types	Components	Ref
Triterpenoid saponins	Ginsenoside Rf, Ginsenoside Rb_1, Ginsenoside Rb_2, Ginsenoside Rb_3, Ginsenoside Rg_3, Ginsenoside Rd, 20(S)-ginsenoside F_2, 20-glc-Ginsenoside Rf, Notoginsenoside R_1, Ginsenoside Re, Ginsenoside Ra_3, Ginsenoside F_3, Ginsenoside Ra_1, Ginsenoside Rg_1, Ginsenoside Rg_2, Ginsenoside Rh_1, Ginsenoside Rc, Ginsenoside Rd, Notoginsenoside R_2, S-Ginsenoside Rg_2, S-Ginsenoside Rg_3, R-Ginsenoside Rg_3, S-Ginsenoside Rs_3, Ginsenoside F_1, Ginsenoside F_2, Ginsenoside Ro, Saponin Rb-2, Chikusetsu saponin Iva, ManoylGinsenoside, S-Ginsenoside Rh_2, R-Ginsenoside Rh_2, et al	Zhou et al. (2009) Liu et al. (2018); Liu et al. (2016); Zhou et al. (2018); Zhou et al. (2011); Zhang et al. (2018); Zheng et al. (2018)
Steroidal saponins	Ophiopojaponin C, Ophiopojaponin B, Ophiopojaponin E, Ophiopojaponin Ra, Ophiopojaponin A, 14-hydroxyophiopojaponin C, Ophiogenin-3-O-α-L-rhamnopyranosyl-(1→2)-β-D-glucopyranoside, Ophiogenin-3-O-α-L-rhamnopyranosyl-(1→4)-β-D- xylopyranosyl-(1→4)-β-D-glucopyranoside, Pennogenin-3-O-α-L-rhamnopyranosyl-(1→2)-β-D-xylopyranosyl-(1→4)-β-D-glucopyranoside, et al	Liu et al. (2018); Liu et al. (2016); Zhou et al. (2018)
Lignans	Schizandrol A, Schizandrol B, Gomisin D, Gomisin M_1, Gomisin N, g-schizandrol, Gomisin E, Gomisin S, Tigloylaomisin H, Isoschizandrol, Schisantherin A, Schizantherin B, Schizantherin C, Benzoylgomisin Q, Gomisin O, Gomisin L_1, Gomisin F, Gomisin J, Gomisin K_1, et al	Zhou et al. (2009); Liu et al. (2018); Liu et al. (2016); Zhou et al. (2018); Zhang et al. (2018)
Flavones	Ophiopogonone E, Ophiopogonone B, 6-aldehydo-isophiopogonone, Ophiopogone A, Ophiopogonanone A, Methylophiopogonone A, Methylophiopogonone B, 2′-hydroxyisoophiopogonin A, et al	Liu et al. (2016); Zhou et al. (2018)
Sugars	Fructose, Glucose, Sucrose, Maltose, et al	Wang Y. et al. (2020)

chromatography-ion trap time-of-flight MS (UFLC-IT-TOF/MS) but also quantitatively analyzed 21 compounds, including three Ophiopogon japonicus, 15 ginsenosides, and three lignans (Liu et al., 2016). Zhou et al. have determined 145 compounds of YQFM by ultra-performance liquid chromatography coupled with quadrupole time-of-flight tandem mass spectrometry (UPLC-Q-TOF/MS), including 20 flavonoids, 24 lignans, 27 saponins, 15 carbohydrates, 38 organic acids, and 22 sterols, peptides, and esters (Zhou et al., 2018). Additionally, using saikosaponin A as the internal reference, Zhou et al. detected nine ginsenosides in the plasma of Wistar rats after the intravenous injection of YQFM by LC-electrospray ionization (ESI)-MS (Zhou et al., 2011). Zhang et al. reported eight ginsenosides and four lignans detected by LC-ESI-MS/MS in the plasma of Beagle dogs after intravenous injection of YQFM (Zhang et al., 2018). According to the research of Zheng et al., 10 ginsenosides were identified by UFLC-MS/MS in the plasma of rats with chronic heart failure after the intervention of YQFM (Zheng et al., 2018). From the view of chemical components, pharmacodynamics, network pharmacology, pharmacokinetics, and properties, Li et al. has demonstrated quality markers of YQFM, including ginsenosides (Rb1, Rg1, Rf, Rh1, Rc, Rb2, Ro, and Rg3), Ophiopogon saponin C, phiogenin-3-O-α-L-rhamnopyranosyl-(1→2)-β-D-glucopyranoside, pennogenin-3-O-α-L-rhamnopyranosyl-(1→2)-β-D-xylopyranosyl-(1→4)-β-D-glucopyranoside, fructose, and schisandrin, representing the transfer and change of main substances during the preparation of YQFM, which are the main medicinal chemical components of YQFM (Li D. K. et al., 2019).

1.2 Action mechanisms of YiQiFuMai injection in the treatment of heart failure

Heart failure is a chronic and progressive disease, and myocardial remodeling is a critical factor in the initiation and progression of heart failure.

1.2.1 Improving cardiac function

In HF mice induced by the permanent coronary artery ligation (CAL) with the intervention of YQFM for 2 weeks (0.13 g/kg, 0.26 g/kg, and 0.53 g/kg) showed that YQFM (0.53 g/kg) improved left ventricular function and ameliorated structural injury. It was reported that YQFM restrained the activity of serum lactic dehydrogenase (LDH) and creatine kinase (CK), lowered the levels of serum malondialdehyde (MDA), amino-terminal pro-peptide of pro-collagen type III (PIIINP), NT-proBNP, and myocardial hydroxyproline (HYP). And YQFM appears to reduce oxidation stress, suppress myocardial collagen deposition and fibrosis, and ameliorate cardiac remodeling by the of the blocking effect on mitogen-activated protein kinases (MAPKs) signaling pathway (Pang et al., 2017). Wistar rats were subjected to abdominal aortic coarctation to establish a chronic heart failure model. And the indications for successful modeling was determined by LVEF% ≤ 60% at 8 weeks after the operation. After 14 days of continuous treatment with YQFM (520, 260 and 1,040 mg/kg), the results indicated that YQFM increased the left ventricular posterior wall in the systolic (LVPWs), ejection fraction (EF), fractional shortening (FS), reduced left ventricular end-systolic diameter (LVESD), the levels of serum brain natriuretic peptide (BNP) and

copeptin (CPP), whereby improving cardiac function and delaying ventricular remodeling in rats (Zhang et al., 2015).

1.2.2 Reducing myocardial injury

SD rats were given the intervention of YQFM (0.28, 0.55 and 1.10 g/kg) *via* tail vein injection for 7 days followed by the intraperitoneal injection of doxorubicin (25 mg/kg) for 5 days to establish acute myocardial injury model. The results manifested that YQFM alleviated doxorubicin-induced myocardial injury and improved cardiac function in rats by reducing the serum levels of LDH, CK, and AST, decreasing left ventricular end-diastolic diameter (LVEDD), and elevating FS (Wang XD. et al., 2020). Vitro experiment has also confirmed the cardioprotective effects of YQFM that the application of YQFM (5 mg/ml) boosted the viability of H9c2 cells exposed to H_2O_2 (0.2 mmol/L, 5 h) (Li et al., 2020).

1.2.3 Improving mitochondrial function

ICR mice were treated with different concentrations of YQFM (0.13, 0.26 and 0.53 g/kg, intraperitoneal) for 2 weeks after CAL. The results showed that YQFM redressed mitochondrial dysfunction by normalizing mitochondrial morphology, increasing mitochondrial membrane potential ($\Delta\psi m$), inhibiting the generation of reactive oxygen species (ROS), up-regulating the expression of mitochondrial fusion protein 2 (Mfn2), and reducing the phosphorylation of dynamin-related protein 1 (Drp1), which was related to reduction in NADPH oxidase 2 (NOX2), $p67^{phox}$, NOX4, calcium voltage-gated channel subunit α1C (CACNA1C) and phosphorylation of calmodulin dependent protein kinase II (p-CaMKII) (Zhang et al., 2019).

1.2.4 Ameliorating myocardial apoptosis

In HF mouse models induced by CAL, after the intraperitoneal injection of YQFM (0.13 g/kg, 0.26 g/kg, 0.53 g/kg) for 14 days, the results showed that the levels of serum creatine kinase-MB (CK-MB), aspartate aminotransferase (AST), interleukin-6 (IL-6), troponin, myosin, and myoglobin were down-regulated, and the omentin level elevated. And the study indicated that YQFM improved left ventricular systolic function and suppressed apoptosis on account of boosting the expression of phosphatidylinositol 3-kinase (PI3K), the phosphorylation of protein kinase B (Akt) and adenine monophosphate activated protein kinase (AMPK) and inhibiting the phosphorylation of p38, C-Jun Kinase enzyme (JNK), and extracellular signal-regulated kinase 1/2 (ERK1/2) (Li F. et al., 2019). *In vitro* experiments, compared with the control group, namely injured H9c2 cells induced by doxorubicin (0.3 μmol/L), the intervention of YQFM (125, 625, 3,125 μg/ml) reduced cytotoxicity, increased cell viability, inhibited the activity of LDH, elevated adenosine triphosphate (ATP) content and restored mitochondrial membrane potential, which played an anti-apoptotic effect (Zeng et al., 2018). Furthermore, the application of YQFM(2.5 mg/ml) on H9c2 cells significantly boosted cell viability and ATP content in apoptotic cells induced by tert-butyl hydroperoxide, and enhanced the phosphorylation of Akt. It also ameliorated the extent of hypertrophy in H9c2 cells induced by angiotensin II (0.1 μM) and elevated the expression of atrial natriuretic peptide (ANP) mRNA (Zhao C. et al., 2018).

1.2.5 Suppressing inflammatory mediators

In chronic heart failure models induced by the ligation of rats' left anterior descending coronary artery, after the treatment of YQFM (100 mg/kg/d) for 8 weeks, UPLC-Q-TOF-MS combined with nuclear factor kappa-B (NF-κB) active luciferase reporter analyzed potential anti-inflammatory components. It was further demonstrated that YQFM reduced the size of myocardial infarction, improved cardiac function, and inhibited the expression of inflammatory cytokines, such as tumor necrosis factor-alpha (TNF-α), NF-κB, IL-6, and interleukin-1β (IL-1β). And eight potential anti-inflammatory components have been confirmed, including ginsenosides Rb1, Rg1, Rf, Rh1, Rc, Rb2, Ro and Rg3 (Xing et al., 2013).

1.2.6 Anti-hypoxia effect

To investigate the anti-hypoxia effect of the extraction of YQFM, an animal model of chronic intermittent hypoxia was constructed, treated with YQFM (1.4, 2.8, and 5.5 g/kg/d) for 28 days, and betaloc (0.1516 g/kg/d) served as the positive control. The results manifested that YQFM reversed endothelial cell swelling and cardiac vacuolation, improved myocardial hypoxia tolerance and attenuated myocardial damage by increasing EF and stroke volume (SV), inhibiting the activity of CK and LDH, reducing MDA content, and boosting superoxide dismutase (SOD) (Feng et al., 2016).

1.2.7 Anti-oxidative effect

In ICR mice that were given intraperitoneal injection with isoproterenol (0.02 g/kg/d) for 3 days followed by YQFM (1.352, 0.676 and 0.338 g/kg/d), the results showed that the serum levels of MDA, CK, and LDH and the activity of myeloperoxidase (MPO) decreased, while the serum SOD level elevated, indicating that YQFM exerted great cardioprotective effect (Wang et al., 2013).

1.2.8 Maintaining the balance of matrix metalloproteinases/tissue inhibitor of metalloproteinases

In Wistar rats with chronic heart failure that underwent abdominal aorta contraction, after the intervention of QYFM (520 mg/kg, 260 mg/kg, 1,040 mg/kg) for 14 days, there were significant changes of contents in myocardium, including MMP-2, MMP-3, MMP-9, TIMP-1, TIMP-2. The study reported that YQFM decreased the levels of MMP-2, MMP-3,

TABLE 2 Myocardial protective effects and mechanisms of YiQiFuMai injection.

Models	Animal/ cell	Effects	Mechanisms	Ref
CAL	ICR mice	Improving cardiac function	LDH, CK, MDA, PIIINP, NT-proBNP, HYP↓ Inhibiting the MAPKs signaling pathways	Pang et al. (2017)
CAL	ICR mice	Improving mitochondrial function	p-Drp1, NOX2, $p67^{phox}$, NOX4, CACNA1C, p-CaMKII, ROS↓ Mfn2↑	Zhang et al. (2019)
CAL	ICR mice	Ameliorating myocardial apoptosis	p-p38, p-JNK, p-ERK1/2↓ PI3K, p-Akt, p-AMPK↑	Li F. et al. (2019)
CAL	SD rat	Suppressing inflammatory mediators	TNF-α, NF-κB, IL-6, IL-1β↓	Xing et al. (2013)
CAL	Wistar rat	Regulating the expression of miRNAs	miR-219a-2-3p, miR-466c-5p, miR-702-5p↓ miR-21-3p, miR-216b-5p, miR-381-3p, miR-542-3p↑	Zhao Y. et al. (2018)
Abdominal aortic banding	Wistar rat	Improving cardiac function	LVIDs, BNP, CCP↓ LVPWs, LVEF, LVFS↑	Zhang et al. (2015)
Abdominal aortic banding	Wistar rat	Improving ventricular remodeling	MMP-2, MMP-3, MMP-9↓ TIMP-1, TIMP-2↑	Zhang et al. (2016)
Chronic intermittent hypoxia	ICR mice	Anti-hypoxia	CK, LDH, MDA↓ EF, SV, SOD↑	Feng et al. (2016)
Adriamycin	SD rat	Reducing myocardial injury	CK, LDH, AST, LVEDD↓ FS↑	Wang X. D. et al. (2020)
Isoprenaline	ICR mice	Anti-oxidative	CK, LDH, MDA, MPO↓ SOD↑	Wang et al. (2013)
H_2O_2	H9c2 cells	Protecting myocardial cells	Cell survival rate↑	Li et al. (2020)
Adriamycin	H9c2 cells	Anti-apoptosis	LDH, Caspase-3↓ Cell survival rate, ATP↑	Zeng et al. (2018)
Angiotensin II	H9c2 cells	Anti-hypertrophy	Surface area of cells, ANP↓	Zhao Y. et al. (2018)
Tert-butyl hydroperoxide	H9c2 cells	Anti-apoptosis	Cell survival rate, ATP, p-Akt↑	Zhao Y. et al. (2018)

Note: ANP, atrialnatriureticpeptide; AST, spartate aminotransferase; ATP, adenosinetriphosphate; BNP, brain natriuretic peptide; CACNA1C, calcium voltage-gated channel subunit α1C; CAL, coronary artery ligation; CK, creatine kinase; CPP, copeptin; EF, ejection fractions; FS, fractional shortening; HYP, hydroxyproline; ICR, institute of cancer research; IL-1β, interleukin-1β; IL-6, interleukin-6; LDH, lactate dehydrogenase; LVEDD, left ventricular end-diastolic diameter; LVEF, left ventricular ejection fraction; LVFS, left ventricular fractional shortening; LVIDs, left ventricular internal diameter in end systole; LVPWs, left ventricular posterior wall in the systolic; MAPKs, mitogen-activated protein kinases; MDA, malondialdehyde; Mfn2, Mitofusin-2; MMP, matrix metalloproteinases; MPO, myeloperoxidase; NADPH, nicotinamide adenine dinucleotide phosphate; NF-κB, nuclear factor kappa-B; NOX2, NADPH, oxidase 2; NOX4, NADPH, oxidase4; NT-proBNP, N-terminal pro-B-type natriuretic peptide; p-Akt, p-protein kinase B; p-AMPK, p-adenine monophosphate activated protein kinase; p-CaMKII, phosphorylation of calmodulin dependent protein kinase II; p-Drp1, phosphorylation of dynamin-related protein 1; p-ERK1/2, p-extracellular signal-regulated kinase 1/2; PI3K, phosphatidylinositol 3-kinase; PIIINP, amino-terminal pro-peptide of pro-collagen type III; p-JNK, p-C-Jun Kinase enzyme; ROS, reactive oxygen species; SOD, superoxide dismutase; SV, stroke volume; TIMP, tissue inhibitor of metalloproteinases; TNF-α, tumor necrosis factor-alpha.

and MMP-9, and elevated the levels of TIMP-1 and TIMP-2, whereby improving cardiac function and delaying ventricular remodeling (Zhang et al., 2016).

1.2.9 Regulating the expression of miRNAs

In chronic heart failure models established by the ligation of rats' the left anterior descending coronary artery, after the administration of YQFM (YQFM, 5 mg/kg/d, ip) for 28 days, the differential expression of microRNAs was studied *via* rat miRNA microarray and bioinformatics analysis. And the results manifested that YQFM increased left ventricular ejection fraction (LVEF) and left ventricular fractional shortening (LVFS), decreased left ventricular diameter, and boosted cardiac output (CO) by down-regulating the expression of miR-219a-2-3p, miR-466c-5p, and miR-702-5p, and up-regulating the expression of miR-21-3p, miR-216b-5p, miR-381-3p, and miR-542-3p (Zhao Y. et al., 2018).

Taken together, YQFM reveals great efficacy on delaying myocardial remodeling and improving cardiac function in injured myocardium induced by coronary artery ligation, abdominal aortic constriction, chronic intermittent hypoxia, and doxorubicin. The underlying mechanisms lie in the regulation of mitochondrial function, anti-apoptotic effect on cardiomyocytes, anti-oxidative effect, anti-inflammation, the modulation of the expression of miRNAs, maintenance of MMP/TIMP balance, and anti-hypoxic effect (Table 2).

1.3 Clinical evidences of YiQiFuMai injection in the treatment of heart failure

1.3.1 Clinical trials

A clinical study involving 1,134 patients with coronary heart disease and heart failure performed by 35 research centers, who were treated with YQFM (5.2 g/d) for 14 days, revealed that the application of YQFM on routine treatment for heart failure contributed to the reduction of Lee's heart failure score, Minnesota heart failure quality of life score, and cardiothoracic ratio, elevated SV, CO, EF, and FS, and decreased LVESD. Therefore, YQFM exerted great efficacy on improving the cardiac pumping performance and quality of life of patients and reversing ventricular remodeling (Sun et al., 2012). In addition, research has evaluated the clinical efficacy of YQFM combined with western medicine *via* stress echocardiography. A study involving 52 patients with ischemic heart failure showed that, compared with the conventional treatment group, YQFM combined with conventional treatment increased EF and early diastolic peak flow velocity/late diastolic peak flow velocity (E/A) value and reduced early mitral filling velocity/early diastolic mitral annular velocity (E/e') ratio and NT-proBNP levels, indicating that YQFM could improve cardiac function (Hu et al., 2014). Two randomized controlled trials concerning 60 elderly patients with chronic heart failure have illustrated that YQFM combined with basic treatment effectively reduced serum NT-proBNP levels and increased EF and 6-min walking distance (6 MWD) compared to basic treatment alone, suggesting the positive effects of YQFM on cardiac function and exercise tolerance (Zhang et al., 2015; Yang et al., 2016). In another randomized controlled trial involving 108 patients with ischemic cardiomyopathy and heart failure, the treatment group was given YQFM combined with Qiliqiangxin Capsules, while the control group was given Qiliqiangxin Capsules alone. And the results manifested that the application of YQFM lowered serum NT-proBNP levels and elevated EF, CO, and 6 MWD, indicating that YQFM combined with Qiliqiangxin Capsules enhanced clinical efficacy, improved clinical symptoms, and promoted the recovery of cardiac function (Jiang et al., 2018). In a study including 103 patients with chronic heart failure and atrial fibrillation, based on the conventional treatment, the control group was given rosuvastatin while the treatment group was given rosuvastatin and YQFM. Compared to the control group, there were significant improvement of cardiac function and 6 MWD performance, increased FS and EF, and reduction in the level of NT-proBNP, LVEDD, the recurrence rate of atrial fibrillation, and risk of permanent atrial fibrillation in the treatment group (Su and Wang, 2018). In a randomized controlled trial of 118 patients with coronary heart disease and chronic heart failure, the application of YQFM combined with atorvastatin improved cardiac function and delayed ventricular remodeling by decreasing LVEDD, lowering the levels of NT-proBNP, soluble CD40 (sCD40) and soluble CD146 (sCD146), and increasing nitric oxide (NO) levels (Li Y. et al., 2019). Furthermore, in a randomized controlled study involved 40 patients who underwent cardiac valve replacement surgery, based on the cardiac rehabilitation, the treatment group received YQFM immediately after surgery. And the results showed that YQFM effectively improved exercise tolerance and 6 MWD performance (Zhang et al., 2020).

Collectively, YQFM exerts great efficacy in the treatment of heart failure, including improving cardiac function, inhibiting ventricular remodeling, and elevating the quality of life. However, the quality of clinical trials of YQFM in the treatment of heart failure remains relatively low. Thus large-sample, multi-center, randomized controlled trials and real world research are vital to provide the evidence-based data (Table 3).

1.3.2 Meta-analyse and systematic reviews

Meta-analysis evaluating clinical efficacy of YQFM combined with conventional western medicine in the treatment of heart failure has revealed that the intervention of YQFM increased EF, CO and 6 MWD, shortened LVEDD and LVESD, and reduced the serum levels of NT-proBNP and BNP, suggesting that on the basis of conventional western medicine treatment, YQFM further improved cardiac function and the quality of life (Wang XL. et al., 2016; Lian et al., 2016; Zhou et al., 2016; Xiong et al., 2017; Xie and Dai, 2019; Fan et al., 2021). Whereas, lacking of the calculation of sample size, details concerned the western medicine treatment and endpoint indicators, unclear random method, and non-uniform dosages and periods of YQFM weaken the quality of the clinical evidence (Table 4).

1.4 Safety of YiQiFuMai injection in the treatment of heart failure

Li *et al.* analyzed 240 patients with coronary heart disease who received YQFM in retrospect, and the results showed that none of the patients had the symptoms or signs of hepatic and renal injury. It was merely reported one case of pharyngeal pain with the injection of YQFM infusion, and the symptom subsided gradually after the withdrawn of YQFM (Li et al., 2018). An analysis involving 998 patients treated with YQFM (>70 years old accounting for 50.69%) exhibited that the incidence of untoward effects was 0.2%, and most of these symptoms and signs were transient without additional treatment (Li K. et al., 2019). Wang *et al.* analyzed the safety of YQFM on 106 elderly patients (≥80 years old) with cardiovascular diseases, and it was found that YQFM had little impact on the levels of serum alanine aminotransferase (ALT), AST, total bilirubin (TBil), and creatinine (Cr), and only one case (accounting for 0.94%) reported mild palpitation and precordial discomfort (Wang et al., 2018). Sun *et al.* retrospectively analyzed the performance of YQFM on 2,476 hospitalized patients by the prescription automatic screening system. The study reported that 31 cases had adverse reactions (accounting for 1.25%) that mainly manifested as general damage and skin lesion, such as rash, pruritus,

TABLE 3 Clinical trials of YiQiFuMai injection in the treatment of heart failure.

Studies	Control	Treatment	Doses	Periods	Results
Self Controlled Trial					
Sun et al. (2012)		n = 1,134	5.2 g	14 d	LVESD, cardiothoracic ratio, Lee's heart failure score, Minnesota heart failure score↓ SV, CO, LVEF, LVFS↑
Hu et al. (2014)		n = 52	5.2 g	14 d	LVEF, E/A↑ NT-proBNP, E/e'↓
Randomized Controlled Trial					
Zhang P. (2015)	n = 30	n = 30	5.2 g	14 d	NT-proBNP↓ LVEF, 6 MWD↑
Yang et al. (2016)	n = 30	n = 30	5.2 g	14 d	NT-proBNP↓ LVEF↑
Jiang et al. (2018)	n = 54	n = 54	5.2 g	14 d	NT-proBNP↓ LVEF, CO, 6 MWD↑
Su and Wang, (2018)	n = 51	n = 52	2.6–3.9 g	14 d	LVFS, LVEF, 6 MWD↑ NT-proBNP, LVEDD↓
Li Y. et al. (2019)	n = 59	n = 59	5.2 g	14 d	LVEDD, NT-proBNP, sCD40, sCD146, PAPP-A↓ NO↑
Zhang et al. (2020)	n = 20	n = 20	5.2 g	(9.05 ± 2.74)d	6 MWD↑

Note: CO, cardiac output; E/A, early diastolic peak flow velocity/late diastolic peak flow velocity; E/e', early mitral filling velocity/early diastolic mitral annular velocity; LVEDD, left ventricular end diastolic inner diameter; LVESD, left ventricular end systolic diameter; LVEF, left ventricular ejection fraction; LVFS, left ventricular fractional shortening; NT-proBNP, N-terminal pro-B-type natriuretic peptide; NO, nitric oxide; PAPP-A, pregnancy associated plasma protein-A; sCD146, soluble CD146; sCD40, soluble CD40; SV, stroke volume; 6 MWD, 6-min walking distance.

TABLE 4 Meta-analyse and systematic reviews of YiQiFuMai injection in the treatment of heart failure.

Studies	Populations	Control	Treatment	Outcome indicators	Clinical efficacy
Wang Y. et al. (2016)	Chronic heart failure	893	1,046	Clinical comprehensive efficacy, NYHA classification, LVEF, LVEDD, NT-proBNP	OR = 3.63 95%*CI* (2.22, 5.93)
Lian et al. (2016)	Heart failure	493	508	Clinical comprehensive efficacy, LVEF, LVESD, CO, NT-proBNP, 6 MWD	OR = 3.09 95%*CI* (2.05, 4.67)
Zhou et al. (2016)	Heart failure	433	446	Overall effective rate, LVEF, LVEDD, BNP	OR = 4.45 95%*CI* (2.62, 7.56)
Xiong et al. (2017)	Heart failure	1,180	1,201	Overall effective rate, LVEF, LVEDD, CO, BNP, 6 MWD	OR = 2.96 95%*CI* (2.23, 3.94)
Xie and Dai, (2019)	Heart failure	961	976	Clinical comprehensive efficacy, LVEF, LVEDD, 6 MWD, NT-pro BNP, BNP	RR = 3.06 95%*CI* (2.27, 4.12)
Fan et al. (2021)	Heart failure	1,475	1,502	Clinical comprehensive efficacy, LVEF, BNP, NT-proBNP, E/A ratio, CO, LVEDD, 6 MWT	RR = 1.21 95%*CI* (1.16, 1.25)

Note: BNP, B-type natriuretic peptide; CO, cardiac output; LVEDD, left ventricular end diastolic inner diameter; LVEF, left ventricular ejection fraction; LVESD, left ventricular end systolic diameter; NT-pro BNP, N-terminal pro-B-type natriuretic peptide; 6 MWD, 6-min walking distance.

chills, high fever, *etc.* Additionally, most adverse reactions occurred within 7 days after the medication (Sun et al., 2019). Cao *et al.* conducted a prospective, large-sample, multi-center analysis involving 44 medical institutions, including 10,767 hospitalized patients treated with YQFM. The research reported 19 cases of adverse reactions (0.176%), and among them, skin lesion was the main one (36.98%). At the same time, it seemed that adverse reactions were more common in the group with higher infusion rate ($p < 0.05$), indicating that immoderate infusion rate was one of the risk factors for untoward effects (Cao H. B. et al., 2019). Ma *et al.* analyzed 51 pieces of clinical research involving 7,824 patients who were given YQFM. There were no serious adverse event, and only 23 study mentioned 42 cases of mildly untoward effects in total. Among them, adverse cardiovascular events, adverse neural damage,

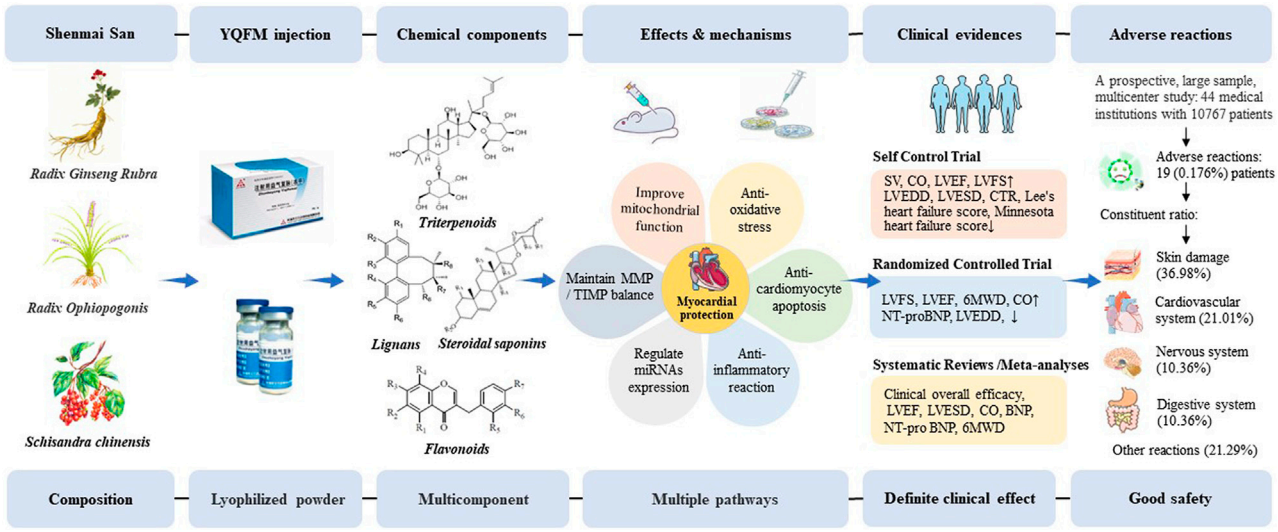

FIGURE 1
The process of YQFM in treating heart failure. BNP, brain natriuretic peptide; CO, cardiac output; CTR, calcitonin receptor; LVEDD, left ventricular end-diastolic diameter; LVEF, left ventricular ejection fraction; LVESD, left ventricular end-systolic diameter; LVFS, left ventricular fractional shortening; MMP/TIMP, matrix metalloproteinases/tissue inhibitor of metalloproteinases; NT-proBNP, N-terminal pro-B-type natriuretic peptide; SV, stroke volume; 6MWD, 6-min walking distance.

skin lesion, and gastrointestinal reactions accounted for 28.6%, 20.4%, 22.5%, and 20.3% respectively (Ma et al., 2015). *In vitro* experiments, YQFM not only inhibited the autonomic contraction of the isolated intestine, but also supressed the spasm of isolated intestine triggered by acetylcholine (Ach) and histamine (His). *In vivo* experiments the blue staining rate and the levels of His and 5-hydroxytryptamine (5-HT) in mice administered with low-dose YQFM were within the normal range without evident pulmonary injury and auricularinfection. By contrast, only when the mice were given 3.43 times the clinical equivalent dose of YQFM, there were mild increase in the blue staining rate and the levels of His and 5-hydroxytryptamine (5-HT) and inflammation, indicating that YQFM had few allergic reactions within a proper dosage range (Gu et al., 2018). Clinical studies have also verified that adverse reactions of YQFM mainly correlated with inappropriate prescription, including beyond indications and dosages, unnecessary treatment, contraindications, and excessive quantities of solvent, etc (Zhao C. et al., 2018). Though YQFM reveals great safety and efficacy, it is worth noting that following the instructions strictly is the key to avoid adverse events.

2 Conclusion

Heart failure, the cumulative effect and endpoint of various cardiac abnormalities, eventually leads to the decline of cardiac pump function, putting up with the challenge to the exploration of effective strategy for the prevention and treatment of heart failure (Committee of Exports on Rational Drug Use National Health and Family Planning Commission of The People'Republic of China and Chinese Pharmacists Association, 2019). Long-term clinical practice verified that Traditional Chinese medicine exerts the composite effect through the multi-target and multi-link ways (Zhang RP., 2015). At present, there are plenty of fundamental research and clinical trials on YQFM, involving pharmacodynamic components, pharmacological effects, clinical application and quality markers. Research has demonstrated that YQFM improved cardiac function, inhibited ventricular remodeling, exerted great anti-inflammatory and anti-oxidative effect, regulated mitochondrial function, thereby improving the quality of life of patients with heart failure (Du et al., 2021). YQFM is widely used in the treatment of heart failure, with definite clinical efficacy and fewer adverse reactions, which provides a reference for rational clinical drug use (Figure 1).

However, there are great gaps referring to the dose-effect relationship, pharmacological targets and mechanism of YQFM in the treatment of cardiovascular diseases waiting to be filled in. The multi-component and multi-target characteristics of Traditional Chinese Medicine raise the bar for the exploration of pharmacological mechanism of YQFM in the treatment of heart failure. At present, the pharmacological effects of different components of YQFM on heart failure remains unclear, and the research merely focuses on the study of ginsenosides. However, there are few studies on the pharmacological effects, mechanisms and targets of the two traditional Chinese medicines of Radix of *Ophiopogon japonicus* (Thunb.) Ker Gawl (Liliaceae), and Fructus of *Schisandra chinensis* (Turcz.) Baill (Schisandraceae), as well as the important active components of Ophiopogonins,

Ophiopogon japonicus polysaccharide and Schizandrin A. What's more, in some studies the dosage of YQFM is not adaptive for the clinical treatment, resulting in the mismatch between clinical practice and basic science. In the future, research ought to reveal the targets and related signaling pathways of YQFM and differ active components so as to provide scientific guidance for the application of YQFM in clinical practice. Besides, owning to the relatively low quality of clinical trials on YQFM in the treatment of heart failure, large-scale, multi-center, high-quality randomized controlled clinical trials and real world studies are badly in need. Finally, although there are few reports about the adverse effects of YQFM, non-standard prescription still an annoying epidemic in the clinical practice. Therefore, it is necessary to improve the legal system of drug reevaluation and the post-marketing supervision to guard the safety and efficacy of the application of drugs, so as to improve the efficacy of YQFM in the treatment of heart failure.

Author contributions

SL wrote the manuscript. YW and WZ searched and reviewed literature. HS conceived and designed the manuscript.

Funding

This work was supported by the China Postdoctoral Science Foundation (2022M710473) and National Key R&D Program of China (2017YFC1700400).

Conflict of interest

The authors declare that the research was conducted in the absence of any commercial or financial relationships that could be construed as a potential conflict of interest.

Publisher's note

All claims expressed in this article are solely those of the authors and do not necessarily represent those of their affiliated organizations, or those of the publisher, the editors and the reviewers. Any product that may be evaluated in this article, or claim that may be made by its manufacturer, is not guaranteed or endorsed by the publisher.

References

Cao, H. B., Hao, C. Y., Bi, J. F., Luo, R. Z., Xie, A. L., Xie, W., et al. (2019). Clinical safety monitoring study of yiqi fumai lyophilized injection. *Drug Eval. Res.* 42, 467–471. doi:10.7501/j.issn.1674-6376.2019.03.015

Cao, Z. H., Pan, J. H., Li, N., Qu, X. B., and Han, D. (2019). Modern pharmacological effect and mechanism of Shengmai san. *Chin. J. Exp. Tradit. Med. Form.* 25, 212–218. doi:10.13422/j.cnki.syfjx.20192208

Chinese Association of Integrative MedicineDoctor Society of integrative MedicineChinese Medical Doctor Association (2016). Expert consensus on Integrated Traditional Chinese and Western medicine diagnosis and treatment of chronic heart failure. *Chin. J. Integr. Tradit. West Med.* 36, 133–141. doi:10.7661/CJIM.2016.02.0133

Committee of Exports on Rational Drug Use National Health and Family Planning Commission of The People'Republic of ChinaChinese Pharmacists Association (2019). Guidelines for rational use of drugs of heart failure(2 edition). *Chin. J. Front. Med. Sci.* 11, 1–78. doi:10.12037/YXQY.2019.07-01

Du, H., Meng, Z. P., Yuan, J., Wan, M. X., Zhang, Y. X., Li, Z., et al. (2021). Pharmacological effects and clinical research progress of Yiqi Fumai Lyophilized Injection on cardiovascular diseases. *Drug Eval. Res.* 44, 2300–2307. doi:10.7501/j.issn.1674-6376.2021.11.002

Fan, G. H., Xing, Z. Y., Liu, M. L., Chen, S. Q., and Wang, M. X. (2021). Systematic evaluation and sequential analysis of efficacy and safety of yiqi fumai(lyophilization) injection in treatment of heart failure. *J. Pract. Tradit. Chin. Intern Med.* 35, 8–18. doi:10.13729/j.issn.1671-7813.Z20200508

Fan, M. M., Zhang, J. Y., Zhang, X. L., and Wang, S. (2020). Research progress on chemical components and pharmacological action of Radix ophiopogonis. *Inf. Tradit. Chin. Med.* 37, 130–134. doi:10.19656/j.cnki.1002-2406.200118

Feng, Y. Q., Ju, A. C., Liu, C. H., Wang, T., Yu, B. Y., and Qi, J. (2016). Protective effect of the extract of Yi-Qi-Fu-Mai preparation on hypoxia-induced heart injury in mice. *Chin. J. Nat. Med.* 14, 401–406. doi:10.1016/S1875-5364(16)30035-8

Fu, C. G., Liu, L. T., and Huang, M. Y. (2020). Chinese experts consensus on clinical applicat ion of Shengmai lnjection. *Chin. J. Integr. Tradit. West Med.* 40, 1430–1438. doi:10.7661/j.cjim.202001009.045

Gu, Y., Ju, A. C., Man, S. L., Wan, X. M., Li, D. K., and Gao, W. Y. (2018). Evaluating safety of yiqi fumai lyophilized injection. *Drug Eval. Res.* 41, 399–404. doi:10.7501/j.issn.1674-6376.2018.03.008

Hao, G., Wang, X., Chen, Z., Zhang, L., Zhang, Y., Wei, B., et al. (2019). Prevalence of heart failure and left ventricular dysfunction in China: The China hypertension survey, 2012-2015. *Eur. J. Heart Fail.* 21, 1329–1337. doi:10.1002/ejhf.1629

Hu, M. F., Kang, W. Q., Hu, X. Y., Zhang, H., and Song, D. L. (2014). An assessment of the curative effect of yiqi fumai (lyophilized) in the treatment of ischemic diastolic heart failure. *Chin. Med. Pharm.* 4, 7–11. doi:10.3969/j.issn.2095-0616.2014.16.003

Jiang, W. J., Zhao, Z. H., and Luo, J. (2018). Clinical observation on the treatment of ischemic cardiomyopathy and heart failure by injecting yiqi fumai (Freeze-dried) and Qiliqiangxin capsule. *Hebei J. Tradit. Chin. Med.* 40, 703–706. doi:10.3969/j.issn.1002-2619.2018.05.014

Ju, A. C., Luo, R. Z., Qin, X. P., Su, X. Q., Li, D. K., Zhou, D. Z., et al. (2018). Pharmacological effects and clinical research progress of Yiqi Fumai Lyophilized lnjection. *Drug Eval. Res.* 41, 354–364. doi:10.7501/j.issn.1674-6376.2018.03.002

Li, D. K., Su, X. Q., Li, Z., Li, L., Wan, M. X., Zhou, X. Q., et al. (2019). Study on quality marker of yiqi fumai lyophilized injection. *Chin. Tradit. Herb. Drug* 50, 290–298. doi:10.7501/j.issn.0253-2670.2019.02.004

Li, F., Pang, L. Z., Zhang, L., Zhang, Y., Zhang, Y. Y., Yu, B. Y., et al. (2019). YiQiFuMai powder injection ameliorates chronic heart failure through cross-talk between adipose tissue and cardiomyocytes via up-regulation of circulating adipokine omentin. *Biomed. Pharmacother.* 119, 109418. doi:10.1016/j.biopha.2019.109418

Li, K., Liu, Y. X., Shi, B. S., Peng, L. H., and Tao, J. Y. (2019). Analysis of yiqi fumai lyophilized injection application and adverse reaction. *Drug Eval. Res.* 42, 2075–2078. doi:10.7501/j.issn.1674-6376.2019.10.032

Li, K., Shi, B. S., Peng, L. H., and Tao, J. Y. (2018). Effect of Yiqi Fumai Lyophilized Injection on liver and kidney function in clinical application. *Drug Eval. Res.* 41, 425–427. doi:10.7501/j.issn.1674-6376.2018.03.013

Li, X. F., Wang, X. D., Wan, M. X., Li, Z., Li, D. K., Zhang, Y. W., et al. (2020). Establishment and preliminary verification of protective model of H9C2 cell injury induced by H2O2by Yiqi Fumai Lyophilized Injection. *Drug Eval. Res.* 43, 1510–1514. doi:10.7501/j.issn.1674-6376.2020.08.007

Li, Y., Jia, X. W., Liu, S. H., Feng, C. N., and Feng, H. P. (2019). Effect of yiqi fumai injection combined with atorvastatin on chronic heart failure patients with coronary heart disease and its effects on sCD40, sCD146 and PAPP-A. *Chin. Arch. Tradit. Chin. Med.* 37, 1225–1228. doi:10.13193/j.issn.1673-7717.2019.05.049

Lian, B. T., Li, Z. Z., Chen, J. C., Cai, Y. Y., and Ye, X. Q. (2016). Systematic review of yiqi fumai injection for patients with heart failure. *Chin. J. Exp. Tradit. Med. Form.* 22, 215–220. doi:10.13422/j.cnki.syfjx.2016080215

Liu, C., Ju, A., Zhou, D., Li, D., Kou, J., Yu, B., et al. (2016). Simultaneous qualitative and quantitative analysis of multiple chemical constituents in YiQiFuMai injection by ultra-

fast liquid chromatography coupled with ion trap time-of-flight mass spectrometry. *Molecules* 21, 640. doi:10.3390/molecules21050640

Liu, H. Y., Xu, Y. Q., Ouyang, T., Liu, W. L., Zhang, Y. M., and Xiao, X. H. (2018). Identification of saponins in yiqi fumai freeze-dried powder for injection by HPLC-Q-TOF-MS. *Chin. J. Exp. Tradit. Med. Form.* 24, 7–12. doi:10.13422/j.cnki.syfjx.2018050007

Loehr, L. R., Rosamond, W. D., Chang, P. P., Folsom, A. R., and Chambless, L. E. (2008). Heart failure incidence and survival (from the Atherosclerosis Risk in Communities study). *Am. J. Cardiol.* 101, 1016–1022. doi:10.1016/j.amjcard.2007.11.061

Ma, N., Hou, Y. Z., Wang, X. L., and Mao, J. Y. (2015). Literature-based study of adverse effects of Yi-Qi-Fu-Mai sterile powder. *Chin. J. New Drugs* 24, 1197–1200.

Maggioni, A. P., Dahlström, U., Filippatos, G., Chioncel, O., Crespo Leiro, M., Drozdz, J., et al. (2013). EURObservational research programme: Regional differences and 1-year follow-up results of the heart failure pilot survey (ESC-HF pilot). *Eur. J. Heart Fail.* 15, 808–817. doi:10.1093/eurjhf/hft050

McDonagh, T. A., Metra, M., Adamo, M., Gardner, R. S., Baumbach, A., Böhm, M., et al. (2021). 2021 ESC Guidelines for the diagnosis and treatment of acute and chronic heart failure. *Eur. Heart J.* 42, 3599–3726. doi:10.1093/eurheartj/ehab368

Pang, L. Z., Ju, A. C., Zheng, X. J., Li, F., Song, Y. F., Zhao, Y., et al. (2017). YiQiFuMai Powder Injection attenuates coronary artery ligation-induced myocardial remodeling and heart failure through modulating MAPKs signaling pathway. *J. Ethnopharmacol.* 202, 67–77. doi:10.1016/j.jep.2017.02.032

Stewart, S., MacIntyre, K., Hole, D. J., Capewell, S., and McMurray, J. J. (2001). More 'malignant' than cancer? Five-year survival following a first admission for heart failure. *Eur. J. Heart Fail.* 3, 315–322. doi:10.1016/s1388-9842(00)00141-0

Su, H. Y., and Wang, K. L. (2018). Clinical effect of Yiqi Fumai Injection combined with statins in the treat-ment of chronic heart failure complicated with atrial fibrillation. *Chin. Med. Her.* 15, 70–73. CNKI:SUN:YYCY.0.2018-35-017.

Sun, J., Qi, X. F., Zhang, L., Chen, X. M., and Ma, P. Z. (2019). A post-marketing surveillance study on patients using Yiqi Fumai Injection (freeze-dried) in a hospital. *Chin. J. Hosp. Pharm.* 39, 97–100. doi:10.13286/j.cnki.chinhosppharmacyj.2019.01.22

Sun, L. F., An, D. Q., and Guo, L. L. (2016). Advantages and characteristics of traditional Chinese medicine treatment of heart failure. *J. Emerg. Tradit. Chin. Med.* 25, 452–456. doi:10.3969/j.issn.1004-745X.2016.03.025

Sun, L. J., Zheng, X. K., and Hao, C. Y. (2012). Multicentre clinical research of Yiqifumai Injection in treatment of coronaryheart disease heart failure. *Chin. Mod. Med.* 19, 7–10. doi:10.3969/j.issn.1674-4721.2012.17.003

Wang, L. L., Zhuge, X., and Lv, X. (2018). Safety of yiqi fumai lyophilized injection in elderly patients. *Drug Eval. Res.* 41, 422–424. doi:10.7501/j.issn.1674-6376.2018.03.012

Wang, W., Su, G. Y., Hu, W. Q., and Zhao, Y. Q. (2016). Research progress in pharmacological effects of ginsenoside on cardiovascular diseases in last decade. *Chin. Tradit. Herb. Drug* 47, 3736–3741. doi:10.7501/j.issn.0253-2670.2016.20.029

Wang, X. L., Ma, N., Hou, Y. Z., and Mao, J. Y. (2016). Meta-analysis of the curative effect of Yiqi Fumai for injection (freeze-dried) combined with Western medicine in the treatment of chronic heart failure. *J. Tradit. Chin. Med.* 57, 391–395. doi:10.13288/j.11-2166/r.2016.05.008

Wang, X. D., Wan, M. X., Zuo, N., Xu, Q., Li, Z., Li, D. K., et al. (2020). Rationality of Yiqi Fumai Lyophilized Injection against doxorubicin inducedacute myocardial injury in rats. *Drug Eval. Res.* 43, 1522–1527. doi:10.7501/j.issn.1674-6376.2020.08.009

Wang, Y., Liu, Y. X., Yue, H. S., Xu, W. Y., Cao, J. M., Jin, H. Y., et al. (2020). Comparison between charged aerosol detector and evaporative light scattering detector for analysis of sugar in Zhusheyong Yiqi Fumai and study on accuracy of methods. *Chin. J. Chin. Mater. Med.* 45, 5511–5517. doi:10.19540/j.cnki.cjcmm.20200221.306

Wang, Y. Q., Liu, C. H., Zhang, J. Q., Zhu, D. N., and Yu, B. Y. (2013). Protective effects and active ingredients of yi-qi-fu-mai sterile powder against myocardial oxidative damage in mice. *J. Pharmacol. Sci.* 122, 17–27. doi:10.1254/jphs.12261fp

Wang, Y. Y., Kong, J. J., Yuan, L., Zhu, B., Xi, X. W., Ran, Y. L., et al. (2021). Clinical observation on yiqi fumai lnjection in the treatment of acute heart failure(qi-yin deficiency syndrome). *Chin. J. Integr. Med. Cardio -/Cerebrova Dis.* 19, 2142–2145. doi:10.12102/j.issn.1672-1349.2021.13.004

Wu, H. Y. (1997). Pharmacological study and clinical application of Shengmai powder in the prevention and treatment of cardiovascular diseases. *Chin. Tradit. Pat. Med.* 19, 2. CNKI:SUN:ZCYA.0.1997-03-021.

Xie, N., and Dai, X. H. (2019). Meta analysis on curative effects of yiqi fumai injection (lyophilization) for heart failure. *Chin. J. Integr. Med. Cardio -/Cerebrova Dis.* 17, 1499–1503. doi:10.12102/j.issn.1672-1349.2019.10.016

Xing, L., Jiang, M., Dong, L., Gao, J., Hou, Y., Bai, G., et al. (2013). Cardioprotective effects of the YiQiFuMai injection and isolated compounds on attenuating chronic heart failure via NF-κB inactivation and cytokine suppression. *J. Ethnopharmacol.* 148, 239–245. doi:10.1016/j.jep.2013.04.019

Xing, N. N., Qu, H. D., Ren, W. C., and Ma, W. (2021). Main chemical constituents and modern pharmacological action of schisandrae chinensis Fructus: A review. *Chin. J. Exp. Tradit. Med. Form.* 27, 210–218. doi:10.13422/j.cnki.syfjx.20211407

Xiong, Y., Xu, C., Chen, J. Y., and Yang, Y. (2017). Meta-analysis of Yiqi Fumai for Injection (lyophilized) in the treatment of heart failure. *J. Shenyang Pharm. Univ.* 34, 428–435. doi:10.14066/j.cnki.cn21-1349/r.2017.05.013

Yang, Y. J., Zhang, Y., Lv, J., Xing, K., and Tian, G. (2016). Treatment of 30 cases of senile coronary heart disease complicated with chronic heart failure by yiqi fumai injection. *Shanxi J. Tradit. Chin. Med.* 37, 1325–1326. doi:10.3969/j.issn.1000-7369.2016.10.027

Yin, K. K., Gou, X. B., Wan, M. X., Zhang, Y. X., Li, D. K., Kou, J. P., et al. (2020). Research progress on pharmacological effects of Shengmai prescription on heart failure. *Drug Eval. Res.* 43, 1501–1505. doi:10.7501/j.issn.1674-6376.2020.08.005

Zeng, Y. J., Zhao, X. C., Wan, M. X., Li, D. K., Li, Z., Song, M. Z., et al. (2018). Protective effect of yiqi fumai lyophilized injection against doxorubicin induced cardiotoxicity in H9c2 (2-1) cell. *Drug Eval. Res.* 41, 380–385. doi:10.7501/j.issn.1674-6376.2018.03.005

Zhang, C. X., Wang, S. Y., Zhao, T. F., and Zhang, M. (2020). Effect of Yiqi Fumai for injection (freeze-dried) on 6-min walking test distance of patients after cardiac valve replacement. *Chin. J. Integr. Med. Cardio -/Cerebrova Dis.* 18, 462–465. doi:10.12102/j.issn.1672-1349.2020.03.021

Zhang, F., Qiao, X., Lu, H., Zhang, S., Du, W., and Xiao, X. (2018). Application of a sensitive and specific LC-ESI-MS/MS method for the simultaneous quantification of twelve bioactive components in dog plasma for an intravenous pharmacokinetic study of Yiqifumai Injection in beagle dogs. *Biomed. Chromatogr.* 32, e4256. doi:10.1002/bmc.4256

Zhang, L., Su, X. Q., Li, D. K., Yue, H. S., Ju, A. C., Yang, F., et al. (2021). Verification of quality marker in Yiqi Fumai Lyo ophilized Injection based on clinical efficacy. *Chin. Tradit. Herb. Drug* 52, 5741–5750.

Zhang, P. (2015). Advantages, disadvantages, and trend of integrative medicine in the treatment of heart failure. *Cell biochem. Biophys.* 72, 363–366. doi:10.1007/s12013-014-0466-7

Zhang, P. Y., and Li, Z. G. (2014). Advantages, disadvantages and trends of integrated traditional Chinese and Western medicine in the treatment of heart failure. *J. Tradit. Chin. Med.* 55, 449–450. doi:10.13288/j.11-2166/r.2014.05.025

Zhang, Q. Y., Wang, B. H., Liu, W. S., and Deng, Y. F. (2015). Effect of yiqi fumai recipe on heart function and heart failure markers in rats with chronic heart failure. *Liaoning J. Tradit. Chin. Med.* 42, 2233–2235. doi:10.13192/j.issn.1000-1719.2015.11.070

Zhang, Q. Y., Wang, B. H., Liu, W. S., and Deng, Y. F. (2016). Regulative effects of yiqifumai injection on the activity of matrix metalloproteinase in rats with chronic heart failure. *Chin. J. Integr. Med. Cardio -/Cerebrova Dis.* 14, 825–829. doi:10.3969/j.issn.1672-1349.2016.08.009

Zhang, R. P. (2015). Observation on the curative effect of Yiqi Fumai injection in the treatment of chronic heart failure in the elderly. *Chin. J. Integr. Med. Cardio -/Cerebrova Dis.* 13, 1647–1648. doi:10.3969/j.issn.1672-1349.2015.14.022

Zhang, Y., Zhang, L., Zhang, Y., Fan, X., Yang, W., Yu, B., et al. (2019). YiQiFuMai powder injection attenuates coronary artery ligation-induced heart failure through improving mitochondrial function via regulating ROS generation and CaMKII signaling pathways. *Front. Pharmacol.* 10, 381. doi:10.3389/fphar.2019.00381

Zhang, Y. S. (1978). Yi Xue qi yuan, 198. Beijing: Ren Min Wei Sheng Chu Ban She.

Zhao, C., Zhai, J. H., Zhang, J., and Zhang, Y. K. (2018). An analysis of off label medication in the elderly inpatients in our hospitai with the use of Yiqi-fumai for Injection. *Chin. J. Hosp. Pharm.* 38, 2469–2473. doi:10.13286/j.cnki.chinhosppharmacyj.2018.23.18

Zhao, Y., Li, Y., Tong, L., Liang, X., Zhang, H., Li, L., et al. (2018). Analysis of microRNA expression profiles induced by yiqifumai injection in rats with chronic heart failure. *Front. Physiol.* 9, 48. doi:10.3389/fphys.2018.00048

Zheng, H. R., Chu, Y., Zhou, D. Z., Ju, A. C., Li, W., Li, X., et al. (2018). Integrated pharmacokinetics of ginsenosides after intravenous administration of YiQiFuMai powder injection in rats with chronic heart failure by UFLC-MS/MS. *J. Chromatogr. B Anal. Technol. Biomed. Life Sci.* 1072, 282–289. doi:10.1016/j.jchromb.2017.10.056

Zhou, D. D., Jiang, S. J., Tong, L., Yang, Y. W., Wang, G. L., Ye, Z. L., et al. (2009). Quantitative determination of eight major constituents in the traditional Chinese medicinal Yi-Qi-Fu-Mai preparation by LC. *Chroma.* 70, 969–974. doi:10.1365/s10337-009-1252-3

Zhou, D., Tong, L., Wan, M., Wang, G., Ye, Z., Wang, Z., et al. (2011). An LC-MS method for simultaneous determination of nine ginsenosides in rat plasma and its application in pharmacokinetic study. *Biomed. Chromatogr.* 25, 720–726. doi:10.1002/bmc.1508

Zhou, L., Fan, F. F., Patiguli, A., Zheng, L. L., and Xu, H. S. (2016). A Meta-analysis on effectiveness and safety of Yiqifumai Injection in the treatment of heart failure. *Chin. Med. Her.* 13, 93–96. CNKI:SUN:YYCY.0.2016-22-023.

Zhou, Y. Y., Jiao, Y. T., Wang, Y. S., Hou, Y. Y., Li, D. K., Zhou, D. Z., et al. (2018). Chemical compositions analysis for yiqi fumai lyophilized injection byUPLC-Q-TOF/MS. *Drug Eval. Res.* 41, 446–450. doi:10.7501/j.issn.1674-6376.2018.03.016

Glossary

Ach acetylcholine

Akt protein kinase B

ALT alanine aminotransferase

AMPK adenine monophosphate activated protein kinase

ANP atrialnatriureticpeptide

ARNI angiotensin receptor neprilysin inhibitor

AST aspartate aminotransferase

ATP adenosinetriphosphate

BNP brain natriuretic peptide

CACNA1C calcium voltage-gated channel subunit α1C

CAL coronary artery ligation

CK creatine kinase

CK-MB creatine kinase-MB

CO cardiac output

CPP copeptin

Cr creatinine

Drp1 dynamin-related protein one

E/A early diastolic peak flow velocity/late diastolic peak flow velocity

E/e' early mitral filling velocity/early diastolic mitral annular velocity

EF ejection fraction

ERK1/2 extracellular signal-regulated kinase 1/2

FS fractional shortening

His histamine

HPLC high-performance liquid chromatography

HPLC-Q-TOF-MS HPLC coupled with quadrupole time-of-flight tandem mass spectrometry

HYP hydroxyproline

IL-1β interleukin-1β

IL-6 interleukin-6

JNK C-Jun Kinase enzyme

LC-ESI-MS liquid chromatography electrospray ionization mass spectrometry

LDH lactic dehydrogenase

LMS liquid-mass spectrometry

LVEDD left ventricular end-diastolic diameter

LVEF left ventricular ejection fraction

LVESD left ventricular end-systolic diameter

LVPWs left ventricular posterior wall in the systolic

LVFS left ventricular fractional shortening

MAPKs mitogen-activated protein kinases

MDA malondialdehyde

Mfn2 mitochondrial fusion protein two

MMP/TIMP matrix metalloproteinases/tissue inhibitor of metalloproteinases

MPO myeloperoxidase

NF-κB nuclear factor kappa-B

NO nitric oxide

NOX2 NADPH oxidase two

NT-proBNP N-terminal pro-B-type natriuretic peptide

p-CaMKII phosphorylation of calmodulin dependent protein kinase II

PI3K phosphatidylinositol 3-kinase

PIIINP amino-terminal pro-peptide of pro-collagen type III

ROS reactive oxygen species

sCD146 soluble CD146

sCD40 soluble CD40

SGLT2i sodium glucose cotransporter two inhibitor

SOD superoxide dismutase

SV stroke volume

TBil total bilirubin

TNF-α tumor necrosis factor-alpha

UFLC-IT-TOF/MS ultrafast liquid chromatography-ion trap time-of-flight MS

UPLC-Q-TOF/MS ultra-performance liquid chromatography coupled with quadrupole time-of-flight tandem mass spectrometry

YQFM the YiQiFuMai injection

5-HT 5-hydroxytryptamine

6 MWD 6-min walking distance.

frontiers | Frontiers in Pharmacology

TYPE Review
PUBLISHED 02 December 2022
DOI 10.3389/fphar.2022.1034870

Check for updates

OPEN ACCESS

EDITED BY
Karl Tsim,
Hong Kong University of Science and Technology, Hong Kong SAR, China

REVIEWED BY
Hoi Huen Chan,
Hong Kong Polytechnic University, Hong Kong SAR, China
Prabhu Balan,
Massey University, New Zealand
Ik-Hyun Cho,
Kyung Hee University, South Korea

*CORRESPONDENCE
Jie Wang,
wangjie0103@126.com

†These authors have contributed equally to this work

SPECIALTY SECTION
This article was submitted to Ethnopharmacology, a section of the journal Frontiers in Pharmacology

RECEIVED 02 September 2022
ACCEPTED 24 November 2022
PUBLISHED 02 December 2022

CITATION
Liu L, Hu J, Mao Q, Liu C, He H, Hui X, Yang G, Qu P, Lian W, Duan L, Dong Y, Pan J, Liu Y, He Q, Li J and Wang J (2022), Functional compounds of ginseng and ginseng-containing medicine for treating cardiovascular diseases. *Front. Pharmacol.* 13:1034870. doi: 10.3389/fphar.2022.1034870

COPYRIGHT
© 2022 Liu, Hu, Mao, Liu, He, Hui, Yang, Qu, Lian, Duan, Dong, Pan, Liu, He, Li and Wang. This is an open-access article distributed under the terms of the Creative Commons Attribution License (CC BY). The use, distribution or reproduction in other forums is permitted, provided the original author(s) and the copyright owner(s) are credited and that the original publication in this journal is cited, in accordance with accepted academic practice. No use, distribution or reproduction is permitted which does not comply with these terms.

Functional compounds of ginseng and ginseng-containing medicine for treating cardiovascular diseases

Lanchun Liu[1†], Jun Hu[1†], Qiyuan Mao[2†], Chao Liu[1], Haoqiang He[1], Xiaoshan Hui[1], Guang Yang[1], Peirong Qu[1], Wenjing Lian[3], Lian Duan[1], Yan Dong[1], Juhua Pan[1], Yongmei Liu[1], Qingyong He[1], Jun Li[1] and Jie Wang[1]*

[1]Departmen of Cardiology, Guang'anmen Hospital, China Academy of Chinese Medical Sciences, Beijing, China, [2]Departmen of Oncology, Guang'anmen Hospital, China Academy of Chinese Medical Sciences, Beijing, China, [3]Beijing University of Chinese Medicine, Beijing, China

Ginseng (Panax ginseng C.A.Mey.) is the dry root and rhizome of the Araliaceae ginseng plant. It has always been used as a tonic in China for strengthening the body. Cardiovascular disease is still the main cause of death in the world. Some studies have shown that the functional components of ginseng can regulate the pathological process of various cardiovascular diseases through different mechanisms, and its formulation also plays an irreplaceable role in the clinical treatment of cardiovascular diseases. Therefore, this paper elaborates the current pharmacological effects of ginseng functional components in treating cardiovascular diseases, summarizes the adverse reactions of ginseng, and sorts out the Chinese patent medicines containing ginseng formula which can treat cardiovascular diseases.

KEYWORDS

panax ginseng, ginsenoside, herbal medicine, functional components, cardiovascular disease

Introduction

Cardiovascular-related disease still remains a major public health problem with high morbidity and mortality in some countries. According to the "Global Health Estimates Report 2022" released by WHO (World Health Statistics, 2022), due to population growth and longer life expectancy, the total number of deaths from non-communicable diseases has increased, and about 33.2 million people worldwide died from cancer, cardiovascular disease, diabetes and chronic respiratory diseases. The "China Cardiovascular Health and Disease Report 2021 Summary" also pointed out that the prevalence and mortality of cardiovascular diseases in China are still on the rise, cardiovascular disease in rural and urban areas accounted for 46.74% and 44.26% of the cause of death respectively, and the burden is still increasing (Chinese Cardiovascular Health and Disease Report Writing Group, 2022). According to a 2020 report by the American Heart Association (AHA),

cardiovascular disease kills about 850,000 people and costs more than $300 billion a year, and its main risk factors are high cholesterol, smoking, and diabetes (Virani et al., 2020).

Relevant studies have shown that the occurrence and development of cardiovascular disease CVD is closely related to a variety of pathological processes. For example, coronary artery disease (CAD) is caused by cholesterol deposits and inflammation that damage the coronary arteries, leading to atherosclerosis which results in insufficient oxygen and blood supply. The pathological mechanism depends on dyslipidemia (Borén et al., 2020), inflammation of blood vessels (Ahluwalia et al., 2013), disorder of endothelial function (Davies et al., 1993; Gutiérrez et al., 2013), infiltration and turnover of macrophages (also known as macrophage polarization) (Stöger et al., 2012), etc. Platelets can cause blood clot problems and play an important role in a variety of cardiovascular diseases. During myocardial ischemia, chemicals such as adenosine, bradykinin, lactate, reactive oxygen species (ROS) and histamine are released to stimulate nerve receptors and produce angina symptoms, while the ischemia-reperfusion period will aggravate the accumulation of ROS and cause DNA damage, leading to cardiomyocyte apoptosis (Rezende et al., 2019). Hypertension is emerging as one of the major risk factors for cardiovascular and renovascular disease and also becoming a major risk factor for death worldwide (Ezzati et al., 2002). The main pathological links involved in the occurrence of hypertension include increased endothelin (ET), decreased nitric oxide (NO)/nitric oxide synthase (NOS), and imbalance of renin-angiotensin-aldosterone system (Zhang, 2011). Endothelial dysfunction, arginase activation, decreased NO bioavailability, and increased vascular stiffness are also important factors in leading hypertension (Ryoo et al., 2011; Konukoglu and Uzun, 2017). Another study found that essential hypertension is closely related to an increase in ROS and cell death mediated by defective mitochondrial oxidative phosphorylation (Zhang et al., 2014). Cardiac Arrhythmia is a common cardiovascular disease in clinic. It is a group of disorders that cause abnormal heart beat frequency and/or rhythm due to the origin conduction disorder of cardiac electrophysiology. Arrhythmias is classified as impulse formation abnormality, impulse conduction abnormality, tachyarrhythmias and bradyarrhythmias (Liu, 2021). There are 3.7 million sudden cardiac deaths in the world every year, and a considerable part is caused by severe arrhythmia (Kuriachan et al., 2015). According to the epidemiological survey of sudden cardiac death in China, more than 80% of sudden cardiac death events are caused by malignant arrhythmia every year (Chen et al., 2020). Heart failure (HF) is a serious public health problem and the leading cause of death from cardiovascular disease worldwide. It is a complex clinical syndrome caused by abnormal changes in cardiac structure and function due to various reasons, resulting in dysfunction of ventricular systolic and diastolic functions which mainly manifesting as dyspnea, fatigue, and fluid retention (Heart Failure Group of Cardiology, 2018). According to the "China Cardiovascular Disease Report 2020," there are 8.9 million heart failure patients in China, The China Heart Failure Patient Registration Study (China-HF) shows that the mortality rate of hospitalized patients with heart failure is 4.1% (China Cardiovascular Health and Disease Report Writing Group, 2021), the 5-year survival rate of heart failure patients is comparable to that of malignant tumors (Kannel, 2000). However, with the wider application of drug therapy, patients can benefit from it, but at the same time, some toxic and side effects have gradually become prominent. For example, long-term use of lipid-lowering drugs will have adverse reactions of myopathy and liver. Aspirin and warfarin often cause gastric mucosal damage, severe intracranial hemorrhage, and even death. Calcium channel blocker (CCB) can cause blurred vision and eye pain. Diltiazem can cause auditory hallucinations and vision loss in patients. Verapamil can cause vertigo symptoms (Yi, 2013). Side effects of antihypertensive drugs include gastrointestinal reactions, nervous system toxicity, etc. Antiarrhythmic drugs themselves also have proarrhythmic effects (Liao and Yang, 2008).

The World Health Organization defines the functional components of herbal medicines as "the components that have a therapeutic effect in herbal medicines." Traditional Chinese Medicine (TCM) has played an important role in preventing cardiovascular diseases by applying herbal medicine based on its unique theory and experience (Hao et al., 2017). Several preclinical studies have confirmed that ginseng and its main functional components are involved in the treatment and prevention of cardiovascular disease, and have the potential to reduce cardiovascular risk factors. From 1976 to 1978, Chinese researchers isolated and identified three saponins from ginseng, namely panaxadiol, panaxatriol and oleanolic acid saponins (Li and Teng, 1978; Chen et al., 2002). Subsequently, ginseng polysaccharides, volatile oil and other components were continuously explored. This article aims to clarify the pharmacological mechanism of ginseng functional components in the prevention and treatment of cardiovascular disease, and to sort out the clinical application of ginseng's formulation in detail.

Pharmacological effects of ginsenosides in treating cardiovascular diseases

Ginsenosides belong to triterpenoid saponins and are mainly divided into three types: protopanaxadiol type, such as ginsenoside Ra1, Rbl, Rb2, Rc, Rd, etc. protopanaxatriol type, such as ginsenoside Re, Rf, Rgl, Rg2, Rhl, etc. Oleanolic acid type, such as ginsenoside RO, Rh3, etc (Chu and Zhang, 2009; Cao et al., 2012) (Figure 1). In one study, a variety of ginsenosides at different sites of ginseng were analyzed using ultra performance

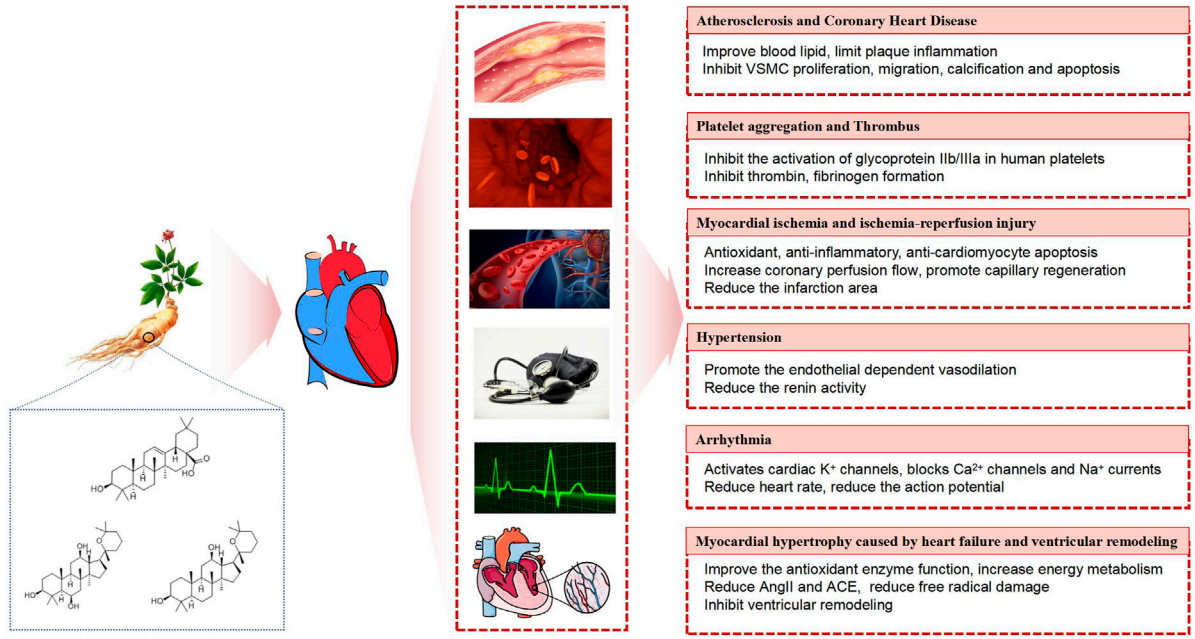

FIGURE 1
Ginsenosides in treating cardiovascular diseases.

liquid chromatography-quadrupole time of flight /mass spectrometry (UPLC-QTOF/MS), and then multivariate analysis was performed on the dataset, according to the results, ginsenosides such as Ra1 and Ra2, are unique among the roots of ginseng (Lee et al., 2017a).

Atherosclerosis and coronary heart disease

Ginseng has shown to involve in the atherosclerotic gene regulation with anti-inflammatory effects and results in the changes in improving in lipid profile (Duan et al., 2017; Cholesterol Treatment Trialists' (CTT) Collaboration O'Connell et al., 2015). Studies have found that protopanaxadiol and protopanaxatriol saponins can improve the lipid profile by reducing the concentrations of cholesterol, triglycerides, low-density lipoprotein and free fatty acids in plasma, while increasing the total concentration of high-density lipoprotein (Deng et al., 2017). This lipid metabolism-modulating effect of ginseng supplementation was also validated in a meta-analysis (Hernández-García et al., 2019). Ginsenosides can also reduce the progression of atherosclerosis by inhibiting the expression of VCAM-1 and enhancing α-smooth muscle actin (α-SMA) (Zhang et al., 2004). In addition to improving blood lipid levels, ginseng extract can also reduce superoxide dismutase (SOD) and catalase (CAT) levels (Kim and Park, 2003). Studies have shown that ginsenoside compounds K and Rb1 are potential active components to restore TNF-α-induced oxidative stress and oxidized low-density lipoprotein (ox-LDL)-induced inflammation and apoptosis (Zhou et al., 2017a; Lu et al., 2019). In animal models, ginsenosides Rg3 and Rb1 are thought to inhibit vascular smooth muscle cell (VSMC) proliferation, migration, calcification, and induce apoptosis (Guo et al., 2018a; Nanao-Hamai et al., 2019). Ginsenoside Re (G-Re) can affect platelet-derived growth factor-BB (PDGF-BB)-induced proliferation of VSMCs by regulating the eNOS/NO/cGMP pathway through G0/G1 cell cycle arrest (Gao et al., 2019). Another study found that ginsenosides Rb1 and Rg1 could inhibit the apoptosis process in atherosclerosis model by increasing autophagy (Zhou et al., 2018; Yang et al., 2018).

Ginseng can also reduce atherosclerosis, or limit intraplaque inflammatory responses by modulating macrophage polarization in order to prevent the occurrence of atherosclerosis (Guo et al., 2018b; Zhang et al., 2018). Recently, a study has proposed that the anti-inflammatory effects of several ginsenosides (Rg3, Rb1, and Rg1) may be due to inducing M2 polarization of macrophages and microglia, which in turn helps to inhibit inflammatory progression and promote inflammation resolution (Im, 2020). By inhibiting the expression of NF-κB and JNK, ginsenosides can not only

reduce the production of inflammatory cytokines such as VCAM-1 and ICAM-1, but also reduce the number of macrophages, thereby controlling the size of atherosclerotic lesions (Su et al., 2016). A study has shown that ginsenosides can reduce the expression of interleukin, inhibit the expression of NF-κB/p65, and exert anti-inflammatory effects (Sun et al., 2013; Zhang et al., 2008). Ginsenoside Rg3 can reduce the expression of cell adhesion molecules and pro-inflammatory cytokines in blood vessels, inhibit the expression of TNF-α, and has anti-inflammatory and anti-atherosclerotic effects (Hien et al., 2010). Another study found that ginsenoside Rb1 can significantly inhibit inflammation, oxidative stress and apoptosis by inhibiting the production of ROS and MDA, reducing the expression levels of IL-6, IL-1, ICAM-1, VCAM-1, VEGF, MMP-2, and MMP-9 (Zhou et al., 2017b). Based on the above research results, it can be found that ginseng has a good effect in treating and preventing atherosclerosis and coronary heart disease caused by inflammation and lipid profile.

Platelet aggregation and thrombus

The existing research results show that ginsenosides can exert antiplatelet and anticoagulant activities through various mechanisms. Ginsenoside Rg1 was found to improve the aggregation of platelets and formation of arterial thrombus, which may be achieved by regulating the ERK/Akt signaling pathway (Zhou et al., 2014). What's more, ginsenoside Rg3 has also been found by two other studies to inhibit the platelet aggregation process through the key signaling pathways such as ERK2 and cAMP (Lee et al., 2008; Kwon, 2018a). Ginsenoside Rg3 can also achieve antithrombotic effect by inhibiting the formation of thrombin (Jeong et al., 2017). For 20(S)-ginsenoside Rg3, its antiplatelet mechanism may be related to the inhibition of glycoprotein IIb/IIIa activation in human platelets (Kwon, 2018b). In another study, ginsenoside Ro was shown to inhibit the binding of fibrinogen to αIIb/β3 in human platelets (Shin et al., 2016). A study evaluated the synergistic effects of different ginsenosides to assess whether structural modifications affect their antiplatelet activity. Ginsenoside Rp3 was prepared from the structural modification of Re by means of reduction with hydrogenation. Rp1 was prepared from other ginsenosides (Rg3, 2h-Rg3, Rg5, and Rk1) with the same method that was used for Rp3 production. 2H-Rg3 is called Dihydroxy-G-Rg3, which is chemically derived from Rg3 by means of reduction with hydrogenation. It was found that G-Rp3 was shown to be effective in inhibiting platelet aggregation by exerting synergistic effects with G-Rp1 and 2H-Rg3 (Irfan et al., 2020). Therefore, the research on ginsenosides will help to develop new antiplatelet and antithrombotic drugs in the cardiovascular system.

Myocardial ischemia and ischemia-reperfusion injury

Ginseng total saponin has antioxidant and anti-inflammatory effects, so it can inhibit oxidative stress and reduce myocardial damage (Aravinthan et al., 2015). For example, the combination of ginsenoside Rb3 and Rb2 has a protective effect on myocardial ischemia-reperfusion injury, and its mechanism may be related to anti-inflammatory response, improve oxidative stress and resist cardiomyocyte apoptosis (Liu et al., 2020a). Studies have found that ginsenoside Rbl can reduce serum aspartate transaminase (AST), Lactic dehydrogenase (LDH) and creatine kinase in myocardial tissue, protect the heart by resisting inflammatory and apoptotic damage (Zheng et al., 2017a). Ginsenoside Rg3 also has similar efficacy, which may be achieved by regulating Akt/eNOS and Bcl/BAx signal transduction pathways (Wang et al., 2015; Zhang et al., 2016). Ginsenosides can protect cardiomyocytes from hypoxia/reoxygenation damage by reducing oxidative damage (Li and Liu, 2006), which may be related to reducing intracellular calcium overload (Xu et al., 2005) and inhibiting the activation of JNK signaling pathway (Li et al., 2012; Li et al., 2017; Sun et al., 2019). Ginsenoside Rg1 can also inhibit autophagy in H9c2 cardiomyocytes (Zhang et al., 2012), improve mitochondrial dynamics imbalance (Dong et al., 2016), and promote capillary regeneration in ischemic myocardial tissue (Wang et al., 2005; Zhang and Liu, 2009). Ginseng can also activate the reperfusion injury salvage kinase (RISK) signaling pathway through glucocorticoid receptor/estrogen receptor (GR/ER) in an endothelium nitric oxide synthase (eNOS)-dependent mechanism (Zhou et al., 2011). Another study stated that ginseng can enhance the PI3K/Akt/eNOS pathway, increase the coronary perfusion flow of the heart, and reduce the infarction size (Yi et al., 2010). It is worth mentioning that ginsenoside Rc as well as Rb1 and Re can also inhibit coronary vascular dysfunction (Chai et al., 2005).

Hypertension

There is substantial evidence that ginsenosides are beneficial in the treatment of hypertension, not only does ginseng lower blood pressure, it also acts as a heart protector (Jeon et al., 2000; Nagar et al., 2016). A study shows that ginsenoside Rb3 can reduce oxidative stress in hypertension and protect endothelial function (Wang et al., 2014). In a spontaneously hypertensive rat model, Rg1 has protective effects not only in large arteries but also in small resistance arteries (Chen et al., 2012). Ginsenosides have been found to inhibit arginase, stimulate endothelial nitric oxide synthase coupling, block homocysteine-induced ROS damage, promote endothelium-dependent vasodilation, and achieve the purpose of lowering blood pressure (Shin et al., 2013; Zhou et al., 2005). In addition to the above studies, ginsenoside Rg3 can reduce renin

activity by stimulating the expression of iNOS/NO, and also reduce blood pressure (Lee et al., 2016).

Ginseng has been shown to lower blood pressure in several studies, but there have also been reports of raising blood pressure, which may be related to the bidirectional effect. In previous literature, a study found ginsenosides can cause biphasic changes in blood pressure without affecting breathing and heart rate (Takagi et al., 1972). Another study found that large doses of ginsenoside Rb1 can cause an increase in blood pressure, and all other ginsenosides except Rb1 showed biphasic changes (Kaku et al., 1975). Although the effect of ginseng in blood pressure has had conflicting results in previous studies, a recent systematic review of randomized, double-blind, placebo-controlled trials has preliminarily resolved the inconsistencies in ginseng evidence for blood pressure regulation, the results of this study provide optimistic evidence for the efficacy of ginseng in reducing prehypertension, acute hypertension and chronic hypertension (Lee et al., 2017b).

Arrhythmia

Ginsenosides can affect the electrophysiology of cardiomyocytes and are used to regulate arrhythmias. Among them, ginsenoside Re is a major phytosterol of ginseng, which can activate the K^+ channel of the heart through the non-genomic pathway of sex hormones (Furukawa et al., 2006), and can also block the Ca^{2+} channel, reduce the heart rate, reduce the action potential plateau phase, and reduce the P wave amplitude (Jin and Liu, 1994). Several other studies have found that ginsenoside Re can regulate K^+ and Ca^{2+} currents in cardiac electrical activity by inducing NO and cyclic guanosine monophosphate pathways (Bai et al., 2003; Bai et al., 2004; Choi et al., 2009). Ginseng Rg2 has been studied in rat models of calcium chloride-induced arrhythmias, and it has been found to have anti-arrhythmic effects, including shortened duration, mortality, and incidence of malignant arrhythmias, which may be related to inhibition of phosphorylation of Ca^{2+} (Gou et al., 2020). Experiments have shown that the use of ginsenosides to intervene in arrhythmias can increase the amplitude of the T wave and reduce the amplitude of the QRS wave, thereby restoring the heart rhythm to normal (Chen and Zhang, 2009; Lu et al., 2012). A study found that ginsenoside Rg3 can change the electrocardiogram (ECG) and monophasic action potential (MAP) of Langendorff perfused rabbit heart, shorten the QT interval, and may be related to alleviating the current inhibition of human ether-related genes (hERG) and accelerating the activation process of potassium channels (Zhang et al., 2021). Another study has shown that ginsenosides can also treat arrhythmias by inhibiting the voltage-dependent Na^+ current in the myocardium and reducing the amplitude of action potentials (Liu et al., 2019). These studies fully demonstrate the antiarrhythmic therapeutic potential of ginsenosides.

Cardiac hypertrophy due to heart failure and ventricular remodeling

Heart failure is a kind of disease that the impaired heart function or structure causes decreased ventricular filling or decreased ejection function, and the heart output is not enough to meet the needs of the body. There are many causes of heart failure, mainly including the excessive pressure overload during cardiac systole, the excessive volume overload during cardiac diastole, the abnormal energy metabolism of cardiomyocytes, the use of cardiotoxic drugs, and the myocardial fibrosis or ventricular remodeling (Lin et al., 2017).

In improving cardiac systolic and diastolic function, a study has found that ginsenoside Rg3 can significantly inhibit the proliferation of middle vascular smooth muscle cell proliferation, reduce stromal hyperplasia, and enhance vasodilation and vasoconstriction function in elderly rats (Liu et al., 2016). It also has found that ginsenosides can enhance the systolic and diastolic functions of the left ventricle after heart failure (Wang et al., 2008). In terms of regulating the energy metabolism, ginsenoside Rb3 can inhibit mitochondria-mediated apoptosis, upregulate energy metabolism, activate fatty acid oxidation, and exert cardioprotective effects (Chen et al., 2019). The active ingredients of ginseng also have a certain therapeutic effect on heart failure caused by cardiotoxicity. For example, ginsenoside Re can improve myocardial fibrosis and heart failure induced by isoproterenol in rats (Wang et al., 2019). It was found that the expression of p-P70S6K, c-Jun N-terminal kinase 1 and Beclin1 decreased in the ginsenoside Rg1 group. These results showed that ginsenoside Rg1 can reduce the expression of doxorubicin-induced cardiac microtubule-associated protein-light chain 3 and autophagy-related 5, reduce doxorubicin-induced endoplasmic reticulum dilation, and improve cardiac insufficiency by inhibiting endoplasmic reticulum stress and autophagy (Xu et al., 2018). Another study found that ginseng can treat adriamycin-induced heart failure, increase the activity of myocardial glutathione peroxidase (GSH-Px), alleviate mitochondrial damage, reduce the production of ROS, and reduce the amount of ascites (You et al., 2005). In addition, ginsenoside Rbl can improve cardiac function and remodeling in patients with heart failure, and the mechanism may be that ginsenoside can not only reduce β-myosin heavy chain (βMHC), angiotensin I converting enzyme (ACE), angiotensin II (AngII) and atrial natriuretic factor (ANF), but also regulate mitochondrial membrane potential (Zheng et al., 2017b). In addition, the active compounds of ginseng can reduce myocardial hypertrophy and oxidative stress (Tsai et al., 2014), and inhibit cardiac fibrosis and heart failure (Guo et al., 2011; Lo et al., 2017). Some studies have also found that ginsenosides can effectively inhibit the right ventricular hypertrophy induced by monocrotaline in rats, suggesting that it has an anti-ventricular hypertrophy effect (Jiang et al., 2007). This effect has also been found to be dependent on phospho-akt

TABLE 1 Chemical structure classification of ginsenoside components.

Name	Component or compound	R1	R2
Protopanaxadiol ginsenosides PPD	Rb1	Glc (2-1)Glc	Glc (6-1)Glc
	Rb2	Glc (2-1)Glc	Glc (6-1)Arap
	Rb3	Glc (2-1)Glc	Glc (6-1)Xyl
	Rc	Glc (2-1)Glc	Glc (6-1) Araf
	Rd	Glc (2-1)Glc	Glc
	Rg3	Glc (2-1)Glc	H
	Ra1	Glc (2-1)Glc	Glc-Arap-Xyl
	Ra2	Glc (2-1)Glc	Glc-Araf-Xyl
Protopanaxatriol ginsenosides PPT	Rg1	Glc	Glc
	Rg2	Glc (2-1)Rha	H
	Re	Glc (2-1)Rha	Glc
	Rf	Glc (2-1)Glc	H
	Rh1	Glc	H
Oleanolic acid ginsenosides	Ro	GlcUA (2-1)glc	Glc

(p-akt) activation and inhibition of p38 mitogen-activated protein kinase (MAPK) (Zhang et al., 2013a), and is often associated with inhibition of vascular mitogenic activity (Qin et al., 2008), both of which have been experimentally verified *in vitro* and *in vivo* (Zhang et al., 2019). The contents of functional compounds of ginsenoside are summarized in Table 1.

Pharmacological effects of ginseng polysaccharides in treating cardiovascular diseases

There are many kinds of polysaccharides which are widely distributed. They can be divided into extracellular and intracellular polysaccharides. Among them, plant polysaccharides and microbial polysaccharides are more studied (Jin and Zhang, 1995). In recent years, ginseng polysaccharides have been paid more and more attention as an important component of ginseng to exert pharmacodynamic activity, and ginseng polysaccharides with different structural characteristics and activities have been reported widely. Ginseng polysaccharides are mainly divided into two categories: neutral sugar and acidic pectin (Li and Zhang, 1986). The main active ingredient is ginseng pectin, which is mainly composed of galactosyl, galacturonic acid, arabinose, and rhamnosyl (Zhang et al., 1982; Li and Zhang, 1984). Ginseng polysaccharide has high antioxidant activity, can significantly scavenge hydroxyl radicals and superoxide anions, its mass concentration has a certain dose-effect relationship with antioxidant activity, and is a good natural antioxidant (Zhou et al., 2015). Studies have shown that ginseng polysaccharides can improve oxidative stress injury in cardiomyocytes by inhibiting ROS and apoptosis (Tian et al., 2018). Another study determined the antioxidant activity of ginseng polysaccharides, and the results showed that the antioxidant activity of neutral polysaccharides was higher than that of acid polysaccharides in the aboveground part of ginseng, while the antioxidant activity of acid polysaccharides in the underground part of ginseng was not large (Chen and Huang, 2019). In addition, ginseng polysaccharide can improve its energy metabolism disorder and increase the vitality of mitochondria (Zhang et al., 2013b). A short review proposed that Rb1 can regulate mitochondrial energy metabolism, mitochondrial fission and fusion, apoptosis, oxidative stress and reactive oxygen species release, mitophagy and mitochondrial membrane potential (Zhou et al., 2019). Other studies have found that ginseng polysaccharides can regulate the activities of GSH and SOD enzymes, significantly reduce the expression levels of B cell lymphoma-2 (Bcl-2) and Bcl-2 Assaciated X protein (Bax) in rats, and improve dyslipidemia in rats with coronary heart disease (Wan et al., 2020).

Pharmacological effects of ginseng volatile oil in treating of cardiovascular disease

Ginseng volatile oil has the special aroma of ginseng. Ginseng stems, leaves and flowers have higher level of volatile oils, while ginseng roots have less volatile oils (Chen et al., 1982). The identification of ginseng volatile oil found that there are many more terpenes (Zhang et al., 1994), followed by oxygenated compounds and long-chain alkanes (Sun and Wang, 1997). Volatile oils include compounds such as pentadecane and n-hexadecanoic acid, etc (Yan et al., 1994; Wu et al., 1996). The results of cell experiments suggest that ginseng volatile oil can inhibit the secretion of inflammatory factors such as TNF-α,

TABLE 2 Mechanism and Clinical Indicators of Ginseng Prescriptions in treating Cardiovascular Diseases.

Ginseng prescriptions	Diseases	Mechanism	Clinical indicators
Xin-su-ning capsule	Tachyarrhythmias atrial fibrillation	prolong APD and increase ERP of cardiac electrical conduction	improve the total effective rate of holter, reduce premature ventricular contractions and the frequency of atrial fibrillation
Yi-xin-shu capsule	angina pectoris diastolic heart failure	lower lipids and anticoagulation, inhibit platelet adhesion and aggregation, improve blood rheology	improve the incidence frequency and degree, echocardiographic indicators, 6-min walking test results, QOL
Tong-xin-luo capsule	unstable angina pectoris myocardial infarction	decrease vWF and Fn, improve blood lipid and hypercoagulability, reduce blood viscosity and level of IL-18, hs- CRP and CK	improve the function of ischemic myocardium, reduce the scope of myocardial infarction
Qili Qiangxin capsule	chronic heart failure	increase ATP, ADP, eNOS and p-AMPK, activate AMPK-eNOS pathway, reduce ICAM-1	increase CO, reduce LVEDP, LVEDD, LVEF and 6-min walk distance, improve exercise tolerance and cardiac function
Qishen capsule	angina pectoris	reduce blood lipids, blood viscosity and fibrinogen, the levels of plasma hs-CRP and BNP	reduce the frequency and myocardial oxygen consumption of angina pectoris, improve the electrocardiogram and cardiac function
Shenshao capsule	unstable angina pectoris myocardial remodeling	reduce CRP, cTnI, IL-6, NO, ET and tPAI-1, decrease WBV, PV, FIB, PAR, TC, TG and LDL-C	reduce the number of carotid plaques, the plaque volume, the cardiac index and arterial intima-media thickness
Shexiang Baoxin pill	ischemic myocardium stable angina pectoris hyperlipidemia	increase VEGF, bFGF, FVIII, SOD, decrease TC, LDL-C	reduce the infarction size of ischemic myocardium, the hyperplasia of arterial intima, decrease all-cause deaths, heart failure events, stroke events
Shensong yangxin capsule	arrhythmia	block IK1, Ito, delay Ik	improve cardiac function, shorten the effective refractory period, reduce the TDR

IL-6 and IL-1β, and inhibit the NF-κB pathway, thereby playing an anti-inflammatory effect (Zuo, 2021). Ginseng volatile oil also has obvious protective effect on ischemic myocardial injury in animals, and can improve blood rheology, anti-platelet aggregation, reduce blood viscosity, and prevent thrombosis (Teng et al., 1989; Zhang, 2016). Ginseng volatile oil can be used for the treatment of coronary heart disease and angina pectoris. It can reduce the content of cardiac troponin I (cTn-I) in serum, reduce the content of Malondialdehyde (MDA), increase the activity of SOD and GSH enzymes, increase the concentration of NO, and protect the myocardium through the mechanism of anti-oxidative damage (Chen, 2015).

Although many studies have proved that ginseng volatile oil has good efficacy on cardiovascular diseases, a recent review concluded that the research on ginseng volatile oil is still in its infancy due to the limitation of the production process (Chen et al., 2022). More large samples and high-quality studies are needed to verify the efficacy of ginseng volatile oil in the treatment of cardiovascular diseases.

Clinical study on the treatment of cardiovascular diseases with ginseng prescriptions

A meta-analysis study using nitrate as a control drug found that ginseng-based drug had a significant effect on symptomatic improvement of angina pectoris and improvement in electrocardiogram (Jia et al., 2012). Another study focused on the efficacy of ginseng prescription in the treatment of patients with coronary angina pectoris, and the study showed that the patients who took the ginseng prescription had greater improvement in ECG results, clinical symptoms and nailfold microcirculation (Yuan et al., 1997). It can be seen that the important role of ginseng-containing prescriptions in the prevention and treatment of cardiovascular diseases should not be ignored. The mechanic and clinical research progress of related drugs is summarized as follows (Table 2).

Xin-su-ning capsule

Xinsuning Capsule can be used to treat tachyarrhythmias. Compared with propafenone and mexiletine hydrochloride, it can effectively improve the total effective rate of holter in patients with premature ventricular contractions, reduce premature ventricular contractions (Wang and Lu, 2008), and significantly improve the clinical symptoms of patients (Yuan, 2000; Song et al., 2022). The frequency of atrial fibrillation was significantly reduced and the incidence of adverse reactions was lower after the addition of Xinsuning Capsules on the basis of conventional western medicine treatment (Li and Zhang, 2015). Xinsuning capsules combined with low-dose betaloc in the treatment of premature ventricular contractions can

significantly reduce the number of premature ventricular contractions, maintain ventricular muscle stability, and improve vascular endothelial function and clinical symptoms (Yang, 2020). It is worth noting that Xinsuning can prolong the action potential duration (APD) and increase the effective refractory period (ERP) of cardiac electrical conduction, thereby inhibiting reentry-induced arrhythmias, and has a good antiarrhythmic effect (Jiao and Ding, 2015).

Yi-xin-shu capsule

Yixinshu Capsule is widely used clinically in coronary heart disease, angina pectoris and chronic heart failure. The capsule has the functions of lowering lipids and anticoagulation, inhibiting platelet adhesion and aggregation, and improving blood rheology (Li and Shi, 2013; Wang and Zhi, 2016). Yixinshu Capsule can also improve the symptoms of shortness of breath, fatigue and dry mouth (Cao, 2009; Cao and Xie, 2010). On the basis of conventional western medicine combined with Yixinshu Capsule in the treatment of diastolic heart failure, it was found that the echocardiographic indicators, 6-min walking test results, the quality of life (QOL)were improved, and were better than those of simple western medicine treatment (Zhang and Zhu, 2011). In the treatment of unstable angina pectoris (UA) of CHD, Yixinshu Capsule is better than the control group which only given antiplatelet aggregation and anticoagulant drugs on the frequency of angina pectoris, the degree of angina pectoris and the electrocardiogram (Tao et al., 2009).

Tong-xin-luo capsule

After the application of Tongxinluo Capsules to treat patients with unstable angina pectoris, the plasma Von Willebrand factor (vWF) and fibronectin (Fn) decreased, which can protect vascular endothelial cells (Xiao et al., 2002). Tongxinluo Capsules can also improve the function of ischemic myocardium in patients undergoing percutaneous coronary intervention (PCI) or thrombolysis after acute myocardial infarction (AMI), and can restore the function of part of the viable myocardium, improve myocardial remodeling after AMI (You et al., 2004), significantly improve blood lipid metabolism, reduce blood viscosity, and improve blood hypercoagulability (Wu et al., 2001). Studies have shown that the addition of Tongxinluo Capsules on the basis of western medicine treatment can improve the clinical efficacy of angina pectoris in elderly patients with coronary heart disease, and reduce the serum levels of interleukin-18 (IL-18) and high-sensitivity C-reactive protein (hs- CRP) level (Wang and Li, 2012). Experimental studies have also found that Tongxinluo Capsule can reduce the scope of myocardial infarction after ischemia-reperfusion in rats, reduce the level of plasma CK, reduce the degree of myocardial necrosis, and have a protective effect on ischemia-reperfusion myocardium (Zhao et al., 2000).

Qili Qiangxin capsule

Studies have found that Qili Qiangxin Capsule can significantly increase the left ventricular myocardial contractility and cardiac output (CO), reduce left ventricular end-diastolic pressure (LVEDP), at the same time can increase renal blood flow, effectively improve cardiac function (Liu et al., 2007). Another study found that Qili Qiangxin Capsule can significantly reduce the left ventricular end-diastolic diameter (LVEDD) in patients with chronic heart failure, reduce the plasma vasopressin (AVP) concentration, significantly increase the plasma brain natriuretic peptide (BNP), left ventricular ejection fraction (LVEF) and 6-min walk distance, improve exercise tolerance (Huang, 2010; Wu et al., 2011; Chen and Zhou, 2015). Qili Qiangxin Capsule can significantly increase the content of ATP and ADP in myocardial tissue, reduce the expression of ICAM-1 mRNA, increase eNOS mRNA, and significantly increase the protein expression of p-AMPK. It is suggested that Qiliqiangxin can protect the myocardial capillary endothelium in rats with pressure overload, and its mechanism may be related to the activation of AMPK-eNOS pathway (Zhang et al., 2013c).

Qishen capsule

Qishen Capsule is one of the effective drugs for the treatment of coronary heart disease angina pectoris. It can improve clinical symptoms, reduce blood lipids, blood viscosity and fibrinogen (Shang, 2003), and can also reduce the levels of plasma hs-CRP and BNP (Deng and Liu, 2013), the frequency of angina pectoris and the rate of vasodilator drugs. It also has a significant effect on patients with myocardial infarction complicated by cardiac insufficiency and coronary artery bypass grafting (Wang, 2010), (Yang and Huang, 2013). On the basis of nicorandil as the control group, combined with Qishen Capsule can improve the total effective rate of patients with coronary heart disease, reduce the frequency and myocardial oxygen consumption of angina pectoris, and improve the electrocardiogram and cardiac function indicators (Li et al., 2022).

Shenshao capsule

Shenshao Capsule can reduce the frequency and shorten the duration of angina attacks, and reduce the levels of serum CRP, cTnI and interleukin-6 (IL-6) in patients with unstable angina pectoris. It also has a decreasing effect on indicators such as

whole blood viscosity (WBV), plasma viscosity (PV), fibrinogen (FIB) and platelet adhesion rate (PAR) (Liu et al., 2020b). Shenshao Capsule not only has a significant clinical effect in the treatment of coronary heart disease, but also can reduce the dosage of nitroglycerin and the blood lipid level of patients. After treatment, the levels of TC, TG and LDL-C were decreased, and HDL-C was increased (Zhang and Ding, 2021). Because of this, Shenshao Capsule can also reduce the number of carotid plaques, the plaque volume, and arterial intima-media thickness (IMT) (Li, 2015). After using Shenshao Capsule, the cardiac index was reduced, and the levels of nitric oxide (NO), endothelin (ET) and tissue plasminogen activation inhibitor (tPAI-1) in myocardium are both decreased (Li et al., 2010).

Shexiang Baoxin pill

Shexiang Baoxin Pill can significantly reduce the infarction size of ischemic myocardium, and there is a dose-effect relationship (Wang et al., 2004). The expression levels of vascular endothelial growth factor (VEGF), basic fibroblast growth factor (bFGF), factor VIII and the surface density of blood vessels in the infarction edge area were significantly increased, suggesting that Shexiang Baoxin Pill can promote the angiogenesis of coronary collaterals (Wang et al., 2002). A prospective, randomized, non-blind controlled clinical trial involving 200 patients with stable angina pectoris also showed that after the treatment of Shexiang Baoxin Pill, the use of nitrates in the treatment group was significantly lower than that before treatment, all-cause deaths, heart failure events, and stroke events also tended to decrease (Zhu et al., 2010). Shexiang Baoxin Pill can also reduce the damage of hyperlipidemia to the artery. It can significantly inhibit the rise of serum total cholesterol (TC) and low-density lipoprotein cholesterol (LDL-C) level and increase the concentration of serum SOD. Reduce the hyperplasia of arterial intima, blood damage to the arterial wall, and inhibit the formation of atherosclerosis (Luo et al., 1998).

Shensong Yangxin capsule

Shensong Yangxin Capsule has a broad-spectrum antiarrhythmic effect, and can block inward rectifier potassium current (IK1), instantaneous outward potassium current (Ito) and delayed rectifier potassium current (Ik) in cardiomyocytes to varying degrees. Importantly, Shensong Yangxin Capsules have fewer proarrhythmic side effects (Li et al., 2007), and may also significantly improve clinical symptoms such as palpitation, insomnia, shortness of breath and fatigue in patients with arrhythmia (Chen et al., 2006; Bai and Wang, 2011). In addition, Shensong Yangxin Capsule can play an anti-arrhythmic effect after heart failure, because it can improve cardiac function, and at the same time, it can not only shorten the effective refractory period of the left and right ventricles, but also reduce the transmural dispersion of repolarization (TDR) (Wang et al., 2012).

Adverse reactions of ginseng medication

Although ginseng has a wide range of clinical applications, it should not be abused. The pharmacopoeia stipulates that the single dose of ginseng is 3–9 g. Taking the recommended dose of ginseng will not cause serious adverse reactions. Studies have shown that high doses of ginseng (15 g/d) will lead to ginseng abuse syndrome (GAS), the specific performance is as follows (Siegel, 1979): ①Nervous system: headache, dizziness, fever, restlessness, easy to wake up, insomnia, sweating, euphoria, mania, confusion, cerebral arteritis, mydriasis. ②Cardiovascular system: arrhythmia, palpitations, slow heart rate, high blood pressure, and even heart failure. ③Endocrine and metabolic system: hypokalemia, gynecomastia, breast pain. ④Blood system: neutropenia, gastrointestinal bleeding, uterine bleeding, cerebral hemorrhage. ⑤Digestive system: abdominal pain, nausea and vomiting, intractable. ⑥Respiratory system: shortness of breath, asthma.

In addition, ginseng will also have an effect on other drugs, and it is particularly important to pay attention to clinical use (Ryu and Chien, 1995). There are literature reports of interactions between ginseng and warfarin, which inhibits the pharmacological effects of warfarin and may increase the risk of blood clotting (Smolinske, 1972; Janetzky and Morreale, 1997). Studies have found that ginseng has an inhibitory effect on monoamine oxidase, similar to monoamine oxidase inhibitors (MAOIs), and should be clinically cautiously combined with antidepressants such as phenylcyprotamine and phenelhydrazine (Dai and Yin, 1987). Studies have reported that ginseng can be used only for mild diabetic patients, for moderate and severe patients, when people participate in the combination of insulin or oral hypoglycemic drugs, it will have a synergistic effect, which may lead to low glucose, and the dose of hypoglycemic drugs needs to be reduced (An et al., 2003).

Summary and prospect

This paper mainly focus on the mechanism of ginsenosides, ginseng polysaccharides, and ginseng volatile oil, summarizes the progress of ginseng-containing drugs, lists the adverse reactions of ginseng medication, and expounds the multi-faceted effects of ginseng functional compounds and composition compatibility in cardiovascular diseases. According to the existing research, ginseng and ginseng-containing drugs can treat coronary heart disease by improving inflammation and lowering blood lipid levels, can inhibit the activation of glycoprotein IIb/IIIa in human

platelets, it can increase coronary perfusion flow and promote capillary regeneration by antioxidant, anti-inflammatory and anticardiomyocyte apoptosis. Ginseng can also reduce heart rate, lower action potential, and suppress arrhythmias by activating K^+ channels, blocking Ca^{2+} channels and Na^+ currents. By improving antioxidant enzyme function, increasing energy metabolism and reducing free radical damage, ginseng can inhibit heart failure and ventricular remodeling. Although the role of ginseng on blood pressure has been controversial in the past, recent studies have shown that ginseng can lower blood pressure by promoting endothelial-dependent vasodilation. It can be seen that ginseng has a good efficacy as a drug for the treatment of cardiovascular diseases and can play a therapeutic role through multiple pathways, which is worth continuing research and development. Besides, there are many related researches on ginsenosides, but relatively few researches on ginseng polysaccharides and volatile oils. Due to the various and complex components of ginseng volatile oils, there are still many unknown unique components of ginseng volatile oils to be separated, identified and developed. At present, there is a lot of clinical evidence for ginseng-containing medicines, but further meta-analysis and quality evaluation are needed to reasonably and clearly explain its therapeutic effects and help the innovative application of botanical medicine.

In order to better explore the natural Chinese herbal medicine represented by ginseng, further develop its functional components, and improve its role in the treatment and prevention of diseases, the following aspects can be achieved: ① Use the theory of traditional Chinese medicine to expand the efficacy and indications of Chinese herbal medicine. Ancient Chinese medicine books are the crystallization of thousands of years of medical practice experience. Tu Youyou was inspired to develop artemisinin from a medical treatise by Ge Hong of the Eastern Jin Dynasty (317–420). Medicine tailored from classic Chinese medicine recipes also play an important role in the fight against COVID-19. ②Pay attention to the combination of ginseng medication. The composition of traditional Chinese medicine prescription is not a simple combination of several drugs, and the rational compatibility and application of rules can improve the clinical efficacy of ginseng. ③Adjust the dosage of Chinese herbal medicine according to the difference of symptoms. The therapeutic effect of Chinese herbal medicine has a dose-effect relationship, and the optimal dose should be selected according to the disease. Taking ginseng as an example, small doses of ginseng are suitable for healthcare people, which can improve physical fitness and enhance disease resistance. Patients with chronic diseases are suitable for medium doses of ginseng, and patients with massive hemorrhagic shock are suitable for large doses of ginseng. ④ Improve the preparation technology of Chinese herbal medicine to promote the development of the industry. There are various types of Chinese herbal preparations in ancient times. In modern times, it is necessary to further use new technologies and methods to design drug delivery systems based on biopharmaceutical characteristics, and to improve the absorption and bioavailability of functional compounds in traditional Chinese medicine preparations, so as to better exert its pharmacological effects.

Author contributions

LL and JH designed the work of review; LH, JH, and QM reviewed the literature available on this topic and wrote the paper; CL, HH, XH, and GY contributed in the scientific writing of the manuscript; PQ and WL polished the formatting of the figures and tables. LD and YD revised the manuscript; JP, YL, QH, JL, and JW defined the framework of the review. All authors approved the paper for publication. LL, JH, and QM contributed equally to this work.

Funding

National Key Research and Development Program (2020YFC2002701): Research on TCM Syndrome Differentiation of Sub-health State, person in charge: JP; State Administration of Traditional Chinese Medicine: The grant number of “Hundreds and Tens of Thousands” Talent Projects for Traditional Chinese Medicine Inheritance and Innovation is (0201000401) (Chief Scientist of Qihuang), person in charge: JW.

Conflict of interest

The authors declare that the research was conducted in the absence of any commercial or financial relationships that could be construed as a potential conflict of interest.

Publisher’s note

All claims expressed in this article are solely those of the authors and do not necessarily represent those of their affiliated organizations, or those of the publisher, the editors and the reviewers. Any product that may be evaluated in this article, or claim that may be made by its manufacturer, is not guaranteed or endorsed by the publisher.

References

Ahluwalia, N., Andreeva, V. A., Kesse-Guyot, E., and Hercberg, S. (2013). Dietary patterns, inflammation and the metabolic syndrome. *Diabetes Metab.* 39 (2), 99–110. doi:10.1016/j.diabet.2012.08.007

An, G. H., Geng, X. F., and Ji, M. C. (2003). Interaction between hypoglycemic drugs and other drugs. *Chin. J. Clin. Pharmacol.* (01), 67–70+74. doi:10.13699/j.cnki.1001-6821.2003.01.016

Aravinthan, A., Kim, J. H., Antonisamy, P., Kang, C. W., Choi, J., Kim, N. S., et al. (2015). Ginseng total saponin attenuates myocardial injury via anti-oxidative and anti-inflammatory properties. *J. Ginseng Res.* 39 (3), 206–212. doi:10.1016/j.jgr.2014.12.001

Bai, Y. R., and Wang, R. Y. (2011). Observation on the curative effect of Shensong Yangxin Capsule in the treatment of arrhythmia. *J. Cardiovasc. Cerebrovasc. Dis. Integr. Traditional Chin. West. Med.* 9 (10), 1170–1171. doi:10.3969/j.issn.1672-1349.2011.10.011

Bai, C. X., Sunami, A., Namiki, T., Sawanobori, T., and Furukawa, T. (2003). Electrophysiological effects of ginseng and ginsenoside Re in Guinea pig ventricular myocytes. *Eur. J. Pharmacol.* 476 (1-2), 35–44. doi:10.1016/s0014-2999(03)02174-5

Bai, C. X., Takahashi, K., Masumiya, H., Sawanobori, T., and Furukawa, T. (2004). Nitric oxide-dependent modulation of the delayed rectifier K+ current and the L-type Ca2+ current by ginsenoside Re, an ingredient of Panax ginseng, in Guinea-pig cardiomyocytes. *Br. J. Pharmacol.* 142 (3), 567–575. doi:10.1038/sj.bjp.0705814

Borén, J., Chapman, M. J., Krauss, R. M., Packard, C. J., Bentzon, J. F., Binder, C. J., et al. (2020). Low-density lipoproteins cause atherosclerotic cardiovascular disease: Pathophysiological, genetic, and therapeutic insights: A consensus statement from the European atherosclerosis society consensus panel. *Eur. Heart J.* 41 (24), 2313–2330. doi:10.1093/eurheartj/ehz962

Cao, C. H., and Xie, F. (2010). Clinical observation of Yixinshu capsule in treating 102 cases of coronary heart disease and angina pectoris. *J. Cardiovasc. Cerebrovasc. Dis. Integr. Traditional Chin. West. Med.* 8 (2), 136–137. doi:10.3969/j.issn.1672-1349.2010.02.005

Cao, Z., Zhang, Y. D., and Xu, Y. H. (2012). New progress in research on active ingredients and pharmacological effects of ginseng. *Ginseng Res.* 24 (2), 39–43. doi:10.3969/j.issn.1671-1521.2012.02.014

Cao, X. J. (2009). Clinical observation of Yixinshu capsule in treating 100 cases of coronary heart disease and angina pectoris. *Eval. Analysis Drugs Chin. Hosp.* 9 (7), 536–538. doi:10.14009/j.issn.1672-2124.2009.07.003

Chai, H., Zhou, W., Lin, P., Lumsden, A., Yao, Q., and Chen, C. (2005). Ginsenosides block HIV protease inhibitor ritonavir-induced vascular dysfunction of porcine coronary arteries. *Am. J. Physiol. Heart Circ. Physiol.* 288 (6), H2965–H2971. doi:10.1152/ajpheart.01271.2004

Chen, F., and Huang, G. (2019). Antioxidant activity of polysaccharides from different sources of ginseng. *Int. J. Biol. Macromol.* 125, 906–908. doi:10.1016/j.ijbiomac.2018.12.134

Chen, C. X., and Zhang, H. Y. (2009). Protective effect of ginsenoside Re on isoproterenol-induced triggered ventricular arrhythmia in rabbits. *Zhongguo Dang Dai Er Ke Za Zhi* 11 (5), 384–388.

Chen, X. D., and Zhou, J. (2015). Combined application of Qili Qiangxin Capsule and trimetazidine in patients with ischemic cardiomyopathy and heart failure. *Chin. J. Exp. Prescr.* 21 (19), 171–175. doi:10.13422/j.cnki.syfjx.2015190171

Chen, Y. J., Huang, Z., and Li, N. P. (1982). Study on volatile oil of ginseng. *China J. Chin. Materia Medica* 7 (4).

Chen, Y. J., Dou, D. Q., and Zhao, C. J. (2002). Research on new components, new activities and quality standardization of ginseng. *Ginseng Res.* 14 (1), 2–19. doi:10.3969/j.issn.1671-1521.2002.01.001

Chen, L. X., Kuang, J. B., and Deng, Y. (2006). Clinical observation of Shensong Yangxin capsule in the treatment of arrhythmia. *Int. Med. Health Her.* 12 (14), 103–104. doi:10.3760/cma.j.issn.1007-1245.2006.14.053

Chen, H., Yin, J., Deng, Y., Yang, M., Xu, L., Teng, F., et al. (2012). The protective effects of ginsenoside Rg1 against hypertension target-organ damage in spontaneously hypertensive rats. *BMC Complement. Altern. Med.* 12, 53. doi:10.1186/1472-6882-12-53

Chen, X., Wang, Q., Shao, M., Ma, L., Guo, D., Wu, Y., et al. (2019). Ginsenoside Rb3 regulates energy metabolism and apoptosis in cardiomyocytes via activating PPARα pathway. *Biomed. Pharmacother.* 120, 109487. doi:10.1016/j.biopha.2019.109487

Chen, X., Wang, Y. F., and Zhang, Z. X. (2020). Current status and treatment progress of arrhythmia in China. *Chin. J. Res. Hosp.* 7 (1), 75198–78201. doi:10.19450/j.cnki.jcrh.2020.01.016

Chen, X. Z., Wang, J., and Fu, D. (2022). Research progress of ginseng active ingredients and preparations in cardiovascular diseases. *Clin. Res. TCM* 14 (09), 140–144. doi:10.3969/j.issn.1674-7860.2022.09.049

Chen, S. W. (2015). *Preclinical study of the new drug "Compound Ginseng Volatile Oil Spray" for the treatment of coronary heart disease and angina pectoris*. Jilin Province: Changchun University of Traditional Chinese Medicine.

China Cardiovascular Health and Disease Report Writing Group (2021). China cardiovascular health and disease report 2020 outline. *Chin. J. Circulation* 36 (6), 521–545. doi:10.3969/j.issn.1000-3614.2021.06.001

Chinese Cardiovascular Health and Disease Report Writing Group (2022). Overview of China cardiovascular health and disease report 2021. *Chin. J. Circulation* 37 (6), 553–578. doi:10.3969/j.issn.1000-3614.2022.06.001

Choi, S. H., Lee, J. H., Pyo, M. K., Lee, B. H., Shin, T. J., Hwang, S. H., et al. (2009). Mutations Leu427, Asn428, and Leu431 residues within transmembrane domain-I-segment 6 attenuate ginsenoside-mediated L-type Ca(2+) channel current inhibitions. *Biol. Pharm. Bull.* 32 (7), 1224–1230. doi:10.1248/bpb.32.1224

Cholesterol Treatment Trialists' (CTT) CollaborationO'Connell, R., Voysey, M., Emberson, J., Blackwell, L., Mihaylova, B., Simes, J., et al. (2015). Efficacy and safety of LDL-lowering therapy among men and women: meta-analysis of individual data from 174, 000 participants in 27 randomised trials. *Lancet* 385 (9976), 1397–1405. doi:10.1016/S0140-6736(14)61368-4

Chu, S. F., and Zhang, J. T. (2009). New achievements in ginseng research and its future prospects. *Chin. J. Integr. Med.* 15 (6), 403–408. doi:10.1007/s11655-009-0403-6

Dai, Y. R., and Yin, Y. (1987). Study on the inhibition effect of B-type monoamine oxidase in traditional Chinese medicine. *Chin. J. Geriatrics* 06 (1), 27–30. doi:10.3760/cma.j.issn.0254-9026.1987.01.114

Davies, M. J., Gordon, J. L., Gearing, A. J., Pigott, R., Woolf, N., Katz, D., et al. (1993). The expression of the adhesion molecules ICAM-1, VCAM-1, PECAM, and E-selectin in human atherosclerosis. *J. Pathol.* 171 (3), 223–229. doi:10.1002/path.1711710311

Deng, Y. F., and Liu, J. L. (2013). Effects of Qishen Capsules on hs-CRP and BNP in patients with angina pectoris. *China Pract. Med.* 8 (25), 150–151. doi:10.3969/j.issn.1673-7555.2013.25.113

Deng, J., Liu, Y., Duan, Z., Zhu, C., Hui, J., Mi, Y., et al. (2017). Protopanaxadiol and protopanaxatriol-type saponins ameliorate glucose and lipid metabolism in type 2 diabetes mellitus in high-fat diet/streptozocin-induced mice. *Front. Pharmacol.* 8, 506. doi:10.3389/fphar.2017.00506

Dong, G., Chen, T., Ren, X., Zhang, Z., Huang, W., Liu, L., et al. (2016). Rg1 prevents myocardial hypoxia/reoxygenation injury by regulating mitochondrial dynamics imbalance via modulation of glutamate dehydrogenase and mitofusin 2. *Mitochondrion* 26, 7–18. doi:10.1016/j.mito.2015.11.003

Duan, L., Xiong, X., Hu, J., Liu, Y., Li, J., and Wang, J. (2017). Panax notoginseng saponins for treating coronary artery disease: A functional and mechanistic overview. *Front. Pharmacol.* 8, 702. doi:10.3389/fphar.2017.00702

Ezzati, M., Lopez, A. D., Rodgers, A., Vander Hoorn, S., and Murray, C. J.Comparative Risk Assessment Collaborating Group (2002). Selected major risk factors and global and regional burden of disease. *Lancet* 360 (9343), 1347–1360. doi:10.1016/S0140-6736(02)11403-6

Furukawa, T., Bai, C. X., Kaihara, A., Ozaki, E., Kawano, T., Nakaya, Y., et al. (2006). Ginsenoside Re, a main phytosterol of Panax ginseng, activates cardiac potassium channels via a nongenomic pathway of sex hormones. *Mol. Pharmacol.* 70 (6), 1916–1924. doi:10.1124/mol.106.028134

Gao, Y., Zhu, P., Xu, S. F., Li, Y. Q., Deng, J., and Yang, D. L. (2019). Ginsenoside Re inhibits PDGF-BB-induced VSMC proliferation via the eNOS/NO/cGMP pathway. *Biomed. Pharmacother.* 115, 108934. doi:10.1016/j.biopha.2019.108934

Gou, D., Pei, X., Wang, J., Wang, Y., Hu, C., Song, C., et al. (2020). Antiarrhythmic effects of ginsenoside Rg2 on calcium chloride-induced arrhythmias without oral toxicity. *J. Ginseng Res.* 44 (5), 717–724. doi:10.1016/j.jgr.2019.06.005

Guo, J., Gan, X. T., Haist, J. V., Rajapurohitam, V., Zeidan, A., Faruq, N. S., et al. (2011). Ginseng inhibits cardiomyocyte hypertrophy and heart failure via NHE-1 inhibition and attenuation of calcineurin activation. *Circ. Heart Fail.* 4 (1), 79–88. doi:10.1161/CIRCHEARTFAILURE.110.957969

Guo, M., Guo, G., Xiao, J., Sheng, X., Zhang, X., Tie, Y., et al. (2018a). Ginsenoside Rg3 stereoisomers differentially inhibit vascular smooth muscle cell proliferation and migration in diabetic atherosclerosis. *J. Cell. Mol. Med.* 22 (6), 3202–3214. doi:10.1111/jcmm.13601

Guo, M., Xiao, J., Sheng, X., Zhang, X., Tie, Y., Wang, L., et al. (2018b). Ginsenoside Rg3 mitigates atherosclerosis progression in diabetic apoE-/- mice by skewing macrophages to the M2 phenotype. *Front. Pharmacol.* 9, 464. doi:10.3389/fphar.2018.00464

Gutiérrez, E., Flammer, A. J., Lerman, L. O., Elízaga, J., Lerman, A., and Fernández-Avilés, F. (2013). Endothelial dysfunction over the course of coronary artery disease. *Eur. Heart J.* 34 (41), 3175–3181. doi:10.1093/eurheartj/eht351

Hao, P., Jiang, F., Cheng, J., Ma, L., Zhang, Y., and Zhao, Y. (2017). Traditional Chinese medicine for cardiovascular disease: Evidence and potential mechanisms. *J. Am. Coll. Cardiol.* 69 (24), 2952–2966. doi:10.1016/j.jacc.2017.04.041

Heart Failure Group of Cardiology (2018). Chinese guidelines for the diagnosis and treatment of heart failure 2018. *Chin. J. Cardiovasc. Dis.* 46, 760–789. doi:10.3760/cma.j.issn.0253-3758.2018.10.004

Hernández-García, D., Granado-Serrano, A. B., Martín-Gari, M., Naudí, A., and Serrano, J. C. (2019). Efficacy of Panax ginseng supplementation on blood lipid profile. A meta-analysis and systematic review of clinical randomized trials. *J. Ethnopharmacol.* 243, 112090. doi:10.1016/j.jep.2019.112090

Hien, T. T., Kim, N. D., Kim, H. S., and Kang, K. W. (2010). Ginsenoside Rg3 inhibits tumor necrosis factor-alpha-induced expression of cell adhesion molecules in human endothelial cells. *Pharmazie* 65 (9), 699–701.

Huang, B. (2010). Effects of Qili Qiangxin Capsule on cardiac function and plasma brain natriuretic peptide level in patients with chronic systolic heart failure. *Chin. J. Exp. Prescr.* 16 (16), 191–193. doi:10.3969/j.issn.1005-9903.2010.16.057

Im, D. S. (2020). Pro-resolving effect of ginsenosides as an anti-inflammatory mechanism of panax ginseng. *Biomolecules* 10 (3), 444. doi:10.3390/biom10030444

Irfan, M., Kim, M., and Rhee, M. H. (2020). Anti-platelet role of Korean ginseng and ginsenosides in cardiovascular diseases. *J. Ginseng Res.* 44 (1), 24–32. doi:10.1016/j.jgr.2019.05.005

Janetzky, K., and Morreale, A. P. (1997). Probable interaction between warfarin and ginseng. *Am. J. Health. Syst. Pharm.* 54 (6), 692–693. doi:10.1093/ajhp/54.6.692

Jeon, B. H., Kim, C. S., Kim, H. S., Park, J. B., Nam, K. Y., and Chang, S. J. (2000). Effect of Korean red ginseng on blood pressure and nitric oxide production. *Acta Pharmacol. Sin.* 21 (12), 1095–1100.

Jeong, D., Irfan, M., Kim, S. D., Kim, S., Oh, J. H., Park, C. K., et al. (2017). Ginsenoside Rg3-enriched red ginseng extract inhibits platelet activation and *in vivo* thrombus formation. *J. Ginseng Res.* 41 (4), 548–555. doi:10.1016/j.jgr.2016.11.003

Jia, Y., Zhang, S., Huang, F., and Leung, S. W. (2012). Could ginseng-based medicines be better than nitrates in treating ischemic heart disease? A systematic review and meta-analysis of randomized controlled trials. *Complement. Ther. Med.* 20 (3), 155–166. doi:10.1016/j.ctim.2011.12.002

Jiang, Q. S., Huang, X. N., Dai, Z. K., Yang, G. Z., Zhou, Q. X., Shi, J. S., et al. (2007). Inhibitory effect of ginsenoside Rb1 on cardiac hypertrophy induced by monocrotaline in rat. *J. Ethnopharmacol.* 111 (3), 567–572. doi:10.1016/j.jep.2007.01.006

Jiao, H. C., and Ding, S. W. (2015). "Clinical and basic research of Chinese medicine Xinsuning capsule in the treatment of premature beat," in The Proceedings of the 2015 Academic Conference of the Heart Disease Branch of the Chinese Society of Traditional Chinese Medicine.

Jin, Z. Q., and Liu, C. M. (1994). Effect of ginsenoside Re on the electrophysiological activity of the heart. *Planta Med.* 60 (2), 192–193. doi:10.1055/s-2006-959452

Jin, C., and Zhang, S. Z. (1995). Rise and prospect of glycobiology and glycoengineering. *Adv. Bioeng.* (3), 12–17. doi:10.13523/j.cb.19950306

Kaku, T., Miyata, T., Uruno, T., Sako, I., and Kinoshita, A. (1975). Chemico-pharmacological studies on saponins of Panax ginseng C. A. Meyer. II. Pharmacological part. *Arzneimittelforschung.* 25 (4), 539–547.

Kannel, W. B. (2000). Incidence and epidemiology of heart failure. *Heart fail. Rev.* 5 (2), 167–173. doi:10.1023/A:1009884820941

Kim, S. H., and Park, K. S. (2003). Effects of Panax ginseng extract on lipid metabolism in humans. *Pharmacol. Res.* 48 (5), 511–513. doi:10.1016/s1043-6618(03)00189-0

Konukoglu, D., and Uzun, H. (2017). Endothelial dysfunction and hypertension. *Adv. Exp. Med. Biol.* 956, 511–540. doi:10.1007/5584_2016_90

Kuriachan, V. P., Sumner, G. L., and Mitchell, L. B. (2015). Sudden cardiac death. *Curr. Probl. Cardiol.* 40 (4), 133–200. doi:10.1016/j.cpcardiol.2015.01.002

Kwon, H. W. (2018a). Inhibitory effect of 20(S)-Ginsenoside Rg3 on human platelet aggregation and intracellular Ca2+ levels via cyclic adenosine monophosphate dependent manner. *Prev. Nutr. Food Sci.* 23 (4), 317–325. doi:10.3746/pnf.2018.23.4.317

Kwon, H. W . (2018b). 20(S)-ginsenoside Rg3 inhibits glycoprotein IIb/IIIa activation in human platelets. *J. Appl. Biol. Chem.* 61 (3), 257–265. doi:10.3839/jabc.2018.037

Lee, W. M., Kim, S. D., Park, M. H., Cho, J. Y., Park, H. J., Seo, G. S., et al. (2008). Inhibitory mechanisms of dihydroginsenoside Rg3 in platelet aggregation: Critical roles of ERK2 and cAMP. *J. Pharm. Pharmacol.* 60 (11), 1531–1536. doi:10.1211/jpp/60.11.0015

Lee, K. H., Bae, I. Y., Park, S. I., Park, J. D., and Lee, H. G. (2016). Antihypertensive effect of Korean Red Ginseng by enrichment of ginsenoside Rg3 and arginine-fructose. *J. Ginseng Res.* 40 (3), 237–244. doi:10.1016/j.jgr.2015.08.002

Lee, J. W., Choi, B. R., Kim, Y. C., Choi, D. J., Lee, Y. S., Kim, G. S., et al. (2017a). Comprehensive profiling and quantification of ginsenosides in the root, stem, leaf, and berry of panax ginseng by UPLC-QTOF/MS. *Molecules* 22 (12), 2147. doi:10.3390/molecules22122147

Lee, H. W., Lim, H. J., Jun, J. H., Choi, J., and Lee, M. S. (2017b). Ginseng for treating hypertension: A systematic review and meta-analysis of double blind, randomized, placebo-controlled trials. *Curr. Vasc. Pharmacol.* 15 (6), 549–556. doi:10.2174/1570161115666170713092701

Li, P., and Liu, Z. X. (2006). Effects of ginsenoside Rb1 on ventricular remodeling in rats with acute myocardial infarction. *J. Pract. Cardiovasc. Cerebrovasc. Dis.* 14 (2), 118–121. doi:10.3969/j.issn.1008-5971.2006.02.017

Li, C. Y., and Shi, Z. X. (2013). Clinical research progress of Yixinshu capsule in the treatment of coronary heart disease angina pectoris. *J. Cardiovasc. Cerebrovasc. Dis.* 11 (3), 351–352. doi:10.3969/j.issn.1672-1349.2013.03.052

Li, X. G., and Teng, F. T. (1978). Study on the active ingredients of ginseng—Extraction, separation and identification of ginsenosides and their sapogenins. *J. Res. Chin. Pat. Med.* (03), 1.

Li, R. Q., and Zhang, Y. S. (1984). Purification and characterization of Panax ginseng C. A. Mey pectin. *Chin. J. Pharm.* 19 (10), 764–768. doi:10.16438/j.0513-4870.1984.10.009

Li, R. Q., and Zhang, Y. Y. (1986). Structural studies of Panax ginseng C. A. Mey pectin. *Chin. J. Pharm.* 21 (12), 912–916. doi:10.16438/j.0513-4870.1986.12.006

Li, F. X., and Zhang, C. F. (2015). Clinical study of Xinsuning capsule in the treatment of paroxysmal atrial fibrillation. *Front. Med.* 55 (26), 95–97. doi:10.3969/j.issn.2095-1752.2015.26.077

Li, N., Wu, X. F., and Ma, K. J. (2007). Effects of Shensong Yangxin Capsules on potassium channels in ventricular myocytes. *J. Difficult Dis.* 6 (3), 133–137. doi:10.3969/j.issn.1671-6450.2007.03.002

Li, Y. Q., Wen, H. J., and Liu, W. M. (2010). Effects of Shenshao Capsule on myocardial remodeling in atherosclerotic rats. *Shandong Med.* 50 (4), 21–23. doi:10.3969/j.issn.1002-266X.2010.04.008

Li, J., Shao, Z. H., Xie, J. T., Wang, C. Z., Ramachandran, S., Yin, J. J., et al. (2012). The effects of ginsenoside Rb1 on JNK in oxidative injury in cardiomyocytes. *Arch. Pharm. Res.* 35 (7), 1259–1267. doi:10.1007/s12272-012-0717-3

Li, Q., Xiang, Y., Chen, Y., Tang, Y., and Zhang, Y. (2017). Ginsenoside Rg1 protects cardiomyocytes against hypoxia/reoxygenation injury via activation of Nrf2/HO-1 signaling and inhibition of JNK. *Cell. Physiol. biochem.* 44 (1), 21–37. doi:10.1159/000484578

Li, F., Long, Y., Ma, H., Qiang, T., Zhang, G., and Shen, Y. (2022). Promoting the reduction of CO_2 to formate and formaldehyde via gas-liquid interface dielectric barrier discharge using a $Zn_{0.5}Cd_{0.5}S$/CoP/multiwalled carbon nanotubes catalyst. *J. Colloid Interface Sci.* 46 (6), 880–891. doi:10.1016/j.jcis.2022.04.125

Li, T. C. (2015). Application of Shenshao Capsule in the treatment of unstable angina pectoris. *Shandong Med.* 55 (38), 34–35. doi:10.3969/j.issn.1002-266X.2015.38.012

Liao, D. N., and Yang, Z. J. (2008). The mechanism of antiarrhythmic drug-induced arrhythmia. *Intern. Med. Theory Pract.* 3 (4), 232–234. doi:10.16138/j.1673-6087.2008.04.006

Lin, G. W., Wang, J. Y., and Ge, J. B. (2017). Practical internal medicine. *J. Sci. Technol.* (12), 2. doi:10.16510/j.cnki.kjycb.2017.12.001

Liu, J. X., Ma, X. B., and Wang, Y. H. (2007). Effects of Qili Qiangxin Capsule on cardiac function in dogs with experimental heart failure. *J. Difficult Difficult Dis.* 6 (3), 141–143. doi:10.3969/j.issn.1671-6450.2007.03.004

Liu, J. J., Li, S. G., Deng, J. J., Ye, M., Zhang, D., Peng, Y., et al. (2016). Effects of ginsenoside Rg3 on vascular structure and function in aged rats. *J. Clin. Cardiovasc. Dis.* 32 (11), 1154–1158. doi:10.13201/j.issn.1001-1439.2016.11.020

Liu, Z., Song, L., Zhang, P., Cao, Z., Hao, J., Tian, Y., et al. (2019). Ginsenoside Rb1 exerts antiarrhythmic effects by inhibiting INa and ICaL in rabbit ventricular myocytes. *Sci. Rep.* 9 (1), 20425. doi:10.1038/s41598-019-57010-9

Liu, X., Jiang, Y., Fu, W., Yu, X., and Sui, D. (2020a). Combination of the ginsenosides Rb3 and Rb2 exerts protective effects against myocardial ischemia reperfusion injury in rats. *Int. J. Mol. Med.* 45 (2), 519–531. doi:10.3892/ijmm.2019.4414

Liu, L. S., Yue, J. B., and Ding, X. (2020b). Clinical study of Shenshao Capsule combined with verapamil in the treatment of unstable angina pectoris. *Mod. Med. Clin.* 35 (1), 83–87. doi:10.7501/j.issn.1674-5515.2020.01.018

Liu, K. (2021). Advances in diagnosis and treatment of arrhythmia. *Chin. J. Prescr. Drugs* 19 (9), 23–26. doi:10.3969/j.issn.1671-945X.2021.09.010

Lo, S. H., Hsu, C. T., Niu, H. S., Niu, C. S., Cheng, J. T., and Chen, Z. C. (2017). Ginsenoside Rh2 improves cardiac fibrosis via pparδ-STAT3 signaling in type 1-like diabetic rats. *Int. J. Mol. Sci.* 18 (7), 1364. doi:10.3390/ijms18071364

Lu, W. J., Zhou, J., and Ma, H. Y. (2012). Effects of astragaloside IV, total ginseng saponins and total American ginseng saponins on arrhythmia in mice induced by

toadstool. *J. Nanjing Univ. Traditional Chin. Med.* 28 (01), 61–64. doi:10.14148/j.issn.1672-0482.2012.01.020

Lu, S., Luo, Y., Zhou, P., Yang, K., Sun, G., and Sun, X. (2019). Ginsenoside compound K protects human umbilical vein endothelial cells against oxidized low-density lipoprotein-induced injury via inhibition of nuclear factor-κB, p38, and JNK MAPK pathways. *J. Ginseng Res.* 43 (1), 95–104. doi:10.1016/j.jgr.2017.09.004

Luo, X. P., Li, Y., and Fan, W. H. (1998). Experimental study on the effect of Shexiang Baoxin pills on reducing the damage of arterial wall caused by hyperlipidemia. *China J. Integr. Traditional Chin. West. Med.* (8). doi:10.3321/j.issn:1003-5370.1998.08.012

Nagar, H., Choi, S., Jung, S. B., Jeon, B. H., and Kim, C. S. (2016). Rg3-enriched Korean Red Ginseng enhances blood pressure stability in spontaneously hypertensive rats. *Integr. Med. Res.* 5 (3), 223–229. doi:10.1016/j.imr.2016.05.006

Nanao-Hamai, M., Son, B. K., Komuro, A., Asari, Y., Hashizume, T., Takayama, K. I., et al. (2019). Ginsenoside Rb1 inhibits vascular calcification as a selective androgen receptor modulator. *Eur. J. Pharmacol.* 859, 172546. doi:10.1016/j.ejphar.2019.172546

Qin, N., Gong, Q. H., Wei, L. W., Wu, Q., and Huang, X. N. (2008). Total ginsenosides inhibit the right ventricular hypertrophy induced by monocrotaline in rats. *Biol. Pharm. Bull.* 31 (8), 1530–1535. doi:10.1248/bpb.31.1530

Rezende, P. C., Ribas, F. F., Serrano, C. V., Jr, and Hueb, W. (2019). Clinical significance of chronic myocardial ischemia in coronary artery disease patients. *J. Thorac. Dis.* 11 (3), 1005–1015. doi:10.21037/jtd.2019.02.85

Ryoo, S., Berkowitz, D. E., and Lim, H. K. (2011). Endothelial arginase II and atherosclerosis. *Korean J. Anesthesiol.* 61 (1), 3–11. doi:10.4097/kjae.2011.61.1.3

Ryu, S. J., and Chien, Y. Y. (1995). Ginseng-associated cerebral arteritis. *Neurology* 45 (4), 829–830. doi:10.1212/wnl.45.4.829

Shang, J. H. (2003). Clinical observation on treating angina pectoris with Qishen capsules. *Chin. Pat. Med.* 25 (4), 303–304. doi:10.3969/j.issn.1001-1528.2003.04.014

Shin, W., Yoon, J., Oh, G. T., and Ryoo, S. (2013). Korean red ginseng inhibits arginase and contributes to endotheliumdependent vasorelaxation through endothelial nitric oxide synthase coupling. *J. Ginseng Res.* 37 (1), 64–73. doi:10.5142/jgr.2013.37.64

Shin, J. H., Kwon, H. W., Cho, H. J., Rhee, M. H., and Park, H. J. (2016). Vasodilator-stimulated phosphoprotein-phosphorylation by ginsenoside Ro inhibits fibrinogen binding to αIIb/β3 in thrombin-induced human platelets. *J. Ginseng Res.* 40 (4), 359–365. doi:10.1016/j.jgr.2015.11.003

Siegel, R. K. (1979). Ginseng abuse syndrome. Problems with the panacea. *JAMA* 241 (15), 1614–1615. doi:10.1001/jama.1979.03290410046024

Smolinske, S. C. (1972). Dietary supplement-drug interactions. *J. Am. Med. Womens Assoc.* 54 (4), 191.

Song, X. L., Yang, X. C., and Lu, N. (2022). A multicenter randomized controlled study of Xinsuning capsules in the treatment of phlegm-heat disturbed heart syndrome with premature ventricular contractions. *China J. Integr. Med.* 42 (4), 438–443. doi:10.7661/j.cjim.20220320.067

Stöger, J. L., Gijbels, M. J., van der Velden, S., Manca, M., van der Loos, C. M., Biessen, E. A., et al. (2012). Distribution of macrophage polarization markers in human atherosclerosis. *Atherosclerosis* 225 (2), 461–468. doi:10.1016/j.atherosclerosis.2012.09.013

Su, P., Du, S., Li, H., Li, Z., Xin, W., and Zhang, W. (2016). Notoginsenoside R1 inhibits oxidized low-density lipoprotein induced inflammatory cytokines production in human endothelial EA.hy926 cells. *Eur. J. Pharmacol.* 770, 9–15. doi:10.1016/j.ejphar.2015.11.040

Sun, Y. X., and Wang, H. (1997). Application of variable temperature infrared spectroscopy in extraction of essential oil from ginseng. *Synth. Chem.* 005 (A10), 759.

Sun, X., Gao, R. L., Lin, X. J., Xu, W. H., and Chen, X. H. (2013). Panax notoginseng saponins induced up-regulation, phosphorylation and binding activity of MEK, ERK, AKT, PI-3K protein kinases and GATA transcription factors in hematopoietic cells. *Chin. J. Integr. Med.* 19 (2), 112–118. doi:10.1007/s11655-012-1306-4

Sun, J., Yu, X., Huangpu, H., and Yao, F. (2019). Ginsenoside Rb3 protects cardiomyocytes against hypoxia/reoxygenation injury via activating the antioxidation signaling pathway of PERK/Nrf2/HMOX1. *Biomed. Pharmacother.* 109, 254–261. doi:10.1016/j.biopha.2018.09.002

Takagi, K., Saito, H., and Nabata, H. (1972). Pharmacological studies of panax ginseng root: Estimation of pharmacological actions of panax ginseng root. *Jpn. J. Pharmacol.* 22 (2), 245–249. doi:10.1254/jjp.22.245

Tao, Y. J., Jiang, B. H., and Qiu, H. (2009). Curative effect observation of Yixinshu capsule in the treatment of unstable angina pectoris. *J. Cardiovasc. Cerebrovasc. Dis. Integr. Traditional Chin. West. Med.* 7 (5), 596–597. doi:10.3969/j.issn.1672-1349.2009.05.046

Teng, C. M., Kuo, S. C., Ko, F. N., Lee, J. C., Lee, L. G., Chen, S. C., et al. (1989). Antiplatelet actions of panaxynol and ginsenosides isolated from ginseng. *Biochim. Biophys. Acta* 990 (3), 315–320. doi:10.1016/s0304-4165(89)80051-0

Tian, Y. B., Zhao, D. Q., and Li, X. Y. (2018). Ginseng polysaccharide protects cardiomyocytes from H2O2-induced oxidative stress injury by inhibiting ROS level and apoptosis. *J. Central China Normal Univ. Nat. Sci. Ed.* 52 (2), 240–247. doi:10.19603/j.cnki.1000-1190.2018.02.014

Tsai, C. C., Chan, P., Chen, L. J., Chang, C. K., Liu, Z., and Lin, J. W. (2014). Merit of ginseng in the treatment of heart failure in type 1-like diabetic rats. *Biomed. Res. Int.* 2014, 484161. doi:10.1155/2014/484161

Virani, S. S., Alonso, A., Benjamin, E. J., Bittencourt, M. S., Callaway, C. W., Carson, A. P., et al. (2020). Heart disease and stroke statistics-2020 update: A report from the American heart association. *Circulation* 141 (9), e139–e596. doi:10.1161/CIR.0000000000000757

Wan, H. F., Ying, J. N., and Guan, Y. (2020). Protective effect of ginseng polysaccharides on mitochondria in myocardial cells of rats with coronary heart disease. *Mod. Food Sci. Technol.* 36 (11), 2460–2528. doi:10.13982/j.mfst.1673-9078.2020.11.0510

Wang, G., and Li, J. P. (2012). Effects of Tongxinluo capsules on serum IL-18 and hs-CRP in elderly patients with coronary heart disease and angina pectoris. *Guangdong Med.* 33 (2), 276–278. doi:10.3969/j.issn.1001-9448.2012.02.053

Wang, C. H., and Lu, J. (2008). Xinsuning capsule in the treatment of 30 cases of viral myocarditis. *Shaanxi Tradit. Chin. Med.* 29 (10), 1362. doi:10.3969/j.issn.1000-7369.2008.10.068

Wang, H. L., and Zhi, J. C. (2016). Clinical observation of Yixinshu capsule combined with isosorbide dinitrate tablets in the treatment of angina pectoris. *Medicine* 000 (004), 285. doi:10.16138/j.1671-5837.2016.04.026

Wang, S. S., Li, Y., and Fan, W. H. (2002). Angiogenesis-promoting effect of Shexiang Baoxin Pill on the heart of rats with experimental myocardial infarction. *Chin. Pat. Med.* 24 (6), 446–449. doi:10.3969/j.issn.1001-1528.2002.06.016

Wang, D. Y., Li, Y., and Fan, W. H. (2004). Effects of Shexiang Baoxin Pill on infarct size and angiogenesis in rats with myocardial infarction. *Chin. Pat. Med.* 26 (11), 912–915. doi:10.3969/j.issn.1001-1528.2004.11.018

Wang, N. Y., Lu, C. J., and Chen, X. H. (2005). Study on effect of ginsenoside Rg1 in promoting myocardiac vascular endothelial cell regeneration through induction on bone marrow stem cell's migration and differentiation in rabbits of myocardial infarction. *China J. Integr. Traditional Chin. West. Med.* 25 (10), 916–919. doi:10.3321/j.issn:1003-5370.2005.10.014

Wang, T. X., Yu, X. F., Qu, S. C., et al. (2008). Effect of ginseng Rb group saponins on ventricular remodeling in rats with stress-loaded myocardial hypertrophy and its mechanism of action. *J. Lishizhen Med. Materia Medica Res.* 19 (7), 1615–1617. doi:10.3969/j.issn.1008-0805.2008.07.032

Wang, X., Duan, H. N., and Hu, J. (2012). Experimental study on the effect of Shensong Yangxin capsule on cardiac function and cardiac electrophysiology. *Chin. J. Cardiac Arrhythmia* 16 (6), 417–421. doi:10.3760/cma.j.issn.1007-6638.2012.06.004

Wang, Y., Dong, J., Liu, P., Lau, C. W., Gao, Z., Zhou, D., et al. (2014). Ginsenoside Rb3 attenuates oxidative stress and preserves endothelial function in renal arteries from hypertensive rats. *Br. J. Pharmacol.* 171 (13), 3171–3181. doi:10.1111/bph.12660

Wang, Y., Hu, Z., Sun, B., Xu, J., Jiang, J., and Luo, M. (2015). Ginsenoside Rg3 attenuates myocardial ischemia/reperfusion injury via Akt/endothelial nitric oxide synthase signaling and the B-cell lymphoma/B-cell lymphoma-associated X protein pathway. *Mol. Med. Rep.* 11 (6), 4518–4524. doi:10.3892/mmr.2015.3336

Wang, Q. W., Yu, X. F., Xu, H. L., Zhao, X. Z., and Sui, D. Y. (2019). Ginsenoside Re improves isoproterenol-induced myocardial fibrosis and heart failure in rats. *Evid. Based Complement. Altern. Med.* 2019, 3714508. doi:10.1155/2019/3714508

Wang, Y. J. (2010). Clinical study of Qishen capsule in the treatment of coronary heart disease and angina pectoris. *Chin. J. Traditional Chin. Med.* 25 (5), 939–940.

World Health Statistics (2022). The global health observatory. Avaliable at: https://www.who.int/data/gho/publications/world-health-statistics.

Wu, J. Z., Li, X. G., and Yang, J. X. (1996). Comparative study on the volatile oil components of fresh ginseng in Hongshen. *Strait Pharm.* (1), 5–6.

Wu, X. L., Li, J. B., and Zhang, Y. (2001). Clinical study of Tongxinluo capsule on blood lipid and blood viscosity. *China J. Basic Med. Traditional Chin. Med.* 7 (5), 32–33. doi:10.3969/j.issn.1006-3250.2001.05.015

Wu, Z. L., Xu, D. L., and Lin, S. (2011). Effects of Qili Qiangxin Capsule on cardiac function and plasma vasopressin in rats with chronic heart failure. *J. Difficult Difficult Dis.* 10 (2), 120–122. doi:10.3969/j.issn.1671-6450.2011.02.020

Xiao, W. L., Dai, H., and Jiang, Z. A. (2002). Study on the protective effect of Tongxinluo capsule on vascular endothelial cells in patients with unstable angina pectoris. *Chin. J. Cardiovasc. Dis.* 30 (5), 268. doi:10.3760/j:issn:0253-3758.2002.05.017

Xu, H., Ge, Y. K., and Deng, T. L., (2005). Protective effect of ginsenoside Rb1 on H2O2-induced cardiomyocyte apoptosis in neonatal rats. *Chin. Pharmacol. Bull.* 21 (7), 803–806. doi:10.3321/j.issn:1001-1978.2005.07.009

Xu, Z. M., Li, C. B., Liu, Q. L., Li, P., and Yang, H. (2018). Ginsenoside Rg1 prevents doxorubicin-induced cardiotoxicity through the inhibition of autophagy and endoplasmic reticulum stress in mice. *Int. J. Mol. Sci.* 19 (11), 3658. doi:10.3390/ijms19113658

Yan, J. C., Zhang, H., and Wei, Y. D. (1994). Extraction and analysis of volatile oil from ginseng. *J. Analysis Test.* 13 (3), 5.

Yang, Q., and Huang, L. (2013). Observation on the efficacy of Qishen Capsules in the treatment of coronary heart disease angina pectoris. *China Emerg. Med.* 22 (9), 1602. doi:10.3969/j.issn.1004-745X.2013.09.070

Yang, P., Ling, L., Sun, W., Yang, J., Zhang, L., Chang, G., et al. (2018). Ginsenoside Rg1 inhibits apoptosis by increasing autophagy via the AMPK/mTOR signaling in serum deprivation macrophages. *Acta Biochim. Biophys. Sin.* 50 (2), 144–155. doi:10.1093/abbs/gmx136

Yang, M. (2020). Clinical observation of Xinsuning capsule combined with Betaloc in the treatment of premature ventricular contractions. *Guizhou Med.* 44 (3), 425–427. doi:10.3969/j.issn.1000-744X.2020.03.033

Yi, X. Q., Li, T., Wang, J. R., Wong, V. K., Luo, P., Wong, I. Y., et al. (2010). Total ginsenosides increase coronary perfusion flow in isolated rat hearts through activation of PI3K/Akt-eNOS signaling. *Phytomedicine* 17 (13), 1006–1015. doi:10.1016/j.phymed.2010.06.012

Yi, D. L. (2013). Analysis of rational use of cardiovascular drugs in the elderly. *Chin. J. Health Nutr.* 23 (3), 1376. doi:10.3969/j.issn.1004-7484(s).2013.03.436

You, S. J., Yang, Y. J., and Chen, K. J. (2004). Efficacy and safety of Tongxinluo capsule after revascularization in acute myocardial infarction. *J. Difficult Difficult Dis.* 3 (4), 193–196. doi:10.3969/j.issn.1671-6450.2004.04.001

You, J. S., Huang, H. F., and Chang, Y. L. (2005). Panax ginseng reduces adriamycin-induced heart failure in rats. *Phytother. Res.* 19 (12), 1018–1022. doi:10.1002/ptr.1778

Yuan, J., Guo, W., Yang, B., Liu, P., Wang, Q., and Yuan, H. (1997). 116 cases of coronary angina pectoris treated with powder composed of radix ginseng, radix notoginseng and succinum. *J. Tradit. Chin. Med.* 17 (1), 14–17.

Yuan, S. W. (2000). Observation on 60 cases of tachyarrhythmia in xinsuning capsule. *J. Shandong Univ. Traditional Chin. Med.* 24 (4), 4. doi:10.3969/j.issn.1007-659X.2000.04.027

Zhang, W., and Ding, J. X. (2021). Clinical effect of Shenshao Capsule in the treatment of coronary heart disease angina pectoris. *J. Clin. Ration. Med.* 14 (35), 38–39. doi:10.15887/j.cnki.13-1389/r.2021.35.013

Zhang, R., and Liu, Y. F. (2009). Effects of ginsenoside Rg1 on angiogenesis and cardiac function after acute myocardial infarction in rats. *Chongqing Med. Sci.* 38 (7), 805–807. doi:10.3969/j.issn.1671-8348.2009.07.026

Zhang, Y. L., and Zhu, X. M. (2011). Clinical observation of Yixinshu Capsule in the treatment of diastolic heart failure. *J. Cardiovasc. Cerebrovasc. Dis. Integr. Traditional Chin. West. Med.* 9 (3), 287–289. doi:10.3969/j.issn.1672-1349.2011.03.015

Zhang, Y. S., Li, R. Q., and Wang, Y. W. (1982). Study on ginseng polysaccharides (I). *J. Northeast Normal Univ. Nat. Sci. Ed.* 14 (02), 100–107. doi:10.16163/j.cnki.22-1123/n.1982.02.014

Zhang, H. G., Yan, J. C., and Wu, G. X. (1994). Study on fatty acid components in ginseng of Changbai. *J. Bethune Med. Univ.* 20 (4), 365. doi:10.13481/j.1671-587x.1994.04.027

Zhang, X. M., Qu, S. C., Sui, D. Y., Yu, X. F., and Lv, Z. Z. (2004). Effects of ginsenoside-Rb on blood lipid metabolism and anti-oxidation in hyperlipidemia rats. *Zhongguo Zhong Yao Za Zhi* 29 (11), 1085–1088. doi:10.3321/j.issn:1001-5302.2004.11.019

Zhang, Y. G., Zhang, H. G., Zhang, G. Y., Fan, J. S., Li, X. H., Liu, Y. H., et al. (2008). Panax notoginseng saponins attenuate atherosclerosis in rats by regulating the blood lipid profile and an anti-inflammatory action. *Clin. Exp. Pharmacol. Physiol.* 35 (10), 1238–1244. doi:10.1111/j.1440-1681.2008.04997.x

Zhang, Z. L., Fan, Y., and Liu, M. L. (2012). Ginsenoside Rg1 inhibits autophagy in H9c2 cardiomyocytes exposed to hypoxia/reoxygenation. *Mol. Cell. Biochem.* 365 (1-2), 243–250. doi:10.1007/s11010-012-1265-3

Zhang, Y. J., Zhang, X. L., Li, M. H., Iqbal, J., Bourantas, C. V., Li, J. J., et al. (2013a). The ginsenoside Rg1 prevents transverse aortic constriction-induced left ventricular hypertrophy and cardiac dysfunction by inhibiting fibrosis and enhancing angiogenesis. *J. Cardiovasc. Pharmacol.* 62 (1), 50–57. doi:10.1097/FJC.0b013e31828f8d45

Zhang, D. L., Liang, L. J., and Zhang, J. (2013b). Effects of ginseng polysaccharide on myocardial hypertrophy and myocardial energy metabolism in rats with abdominal aortic constriction. *China Mod. Appl. Pharm.* 30 (6), 571–575. doi:10.13748/j.cnki.issn1007-7693.2013.06.009

Zhang, J. F., Tang, S. W., and Wang, H. T. (2013c). Effects of Qili Qiangxin Capsule on endothelial injury and energy metabolism in rats with pressure overload heart failure. *J. Traditional Chin. Med.* 54 (14), 5.

Zhang, Y. S., Chen, X., and Li, Y. (2014). Research progress on the correlation between mitochondrial DNA mutations and essential hypertension. *Chin. J. Multiple Organ Dis. Aged* (10), 781–787. doi:10.3724/SP.J.1264.2014.000181

Zhang, L. P., Jiang, Y. C., Yu, X. F., Xu, H. L., Li, M., Zhao, X. Z., et al. (2016). Ginsenoside Rg3 improves cardiac function after myocardial ischemia/reperfusion via attenuating apoptosis and inflammation. *Evid. Based Complement. Altern. Med.* 2016, 6967853. doi:10.1155/2016/6967853

Zhang, X., Liu, M. H., Qiao, L., Zhang, X. Y., Liu, X. L., Dong, M., et al. (2018). Ginsenoside Rb1 enhances atherosclerotic plaque stability by skewing macrophages to the M2 phenotype. *J. Cell Mol. Med.* 22 (1), 409–416. doi:10.1111/jcmm.13329

Zhang, N., An, X., Lang, P., Wang, F., and Xie, Y. (2019). Ginsenoside Rd contributes the attenuation of cardiac hypertrophy *in vivo* and *in vitro*. *Biomed. Pharmacother.* 109, 1016–1023. doi:10.1016/j.biopha.2018.10.081

Zhang, J., Luo, D., Li, F., Li, Z., Gao, X., Qiao, J., et al. (2021). Ginsenoside Rg3 alleviates antithyroid cancer drug vandetanib-induced QT interval prolongation. *Oxid. Med. Cell Longev.* 2021, 3520034. doi:10.1155/2021/3520034

Zhang, Hj (2011). Research progress of traditional Chinese and Western medicine on the pathogenesis of essential hypertension. *Mod. J. Integr. Traditional Chin. West. Med.* 20 (19), 2465–2467. doi:10.3969/j.issn.1008-8849.2011.19.087

Zhang, Y. (2016). *Anti-myocardial ischemia mechanism of compound ginseng volatile oil aerosol and its effect on hemorheology*. Jilin: Changchun University of Traditional Chinese Medicine.

Zhao, M. Z., Gao, C. M., and Zhang, Y. Y. (2000). Experimental study on the protective effect of Tongxinluo capsule on experimental myocardial ischemia-reperfusion injury. *China J. Basic Med.* 6 (1), 36–38. doi:10.3969/j.issn.1006-3250.2000.01.013

Zheng, Q., Bao, X. Y., Zhu, P. C., Tong, Q., Zheng, G. Q., and Wang, Y. (2017a). Ginsenoside Rb1 for myocardial ischemia/reperfusion injury: Preclinical evidence and possible mechanisms. *Oxid. Med. Cell. Longev.* 2017, 6313625. doi:10.1155/2017/6313625

Zheng, X., Wang, S., Zou, X., Jing, Y., Yang, R., Li, S., et al. (2017b). Ginsenoside Rb1 improves cardiac function and remodeling in heart failure. *Exp. Anim.* 66 (3), 217–228. doi:10.1538/expanim.16-0121

Zhou, W., Chai, H., Lin, P. H., Lumsden, A. B., Yao, Q., and Chen, C. (2005). Ginsenoside Rb1 blocks homocysteine-induced endothelial dysfunction in porcine coronary arteries. *J. Vasc. Surg.* 41 (5), 861–868. doi:10.1016/j.jvs.2005.01.054

Zhou, H., Hou, S. Z., Luo, P., Zeng, B., Wang, J. R., Wong, Y. F., et al. (2011). Ginseng protects rodent hearts from acute myocardial ischemia-reperfusion injury through GR/ER-activated RISK pathway in an endothelial NOS-dependent mechanism. *J. Ethnopharmacol.* 135 (2), 287–298. doi:10.1016/j.jep.2011.03.015

Zhou, Q., Jiang, L., Xu, C., Luo, D., Zeng, C., Liu, P., et al. (2014). Ginsenoside Rg1 inhibits platelet activation and arterial thrombosis. *Thromb. Res.* 133 (1), 57–65. doi:10.1016/j.thromres.2013.10.032

Zhou, S. S., Wang, Y. Y., and Liu, D. (2015). Optimization of ultrasonic-assisted extraction of polysaccharide from ginseng flowers and its antioxidant activity. *Food Sci.* 36 (6), 76–81. doi:10.7506/spkx1002-6630-201506014

Zhou, P., Lu, S., Luo, Y., Wang, S., Yang, K., Zhai, Y., et al. (2017). Attenuation of TNF-α-Induced inflammatory injury in endothelial cells by ginsenoside Rb1 via inhibiting NF-κB, JNK and p38 signaling pathways. *Front. Pharmacol.* 8, 464. doi:10.3389/fphar.2017.00464

Zhou, P., Lu, S., Luo, Y., Wang, S., Yang, K., Zhai, Y., et al. (2017). Attenuation of TNF-α-Induced inflammatory injury in endothelial cells by ginsenoside Rb1 via inhibiting NF-κB, JNK and p38 signaling pathways. *Front. Pharmacol.* 8, 464. doi:10.3389/fphar.2017.00464

Zhou, P., Xie, W., Luo, Y., Lu, S., Dai, Z., Wang, R., et al. (2018). Inhibitory effects of ginsenoside Rb1 on early atherosclerosis in ApoE-/- mice via inhibition of apoptosis and enhancing autophagy. *Molecules* 23 (11), 2912. doi:10.3390/molecules23112912

Zhou, P., Xie, W., Sun, Y., Dai, Z., Li, G., Sun, G., et al. (2019). Ginsenoside Rb1 and mitochondria: A short review of the literature. *Mol. Cell ProbesMol Cell Probes*. 4354, 1101626–1101635. doi:10.1016/j.mcp.2018.12.001

Zhu, H., Luo, X. P., and Wang, L. J. (2010). Evaluation on clinical effect of long-term shexiang baoxin pill administration for treatment of coronary heart disease. *China J. Integr. Traditional Chin. West. Med.* 30 (5), 474–477.

Zuo, X. (2021). *Anti-inflammatory activity of ginseng volatile oil*. Changchun, China: Jilin University.

frontiers | Frontiers in Pharmacology

TYPE Systematic Review
PUBLISHED 02 December 2022
DOI 10.3389/fphar.2022.1025104

Check for updates

OPEN ACCESS

EDITED BY
Chen Huei Leo,
Singapore University of Technology and Design, Singapore

REVIEWED BY
Kuo Gao,
Beijing University of Chinese Medicine, China
Jianbo Guo,
The University of Hong Kong, Hong Kong SAR, China
Qiang Tang,
Chengdu University of Traditional Chinese Medicine, China

*CORRESPONDENCE
Kuiwu Yao,
yaokuiwu@126.com

†These authors have contributed equally to this work and share first authorship

SPECIALTY SECTION
This article was submitted to Ethnopharmacology, a section of the journal Frontiers in Pharmacology

RECEIVED 22 August 2022
ACCEPTED 22 November 2022
PUBLISHED 02 December 2022

CITATION
Lin J, Wang Q, Xu S, Zhou S, Zhong D, Tan M, Zhang X and Yao K (2022), Banxia baizhu tianma decoction, a Chinese herbal formula, for hypertension: Integrating meta-analysis and network pharmacology.
Front. Pharmacol. 13:1025104.
doi: 10.3389/fphar.2022.1025104

COPYRIGHT
© 2022 Lin, Wang, Xu, Zhou, Zhong, Tan, Zhang and Yao. This is an open-access article distributed under the terms of the Creative Commons Attribution License (CC BY). The use, distribution or reproduction in other forums is permitted, provided the original author(s) and the copyright owner(s) are credited and that the original publication in this journal is cited, in accordance with accepted academic practice. No use, distribution or reproduction is permitted which does not comply with these terms.

Banxia baizhu tianma decoction, a Chinese herbal formula, for hypertension: Integrating meta-analysis and network pharmacology

Jianguo Lin[1,2†], Qingqing Wang[1†], Siyu Xu[1,3], Simin Zhou[1], Dongsheng Zhong[4], Meng Tan[4], Xiaoxiao Zhang[1] and Kuiwu Yao[1,5*]

[1]Guang'anmen Hospital, China Academy of Chinese Medical Sciences, Beijing, China, [2]Tianjin University of Traditional Chinese Medicine, Tianjin, China, [3]Beijing University of Chinese Medicine, Beijing, China, [4]Guizhou University of Traditional Chinese Medicine, Guizhou, China, [5]Eye Hospital China Academy of Chinese Medical Sciences, Beijing, China

Hypertension is a major cardiovascular risk factor, which seriously affects the quality of life of patients. Banxia Baizhu Tianma Decoction (BXD) is a Chinese herbal formula that is widely used to treat hypertension in China. This study aimed to evaluate the efficacy and potential mechanism of BXD for hypertension by meta-analysis and network pharmacology. Meta-analysis was performed to explore the efficacy and safety of BXD combined with conventional treatment for hypertension. Network pharmacology was used to explore the molecular mechanism of BXD in antihypertension. A total of 23 studies involving 2,041 patients were included. Meta-analysis indicated that compared with conventional treatment, combined BXD treatment was beneficial to improve clinical efficacy rate, blood pressure, blood lipids, homocysteine, endothelial function, inflammation, and traditional Chinese medicine symptom score. In addition, meta-analysis indicated that BXD is safe and has no obvious adverse reactions. Network pharmacology showed that the antihypertensive targets of BXD may be AKT1, NOS3, ACE, and PPARG. The antihypertensive active ingredients of BXD may be naringenin, poricoic acid C, eburicoic acid, and licochalcone B. Due to the poor methodological quality of the Chinese studies and the small sample size of most, the analysis of this study may have been affected by bias. Therefore, the efficacy and safety of BXD for hypertension still need to be further verified by high-quality clinical studies.

Systematic Review Registration: https://www.crd.york.ac.uk/prospero/, identifier CRD42022353666

KEYWORDS

banxia baizhu tianma decoction, hypertension, meta-analysis, network pharmacology, blood pressure, traditional Chinese medicine

1 Introduction

Hypertension is a clinical syndrome characterized by increased systemic arterial blood pressure, which may be accompanied by functional or organic damage of the heart, brain, kidney, and other organs [Hypertension was defined as systolic blood pressure (SBP) ≥ 140 mmHg or diastolic blood pressure (DBP) ≥ 90 mmHg] (Messerli et al., 2007). Hypertension is the leading preventable risk factor for cardiovascular disease and all-cause mortality worldwide (Mills et al., 2020). The prevalence of hypertension will gradually increase with urbanization, population aging, and related lifestyle changes such as unhealthy diets and physical inactivity. In China, the prevalence of hypertension among people over 18 years old is 23.2%, which is about 240 million (Zhao et al., 2019). A 2019 study found that only 30% of people with hypertension were treated with medications, and only 10% had their blood pressure controlled below threshold levels for hypertension. High-income countries generally do better, but most have lower treatment and control rates than developed countries (Geldsetzer et al., 2019). Therefore, prevention and treatment of hypertension are urgent.

Over the past half-century, tremendous progress has been made in the pharmacological treatment of hypertension, but some shortcomings remain (adverse effects, drug resistance, long-term use, economic burden, etc.) (Bramlage and Hasford, 2009; Albasri et al., 2021). Hypertension belongs to the category of headache and vertigo in traditional Chinese medicine (TCM). TCM has a long history in the treatment of hypertension and has accumulated a lot of experience in pre-hypertension, hypertension, obese hypertension, and resistant hypertension (Xiong et al., 2013; Xiong et al., 2015; Zhang et al., 2020). Banxia Baizhu Tianma Decoction (BXD) is a TCM formula that originated from the Qing Dynasty. BXD is composed of 6 types of botanical drugs, including *Pinellia ternata* (Thunb.) Makino [Araceae] (Banxia), *Atractylodes macrocephala* Koidz. [Asteraceae] (Baizhu), *Citrus* × *aurantium* L. [Rutaceae] (Chenpi), *Glycyrrhiza uralensis* Fisch. ex DC. [Fabaceae] (Gancao), *Gastrodia elata* Blume [Orchidaceae] (Tianma), *Wolfiporia cocos* (F.A. Wolf) Ryvarden & Gilb. 1984 (Fulin). BXD has the effects of eliminating dampness and phlegm, dispelling pathogenic wind and eliminating phlegm and is widely used in hypertension and its complications (Xiong et al., 2012), however, there is a lack of high-quality, high-level evidence to further confirm its clinical efficacy. Currently, the active ingredients from BXD have been shown to have anti-inflammatory, antioxidant, vasodilator, and calcium ion regulation effects (Tan et al., 2018; Xu et al., 2022), however, the mechanism of BXD in improving hypertension has not been clarified. Network pharmacology is a new subject based on systems biology and bioinformatics, which can elucidate the mechanism of drug action at the molecular level (Xiao et al., 2021). TCM network pharmacology approach provides a new research paradigm for translating TCM from an experience-based medicine to an evidence-based medicine system, which will accelerate botanical drug discovery, and improve current drug discovery strategies (Luo et al., 2020). In this study, we aimed to validate the efficacy of BXD in hypertensive patients and to explore the underlying molecular and cellular mechanisms from network pharmacology perspective.

2 Materials and methods

This study was conducted and reported according to the guidelines of Preferred Reporting Items for Systematic Reviews and Meta-Analyses (PRISMA) (Liberati et al., 2009). The study protocol (CRD42022353666) was registered in the PROSPERO (https://www.crd.york.ac.uk/prospero/).

2.1 Literature search strategy

The databases used in this study included PubMed, Cochrane, Embase, Wanfang database, China national knowledge infrastructure (CNKI), and China Science and Technology Journal Database (VIP). The retrieval time was set as the establishment of the database until August 2022. The search terms were MeSH terms combined with the keywords: “banxia baizhu tianma” and “hypertension”. The search strategy was shown in Supplementary Table S1.

2.2 Inclusion and exclusion criteria

The inclusion criteria for this study were: 1) The type of study is randomized controlled trials (RCTs). 2) Patients met the diagnostic criteria for hypertension (Hypertension and League, 2019). 3) The experimental group received BXD combined with conventional treatment. The control group received conventional treatment. The treatment dose and course of treatment were unrestricted. Conventional treatment included calcium channel blockers (CCB), angiotensin-converting enzyme inhibitors (ACEI), angiotensin receptor blockers (ARBs), diuretics, and β-receptor blockers.

The exclusion criteria for this study were: 1) Duplicate published studies. 2) Studies with incorrect or incomplete data. 3) Unable to extract data for research. 4) Review or experiment articles.

2.3 Outcome measure

The primary outcome measures were: SBP, DBP, and clinical efficacy rate. The secondary outcome measures were: total

cholesterol (TC), triglyceride (TG), high-density lipoprotein cholesterol (HDL-C), low-density lipoprotein cholesterol (LDL-C), homocysteine (Hcy), endothelial function, inflammatory biomarkers, and TCM symptom score.

2.4 Data extraction

Data were extracted independently from the included literature by SM and SY. A "basic information extraction table" was developed, and the information extracted included: the investigator, year of publication, number of cases, age, intervention, duration of intervention, and outcome measures. Any disputes were resolved through discussion with the third author (QW). When necessary, study details were requested from the corresponding authors *via* email.

2.5 Risk of bias and quality assessment

The quality of the included studies was evaluated with the risk bias assessment by Cochrane collaboration's tool (Higgins et al., 2011), including random sequence generation, allocation hiding, blinding of practitioners and subjects, blinding of outcome evaluators, the integrity of outcome data, selective reporting of results, and other sources of bias. Three evaluation results, namely low risk, high risk, and unclear risk, were made one by one.

2.6 Statistical analysis

The Stata 17.0 software (Stata Corp., College Station, TX, United States) was applied to statistical analysis. Standardized mean difference (SMD) was utilized for continuous outcomes. Risk ratio (RR) was utilized for dichotomous outcomes. All of them were expressed with a 95% confidence interval (CI). Heterogeneity was tested using the Q test, and if $I^2 \leq 50\%$, a fixed-effects model was used, and if $I^2 > 50\%$, indicating greater statistical heterogeneity, a random-effects model was used. Both results were expressed using a forest plot. The publication bias was estimated by Egger's test and funnel plot. It was regarded as a significant difference when $p < 0.05$.

2.7 Identify BXD and hypertension targets

With the Traditional Chinese Medicine Systems Pharmacology Database and Analysis Platform (TCMSP, https://tcmspw.com) (Ru et al., 2014), the active ingredients of BXD were obtained. The TCMSP parameter was set as bioavailability (OB) ≥ 30% and drug-like properties (DL) ≥ 0.18 (Guo et al., 2019). The targets corresponding to the active ingredients were obtained by using the Swiss Target Prediction database (http://swisstargetprediction.ch/). With "hypertension" as the keyword, the targets of hypertension were obtained through four databases. The four different databases and search criteria are as follows: GeneCards (https://www.genecards.org/) (Stelzer et al., 2016), and the screening criterion is relevance score ≥ 4; Comparative Toxicogenomics Database (CTD) (https://ctdbase.org/) (Davis et al., 2019), and the screening criterion is direct evidence or inference score ≥ 100; DisGeNET (https://www.disgenet.org) (Piñero et al., 2020), and the screening standard is gene-disease association score ≥ 0.2. INPUT 2.0 (http://cbcb.cdutcm.edu.cn/INPUT/) (Li Q et al., 2022), and the screening criterion set the default parameters. Subsequently, the intersection of these targets was taken to obtain the crossover targets.

2.8 Protein-protein interaction and gene enrichment analysis

PPI analysis of overlapping targets was conducted through STRING platform (https://string-db.org/) (Szklarczyk et al., 2019), and the calculated results were imported into Cytoscape 3.9.1 software (Shannon et al., 2003) for network topology analysis. CytoHubba plug-in was used to screen key targets. Gene enrichment of overlapping targets was performed through DAVID database (https://david.ncifcrf.gov/) (Huang et al., 2009). It mainly includes molecular function (MF), cellular components (CC), biological process (BP), and kyoto encyclopedia of genes and genomes (KEGG). Hiplot (https://hiplot-academic.com/) was used to visualize the results.

2.9 Molecular docking

Selected key targets and key ingredients for molecular docking. The key target structures were obtained through PDB database (https://www.rcsb.org/). The structure of the key ingredients was obtained through the PubChem database (https://pubchem.ncbi.nlm.nih.gov/). Then used Pymol, Autodock Vina (Trott and Olson, 2010), and PLIP (https://plip-tool.biotec.tu-dresden.de/) (Adasme et al., 2021) for molecular docking.

3 Results

3.1 Eligible studies

A total of 1,747 related studies were retrieved. 1,003 studies remain after the elimination of duplicates by NoteExpress software and manual assistance. After reading the abstract and title, 101 studies remain. After reading the full text, 78 studies were excluded. Finally, a total of 23 studies were included (Wu et al., 2007; Xiong, 2010; Pang, 2013; Huang and Li, 2014; Shen and Jin, 2015; Guan and Chen, 2016; Liu, 2016; Wu and Zhou,

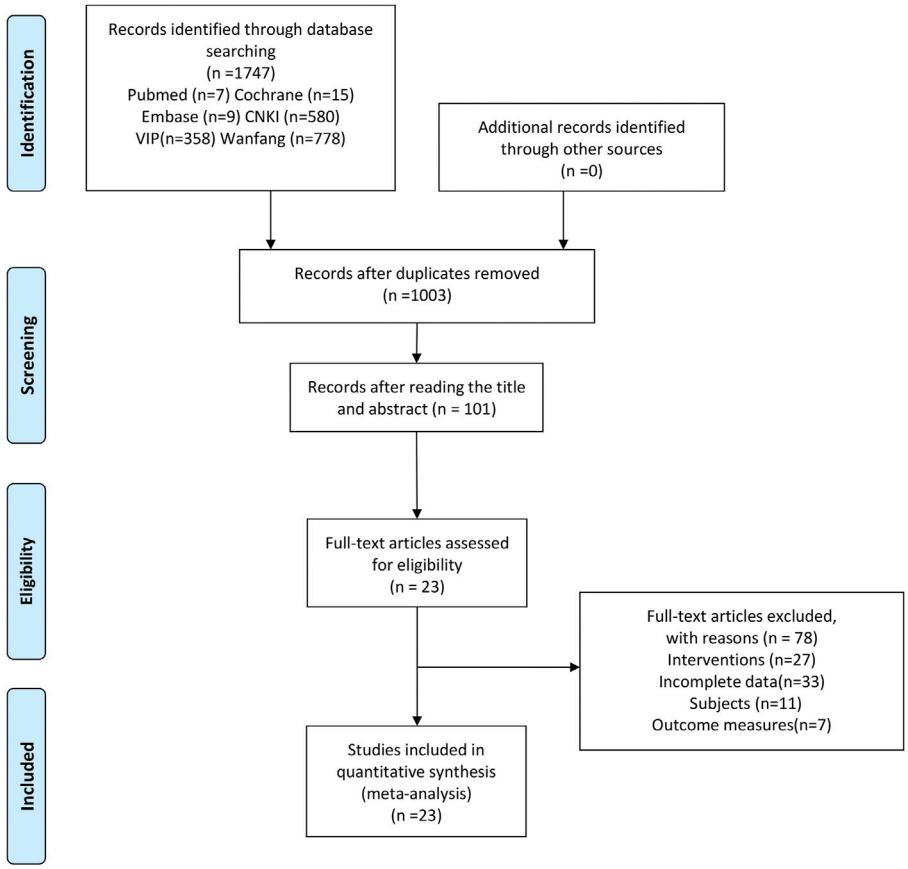

FIGURE 1
Flow diagram of the study selection process.

2016; Zhao et al., 2016; Miao et al., 2017; Song, 2018; Ma et al., 2019; Shi, 2019; Wu, 2019; Liu et al., 2020; Mu, 2020; Tang et al., 2020; Zhang, 2021; Zhang et al., 2021; Zheng, 2021; Dai et al., 2022; Zhang et al., 2022; Zhao, 2022). The flow diagram of screening was shown in Figure 1.

3.2 Characteristics of studies

A total of 23 RCTs involving 2,041 patients (treatment group: 1,025, control group: 1,016) were included. The publication period was from 2007 to 2022. The shortest treatment time was 4 weeks, and the longest treatment time was 12 weeks. Types of hypertension include H-type hypertension (Pang, 2013; Wu and Zhou, 2016; Liu et al., 2020; Zhao, 2022), senile hypertension (Liu et al., 2020; Mu, 2020; Zhang, 2021), hypertensive crisis (Zhang et al., 2021), obesity type hypertension (Huang and Li, 2014; Zhao et al., 2016; Shi, 2019), phlegm-dampness type hypertension (Wu et al., 2007; Xiong, 2010; Huang and Li, 2014; Guan and Chen, 2016; Zhao et al., 2016; Miao et al., 2017; Shi, 2019; Liu et al., 2020; Mu, 2020; Tang et al., 2020; Zhang et al., 2021; Dai et al., 2022; Zhang et al., 2022). In all the studies, BXD was the basic prescription, and botanical drugs (Such as *Alisma plantago-aquatica* L. [Alismataceae] (Zexie), *Neolitsea cassia* (L.) Kosterm. [Lauraceae] (Guizhi), *Arisaema heterophyllum* Blume [Araceae] (Dannanxing), *Conioselinum anthriscoides* '*Chuanxiong*' [Apiaceae] (Chuanxiong), *Chrysanthemum* × *morifolium* (Ramat.) Hemsl. [Asteraceae] (Juhua), *Vitex trifolia* L. [Lamiaceae] (Manjingzi), *Acorus gramineus* Aiton [Acoraceae] (Shichangpu)) were added or subtracted according to syndrome differentiation. The characteristics of the included studies were shown in Table 1. The composition of the prescriptions was shown in Supplementary Table S2.

3.3 Risk of bias and quality assessment of studies

All studies were randomized, and the majority of studies described specific randomization methods. One study (Dai

TABLE 1 Characteristics of the included studies.

Study	Sample size (T/C)	Mean age (years) (T/C)	Intervention (T/C)	Duration	Outcome measures
Dai et al. (2022)	45/45	51.39 ± 6.38 53.78 ± 7.61	BXD + CT/CT	8 weeks	①②⑤
Zhang et al. (2022)	54/54	55.19 ± 16.73 56.51 ± 15.41	BXD + CT/CT	12 weeks	①⑤⑦
Zhao, (2022)	45/45	65.77 ± 8.23 66.12 ± 8.40	BXD + CT/CT	8 weeks	②④
Zhang, (2021)	36/36	72.2 ± 2.1 72.8 ± 2.3	BXD + CT/CT	6 weeks	①②
Zheng, (2021)	54/54	55.12 ± 5.87 55.14 ± 3.27	BXD + CT/CT	4 weeks	②
Zhang et al. (2021)	40/40	52.74 ± 7.71 53.11 ± 8.99	BXD + CT/CT	4 weeks	①②⑦
Liu et al. (2020)	49/48	NA	BXD + CT/CT	8 weeks	②④
Tang et al. (2020)	43/43	56.84 ± 7.69 56.84 ± 7.69	BXD + CT/CT	4 weeks	①②
Mu, (2020)	44/44	77.20 ± 4.18 76.48 ± 3.62	BXD + CT/CT	4 weeks	①②⑤
Ma et al. (2019)	100/100	54.24 ± 12.6 54.14 ± 12.57	BXD + CT/CT	4 weeks	①②③⑥
Wu, (2019)	30/30	52.68 ± 5.25 51.45 ± 4.99	BXD + CT/CT	4 weeks	②④⑦
Shi, (2019)	62/61	53.86 ± 8.37 52.71 ± 8.12	BXD + CT/CT	8 weeks	②③
Song, (2018)	32/32	57.46 ± 11.29 56.85 ± 11.08	BXD + CT/CT	8 weeks	①②⑥
Miao et al. (2017)	44/44	56.52 ± 6.35	BXD + CT/CT	4 weeks	②
Zhao et al. (2016)	40/40	62.34 ± 9.32 64.18 ± 8.67	BXD + CT/CT	12 weeks	①②③
Guan and Chen, (2016)	30/30	63.5 ± 6.8 62.9 ± 6.5	BXD + CT/CT	4 weeks	①②③④
Liu, (2016)	43/43	48.97 ± 6.24 51.08 ± 7.05	BXD + CT/CT	4 weeks	②④
Wu and Zhou, (2016)	50/50	62.8 ± 6.1 63 ± 5.8	BXD + CT/CT	8 weeks	②④⑥
Shen and Jin, (2015)	30/30	55.13 ± 12.05 54.27 ± 11.37	BXD + CT/CT	8 weeks	①②⑥
Huang and Li, (2014)	50/48	58.7 ± 1.8 59.4 ± 1.1	BXD + CT/CT	4 weeks	①②
Pang, (2013)	30/26	63.4 ± 6.6 62.8 ± 6.5	BXD + CT/CT	4 weeks	①②④
Xiong, (2010)	30/30	53.87 ± 5.92 52.87 ± 5.4	BXD + CT/CT	4 weeks	①②
Wu et al. (2007)	44/43	53.6 ± 8 52.8 ± 7.3	BXD + CT/CT	8 weeks	②③

Note: T: treatment group; C: control group; BXD: banxia baizhu tianma decoction; CT: Conventional treatment (including CCB, ACEI, ARB, diuretics, and β-receptor blocker); ①Clinical efficacy rate; ②Blood pressure; ③Blood lipids; ④Hcy; ⑤Endothelial function; ⑥Inflammatory biomarkers; ⑦TCM, symptom score.

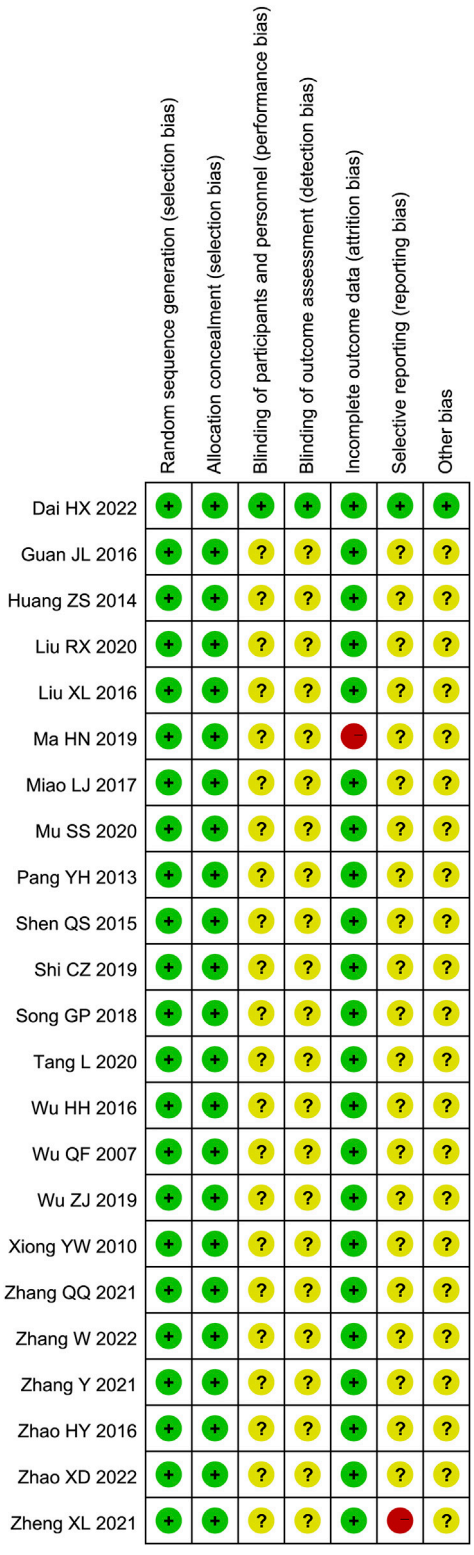

FIGURE 2
Risk of bias assessments of included studies.

et al., 2022) described the implementation of blinding. One study (Liu et al., 2020) did not describe specific baseline characteristics. Overall, the quality of the studies was not high. The risk of bias in the included studies were presented in Figure 2.

3.4 Meta-analysis results

The calculated results of all meta-analyses were shown in Table 2.

3.4.1 Clinical efficacy rate

14 studies reported clinical efficacy rate. There were 604 patients in the treatment group and 598 in the control group. Meta-analysis indicated that BXD combined with conventional treatment had a higher clinical efficacy rate than conventional treatment (RR = 1.25, 95% CI [1.19, 1.32], $I^2 = 0\%$, $p < 0.05$, Figure 3).

3.4.2 Blood pressure

22 studies reported blood pressure. There were 971 patients in the treatment group and 962 in the control group. Meta-analysis indicated that BXD combined with conventional treatment had a better ability to lower SBP than conventional treatment (SMD = −1.21, 95% CI [−1.56, −0.86], $I^2 = 91.81\%$, $p < 0.05$, Figure 4A). Sensitivity analysis indicated that the heterogeneity might be caused by 3 studies (Xiong, 2010; Ma et al., 2019; Zheng, 2021), and heterogeneity was reduced by excluding these studies ($I^2 = 78.27\%$, Supplementary Figure S1). In addition, meta-analysis indicated that BXD combined with conventional treatment had a better ability to lower DBP than conventional treatment (SMD = −1.01, 95% CI [−1.33, −0.69], $I^2 = 90.76\%$, $p < 0.05$, Figure 4B). We speculate that heterogeneity resulted from the use of the post-intervention mean (Supplementary Figure S2).

3.4.3 Blood lipids

5 studies reported blood lipids. There were 276 patients in the treatment group and 274 in the control group. Meta-analysis indicated that compared to the control group, treatment group had a better ability to improve TC(SMD = −0.70, 95% CI [−1.11, −0.28], $I^2 = 81.07\%$, $p < 0.05$, Figure 5A), TG (SMD = -0.80, 95% CI [-1.46, -0.14], $I^2 = 92.50\%$, $p < 0.05$, Figure 5B), LDL-C (SMD = −0.58, 95% CI [−0.75, -0.41], $I^2 = 0\%$, $p < 0.05$, Figure 5C), HDL-C (SMD = 0.51, 95% CI [0.34, 0.68], $I^2 = 47.43\%$, $p < 0.05$, Figure 5D). Sensitivity analysis indicated that the heterogeneity of TC might be caused by 2 studies (Ma et al., 2019; Shi, 2019), and heterogeneity was reduced by excluding these studies ($I^2 = 0\%$, Supplementary Figure S3). Sensitivity analysis indicated that the heterogeneity of TG might be caused

TABLE 2 Calculation results of the meta-analysis.

Outcome measures	Trials	Sample size	SMD/ RR	95% CI	*Z*	*P*	I^2 (%)	*P* For heterogeneity
Clinical efficacy rate	14	1,202	1.25	(1.19, 1.32)	8.72	0.00	0.00	0.78
SBP	22	1933	−1.21	(−1.56, −0.86)	−6.78	0.00	91.81	0.00
DBP	22	1933	−1.01	(−1.33, −0.69)	−6.22	0.00	90.76	0.00
TC	5	550	−0.70	(−1.11, −0.28)	−3.30	0.00	81.07	0.00
TG	5	550	−0.80	(−1.46, −0.14)	−2.37	0.02	92.50	0.00
LDL-C	5	550	−0.58	(−0.75, −0.41)	−6.62	0.00	0.00	0.49
HDL-C	5	550	0.51	(0.34, 0.68)	5.84	0.00	47.43	0.11
Hcy	7	549	−2.26	(−3.43, −1.09)	−3.79	0.00	96.56	0.00
NO	3	286	0.88	(0.63, 1.12)	7.09	0.00	0.00	0.99
ET-1	3	286	−1.09	(−1.33, −0.84)	−8.57	0.00	0.00	0.79
CRP	4	284	−2.19	(−3.30, −1.09)	−3.88	0.00	92.66	0.00
IL-6	3	184	−2.65	(−4.67, −0.63)	−2.57	0.01	95.87	0.00
Vertigo	3	124	−2.57	(−4.09, −1.04)	−3.29	0.00	94.96	0.00
Anorexia	3	124	−2.95	(−4.63, −1.27)	−3.44	0.00	95.21	0.00
Chest tightness and fatigue	3	124	−2.77	(−4.91, −0.62)	−2.53	0.01	97.31	0.00
Adverse reactions	13	1,273	0.52	(0.35, 0.78)	−3.20	0.00	0.00	0.91

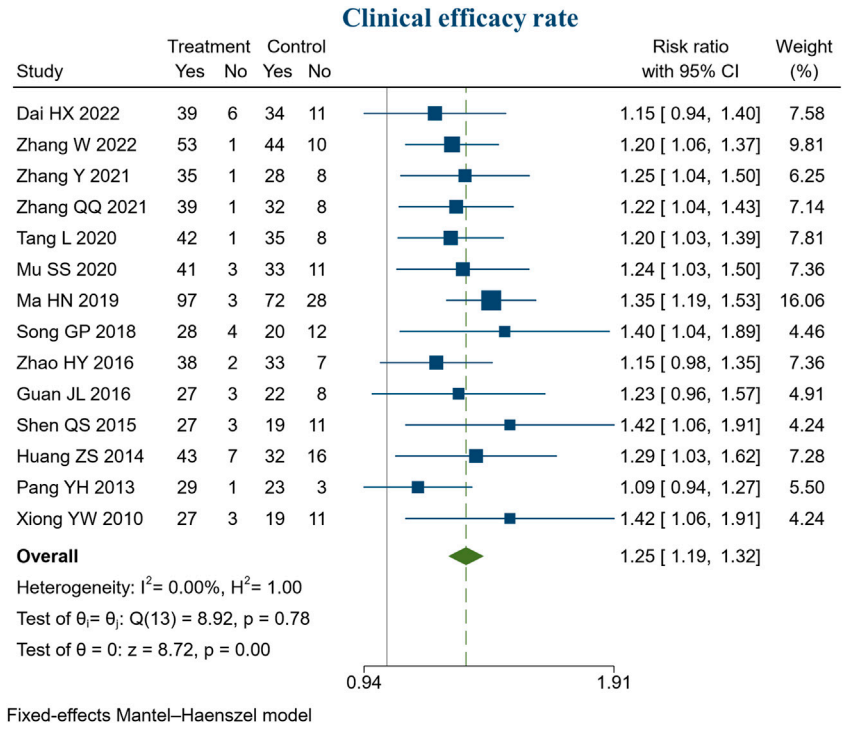

FIGURE 3
Forest plot of clinical efficacy rate.

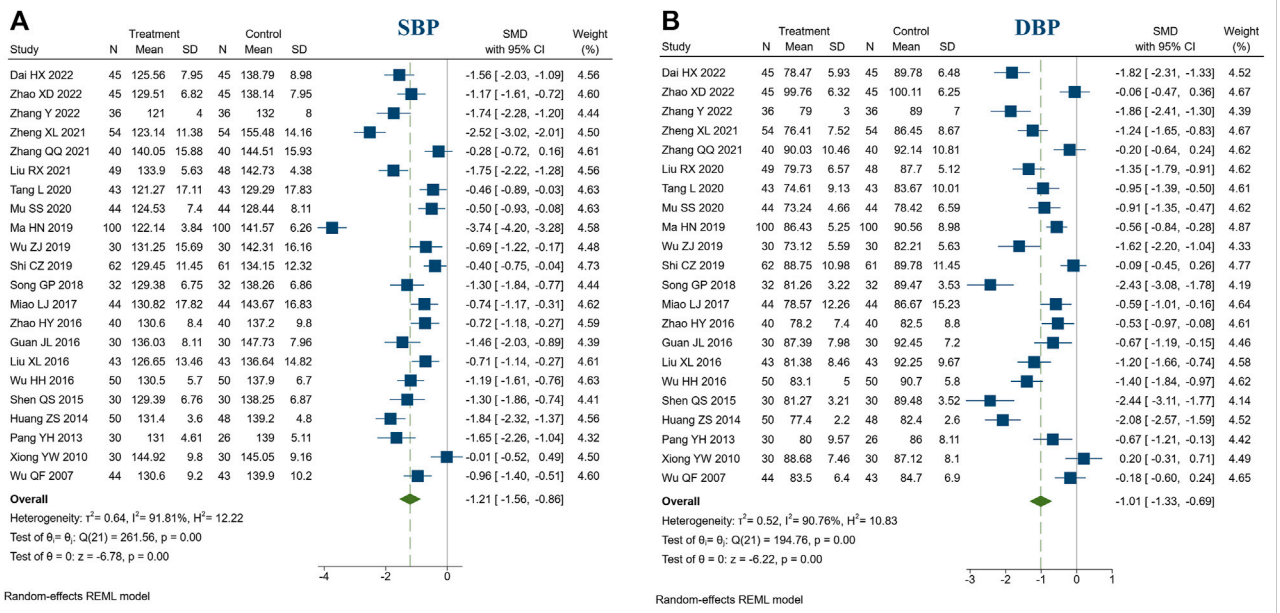

FIGURE 4
Forest plot of blood pressure. **(A)** SBP; **(B)** DBP.

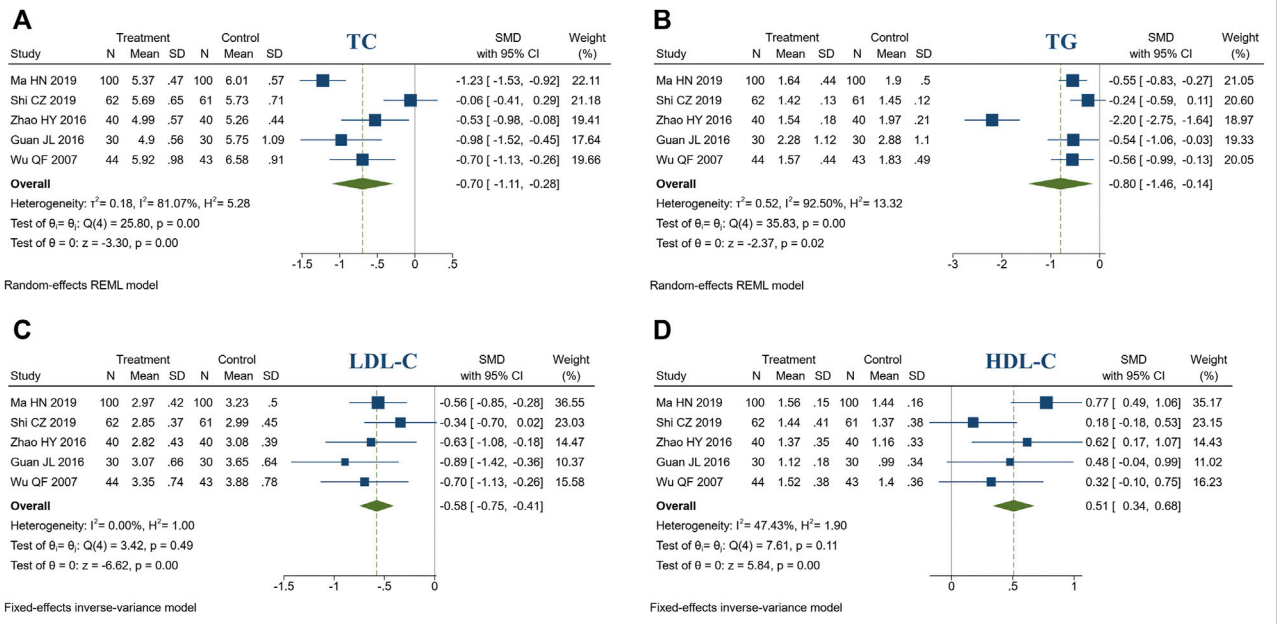

FIGURE 5
Forest plot of blood lipids. **(A)** TC; **(B)** TG; **(C)** LDL-C; **(D)** HDL-C.

by 1 study (Zhao et al., 2016), and heterogeneity was reduced by excluding the studies (I^2 = 0%, Supplementary Figure S4). In addition, we speculated that the heterogeneity was due to different ways of measuring blood lipids.

3.4.4 Homocysteine

7 studies reported Hcy. There were 277 patients in the treatment group and 272 in the control group. Meta-analysis indicated that compared to the control group, the treatment

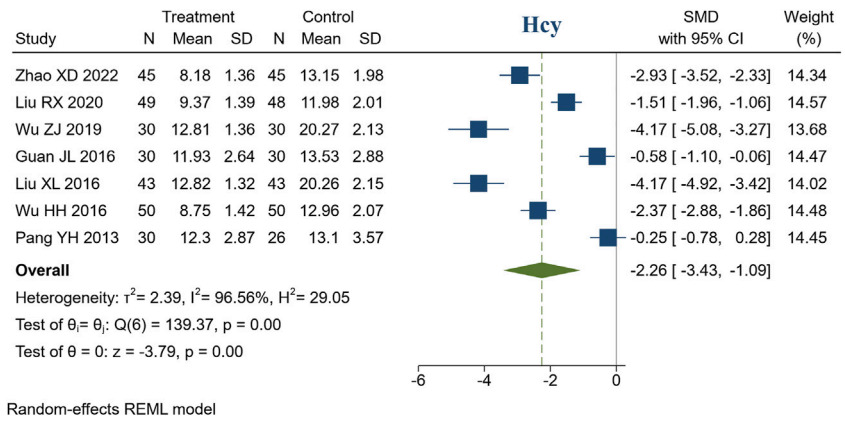

FIGURE 6
Forest plot of Hcy.

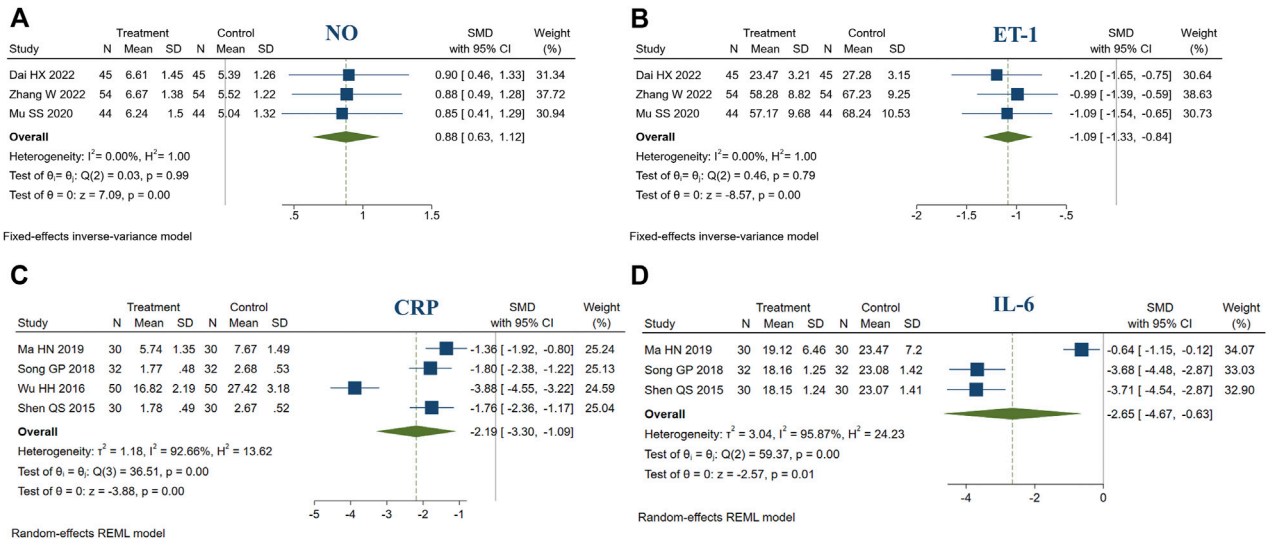

FIGURE 7
Forest plot of endothelial function and inflammatory biomarkers. **(A)** NO; **(B)** ET-1; **(C)** CRP; **(D)** IL-6.

group had a better ability to decrease Hcy (SMD = −2.26, 95% CI [−3.43, −1.09], I^2 = 96.56%, p < 0.05, Figure 6). Sensitivity analysis indicated that the heterogeneity may be caused by different measurement methods of Hcy (Supplementary Figure S5).

3.4.5 Endothelial function

3 studies reported endothelial function (NO, ET-1). There were 143 patients in the treatment group and 143 in the control group. Meta-analysis indicated that compared to the control group, the treatment group had a better ability to increase NO (SMD = 0.88, 95% CI [0.63, 1.12], I^2 = 0%, p < 0.05, Figure 7A). Similarly, compared to the control group, treatment group had a better ability to decrease ET-1 (SMD = −1.09, 95% CI [−1.33, −0.84], I^2 = 0%, p < 0.05, Figure 7B).

3.4.6 Inflammatory biomarkers

4 studies reported CRP. There were 142 patients in the treatment group and 142 in the control group. Meta-analysis indicated that compared to the control group, the treatment

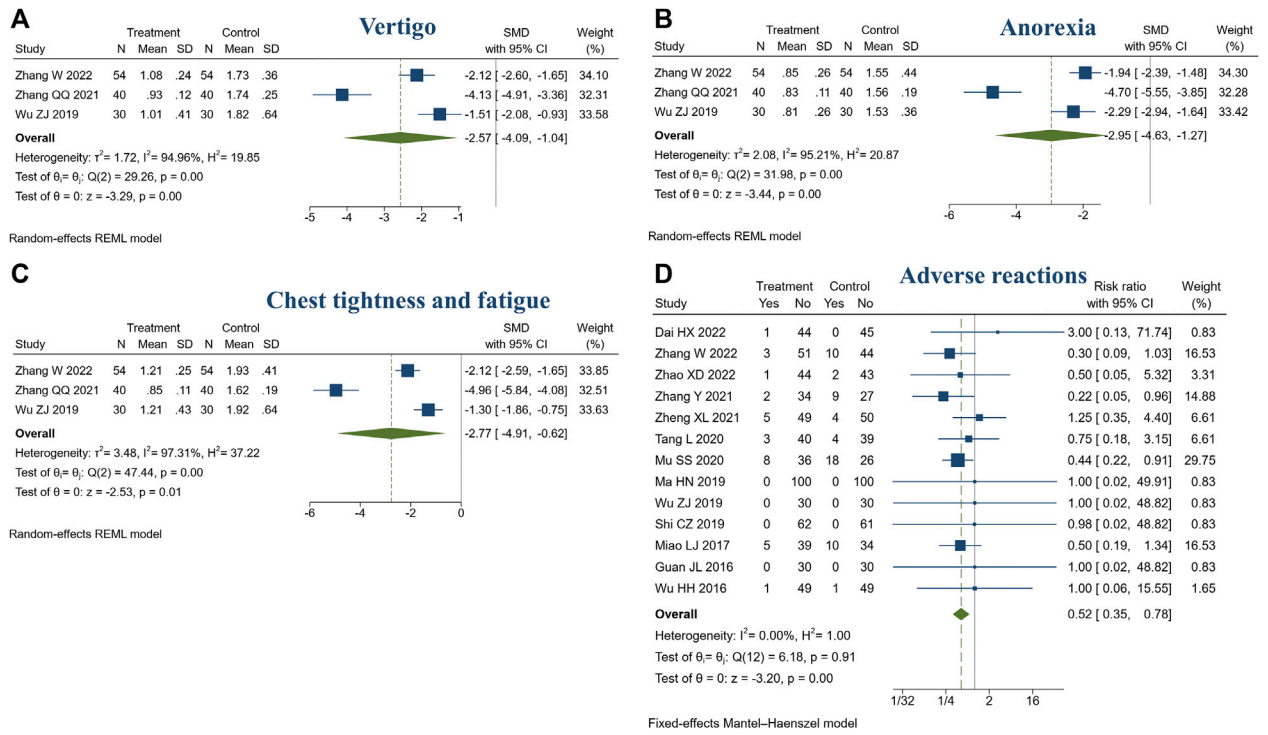

FIGURE 8
Forest plot of TCM symptom score and adverse reactions. **(A)** Vertigo; **(B)** Anorexia; **(C)** Chest tightness and fatigue; **(D)** Adverse reactions.

group had a better ability to decrease CRP (SMD = −2.19, 95% CI [−3.30, −1.09], I^2 = 92.66%, p < 0.05, Figure 7C). In addition, 3 studies reported IL-6. There were 92 patients in the treatment group and 92 in the control group. Meta-analysis indicated that compared to the control group, the treatment group had a better ability to decrease IL-6 (SMD = −2.65, 95% CI [−4.67, −0.63], I^2 = 95.87%, p < 0.05, Figure 7D). Sensitivity analysis suggested that the heterogeneity was caused by the different measurement methods and units of IL-6 and CRP (Supplementary Figures S6, S7).

3.4.7 TCM symptom scores

3 studies reported TCM symptom scores. There were 124 patients in the treatment group and 124 in the control group. Meta-analysis showed that compared with the control group, the treatment group had a stronger ability to improve the TCM symptoms, such as vertigo (SMD = −2.57, 95% CI [−4.09, −1.04], I^2 = 94.96%, p < 0.05, Figure 8A), anorexia (SMD = −2.95, 95% CI [−4.63, −1.27], I^2 = 95.21%, p < 0.05, Figure 8B), chest tightness and fatigue (SMD = −2.77, 95% CI [−4.91, −0.62], I^2 = 97.31%, p < 0.05, Figure 8C). Sensitivity analysis suggested that different TCM syndrome score evaluation criteria may be the cause of heterogeneity (Supplementary Figures S8, S9, S10).

3.4.8 Adverse reactions

In this review, 14 studies reported adverse reactions (14/23, 60.87%) (Huang and Li, 2014; Guan and Chen, 2016; Wu and Zhou, 2016; Miao et al., 2017; Ma et al., 2019; Shi, 2019; Wu, 2019; Mu, 2020; Tang et al., 2020; Zhang, 2021; Zheng, 2021; Dai et al., 2022; Zhang et al., 2022; Zhao, 2022). Among them, no adverse reactions were identified in both treatment or control groups (Guan and Chen, 2016; Ma et al., 2019; Shi, 2019; Wu, 2019). One study did not specifically describe it (Huang and Li, 2014). The adverse reactions included nausea, vomiting, headache, palpitation, loss of appetite, diarrhea, sweating, etc. The symptoms were mild, tolerable, and could be relieved automatically. Meta-analysis showed the treatment group was safer than the control group (RR = 0.52, 95% CI [0.35, 0.78], I^2 = 0%, p < 0.05, Figure 8D).

3.4.9 Publication bias

SBP, DBP, and clinical efficacy rate were evaluated by publication bias. The funnel plot and Egger's test suggested the possibility of publication bias in DBP (Egger's test: p < 0.05, Figure 9A). SBP and clinical efficacy rate did not show publication bias (Egger's test: p = 0.1383, p = 0.2814, Figures 9B,C).

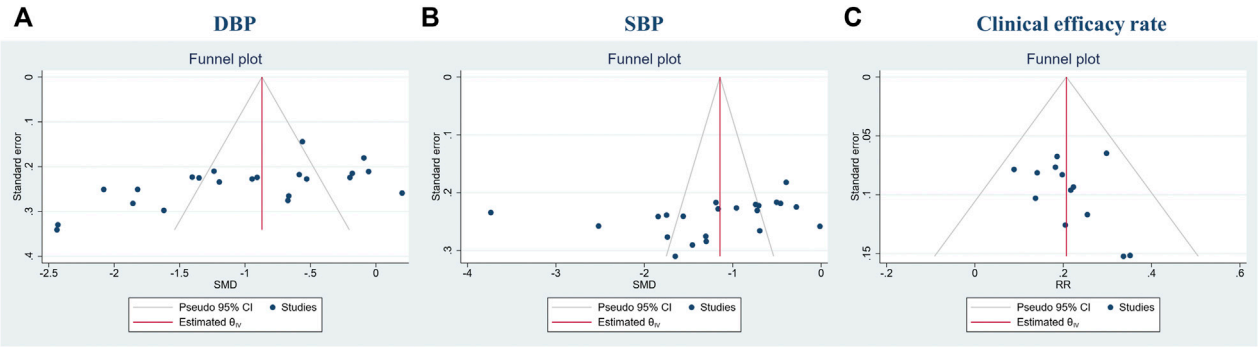

FIGURE 9
Funnel plot. **(A)** DBP; **(B)** SBP; **(C)** Clinical efficacy rate.

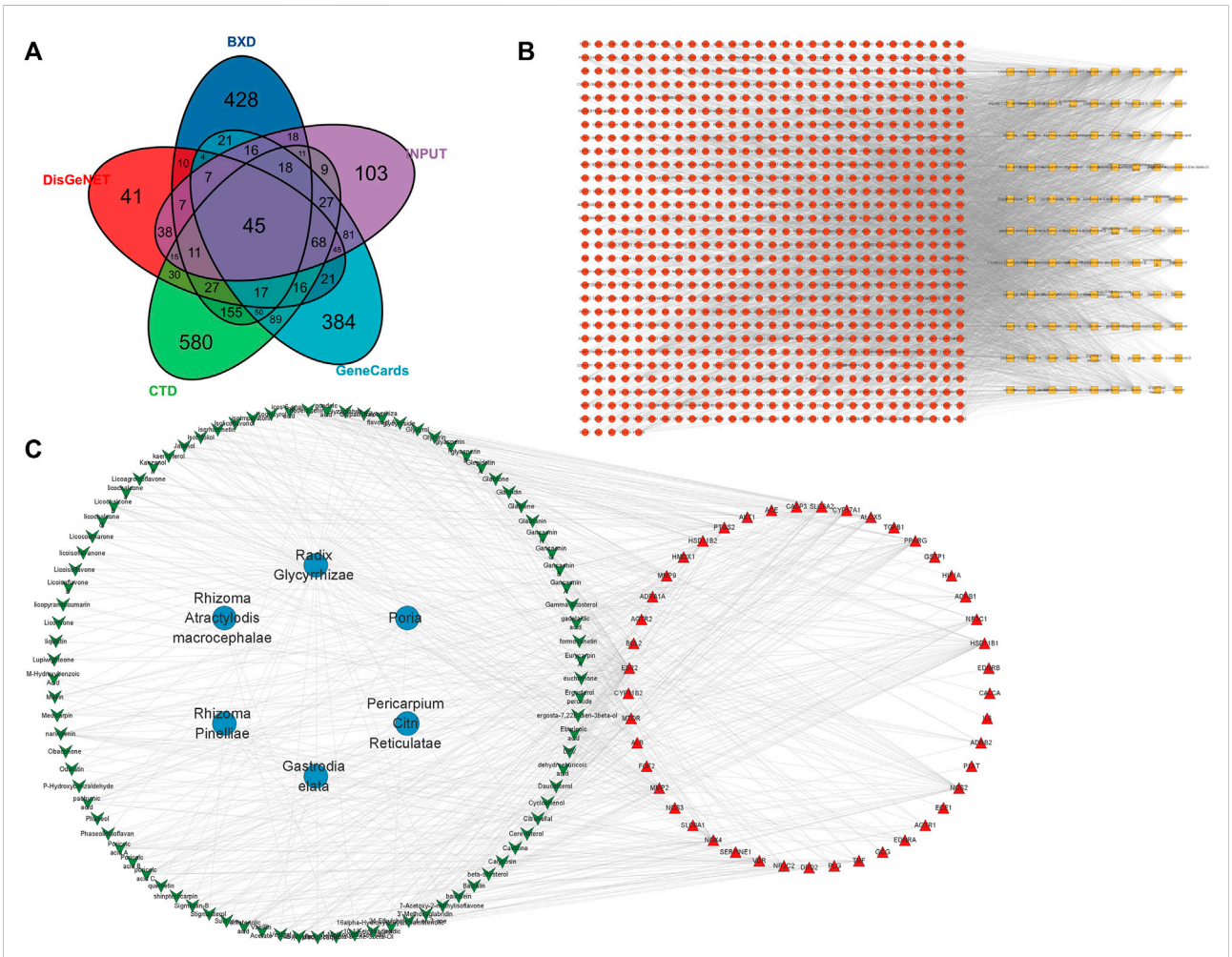

FIGURE 10
Network pharmacology of BXD and hypertension. **(A)** VENN of hypertension and BXD; **(B)** BXD-target network **(C)** BXD and hypertension network.

TABLE 3 Top 20 active ingredients.

Degree	Name
16	16alpha-Hydroxydehydrotrametenolic acid
15	Naringenin
14	Eburicoic acid
14	Poricoic acid C
13	Gondoic acid
13	Trametenolic acid
13	Poricoic acid A
12	Hederagenin
12	Icos-5-enoic acid
12	Gadelaidic acid
11	Dehydroeburicoic acid
10	Cerevisterol
10	Pachymic acid
10	Sigmoidin-B
10	Jaranol
10	Licochalcone B
9	Glypallichalcone
9	Cavidine
9	24-Ethylcholest-4-en-3-one
9	Glepidotin A

3.5 Analysis of BXD and hypertension targets

A total of 99 active ingredients and 845 targets corresponding to the active ingredients were collected. A total of 45 intersection targets of hypertension and BXD were obtained (Figure 10A). After that, the BXD-target network was constructed by Cytoscape (Figure 10B). Finally, the BXD and hypertension network was constructed (Figure 10C) and the key active ingredients were screened by analyzing network function. The list of top 20 active ingredients was listed according to the degree (Table 3).

3.6 PPI and gene enrichment analysis

PPI processing was conducted on the overlapping targets through STRING platform (Figure 11) and using Cytoscape to screen key targets. The key targets were NOS3, ACE, AKT1, TNF, ALB, PPARG, PTGS2, and CASP3 (Table 4). Gene enrichment analysis was conducted on the overlapping targets through DAVID. The results showed that the main BP items were response to hypoxia, positive regulation of smooth muscle cell proliferation, response to xenobiotic stimulus, regulation of blood pressure, inflammatory response, positive regulation of apoptotic process, positive regulation of blood vessel endothelial cell migration (Figure 12A). The main MF items were steroid binding, heme binding, identical protein binding, endopeptidase activity, and oxidoreductase activity (Figure 12B). The main CC items were extracellular space, extracellular region, neuronal cell body, platelet alpha granule lumen, and caveola. (Figure 12C). Visualization of the top 20 KEGG pathways (Figure 12D), involving AGE-RAGE signaling pathway in diabetic complications, HIF-1 signaling pathway fluid shear stress and atherosclerosis, cGMP-PKG signaling pathway, calcium signaling pathway, adrenergic signaling in cardiomyocytes.

3.7 Analysis of molecular docking

Through integrating data of Sections 3.5, 3.6, selected AKT1 (PDBID:1unp), NOS3 (PDBID:1m9j), ACE (PDBID: 1o86), and PPARG (PDBID:1i7i) as molecular docking targets, selected naringenin (CID: 932), 16alpha-Hydroxydehydrotrametenolic acid (CID: 10743008), poricoic acid C (CID:56668247), eburicoic acid (CID: 73402), licochalcone B (CID: 5318999) as binding ligands. The results showed that the docking energy was ≤ -6 kcal·mol^{-1} (Table 5) and the receptor and ligand bind stably. Pymol and PLP were used to draw the result of molecular docking (Figure 13).

4 Discussion

To the best of our knowledge, this is the first article that integrates meta-analysis and network pharmacology to evaluate the efficacy and potential pharmacological mechanisms of BXD in the treatment of hypertension. This article reviews 23 intervention studies of BXD combined with conventional treatment in patients with hypertension, aiming to reveal the clinical effects of BXD. The meta-analysis found that compared with conventional treatment, combined BXD treatment was beneficial to improve clinical efficacy rate, blood pressure, blood lipids, Hcy, endothelial function, and inflammation. Notably, the combined treatment with BXD was effective in improving TCM symptoms which were important for improving the quality of life of patients. The treatment of hypertension should not only lower blood pressure but also improve the patient's symptoms. According to TCM theory, the appearance of symptoms is a response to the imbalance of the internal environment of the body. Through the treatment of BXD, the internal environment of the body can be changed to improve the disease. In addition, BXD is safe and has no obvious adverse reactions. In general, BXD can be used as a complementary and alternative therapy for patients with hypertension on the premise of TCM syndrome differentiation.

Unfortunately, the overall quality of this study was not high. The methodological quality of RCTs was low, and the blinding, selective reporting of results and other biases were not described. In addition, the sample size of these RCTs was small, and they

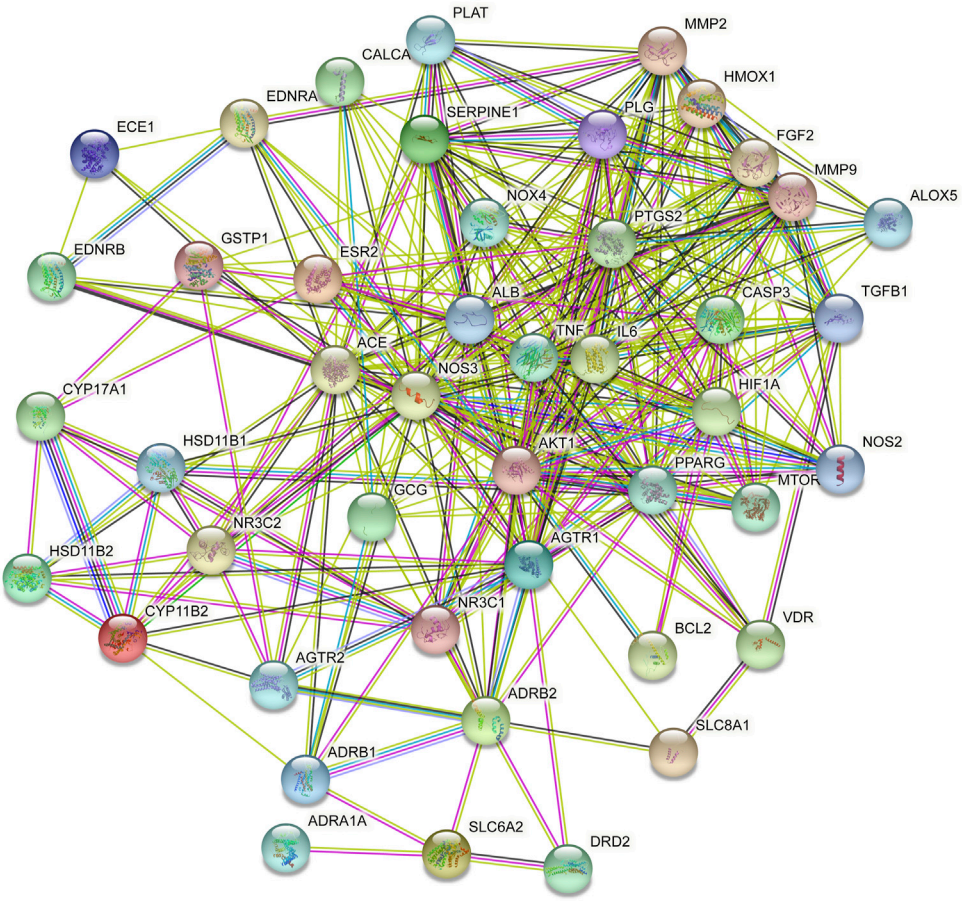

FIGURE 11
PPI of the key target.

were all Chinese studies, and they were positive publications, which suggested a significant publication bias.

The pathological mechanism of hypertension is associated with endothelial dysfunction, increased vasoconstriction, and vascular changes characterized by arterial remodeling. The sympathetic nervous system, the renin-angiotensin-aldosterone system, and the immune system are all involved in the pathogenesis of hypertension (Coffman, 2011; Touyz et al., 2018). Using network pharmacology, we predicted the molecular mechanism of BXD against hypertension. The results showed that the key of BXD active ingredients including naringenin, 16 alpha-Hydroxydehydrotrametenolic acid, poricoic acid C, eburicoic acid, and licochalcone B. Naringenin is a flavanone, aglycone of naringin, exhibits a plethora of pharmacological properties. Studies have shown that naringenin exerts antihypertensive effects by attenuating the MCR/ACE/KIM-1 pathway (Oyagbemi et al., 2020). Recently, Liu et al. found that naringenin can reduce weight, fat, and blood pressure in obesity-associated hypertension rats, and the mechanism is related to the regulation of lipid disorders and oxidative stress (Liu et al., 2022). Eburicoic acid is present in the polyporus. Eburicoic acid has therapeutic potential for hyperlipidemia because it reduces adipose expression levels of lipogenic FAS and PPARγ, resulting in reduced lipolipid accumulation (Lin et al., 2017). Licochalcone B is a flavonoid active ingredient found in *Glycyrrhiza uralensis* Fisch. ex DC. [Fabaceae], which has a strong anti-inflammatory, antioxidant capacity, and can inhibit the production of NO, IL-6, and PGE2 in LPS-induced macrophage cells (Fu et al., 2013). Recent studies have shown that licochalcone B is also a specific NLRP3 (Li X et al., 2022). In conclusion, the active ingredients of BXD have potential pharmacological effects, and the beneficial effects of the active ingredients of BXD will be gradually explored with the development of technology.

In addition, we also found that the key antihypertensive targets of BXD were AKT1, NOS3, ACE, PPARG, TNF, and PTGS2. AKT regulates cell proliferation and growth and is involved in cellular processes including apoptosis and glucose

TABLE 4 Top 20 key targets.

Degree	Name
33	NOS3
32	ACE
32	AKT1
31	TNF
31	ALB
30	IL6
26	PPARG
25	PTGS2
24	CASP3
23	MMP9
22	HIF1A
21	MMP2
21	TGFB1
21	SERPINE1
20	HMOX1
20	AGTR1
18	FGF2
17	PLG
16	MTOR
15	NOX4

metabolism. A study showed that AKT regulated endothelial function in SHR rats (Iaccarino et al., 2004). Cid-Soto et al. investigated the association of the eighth single nucleotide polymorphism in the AKT1 gene with different metabolic traits and found that AKT1 was associated with hypertension in Mestizos (Cid-Soto et al., 2018). NOS3 is important for vasodilation and heart rate (eNOS encoded by the NOS3), and eNOS knockout causes an increase in blood pressure (Shesely et al., 1996). Targeted disruption of the NOS gene in mice has become a useful tool to study cardiovascular endothelial dysfunction, response to vascular injury, and ischemia-reperfusion or atherosclerosis (Rochette et al., 2013). PPARG is a transcription factor that plays an important role in adipocyte differentiation, which is closely related to cardiometabolic diseases. A meta-analysis suggested that PPARG gene polymorphisms may be associated with the risk of hypertension (Cai et al., 2017). Similarly, Li et al. found that PPARG may also be involved in folic acid treatment of H-type hypertension (Liang et al., 2022). Subsequently, we performed validation by molecular docking and the results showed good affinity of the ligand and receptor. In addition, the possibility of combining targets and ingredients was further demonstrated by the literature review. For example, Liao et al. (2014) found demonstrated that naringenin could act by down-regulating

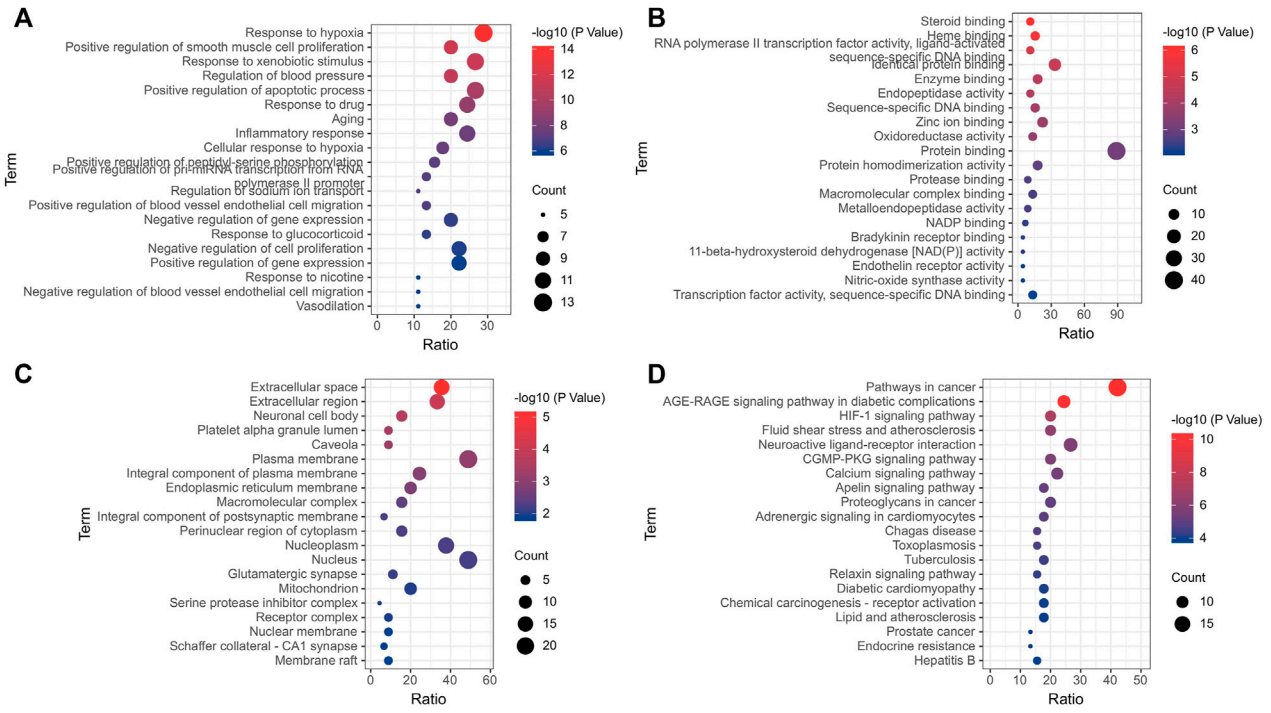

FIGURE 12
Enrichment analysis of gene. **(A)** Biological process; **(B)** Molecular function; **(C)** Cellular components; **(D)** KEGG.

TABLE 5 Docking energy of the active ingredients and targets (kcal·mol^{-1}).

Compounds	AKT1	NOS3	ACE	PPARG
Naringenin	−6.8	−9.4	−8.1	−7.6
16alpha-Hydroxydehydrotrametenolic acid	−7.3	−9.2	−8.6	−8.2
Poricoic acid C	−6.8	−9.3	−7.7	−7.6
Eburicoic acid	−6.8	−9.2	−7.8	−8.3
Licochalcone B	−6.4	−8.8	−7.7	−7.4

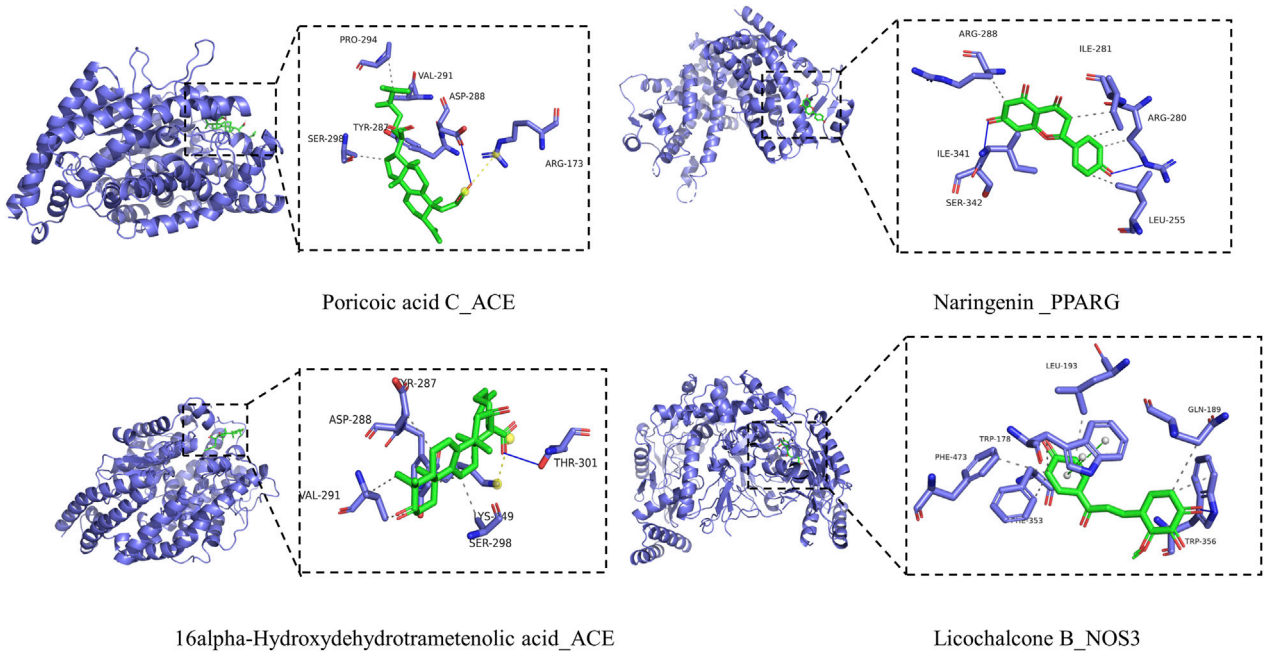

FIGURE 13
Molecular docking of key targets and key ingredients.

AKT, and similarly, Zhang et al. (2015) found that naringenin inhibited the PI3K/AKT pathway, which in turn improved left ventricular function in pressure overload mice. Furthermore, it has been shown that naringenin treatment restored the impaired endothelium-dependent vasodilation by significantly increasing eNOS activity and NO levels. It is undeniable that the results of molecular docking still need to be verified by more experiments (Qin et al., 2016).

Finally, we also performed gene enrichment analysis for these targets. We found that these genes were mainly enriched in HIF-1 signaling pathway, fluid shear stress and atherosclerosis, calcium signaling pathway, cGMP-PKG signaling pathway. HIF-1 signaling pathway regulates oxygen homeostasis and plays an important role in the circulatory system. Evidence suggested that transcriptional changes in HIFs are an important molecular mechanism of hypertension (Semenza, 2014). Studies from Cowburn et al. found that the balance between HIF-1α and HIF-2α expression is a potential mechanism for the body to control blood pressure. They found that HIFs modulate macrophage production of NO *via* iNOS/NOS2 and arginase 1 (Takeda et al., 2010; Cowburn et al., 2013). Intracellular calcium signaling plays a crucial role in cardiovascular activity. The production of endothelium-derived vasoactive factors and the activation of endothelial potassium channels require elevated intracellular Ca^{2+}levels. Disruption of Ca^{2+}signaling circuits may contribute to endothelial dysfunction in hypertension (Sonkusare et al., 2014; Wilson et al., 2019). In summary, the above evidence suggested that BXD has the characteristics of regulating multiple pathways and multiple targets.

5 Conclusion

In conclusion, meta-analysis indicated that BXD combined with conventional treatment for hypertension is effective and safe. BXD has the characteristics of multi-pathway, multi-component, and multi-target in the treatment of hypertension. The antihypertensive targets of BXD may be AKT1, NOS3, ACE, and PPARG. The antihypertensive active ingredients of BXD may be naringenin, poricoic acid C, eburicoic acid, and licochalcone B. However, the evidence of BXD for hypertension should be carefully interpreted due to the low methodological quality, small sample size, limited number of trials, and other unidentified risks of bias. The efficacy and safety of BXD for hypertension still need to be further proved by high-quality clinical and basic studies.

Data availability statement

The original contributions presented in the study are included in the article/Supplementary Material, further inquiries can be directed to the corresponding author.

Author contributions

JL and KY designed the manuscript. JL and QW edited the manuscript. SX, SZ, XZ, and QW collected the data. DZ and MT revised the manuscript. All authors contributed to manuscript revision, read, and approved the submitted version.

Funding

This study was funded by grants from CACMS Innovation Fund (CI 2021A00906).

Conflict of interest

The authors declare that the research was conducted in the absence of any commercial or financial relationships that could be construed as a potential conflict of interest.

The reviewer KG declared a shared affiliation with the author SX to the handling editor at the time of review.

Publisher's note

All claims expressed in this article are solely those of the authors and do not necessarily represent those of their affiliated organizations, or those of the publisher, the editors and the reviewers. Any product that may be evaluated in this article, or claim that may be made by its manufacturer, is not guaranteed or endorsed by the publisher.

Supplementary material

The Supplementary Material for this article can be found online at: https://www.frontiersin.org/articles/10.3389/fphar.2022.1025104/full#supplementary-material

References

Adasme, M. F., Linnemann, K. L., Bolz, S. N., Kaiser, F., Salentin, S., Haupt, V. J., et al. (2021). PLIP 2021: expanding the scope of the protein-ligand interaction profiler to DNA and RNA. *Nucleic Acids Res.* 49 (W1), W530–W534. doi:10.1093/nar/gkab294

Albasri, A., Hattle, M., Koshiaris, C., Dunnigan, A., Paxton, B., Fox, S. E., et al. (2021). Association between antihypertensive treatment and adverse events: systematic review and meta-analysis. *BMJ* 372, n189. doi:10.1136/bmj.n189

Bramlage, P., and Hasford, J. (2009). Blood pressure reduction, persistence and costs in the evaluation of antihypertensive drug treatment--a review. *Cardiovasc. Diabetol.* 8, 18. doi:10.1186/1475-2840-8-18

Cai, G., Zhang, X., Weng, W., Shi, G., Xue, S., and Zhang, B. (2017). Associations between PPARG polymorphisms and the risk of essential hypertension. *PLoS One* 12 (7), e0181644. doi:10.1371/journal.pone.0181644

Cid-Soto, M. A., Martínez-Hernández, A., García-Ortíz, H., Córdova, E. J., Barajas-Olmos, F., Centeno-Cruz, F., et al. (2018). Gene variants in AKT1, GCKR and SOCS3 are differentially associated with metabolic traits in Mexican Amerindians and Mestizos. *Gene* 679, 160–171. doi:10.1016/j.gene.2018.08.076

Coffman, T. M. (2011). Under pressure: the search for the essential mechanisms of hypertension. *Nat. Med.* 17 (11), 1402–1409. doi:10.1038/nm.2541

Cowburn, A. S., Takeda, N., Boutin, A. T., Kim, J. W., Sterling, J. C., Nakasaki, M., et al. (2013). HIF isoforms in the skin differentially regulate systemic arterial pressure. *Proc. Natl. Acad. Sci. U. S. A.* 110 (43), 17570–17575. doi:10.1073/pnas.1306942110

Dai, H., Zai, W., and Xiang, Y. (2022). Clinical effect of Banxia Baizhu Tianma Decoction flexible modification in the treatment of essential hypertension with phlegm-dampness syndrome. *Chin. Mod. Med.* 29 (01), 141–144.

Davis, A. P., Grondin, C. J., Johnson, R. J., Sciaky, D., Mcmorran, R., Wiegers, J., et al. (2019). The comparative Toxicogenomics database: update 2019. *Nucleic Acids Res.* 47 (D1), D948–D954. doi:10.1093/nar/gky868

Fu, Y., Chen, J., Li, Y. J., Zheng, Y. F., and Li, P. (2013). Antioxidant and anti-inflammatory activities of six flavonoids separated from licorice. *Food Chem.* 141 (2), 1063–1071. doi:10.1016/j.foodchem.2013.03.089

Geldsetzer, P., Manne-Goehler, J., Marcus, M. E., Ebert, C., Zhumadilov, Z., Wesseh, C. S., et al. (2019). The state of hypertension care in 44 low-income and middle-income countries: a cross-sectional study of nationally representative individual-level data from 1·1 million adults. *Lancet* 394 (10199), 652–662. doi:10.1016/S0140-6736(19)30955-9

Guan, J., and Chen, X. (2016). Effects of modified Banxia Baizhu Tianma decoction on lipid and homocysteine of patients with hypertension induced by accumulation of excessive phlegm and dampness. *Pharm. Clin. Chin. Mat. Med.* 7 (05), 42–44.

Guo, W., Huang, J., Wang, N., Tan, H. Y., Cheung, F., Chen, F., et al. (2019). Integrating network pharmacology and pharmacological evaluation for deciphering the action mechanism of herbal formula zuojin pill in suppressing hepatocellular carcinoma. *Front. Pharmacol.* 10, 1185. doi:10.3389/fphar.2019.01185

Higgins, J. P., Altman, D. G., Gøtzsche, P. C., Jüni, P., Moher, D., Oxman, A. D., et al. (2011). The Cochrane Collaboration's tool for assessing risk of bias in randomised trials. *BMJ* 343, d5928. doi:10.1136/bmj.d5928

Huang, D. W., Sherman, B. T., and Lempicki, R. A. (2009). Systematic and integrative analysis of large gene lists using DAVID bioinformatics resources. *Nat. Protoc.* 4 (1), 44–57. doi:10.1038/nprot.2008.211

Huang, S., and Li, H. (2014). Efficacy of hypertension Banxiabaizhutianma soup combined with captopril in the treatment of obesity with hypertension disease. *Jilin Med. J.* 35 (28), 6245–6246.

Hypertension, W. G. O. C., and League, C. H. (2019). Guidelines for the prevention and treatment of hypertension in China (revised in 2018). *Chin. J. Cardiovasc. Med.* 24 (01), 24–56. doi:10.3969/j.issn.1007-5410.2019.01.002

Iaccarino, G., Ciccarelli, M., Sorriento, D., Cipolletta, E., Cerullo, V., Iovino, G. L., et al. (2004). AKT participates in endothelial dysfunction in hypertension. *Circulation* 109 (21), 2587–2593. doi:10.1161/01.CIR.0000129768.35536.FA

Li, Q., Feng, H., Wang, H., Wang, Y., Mou, W., Xu, G., et al. (2022). Licochalcone B specifically inhibits the NLRP3 inflammasome by disrupting NEK7-NLRP3 interaction. *EMBO Rep.* 23 (2), e53499. doi:10.15252/embr.202153499

Li, X., Tang, Q., Meng, F., Du, P., and Chen, W. (2022). INPUT: An intelligent network pharmacology platform unique for traditional Chinese medicine. *Comput. Struct. Biotechnol. J.* 20, 1345–1351. doi:10.1016/j.csbj.2022.03.006

Liang, X., He, T., Gao, L., Wei, L., Rong, D., Zhang, Y., et al. (2022). Explore the role of the rs1801133-PPARG pathway in the H-type hypertension. *PPAR Res.* 2022, 2054876. doi:10.1155/2022/2054876

Liao, A. C., Kuo, C. C., Huang, Y. C., Yeh, C. W., Hseu, Y. C., Liu, J. Y., et al. (2014). Naringenin inhibits migration of bladder cancer cells through downregulation of AKT and MMP-2. *Mol. Med. Rep.* 10 (3), 1531–1536. doi:10.3892/mmr.2014.2375

Liberati, A., Altman, D. G., Tetzlaff, J., Mulrow, C., Gøtzsche, P. C., Ioannidis, J. P., et al. (2009). The PRISMA statement for reporting systematic reviews and meta-analyses of studies that evaluate health care interventions: explanation and elaboration. *PLoS Med.* 6 (7), e1000100. doi:10.1371/journal.pmed.1000100

Lin, C. H., Kuo, Y. H., and Shih, C. C. (2017). Eburicoic acid, a triterpenoid compound from antrodia camphorata, displays antidiabetic and antihyperlipidemic effects in palmitate-treated C2C12 myotubes and in high-fat diet-fed mice. *Int. J. Mol. Sci.* 18 (11), 2314. doi:10.3390/ijms18112314

Liu, H., Zhao, H., Che, J., and Yao, W. (2022). Naringenin protects against hypertension by regulating lipid disorder and oxidative stress in a rat model. *Kidney Blood Press. Res.* 47 (6), 423–432. doi:10.1159/000524172

Liu, R., Fu, B., and Ji, Y. (2020). Clinical study of banxia baizhu tianma decoction in the treatment of senile patients with H-type hypertension and carotid atherosclerotic plaque. *Jilin J. Tradit. Chin. Med.* 40 (06), 758–761. doi:10.13463/j.cnki.jlzyy.2020.06.017

Liu, X. (2016). Effect of Banxia Baizhu Tianma decoction combined with Western medicine on serum Hcy, CysC and UA levels in patients with essential hypertension. *Mod. J. Intergr. Tradit. Chin. West. Med.* 25 (32) , 3584 –3586. doi:10.3969/j.issn.1008-8849.2016.32.017

Luo, T. T., Lu, Y., Yan, S. K., Xiao, X., Rong, X. L., and Guo, J. (2020). Network pharmacology in research of Chinese medicine formula: Methodology, application and prospective. *Chin. J. Integr. Med.* 26 (1), 72–80. doi:10.1007/s11655-019-3064-0

Ma, H., Su, W., Xia, J., and Shen, Y. (2019). Clinical study on Banxia Baizhu Tianma Decoction in the treatment of primary hypertension with syndrome of wind - phlegm invading upward. *World J. Integr. Tradit. West. Med.* 14 (11), 1579–1583. doi:10.13935/j.cnki.sjzx.191124

Messerli, F. H., Williams, B., and Ritz, E. (2007). Essential hypertension. *Lancet* 370 (9587), 591–603. doi:10.1016/S0140-6736(07)61299-9

Miao, L., Yang, Y., and Xing, H. (2017). Clinical observation of Banxia Baizhu Tianma decoction combined with captopril in treating hypertension. *Inn. Mong. Med. J.* 49 (05), 601–604. doi:10.16096/j.cnki.nmgyxzz.2017.49.05.041

Mills, K. T., Stefanescu, A., and He, J. (2020). The global epidemiology of hypertension. *Nat. Rev. Nephrol.* 16 (4), 223–237. doi:10.3969/j.issn.1002-7386.2020.24.013

Mu, S. (2020). Effects of Banxia Baizhu Tianma decoction combined with nifedipine in treatment of hypertension in elderly patients and its influences on adverse reactions of patients. *Hebei Med. J.* 42 (24), 3746–3749.

Oyagbemi, A. A., Omobowale, T. O., Adejumobi, O. A., Owolabi, A. M., Ogunpolu, B. S., Falayi, O. O., et al. (2020). Antihypertensive power of Naringenin is mediated via attenuation of mineralocorticoid receptor (MCR)/angiotensin converting enzyme (ACE)/kidney injury molecule (Kim-1) signaling pathway. *Eur. J. Pharmacol.* 880, 173142. doi:10.1016/j.ejphar.2020.173142

Pang, Y. (2013). Clinical effect of modified banxia baizhu tianma decoction in treatment of H -type hypertension. *J. N. Chin. Med.* 45 (06) , 16 –18. doi:10.13457/j.cnki.jncm.2013.06.009

Piñero, J., Ramírez-Anguita, J. M., Saüch-Pitarch, J., Ronzano, F., Centeno, E., Sanz, F., et al. (2020). The DisGeNET knowledge platform for disease genomics: 2019 update. *Nucleic Acids Res.* 48 (D1), D845–D855. doi:10.1093/nar/gkz1021

Qin, W., Ren, B., Wang, S., Liang, S., He, B., Shi, X., et al. (2016). Apigenin and naringenin ameliorate PKCβII-associated endothelial dysfunction via regulating ROS/caspase-3 and NO pathway in endothelial cells exposed to high glucose. *Vasc. Pharmacol.* 85, 39–49. doi:10.1016/j.vph.2016.07.006

Rochette, L., Lorin, J., Zeller, M., Guilland, J. C., Lorgis, L., Cottin, Y., et al. (2013). Nitric oxide synthase inhibition and oxidative stress in cardiovascular diseases: possible therapeutic targets? *Pharmacol. Ther.* 140 (3), 239–257. doi:10.1016/j.pharmthera.2013.07.004

Ru, J., Li, P., Wang, J., Zhou, W., Li, B., Huang, C., et al. (2014). TCMSP: a database of systems pharmacology for drug discovery from herbal medicines. *J. Cheminform.* 6, 13. doi:10.1186/1758-2946-6-13

Semenza, G. L. (2014). Oxygen sensing, hypoxia-inducible factors, and disease pathophysiology. *Annu. Rev. Pathol.* 9, 47–71. doi:10.1146/annurev-pathol-012513-104720

Shannon, P., Markiel, A., Ozier, O., Baliga, N. S., Wang, J. T., Ramage, D., et al. (2003). Cytoscape: a software environment for integrated models of biomolecular interaction networks. *Genome Res.* 13 (11), 2498–2504. doi:10.1101/gr.1239303

Shen, Q., and Jin, Y. (2015). Clinical observation of banxiabaizhutianma decoction combined with western medicine in treatement of hypertension and its effect on renal function and levels of inflammatory factors. *J. Hubei Univ. Chin. Med.* 17 (6), 28–30. doi:10.3969/j.issn.1008-987x.2015.06.10

Shesely, E. G., Maeda, N., Kim, H. S., Desai, K. M., Krege, J. H., Laubach, V. E., et al. (1996). Elevated blood pressures in mice lacking endothelial nitric oxide synthase. *Proc. Natl. Acad. Sci. U. S. A.* 93 (23), 13176–13181. doi:10.1073/pnas.93.23.13176

Shi, C. (2019). Clinical observation of modified banxia baizhu tianma decoction in treating obesity related hypertension with phlegm dampness syndrome. *Guangxi J. Tradit. Chin. Med.* 42 (02), 25–27.

Song, G. (2018). Clinical observation on banxia baizhu tianma decoction combined with western medicine in the treatment of hypertension. *Guangming J. Tradit. Chin. Med.* 33 (05), 708–710. doi:10.3969/j.issn.1003-8914.2018.05.049

Sonkusare, S. K., Dalsgaard, T., Bonev, A. D., Hill-Eubanks, D. C., Kotlikoff, M. I., Scott, J. D., et al. (2014). AKAP150-dependent cooperative TRPV4 channel gating is central to endothelium-dependent vasodilation and is disrupted in hypertension. *Sci. Signal.* 7 (333), ra66. doi:10.1126/scisignal.2005052

Stelzer, G., Rosen, N., Plaschkes, I., Zimmerman, S., Twik, M., Fishilevich, S., et al. (2016). The GeneCards suite: From gene data mining to disease genome sequence analyses. *Curr. Protoc. Bioinforma.* 54, 1. doi:10.1002/cpbi.5

Szklarczyk, D., Gable, A. L., Lyon, D., Junge, A., Wyder, S., Huerta-Cepas, J., et al. (2019). STRING v11: protein-protein association networks with increased coverage, supporting functional discovery in genome-wide experimental datasets. *Nucleic Acids Res.* 47 (D1), D607–D613. doi:10.1093/nar/gky1131

Takeda, N., O'Dea, E. L., Doedens, A., Kim, J. W., Weidemann, A., Stockmann, C., et al. (2010). Differential activation and antagonistic function of HIF-{alpha} isoforms in macrophages are essential for NO homeostasis. *Genes Dev.* 24 (5), 491–501. doi:10.1101/gad.1881410

Tan, C. S., Loh, Y. C., Ng, C. H., Ch'Ng, Y. S., Asmawi, M. Z., Ahmad, M., et al. (2018). Anti-hypertensive and vasodilatory effects of amended banxia baizhu tianma Tang. *Biomed. Pharmacother.* 97, 985–994. doi:10.1016/j.biopha.2017.11.021

Tang, L., Li, Z., and Bai, R. (2020). Study on the mechanism of banxia baizhu tianma decoction on essential hypertension. *Word J. Chin. Tradit. Med.* 15 (16), 2458–2461+2465. doi:10.3969/j.issn.1673-7202.2020.16.022

Touyz, R. M., Alves-Lopes, R., Rios, F. J., Camargo, L. L., Anagnostopoulou, A., Arner, A., et al. (2018). Vascular smooth muscle contraction in hypertension. *Cardiovasc. Res.* 114 (4), 529–539. doi:10.1093/cvr/cvy023

Trott, O., and Olson, A. J. (2010). AutoDock Vina: improving the speed and accuracy of docking with a new scoring function, efficient optimization, and multithreading. *J. Comput. Chem.* 31 (2), 455–461. doi:10.1002/jcc.21334

Wilson, C., Zhang, X., Buckley, C., Heathcote, H. R., Lee, M. D., and Mccarron, J. G. (2019). Increased vascular contractility in hypertension results from impaired endothelial calcium signaling. *Hypertension* 74 (5), 1200–1214. doi:10.1161/HYPERTENSIONAHA.119.13791

Wu, H., and Zhou, X. (2016). H type hypertensive patients using banxia baizhu tianma decoction combined therapy to improve blood pressure and plasma hcy.*Arch. Tradit. Chin. Med.* 34 (09), 2295–2297. doi:10.13193/j.issn.1673-7717.2016.09.070

Wu, Q., Wen, M., and Lan, D. (2007). Effects of Banxiabaizhutianma decoction on salt-sensitivity and blood lipid in Tanshiyongsheng group hypertensive patients. *Fujian Med. J.* (01), 146–148.

Wu, Z. (2019). The effect of Banxia Baizhu Tianma Decoction on essential hypertension and its influence on serum Hcy, CysC and UA levels. *J. Chron. Pathem.* 20 (07), 1104–1106. doi:10.16440/j.cnki.1674-8166.2019.07.052

Xiao, P. T., Liu, S. Y., Kuang, Y. J., Jiang, Z. M., Lin, Y., Xie, Z. S., et al. (2021). Network pharmacology analysis and experimental validation to explore the mechanism of sea buckthorn flavonoids on hyperlipidemia. *J. Ethnopharmacol.* 264, 113380. doi:10.1016/j.jep.2020.113380

Xiong, X., Li, X., Zhang, Y., and Wang, J. (2015). Chinese herbal medicine for resistant hypertension: a systematic review. *BMJ Open* 5 (1), e005355. doi:10.1136/bmjopen-2014-005355

Xiong, X., Yang, X., Liu, W., Feng, B., Ma, J., Du, X., et al. (2012). Banxia baizhu tianma decoction for essential hypertension: a systematic review of randomized controlled trials. *Evid. Based. Complement. Altern. Med.* 2012, 271462. doi:10.1155/2012/271462

Xiong, X., Yang, X., Liu, Y., Zhang, Y., Wang, P., and Wang, J. (2013). Chinese herbal formulas for treating hypertension in traditional Chinese medicine: perspective of modern science. *Hypertens. Res.* 36 (7), 570–579. doi:10.1038/hr.2013.18

Xiong, Y. (2010). Clinical effect of the modified banxia baizhu tianma decoction combining western medicine on 60 patients with phlegm-dampness type primary hypertension. *Chin. Med. Mod. Dist. Educ. Chin.* 8 (13), 67–68.

Xu, N., Li, M., Wang, P., Wang, S., and Shi, H. (2022). Spectrum-Effect relationship between antioxidant and anti-inflammatory effects of banxia baizhu tianma decoction: Aa identification method of active substances with endothelial cell protective effect. *Front. Pharmacol.* 13, 823341. doi:10.3389/fphar.2022.823341

Zhang, D. Y., Cheng, Y. B., Guo, Q. H., Shan, X. L., Wei, F. F., Lu, F., et al. (2020). Treatment of masked hypertension with a Chinese herbal formula: a randomized, placebo-controlled trial. *Circulation* 142 (19), 1821–1830. doi:10.1161/CIRCULATIONAHA.120.046685

Zhang, N., Yang, Z., Yuan, Y., Li, F., Liu, Y., Ma, Z., et al. (2015). Naringenin attenuates pressure overload-induced cardiac hypertrophy. *Exp. Ther. Med.* 10 (6), 2206–2212. doi:10.3892/etm.2015.2816

Zhang, Q., Zhao, Y., Wu, K., Wu, Y., Hu, B., and Cao, W. (2021). Efficacy of banxia baizhu tianma decoction in treating hypertension crisis. *J. Emerg. Tradit. Chin. Med.* 30 (06), 1034–1037. doi:10.3969/j.issn.1004-745X.2021.06.024

Zhang, W., Zhang, J., and Wang, X. (2022). Clinical study on banxia baizhu tianma Tang combined with irbesartan for hypertension. *J. N. Chin. Med.* 54 (05), 49–52. doi:10.13457/j.cnki.jncm.2022.05.010

Zhang, Y. (2021). Effect of banxia baizhu tianma decoction combined with levamlodipine besylate tablets in the treatment of senile hypertension. *Chin. For. Med. Res.* 19 (13), 20–22. doi:10.14033/j.cnki.cfmr.2021.13.007

Zhao, D., Liu, J., Wang, M., Zhang, X., and Zhou, M. (2019). Epidemiology of cardiovascular disease in China: current features and implications. *Nat. Rev. Cardiol.* 16 (4), 203–212. doi:10.1038/s41569-018-0119-4

Zhao, H., Huang, J., Wang, W., and Luo, C. (2016). Observation of the clinical efficacy of banxia baizhu tianma decoction in the treatment of obese hypertension patients. *J. Liaoning Univ. Tradit. Chin. Med.* 18 (12), 14–17. doi:10.13194/j.issn.1673-842x.2016.12.004

Zhao, X. (2022). Clinical effect of banxia baizhu tianma decoction on type H hypertension. Nei mongol. *J. Tradit. Chin. Med.* 41 (06), 39–40. doi:10.16040/j.cnki.cn15-1101.2022.06.078

Zheng, X., Hu, B., Zheng, C. Y., Huang, F. Y., and Gao, F. (2021). Correction to: Improvement of analgesic efficacy for total hip arthroplasty by a modified ultrasound-guided supra-inguinal fascia iliaca compartment block. *Clin. Res. Tradit. Chin. Med.* 13 (10), 99–101. doi:10.1186/s12871-021-01314-9

frontiers | Frontiers in Pharmacology

TYPE Mini Review
PUBLISHED 23 December 2022
DOI 10.3389/fphar.2022.1070567

Check for updates

OPEN ACCESS

EDITED BY
Qing Yong He,
Guang'anmen Hospital (CAS), China

REVIEWED BY
Suxiang Feng,
Henan University of Traditional Chinese Medicine, China
Shoudong Guo,
Weifang Medical University, China
Yali Yu,
Jilin University, China
Yuanqiang Guo,
Nankai University, China
Lu Yang,
Beijing University of Chinese Medicine, China

*CORRESPONDENCE
Wenlan Li,
lwldzd@163.com

†These authors have contributed equally to this work

SPECIALTY SECTION
This article was submitted to Ethnopharmacology, a section of the journal Frontiers in Pharmacology

RECEIVED 15 October 2022
ACCEPTED 15 December 2022
PUBLISHED 23 December 2022

CITATION
Guo Y, Zhang R and Li W (2022), Emodin in cardiovascular disease: The role and therapeutic potential.
Front. Pharmacol. 13:1070567.
doi: 10.3389/fphar.2022.1070567

COPYRIGHT
© 2022 Guo, Zhang and Li. This is an open-access article distributed under the terms of the Creative Commons Attribution License (CC BY). The use, distribution or reproduction in other forums is permitted, provided the original author(s) and the copyright owner(s) are credited and that the original publication in this journal is cited, in accordance with accepted academic practice. No use, distribution or reproduction is permitted which does not comply with these terms.

Emodin in cardiovascular disease: The role and therapeutic potential

Yuanyuan Guo[1,2†], Rongzhen Zhang[3†] and Wenlan Li[1*]

[1]School of Pharmacy, Harbin University of Commerce, Harbin, China, [2]Department of Cardiology, Geriatrics, and General Medicine, The First Affiliated Hospital of Harbin Medical University, Harbin, China, [3]Department of Heart Failure, Shanghai East Hospital, School of Medicine, Tongji University, Shanghai, China

Emodin is a natural anthraquinone derivative extracted from Chinese herbs, such as *Rheum palmatum L*, *Polygonum cuspidatum*, and *Polygonum multiflorum*. It is now also a commonly used clinical drug and is listed in the Chinese Pharmacopoeia. Emodin has a wide range of pharmacological properties, including anticancer, antiinflammatory, antioxidant, and antibacterial effects. Many *in vivo* and *in vitro* experiments have demonstrated that emodin has potent anticardiovascular activity. Emodin exerts different mechanisms of action in different types of cardiovascular diseases, including its involvement in pathological processes, such as inflammatory response, apoptosis, cardiac hypertrophy, myocardial fibrosis, oxidative damage, and smooth muscle cell proliferation. Therefore, emodin can be used as a therapeutic drug against cardiovascular disease and has broad application prospects. This paper summarized the main pharmacological effects and related mechanisms of emodin in cardiovascular diseases in recent years and discussed the limitations of emodin in terms of extraction preparation, toxicity, and bioavailability-related pharmacokinetics in clinical applications.

KEYWORDS

emodin, cardiovascular disease, pharmacological, effect, limitation

1 Introduction

Cardiovascular disease (CVD), primarily ischemic heart disease and stroke, is the leading cause of death and disability worldwide (Roth et al., 2020; Tsao et al., 2022). CVD and mortality have been increasing globally since 1990, with the highest cardiovascular mortality in China. Hypertension is the most significant modifiable cardiovascular risk factor (Roth et al., 2020; China, 2022). Cardiovascular complications have been common in patients with coronavirus disease-2019 (COVID-19) pneumonia since the outbreak of the pandemic. Multiple studies have demonstrated that comorbid CVD is associated with a more severe course and higher mortality in COVID-19 pneumonia (Ma et al., 2021). In exploring its treatment, herbal remedies have made many positive contributions, demonstrating the unique efficacy of herbal medicine.

Chinese herbal medicines have been used in China for at least a 1000 years, and rhubarb is the collective name of a variety of perennial plants of the genus *Polygonaceae*. In China, rhubarb is primarily used for medicinal purposes. The Chinese herb rhubarb attacks stagnation, clears dampness and heat, dips fire, cools the blood, removes blood stasis, and detoxifies harmful toxins. Emodin, 1,3,8-trihydroxy-6-methylanthracene-9,10-dione (the structure of emodin is shown in Figure 1), is an anthraquinone compound extracted from rhubarb, with a molecular formula of $C_{15}H_{10}O_5$. Emodin is a tricyclic planar structure with multiple modification sites: a hydroxyl group at position 3, an anthraquinone ring mainly at positions 2 and 4, and a methyl group at position 6 (Ghimire et al., 2015; Qiu et al., 2021). It is used abroad as a light laxative (Li et al., 2008). The pharmacokinetics of emodin show that emodin glucuronide/sulfate is present only in the plasma. Emodin is present in the kidney and lungs mainly as glucuronide/sulfate, and free emodin is present in high levels in the liver (Lin et al., 2012; Zhu et al., 2014). Wine processing increases the distribution of emodin in cardiopulmonary tissue (Wu et al., 2017). Polyethylene glycolytic drugs combined with emodin form stable emodin liposomes that can effectively increase emodin content in the heart (Wang et al., 2012). Laser confocal microscopy has shown that emodin is mostly dispersed in the cytoplasm and in small amounts in the nucleus (Wang et al., 2007). However, emodin has poor water solubility. Therefore, the modification of various points in its chemical structure could improve its water solubility appropriately, which is also a reasonable way to improve its bioavailability (Zheng et al., 2021). In this study, we integrated 18β-glycyrrhetinic acid and emodin, which not only improved emodin bioavailability but also reduced drug toxicity. This innovative one-step route has been shown to improve the hatching and survival rates of zebrafish embryos and reduce malformation and apoptosis rates of cardiomyocytes (Zhong et al., 2022). Emodin has shown many potential health benefits in preclinical models, with no significant toxicity to the cardiovascular system in rats, either through intraperitoneal or oral (20–80 mg/kg) administration (Sougiannis et al., 2021).

We first searched the National Library of Medicine website for the medical subject headings as subject terms “emodin” and “cardiovascular disease,a and then obtained the relevant professional subject terms and added them to the PubMed Search Builder to search the literature. It was found that emodin has cardioprotective activity (Tao et al., 2015) in atherosclerosis, myocardial ischemia-reperfusion (I/R) injury, myocardial hypertrophy, hypertension, and hyperlipidemia. The most recent results are shown in Table 1. In addition, multiple studies have confirmed that emodin has a series of protective effects in CVDs, such as antiinflammatory, immunomodulatory, antiviral, antioxidant and oxygen-free radical scavenging, antifibrosis, and bidirectional regulation of intracellular calcium and L-type calcium channels in cardiac muscle (as shown in Figure 2). This study summarized the effects of emodin on CVDs to provide a theoretical basis for clinical treatment.

2 The role and mechanism of emodin in CVDs

2.1 Atherosclerosis

Coronary heart disease seriously affects human health, and its pathogenesis is closely related to atherosclerosis. The process of atherosclerosis includes endothelial cell injury, subendothelial lipid deposition, proliferation and migration of vascular smooth muscle cells (VSMCs), and monocyte adhesion, migration, and differentiation into macrophages. The therapeutic effect of emodin on coronary heart disease is closely associated with the process of atherosclerosis (Li et al., 2021). In addition, emodin can be used as an acoustic sensitizer for sonodynamic therapy as a potential approach for atherosclerosis treatment by exerting sonodynamic effects on THP-1 macrophages, inducing increased reactive oxygen species (ROS) production, cytoskeletal filament disruption, and apoptosis in THP-1-derived macrophages (Gao et al., 2011; Qian and Gao, 2018). *In vivo* experiments have also demonstrated that emodin-mediated sonodynamic therapy can significantly reduce the size of atherosclerotic plaques by decreasing the inflammatory response in them. At the same time, the expression of matrix metalloproteinase (MMP)-2 and MMP-9 in atherosclerotic plaques in mice was decreased, and the expression of TIMP-1 was increased, suggesting that emodin-mediated sonodynamic therapy can, to some extent, change the histological composition of plaques and exert a stabilizing effect on them (Limin et al., 2018). In a zebrafish model established on a high-fat diet, emodin treatment was effective in reducing lipid accumulation in blood vessels and liver and inhibiting the inflammatory response of vascular neutrophils. The specific mechanism was found to enhance low-density lipoprotein uptake, reverse cholesterol

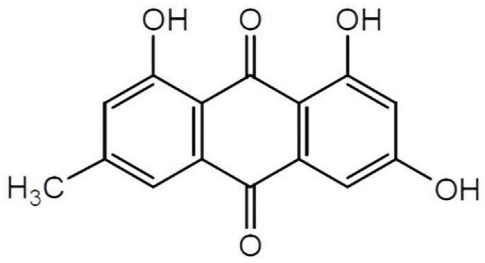

FIGURE 1
The structure of emodin. Emodin, 1,3,8-trihydroxy-6-methylanthracene-9,10-dione, molecular Formula is $C_{15}H_{10}O_5$. Emodin is a tricyclic planar structure with multiple modification sites, hydroxyl group at position 3, anthraquinone ring mainly at positions 2 and 4, and methyl group at position 6.

TABLE 1 Role of emodin in cardiovascular diseases.

Disease	Bioactivity	Mechanism	References
Atherosclerosis	Anti-Inflammation	decrease the expression of MMP-2 and MMP-9 increase the expression of TIMP-1	Limin et al. (2018)
Myocardial infarction	Anti-apoptosis	up-regulation of miR-138, inactivated Sirt1/AKT and Wnt/β-catenin pathways. inhibit caspase-3 activation	Zhang et al. (2019), Wu et al. (2007)
	Anti-Inflammation	suppress the TLR4/MyD88/NF-κB/NLRP3 inflammasome pathway, inhibit gasdermin D-mediated pyroptosis. suppress TNF-α expression and NF-kκB activation	Ye et al. (2019), Wu et al. (2007)
	Anti-oxidant	enhancement in mitochondrial antioxidant components	Du and Ko (2006)
Heart failure	Anti-apoptosis	suppress complex I and p-ERK	Liu and Ning (2021)
	Anti-cardiac hypertrophy	inhibits histone deacetylase activity	Evans et al. (2020)
		activate SIRT3 signaling	Gao et al. (2020)
Hypertension	Suppression of tonic tension	inhibition of PKCδ	Lim et al. (2014)
	Anti-fibrosis	reduce TGF-β1,CTGF,MMP-2 and TIMP-2 expression	Chen et al. (2012a), Chen et al. (2014)
Valvular calcification	Anti-calcium accumulation	suppress AKT/FOXO1 signaling	Luo et al. (2022)
	Anti-proliferation	*via* the NF-κB signaling pathway by inhibiting the gene expression of BMP2, TNF, TRAF1, and RELA.	Xu et al. (2018b)
Viral myocarditis	Anti-virus	differentially regulate multiple signal cascades, including Akt/mTORC1/p70(S6K) (p70 S6 kinase), ERK1/2 (extracellular-signal-regulated kinase 1/2)/p90(RSK) (p90 ribosomal S6 kinase) and Ca(2+)/calmodulin	Zhang et al. (2016a)
	Anti-Inflammation	inhibiti IL-23/IL-17 inflammatory axis, Th17 cell proliferation and viral replication	Jiang et al. (2014)
	Anti-Inflammation	decrease the production of proinflammatory cytokines TNF-α and IL-1β	Song et al. (2012)
Septic myocardial injury	Anti-Inflammation	Inhibit NLRP3	Dai et al. (2021)
Diabetic cardiomyopathy	Anti-Inflammation	upregulation the AKT/GSK-3β Signaling Pathway	Wu et al. (2014)
Hyperlipidaemia	Anti-Inflammation	AMPK activation and PPARγ activation	Chen et al. (2012b), Tzeng et al. (2012)
		inhibits 11beta-hydroxysteroid dehydrogenase type 1	Feng et al. (2010)
	Calcium regulation	upregulation of L-type calcium channel expression	Zhao et al. (2009)

transport, and inhibit cholesterol synthesis (Wang et al., 2016; He et al., 2022). The lipid-lowering effect of emodin is similar to that of simvastatin, and additionally, it also restores aortic endothelial function and improves antioxidant capacity (Wu et al., 2021). Emodin induces apoptosis in VSMCs and exerts antismooth muscle cell proliferation effects. It also increases the production of ROS in cells and upregulates the level of p53 protein in a dose-dependent manner and has therapeutic potential for progressive arterial restenosis caused by abnormal proliferation and migration of vascular smooth muscle (Wang et al., 2007). Thus, emodin exerts antiatherosclerotic effects by exerting lipid-modulating, endothelial-protective, and antiinflammatory effects to attenuate and stabilize atherosclerotic plaques.

2.2 Myocardial infarction

Acute myocardial infarction (AMI) is characterized by an intense inflammatory response and increased apoptosis. Apoptosis is a mechanism that removes debris during tissue injury, and the amount of apoptosis after myocardial infarction is positively correlated with the extent of myocardial infarction. The degree of inflammatory response is also a major determinant of cardiac remodeling and function. *In vivo* experiments showed that emodin significantly increased the levels of cTnI and PGC-1 (specific markers directly reflecting cardiomyocyte energy metabolism) as well as the expression of complex I and p-ERK in the myocardial tissue from myocardial infarction

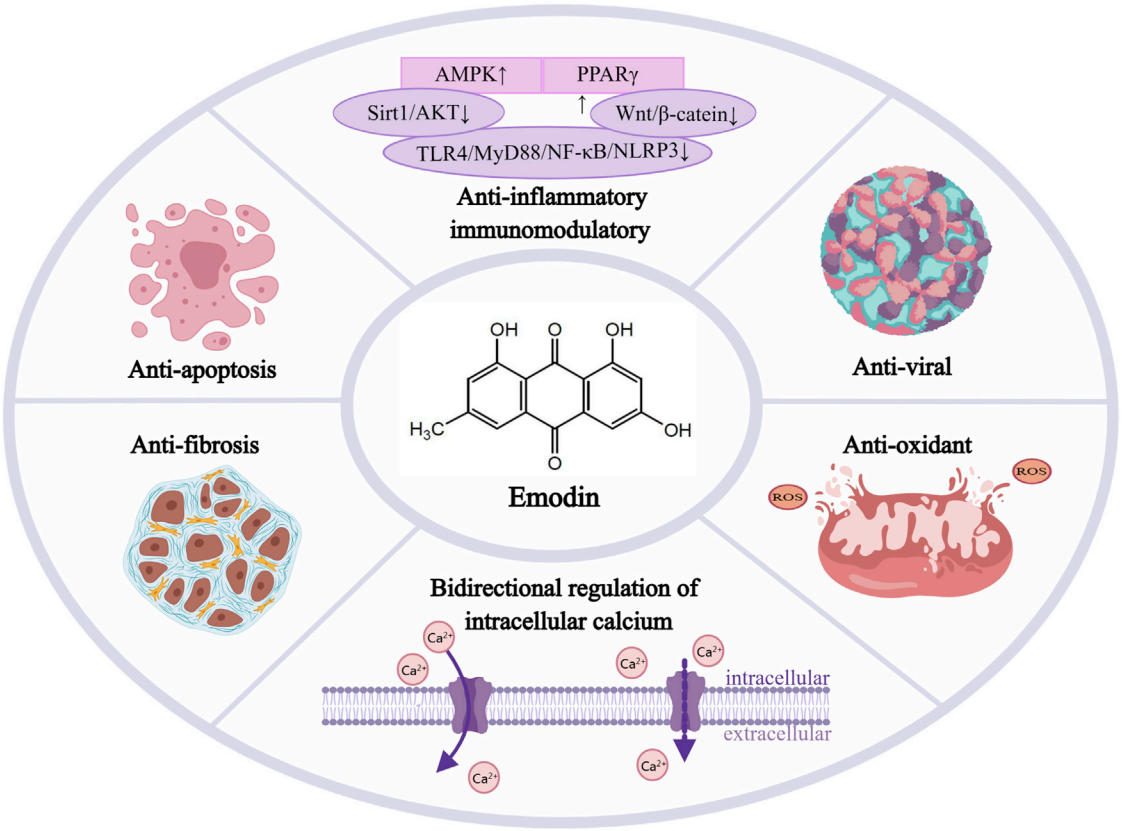

FIGURE 2
Emodin's potent protective effects in cardiovascular diseases, Emodin has a series of protective effects in CVDs such as anti-inflammatory and immunomodulatory, anti-viral,anti-apoptosis, antioxidant and oxygen free radical scavenging, anti-fibrosis, and bidirectional regulation of intracellular calcium and L-type calcium electrodes in cardiac muscle. AMPK, activated protein kinase; PPARγ, peroxisome proliferator-activated receptor γ; Sirt1,sirtuin1; AKT, protein kinase B; TLR4,toll-like receptor-4; MyD88,myeloiddifferentiationfactor88; NF-κB, nuclear factor kappa-B; NLRP3,Nod-like receptors protein-3.

mice. It also significantly improved myocardial energy metabolism, reduced myocardial apoptosis, and improved cardiac function in a dose-dependent manner (Liu and Ning, 2021). Emodin prevents myocardial cell injury by inhibiting local inflammatory responses and apoptosis. Administration of emodin reduced myocardial infarct size in a dose-dependent manner in mice with AMI, significantly inhibited tumor necrosis factor (TNF)-α expression and NF-κB activation in localized myocardial infarct areas, and inhibited cardiomyocyte apoptosis by inhibiting caspase-3 activation (Wu et al., 2007).

Reactive oxygen and calcium overload are involved in the mechanism of I/R injury, and emodin not only attenuates I/R injury in the heart, brain, kidney, and small intestine of rats and mice through antiinflammatory effects but also has antioxidant and calcium-modulating effects (Wang et al., 2022). After myocardial I/R injury, the expression level of gasdermin D-N domains is elevated in myocardial tissue, and emodin treatment inhibits the onset of cellular pyroptosis, attenuates the release of inflammatory mediators, and reduces the expression of gasdermin D-N domains by inhibiting the TLR4/MyD88/NF-κB/NLRP3 inflammatory vesicle pathway. These results suggest a new therapeutic target for emodin to improve myocardial I/R injury (Ye et al., 2019). In Sprague–Dawley rats administered with emodin, MDA production in the heart is significantly reduced after I/R, left ventricular function is improved, and infarct size is reduced (Sato et al., 2000). Emodin exhibits powerful free radical scavenging activity. Similarly, emodin has myocardial protective effects in both male and female rat heart models of myocardial I/R by enhancing the mitochondrial antioxidant components (Du and Ko, 2005). Low-dose emodin pretreatment and ischemic preconditioning prevent myocardial I/R injury through similar but not identical biochemical mechanisms (Du and Ko, 2006). In conclusion, emodin can reduce the apoptosis rate in the myocardial tissue, improve cardiac function, and alleviate post-myocardial

infarction heart failure by regulating apoptosis and the oxidative stress response in a myocardial infarction model. However, whether emodin affects disease progression through other mechanisms remains to be explored in future studies.

2.3 Hypertension

Hypertension is an important risk factor for CVDs and VSMCs, and their contraction mechanisms are closely related to the development of hypertension. It was demonstrated that emodin inhibited phenylephrine-induced, deendothelialized aortic vasoconstriction in a concentration- and time-dependent manner, and its diastolic mechanism was verified in primary VSMCs. Emodin was found to inhibit myosin light chain kinase activity, attenuate contraction, and suppress calcium by blocking PKC-δ sensitization, leading to relaxation of VSMCs and vasodilation (Lim et al., 2014). This finding could contribute to the development of emodin as a tonicity modulator for the treatment of hypertension.

In addition, renal hypertension accounts for approximately 1–5% of the total number of patients with hypertension. Renal hypertensive rats were prepared by two-kidney one-clip surgeries and then treated with emodin, irbesartan, or their combination. The results showed that in the emodin treatment group, the left ventricular mass index, hydroxyproline, collagen content, MMP-2, and TIMP-2 expressions were significantly decreased; however, systolic blood pressure and angiotensin II (Ang II) content remained stable to some extent. The application of irbesartan alone or the combination of emodin and irbesartan significantly reduced systolic blood pressure and Ang II content. This finding suggests that emodin has no significant hypotensive effect on renal hypertension, but its combination with irbesartan inhibits ventricular fibrosis in Goldblatt hypertensive rats by reducing the expression of MMP-2 and TIMP-2 tissue inhibitors (Chen C. et al., 2012; Chen et al., 2014). Moreover, the combination of irbesartan and emodin provides better antifibrotic effects than single applications. Therefore, not only can emodin produce many beneficial effects on its own, but it can also be researched and developed as a compound drug in the future so that it can be used as an auxiliary drug ingredient to reduce the side-effects of other drugs and increase their efficacy.

2.4 Valvular heart disease

Calcific heart valve disease is a prevalent valve disease that usually occurs in older adults and is increasingly being recognized as a significant financial and health burden. In one study, human aortic valve interstitial cells were isolated and cultured from patients with calcific heart valve disease. The addition of TNF-α to the culture medium induced calcification in the cells, and the addition of emodin to the TNF-α conditioned medium did not cause severe toxicity to the cells. Rather, it was found to interfere with cell proliferation and inhibit the formation of calcific deposits in a dose-dependent manner. Treatment with emodin can reduce the serum levels of the proinflammatory cytokines, such as TNF-α and interleukin (IL)-1β, and inhibit TNF-α-induced calcification in human aortic valve interstitial cells *via* the NF-κB pathway (Xu et al., 2018b). Emodin also attenuates aortic valve calcification associated with high calcium, inhibits elevated calcium levels, and upregulates osteogenic genes and calcium accumulation in porcine aortic valve interstitial cells under high calcium conditions. p-AKT and p-FOXO1 were upregulated in porcine aortic valve interstitial cells under hypercalcemic conditions, and this upregulation could be reversed through emodin treatment. The inhibitory effect of emodin was reversed by the addition of AKT activator, suggesting that emodin alleviated hypercalcemia-associated valve calcification by inhibiting AKT/FOXO1 signaling (Luo et al., 2022). These findings provide new insights into the treatment strategies for clinical valve calcification.

2.5 Myocarditis

The inflammatory response is a double-edged sword, and current evidence shows that it has become a key point in regulating the pathogenesis and progression of CVDs. Emodin inhibits NF-κB levels in the myocardial tissue of rats with autoimmune myocarditis, improves left heart function, and reduces the severity of myocarditis (Song et al., 2012). Lipopolysaccharide (LPS) stimulates the inflammatory response of cells, which can reduce the viability of H9c2 cells, downregulate the expression of cyclin D1 in cells, induce apoptosis, and increase the release of IL-1β, IL-6, and TNF-α. High concentrations of emodin (≥20 μM) can reduce H9c2 cell viability, while low doses (10 μM) of emodin can reduce LPS-induced cardiomyocyte inflammatory damage, mainly by downregulating miR-223 to inactivate the JNK signaling pathway. Overexpression of miR-223 can weaken the myocardial protective effect of emodin on H9c2 cells. Therefore, miR-223 is considered to be the target of emodin antiinflammatory therapy, providing *in vitro* evidence that emodin has the potential for clinical treatment of myocarditis (Yang et al., 2019). Similarly, emodin ameliorates LPS-induced myocardial injury and cardiac insufficiency by inhibiting NLRP3 inflammasome activation to attenuate inflammatory response and cardiomyocyte scorching (Dai et al., 2021). Thus, emodin exerts antiinflammatory and protective effects against myocardial injury.

Emodin has an anthraquinone ring structure and belongs to the anthraquinone group, which has been shown to have virucidal and antiviral activity against RNA, DNA, enveloped, non-enveloped, ph-dependent, and independent viruses, such as

hepatitis viruses, herpes viruses, and influenza viruses (Parvez et al., 2019). Viral myocarditis is an excessive inflammation caused by viral myocardial infection. The main pathogen is the coxsackie group B virus, but the antiviral effect of emodin is not direct inactivation of the virus. Emodin prevents coxsackie virus B3 (CVB3) myocarditis by inhibiting the IL-23/IL-17 inflammatory axis, Th17 cell proliferation, and viral replication in mice, significantly reducing IL-23, IL-17, IL-6, and IL-1β expression levels in the myocardium and serum of CVB3-infected mice (Jiang et al., 2014). Studies have shown that emodin inhibits CVB3 replication by impairing the translation machinery and inhibiting viral translation elongation (Zhang H. M. et al., 2016). For CVB4 infection, *in vitro* experiments showed that emodin inhibited CVB4 entry and replication in a concentration- and time-dependent manner and inhibited CVB4 infection-induced apoptosis. *In vivo* studies have shown a dose-dependent increase in survival, body weight, and mean time to death in mice orally administered different doses of emodin as well as a significant decrease in myocardial virus titers and pathological scores/lesions (Liu et al., 2013). Emodin also has strong inhibitory activity against CVB5, and studies have shown that emodin reduced IFN-α mRNA expression but significantly enhanced TNF-α expression during the first 0–4 h after infection in a concentration- and time-dependent manner (Liu et al., 2015). Furthermore, in a study of 92 patients with viral myocarditis, control and observation groups were set up. In the observation group, rhubarb was administered orally in combination with the therapeutic drugs, and it was found that rhubarb treatment effectively reduced the serum levels of IL-23, IL-17, and sCD40L in patients with viral myocarditis and at the same time improved the myocardial enzymatic levels and cardiac function in patients. This confirmed the antiviral effect of rhubarb in patients with viral myocarditis (Wu and Yang, 2018). Emodin exerts antiviral effects by blocking the replication process of the virus. Future clinical applications still need more accurate extraction of the active ingredients in rhubarb to better exploit the effects of the emodin components and reduce the side-effects caused by other impurities.

2.6 Diabetic cardiomyopathy

Emodin exerts antidiabetic and lipid-regulating effects by upregulating the expression of L-type calcium channels in the pancreas and heart of hyperlipidemic diabetic rats (Zhao et al., 2009). Currently, the leading cause of death in people with diabetes is CVD, and this complication of diabetes and CVD is known as diabetic cardiomyopathy. Emodin induced a dose-dependent increase in plasma superoxide dismutase activity in dyslipidemia-diabetic rats (Zhao et al., 2009). In addition, emodin was able to induce increased phosphorylation of protein kinase B and glycogen synthase kinase-3β in the myocardium of type 2 diabetic rats and improve cardiac function (Wu et al., 2014). It was also found that emodin exerts an antiinsulin resistance effect by downregulating miR-20b and thus, upregulating SMAD7, which improves glucose metabolism (Xiao et al., 2019a). Thus, emodin may not only lower glucose and blood lipids but may also have great therapeutic potential in diabetic cardiomyopathy and metabolic syndrome.

2.7 Heart failure

Pathological myocardial hypertrophy is a prominent feature of cardiac remodeling. It is an initial compensatory response to increased ventricular wall tension, in which sustained myocardial hypertrophy leads to cardiac malformations and dysfunction, eventually leading to ventricular dilatation and heart failure. In recent years, cardiac function has been found to be closely associated with mitochondrial metabolism. Sirt3 is a major member of the mitochondrial sirtuin family, a key regulator of mitochondrial metabolism and function. Overall deficiency of Sirt3 exacerbates cardiac function and is associated with hyperacetylation of key enzymes in the cardiac tricarboxylic acid cycle and production of lactate and NADH (Xu et al., 2020). Emodin blocks agonist-induced and pressure overload-mediated myocardial hypertrophy (Evans et al., 2021) and plays an important role in alleviating myocardial hypertrophy by regulating the mitochondrial Sirt3 signaling pathway (Gao et al., 2020; Guo et al., 2020). Inhibition of histone deacetylase enzyme attenuates pathological cardiac hypertrophy and enhances myofibril relaxation *in vitro* and *in vivo* at the molecular level (Travers et al., 2021). Emodin blocks cardiomyocyte hypertrophy induced by phenylephrine or the intracellular agonist fipronil (Evans et al., 2020). *In vitro* experiments have demonstrated that emodin is a histone deacetylase inhibitor that decreases histone deacetylase activity in cardiomyocytes to increase histone acetylation. *In vivo* experiments have also demonstrated that emodin inhibits histone deacetylase activity in Ang II-exposed mouse hearts, reducing pathological myocardial hypertrophy and myocardial fibrosis (Evans et al., 2020). Therefore, antimyocardial hypertrophy is an important target of emodin for preventing the development of heart failure.

Myocardial fibrosis has been implicated as a causative factor for the eventual development of heart failure. The hyperactivation of cardiac fibroblasts, including increased proliferation, migration, and collagen synthesis, is a key step in cardiac fibrosis. Emodin attenuates aortic constriction model-induced cardiac fibrosis in mice, inhibits Ang II-stimulated cardiac fibroblast activation and migration capacity, and significantly attenuates the upregulation of α-SMA expression and collagen I synthesis in fibroblasts (Xiao

et al., 2019b). Studies have shown that metastasis-associated protein 3(MTA3) expression is associated with cardiac fibrosis, and that MTA3 inhibits the proliferation and migration of cardiac fibroblasts (Qin et al., 2015). In a model of fibrosis treated with emodin, the expression of MTA3 was found to be significantly upregulated, which was confirmed by both gene knockdown and overexpression. Emodin inhibited the activation of cardiac fibroblasts by upregulating MTA3, thereby reducing cardiac fibrosis (Xiao et al., 2019b). In addition, the activation of TGF-β and its signaling pathway is a major factor leading to fibrosis in several organs (Khalil et al., 2017). Emodin attenuated TGF-β1-mediated activation and fibrosis in cardiac fibroblasts. Further, in a TGF-β1-induced cardiac fibroblast model, emodin inhibited the activation of Erk1/2 and attenuated the expression of phosphorylated smad2/3, while phosphorylated p38 increased in a dose-dependent manner (Carver et al., 2021). These studies found that emodin can act as an effective antifibrotic agent by modulating multiple signaling pathways, thus reinforcing the idea that traditional Chinese medicine may provide a novel agent for improving the clinical management of cardiac fibrosis.

Calcium plays a crucial role in the maintenance of intracellular and extracellular homeostatic networks. Calcium homeostasis is critical for myocardial synchronization in heart failure. Abnormal cardiac diastolic calcium homeostasis can lead to impaired myocardial diastolic function, and abnormal myocyte calcium homeostasis in heart failure with reduced ejection fraction is associated with t-tubule disruption (Frisk et al., 2021). Emodin has a bidirectional effect on intracellular calcium concentrations and L-type calcium currents in adult guinea pig cardiomyocytes. At rest, intracellular calcium concentration was not affected by emodin concentration, whereas with the addition of potassium chloride, different emodin concentrations had different effects on intracellular calcium concentration and L-type calcium current in guinea pig cardiomyocytes, with inhibition of respective current at low concentrations (100 μm). At high concentrations (1 mm), it increased intracellular calcium concentration and L-type calcium current (Liu et al., 2004). In addition, experiments in isolated perfused beating rabbit atria showed that emodin also increased atrial natriuretic peptide secretion in a concentration-dependent manner, while decreasing atrial pulse pressure and beat-to-beat output. Inhibition of L-type calcium channels with nifedipine attenuates emodin-induced changes in atrial natriuretic peptide secretion and atrial kinetics (Zhou et al., 2022). This shows that the protective effect of emodin against CVDs and impaired regulation of cardiovascular endocytosis may be related to intracellular calcium ion levels and L-type calcium channels in cardiac myocytes. Experiments have only been performed under normal physiological conditions, and further exploration in disease models is needed.

3 Limitations of emodin application

Controversy still exists regarding the effects of emodin on tissue and cell toxicity, proliferation, and apoptosis, as well as the process of emodin preparation in preclinical trials. This included the dose of application, mode of administration, absorption and distribution, and the side-effects of diarrhea. All this leads to difficulties in initiating clinical trials with emodin.

3.1 Extraction technology

Emodin is a natural anthraquinone derivative that is widely found in Chinese herbal medicines, such as *Rheum palmatum*, *Rhizoma tigrinum*, and *Polygonum officinale*. Therefore, it has a wide range of sources and is widely used in medicine, health, food, and dye stuffs. Traditional extraction methods, such as marinated extraction, heat reflux extraction, and Soxhlet extraction, are very time-consuming and labor-intensive owing to the solubility properties of emodin. Modern extraction techniques, such as microwave-assisted extraction, can have harmful effects on the environment and human health because of the solubility properties of emodin, although this method is more efficient, faster, and consumes less solvent (Sun and Liu, 2008). A previous study proposed an ultrasound-assisted extraction method using natural deep eutectic solvents consisting of lactic acid, glucose, and water (Wu et al., 2018). Based on this, another study developed a more effective, rapid, simple, and economical extraction method by converting deep eutectic solvents into protic ionic liquids and using a microwave-assisted extraction method instead of ultrasound-assisted extraction (Fan et al., 2019). The extraction and preparation of emodin is still under further innovation and development.

3.2 Bioavailability

Regarding the pharmacokinetics and metabolism of emodin, after the administration of 20 mg/kg emodin by gavage, it can be rapidly absorbed by the circulatory system with a half-life of 6.44 h. However, the oral absorption bioavailability is only 2.83–3.2%, and about 56% of emodin is not absorbed and is excreted out of the body through feces. The absorbed components can be rapidly metabolized to hydroxylated and glucuronidated metabolites, which are mainly distributed in the kidney (Song et al., 2022; Zhou et al., 2022). When rats were given intravenous emodin 0.4 mg/kg, it was rapidly metabolized and eliminated, with a half-life of 1.82 h (Song et al., 2022). To improve the oral utilization of emodin, a study was conducted to prepare emodin nanoemulsions enriched with polyoxyethylene castor oil (Zhang T. et al., 2016). Given the lipid solubility of emodin,

some studies have also configured emodin-liposome coupling agents, in which D-α-tocopheryl polyethylene glycol 1,000 succinate and a pegylated agent improved the encapsulation efficiency and stability of emodin egg phosphatidylcholine/cholesterol liposomes. This also prolonged the residence time of emodin in the circulatory system and increased its content in the heart (Wang et al., 2012). In addition, it was found that the distribution of emodin in the heart and lung tissues of rats was significantly altered by wine processing—a traditional Chinese method of "wine processing" (Wu et al., 2017). The encapsulation of drugs by nanoparticles is beneficial for improving the targeting and bioavailability of drugs and reducing their toxic side-effects (Li et al., 2017). For emodin to play a more targeted role in the cardiovascular system, additional preparation processes are still under development, such as increasing the anticardiovascular activity of emodin by adding modifications and loading in combination with nano-targeting systems. A large number of experiments are required to validate this in the future to lay the foundation for clinical applications.

3.3 Toxicity

In a wide variety of disease models, the effects of different emodin concentrations are not the same, and according to previous experimental analyses, most of the different effects of emodin are concentration-dependent and act differently in different cells. Because the anthracycline ring in the structure of emodin is very similar to the core of anthracyclines used in cancer therapy (adriamycin, erythromycin, etc.), emodin has cytotoxic and growth-inhibitory effects on different types of cancer cells. Additionally, long-term high doses of emodin may cause nephrotoxicity, hepatotoxicity, and reproductive toxicity (Akkol et al., 2021). At low concentrations (less than 20 μm), emodin did not affect the viability of cardiomyocytes and protected them from damage in a hypoxic environment (Yang et al., 2019; Zhang et al., 2019). In contrast, at the same low concentration (5 μm), emodin significantly inhibited the proliferation of VSMCs and vascular endothelial cells. The inhibition of mitochondrial activity in VSMCs was more pronounced than that in vascular endothelial cells (Xu et al., 2018a). *In vitro* experiments have shown that when emodin affects cardiomyocyte viability at a concentration of 20 μm, it also inhibits fibroblast proliferation; at 10 μm, it protects cardiomyocytes from ischemic and hypoxic injury, and attenuates TG-β-induced fibroblast proliferation (Carver et al., 2021). Therefore, the therapeutic application of emodin requires careful evaluation of its effects on specific cell types and exploration of the appropriate and most beneficial therapeutic concentrations. In addition, a deeper study of the specific mechanisms of emodin in different cells and tissues is needed when targeting different diseases for treatment.

4 Conclusion

Emodin is a natural bioactive drug that exerts its anticardiovascular activity through different molecular targets in vascular cells. Emodin regulates the inflammatory response, suppresses apoptosis, alleviates hypertrophy, and reduces myocardial fibrosis. It has promising prospects in myocardial ischemia, atherosclerosis, viral myocarditis, hypertension, and heart failure. Although encouraging results have been achieved in this research field, most are still in the preclinical experimental stage. Notably, clinical data supporting the safety and pharmacokinetics of emodin in humans are lacking. Therefore, there may be undetermined drawbacks in the clinical use of emodin. In conclusion, the current study represents an important step in the clinical development of emodin as an active agent against CVD.

Author contributions

YG and WL guided the scope and research background of the research, RZ wrote the original version of this manuscript, YG and WL critically revised the manuscript.

Funding

This work was supported by the China Heilongjiang Province Postdoctoral Foundation General Fund (LBHZ20022) and Central support for local universities reform and development funds for talent training projects (Key technology and product creation for the discovery of quality markers of Ganoderma lucidum, an authentic medicinal herb of Longjiang).

Conflict of interest

The authors declare that the research was conducted in the absence of any commercial or financial relationships that could be construed as a potential conflict of interest.

Publisher's note

All claims expressed in this article are solely those of the authors and do not necessarily represent those of their affiliated organizations, or those of the publisher, the editors and the reviewers. Any product that may be evaluated in this article, or claim that may be made by its manufacturer, is not guaranteed or endorsed by the publisher.

References

Akkol, E. K., Tatli,II, Karatoprak, G. S., Agar, O. T., Yucel, C., Sobarzo-Sanchez, E., et al. (2021). Is emodin with anticancer effects completely innocent? Two sides of the coin. *Cancers (Basel)* 13 (11), 2733. doi:10.3390/cancers13112733

Carver, W., Fix, E., Fix, C., Fan, D., Chakrabarti, M., and Azhar, M. (2021). Effects of emodin, a plant-derived anthraquinone, on TGF-β1-induced cardiac fibroblast activation and function. *J. Cell Physiol.* 236 (11), 7440–7449. doi:10.1002/jcp.30416

Chen, C., Liang, Z., Chen, Q., and Li, Z. G. (2012a). Irbesartan and emodin on myocardial remodeling in Goldblatt hypertensive rats. *J. Cardiovasc Pharmacol.* 60 (4), 375–380. doi:10.1097/FJC.0b013e3182650f1c

Chen, Q., Pang, L., Huang, S., Lei, W., and Huang, D. (2014). Effects of emodin and irbesartan on ventricular fibrosis in Goldblatt hypertensive rats. *Pharmazie* 69 (5), 374–378.

Chen, Z., Zhang, L., Yi, J., Yang, Z., Zhang, Z., and Li, Z. (2012b). Promotion of adiponectin multimerization by emodin: A novel AMPK activator with pparγ-agonist activity. *J. Cell Biochem.* 113 (11), 3547–3558. doi:10.1002/jcb.24232

China (2022). China cardiovascular health and disease report 2021 summary. *Chin. Circulation J.* 37 (06), 553–578.

Dai, S., Ye, B., Chen, L., Hong, G., Zhao, G., and Lu, Z. (2021). Emodin alleviates LPS-induced myocardial injury through inhibition of NLRP3 inflammasome activation. *Phytother. Res.* 35 (9), 5203–5213. doi:10.1002/ptr.7191

Du, Y., and Ko, K. M. (2005). Effects of emodin treatment on mitochondrial ATP generation capacity and antioxidant components as well as susceptibility to ischemia-reperfusion injury in rat hearts: Single versus multiple doses and gender difference. *Life Sci.* 77 (22), 2770–2782. doi:10.1016/j.lfs.2005.03.027

Du, Y., and Ko, K. M. (2006). Effects of pharmacological preconditioning by emodin/oleanolic acid treatment and/or ischemic preconditioning on mitochondrial antioxidant components as well as the susceptibility to ischemia-reperfusion injury in rat hearts. *Mol. Cell Biochem.* 288 (1-2), 135–142. doi:10.1007/s11010-006-9129-3

Evans, L., Shen, Y., Bender, A., Burnett, L. E., Li, M., Habibian, J. S., et al. (2021). Divergent and overlapping roles for selected phytochemicals in the regulation of pathological cardiac hypertrophy. *Molecules* 26 (5), 1210. doi:10.3390/molecules26051210

Evans, L. W., Bender, A., Burnett, L., Godoy, L., Shen, Y., Staten, D., et al. (2020). Emodin and emodin-rich rhubarb inhibits histone deacetylase (HDAC) activity and cardiac myocyte hypertrophy. *J. Nutr. Biochem.* 79, 108339. doi:10.1016/j.jnutbio.2019.108339

Fan, Y., Niu, Z., Xu, C., Yang, L., and Yang, T. (2019). Protic ionic liquids as efficient solvents in microwave-assisted extraction of rhein and emodin from Rheum palmatum L. *Molecules* 24 (15), 2770. doi:10.3390/molecules24152770

Feng, Y., Huang, S. L., Dou, W., Zhang, S., Chen, J. H., Shen, Y., et al. (2010). Emodin, a natural product, selectively inhibits 11beta-hydroxysteroid dehydrogenase type 1 and ameliorates metabolic disorder in diet-induced obese mice. *Br. J. Pharmacol.* 161 (1), 113–126. doi:10.1111/j.1476-5381.2010.00826.x

Frisk, M., Le, C., Shen, X., Roe, A. T., Hou, Y., Manfra, O., et al. (2021). Etiology-dependent impairment of diastolic cardiomyocyte calcium homeostasis in heart failure with preserved ejection fraction. *J. Am. Coll. Cardiol.* 77 (4), 405–419. doi:10.1016/j.jacc.2020.11.044

Gao, J., Zhang, K., Wang, Y., Guo, R., Liu, H., Jia, C., et al. (2020). A machine learning-driven study indicates emodin improves cardiac hypertrophy by modulation of mitochondrial SIRT3 signaling. *Pharmacol. Res.* 155, 104739. doi:10.1016/j.phrs.2020.104739

Gao, Q., Wang, F., Guo, S., Li, J., Zhu, B., Cheng, J., et al. (2011). Sonodynamic effect of an anti-inflammatory agent--emodin on macrophages. *Ultrasound Med. Biol.* 37 (9), 1478–1485. doi:10.1016/j.ultrasmedbio.2011.05.846

Ghimire, G. P., Koirala, N., Pandey, R. P., Jung, H. J., and Sohng, J. K. (2015). Modification of emodin and aloe-emodin by glycosylation in engineered Escherihia coli. *World J. Microbiol. Biotechnol.* 31 (4), 611–619. doi:10.1007/s11274-015-1815-4

Guo, R., Liu, N., Liu, H., Zhang, J., Zhang, H., Wang, Y., et al. (2020). High content screening identifies licoisoflavone A as a bioactive compound of Tongmaiyangxin Pills to restrain cardiomyocyte hypertrophy via activating Sirt3. *Phytomedicine* 68, 153171. doi:10.1016/j.phymed.2020.153171

He, L. F., Wang, C., Zhang, Y. F., Guo, C. C., Wan, Y., and Li, Y. X. (2022). Effect of emodin on hyperlipidemia and hepatic lipid metabolism in zebrafish larvae fed a high-cholesterol diet. *Chem. Biodivers.* 19 (2), e202100675. doi:10.1002/cbdv.202100675

Jiang, N., Liao, W., and Kuang, X. (2014). Effects of emodin on IL-23/IL-17 inflammatory axis, Th17 cells and viral replication in mice with viral myocarditis. *Nan Fang. Yi Ke Da Xue Xue Bao* 34 (3), 373–378.

Khalil, H., Kanisicak, O., Prasad, V., Correll, R. N., Fu, X., Schips, T., et al. (2017). Fibroblast-specific TGF-beta-Smad2/3 signaling underlies cardiac fibrosis. *J. Clin. Invest.* 127 (10), 3770–3783. doi:10.1172/JCI94753

Li, D., Liu, L., Yang, S., Xing, Y., Pan, L., Zhao, R., et al. (2021). Exploring the therapeutic mechanisms of huzhang-shanzha herb pair against coronary heart disease by network pharmacology and molecular docking. *Evid. Based Complement. Altern. Med.* 2021, 5569666. doi:10.1155/2021/5569666

Li, F., Wang, S. C., Wang, X., Ren, Q. Y., Wang, W., Shang, G. W., et al. (2008). Novel exploration of cathartic pharmacology induced by rhubarb. *Zhongguo Zhong Yao Za Zhi* 33 (4), 481–484.

Li, L., Sheng, X., Zhao, S., Zou, L., Han, X., Gong, Y., et al. (2017). Nanoparticle-encapsulated emodin decreases diabetic neuropathic pain probably via a mechanism involving P2X3 receptor in the dorsal root ganglia. *Purinergic Signal* 13 (4), 559–568. doi:10.1007/s11302-017-9583-2

Lim, K. M., Kwon, J. H., Kim, K., Noh, J. Y., Kang, S., Park, J. M., et al. (2014). Emodin inhibits tonic tension through suppressing PKCδ-mediated inhibition of myosin phosphatase in rat isolated thoracic aorta. *Br. J. Pharmacol.* 171 (18), 4300–4310. doi:10.1111/bph.12804

Limin, W., youwang, L., Enbo, W., Zhaolong, Y., and Yalin, L. (2018). Study on the effect of emodin as acoustic sensitizer mediating acoustic dynamic therapy on atherosclerosis in mice. *Med. Inf.* 31 (06), 58–60.

Lin, S. P., Chu, P. M., Tsai, S. Y., Wu, M. H., and Hou, Y. C. (2012). Pharmacokinetics and tissue distribution of resveratrol, emodin and their metabolites after intake of Polygonum cuspidatum in rats. *J. Ethnopharmacol.* 144 (3), 671–676. doi:10.1016/j.jep.2012.10.009

Liu, J., and Ning, L. (2021). Protective role of emodin in rats with post-myocardial infarction heart failure and influence on extracellular signal-regulated kinase pathway. *Bioengineered* 12 (2), 10246–10253. doi:10.1080/21655979.2021.1983977

Liu, Z., Ma, N., Zhong, Y., and Yang, Z. Q. (2015). Antiviral effect of emodin from Rheum palmatum against coxsakievirus B5 and human respiratory syncytial virus *in vitro*. *J. Huazhong Univ. Sci. Technol. Med. Sci.* 35 (6), 916–922. doi:10.1007/s11596-015-1528-9

Liu, Z., Wei, F., Chen, L. J., Xiong, H. R., Liu, Y. Y., Luo, F., et al. (2013). *In vitro* and *in vivo* studies of the inhibitory effects of emodin isolated from Polygonum cuspidatum on Coxsakievirus B4. *Molecules* 18 (10), 11842–11858. doi:10.3390/molecules181011842

Luo, M., Sun, W., Bin, Z., and Kong, X. (2022). Emodin alleviates aortic valvular calcification by inhibiting the AKT/FOXO1 pathway. *Ann. Anat.* 240, 151885. doi:10.1016/j.aanat.2021.151885

Ma, L., Song, K., and Huang, Y. (2021). Coronavirus disease-2019 (COVID-19) and cardiovascular complications. *J. Cardiothorac. Vasc. Anesth.* 35 (6), 1860–1865. doi:10.1053/j.jvca.2020.04.041

Parvez, M. K., Al-Dosari, M. S., Alam, P., Rehman, M., Alajmi, M. F., and Alqahtani, A. S. (2019). The anti-hepatitis B virus therapeutic potential of anthraquinones derived from Aloe vera. *Phytother. Res.* 33 (11), 2960–2970. doi:10.1002/ptr.6471

Qian, J., and Gao, Q. (2018). Sonodynamic therapy mediated by emodin induces the oxidation of microtubules to facilitate the sonodynamic effect. *Ultrasound Med. Biol.* 44 (4), 853–860. doi:10.1016/j.ultrasmedbio.2017.12.016

Qin, W., Du, N., Zhang, L., Wu, X., Hu, Y., Li, X., et al. (2015). Genistein alleviates pressure overload-induced cardiac dysfunction and interstitial fibrosis in mice. *Br. J. Pharmacol.* 172 (23), 5559–5572. doi:10.1111/bph.13002

Qiu, X., Pei, H., Ni, H., Su, Z., Li, Y., Yang, Z., et al. (2021). Design, synthesis and anti-inflammatory study of novel N-heterocyclic substituted Aloe-emodin derivatives. *Chem. Biol. Drug Des.* 97 (2), 358–371. doi:10.1111/cbdd.13788

Roth, G. A., Mensah, G. A., Johnson, C. O., Addolorato, G., Ammirati, E., Baddour, L. M., et al. (2020). Global burden of cardiovascular diseases and risk factors, 1990-2019: Update from the GBD 2019 study. *J. Am. Coll. Cardiol.* 76 (25), 2982–3021. doi:10.1016/j.jacc.2020.11.010

Sato, M., Maulik, G., Bagchi, D., and Das, D. K. (2000). Myocardial protection by protykin, a novel extract of trans-resveratrol and emodin. *Free Radic. Res.* 32 (2), 135–144. doi:10.1080/10715760000300141

Song, Y., Yang, J., Wang, X., Chen, J., Si, D., Gao, H., et al. (2022). Pharmacokinetics and metabolism of trans-emodin dianthrones in rats. *J. Ethnopharmacol.* 290, 115123. doi:10.1016/j.jep.2022.115123

Song, Z. C., Wang, Z. S., Bai, J. H., Li, Z., and Hu, J. (2012). Emodin, a naturally occurring anthraquinone, ameliorates experimental autoimmune myocarditis in rats. *Tohoku J. Exp. Med.* 227 (3), 225–230. doi:10.1620/tjem.227.225

Sougiannis, A. T., Enos, R. T., VanderVeen, B. N., Velazquez, K. T., Kelly, B., McDonald, S., et al. (2021). Safety of natural anthraquinone emodin: An assessment in mice. *BMC Pharmacol. Toxicol.* 22 (1), 9. doi:10.1186/s40360-021-00474-1

Sun, C., and Liu, H. (2008). Application of non-ionic surfactant in the microwave-assisted extraction of alkaloids from Rhizoma Coptidis. *Anal. Chim. Acta* 612 (2), 160–164. doi:10.1016/j.aca.2008.02.040

Tao, S., Liang, X. Y., Wang, Y., and Wang, Y. (2015). Screening of active compounds with myocardial protective effects from Tongmai Yangxin pill. *Zhejiang Da Xue Xue Bao Yi Xue Ban.* 44 (2), 145–153. doi:10.3785/j.issn.1008-9292.2015.03.005

Travers, J. G., Wennersten, S. A., Pena, B., Bagchi, R. A., Smith, H. E., Hirsch, R. A., et al. (2021). HDAC inhibition reverses preexisting diastolic dysfunction and blocks covert extracellular matrix remodeling. *Circulation* 143 (19), 1874–1890. doi:10.1161/CIRCULATIONAHA.120.046462

Tsao, C. W., Aday, A. W., Almarzooq, Z. I., Alonso, A., Beaton, A. Z., Bittencourt, M. S., et al. (2022). Heart disease and stroke statistics-2022 update: A report from the American heart association. *Circulation* 145 (8), e153–e639. doi:10.1161/CIR.0000000000001052

Tzeng, T. F., Lu, H. J., Liou, S. S., Chang, C. J., and Liu, I. M. (2012). Emodin, a naturally occurring anthraquinone derivative, ameliorates dyslipidemia by activating AMP-activated protein kinase in high-fat-diet-fed rats. *Evid. Based Complement. Altern. Med.* 2012, 781812. doi:10.1155/2012/781812

Wang, J., Ji, J., Song, Z., Zhang, W., He, X., Li, F., et al. (2016). Hypocholesterolemic effect of emodin by simultaneous determination of *in vitro* and *in vivo* bile salts binding. *Fitoterapia* 110, 116–122. doi:10.1016/j.fitote.2016.03.007

Wang, T., Yin, X., Lu, Y., Shan, W., and Xiong, S. (2012). Formulation, antileukemia mechanism, pharmacokinetics, and biodistribution of a novel liposomal emodin. *Int. J. Nanomedicine* 7, 2325–2337. doi:10.2147/ijn.S31029

Wang, X., Zou, Y., Sun, A., Xu, D., Niu, Y., Wang, S., et al. (2007). Emodin induces growth arrest and death of human vascular smooth muscle cells through reactive oxygen species and p53. *J. Cardiovasc Pharmacol.* 49 (5), 253–260. doi:10.1097/FJC.0b013e318033dfb3

Wang, Y., Liu, Q., Cai, J., Wu, P., Wang, D., Shi, Y., et al. (2022). Emodin prevents renal ischemia-reperfusion injury via suppression of CAMKII/DRP1-mediated mitochondrial fission. *Eur. J. Pharmacol.* 916, 174603. doi:10.1016/j.ejphar.2021.174603

Wu, c., and Yang, H. (2018). Effect of rhodopsin on the efficacy and serum indices of patients with viral myocarditis. *Clin. Medicat. J.* 16 (09), 39–42+47.

Wu, J. H., Lv, C. F., Guo, X. J., Zhang, H., Zhang, J., Xu, Y., et al. (2021). Low dose of emodin inhibits hypercholesterolemia in a rat model of high cholesterol. *Med. Sci. Monit.* 27, e929346. doi:10.12659/MSM.929346

Wu, Y. C., Wu, P., Li, Y. B., Liu, T. C., Zhang, L., and Zhou, Y. H. (2018). Natural deep eutectic solvents as new green solvents to extract anthraquinones from Rheum palmatum L. *RSC Adv.* 8 (27), 15069–15077. doi:10.1039/c7ra13581e

Wu, Y., Peng, X. Q., Jiang, X. Y., Shi, M. Q., Yang, S. Y., Fu, Y. J., et al. (2017). Effects of wine processed Rheum palmatum on tissue distribution of aloe-emodin, rhein and emodin in rats. *Zhongguo Zhong Yao Za Zhi* 42 (8), 1603–1608. doi:10.19540/j.cnki.cjcmm.20170224.014

Wu, Y., Tu, X., Lin, G., Xia, H., Huang, H., Wan, J., et al. (2007). Emodin-mediated protection from acute myocardial infarction via inhibition of inflammation and apoptosis in local ischemic myocardium. *Life Sci.* 81 (17-18), 1332–1338. doi:10.1016/j.lfs.2007.08.040

Wu, Z., Chen, Q., Ke, D., Li, G., and Deng, W. (2014). Emodin protects against diabetic cardiomyopathy by regulating the AKT/GSK-3β signaling pathway in the rat model. *Molecules* 19 (9), 14782–14793. doi:10.3390/molecules190914782

Xiao, D., Hu, Y., Fu, Y., Wang, R., Zhang, H., Li, M., et al. (2019a). Emodin improves glucose metabolism by targeting microRNA-20b in insulin-resistant skeletal muscle. *Phytomedicine* 59, 152758. doi:10.1016/j.phymed.2018.11.018

Xiao, D., Zhang, Y., Wang, R., Fu, Y., Zhou, T., Diao, H., et al. (2019b). Emodin alleviates cardiac fibrosis by suppressing activation of cardiac fibroblasts via upregulating metastasis associated protein 3. *Acta Pharm. Sin. B* 9 (4), 724–733. doi:10.1016/j.apsb.2019.04.003

Xu, K., Al-Ani, M. K., Wang, C., Qiu, X., Chi, Q., Zhu, P., et al. (2018a). Emodin as a selective proliferative inhibitor of vascular smooth muscle cells versus endothelial cells suppress arterial intima formation. *Life Sci.* 207, 9–14. doi:10.1016/j.lfs.2018.05.042

Xu, K., Zhou, T., Huang, Y., Chi, Q., Shi, J., Zhu, P., et al. (2018b). Anthraquinone emodin inhibits tumor necrosis factor alpha-induced calcification of human aortic valve interstitial cells via the NF-κB pathway. *Front. Pharmacol.* 9, 1328. doi:10.3389/fphar.2018.01328

Xu, Y., Zhang, S., Rong, J., Lin, Y., Du, L., Wang, Y., et al. (2020). Sirt3 is a novel target to treat sepsis induced myocardial dysfunction by acetylated modulation of critical enzymes within cardiac tricarboxylic acid cycle. *Pharmacol. Res.* 159, 104887. doi:10.1016/j.phrs.2020.104887

Yang, Y., Jiang, Z., and Zhuge, D. (2019). Emodin attenuates lipopolysaccharide-induced injury via down-regulation of miR-223 in H9c2 cells. *Int. Heart J.* 60 (2), 436–443. doi:10.1536/ihj.18-048

Ye, B., Chen, X., Dai, S., Han, J., Liang, X., Lin, S., et al. (2019). Emodin alleviates myocardial ischemia/reperfusion injury by inhibiting gasdermin D-mediated pyroptosis in cardiomyocytes. *Drug Des. Devel Ther.* 13, 975–990. doi:10.2147/dddt.S195412

Zhang, H. M., Wang, F., Qiu, Y., Ye, X., Hanson, P., Shen, H., et al. (2016a). Emodin inhibits coxsackievirus B3 replication via multiple signalling cascades leading to suppression of translation. *Biochem. J.* 473 (4), 473–485. doi:10.1042/bj20150419

Zhang, T., Dong, D., Lu, D., Wang, S., and Wu, B. (2016b). Cremophor EL-based nanoemulsion enhances transcellular permeation of emodin through glucuronidation reduction in UGT1A1-overexpressing MDCKII cells. *Int. J. Pharm.* 501 (1-2), 190–198. doi:10.1016/j.ijpharm.2016.01.067

Zhang, X., Qin, Q., Dai, H., Cai, S., Zhou, C., and Guan, J. (2019). Emodin protects H9c2 cells from hypoxia-induced injury by up-regulating miR-138 expression. *Braz J. Med. Biol. Res.* 52 (3), e7994. doi:10.1590/1414-431x20187994

Zhao, X. Y., Qiao, G. F., Li, B. X., Chai, L. M., Li, Z., Lu, Y. J., et al. (2009). Hypoglycaemic and hypolipidaemic effects of emodin and its effect on L-type calcium channels in dyslipidaemic-diabetic rats. *Clin. Exp. Pharmacol. Physiol.* 36 (1), 29–34. doi:10.1111/j.1440-1681.2008.05051.x

Zheng, Q., Li, S., Li, X., and Liu, R. (2021). Advances in the study of emodin: An update on pharmacological properties and mechanistic basis. *Chin. Med.* 16 (1), 102. doi:10.1186/s13020-021-00509-z

Zhong, Y., Ding, Y., Xiao, D., Hu, D., and Li, Y. (2022). New 18β-glycyrrhetinic acid-emodin esters synthetized by a one-step innovative route, its structural characterization, and *in vivo* toxicity assessed on zebrafish models. *Chem. Biodivers.* 19 (4), e202100928. doi:10.1002/cbdv.202100928

Zhou, L., Hu, X., Han, C., Niu, X., Han, L., Yu, H., et al. (2022). Comprehensive investigation on the metabolism of emodin both *in vivo* and *in vitro*. *J. Pharm. Biomed. Anal.* 223, 115122. doi:10.1016/j.jpba.2022.115122

Zhu, L., Zhao, J. L., Peng, X. H., Wan, M. H., Huang, X., and Tang, W. F. (2014). Pharmacological study on free anthraquinones compounds in rhubarb in rats with experimental acute pancreatitis. *Zhongguo Zhong Yao Za Zhi* 39 (2), 304–308.

Glossary

CVD Cardiovascular disease

ROS reactive oxygen species

THP-1 human acute monocytic leukemia cell

MMP matrix metalloproteinase

TIMP tissue inhibitor of metalloproteinase-1

cTnI cardiac troponin I

PGC-1 peroxisome proliferator-activated receptor-γ coactivator-1

p-ERK phosphorylated-extracellular signal-regulated kinase

JNK Jun kinase enzyme

TNF-α tumor necrosis factor-alpha

NF-κB nuclear factor kappa-B

IR Ischemia-Reperfusion

TLR4 toll-like receptor-4

MyD88 myeloiddifferentiationfactor88

NLRP3 Nod-like receptors protein-3

MDA malondialdehyde

VSMCs vascular smooth muscle cells

PKC protein kinase C

Ang II angiotensin II

IL-1b interleukin-1b

IL-6 interleukin-6

IL-23 interleukin-23

IL-17 interleukin-17

p-AKT phosphorylated-protein kinase B

p-FOXO1 forkhead box protein O1

LPS Lipopolysaccharide

miR micro RNA

Th17CVB3 CVB3coxsackievirus B3

CVB4 coxsackievirus B4

CVB5 coxsackievirus B5

IFN-α interferon-alpha

TNF-γ tumor necrosis factor-gama

SMAD7 small mother against decapentaplegic-7

Sirt3 sirtuin 3

NADH reduced form of nicotinamide-adenine dinucleotid

α-SMA alpha-smooth muscle actin

MTA3 metastasis-associated protein 3

TGF-β transforming growth factor-beta

frontiers | Frontiers in Pharmacology

TYPE Clinical Trial
PUBLISHED 23 December 2022
DOI 10.3389/fphar.2022.1017734

Check for updates

OPEN ACCESS

EDITED BY
Qing Yong He,
China Academy of Chinese Medical Sciences, China

REVIEWED BY
Xiangjun Yin,
Zhejiang Chinese Medical University, China
Yu-Qing Zhang,
McMaster University, Canada

*CORRESPONDENCE
Huihui Zhao,
hh686@126.com
Wei Wang,
wangwei26960@126.com

†These authors share first authorship

SPECIALTY SECTION
This article was submitted to Ethnopharmacology, a section of the journal Frontiers in Pharmacology

RECEIVED 12 August 2022
ACCEPTED 08 December 2022
PUBLISHED 23 December 2022

CITATION
Du K, Liu J, Tan N, Huang X, Wang J, Zhao H and Wang W (2022), The effects of qishen granules for patients with chronic heart failure: A multicenter randomized double-blind placebo-controlled trial.
Front. Pharmacol. 13:1017734.
doi: 10.3389/fphar.2022.1017734

COPYRIGHT
© 2022 Du, Liu, Tan, Huang, Wang, Zhao and Wang. This is an open-access article distributed under the terms of the Creative Commons Attribution License (CC BY). The use, distribution or reproduction in other forums is permitted, provided the original author(s) and the copyright owner(s) are credited and that the original publication in this journal is cited, in accordance with accepted academic practice. No use, distribution or reproduction is permitted which does not comply with these terms.

The effects of qishen granules for patients with chronic heart failure: A multicenter randomized double-blind placebo-controlled trial

Kangjia Du[1†], Junjie Liu[2†], Nannan Tan[1], Xinyi Huang[1], Juan Wang[1], Huihui Zhao[1*] and Wei Wang[1*]

[1]Department of Chinese medicine, Beijing University of Chinese Medicine, Beijing, China, [2]Department of Cardiology, Nanjing Pukou Hospital of Traditional Chinese Medicine, Nanjing, China

Background: Despite advancements in chronic heart failure (CHF) treatment, the effect often remains unsatisfactory and unstable. More effective therapies are needed. Qishen granules (QSG) are a novel Chinese botanical drug effective in treating CHF in animal models, but clinical evidence remains inadequate.

Objective: This study aims to evaluate the effects of QSG on patients with CHF.

Methods: We enrolled CHF patients in this 12-week, randomized, double-blind, placebo-controlled trial and randomly assigned them to the QSG (twice a day, 6.8 g granules at once) or placebo group. The primary endpoint was a change in the plasma N-terminal pro-B-type natriuretic peptide (NT-proBNP) level after treatment. The secondary outcome consists of the New York Heart Association (NYHA) functional classification, 6-min walking distance (6MWD), TCM syndrome integral scale, quality of life, and echocardiographic index.

Results: A total of 191 patients completed the 12-week follow-up period, with 94 in the QSG group and 97 in the placebo group. The Qishen granules group demonstrated a considerably greater reduction in NT-proBNP than the placebo group (50% vs 32% for QSG vs placebo, respectively; $p = 0.011$). Patients who received QSG performed better in the NYHA functional rank, 6MWD, TCM syndrome integral scale, and quality of life ($p < 0.05$). The QSG group performed better in HFrEF patients regarding the efficiency of NT-proBNP. There was no statistical significance in the change in evaluated safety parameters, such as blood routine and biochemistry.

Conclusion: Based on standard treatment, Qishen granules further reduced the levels of NT-proBNP when compared with placebo. Together with other

Abbreviations: CHF, chronic heart failure; FS, fractional shortening; HFrEF, heart failure with reduced ejection fraction; HFmrEF, heart failure with mild reduced ejection fraction; HFpEF, heart failure with preserved ejection fraction; LVEDD, left ventricular end-diastolic dimension; LVEF, left ventricle ejection fraction; LVESD, left ventricular end-systolic dimension; MLHFQ, minnesota living with heart failure questionnaire; NT-proBNP, N-terminal pro-B-type natriuretic peptide; NYHA, new york heart association; QSG, Qi Shen granules; 6 MWD, 6-min walk distance.

outcomes, our findings suggest that QSG could be used in combination therapy for CHF.

Clinical Trial Registration: www.clinicaltrials.gov, identifier NCT03027375. Registered 9 October 2017

KEYWORDS

chronic heart failure, qi shen granules, randomized controlled trial, detoxification, NT-probnp

Introduction

Chronic heart failure (CHF), the final stage of various myocardial diseases, is a comprehensive clinical syndrome that occurs when the heart chamber cannot pump enough blood for organs (Groenewegen et al., 2020). According to recent epidemiological data, the prevalence of heart failure in China is 3.5% (Guo et al., 2016). Despite advances in the standard treatment strategy for heart failure, the effect often remains unsatisfactory and unstable. An international prospective cohort study data prove that 16.5% of people die of CHF within a year (Dokainish et al., 2017). Traditional Chinese medicine (TCM) has been widely used to treat CHF in China for years due to mechanisms of multitarget effects and a significant curative effect in alleviating symptoms (Li et al., 2013). From the general perspective of TCM, the primary cause of heart failure is heart Qi deficiency and blood stasis, which refers to a pathological state in which Qi cannot promote blood circulation, resulting in poor or even stagnant blood circulation. The current treatment has successfully improved symptoms and quality of life but has performed poorly in delaying ventricular remodeling and improving long-term prognosis. Researchers increasingly recognize that other unnoticed pathologies may play an essential role in the progression of heart failure. Heat toxicity is unnoticed pathogenesis closely related to inflammation. Heat toxicity is thought to induce acute episodes of heart failure, exacerbate symptoms and promote ventricular remodeling. It has been gradually considered an essential factor in heart failure (Yuan et al., 2014; Wang et al., 2021). Therefore, heat-clearing and detoxifying might be an effective therapy to complement the classical treatment of tonifying Qi and removing blood stasis. Qi Shen granules (QSG) are the representative drug for this innovative therapy.

QSG evolved from two well-known prescriptions (Simiaoyongan Decoction and Zhenwu Decoction). Researchers conducted experiments in animal and cell models to validate the effects of QSG and explore its mechanism of action. These studies indicated that QSG could treat CHF by facilitating cardiac contractile function, improving hemodynamics, and attenuating remodeling (Yang et al., 2020; Zhang et al., 2020; Chen et al., 2021). However, no clinical studies have been reported. Therefore, we designed a randomized control study to assess the efficacy and safety of QSG.

Methods

Design

This was a 12-week, randomized, double-blind, placebo-controlled, multicenter study. This study aimed to determine whether QSG reduces NT-proBNP, improves cardiac function and exercise performance, and alleviates clinical symptoms in heart failure patients. The participants could quit at any time for any reason. The appropriate ethics committees approved all studies. This study has been registered at Clinical Trials. gov (NCT: 03027375). More detailed design information was previously reported in 2017 (Wang et al., 2017).

Drug composition

QSG consists of six TCM botanical drugs: Astragalus mongholicus Bunge [*Leguminosae*; *Astragali Radix*], Salvia miltiorrhiza Bunge [*Lamiaceae; Salviae miltiorrhizae radix et rhizoma*], Aconitum carmichaeli Debeaux [*Ranunculaceae*; *Aconiti Lateralis Radix Praeparata*], *Scrophularia ningpoensis Hemsl* [*Scrophulariaceae*; *Scrophulariae Radix*], *Lonicera japonica* Thunb *[Caprifoliaceae; Lonicerae Japonicae Flos*], Glycyrrhiza glabra L [*Leguminosae; Glycyrrhizae Radix et Rhizoma*]. The quantity of each drug is 6 g, 1.5 g, 0.9 g, 2 g, 2 g, and 1.2 g in sequence.

All drugs were extracted by water extraction and alcohol sedimentation. Water extraction process conditions: add eight times the amount of water, and extract three times, each time for 1 h. Alcoholic sedimentation process: concentrate the aqueous extract to a relative density of 1.10~1.15 (60°C), add ethanol until its concentration is 70%, let it stand and refrigerate for 16 h, centrifuge, separate, take the supernatant, concentrate under reduced pressure and dry under vacuum (60°C, −0.8 MPa). The excipient is lactose.

Population

CHF patients from three hospitals (China-Japan Friendship Hospital, Hubei Provincial Hospital of Traditional Chinese Medicine, and The First Affiliated Hospital of Beijing University of Traditional Chinese Medicine) were screened following eligibility and exclusion criteria. The eligibility criteria were as follows (Groenewegen et al., 2020): age between 18 and 75 years (Guo et al., 2016), clinically diagnosed with heart failure for more than 3 months (Dokainish et al., 2017), CHF caused by coronary heart disease and hypertension, which was diagnosed according to the Chinese guidelines published in 2014 (Li et al., 2013), New York Heart Association (NYHA) functional class from II to IV (Wang et al., 2021), a serum N-terminal pro-B type natriuretic peptide (NT-proBNP) level ≥450 pg/ml (Yuan et al., 2014), provision of written informed consent (Chen et al., 2021), inclusion of all types of ejection fraction. The exclusion criteria were as follows (Groenewegen et al., 2020): CHF accompanied by severe valvular heart disease, congenital heart disease, pericardial disease, cardiomyopathy, unstable angina, acute myocardial infarction (within the previous 4 weeks), cardiogenic shock, acute myocarditis, infective endocarditis, or uncontrolled severe cardiac arrhythmia with hemodynamic changes (Guo et al., 2016); pulmonary heart disease, pulmonary hypertension caused by acute or chronic pulmonary embolism or cerebral apoplexy in the last 6 months (Dokainish et al., 2017); severe hepatic inadequacy with alanine aminotransferase or alkaline phosphatase levels more than twice the upper normal limit, renal inadequacy with a serum creatinine level >3 mg/dl (>265 μmol/L), severe electrolyte imbalance, severe hematologic disease, malignant tumor, diabetes mellitus with severe complications, or severe endocrine diseases such as hyperthyroidism and hypothyroidism (Li et al., 2013); acute infection confirmed by any one of the following three indicators: a) fever, b) a white blood cell count>10 × 10^9/L and a percentage of neutrophils> 75%, c) shadow on chest X-ray (Wang et al., 2021); uncontrolled blood pressure (systolic≥180 mmHg or diastolic≥110 mmHg) or fibrosis in other organs (Yuan et al., 2014); pregnancy or breastfeeding (Chen et al., 2021); psychiatric or infectious disease.

Treatment

Qualified patients were randomized in a 1:1 ratio to receive either QSG or a matching placebo for 12 weeks, twice a day, 6.8 g granules at a time. Patients in both groups received internal medicine treatment according to the 2014 guidelines (Zhang and Zhang, 2014). Participants were prohibited from taking other Chinese medicines during the trial period. Beijing KangRenTang Pharmaceutical Co., Ltd. manufactured the QSG and placebo.

Outcomes and clinical visit

The primary outcome is the proportion of patients demonstrating a more than 30% (4) decrease in NT-proBNP levels after 12 weeks of treatment. The secondary outcomes are changes in NYHA functional degree, 6-min walking distance, echocardiogram data, quality of life measured with the Minnesota Living with Heart Failure Questionnaire (MLHFQ, Table MLHFQ, ©1986 Regents of the University of Minnesota), and symptoms with TCM syndrome integral scale (SIS). We collected their NYHA functional degree, 6 MWD, MLHFQ, and TCM syndrome integral scale information at each visit point (week 0 ± 3 days, week 4 ± 3 days, week 8 ± 3 days, and week 12 ± 3 days). We measured the NT-proBNP and echocardiogram data only at the first and last visits.

TCM SIS is determined based on preliminary clinical research results and expert opinion (Table scale). All laboratory tests were carried out at local participating units. Plasma NT-proBNP was tested using electrochemiluminescence (Roche Diagnostics, Basel, Switzerland).

Any adverse medical event that occurs in a subject during the observation period of a clinical study, regardless of whether it is causally related to the test drug, is considered an adverse event (AE). Serious adverse event (SAE) includes death, life-threatening hospitalization, prolonged hospitalization, or causing a permanent disability, cancer, congenital disabilities, and drug overdose.

Randomization

An independent statistician who was unaware of the design and purpose of the study generated the randomization table using the Statistical Analysis System (SAS, version 9.4). The 200 eligible patients were randomly allocated in a 1:1 ratio to either the QSG treatment group or the placebo group. The randomization was stratified by the study site. The statistician was not involved in patient recruitment. The random assignment form was sealed in an opaque envelope, and the project leader and statistician kept a copy. Participants received the number in the enrollment order and took the corresponding drugs.

Blinding

Both participants and investigators were blinded to the treatment allocation throughout the study. QSG and placebo were identical in packaging, particle appearance, and taste. The manufacturer labeled the random codes on the packaging. The clinical trial pharmacist at each center provided packaged drugs to the participants according to the randomization number.

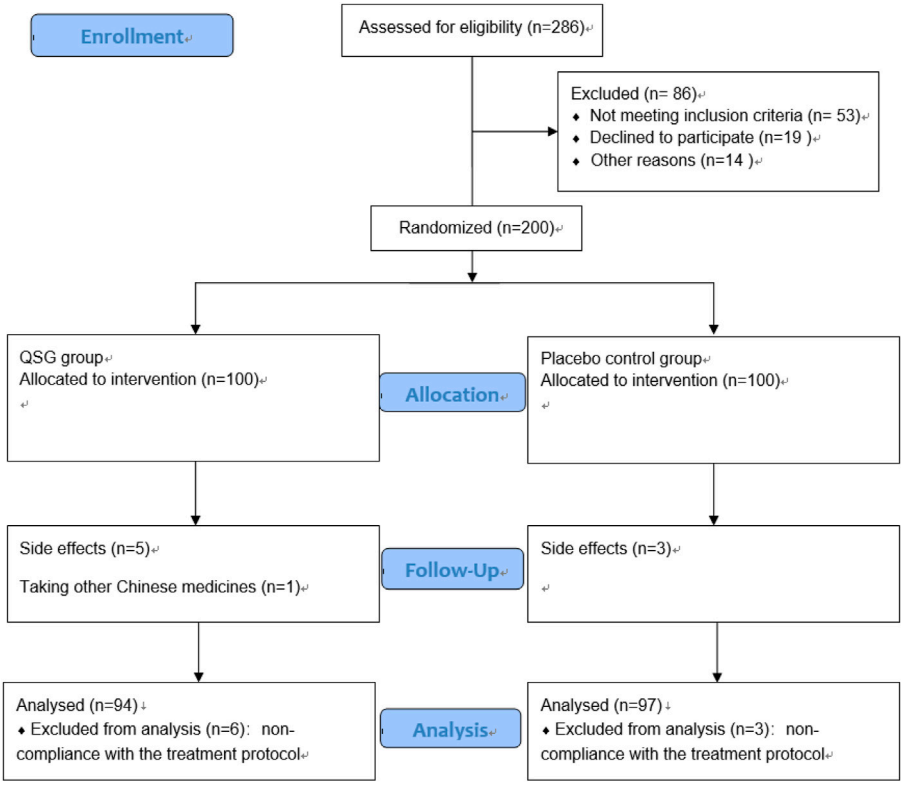

FIGURE 1
Study flow chart.

Sample size calculation

The sample size was calculated based on the primary outcome. According to a previous trial on treating CFH with TCM (4), we assumed that the proportion of patients demonstrating a more than 30% NT-proBNP decrease in the QSG group would be 53% (P2), and the other ratio in the placebo group would be 31.98% (P1). Given a type-I error rate of $\alpha = 0.05$ and a type-II error rate of $\beta = 0.2$, each group required 80 patients. Considering a drop rate of 20% among recruited patients, the total sample size needed 200 to achieve efficacy analysis results.

Data analysis

Two researchers entered the data independently. We used the per-protocol analysis to analyze the data and the Shapiro-Wilk test to identify data distribution. Normally distributed variables were analyzed by two-tailed t-test between two groups, and paired t-test were used for intragroup data comparisons. Other distribution-type variables were analyzed by the Wilcoxon or Chi-Square test. The MLHFQ and syndrome integral data were analyzed with repeated measures models using time and treatment as the main factors. $p < 0.05$ is a statistically significant criterion.

A subgroup analysis was performed for patients with different levels of LVEF, heart failure with reduced ejection (HFrEF), heart failure with mildly reduced ejection fraction (HFmrEF), and heart failure with preserved ejection fraction (HFpEF). The criteria (Heidenreich et al., 2022) are as follows: HFrEF (LVEF≤40%), HFmrEF (LVEF41%–49%), and HFpEF (LVEF≥50%). First, we compared patients' baseline age, sex, BMI, and NT-proBNP of patients within each subgroup and confirmed no significant differences. We then compared between-group differences in NT-proBNP and echocardiographic markers in different ejection fraction populations.

All statistical analyses were performed with SAS version 9.4 (SAS Institute Inc., Cary, NC, United States).

Results

Demographic and clinical characteristics

From January 2017 to March 2021, 200 patients were recruited to participate in this trial. Nine patients were excluded for non-compliance with the treatment protocol. Finally, there were 94 patients in the QSG group and 97 in the placebo group (Figure 1). The mean age of all patients was 67.95 years, and

TABLE 1 Baseline characteristics of patients.

Characteristics	All n = 191	QSG, n = 94	Placebo, n = 97	*p*-value[a]
Male/Female	122/69	59/35	63/34	0.692
Age	70 (63,75)	69 (61,75)	70 (63,75)	0.450
Height (cm)	167 (158,173)	167 (157,173)	166 (158,173)	0.802
Weight (kg)	69.2 ± 11.8	69.0 ± 12.0	69.2 ± 11.5	0.944
BMI	24.9 ± 3.4	24.9 ± 3.6	24.8 ± 3.1	0.775
Heart rate	75 (66,86)	75 (68,85)	76 (65,87)	0.485
Breath	19 (18,20)	19 (18,20)	19 (18,20)	0.575
Sbp	135.6 ± 20.2	136.1 ± 19.2	135.1 ± 21.1	0.389
Dbp	80 (70,88)	80 (70,90)	77 (70,88)	0.115
Mean LVEF	50.5 ± 16.3	51.1 ± 16.2	49.8 ± 16.4	0.591
Course (month)	65.32 ± 65.8	65.5 ± 68.26	65.11 ± 63.70	0.965
NYHA				
II	28 (14.7%)	15	13	0.999
III	112 (58.6%)	54	58	0.999
IV	51 (26.7%)	25	26	0.999
Comorbidity				
Diabetes	96 (50.3%)	47	49	0.943
Hyperlipidemia	85 (44.5%)	45	40	0.356
Arrhythmia	80 (41.9%)	39	41	0.913
Hypertension	146 (76.4%)	72	74	0.960
Hyperuricemia	15 (7.9%)	9	6	0.384
Valve disease	7 (3.7%)	3	4	0.732
Medications				
Statin	122 (63.9%)	63	59	0.373
ACEI/ARB	115 (60.2%)	62	53	0.058
B-blockers	149 (78.0%)	75	74	0.559
Diuretics	132 (69.1%)	56	76	0.260
Ca-blockers	38 (19.9%)	19	19	0.914
Anticoagulants	127 (66.5%)	69	58	0.300
Spironolactone	93 (48.7%)	40	53	0.095
Nitrates	49 (25.7%)	28	21	0.198

Normally distributed data are presented as the mean ± SD, or the percentage of patients. Non-normally distributed data are presented as the median (Q1, Q3). 'Course' means chronic heart failure duration.

Sbp = systolic blood pressure; Dbp = diastolic blood pressure; NYHA, new york heart association.

[a]Based on independent t-test or Wilcoxon test.

62.8% were male. The average course of CHF was 65.32 months. The detailed baseline information is shown in Table 1. No significant difference was found between the two groups at baseline.

Primary outcome

The baseline NT-proBNP levels in the QSG and placebo groups were comparable. After 12 weeks of treatment, 47 patients (50%) in the QSG group and 31 patients (32%) in the placebo group were defined as effective according to the previous standard (Chi-square 6.431, $p = 0.011$, Table 2). The NT-proBNP numerical value in the two groups demonstrated a significant difference (891.0 (481.8,2443.5) vs. 1,649.0 (659.4,3179.0), pg/ml, $p = 0.027$, Table 3).

We analyzed the results sorted by LVEF level. First, we compared baseline data, including age, gender BMI, and NT-proBNP, to ensure that the subsequent analysis was reasonable and reliable (Table 4). No significant difference was found in a subset. In the HFrEF subgroup, the treatment efficiency of QSG was better than the control group. At the same time, the rest of the population did not show differences (Table 5).

TABLE 2 Treatment efficiency in NT-proBNP.

	QSG, n = 94	Placebo, n = 97	Chi-square value	*p*-value
Valid (≥30%)	47 (50.0%)	31 (32.0%)	6.431	0.011
Invalid (<30%)	47 (50.0%)	66 (68.0%)		

QSG, Qi shen granules. The effective standard is that the reduction ratio is greater than or equal to 30%.

TABLE 3 numerical value change in NT-proBNP.

	QSG, n = 94	Placebo, n = 97	Z	*p*-value
NT-ProBNP baseline	1,633.0 (741.5,3677.7)	1,607.2 (736.0,4682.5)	−0.181	0.857
NT-ProBNP after treat	891.0 (481.8,2443.5)	1,649.0 (659.4,3179.0)	−2.214	0.027

QSG, Qi shen granules. *p* values determined by the Wilcoxon test.

TABLE 4 subgroup baseline characteristics of patients.

Subgroup	Characteristics	t/Z	*p*-value
HFrEF	Age	−0.536	0.562
	Sex	−1.320	0.187
	BMI	0.689	0.494
	NT-proBNP	0.106	0.916
HFmrEF	Age	−1.909	0.056
	Sex	−0.410	0.682
	BMI	−0.616	0.541
	NT-proBNP	−0.828	0.413
HFpEF	Age	−0.534	0.593
	Sex	−0.710	0.478
	BMI	0.346	0.730
	NT-proBNP	0.324	0.746

HFrEF, heart failure with reduced ejection fraction; HFmrEF, heart failure with mildly reduced ejection fraction; HFpEF, heart failure with preserved ejection fraction.

TABLE 5 subgroup Treatment efficiency in NT-proBNP.

	Group	Invalid	Valid	*p*-value
HFrEF (56)	QSG	13	14	0.006
	Placebo	24	5	
HFmrEF (38)	QSG	9	3	0.900
	Placebo	19	7	
HFpEF (97)	QSG	25	30	0.364
	Placebo	23	19	

QSG, Qi shen granules; HFrEF, heart failure with reduced ejection fraction; HFmrEF, heart failure with mildly reduced ejection fraction; HFpEF, heart failure with preserved ejection fraction.
The effective standard is that the NT-proBNP, reduction ratio is greater than or equal to 30%.

TABLE 6 Echocardiographic indices.

		QSG, n = 94	Placebo, n = 97	*p*-value
LVEF	0 W	51 ± 16	50 ± 16	0.597
	12 W	53 ± 14	51 ± 15	0.297
FS	0 W	28 ± 10	26 ± 10	0.382
	12 W	30 ± 11	27 ± 10	0.090
LVEDD	0 W	53 ± 11	55 ± 12	0.222
	12 W	52 ± 12	55 ± 11	0.074
LVESD	0 W	39 ± 12	42 ± 13	0.212
	12 W	39 ± 11	41 ± 13	0.345

QSG, Qi shen granules; LVEDD, left ventricular end-diastolic dimension; LVEF, left ventricle ejection fraction; FS, fractional shortening; LVESD, left ventricular end-systolic dimension.

TABLE 7 6 MWD.

6 MWD, m	QSG, n = 75	Placebo, n = 84	Z	*p*-value
0 W	330.7 (217.0,384.3)	316.0 (249.2,359.0)	−0.359	0.720
12 W	367.0 (249.2,359.0)	333.5 (282.0,388.0)	−2.854	0.004
Z	−3.604	−2.544		
p-value	<0.001	0.011		

Secondary outcome

Echocardiography measurements. In the overall population, echocardiography did not significantly change from baseline to the end. No significant changes were observed between groups ($p > 0.05$ for all, Table 6).

6MWD. Some participants refused to undergo the 6-min walk test due to physical intolerance or concerns about possible risks. Both groups showed improvements after treatment for 12 weeks ($p < 0.001$ and $p = 0.050$, respectively). Compared to placebo group patients, QSG patients exhibited more significant improvements (Table 7, $p = 0.001$).

We observed the NYHA class at each visit. There was no significant difference between the two groups at 0 and 4 weeks. As the number of NYHA I-II patients gradually increased, whereas the number of NYHA III-IV patients decreased, the difference between the two groups came up at 8 and 12 weeks (Figure 2). Both patients promoted NYHA function, and the QSG group showed better improvement ($p < 0.001$ at both sites).

Quality of life was assessed using the MLHFQ at each visit. The two groups demonstrated a similar mean at 0 weeks and 4 weeks. Significant effects were observed from 8 to 12 weeks (Table 8; Figure 3, $p < 0.001$ for all). In the repeated measures model analysis, patients in the QSG group demonstrated a more significant decrease in the MNSN score ($F = 11.669$, $p = 0.001$), and the time effect was substantial ($F = 98.93$, $p < 0.01$).

The TCM SIS was used to collect syndrome information at each visit. Syndrome scores remained similar in the two groups until 8 weeks. The QSG group exhibited lower scores, meaning that patients alleviated symptoms better than those in the placebo group. (Table 9; Figure 4). In the repeated measures model analysis, significant effects were observed in treatment and time (treatment $p = 0.0083$, time $p < 0.0001$).

Adverse events

The safety set analyses included a total of 191 patients in each group. For adverse events, the total number was five in the QSG group and three in the placebo group. In the QSG group, two patients reported stomachache, two reported nausea, and one reported diarrhea after taking medicine. In the placebo group, two reported nausea, and one reported dry cough. The analysis of drug-induced adverse events revealed no difference between the study groups (Table 10). No serious adverse events (SAEs) related to the study drugs were reported.

Discussion

This is the first clinical study demonstrating the QSG effect in heart failure patients. There were changes in the study

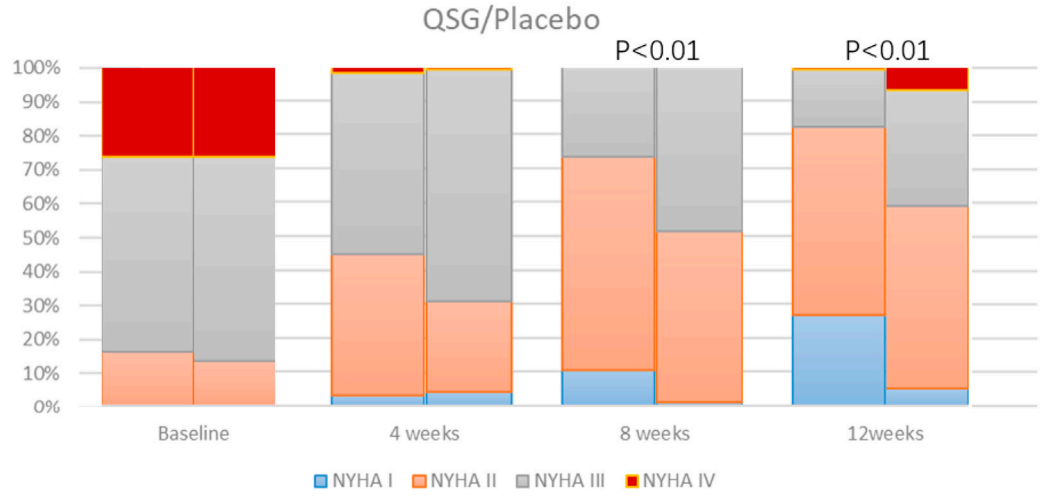

FIGURE 2
NYHA cardiac function class distribution.

TABLE 8 MLHFQ.

OB (W)	QSG, n = 94	Placebo, n = 97	T Value	*p*-value
0	68.3 ± 14.9	67.7 ± 14.9	0.273	0.785
4	54.1 ± 15.6	59.0 ± 18.7	−1.933	0.055
8	43.5 ± 19.4	55.2 ± 21.2	−3.968	<0.001
12	37.9 ± 21.5	50.7 ± 24.3	−3.860	<0.001

MLHFQ, minnesota living with heart failure Questionnaire; QSG, Qi Shen granules.; OB, observation time.
p values were determined by repeated-measures analysis of variance.

implementation compared to the previously published protocol: 1) the inclusion criteria added patients with class IV heart function, 2) all patients with TCM diagnosis were included, and 3) a more authoritative and reliable sample size calculation formula was used. We expected to obtain comprehensive and objective information on QSG for heart failure, so the study population was appropriately expanded so that the study results were closer to clinical reality.

The main findings of this study are that QSG could significantly reduce the NT-proBNP level of patients, improve quality of life and the 6-min walk test scores, and alleviate the symptoms of patients. There were no severe adverse reactions during this study. Our observations suggest that QSG could be a supplementary therapeutic strategy for treating heart failure patients.

As mentioned before, the clinical innovation of TCM treatment of heart failure has essential theoretical and practical significance. Currently, TCM treatment of heart failure is limited to tonifying qi, warming yang, and promoting blood circulation. We believe that boosting the effectiveness of TCM treatment of heart failure requires innovation in the therapy. In recent years, the role of heat toxicity in heart failure has attracted attention, partly because the corresponding concept of inflammatory pathways has been valued in the mechanism of heart failure. Based on this theoretical innovation, heat-clearing and detoxifying treatment methods were added to tonifying qi, warming yang, and promoting blood circulation. Due to the lack of comparison with classical treatment methods, the experiment still cannot explain whether the treatment of heat-clearing and detoxification has advantages. However, this research still achieves innovations in therapy.

The role of QSG in treating heart failure has been demonstrated in several animal experiments. Qiu Qi et al. (Qiu et al., 2014) studied the effects on miniature pig models and found that Qishen granules can significantly alleviate the symptoms. QSG have the same effect on heart failure mice and rat models (Xuanchao et al., 2015). Further studies have

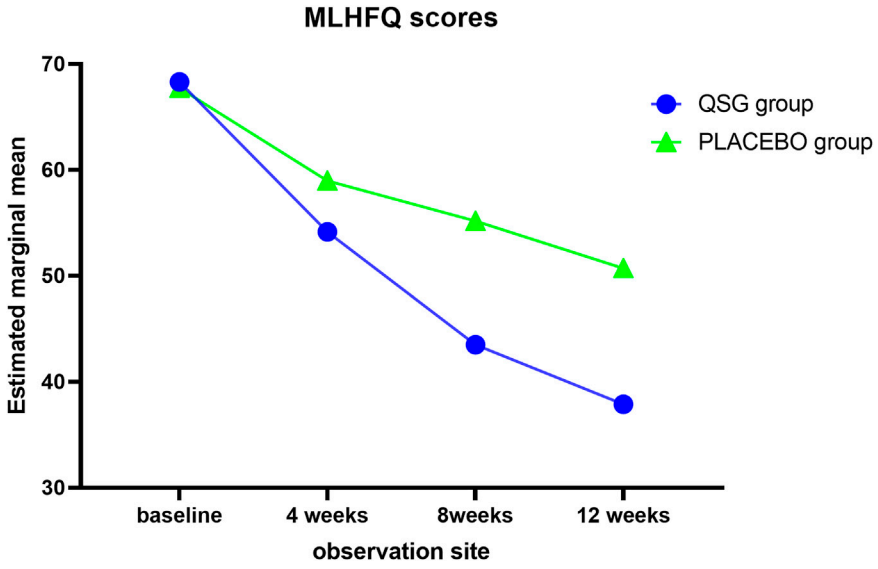

FIGURE 3
MLHFQ scores.

TABLE 9 TCM syndrome integral scale.

OB (W)	QSG, n = 94	Placebo, n = 97	T Value	*p*-value
0	62.8 ± 14.2	64.2 ± 14.8	−0.686	0.494
4	53.2 ± 18.0	55.7 ± 20.7	−0.885	0.378
8	42.1 ± 19.1	49.4 ± 22.4	−2.412	0.017
12	32.4 ± 23.4	44.8 ± 27.2	−3.380	0.001

QSG, Qi Shen granules.
OB, observation time.
p values were determined by repeated-measures analysis of variance.

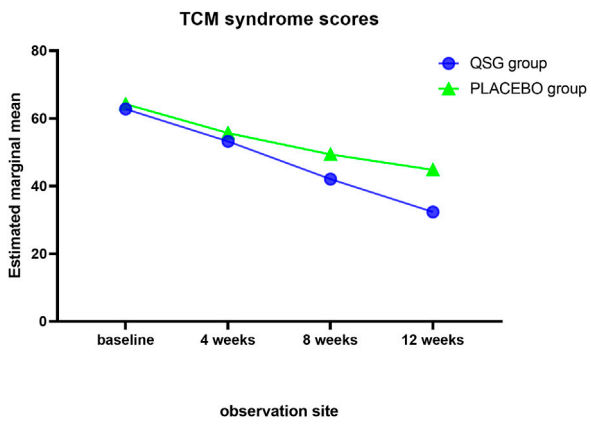

FIGURE 4
TCM syndrome scores.

confirmed that Qishen Granules can inhibit the apoptosis of cardiomyocytes (Chang et al., 2018), the oxidative stress effect induced by p47phox and RAC1, and myocardial fibrosis (Zeng et al., 2018). The regulation mechanism is diverse and resultful. These solid research foundations provide a basis for the clinical use of Qishen Granules.

NT-proBNP is an internationally recognized indicator for the assessment of heart failure. It is effective for both acute and chronic heart failure (Najbjerg et al., 2019). Compared with BNP, NT-proBNP has a longer half-life and a more stable state. It is less affected by renal function indicators (Farnsworth et al., 2018), so NT-proBNP is generally used to evaluate heart failure in clinical practice. As an indicator, a 30% decrease in NT-proBNP is defined as an adequate criterion (Li et al., 2013). This experiment follows this research line of thought, and the results show that QSG can effectively reduce the level of NT-proBNP in patients with chronic heart failure. QSG showed

TABLE 10 Adverse event.

Adverse event	QSG, n = 94	Placebo, n = 97	Chi-square	*p*-value
Yes	5	3	0.590	0.443
No	89	94		

QSG, Qi Shen granules;QSG, for heart failure.

promising results in lowering NT-proBNP in the HFrEF population. However, no significant differences were seen in other patients, suggesting that QSG may be more suitable for application in patients with reduced ejection fraction.

Echocardiography can provide real-time heart function evaluation, tube diameter, ventricular wall and septal thickness, and fractional shortening. It is the preferred method for evaluating cardiac structure and function (Expert Consensus on Standardized Echocardiography, 2019). After treatment, although there was no statistically significant difference in left ventricular ejection fraction between groups, the LVEF value increased, which may be related to the small sample size. There are no apparent differences in many ultrasound indicators, indicating that the changes in the ventricular structure are slowly developing and relatively stable. A significantly different effect on this process may require a longer medication cycle, suggesting the importance of early intervention for heart failure.

Heart function classification can reflect the severity of heart failure as a whole. The results show that the distribution of heart function between groups at baseline is comparable. There was a statistically significant difference between groups at 8 weeks, and the distinction still existed at 12 weeks. This demonstrates that QSG can improve heart function.

Heart failure is a complex and severe disease, and TCM is good at reducing the symptoms of the disease. In this study, QSG reduced heart failure symptoms, enhanced exercise capacity, and improved patients' quality of life. These metrics may not be solid evidence of efficacy, but patients did benefit from improvements in these metrics. In recent years these soft indicators have played a more critical role in the evaluation of the effectiveness of heart failure (Freedland et al., 2021; Johansson et al., 2021). The main adverse reactions are gastrointestinal types. It is related to the application of aspirin, clopidogrel, and digoxin. The appearance of dry cough may be related to the use of hydrochlorothiazide. There was no difference in adverse reactions between the treatment and control groups, indicating that Qishen granules have good safety.

Study limitations

Patients with multiple types of ejection fractions were included in this study, and the study population was highly heterogeneous. Unfortunately, there was a lack of positive drug control. Only a comparison with placebo indicated that QSG granules effectively treated chronic heart failure, making it difficult to assess the drug's actual value in treating heart failure. In future studies, we will optimize the composition and dosage of QSG granules, using qiliqiangxin capsules as a controlled drug, and evaluate the efficacy of QSG granules in treating HFrEF.

Conclusion

Based on conventional treatment, the randomized, placebo-controlled trial demonstrates the benefits of QSG on the levels of NT-proBNP, symptoms, heart function, 6 MWD, and quality of life for all heart failure patients. Our data suggest that QSG could be used in combination therapy for CHF.

Data availability statement

The raw data supporting the conclusion of this article will be made available by the authors, without undue reservation.

Ethics statement

The studies involving human participants were reviewed and approved by the Ethics Committee of Beijing University of TCM (No. 2017BZHYLL0101), China-Japan Friendship Hospital (No. 2016-112) and Hubei Provincial Hospital of Traditional Chinese Medicine (No. HBZY22019-C47-01). The patients/participants provided their written informed consent to participate in this study.

Author contributions

KD and JL contributed equally to this research. WW proposed the project notion. KD, JL, NT, XH, HZ, and JW conducted the research. KD and JL analyzed data and wrote the manuscript. All participants discussed and approved the final manuscript.

Funding

This study was supported by National Natural Science Foundation of China (No. 81973697), the Beijing University of Chinese Medicine, Research and Development Fund Project (2016-ZXFZJJ-003), National Key R&D Program (2017YFC1700102), and Jiangsu Provincial Double-Innovation Doctor Program (JSSCBS20211613).

Acknowledgments

The authors would like to thank all the patients who participated in this study. The authors thank colleagues who contributed to the design of the study protocol.

Conflict of interest

The authors declare that the research was conducted in the absence of any commercial or financial relationships that could be construed as a potential conflict of interest.

Publisher's note

All claims expressed in this article are solely those of the authors and do not necessarily represent those of their affiliated organizations, or those of the publisher, the editors and the reviewers. Any product that may be evaluated in this article, or claim that may be made by its manufacturer, is not guaranteed or endorsed by the publisher.

References

Chang, H., Wang, Y., Li, C., Huo, K., and Wang, W. (2018). Mechanism of inhibition of apoptosis in H9C2 cardiomyocytes by yixin detoxification formula. *J. Beijing Univ. Traditional Chin. Med.* 41 (01), 25–30.

Chen, X., Li, Y., Li, J., Liu, T., Jiang, Q., Hong, Y., et al. (2021). Qishen granule (QSG) exerts cardioprotective effects by inhibiting NLRP3 inflammasome and pyroptosis in myocardial infarction rats. *J. Ethnopharmacol.* 285, 114841. doi:10.1016/j.jep.2021.114841

Dokainish, H., Teo, K., Zhu, J., Roy, A., AlHabib, K. F., ElSayed, A., et al. (2017). Global mortality variations in patients with heart failure: Results from the international congestive heart failure (INTER-CHF) prospective cohort study. *Lancet Glob. Health* 5 (7), e665–e672. doi:10.1016/S2214-109X(17)30196-1

Expert Consensus on standardized echocardiography in Chinese adults with heart failure. *Chin. J. Circulation*. 2019;34(05):422–436.

Farnsworth, C. W., Bailey, A. L., Jaffe, A. S., and Scott, M. G. (2018). Diagnostic concordance between NT-proBNP and BNP for suspected heart failure. *Clin. Biochem.* 59, 50–55. doi:10.1016/j.clinbiochem.2018.07.002

Freedland, K. E., Rich, M. W., and Carney, R. M. (2021). Improving quality of life in heart failure. *Curr. Cardiol. Rep.* 23 (11), 159. doi:10.1007/s11886-021-01588-y

Groenewegen, A., Rutten, F. H., Mosterd, A., and Hoes, A. W. (2020). Epidemiology of heart failure. *Eur. J. Heart Fail* 22 (8), 1342–1356. doi:10.1002/ejhf.1858

Guo, L., Guo, X., Chang, Y., Yang, J., Zhang, L., Li, T., et al. (2016). Prevalence and risk factors of heart failure with preserved ejection fraction: A population-based study in northeast China. *Int. J. Environ. Res. Public Health* 13 (8), 770. doi:10.3390/ijerph13080770

Heidenreich, P. A., Bozkurt, B., Aguilar, D., Allen, L. A., Byun, J. J., Colvin, M. M., et al. (2022). AHA/ACC/HFSA guideline for the management of heart failure: A report of the American college of cardiology/American heart association joint committee on clinical practice guidelines. *Circulation* 145 (18), e1033. doi:10.1161/CIR.0000000000001063

Johansson, I., Joseph, P., Balasubramanian, K., McMurray, J. J. V., Lund, L. H., Ezekowitz, J. A., et al. (2021). Health-related quality of life and mortality in heart failure: The global congestive heart failure study of 23 000 patients from 40 countries. *Circulation* 143 (22), 2129–2142. doi:10.1161/CIRCULATIONAHA.120.050850

Li, X., Zhang, J., Huang, J., Ma, A., Yang, J., Li, W., et al. (2013). A multicenter, randomized, double-blind, parallel-group, placebo-controlled study of the effects of qili qiangxin capsules in patients with chronic heart failure. *J. Am. Coll. Cardiol.* 62 (12), 1065–1072. doi:10.1016/j.jacc.2013.05.035

Najbjerg, A. G., Bruhn, L. V., Sandbaek, A., and Hornung, N. (2019). NT-proBNP to exclude heart failure in primary care - a pragmatic, cluster-randomized study. *Scand. J. Clin. Lab. Invest.* 79 (5), 334–340. doi:10.1080/00365513.2019.1622034

Qiu, Q., Wang, Y., Yang, K., Li, C., Shu, W., Si, W., et al. (2014). Effect of yixin detoxification formula on the symptomatology of ameroid narrowing ring-induced qi deficiency and blood stasis in small pigs. *Chin. J. Basic Chin. Med.* 20 (05), 589–592.

Wang, J., Shi, J., Wei, J., Wang, J., Gao, K., Li, X., et al. (2017). Safety and efficacy of qishen granules in patients with chronic heart failure: Study protocol for a randomized controlled trial. *Trials* 18 (1), 468. doi:10.1186/s13063-017-2193-z

Wang, W., Liu, J., Yang, S., Gong, M., Xu, Z., Wang, J., et al. (2021). Exploring the relationship between "toxicity" and chronic heart failure. *J. Chin. Med.* 36 (06), 1143–1146.

Xuanchao, Feng, Guo, Shuzhen, Lian, Hongjian, and Wang, Wei (2015). Effects of Yixin Detoxification Formula on NOX2 and NOX4 in myocardial tissue of rats with heart failure due to Qi deficiency and blood stasis. *Chin. J. Traditional Chin. Med.* 30 (07), 2535–2538.

Yang, X., Wang, Q., Zeng, Z., Zhang, Q., Liu, F., Chang, H., et al. (2020). The protective effect of qishen granule on heart failure after myocardial infarction through regulation of calcium homeostasis. *Evid. Based Complement. Altern. Med.* 2020, 1868974. doi:10.1155/2020/1868974

Yuan, T., Xian, S., Yang, Z., Wang, Z., Li, X., Wang, L., et al. (2014). Preliminary investigation of the theoretical basis of "poison" evil causing chronic heart failure. *Chin. J. Traditional Chin. Med.* 29 (06), 1785–1790.

Zeng, Z., Zhang, H., Ren, Y., Jiao, S., and Wang, W. (2018). Study on the mechanism of intervention of Astragalus granules in heart failure rats based on the regulation of oxidative stress. *World TCM* 13 (05), 1229–1232.

Zhang, J., and Zhang, Y. (2014). Chinese guidelines for diagnosing and treating heart failure 2014. *Chin. J. Cardiovasc. Dis.* 42 (02), 98–122.

Zhang, Q., Shi, J., Guo, D., Wang, Q., Yang, X., Lu, W., et al. (2020). Qishen Granule alleviates endoplasmic reticulum stress-induced myocardial apoptosis through IRE-1-CRYAB pathway in myocardial ischemia. *J. Ethnopharmacol.* 252, 112573. doi:10.1016/j.jep.2020.112573

frontiers | Frontiers in Pharmacology

TYPE Review
PUBLISHED 17 January 2023
DOI 10.3389/fphar.2023.1082817

Check for updates

OPEN ACCESS

EDITED BY
Jian Zhang,
Tianjin Medical University, China

REVIEWED BY
Yuanli Chen,
Hefei University of Technology, China
Shiyu Song,
Nanjing University, China
Chuanbin Liu,
People's Liberation Army General Hospital, China

*CORRESPONDENCE
Min Wu,
wumin19762000@126.com

SPECIALTY SECTION
This article was submitted to Ethnopharmacology, a section of the journal Frontiers in Pharmacology

RECEIVED 28 October 2022
ACCEPTED 06 January 2023
PUBLISHED 17 January 2023

CITATION
Li Y, Yang S, Jin X, Li D, Lu J, Wang X and Wu M (2023), Mitochondria as novel mediators linking gut microbiota to atherosclerosis that is ameliorated by herbal medicine: A review. *Front. Pharmacol.* 14:1082817. doi: 10.3389/fphar.2023.1082817

COPYRIGHT
© 2023 Li, Yang, Jin, Li, Lu, Wang and Wu. This is an open-access article distributed under the terms of the Creative Commons Attribution License (CC BY). The use, distribution or reproduction in other forums is permitted, provided the original author(s) and the copyright owner(s) are credited and that the original publication in this journal is cited, in accordance with accepted academic practice. No use, distribution or reproduction is permitted which does not comply with these terms.

Mitochondria as novel mediators linking gut microbiota to atherosclerosis that is ameliorated by herbal medicine: A review

Yujuan Li[1], Shengjie Yang[1], Xiao Jin[1], Dan Li[1], Jing Lu[1,2], Xinyue Wang[1] and Min Wu[1]*

[1]Guang'an Men Hospital, China Academy of Chinese Medical Sciences, Beijing, China, [2]Beijing University of Chinese Medicine, Beijing, China

Atherosclerosis (AS) is the main cause of cardiovascular disease (CVD) and is characterized by endothelial damage, lipid deposition, and chronic inflammation. Gut microbiota plays an important role in the occurrence and development of AS by regulating host metabolism and immunity. As human mitochondria evolved from primordial bacteria have homologous characteristics, they are attacked by microbial pathogens as target organelles, thus contributing to energy metabolism disorders, oxidative stress, and apoptosis. Therefore, mitochondria may be a key mediator of intestinal microbiota disorders and AS aggravation. Microbial metabolites, such as short-chain fatty acids, trimethylamine, hydrogen sulfide, and bile acids, also affect mitochondrial function, including mtDNA mutation, oxidative stress, and mitophagy, promoting low-grade inflammation. This further damages cellular homeostasis and the balance of innate immunity, aggravating AS. Herbal medicines and their monomers can effectively ameliorate the intestinal flora and their metabolites, improve mitochondrial function, and inhibit atherosclerotic plaques. This review focuses on the interaction between gut microbiota and mitochondria in AS and explores a therapeutic strategy for restoring mitochondrial function and intestinal microbiota disorders using herbal medicines, aiming to provide new insights for the prevention and treatment of AS.

KEYWORDS

atherosclerosis, mitochondria, gut microbiota, metabolism, herbal medicine

1 Introduction

Atherosclerosis (AS) is an inflammatory disease characterized by endothelial cell damage, lipid deposition, and smooth muscle cell proliferation. It is one of the leading causes of cardiovascular disease (CVD) and is responsible for morbidity and mortality worldwide (Cai et al., 2020; Dagenais et al., 2020). Recent studies have focused on the intestinal flora and mitochondrial dysfunction as risk factors for AS (Witkowski et al., 2020). In the distal gastrointestinal tract, gut flora plays an important role in host physiology by establishing bacterial–host symbiosis, whereas its imbalance regulates host inflammation and metabolic and immune disorders, triggering the development of AS (Barrington and Lusis, 2017; Jonsson and Bäckhed, 2017). Moreover, bacterial translocation and metabolites entering circulation aggravate atherosclerotic plaque severity by directly invading arteries, increasing lipid deposition and insulin resistance, and activating the innate immune system (Witkowski et al., 2020). The predominant intestinal flora metabolites include short-chain fatty acids (SCFAs), trimethylamine (TMA), amino acids and their derivatives, secondary bile acids, and vitamins, all of which are associated with AS (Koeth et al., 2013). Although the mechanism and relationship

between the gut flora and AS are complex, mitochondria could be an intermediate link, which might explain why AS occurs locally. As the center of cellular aerobic respiration, mitochondria synthesize 90% adenosine triphosphate (ATP) to provide the energy required by cells (Rossmann et al., 2021). Owing to an endosymbiotic relationship with ancient proteobacteria (Roger et al., 2017), mitochondria are also responsible for the signal transduction of innate immunity, oxidative stress, and cell death (Forrester et al., 2018). Thus, mitochondria are often targeted for bacterial attack and show functional abnormalities, including mitochondrial reactive oxygen species (mtROS)-induced oxidative stress, mitochondrial DNA (mtDNA) mutation and release, and imbalance of mitochondrial dynamics, further contributing to arterial wall cell damage, inflammation, and AS (Yu and Bennett, 2014; Oliveira and Vercesi, 2020).

Current treatments for AS mainly aim at improving known risk factors. Despite significant developments in disease control and prevention, there is no clear, effective treatment for these novel mechanisms (Pursnani et al., 2017; Lawton et al., 2022). Herbal medicines have been widely used to treat AS, and a possible therapeutic target is to regulate gut microbiota homeostasis, which is regarded as prebiotics (Anlu et al., 2019). Herbal medicines and their natural compounds can effectively improve mitochondrial function to protect vascular cell homeostasis and survival (Zhou et al., 2022). In this review, we discussed the emerging mechanisms of mitochondria as the key mediator linking gut microbiota to AS and systematically reviewed the role of herbal medicine and their natural compounds in improving AS through the microbiota–mitochondrial axis.

2 Vital role of mitochondria in AS

2.1 Mitochondrial dysfunction

During AS progression, mitochondrial dysfunction is associated with progressive deleterious changes, including 1) the accumulation of mtDNA mutations, 2) excessive production of mtROS and diminished antioxidant defense, leading to increased oxidative damage, and 3) mitophagy inhibition, leading to a decline in mitochondrial renewal.

2.1.1 mtDNA mutation

The genetic mechanisms of atherogenesis depend on the nuclear and mitochondrial genomes. In contrast, mtDNA is more vulnerable to damage from mtROS owing to its lack of introns and histones, leaving DNA exposed, and lack of DNA polymerase, leading to a high error rate and poor stability during mtDNA replication proximate to the site of ROS production (Valente et al., 2016; Stewart and Chinnery, 2021). mtDNA encodes protein subunits necessary for oxidative phosphorylation (Fontana and Gahlon, 2020), resulting in abnormal complex expression, subsequently leading to the generation of excessive mtROS vicious cycle between mtDNA mutation and mtROS (Yang et al., 2020). The other accepted reason for the occurrence of mtDNA mutations is replication errors resulting from *de novo* events and clonal expansion, and the two have an additive effect and are detrimental to overall health (Ross et al., 2014). Many somatic mtDNA mutations originate from early adulthood to clonally expand preexisting mutations (Greaves et al., 2014) and increase dramatically with age through spontaneous replication errors of mtDNA polymerase γ (Pol γ), accelerate mtDNA turnover, and direct repeats (Khrapko, 2011). The frequency of *de novo* mtDNA mutation is elevated in mouse female germ cells, being associated with age and parity or sexual maturity (Arbeithuber et al., 2020). All of these factors lead to a high mutation rate and heteroplasmy of mtDNA.

mtDNA mutations occur in the local disturbance of plaques (Sazonova et al., 2015), and the number of mtDNA mutations in the arterial wall cells increases as the lesions become more severe (Ballinger et al., 2002). mtDNA mutations, such as m.1555A>G, m.14459G>A, m.12315G>A, and m.13513G>A occur in plasma leukocytes or aortic plaques, (Sazonova et al., 2015; Sazonova et al., 2017), which may uncouple oxidative phosphorylation (OXPHOS), inactivate ATP synthase, and enhance the basal rate of oxygen consumption (Gilkerson et al., 2012; Orekhov et al., 2020b). High levels of mtDNA^{4977} deletion are independent risk factors for adverse cardiovascular events and cause mortality in patients with stable coronary heart disease (CHD) (Vecoli et al., 2018; Vecoli et al., 2019). In three cohort studies, mtDNA copy number (mtDNA-CN), which reflects normal mtDNA expression, is negatively correlated with CHD (Ashar et al., 2017; Zhang Y et al., 2017). PolG$^{-/-}$/ApoE$^{-/-}$ mice lacking mtDNA polymerase γ exhibit extensive mtDNA damage, OXPHOS defects, and severe AS (Yu et al., 2013). ApoE$^{-/-}$ mice overexpressing the mitochondrial helicase Twinkle (Tw^{+}/ApoE$^{-/-}$) showed increased mtDNA-CN, respiratory complex abundance and respiration, decreased plaque necrotic core, and increased fibrous cap area (Yu et al., 2017). mtDNA mutation contribute to induction of proton leakage, transmembrane potential loss, reduced mitochondrial Ca^{2+} uptake (Granatiero et al., 2016), and activation of the adenosine monophosphate-activated protein kinase (AMPK) signaling pathway (Orekhov et al., 2020b), promoting arterial wall cell apoptosis and vascular inflammation. Consequently, mtDNA mutations contribute significantly to AS and CHD by disrupting the intracellular environment.

2.1.2 Excessive production of mtROS

Mitochondrial complexes are the main producers of mtROS (Yin et al., 2021), and the excessive production of mtROS and inhibition of antioxidase cause an imbalance in redox reactions (Springo et al., 2015), which promotes mtDNA mutations (Fontana and Gahlon, 2020), aggravates NF-κB activation (Csiszar et al., 2014), excites NAD(P)H oxidase (NOX) in the cytoplasm (Canugovi et al., 2019), and develops vascular oxidative stress and inflammation. Cho et al. (Cho et al., 2013) determined that mtROS significantly increased and augmented superoxide dismutase 2 (SOD2) ubiquitination in coronary endothelial cells (ECs) from type 2 diabetic mice, leading to abnormal vascular relaxation and EC damage. mtROS attenuates nitric oxide (NO) bioavailability, impairs endothelium-dependent dilation, and uncouples nitric oxide synthase (eNOS), contributing to vasodilation inhibition (Robert et al., 2021). Apoe$^{-/-}$/SOD2$^{+/-}$ mice treated with MitoTEMPO targeting mtROS showed reduced smooth muscle cell apoptosis, necrotic core expansion, and matrix degradation to stabilize plaques (Vendrov et al., 2017). Mitochondria-derived H_2O_2 induces NF-κB activation in aged endothelial cells, which elevates low-grade vascular inflammation, such as increased levels of proinflammatory cytokines and adhesion molecules (Li Z et al., 2021). Mitochondrial H_2O_2 also induces endothelial-to-mesenchymal transition (EndoMT) *via* the p38 MAPK or NF-κB signaling pathways to cause vascular dysfunction and AS (Ko et al., 2019; Xu et al., 2020). EndoMT is a dynamic process that loses characteristic endothelial tight junctions and markers, including CD31, VE-cadherin, and

eNOS, and acquires the mesenchymal phenotype (Xu et al., 2020). Administration of natural compounds, such as Baicalein (Shi R et al., 2018) and schizandrin B (You et al., 2019), attenuates EndoMT by suppressing the NF-κB pathway. Mitochondria-targeted antioxidants, including mitoquinone (MitoQ), MitoTEMPO, and coenzyme Q 10 (CoQ10) effectively ameliorate AS (Rossman et al., 2018). MitoQ intervention inhibits nitrotyrosine concentration and improves mitochondrial and endothelial functions (Braakhuis et al., 2018). MitoQ also decreases aortic stiffness in old mice by weakening the aortic pulse wave velocity and restoring the elastin region elastic modulus and elastin expression (Gioscia-Ryan et al., 2018). CoQ10 treatment of AS attenuates mtROS generation and activates the AMPK–YAP–OPA1 pathway to improve mitochondrial function (Xie et al., 2020). Therefore, mitochondria-derived ROS are key risk factors for cell damage, inflammation, and AS. Decreased mtROS production effectively mitigates atherosclerotic lesions.

2.1.3 Inhibition of mitophagy

Mitophagy is a selective type of autophagy that acts by removing unnecessary or aberrant mitochondria and its harmful metabolites, such as mtROS, ensuring mitochondrial quality control and stabilizing cell homeostasis (Kubli and Gustafsson, 2012). Autophagy can be divided into ubiquitin-dependent mitophagy and receptor-regulated mitophagy (Song et al., 2021). Mitophagy is inhibited in plaque lesions. Under high-glucose conditions, putative kinase 1 (PINK)/Parkin acetylation is defective in aortas regulated by sirtuin 3 (SIRT3) or uncoupling protein 2 (UCP2) (Wei et al., 2017), triggering impaired endothelial cells and aggravating AS by excessive mtROS, loss of mitochondrial membrane potential (MMP), and ATP reduction (Zhu W et al., 2018; Forte et al., 2021). Deficiencies in PINK1 or Parkin proteins result in vascular smooth muscle cell (VSMC) apoptosis by inhibiting mitophagy (Swiader et al., 2016) and increasing the occurrence of myocardial infarction by the accumulation of swollen and dysfunctional mitochondria (Kubli et al., 2013). Activation of the PINK1/Parkin pathway maintains mitochondrial integrity and avoids damage to the endothelial cells of obese mice (Wu W et al., 2015), leading to reduced apoptosis by mitigating B Cell lymphoma-associated X (BAX). Apolipoprotein A–I binding protein (AIBP) located at the inner mitochondrial membrane (IMM) is expressed in human and mouse atherosclerotic plaques (Choi et al., 2021). AIBP regulates PINK/parkin-related mitophagy and stimulates mitofusin 1 (MFN1) and MFN2 ubiquitination, improving mitophagy and fission to prevent further cell damage in AS. Therefore, enhanced mitophagy is beneficial for diminishing apoptosis, restoring endothelial function, and protecting the vasculature from sclerosis. In conclusion, the effects of mitochondrial dysfunction on AS have gradually become a focus of research. Injury to mtDNA, mtROS, and mitophagy are all involved in inflammation, disruption of cell homeostasis, and the development of AS.

2.2 Mitochondrial regulation of innate immunity and inflammation

Mitochondria are mostly known for immunity, inflammation, and apoptosis. For example, mitochondrial energy supply depends on the tricarboxylic acid cycle, and its disruption generates metabolites involved in the inflammatory response and modulates the innate immune response in immune cells (Banoth and Cassel, 2018). Downregulation of isocitrate dehydrogenase leads to the conversion of citrate to itaconate (Lampropoulou et al., 2016), which has direct antimicrobial characteristics that stimulate the innate immune response and enhance the proinflammatory properties of M1 (Peace and O'Neill, 2022). Succinate is also proinflammatory and induces mtROS production and IL-1β expression (Banoth and Cassel, 2018).

2.2.1 Mitochondrial damage-associated molecular patterns

As mitochondria evolved from ancient eubacteria, mtDNA contains hypomethylated cytosine-phosphate-guanine sequences similar to those in bacterial DNA (Fang et al., 2016). In addition to mtDNA, mitochondria-derived DAMPs (mtDAMPs) also include other mitochondrial metabolites, such as mtROS, phospholipid cardiolipin, and formyl peptides, which can be recognized as pathogens, elicit inflammation, and induce an innate immune response (Zhang et al., 2010). They are released from impaired mitochondria and activate formyl peptide receptor or pattern recognition proteins (PRPs), which respond to multiple inflammatory signaling pathways, including the nod-like receptor family pyrin domain containing 3 (NLRP3) inflammasome, NF-κB activation, and stimulator of interferon genes (STING) pathways (Misawa et al., 2017). Therefore, mitochondria are crucial elements in sterile inflammation, leading to chronic inflammation in AS.

Mitochondrial permeability transition pores (mPTP) and voltage-dependent anion channel (VDAC) oligomers are responsible for mtDAMP release (Sprenger et al., 2021; Picca et al., 2022). mPTP opening occurs in cells subjected to disrupted calcium levels or oxidative stress (Kim et al., 2019). Binding of mtDNA with charged residues in the N-terminal domain of VDAC1 facilitates VDAC1 oligomerization, which is instrumental in the release of mtDNA fragments over the outer membrane and increases outer membrane permeabilization mediated by BAX and B Cell lymphoma antagonist/killer (BAK) (McArthur et al., 2018). In addition to releasing large molecules from the mitochondria, VDAC also affects ROS production. When VDAC is inhibited by hexokinase, mtROS expression and NLRP3 activation are downregulated (Kim et al., 2019; Xian et al., 2022). Ultimately, mtDAMP, in the form of mitochondrial-derived extracellular vesicles, crosses the cytomembrane (Zhao et al., 2021).

2.2.2 mtDAMPs activate NLRP3 inflammasome

NLRP3 inflammasome is a protein complex of the NLR family. Activated NLRP3 is regulated by the adaptors of damaged mitochondria and endoplasmic reticulum (ER), further inducing caspase-1 expression and promoting interleukin (IL)-1β and IL-18 secretion, further causing inflammation and pyroptosis (Zhou et al., 2011; Song et al., 2020), which can be demonstrated by the colocalization of mitochondria with NLRP3–ASC–caspase–1 (Mohanty et al., 2019). Oxidative stress is a proinflammatory characteristic of impaired mitochondria (Heid et al., 2013). Oxidized mtDNA and mtROS interact with NLRP3 on being released into the cytoplasm (Xian et al., 2022). Depletion of mtDNA using ethidium bromide or knockout of mitochondrial transcription factor A (TFAM) suppresses NLRP3 activation and IL-1β expression (Salnikova et al., 2021).

Mitochondria also provide other key signals to recruit and activate the NLRP3 inflammasome, including translocation of cardiolipin,

mitochondrial antiviral signaling proteins (MAVS), and cytosolic potassium ion (K^+) efflux (Bird, 2012). Cardiolipin plays a key role in triggering NLRP3 owing to its role as a relic of the prokaryotic cell membrane (Iyer et al., 2013). Cardiolipin is located in the IMM and is transferred to the outer mitochondrial membrane (OMM) after depolarization to recruit NLRP3 (Gkikas et al., 2018). After knockout of cardiolipin synthase to inhibit cardiolipin, the NLRP3 inflammasome is effectively downregulated, and the inflammatory response is attenuated, indicating that cardiolipin triggers NLRP3 (Toksoy et al., 2017). MAVS, located in the OMM, is a critical signal for antiviral infection. MAVS is also involved in NLRP3 activation (Subramanian et al., 2013). Specifically, it recruits NLRP3 to the OMM and mediates its oligomerization and activation by targeting mtROS (Park et al., 2013). MAVS is a key sensor of mtROS, contributing to the production of type I interferon (IFN) and activation of caspase-1, and is responsible for host immunity and inflammation (Buskiewicz et al., 2016). Furthermore, ATP and K^+ efflux are regarded as two key NLRP3 activators caused by impaired mitochondria and induce Ca^{2+} influx and direct damage to mitochondrial Ca^{2+} homeostasis (Yaron et al., 2015; Katsnelson et al., 2016), further affecting Krebs cycle enzyme activity, leading to a loss of MMP and mitochondrial network fragmentation (Hawkins et al., 2007; Liu et al., 2018). Mitochondrial Ca^{2+} homeostasis plays a crucial role in plaque calcification and unstable lesions in AS (Forrester et al., 2018).

Mitophagy mediates innate immunity and prevents hyperstimulation of NLRP3 and superfluous inflammation (Orekhov et al., 2020b). As defective mitophagy constantly emits inflammatory signals, cells cannot bear the ongoing stress and undergo apoptosis (Jin et al., 2022). Melatonin inhibits mtROS expression and suppresses NLRP3 inflammasome activation by enhancing mitophagy in lipopolysaccharide-treated (LPS)-treated macrophages, thereby preventing AS progression (Ma S et al., 2018). Accordingly, NLRP3 may be sensitive to mitochondrial dysfunction, explaining the correlation between mitochondrial dysfunction and chronic inflammatory diseases. Furthermore, NLRP3 exacerbates mitochondrial dysfunction. For example, caspase-1 induced by NLRP3 enhances mitochondrial membrane permeabilization and mtROS generation, and NLRP3 disturbs mitochondrial Ca^{2+} homeostasis (Yu et al., 2014). These suggest a positive feedback loop between NLRP3 and mitochondria (Orekhov et al., 2020a).

2.2.3 mtDAMPs induce other inflammatory pathways

Cyclic guanosine monophosphate–adenosine monophosphate synthase (cGAS) effectively senses and recognizes viral and bacterial DNA in the cytoplasm. Released mtDNA is also an endogenous cGAS ligand that binds to cGAS and catalyzes the generation of cyclic guanosine monophosphate–adenosine monophosphate (cGAMP) (Chowdhury et al., 2022). cGAMP is a secondary messenger that recruits STING (Yu et al., 2020), which stimulates tank-binding kinase in perinuclear endosomes to mediate the phosphorylation of the transcription factor interferon regulatory factor 3 (IRF-3) and transposition into the nucleus (West et al., 2015), promoting type I and III IFN responses and interferon-stimulated gene activation (Puhm et al., 2019). cGAMP expression is elevated in the arteries of $ApoE^{-/-}$ mice, stimulating the accumulation of lipids and macrophages and the secretion of inflammatory cytokines (Pham et al., 2021). However, STING deficiency prevents the progression of atherosclerotic plaques by inhibiting inflammation (Pham et al., 2021). Thus, the cGAS–STING pathway enhances vascular inflammation induced by mtDNA to aggravate AS.

Mitochondria engage in antimicrobial processes of toll-like receptor (TLR) signaling cascades. Activated TLR send signals to the mitochondria by translocating tumor necrosis factor receptor associated factor 6 (TRAF6) and ubiquitinate the evolutionarily conserved mitochondrial signaling intermediate in toll pathways (ECSIT) to stimulate mtROS production and move mitochondria to phagosomes, enhancing antimicrobial activity (West et al., 2011). Depletion of ECSIT and TRAF6 decreases the expression of mtROS and attenuates antimicrobial ability (Banoth and Cassel, 2018). TLR9 is an innate immune receptor that recognizes CpG motifs in bacterial or viral DNA and releases mtDNA (Hotz et al., 2018). Extracellular mtDNA triggers NF-κB nuclearization, induces proinflammatory cytokines, augments type I IFN responses, and provokes a sterile systemic inflammatory response syndrome mediated by TLR9 activation (Zhang et al., 2014; Bliksøen et al., 2016). Circulating oxidative mtDNA triggers TLR9 activation and upregulates proinflammatory cytokines in macrophages of $ApoE^{-/-}$ mice undergoing e-cigarette intervention, which leads to AS. Inhibition of the inflammatory cascade depends on normal mitophagy (Li J et al., 2021). Mitophagy is suppressed *via* PINK degradation, promoting macrophage polarization of the proinflammatory phenotype M1 and the development of AS (Hung et al., 2021). Consequently, TLRs are recognized and stimulated by mitochondria-derived DAMPs, such as mtDNA, and further trigger amplification of the inflammatory cascade to exacerbate AS progression.

2.3 Mitochondrial regulation in vascular cells

Various cells play different roles in AS progression, including barrier protection function of ECs, vasoconstriction and remodeling function of VSMCs, phagocytosis of lipids and immune function in macrophages, with mitochondria participating in all.

2.3.1 Cholesterol metabolism in macrophages

Mitochondria play a crucial role in lipid metabolism during AS progression. Modified low-density lipoprotein (LDL) is phagocytosed by macrophages and focally stimulates vascular innate immunity, where the mitochondria-associated immune barrier is compromised, contributing to lipid deposition, accumulation of proinflammatory mediators, and transformation of lipid-rich foam cells (Duan et al., 2022). In ECs, intervention with oxidized LDL (ox-LDL) causes mtROS significantly increase, reduction in complex I and III enzyme activity, mPTP opening, cytosolic Ca^{2+} influx, promoting mitochondrial damage and cell apoptosis, triggering vascular inflammation, and the occurrence of AS (Orekhov et al., 2020b). Mitochondrial respiratory dysfunction negatively influences cholesterol efflux in macrophages. Reverse cholesterol transport (RCT) is mediated by ATP-binding cassette cholesterol transporter proteins (ABCA1) and apolipoprotein A–I (ApoAI) in macrophages, leading to the accumulation of cholesterol and an increase in foam cells (Dumont et al., 2021; Dorighello et al., 2022). ATP is the energy provider for ABCA1-dependent cholesterol efflux. miR-33 also controls cholesterol efflux by limiting ATP production (Karunakaran et al., 2015).

Excessive accumulation of cholesterol stimulates mPTP to open and enter the mitochondria, subsequently generating multiple oxysterols *via* CYP27A1 (a cytochrome p450 oxidase), such as 25- and 27-hydroxycholesterol (25-/27-OH) in the mitochondria, and constantly esterifies oxysterol in atherosclerotic plaques (Korytowski et al., 2015). Cholesterol oxides inhibit ABCA1 and ABCG1 expression and diminish 27-OH efflux inside the mitochondria of macrophages, leading to RCT impairment and peroxidation damage in the mitochondria (Karunakaran et al., 2015). AIBP binds to ApoAI and induces mitophagy and NADPH, whereas a deficiency in AIBP leads to the accumulation of damaged mitochondria and polarization in M1 macrophages to promote inflammation. Furthermore, interventions targeting the mitochondria can recover cholesterol trafficking in AS. Mitochondrial antioxidant Mito-Tempol attenuates cholesteryl accumulation by activating ABCA1 expression to export cholesterol (Ma Y et al., 2018). Pravastatin is involved in mitochondrial fusion and the formation of mitochondria-associated membranes to strengthen the correlation between mitochondria and the ER, further decreasing foam cell generation in a high-lipid environment (Assis et al., 2022). Therefore, recovering mitochondrial respiratory function and providing efficient energy ameliorates cholesterol trafficking, decreases foam cell numbers, and reverses AS progression.

2.3.2 VSMC proliferation, migration, and phenotype switching

VSMC proliferation, migration, and phenotype switching are critical features of AS and contribute to intimal hyperplasia and restenosis in the arteries. VSMC exhibit a contractile phenotype that modulates vascular dilation and contraction under physiological conditions. After vascular injury from various stresses, VSMC convert to a synthetic phenotype, minimizing contractile function and migrating and proliferating from the medial layer to the arterial lumen (Chen et al., 2022). VSMC phenotype switching is closely associated with mitochondrial functions, including fission, oxidative stress, mitophagy, and Ca^{2+} influx. Mitochondrial fission regulates the quantity and quality of mitochondria in cells and is mediated by dynamin-related GTPases, such as dynamin-related protein 1 (Drp1) (Maimaitijiang et al., 2016). Drp1 activated by AngII, PGDF-BB, or H_2O promotes VSMC proliferation by accelerating the cell cycle, whereas mitochondrial division inhibitor-1 (Mdivi-1) stops the cell cycle at the G0 (quiescent)/G1 (long growth) phase by inhibiting Drp1 (Lim et al., 2015), attenuating VSMC proliferation and migration (Zhang X et al., 2018). High glucose induces mitochondrial fragmentation, leading to mtROS production, oxidative stress, and VSMC proliferation, which was reversed by reducing Drp1 expression *via* Mdivi (Maimaitijiang et al., 2016) or H_2S (Sun et al., 2016). Meanwhile, knockdown of the dominant-negative mutant Drp1-K38A or Drp1 also inhibits PDGF-induced mitochondrial fission and mtROS levels, resulting in the suppression of VSMC migration. Mitochondrial Ca^{2+} uptake by activating Ca^{2+}-dependent kinase II and mitochondrial Ca^{2+} uniporter also affects mitochondrial translocation to the leading edge of migrating VSMC (Nguyen et al., 2018). Apelin-13 triggers mitochondrial Ca^{2+} influx and facilitates mtROS expression and mitophagy mediated by the PINK1/Parkin pathway, leading to the proliferation of VSMCs, whereas using mito-TEMPO, Mdivi-1, siRNA-PINK1, or siRNA-Parkin can ameliorate VSMC proliferation (Chen et al., 2022). Thus, VSMC proliferation and migration are mediated by excessive mitochondrial fission, mtROS, Ca^{2+} influx, and mitophagy, which aggravate vascular intimal remodeling and AS progression.

2.3.3 Cell death

Mitochondria are strongly associated with programmed cell death, and their related mechanisms include apoptosis and pyroptosis (Bock and Tait, 2020), which is a cascade of amplified inflammatory reactions mediated by caspase-1 and inflammasome (Yu et al., 2014). Mitochondria are crucial promoters of inflammasome activation and pyroptosis, and the inhibition of mitophagy exacerbates pyroptosis. NIP3-like protein X (NIX) engages in mitophagy with microtubule-associated protein 1 light chain 3 (LC3) (Peng et al., 2020), suppresses mtROS and NLRP3 expression, inhibits caspase-1 and IL-1β activation, and induces macrophage pyroptosis in AS progression (Peng et al., 2022; Tian et al., 2022).

The main mechanism of apoptosis is the enhancement of OMM permeabilization mediated by the accumulation of Ca^{2+} and activation of the proapoptotic proteins BAX and BAK (Jeong and Seol, 2008). BAX and BAK oligomerize at the OMM and for a transmembrane pore, resulting in mPTP opening, loss of MMP, and release of mitochondrial intermembrane space proteins, such as cytochrome c, apoptosis-inducing factor, and endonuclease G (Schellenberg et al., 2013). Water moves into the mitochondrial matrix *via* the opening of the mPTP, causing mitochondrial matrix swelling and OMM rupture, releasing more intermembrane space proteins into the cytoplasm and inducing apoptosis (Han et al., 2019; Liang et al., 2022). After exporting into the cytosol, cytochrome C combines with apoptotic protease-activating factor-1 and procaspase-9, composing the apoptosome structure and initiating an irreversible apoptosis cascade (Zhao Y et al., 2020). Furthermore, nitrosylation of Drp1 regulates fission and triggers the release of proapoptotic factors into the cytoplasm (Kleele et al., 2021; Jenner et al., 2022). Expression of the fusion protein optic atrophy protein 1(OPA1) suppresses apoptosis by limiting cristae remodeling, and OPA1 knockout exacerbates VSMC apoptosis and aggravates AS (Peng et al., 2020). Therefore, owing to their unique structure and function, mitochondria are responsible for the activity and death of vascular cells through the regulation of inflammation, permeability, dynamics, and activation of proapoptotic cytokines (Figure 1). However, the gut microbiota and its metabolites may be potential predisposing factors for these results.

3 Gut microbiota disorders target mitochondria and are closely correlated with AS

There are 100 trillion microbes in the human gastrointestinal tract, including 1000 different bacterial species comprising five phyla: *Bacteroidetes, Firmicutes, Proteobacteria, Actinobacteria,* and *Verrucomicrobia*, collectively regarded as "gut microbiota" (Li et al., 2014; Yoo et al., 2022). Gut microbiota and host symbiotic interactions commonly form an intestinal microenvironment to digest indigestible substances and secrete biologically active metabolites, and together

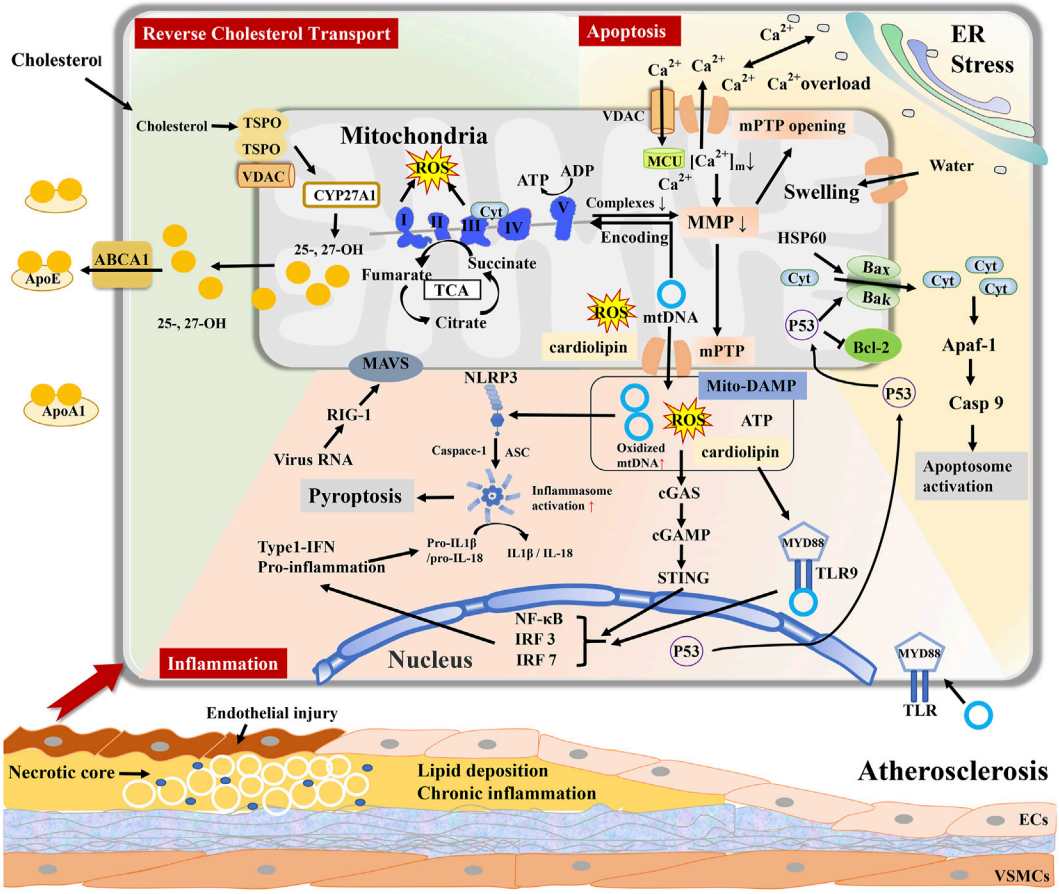

FIGURE 1
Mitochondria regulate reverse cholesterol transport (RCT), cell apoptosis, and inflammatory response during atherosclerosis. Excessive accumulation of cholesterol entry into mitochondria generate and esterify 25- and 27-hydroxycholesterol ((25-/27-OH)) by CYP27A1. Inhibition of ABCA1 results in RCT impairment and peroxidation damage in the mitochondria of macrophages. Mitochondria-DAMPs include mtDNA, mtROS, ATP, and cardiolipin, and export *via* mPTP. Mito-DAMPs are recognized as a pathogen to elicit inflammation, such as TLR9 signaling, cGAS–cGAMP–STING pathway, and inducing NLRP3 inflammasome to stimulate inflammatory cascade response. mPTP opening causes Ca^{2+} and cytochrome C (Cyt) efflux and mitochondrial swelling, leading to cellular apoptosis. Mitochondrial dysfunction contributes to lipid deposition, inflammation, and cellular apoptosis in the vascular wall, jointly promoting atherosclerosis progression.

maintain host energy metabolism, promote immune homeostasis, and sustain the normal function of distal organs (Gregory et al., 2015; Lian W S et al., 2022). When the intestinal flora and some of its metabolites, such as LPS, enter the bloodstream, they act as PAMP to bind to PRPs in host cells, activate immune cells, induce the production of inflammatory cytokines and chemokines necessary for protective immune responses, and present antigens to antigen-presenting cells in lymphoid tissues, resulting in systemic inflammation and excessive immune response (Verhaar et al., 2020). Meanwhile, the proliferation of opportunistic pathogens or facultative anaerobic bacteria in the intestinal tract causes gut dysbiosis and secretion of numerous abnormal metabolites, which facilitate host fat mass gain, insulin resistance, and various metabolic diseases such as obesity, diabetes, metabolic syndrome, and AS (Le Roy et al., 2022). An imbalance in the proportion of microbiota species is closely correlated with the host's age, dietary habits, emotional stress, and antibiotic application (Boulangé et al., 2016). Thus, the gut microbiota is not only a digestive apparatus but also a dynamic endocrine organ that regulates the physiological and pathological conditions of the host (Vezza et al., 2020).

3.1 Gut microbiota-mediated damage to mitochondria and AS

3.1.1 Flora translocation in the atherosclerotic plaque

Gut dysbiosis is strongly associated with AS and CVD, mainly through microbiota translocation into atherosclerotic plaques and microbial metabolites from the gut, which act on distal arteries to affect AS progression (Lindskog Jonsson et al., 2017). DNA from *Bacteroides forsythus, Prevotella intermedia, Porphyromonas gingivalis, genus Curvibacter,* and *Actinobacillus actinomycetem comitans* have been detected in human endarterectomy plaques (Koren et al., 2011; Ziganshina et al., 2016). *Burkholderiales* and *Propionibacterium* are the most abundant taxa in atherosclerotic plaques (Ziganshina et al., 2016). Several structural components of the gut microbiota directly stimulate the expression of proinflammatory cytokines and chemokines, such as LPS, peptidoglycan, flagellin, and bacterial DNA. These bacteria that invade arteries not only contribute to local infections and inflammation but also aggravate the total cholesterol and

fibrinogen levels to exacerbate atherosclerotic plaque ruptures (Brown and Hazen, 2018).

Gut bacterial abundance and diversity are altered in ApoE$^{-/-}$mice with AS, including decreased α-diversity (Kappel et al., 2020) and increased abundance of *Verrucomicrobia,* Bacteroidaceae*, Bacteroides, Akkermansia,* and *phylum Actinobacteria*, which positively correlate with serum cholesterol, triglycerides, and LDL levels, inducing TLR signaling and cytokine receptor interactions (Liu Q et al., 2020). Similar alterations in the gastrointestinal tract of human atherosclerotic patients have also been found, such as enrichment in *Collinsella* or *phylum Actinobacteria*, which increase gut permeability and triglyceride synthesis, recruit neutrophils, and trigger the NF-κB pathway (Chen J et al., 2016; Gomez-Arango et al., 2018). In contrast, probiotics are involved in multiple key processes of AS development by attenuating intestinal flora disorders and the risk of infection (Zhai et al., 2022). L*actobacillus strains,* such as *Lactobacillus rhamnosus JL1* (Yang et al., 2021), *Lactobacillus pentosus* (Huang et al., 2014), and *Lactobacillus acidophilus* (Michael et al., 2017), decrease total cholesterol, triglyceride, and LDL levels in mice fed a high-fat diet. *Lactobacillus cfermentum* effectively protects endothelial function and prevents oxidative stress by maintaining intestinal homeostasis and inhibiting eNOS uncoupling and NOX2 activation (Toral et al., 2018). Moreover, *Bifidobacterium* ameliorates inflammatory factors, such as TNF-α and IL-6, resulting in the reversal of AS progression (Primec et al., 2019; Zaharuddin et al., 2019).

3.1.2 Mitochondrial injury from gut microbiota

The correlation between the gut microbiota and mitochondria can be traced back to α-Proteobacteria as the origin of the mitochondria (Roger et al., 2017). Mitochondria have homologous characteristics with bacteria; therefore, bacterial and mitochondrial protein-targeting sequences exhibit similarities and close lineage, leading to mitochondria becoming a target for gut microbiota (Degli Esposti et al., 2014). Similar autophagic methods eliminate both mitochondria and bacterial membranes, whereas abnormal autophagy contributes to chronic inflammation by inducing cytokine and inflammasome expression in the host (Kalghatgi et al., 2013). Consequently, mitochondria-related innate immunity activation is an important target of the gut microbiota (Jackson and Theiss, 2020). *Clostridium difficile* toxin A triggers mtROS production and ATP dissipation, which are associated with upregulation of NF-κB and IL-8 (He et al., 2002). *Salmonella enterica* serovar *Typhimurium* stimulates macrophage activation and induces an innate immune response by releasing mtDNA into the cytosol to induce a type I IFN response and the cGAS–STING pathway (Xu L et al., 2022). During these processes, gut bacterial effector proteins transit to the mitochondrial subcompartments *via* complex import systems and are precisely located in the mitochondria by targeting the sequence domain (Mahmud et al., 2021). Specifically, bacterial effector proteins are recognized and translocated by the translocase of the OMM complex and transported to the OMM, mediated by the sorting and assembly machinery complex. The effector proteins are subsequently transferred into the IMM and matrix by the translocase of the inner membrane 22 (TIM22) and TIM23 complexes, resulting in mitochondrial dysfunction and risk of bacterial survival and infectivity (Mahmud et al., 2021).

Furthermore, as mitochondria are organelles that regulate apoptosis, the consequences of infection from the gut microbiota usually target mitochondria-mediated apoptosis to enhance its virulence. enteropathogenic *E coli* produces the cytotoxins Maps EspZ and EspF, precisely targeting the mitochondria. EspF induces apoptosis *via* the release of cytochrome c from the mitochondria, whereas EspZ inhibits apoptosis to sustain MMP (Shames et al., 2011). Maps are also transported to the mitochondria *via* the import system, further stimulating Drp1 to promote fission, depleting MMP to cause Ca^{2+} efflux, cytochrome c release, endogenous apoptosis, and triggering p38 MAPK cascades to increase the inflammatory response (Ramachandran et al., 2020). VacA generated by *Helicobacter pylori* exacerbates apoptosis through similar stimulation, including the formation of anion-selective channels at the OMM to release cytochrome c into the cytosol and activate caspase 3 (Rassow, 2011). Host cell survival or death depends on mechanisms that are conducive to bacterial colonization. FimA, an effector protein produced by *Salmonella enterica*, maintains the relationship between VDAC1 and the glycolytic enzyme hexokinase to inhibit cytochrome c release by binding to VDAC1 at the OMM (Sukumaran et al., 2010). Another effector protein, SipB, facilitates autophagy-dependent cell death by disrupting the mitochondrial cristae morphology and imbalanced dynamics (Hernandez et al., 2003). In contrast, mitochondrial function also improves gut health and microbiota stability. In mice with increased mitochondrial activity, the relative abundance of *Dorea* and *Oscillospira* genera is enhanced and expression of SCFA, NAD, and sirtuin is elevated, leading to facilitation of fatty acid oxidation and reduction of metabolic disorders (Juárez-Fernández et al., 2022). Mitochondrial dysfunction in intestinal epithelial cells aggravates inflammation and oxygenation in the gut barrier and increases the abundance of facultative anaerobes, which are further involved in metabolic disorders (Zhang Y et al., 2022). Moreover, mitochondria also participate in the amelioration of lipid metabolism in the liver and reverse HFD-induced type 2 diabetes (Rodrigues et al., 2021). These data indicate that mitochondria outside vascular cells also respond to AS progression by regulating the gut microbiota. Therefore, gut bacteria not only regulate cell death by secreting toxins targeting mitochondria to promote bacterial colonization and reproduction but also activate the host's innate immunity mediated by mitochondria to resist gut bacterial infections, subsequently leading to chronic inflammation and systemic diseases, including AS.

3.2 SCFA effects on mitochondria during AS

SCFAs are the most abundant type of gut microbiota metabolites derived from the colon and cecum of non-digestible carbohydrates, including acetate, butyrate, and propionate, which not only serve as ingredients for mitochondrial energy metabolism but are also involved in improving mitochondrial function (den Besten et al., 2013). Most SCFAs are absorbed by the host mainly through active transport mediated by translocated proteins in colonocytes, and the effects of SCFAs on mitochondria may depend on the SCFA concentration. Zhao et al. (Zhao T et al., 2020) found that butyrate mediates 54 genes associated with mitochondrial energy metabolism and exerts protective effects by increasing mtDNA and ATP contents under high insulin conditions. Butyrate also defends islet β cell activity *via* the depletion of mtROS and activation of antioxidant enzymes to inhibit oxidative and nitrosative stresses, lipogenesis, and loss of excess weight by stimulating GPR43 and beta-arrestin2 activity to favor

mitochondrial biogenesis and energy expenditure, including triggering AMPK and the expression of PGC-1α and OXPHOS pathways, reducing the risk factors for AS (Tang et al., 2020). Administration of 3-hydroxybutyrate (3-HT) is beneficial and ameliorates atherogenesis (Zhang et al., 2021). Possibly, 3-HT binds to G-protein-coupled receptor 109a in macrophages to functionally facilitate cholesterol efflux and extracellular Ca^{2+} influx, leading to a decrease in the proportion of M1 macrophages *via* the suppression of NLRP3 and inactivation of ER stress *via* the inhibition of Ca^{2+} depletion (Zhang et al., 2021). The antioxidant response of butyrate significantly contributes to the induction of mitochondrial manganese–superoxide dismutase (MnSOD) and glutathione peroxidase expression by downregulating glycogen synthase kinase-3 beta and upregulating the nuclear translocation of nuclear factor erythroid 2-related factor 2 (Nrf2) (Tang et al., 2020). Propionic acid also regulates the redox state of the microenvironment through the mtROS content to influence chronic inflammatory diseases. Butyrate and its derivative butyramide attenuate insulin resistance and fat accumulation in the liver cells of obese mice by promoting mitochondrial fusion and the AMPK–acetyl–coenzyme A (CoA) carboxylase pathway to increase the utilization of fatty acids, glucose homeostasis, and mitochondrial respiratory rate (Mollica et al., 2017). SCFAs also suppress blood vessel cell death and chromatin modification by inactivating histone deacetylase, decreasing $CD4^+$ and $CD8^+$ T cell proliferation to inhibit vascular inflammation by delaying the maturation of dendritic cells, ultimately controlling AS progression (Andrade-Oliveira et al., 2015); therefore, SCFAs, especially butyrate, exert protective effects on mitochondria in vascular cells at a certain concentration (Table 1).

3.3 Trimethylamine-N-oxide effects on mitochondria during AS

TMAO is a harmful bacterial metabolite associated with AS. After consuming dietary components containing carnitine, choline, and betaine, TMA derived from the gut microbiota is subsequently oxidized to TMAO *via* flavin-containing monooxygenases in the liver (Wang et al., 2011). After transplanting the cecal microbiota of C57BL/6J mice with a choline diet and high TMAO levels into germ-free $ApoE^{-/-}$ mice, the recipients bore a greater atherosclerotic plaque burden and a positive association between TMAO levels in the plasma and atherosclerotic lesion area (Gregory et al., 2015). This indicates that choline diet-dependent TMAO levels may enhance atherosclerotic susceptibility. In a 3-year follow-up of 4,007 healthy participants with phosphatidylcholine challenges, the plasma levels of TMAO decreased with oral broad-spectrum antibiotics but increased after the withdrawal of antibiotics, which elevated the risk of major adverse cardiovascular events (MACE) (Tang et al., 2013), demonstrating the crucial role of gut microbiota in AS.

Mitochondria can be a target mediating TMAO effects on AS (Table 1). TMAO enhances aortic valve thickness and osteogenic differentiation by facilitating mitochondrial stress, including stimulation of mitochondrial swelling and NF-κB signaling (Li et al., 2022). TMAO also participates in the inhibition of mitochondrial respiration and OXPHOS. TMAO-treated cardiac fibers contribute to the decline in substrate-dependent respiration with pyruvate by 30% and negatively to β-oxidation, with declines in palmitoyl-CoA-related respiration and energy production (Makrecka-Kuka et al., 2017). TMAO also inhibits phosphocreatine and ATP levels by downregulating complex IV, further aggravating cardiac dysfunction and left ventricular pressure overload (Yoshida et al., 2022). Additionally, TMAO promote vascular endothelial injury by mitochondrial mediation. In ECs, TMAO administration increases succinate dehydrogenase complex subunit B overexpression, which promotes mtROS production and mitochondrial dysfunction, resulting in pyroptosis (Wu et al., 2020). TMAO upregulates mtROS levels and activates NLRP3 expression, likely by inhibiting SOD2 and SIRT3, further aggravating the inflammatory cascade in the blood vessels (Chen et al., 2017). TMAO mediates vascular cell adhesion molecule-1 expression in ECs to enhance monocyte adhesion, trigger scavenger receptors in macrophages, and recruit macrophages to promote the secretion of the inflammatory cytokines TNF-α and IL-6 (Mohammadi et al., 2016; Al-Obaide et al., 2017). In addition to increasing mtROS levels, TMAO-induced endothelial damage is strongly associated with other mitochondrial functions, such as the loss of MMP and Ca^{2+} influx, which affects NO release and eNOS phosphorylation (Querio et al., 2022). TMAO also induces Ca^{2+} and mtDNA release from platelets, causing dose-dependent platelet hyperreactivity and thrombus formation, which may be induced by ADP in the mitochondria (Querio et al., 2019). Moreover, TMAO might be reduced by the mitochondrial hmARC1.(Schneider et al., 2018). hmARC1 is an effective constituent of the mitochondrial amidoxime-reducing component protein that can translate TMAO into precursor TMA (Schneider et al., 2018). Overexpression of hmARC1 is correlated with the decline in TMAO in the liver as well as the enrichment of N-reductive activity in OMM. Collectively, mitochondria play a crucial role in mediating the effects of TMAO on AS progression, expanding the negative effects of TMAO on energy metabolism, oxidative stress, inflammatory cascade reactions, EC injury and death, and thrombus formation.

3.4 Hydrogen sulfide effects on mitochondria during AS

The bacterial metabolite H_2S, which is generated by the gut microbiota or host cells and is the third physiologic signaling gas after CO and NO, shows dose-dependent effects on vessels, such as facilitating vasodilation and angiogenesis, decreasing monocyte adhesion, and attenuating apoptosis (Paul et al., 2021). The aorta has the highest H_2S bioavailability and most H_2S bioequivalents (Shen et al., 2013). H_2S triggers cGMP synthesis, inhibits the degradation of cGMP and cAMP to promote NO release and vasodilatation, and activates NAD+ in ECs to delay endothelial senescence. Moreover, H_2S has a pro-angiogenic effect partly through the regulation of electron transport, OXPHOS, and sulfhydration with mitochondria to elevate glucose uptake and glycolysis (Longchamp et al., 2018).

As H_2S is sensitive to oxygen, the metabolic site of H_2S is mainly in the mitochondria. The anaerobic microbiota generates a non-negligible amount of H_2S in the colon, which is oxidized into detoxicated thiosulfate and sulfate mediated by mitochondria and excreted. The released electrons can be transferred to the electron transport chain (ETC), further improving ATP production during this metabolic process (Libiad et al., 2019). H_2S reduces oxidative stress and mitochondrial swelling while enhancing mitophagy and mitochondrial biogenesis and mediates the sulfidation of the

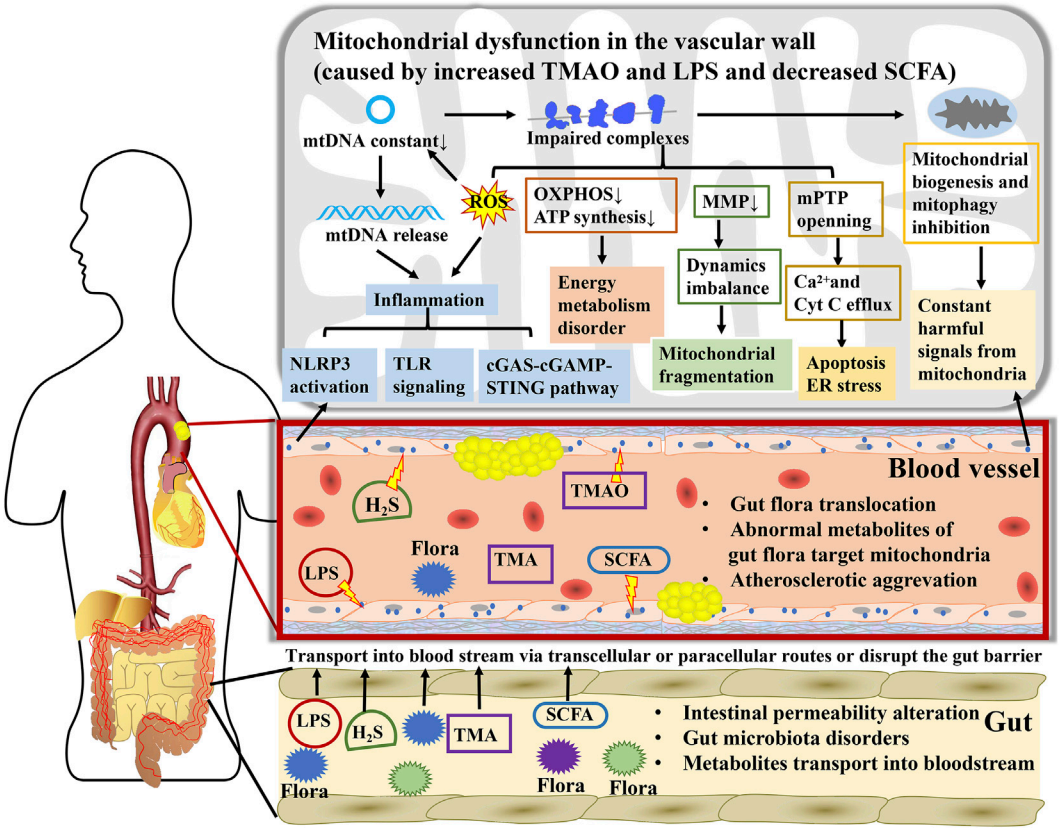

FIGURE 2
A key mediator linking gut microbiota to atherosclerosis, mitochondria participate in the interaction between numerous metabolites from gut microbiota and atherosclerosis. During atherosclerosis, gut microbiota disorders and intestinal permeability alteration contribute to direct transposition of flora to arteries. Microbial metabolites are transported into the bloodstream *via* transcellular or paracellular routes or disrupting the gut barrier and subsequently affect mitochondrial function in blood vessels cells. Mitochondria expand the influence of TMAO, LPS, H_2S, and SCFA on energy metabolism, oxidative stress, inflammatory cascade reaction, and endothelial cell injury through regulating mtDNA release, ATP synthesis, MMP, mPTP, mitochondrial biogenesis, and mitophagy, further promoting or opposing the atherogenic process.

mitophagy protein parkin, further activating E3 ubiquitin ligase and inducing mitophagy (Sun et al., 2020). It also improves mitochondrial biogenesis in myocardial cells following ischemia/reperfusion (I/R) injury by downregulating protein phosphatase 2A and upregulating peroxisome PGC-1α (Calvert et al., 2010; Untereiner et al., 2016). In H_2O_2-treated cardiomyocytes, NaHS effectively attenuates mtROS production, reduces damage from oxidative stress, and enhances cardiomyocyte viability and activity *via* a SIRT1-dependent pathway (Wu D et al., 2015). SIRT1 is a significant element in mediating the effects of NaHS on reversing oxidative stress and depleting ATP. These effects can be eliminated by SIRT1 silencing (Ma et al., 2019). Furthermore, NaHS ameliorates EC senescence by upregulating SIRT1 and antioxidant defenses (Zheng et al., 2014). Low doses of H_2S are beneficial to cells as they promote mitochondrial biological function and ameliorate apoptosis, whereas high concentrations inactivate complex III at the ETC and even lead to apoptosis of aortic SMCs (Murphy et al., 2019). Excess H_2S is cytotoxic and harmful to cellular energy metabolism and causes DNA injury through the inhibition of mitochondrial respiration and ATP synthesis (Borisov and Forte, 2021). High concentrations of H_2S bind to the copper center of cytochrome c oxidase to inhibit its activation and suppress mitochondrial activity (Módis et al., 2014). This further confirms that mitochondria play a crucial role in regulating the interaction between H_2S from the gut microbiota and vascular damage (Table 1).

3.5 Other intestinal flora metabolites

Other metabolites from the gut microbiota also correlate with the development of AS (Table 1). Small metabolites are transported into the bloodstream *via* transcellular or paracellular routes, whereas large metabolites disrupt the gut barrier and are released into the body (Kirichenko et al., 2020). Indole derivatives, such as indoxyl sulfate, indole ethanol, and indole acrylic acid, are produced by the gut microbiota from tryptophan and induce proinflammatory activity after entering the bloodstream (Xu H et al., 2022). In addition, indolepropionic acid (IPA), which is metabolized from tryptophan, is substantially reduced in patients with coronary artery disease. Oral IPA administration mitigates the extent of atherosclerotic lesions by activating ABCA1 and promoting RCT (Xue et al., 2022). Another amino acid derivative metabolized by the gut microbiota is phenylacetylglutamine, which induces platelet hyper-responsiveness and thrombotic action (Liu et al., 2021) and is positively associated with MACE (Bogiatzi et al., 2018). Furthermore, secondary bile acids (BAs) and LPS are microbiota-dependent proatherogenic molecules.

TABLE 1 Effects of intestinal microbiota metabolites on mitochondria and AS.

Metabolite	Subject	Effects on mitochondria	Effects on vessels	Ref
propionate	rats/Heart perfusions	increase glucose uptake and oxidation; promote mitochondrial CoA trapping and inhibit fatty acid oxidation	mediate perturbation of cardiac energy metabolism	Wang et al. (2018)
3–HB	$ApoE^{-/-}$ mice	reduce the release of Ca^{2+} from the ER to mitochondria, inhibits ER stress	reduce systemic inflammatory and AS, increase cholesterol efflux	Zhang et al. (2021)
TMAO	patients with CAVD; AVICs	promote ER stress, mitochondrial stress, and NF–κB activation	increase aortic valve thicknesses	Li et al. (2022)
TMAO	HUVECs or aortas from $ApoE^{-/-}$ mice	stimulate mtROS generation, inhibit SOD2 activation and SIRT3 expression	induce vascular inflammation and promote AS.	Chen et al. (2017)
TMAO	cardiac fibers	decrease LEAK and OXPHOS mitochondrial respiration with pyruvate and impair substrate flux *via* pyruvate dehydrogenase	induce disturbances in cardiac mitochondrial energy metabolism	Makrecka-Kuka et al. (2017)
TMAO	Wistar rats	prevent MCT–impaired mitochondrial energy metabolism by preserving fatty acid oxidation and decreasing pyruvate metabolism	restore right ventricular function, reduce heart failure severity, and maintain cardiac functionality	Videja et al. (2020)
TMAO	endothelial cells	modify the purinergic response affecting intracellular ATP–induced calcium increase, nitric oxide release, and $eNOS^{Ser1179}$	impacts on endothelial eNOS phosphorylation	Querio et al. (2022)
TMAO	cardiac tissues from mice	significant reduction of phosphocreatine and ATP levels in cardiac tissue *via* suppression of mitochondrial complex IV activity	cause cardiac dysfunction with LV pressure overload	Yoo et al. (2022)
LPS	VSMC	stimulate PCSK9 release and induce mtDNA damage	cellular injury and apoptosis, promote AS	Ding et al. (2016)
LPS	HUVECs	decrease ATP content, MMP, and maximal respiration rate; increase expression of Drp1 with excessive mitochondrial fission	HUVECs injury	Lian N et al. (2022)
LPS	HUVECs	cause the mitochondrial permeability transition, cytosolic release of cytochrome c, and activation of caspases	induce apoptosis	Lim et al. (2009)
LPS	HUVECs	promote Drp1 phosphorylation, initiate the mitochondrial fission contributing to the caspase 9–dependent mitochondrial apoptosis	apoptosis of HUVEC	Cui et al. (2018)
H_2S	ischemia–induced heart failure mice	increase ADP–stimulated oxygen consumption and ATP synthesis, elevate respiratory control ratios; attenuate oxidative stress	decrease infarct area/area at risk; decrease infarct area/LV.	Calvert et al. (2010)
H_2S	aorta and VSMC	increase mtDNA–CN and mitochondrial maker gene expression, inhibit TFAM promoter methylation	regulate arterial tension	Li and Yang, (2015)
H_2S	HUVEC	promote glucose uptake and ATP generation by glycolysis; shifts oxidative/glycolytic balance concomitant with inhibition of mitochondrial electron transport and OXPHOS.	trigger angiogenesis and improve vascular health	Longchamp et al. (2018)
H_2S	H9c2 cardiomyocytes	increased ATP level and the expression of ATPase, decrease in ROS production and the enhancement in SOD, GPx, GST and SIRT1 expression	increase the cell viability and inhibit the cell apoptosis	Wu D et al. (2015)

Note: 3–HB, Ketone Body 3-Hydroxybutyrate; HUVEC, human umbilical vein endothelial cells; CAVD, calcified aortic valve disease; AVICs, human aortic valve interstitial cells; LEAK, substrate–dependent respiration; OXPHOS, oxidative phosphorylation; MCT, monocrotaline; PCSK9, proprotein convertase subtilisin/kexin type 9; LV, left ventricular.

BAs are converted by the gut microbiota from primary BAs and further mediate lipid and glucose metabolic pathways by binding to receptor farnesoid X and membrane receptor Takeda G-protein-coupled receptor 5, resulting in the development of vascular inflammation, lipid deposition, and AS (Pols et al., 2011; Kuipers et al., 2014). Indole-3-carboxylic acid and BAs contribute to mitochondrial swelling and increase mitochondrial permeability by changing the Ca^{2+} concentration threshold for mPTP opening (Fedotcheva et al., 2021). Binding of secondary BAs to the G-coupled membrane protein 5 and farnesoid X receptor triggers mitochondrial fission *via* the ERK/DRP1 pathway and mediates fatty acid uptake and β-oxidation, further causing energy metabolism disorders and apoptosis (Mikó et al., 2018). LPS, a large molecule derived from Gram-negative bacteria, translocates into the bloodstream by compromising the intestinal mucosa, leading to metabolic endotoxemia (Giusti et al., 2017). LPS subsequently stimulates the TLR 4 and TLR4/MyD88/TRIF signaling pathways to trigger macrophages and systemic inflammation (Caesar et al., 2015). Additionally, some Gram-negative bacteria can translocate to the arterial intima and directly release LPS, leading to AS progression (Verhaar et al., 2020). Consequently, the gut microbiota–mitochondria axis acts as a significant endocrine

TABLE 2 Effects of natural compounds from herbs on gut flora, mitochondria, and AS.

Natural compound	Model	Administration	Effects on gut flora/mitochondria	Effects on vessels	Ref
BBR	HFD–fed Apoe$^{-/-}$ mice	0.5 g/L in drinking water for 14w	increase the abundance of Akkermansia spp; increase intestinal expression of tight junction proteins and the thickness of the colonic mucus layer	decrease arterial and intestinal expression of proinflammatory cytokines and chemokines; have antiatherosclerotic and metabolic protective effects	Zhu L et al. (2018)
BBR	HFD–fed Apoe$^{-/-}$ mice	50 mg/kg twice weekly by gavage; FMT	increase Firmicutes and Verrucomicrobia; decrease Bacteroidetes and Proteobacteria; reduce TMAO level and FMO3 expression	reduce collagen content in atherosclerotic plaque and MMP–2, IL–6 and ICAM–1 expression	Shi Y et al. (2018)
BBR	Ang II– infused C57BL/6 J mice	150 mg/kg/d for 4 w	reduce the Firmicutes/Bacteroidetes ratio and increase the abundances of *Lactobacillus* and plasma TMA/TMAO production; inhibit FMO3 expression	alleviate the elevated blood pressure, vascular dysfunction, and vascular pathological remodeling	Wang Z et al. (2022)
BBR	choline– fed ApoE$^{-/-}$ mice	200 mg/kg/d for 6w	attenuate TMA/TMAO production and abundance of CutC and CntA genes; inhibit the choline–to–TMA transformation in the strains of C. sporogenes and A. hydrogenalis	mitigate atherosclerotic lesion areas	Li X et al. (2021)
BBR	HFD–fed Apoe$^{-/-}$ mice	50 mg/kg/d by gavage	adjust the composition of intestinal flora; elevate lipid and glycan metabolism and synthesis of SCFAs; reduce TMAO production	decrease pro–inflammatory cytokines, lipid level in plasma, and atherosclerotic lesions	Wu et al. (2020)
BBR	HFD–fed hamsters	100 mg/kg orally; FMT	reduce the TMA production in the *E. coli* and Eubacterium and TMAO in plasma and faecal samples; suppress FMOs activity; adjust the composition of intestinal flora	decrease blood glucose and lipids; reduce development of plaques in AS patients	Ma et al. (2022)
BBR	AS patients	orally 1 g/d for 4m	decline of Eubacterium_hallii_group, Anaerostipes, Faecalibacterium, Dialister, Eubacterium_coprostanoligenes_group, Coprococcus_3, Butyricicoccus and *Clostridium*_sensu_strito_1		Ma et al. (2022)
BBR	TAC–induced chronic HF	50 mg/kg/d for 4w by gavage	upregulate PINK1/Parkin–mediated mitophagy	ameliorate cardiac dysfunction, cardiac hypertrophy, interstitial fibrosis, and cardiomyocyte apoptosis	Abudureyimu et al. (2020)
BBR	MI/R; H9C2 cells	300 mg/kg/d for 3d	increase MMP; regulate autophagy–related protein expression; induce cell proliferation and autophagosome formation	reduce the myocardial infarct size, cardiomyocyte apoptosis, and the expression of myocardial enzyme (CK–MB, LDH, and AST)	Zhu et al. (2020)
RSV	HFHSD–fed C57Bl/6N mice	chow with 0.4% RSV; FMT for 8w	decrease relative abundance of Turicibacteraceae, Moryella, Lachnospiraceae, and Akkermansia; increase relative abundance of *Bacteroides* and Parabacteroides	improve glucose homeostasis in obese mice	Sung et al. (2017)
RSV	HFHSD–fed C57Bl/6N mice	FMT	few changes in fecal metabolites and the metabolic profile; reduce inflammatory cytokine level	decrease inflammation in the colon; reduce the systolic blood pressure of hypertensive mice	Kim et al. (2018)
RSV	Choline– or TMA–fed in mice	chow with 0.4% RSV	increase Bacteroidetes; decrease Firmicutes; reduce TMAO synthesis and ileal BA content; enhance BA deconjugation and fecal excretion; repress the enterohepatic FXR– FGF15 axis; increase CYP7A1 expression and hepatic BA neosynthesis	decrease the atherosclerotic lesion area and the cholesterol content in the whole aorta	Chen M L et al. (2016)
RSV	t–BHP–induced HUVECs	0.1, 1, 10, 15 μM 2h	repress collapse of MMP and mtROS generation; increase enzymatic activities of IDH2, GSH–Px and SOD2	increase cell viability; inhibit cell apoptosis	Yang et al. (2019)
RSV	PA–induced HUVECs	10 μM for 8 h	improve expression of MFN1, MFN2, and OPA1; inhibit fragmentation of mitochondria; reduce oxidative stress	attenuate endothelial oxidative injury	Zhou et al. (2014)
RSV	ox–LDL induced HUVEC	5, 10, 20, 40, 80, 120 μg/ml 24 h	increase MMP, Bcl–2/BAX ratio and SOD2; decrease the release of mitochondrial cytochrome c into the cytoplasm; reduce the activation of caspase and lipid peroxidation	possess protective effects against endothelial cell apoptosis and oxidative damage	Liu et al. (2017)
RSV	older glu–intolerant adults	2–3 g/d for 6 w	increase OXPHOS perturbed pathways and mitochondrial content	have beneficial effects on vascular function	Pollack et al. (2017)

(Continued on following page)

TABLE 2 (*Continued*) Effects of natural compounds from herbs on gut flora, mitochondria, and AS.

Natural compound	Model	Administration	Effects on gut flora/mitochondria	Effects on vessels	Ref
allicin	L–carnitine –fed ApoE$^{-/-}$ mice	orally 10 mg/kg/d in 0.5% CMC	inhibit γBB and TMA; reduce serum d9–TMA and d9–TMAO; inhibit microbial carnitine→γBB→TMA pathways	reduce aortic plaques	Panyod et al. (2022)
allicin	OCCT in Nine volunteers	garlic: water (ratio 1:3) were mixed	reduce TMAO formation; improve gut microbial diversity; increase the relative abundances of beneficial bacteria; increase γBB; prevent the microbial transformation of γBB into TMA	reduction in platelet aggregation	Panyod et al. (2022)
allicin	LPS–induced HUVECs	0–40 μg/ml 24 h	decrease the MMP collapse, cytochrome c synthesis and mitochondrial ATP release; suppress ROS overproduction; reduce lipid peroxidation the endogenous antioxidant enzyme activities	enhance HUVEC proliferation; ameliorate apoptosis	Zhang M et al. (2017)
allicin	HFD–fed C57BL/6 mice	100 mg/kg/d	increase the abundance of Bacteroidales and Clostridiales at the order level; increase the abundance of Akkermansia at the genus level	improve lipolysis and insulin sensitivity by suppressing hepatic lipid synthesis and increasing thermogenesis	Shi et al. (2019)
curcumin	HFD–fed Apoe$^{-/-}$ mice	0.1% for 16w	decrease intestinal cholesterol absorption	reduce the extent of atherosclerotic lesions by 45%; reduce cholesterol accumulation in the aortas by 56%	Zou et al. (2018)
curcumin	Aging mice	dietary 0.2%	promote eNOS and AMPK phosphorylation; upregulate UCP2 and reduced ROS production	improve cerebrovascular endothelium–dependent relaxation in aging	Pu et al. (2013)
THC	MI/R injury	50 mg/kg/day	increase SOD and CAT activities; decrease MDA level; enhance MMP; diminish the Bax/Bcl–2 ratio and cleave caspase–3 level	increase EF and FS; decrease LVESD and LVESV	Chen et al. (2021)
QUE	HCD–fed ApoE$^{-/-}$ mice	100 mg/kg/d. for 12w	decrease the abundance of Phascolarctobacterium and Anaerovibrio genera	protect damaged vessels; exhibit a thinner intima hyperplasia; less inflammatory cells	Wu et al. (2019)
QUE	HUVECs	10 μM 1 h	depolarize the mitochondrial membrane; increase level of the mitoBK$_{Ca}$ β3 regulatory subunit	enhance cellular migration; beneficial for vascular endothelial cells	Kampa et al. (2021)
QUE	50 μM iron	20 μM for 48 h	decrease mitochondrial oxidative stress and mPTP opening, increase mitochondrial membrane potential	attenuate iron overload induced HUVECs mitochondrial dysfunction	Chen et al. (2020)
QUE	Ldlr$^{-/-}$ mice	100 ug/d in an aqueous solution containing 1% sodium lauryl sulphate	reduce the abundance of Verrocomicrobia; increase microbiome diversity and the abundances of Actinobacteria, Cyanobacteria and Firmicutes	reduce the extent of atherosclerotic lesions in the aortic sinus	Nie et al. (2019)
QUE	Pi–induce VSMCs	50 μM 6 d	inhibit oxidative stress; decrease mitochondrial fission by inhibiting the expression and phosphorylation of Drp1	block apoptosis and calcification of VSMCs; ameliorate aortic calcification	Cui et al. (2017)
QUE	apoE$^{-/-}$ mice	20 mg/kg/d 8 w	increase MMP; decrease ROS generation	decrease lipid deposition in arterial lumina, serum sIcam–1, and IL–6 and Vcam–1 in aorta, while increase the density of SIRT1 in aorta	Jiang et al. (2020)
QUE	ox–LDL–induced HAECs	0.3, 1, or 3 μM 48 h		decrease the expression of SaβG; improve cell morphology	

Note: BBR, berberine; RSV, resveratrol; Que, Quercetin; HFD, high–fat diet; HCD, high cholesterol diet; Ang II, Angiotensin II; TAC, transverse aortic contraction; HF, heart failure; HFHSD, high fat/high sugar; t–BHP, tert–butyl hydroperoxide; HUVECs, human umbilical vein endothelial cells; PA, palmitic acid; OCCT, oral carnitine challenge test; MI/R, myocardial ischemia–reperfusion; Ldlr$^{-/-}$.

low–density lipoprotein receptor–null; Pi, inorganic phosphate; THC, tetrahydrocurcumin; FGF15, fibroblast growth factor 15; CYP7A1, cholesterol 7a–hydroxylase; IDH2, isocitrate dehydrogenase 2; γBB, γ–butyrobetaine; SaβG, senescence–associated β–galactosidase; FMT, fecal microbiota transplantation; CutC, enzyme/co–enzyme of choline–trimethylamine lyase; MDA, malondialdehyde; EF, ejection fraction; FS, fractional shortening; LVESD, left ventricular end systolic diameter; LVESV, left ventricular end systolic volume; mitoBK$_{Ca}$, mitochondrial large–conductance Ca^{2+}–regulated potassium; IDH, isocitrate dehydrogenase; CK–MB, creatine kinase–MB; LDH, lactate dehydrogenase; AST, aspartate aminotransferase; HF, heart failure; TAC, transverse aortic contraction; h, hours; d, days; w, weeks; m, months.

metabolic pathway to regulate the host's systemic chronic diseases, especially AS. The specific mechanism might also be affected by the dominant bacteria in the gut, concentration of metabolites, and other atherosclerotic risk factors. Further studies are necessary to determine the long-distance interactions between the gut microbiota, mitochondria, and AS completely and accurately (Figure 2).

4 Natural compounds in herbal medicine regulating intestinal flora and mitochondria to treat AS

Intervention of gut microbiota and mitochondria is a novel therapeutic target for AS. Lifestyle adjustments may simultaneously regulate gut microbiota and mitochondria (Najjar and Feresin, 2019). Endurance exercise maintains the stability of intestinal flora and reverses host mitochondrial functions by inhibiting enteric inflammation and diminishing the reproduction of pathobionts in the intestinal tract (Clark and Mach, 2017). Plant-based diets or consumption of unsaturated fatty acids can improve gut microbiota diversity and symbiotic homeostasis and recover mitochondrial respiration and fatty acid oxidation (López-Salazar et al., 2021), resulting in enhanced satiety, increased energy expenditure, and elevated insulin sensitivity, ultimately ameliorating AS by reducing body fat and maintaining glycemic stability. However, the therapeutic effects of exercise and dietary changes are limited. Herbal medicine has been used to treat CVDs in China for many years because of the advantages of multi-target, synergistic, and systemic therapy. Herbs are closely related to gut microbiota and mitochondria (Zhou et al., 2022). Gut microbiota converts herbs into active metabolites with higher bioavailability, and herbs regulate gut microbiota biodiversity to ameliorate CVD in the host, similar to prebiotics (Table 2) (Ma et al., 2022; Qi et al., 2022).

4.1 Berberine

Berberine (BBR) is an isoquinoline alkaloid found mainly in *Coptis chinensis* and *Berberis pruinosa var. pruinosa* (Habtemariam, 2020). BBR has low oral bioavailability and absorption owing to its poor solubility. Modulating the gut microbiota to some extent increases the efficiency of BBR in CVDs. BBR effectively mitigates AS in high-fat diet-fed ApoE$^{-/-}$ mice by upregulating the abundance of intestinal *Akkermansia* (Zhu L et al., 2018), *Verrucomicrobia, Firmicutes* (Shi Y et al., 2018), *Alistipes,* and *Roseburia* (Wu et al., 2020), while downregulating that of Lachnospiraceae*, Bacteroidales,* and *Eubacterium*. Changes in the intestinal microbiota recover gut barrier integrity, affect serum TMAO (Shi Y et al., 2018), secondary BAs, and SCFA levels, and attenuate proinflammatory cytokines, chemokines, total cholesterol, and very low-density lipoprotein (Wu et al., 2020), thereby reversing atherosclerotic lesions. BBR is metabolized to dihydroberberine by the gut microbiota (Ma et al., 2022), and dihydroberberine further inactivates the enzymes choline-trimethylamine lyase and flavin monooxygenase, enhancing the diversity of the microbiome to suppress TMAO production and decreasing atherosclerotic lesion (Li X et al., 2021). Moreover, BBR ameliorates the risk factors for AS, including obesity (Hu et al., 2012), hyperglycemia (Li M et al., 2020), and hyperlipidemia (Yang et al., 2022), by maintaining the balance of intestinal flora.

BBR might target mitochondria to exert a protective effect on AS mediated by the gut microbiota. BBR protects ECs from oxidative stress by inhibiting Nox4 protein and ROS expression to improve vasodilation (Cheng et al., 2013). Nox4 in vessels is mainly distributed in the mitochondrial membrane and is involved in stimulating mtROS production. A decline in mtROS caused by BBR further elicits a lower expression of the NLRP3 inflammasome and increases MMP. BBR greatly improves mitophagy by preserving myocardial function and suppressing apoptosis. For example, BBR improves cardiac hypertrophy and cardiomyocyte apoptosis *via* the PINK1/parkin pathway (Abudureyimu et al., 2020), induces mitophagy to inhibit NLRP3 activation by reducing P62 and recruiting LC3 to mitochondria (Liu H et al., 2020), restores cardiomyocyte senescence by activating prohibitin 2 (Wang L et al., 2022), and defends the myocardium from I/R injury *via* the hypoxia-induced factor (HIF)-1α/BCL2-interacting protein 3(BNIP3) pathway (Zhu et al., 2020). Furthermore, BBR also decreases basal oxygen consumption rates and facilitates fatty acid oxidation by diminishing mitochondrial swelling and upregulating mitochondrial biogenesis mediated by the AMPK/PGC-1α pathway to attenuate lipid deposition and weight in obese mice (Yao et al., 2020; Yu et al., 2021). BBR exerts a protective effect on fatty acid oxidation enzymes, mitochondrial dynamics balance, and ATP synthesis in cells induced by high glucose (Rong et al., 2021). Collectively, BBR remarkably recovered the gut flora and metabolic balance and preserved mitochondrial function, contributing to the inhibition of AS progression.

4.2 Resveratrol

Resveratrol (RSV) is a plant-derived polyphenol extracted from grapes, peanuts, blueberries, and mulberries and has been used as a potential prebiotic in the intervention of AS. RSV attenuates atherosclerotic plaques by enriching *Bacteroides, Lactobacillus, Parabacteroides,* and *Bifidobacterium* (Chen M L et al., 2016; Sung et al., 2017), reducing TMAO levels and increasing BA excretion. However, a combination of antibiotics and RSV cannot suppress TMAO or mitigate AS. These results revealed the important role of the gut microbiota in the anti-atherosclerosis treatment of RSV (Chen M L et al., 2016). RSV also mitigates insulin resistance and triglyceride deposition in the liver to suppress the effects of metabolic syndrome on AS by increasing the proportion of *Akkermansia spp.* in the intestine (Anhê et al., 2015). Fecal transplantation following resveratrol treatment in mice is beneficial for improving glucose metabolism and low-grade inflammation in obese mice (Sung et al., 2017). In turn, the gut microbiota converts resveratrol into its derivatives to enhance bioavailability, such as dihydroresveratrol, 3,4′-dihydroxy-trans-stilbene and 3,4′-dihydroxybibenzyl (Bode et al., 2013), which is the predominant form in the plasma and effectively protects ECs and VSMCs.

RSV induces endothelial relaxation by activating eNOS and NO synthesis, diminishing ET-1, and inhibits VSMCs proliferation and senescence by decreasing β-galactosidase and pro-fibrotic proteins to ameliorate vascular remodeling and sclerosis (Kim et al., 2018). Possible mechanisms are closely related to mitochondrial function. In human coronary arterial ECs, RSV exerts protective effects on

mitochondrial biogenesis by upregulating PGC-1α, Nrf-1, and TFAM, and triggering eNOS expression and NO release by inducing SIRT1 (Csiszar et al., 2009; Davinelli et al., 2013). RSV also improves complex I and III expression in the ETC and BNIP3-related mitophagy by triggering HIF1 and AMPK, leading to mitochondrial redox balance and mitochondrial renewal in ox-LDL-induced ECs (Li C et al., 2020). RSV is well-known for its antioxidant properties. It ameliorates mitochondrial fragmentation to diminish mtROS levels by enhancing Mfn1/2 and OPA1 activation (Yang et al., 2019). RSV significantly decreases mtROS levels by activating AMPK-PGC-1α-ERRα-SIRT3 signaling (Zhou et al., 2014) and inhibiting antioxidant enzymes to defend EC activity from H_2O_2 and deplete apoptosis by attenuating cytochrome c efflux from the mitochondria and Bcl-2 expression (Liu et al., 2013; Liu et al., 2017). SIRT1 is also involved in the antioxidant activity of RSV. RSV is a well-known activator of SIRT1 (Csiszar et al., 2008; Wellman et al., 2017) that can stimulate MnSOD and glutathione (GSH) to reduce the levels of $O_2^{\bullet-}$and H_2O_2 in the endothelial mitochondria (Ungvari et al., 2009). In clinical trials, RSV-treated older adults with glucose intolerance exhibited symptoms of an enhanced fasting reactive hyperemia index, showing a restoration of endothelial function, probably caused by increasing mitochondrial content and facilitating OXPHOS (Pollack et al., 2017). Consequently, RSV can simultaneously improve endothelial injury, vascular thickening, and fibrosis by modulating intestinal microbiota homeostasis and the mitochondrial redox balance.

4.3 Allicin

Allicin is a thioester of sulfenic acid isolated from *Allium sativum L.* [Amaryllidaceae] and effectively crosses cell membranes to play antibacterial and antioxidant roles owing to its hydrophobic characteristics. Garlic is a recognized prebiotic; thus, allicin can be metabolized into diallyl disulfide (DAD) and diallyl trisulfide (DAT) to regulate gut microbiota composition and disrupt TMA production in ApoE$^{-/-}$ mice with high concentrations of carnitine (Panyod et al., 2022). Following allicin treatment, the proportions of *Bifidobacterium, Lactobacillus, Bacteroidales,* and *Clostridiales* significantly increased in the gut (Shi et al., 2019), while those in some pathogenic bacteria, such as *Proteobacteria, Escherichia–Shigella,* and *Streptococcus,* drastically reduced (Hu et al., 2021). Moreover, allicin also regulates the metabolites of gut microbiota, such as upregulating SCFA, while downregulating secondary BAs, TMAO, and indoles, stimulating brown adipose tissue activation, browning in white adipose tissues (Zhang et al., 2020), decline in lipid accumulation in the liver, and weight loss in obese mice (Shi et al., 2019).

Allicin can recover mitochondrial function in ECs and ameliorate AS. DAT contributes to protecting ECs from oxidative stress under high-glucose conditions by facilitating mitochondrial respiration, triggering MnSOD and glutathione peroxidase (GSH-Px) expression, and suppressing lipid peroxidation (Liu et al., 2014). Moreover, allicin is involved in elevating MMP and inhibiting cytochrome c release and ATP export as a DAMP by inactivating antioxidant enzymes and stimulating Nrf2 activation, resulting in the reversal of endothelial apoptosis and vascular inflammation (Zhang M et al., 2017). DAD can prevent cardiac hypertrophy by improving mitochondrial biogenesis, including activation of the mitochondrial complex and the eNOS–Nrf2–TFAM signaling pathway (Khatua et al., 2016). This demonstrated the antibacterial and antioxidant properties of allicin. Allicin, DAD, and DAT are the main probiotic compounds that preserve cardiovascular diastolic function and cell activity by resisting mitochondria-related oxidative stress.

4.4 Quercetin

Quercetin (Que) is a flavonoid naturally found in various vegetables, fruits, nuts, tea, and wine. Que has become an increasingly popular natural dietary supplement owing to its association with CVDs. The anti-atherosclerotic effects of Que in maintaining intestinal homeostasis have been widely reported. Oral administration of Que reduces lipid metabolites, such as atherogenic lysophosphatidyl choline, in the plasma and artery wall, which are negatively correlated with the abundance of *Actinobacteria, Firmicutes,* and *Cyanobacteria* in the gut (Nie et al., 2019). Que notably diminishes plasma lipid levels (TC, TG, HDL, and LDL) and plasma inflammation (TNF-α and IL-6) through the BA biosynthesis pathway metabolized by the gut microbiota with a KEGG analysis (Wu et al., 2019). Que also prevents lipid accumulation in vascular macrophages and elevates foam cell survival rates by inducing autophagy and oxidative resistance (Cao et al., 2019). Que is involved in many aspects of lipid metabolism, from the gut to vessels, to attenuate AS.

Que plays a protective role by increasing mitochondria-related cellular viability. Que opens the mitochondrial large-conductance Ca^{2+}-regulated potassium channel, leading to MMP depolarization and maintenance of EC environmental homeostasis (Kampa et al., 2021). Alterations in MMP and permeability caused by oxidative damage could contribute to apoptosis and direct damage to NO content, while Que could reverse these phenomena to preserve EC activity induced by iron or angiotensin II (Lu et al., 2016; Chen et al., 2020). Que also has potential benefits against mitochondrial fragmentation mediated by Drp1 overexpression, which enhances mtROS levels and exacerbates VSMCs apoptosis *via* cytochrome c release and caspase-3 activation, further causing vascular calcification (Cui et al., 2017). The mitochondrial protective effects have also been confirmed *in vivo*. Que remarkably mitigated the extent of atherosclerotic plaque area and decreased lipid deposition in the aorta and soluble intercellular adhesion molecule-1 in ApoE$^{-/-}$ mice, probably because of increased MMP and decreased mtROS levels to resist endothelial senescence and apoptosis (Jiang et al., 2020). Briefly, the cardiovascular targets of Que treatment have been established along the gut microbiota–mitochondrial axis.

4.5 Curcumin

Curcumin, a bioactive polyphenolic of *Curcuma longa L.* [Zingiberaceae], is involved in anti-atherosclerosis by remodeling gut microbiota dysbiosis, altering the level of metabolites, and cytoprotection targeting mitochondria. Curcumin can reduce TMAO levels to diminish atherosclerotic lesions induced by cadmium exposure (Zhang J et al., 2022), probably by increasing bacterial richness (McFadden et al., 2015) and improving the defense of the intestinal barrier (Wang et al., 2017). Effective regulation of intestinal microbiota using curcumin can further inhibit the absorption of intestinal cholesterol (Hong et al., 2022) and mitigate low-grade systemic inflammation (Cox et al., 2022), including a 56%

reduction in cholesterol deposition in the aorta (Zou et al., 2018) and a decline in monocyte chemoattractant protein 1 (Zhou et al., 2021), lipocalin 2 (Wan et al., 2016), TNFα, NFκB, and C-reactive protein expression. The therapeutic effect of curcumin on AS also depends on improving bioavailability mediated by the gut microbiota (Lopresti, 2018), further strengthening its positive influence on the distal mitochondria. Curcumin protects ECs and cardiomyocytes from mitochondrial oxidative stress and MMP loss (Gupta et al., 2016; Chen et al., 2021). Specifically, curcumin can upregulate UCP2 to reduce the generation of downstream mtROS, leading to enhanced eNOS and AMPK phosphorylation and recovery of endothelial functions (Gupta et al., 2016). Curcumin inhibits cardiomyocyte autophagy and apoptosis induced by hypoxia and reoxygenation injury by facilitating the expression of antioxidant enzymes, increasing MMP, and suppressing mitochondria-related apoptosis (Chen et al., 2021). Therefore, curcumin acts as an anti-atherogenic agent by ameliorating the intestinal flora and mitochondria to prevent lipid accumulation, inflammation, and oxidative stress.

There are multiple other bioactive compounds extracted from herbal medicines, including ginkgolide B (Lv et al., 2021), pterostilbene (Zhang et al., 2012), and catalpol (Zhang Y et al., 2018), which are beneficial for maintaining the connection between the bacterial flora, metabolites, and mitochondria and contribute to the recovery of vascular stability and inhibition of AS progression. Thus, herbal medicines and their natural compounds can sustain the balance between the microbiota and the host. However, further research is necessary to reveal the therapeutic effects of herbal medicines on the immune and metabolic networks between gut microbiota and mitochondria.

5 Conclusion

Although the risk factors and therapeutic methods for AS have been constantly improving, atherosclerotic CVD remains the leading cause of death worldwide. This review focuses on the close association between gut microbiota and mitochondria during AS progression and simultaneously enumerates several common herbal medicines and their natural compounds to prevent AS by adjusting the intestinal flora and sustaining mitochondrial function. Derived from the endosymbiotic α-proteobacterium, mitochondria possess characteristics similar to those of bacteria, such as exporting DAMP to activate innate immunity, which makes mitochondria a target for the gut microbiota and its metabolites, including SCFA, TMAO, and H_2S. Mitochondria not only participate in providing energy but also act as activators of cholesterol metabolism, inflammation, and apoptosis, facilitating the development of AS. Herbal medicines are widely used in China owing to their advantages of multi-target and systemic treatments, which enable the simultaneous regulation of the intestinal flora and vascular mitochondria. Gut microbiota have not only been shown to be endocrine organs that regulate metabolism but are also significantly responsible for reversing the poor bioavailability of natural compounds. Importantly, the interactions between the gut microbiota and mitochondria collectively establish an immune and metabolic network that influences AS progression, which could be a potential target of herbal medicine to prevent AS. However, the causal relationships among microbiota, mitochondria, and AS remain unclear. The safety of herbs, including safe dosage, treatment duration, and potential side effects, has not been investigated in detail. Subsequent analyses are required to systematically elucidate a complete and accurate picture of gut microbiota, metabolites, mitochondria, and local atherosclerotic changes *via* metagenomic, metabolomic, and cytological methods.

Author contributions

YL and MW designed and directed the manuscript. YL wrote the manuscript. SY: revised the manuscript. JX and DL searched for relevant literature. JL and XW edited the figures and tables. All authors have read and approved the final manuscript.

Funding

The work was supported by the National Natural Science Foundation of China (No. 81202805, 82074254), the Beijing Natural Science Foundation (No.7172185), and Science and Technology Innovation Project of China Academy of Chinese Medical Sciences (No. C12021A01413).

Conflict of interest

The authors declare that the research was conducted in the absence of any commercial or financial relationships that could be construed as a potential conflict of interest.

Publisher's note

All claims expressed in this article are solely those of the authors and do not necessarily represent those of their affiliated organizations, or those of the publisher, the editors and the reviewers. Any product that may be evaluated in this article, or claim that may be made by its manufacturer, is not guaranteed or endorsed by the publisher.

References

Abudureyimu, M., Yu, W., Cao, R. Y., Zhang, Y., Liu, H., and Zheng, H. (2020). Berberine promotes cardiac function by upregulating PINK1/parkin-mediated mitophagy in heart failure. *Front. Physiol.* 11, 565751. doi:10.3389/fphys.2020.565751

Al-Obaide, M. A. I., Singh, R., Datta, P., Rewers-Felkins, K. A., Salguero, M. V., Al-Obaidi, I., et al. (2017). Gut microbiota-dependent trimethylamine-N-oxide and serum biomarkers in patients with T2DM and advanced CKD. *J. Clin. Med.* 6 (9), 86. doi:10.3390/jcm6090086

Andrade-Oliveira, V., Amano, M. T., Correa-Costa, M., Castoldi, A., Felizardo, R. J., de Almeida, D. C., et al. (2015). Gut bacteria products prevent AKI induced by ischemia-reperfusion. *J. Am. Soc. Nephrol.* 26 (8), 1877–1888. doi:10.1681/asn.2014030288

Anhê, F. F., Roy, D., Pilon, G., Dudonné, S., Matamoros, S., Varin, T. V., et al. (2015). A polyphenol-rich cranberry extract protects from diet-induced obesity, insulin resistance and intestinal inflammation in association with increased Akkermansia spp. population in the gut microbiota of mice. *Gut* 64 (6), 872–883. doi:10.1136/gutjnl-2014-307142

Anlu, W., Dongcheng, C., He, Z., Qiuyi, L., Yan, Z., Yu, Q., et al. (2019). Using herbal medicine to target the "microbiota-metabolism-immunity" axis as possible therapy for cardiovascular disease. *Pharmacol. Res.* 142, 205–222. doi:10.1016/j.phrs.2019.02.018

Arbeithuber, B., Hester, J., Cremona, M. A., Stoler, N., Zaidi, A., Higgins, B., et al. (2020). Age-related accumulation of de novo mitochondrial mutations in mammalian oocytes and somatic tissues. *PLoS Biol.* 18 (7), e3000745. doi:10.1371/journal.pbio.3000745

Ashar, F. N., Zhang, Y., Longchamps, R. J., Lane, J., Moes, A., Grove, M. L., et al. (2017). Association of mitochondrial DNA copy number with cardiovascular disease. *JAMA Cardiol.* 2 (11), 1247–1255. doi:10.1001/jamacardio.2017.3683

Assis, L. H. P., Dorighello, G. G., Rentz, T., de Souza, J. C., Vercesi, A. E., and de Oliveira, H. C. F. (2022). *In vivo* pravastatin treatment reverses hypercholesterolemia induced mitochondria-associated membranes contact sites, foam cell formation, and phagocytosis in macrophages. *Front. Mol. Biosci.* 9, 839428. doi:10.3389/fmolb.2022.839428

Ballinger, S. W., Patterson, C., Knight-Lozano, C. A., Burow, D. L., Conklin, C. A., Hu, Z., et al. (2002). Mitochondrial integrity and function in atherogenesis. *Circulation* 106 (5), 544–549. doi:10.1161/01.cir.0000023921.93743.89

Banoth, B., and Cassel, S. L. (2018). Mitochondria in innate immune signaling. *Transl. Res.* 202, 52–68. doi:10.1016/j.trsl.2018.07.014

Barrington, W. T., and Lusis, A. J. (2017). Atherosclerosis: Association between the gut microbiome and atherosclerosis. *Nat. Rev. Cardiol.* 14 (12), 699–700. doi:10.1038/nrcardio.2017.169

Bird, L. (2012). Innate immunity: Linking mitochondria and microbes to inflammasomes. *Nat. Rev. Immunol.* 12 (4), 229. doi:10.1038/nri3195

Bliksøen, M., Mariero, L. H., Torp, M. K., Baysa, A., Ytrehus, K., Haugen, F., et al. (2016). Extracellular mtDNA activates NF-κB via toll-like receptor 9 and induces cell death in cardiomyocytes. *Basic Res. Cardiol.* 111 (4), 42. doi:10.1007/s00395-016-0553-6

Bock, F. J., and Tait, S. W. G. (2020). Mitochondria as multifaceted regulators of cell death. *Nat. Rev. Mol. Cell Biol.* 21 (2), 85–100. doi:10.1038/s41580-019-0173-8

Bode, L. M., Bunzel, D., Huch, M., Cho, G. S., Ruhland, D., Bunzel, M., et al. (2013). *In vivo* and *in vitro* metabolism of trans-resveratrol by human gut microbiota. *Am. J. Clin. Nutr.* 97 (2), 295–309. doi:10.3945/ajcn.112.049379

Bogiatzi, C., Gloor, G., Allen-Vercoe, E., Reid, G., Wong, R. G., Urquhart, B. L., et al. (2018). Metabolic products of the intestinal microbiome and extremes of atherosclerosis. *Atherosclerosis* 273, 91–97. doi:10.1016/j.atherosclerosis.2018.04.015

Borisov, V. B., and Forte, E. (2021). Terminal oxidase cytochrome bd protects bacteria against hydrogen sulfide toxicity. *Biochem. Mosc.* 86 (1), 22–32. doi:10.1134/S000629792101003X

Boulangé, C. L., Neves, A. L., Chilloux, J., Nicholson, J. K., and Dumas, M. E. (2016). Impact of the gut microbiota on inflammation, obesity, and metabolic disease. *Genome Med.* 8 (1), 42. doi:10.1186/s13073-016-0303-2

Braakhuis, A. J., Nagulan, R., and Somerville, V. (2018). The effect of MitoQ on aging-related biomarkers: A systematic review and meta-analysis. *Oxid. Med. Cell Longev.* 2018, 8575263. doi:10.1155/2018/8575263

Brown, J. M., and Hazen, S. L. (2018). Microbial modulation of cardiovascular disease. *Nat. Rev. Microbiol.* 16 (3), 171–181. doi:10.1038/nrmicro.2017.149

Buskiewicz, I. A., Montgomery, T., Yasewicz, E. C., Huber, S. A., Murphy, M. P., Hartley, R. C., et al. (2016). Reactive oxygen species induce virus-independent MAVS oligomerization in systemic lupus erythematosus. *Sci. Signal* 9 (456), ra115. doi:10.1126/scisignal.aaf1933

Caesar, R., Tremaroli, V., Kovatcheva-Datchary, P., Cani, P. D., and Bäckhed, F. (2015). Crosstalk between gut microbiota and dietary lipids aggravates WAT inflammation through TLR signaling. *Cell Metab.* 22 (4), 658–668. doi:10.1016/j.cmet.2015.07.026

Cai, X., Zhang, Y., Li, M., Wu, J. H., Mai, L., Li, J., et al. (2020). Association between prediabetes and risk of all cause mortality and cardiovascular disease: Updated meta-analysis. *Bmj* 370, m2297. doi:10.1136/bmj.m2297

Calvert, J. W., Elston, M., Nicholson, C. K., Gundewar, S., Jha, S., Elrod, J. W., et al. (2010). Genetic and pharmacologic hydrogen sulfide therapy attenuates ischemia-induced heart failure in mice. *Circulation* 122 (1), 11–19. doi:10.1161/circulationaha.109.920991

Canugovi, C., Stevenson, M. D., Vendrov, A. E., Hayami, T., Robidoux, J., Xiao, H., et al. (2019). Increased mitochondrial NADPH oxidase 4 (NOX4) expression in aging is a causative factor in aortic stiffening. *Redox Biol.* 26, 101288. doi:10.1016/j.redox.2019.101288

Cao, H., Jia, Q., Yan, L., Chen, C., Xing, S., and Shen, D. (2019). Quercetin suppresses the progression of atherosclerosis by regulating MST1-mediated autophagy in ox-LDL-induced RAW264.7 macrophage foam cells. *Int. J. Mol. Sci.* 20 (23), 6093. doi:10.3390/ijms20236093

Chen, J., Wright, K., Davis, J. M., Jeraldo, P., Marietta, E. V., Murray, J., et al. (2016). An expansion of rare lineage intestinal microbes characterizes rheumatoid arthritis. *Genome Med.* 8 (1), 43. doi:10.1186/s13073-016-0299-7

Chen, M. L., Yi, L., Zhang, Y., Zhou, X., Ran, L., Yang, J., et al. (2016). Resveratrol attenuates trimethylamine-N-oxide (TMAO)-Induced atherosclerosis by regulating TMAO synthesis and bile acid metabolism via remodeling of the gut microbiota. *mBio* 7 (2), e02210–e02215. doi:10.1128/mBio.02210-15

Chen, M. L., Zhu, X. H., Ran, L., Lang, H. D., Yi, L., and Mi, M. T. (2017). Trimethylamine-N-Oxide induces vascular inflammation by activating the NLRP3 inflammasome through the SIRT3-SOD2-mtROS signaling pathway. *J. Am. Heart Assoc.* 6 (9), e006347. doi:10.1161/jaha.117.006347

Chen, X., Li, H., Wang, Z., Zhou, Q., Chen, S., Yang, B., et al. (2020). Quercetin protects the vascular endothelium against iron overload damages via ROS/ADMA/DDAHII/eNOS/NO pathway. *Eur. J. Pharmacol.* 868, 172885. doi:10.1016/j.ejphar.2019.172885

Chen, X., Xie, Q., Zhu, Y., Xu, J., Lin, G., Liu, S., et al. (2021). Cardio-protective effect of tetrahydrocurcumin, the primary hydrogenated metabolite of curcumin *in vivo* and *in vitro*: Induction of apoptosis and autophagy via PI3K/AKT/mTOR pathways. *Eur. J. Pharmacol.* 911, 174495. doi:10.1016/j.ejphar.2021.174495

Chen, Z., Zhou, Q., Chen, J., Yang, Y., Chen, W., Mao, H., et al. (2022). MCU-dependent mitochondrial calcium uptake-induced mitophagy contributes to apelin-13-stimulated VSMCs proliferation. *Vasc. Pharmacol.* 144, 106979. doi:10.1016/j.vph.2022.106979

Cheng, F., Wang, Y., Li, J., Su, C., Wu, F., Xia, W. H., et al. (2013). Berberine improves endothelial function by reducing endothelial microparticles-mediated oxidative stress in humans. *Int. J. Cardiol.* 167 (3), 936–942. doi:10.1016/j.ijcard.2012.03.090

Cho, Y. E., Basu, A., Dai, A., Heldak, M., and Makino, A. (2013). Coronary endothelial dysfunction and mitochondrial reactive oxygen species in type 2 diabetic mice. *Am. J. Physiol. Cell Physiol.* 305 (10), C1033–C1040. doi:10.1152/ajpcell.00234.2013

Choi, S. H., Agatisa-Boyle, C., Gonen, A., Kim, A., Kim, J., Alekseeva, E., et al. (2021). Intracellular AIBP (apolipoprotein A-I binding protein) regulates oxidized LDL (Low-Density lipoprotein)-induced mitophagy in macrophages. *Arterioscler. Thromb. Vasc. Biol.* 41 (2), e82–e96. doi:10.1161/atvbaha.120.315485

Chowdhury, A., Witte, S., and Aich, A. (2022). Role of mitochondrial nucleic acid sensing pathways in health and patho-physiology. *Front. Cell Dev. Biol.* 10, 796066. doi:10.3389/fcell.2022.796066

Clark, A., and Mach, N. (2017). The crosstalk between the gut microbiota and mitochondria during exercise. *Front. Physiol.* 8, 319. doi:10.3389/fphys.2017.00319

Cox, F. F., Misiou, A., Vierkant, A., Ale-Agha, N., Grandoch, M., Haendeler, J., et al. (2022). Protective effects of curcumin in cardiovascular diseases-impact on oxidative stress and mitochondria. *Cells* 11 (3), 342. doi:10.3390/cells11030342

Csiszar, A., Gautam, T., Sosnowska, D., Tarantini, S., Banki, E., Tucsek, Z., et al. (2014). Caloric restriction confers persistent anti-oxidative, pro-angiogenic, and anti-inflammatory effects and promotes anti-aging miRNA expression profile in cerebromicrovascular endothelial cells of aged rats. *Am. J. Physiol. Heart Circ. Physiol.* 307 (3), H292–H306. doi:10.1152/ajpheart.00307.2014

Csiszar, A., Labinskyy, N., Pinto, J. T., Ballabh, P., Zhang, H., Losonczy, G., et al. (2009). Resveratrol induces mitochondrial biogenesis in endothelial cells. *Am. J. Physiol. Heart Circ. Physiol.* 297 (1), H13–H20. doi:10.1152/ajpheart.00368.2009

Csiszar, A., Labinskyy, N., Podlutsky, A., Kaminski, P. M., Wolin, M. S., Zhang, C., et al. (2008). Vasoprotective effects of resveratrol and SIRT1: Attenuation of cigarette smoke-induced oxidative stress and proinflammatory phenotypic alterations. *Am. J. Physiol. Heart Circ. Physiol.* 294 (6), H2721–H2735. doi:10.1152/ajpheart.00235.2008

Cui, J., Li, Z., Zhuang, S., Qi, S., Li, L., Zhou, J., et al. (2018). Melatonin alleviates inflammation-induced apoptosis in human umbilical vein endothelial cells via suppression of Ca(2+)-XO-ROS-Drp1-mitochondrial fission axis by activation of AMPK/SERCA2a pathway. *Cell Stress Chaperones* 23 (2), 281–293. doi:10.1007/s12192-017-0841-6

Cui, L., Li, Z., Chang, X., Cong, G., and Hao, L. (2017). Quercetin attenuates vascular calcification by inhibiting oxidative stress and mitochondrial fission. *Vasc. Pharmacol.* 88, 21–29. doi:10.1016/j.vph.2016.11.006

Dagenais, G. R., Leong, D. P., Rangarajan, S., Lanas, F., Lopez-Jaramillo, P., Gupta, R., et al. (2020). Variations in common diseases, hospital admissions, and deaths in middle-aged adults in 21 countries from five continents (PURE): A prospective cohort study. *Lancet* 395 (10226), 785–794. doi:10.1016/s0140-6736(19)32007-0

Davinelli, S., Sapere, N., Visentin, M., Zella, D., and Scapagnini, G. (2013). Enhancement of mitochondrial biogenesis with polyphenols: Combined effects of resveratrol and equol in human endothelial cells. *Immun. Ageing* 10 (1), 28. doi:10.1186/1742-4933-10-28

Degli Esposti, M., Chouaia, B., Comandatore, F., Crotti, E., Sassera, D., Lievens, P. M., et al. (2014). Evolution of mitochondria reconstructed from the energy metabolism of living bacteria. *PLoS One* 9 (5), e96566. doi:10.1371/journal.pone.0096566

den Besten, G., van Eunen, K., Groen, A. K., Venema, K., Reijngoud, D. J., and Bakker, B. M. (2013). The role of short-chain fatty acids in the interplay between diet, gut microbiota, and host energy metabolism. *J. Lipid Res.* 54 (9), 2325–2340. doi:10.1194/jlr.R036012

Ding, Z., Liu, S., Wang, X., Mathur, P., Dai, Y., Theus, S., et al. (2016). Cross-talk between PCSK9 and damaged mtDNA in vascular smooth muscle cells: Role in apoptosis. *Antioxid. Redox Signal* 25 (18), 997–1008. doi:10.1089/ars.2016.6631

Dorighello, G. G., Assis, L. H. P., Rentz, T., Morari, J., Santana, M. F. M., Passarelli, M., et al. (2022). Novel role of CETP in macrophages: Reduction of mitochondrial oxidants production and modulation of cell immune-metabolic profile. *Antioxidants (Basel)* 11 (9), 1734. doi:10.3390/antiox11091734

Duan, M., Chen, H., Yin, L., Zhu, X., Novák, P., Lv, Y., et al. (2022). Mitochondrial apolipoprotein A-I binding protein alleviates atherosclerosis by regulating mitophagy and macrophage polarization. *Cell Commun. Signal* 20 (1), 60. doi:10.1186/s12964-022-00858-8

Dumont, A., Lee, M., Barouillet, T., Murphy, A., and Yvan-Charvet, L. (2021). Mitochondria orchestrate macrophage effector functions in atherosclerosis. *Mol. Asp. Med.* 77, 100922. doi:10.1016/j.mam.2020.100922

Fang, C., Wei, X., and Wei, Y. (2016). Mitochondrial DNA in the regulation of innate immune responses. *Protein Cell* 7 (1), 11–16. doi:10.1007/s13238-015-0222-9

Fedotcheva, N., Olenin, A., and Beloborodova, N. (2021). Influence of microbial metabolites on the nonspecific permeability of mitochondrial membranes under conditions of acidosis and loading with calcium and iron ions. *Biomedicines* 9 (5), 558. doi:10.3390/biomedicines9050558

Fontana, G. A., and Gahlon, H. L. (2020). Mechanisms of replication and repair in mitochondrial DNA deletion formation. *Nucleic Acids Res.* 48 (20), 11244–11258. doi:10.1093/nar/gkaa804

Forrester, S. J., Kikuchi, D. S., Hernandes, M. S., Xu, Q., and Griendling, K. K. (2018). Reactive oxygen species in metabolic and inflammatory signaling. *Circ. Res.* 122 (6), 877–902. doi:10.1161/circresaha.117.311401

Forte, M., Bianchi, F., Cotugno, M., Marchitti, S., Stanzione, R., Maglione, V., et al. (2021). An interplay between UCP2 and ROS protects cells from high-salt-induced injury through autophagy stimulation. *Cell Death Dis.* 12 (10), 919. doi:10.1038/s41419-021-04188-4

Gilkerson, R. W., De Vries, R. L., Lebot, P., Wikstrom, J. D., Torgyekes, E., Shirihai, O. S., et al. (2012). Mitochondrial autophagy in cells with mtDNA mutations results from synergistic loss of transmembrane potential and mTORC1 inhibition. *Hum. Mol. Genet.* 21 (5), 978–990. doi:10.1093/hmg/ddr529

Gioscia-Ryan, R. A., Battson, M. L., Cuevas, L. M., Eng, J. S., Murphy, M. P., and Seals, D. R. (2018). Mitochondria-targeted antioxidant therapy with MitoQ ameliorates aortic stiffening in old mice. *J. Appl. Physiol.* 124 (5), 1194–1202. doi:10.1152/japplphysiol.00670.2017

Giusti, L., Gabriele, M., Penno, G., Garofolo, M., Longo, V., Del Prato, S., et al. (2017). A fermented whole grain prevents lipopolysaccharides-induced dysfunction in human endothelial progenitor cells. *Oxid. Med. Cell Longev.* 2017, 1026268. doi:10.1155/2017/1026268

Gkikas, I., Palikaras, K., and Tavernarakis, N. (2018). The role of mitophagy in innate immunity. *Front. Immunol.* 9, 1283. doi:10.3389/fimmu.2018.01283

Gomez-Arango, L. F., Barrett, H. L., Wilkinson, S. A., Callaway, L. K., McIntyre, H. D., Morrison, M., et al. (2018). Low dietary fiber intake increases Collinsella abundance in the gut microbiota of overweight and obese pregnant women. *Gut Microbes* 9 (3), 189–201. doi:10.1080/19490976.2017.1406584

Granatiero, V., Giorgio, V., Calì, T., Patron, M., Brini, M., Bernardi, P., et al. (2016). Reduced mitochondrial Ca(2+) transients stimulate autophagy in human fibroblasts carrying the 13514A>G mutation of the ND5 subunit of NADH dehydrogenase. *Cell Death Differ.* 23 (2), 231–241. doi:10.1038/cdd.2015.84

Greaves, L. C., Nooteboom, M., Elson, J. L., Tuppen, H. A., Taylor, G. A., Commane, D. M., et al. (2014). Clonal expansion of early to mid-life mitochondrial DNA point mutations drives mitochondrial dysfunction during human ageing. *PLoS Genet.* 10 (9), e1004620. doi:10.1371/journal.pgen.1004620

Gregory, J. C., Buffa, J. A., Org, E., Wang, Z., Levison, B. S., Zhu, W., et al. (2015). Transmission of atherosclerosis susceptibility with gut microbial transplantation. *J. Biol. Chem.* 290 (9), 5647–5660. doi:10.1074/jbc.M114.618249

Gupta, P., Jordan, C. T., Mitov, M. I., Butterfield, D. A., Hilt, J. Z., and Dziubla, T. D. (2016). Controlled curcumin release via conjugation into PBAE nanogels enhances mitochondrial protection against oxidative stress. *Int. J. Pharm.* 511 (2), 1012–1021. doi:10.1016/j.ijpharm.2016.07.071

Habtemariam, S. (2020). Berberine pharmacology and the gut microbiota: A hidden therapeutic link. *Pharmacol. Res.* 155, 104722. doi:10.1016/j.phrs.2020.104722

Han, J. H., Park, J., Myung, S. H., Lee, S. H., Kim, H. Y., Kim, K. S., et al. (2019). Noxa mitochondrial targeting domain induces necrosis via VDAC2 and mitochondrial catastrophe. *Cell Death Dis.* 10 (7), 519. doi:10.1038/s41419-019-1753-4

Hawkins, B. J., Solt, L. A., Chowdhury, I., Kazi, A. S., Abid, M. R., Aird, W. C., et al. (2007). G protein-coupled receptor Ca2+-linked mitochondrial reactive oxygen species are essential for endothelial/leukocyte adherence. *Mol. Cell Biol.* 27 (21), 7582–7593. doi:10.1128/mcb.00493-07

He, D., Sougioultzis, S., Hagen, S., Liu, J., Keates, S., Keates, A. C., et al. (2002). *Clostridium difficile* toxin A triggers human colonocyte IL-8 release via mitochondrial oxygen radical generation. *Gastroenterology* 122 (4), 1048–1057. doi:10.1053/gast.2002.32386

Heid, M. E., Keyel, P. A., Kamga, C., Shiva, S., Watkins, S. C., and Salter, R. D. (2013). Mitochondrial reactive oxygen species induces NLRP3-dependent lysosomal damage and inflammasome activation. *J. Immunol.* 191 (10), 5230–5238. doi:10.4049/jimmunol.1301490

Hernandez, L. D., Pypaert, M., Flavell, R. A., and Galán, J. E. (2003). A Salmonella protein causes macrophage cell death by inducing autophagy. *J. Cell Biol.* 163 (5), 1123–1131. doi:10.1083/jcb.200309161

Hong, T., Zou, J., Jiang, X., Yang, J., Cao, Z., He, Y., et al. (2022). Curcumin supplementation ameliorates bile cholesterol supersaturation in hamsters by modulating gut microbiota and cholesterol absorption. *Nutrients* 14 (9), 1828. doi:10.3390/nu14091828

Hotz, M. J., Qing, D., Shashaty, M. G. S., Zhang, P., Faust, H., Sondheimer, N., et al. (2018). Red blood cells homeostatically bind mitochondrial DNA through TLR9 to maintain quiescence and to prevent lung injury. *Am. J. Respir. Crit. Care Med.* 197 (4), 470–480. doi:10.1164/rccm.201706-1161OC

Hu, W., Huang, L., Zhou, Z., Yin, L., and Tang, J. (2021). Diallyl disulfide (DADS) ameliorates intestinal Candida albicans infection by modulating the gut microbiota and metabolites and providing intestinal protection in mice. *Front. Cell Infect. Microbiol.* 11, 743454. doi:10.3389/fcimb.2021.743454

Hu, Y., Ehli, E. A., Kittelsrud, J., Ronan, P. J., Munger, K., Downey, T., et al. (2012). Lipid-lowering effect of berberine in human subjects and rats. *Phytomedicine* 19 (10), 861–867. doi:10.1016/j.phymed.2012.05.009

Huang, Y., Wang, J., Quan, G., Wang, X., Yang, L., and Zhong, L. (2014). Lactobacillus acidophilus ATCC 4356 prevents atherosclerosis via inhibition of intestinal cholesterol absorption in apolipoprotein E-knockout mice. *Appl. Environ. Microbiol.* 80 (24), 7496–7504. doi:10.1128/aem.02926-14

Hung, C. H., Lin, Y. C., Tsai, Y. G., Lin, Y. C., Kuo, C. H., Tsai, M. L., et al. (2021). Acrylamide induces mitophagy and alters macrophage phenotype via reactive oxygen species generation. *Int. J. Mol. Sci.* 22 (4), 1683. doi:10.3390/ijms22041683

Iyer, S. S., He, Q., Janczy, J. R., Elliott, E. I., Zhong, Z., Olivier, A. K., et al. (2013). Mitochondrial cardiolipin is required for Nlrp3 inflammasome activation. *Immunity* 39 (2), 311–323. doi:10.1016/j.immuni.2013.08.001

Jackson, D. N., and Theiss, A. L. (2020). Gut bacteria signaling to mitochondria in intestinal inflammation and cancer. *Gut Microbes* 11 (3), 285–304. doi:10.1080/19490976.2019.1592421

Jenner, A., Peña-Blanco, A., Salvador-Gallego, R., Ugarte-Uribe, B., Zollo, C., Ganief, T., et al. (2022). DRP1 interacts directly with BAX to induce its activation and apoptosis. *Embo J.* 41 (8), e108587. doi:10.15252/embj.2021108587

Jeong, S. Y., and Seol, D. W. (2008). The role of mitochondria in apoptosis. *BMB Rep.* 41 (1), 11–22. doi:10.5483/bmbrep.2008.41.1.011

Jiang, Y. H., Jiang, L. Y., Wang, Y. C., Ma, D. F., and Li, X. (2020). Quercetin attenuates atherosclerosis via modulating oxidized LDL-induced endothelial cellular senescence. *Front. Pharmacol.* 11, 512. doi:10.3389/fphar.2020.00512

Jin, Y., Liu, Y., Xu, L., Xu, J., Xiong, Y., Peng, Y., et al. (2022). Novel role for caspase 1 inhibitor VX765 in suppressing NLRP3 inflammasome assembly and atherosclerosis via promoting mitophagy and efferocytosis. *Cell Death Dis.* 13 (5), 512. doi:10.1038/s41419-022-04966-8

Jonsson, A. L., and Bäckhed, F. (2017). Role of gut microbiota in atherosclerosis. *Nat. Rev. Cardiol.* 14 (2), 79–87. doi:10.1038/nrcardio.2016.183

Juárez-Fernández, M., Goikoetxea-Usandizaga, N., Porras, D., García-Mediavilla, M. V., Bravo, M., Serrano-Maciá, M., et al. (2022). Enhanced mitochondrial activity reshapes a gut microbiota profile that delays NASH progression. *Hepatology*. doi:10.1002/hep.32705

Kalghatgi, S., Spina, C. S., Costello, J. C., Liesa, M., Morones-Ramirez, J. R., Slomovic, S., et al. (2013). Bactericidal antibiotics induce mitochondrial dysfunction and oxidative damage in Mammalian cells. *Sci. Transl. Med.* 5 (192), 192ra85. doi:10.1126/scitranslmed.3006055

Kampa, R. P., Sęk, A., Szewczyk, A., and Bednarczyk, P. (2021). Cytoprotective effects of the flavonoid quercetin by activating mitochondrial BK(Ca) channels in endothelial cells. *Biomed. Pharmacother.* 142, 112039. doi:10.1016/j.biopha.2021.112039

Kappel, B. A., De Angelis, L., Heiser, M., Ballanti, M., Stoehr, R., Goettsch, C., et al. (2020). Cross-omics analysis revealed gut microbiome-related metabolic pathways underlying atherosclerosis development after antibiotics treatment. *Mol. Metab.* 36, 100976. doi:10.1016/j.molmet.2020.100976

Karunakaran, D., Thrush, A. B., Nguyen, M. A., Richards, L., Geoffrion, M., Singaravelu, R., et al. (2015). Macrophage mitochondrial energy status regulates cholesterol efflux and is enhanced by anti-miR33 in atherosclerosis. *Circ. Res.* 117 (3), 266–278. doi:10.1161/circresaha.117.305624

Katsnelson, M. A., Lozada-Soto, K. M., Russo, H. M., Miller, B. A., and Dubyak, G. R. (2016). NLRP3 inflammasome signaling is activated by low-level lysosome disruption but inhibited by extensive lysosome disruption: Roles for K+ efflux and Ca2+ influx. *Am. J. Physiol. Cell Physiol.* 311 (1), C83–c100. doi:10.1152/ajpcell.00298.2015

Khatua, T. N., Dinda, A. K., Putcha, U. K., and Banerjee, S. K. (2016). Diallyl disulfide ameliorates isoproterenol induced cardiac hypertrophy activating mitochondrial biogenesis via eNOS-Nrf2-Tfam pathway in rats. *Biochem. Biophys. Rep.* 5, 77–88. doi:10.1016/j.bbrep.2015.11.008

Khrapko, K. (2011). The timing of mitochondrial DNA mutations in aging. *Nat. Genet.* 43 (8), 726–727. doi:10.1038/ng.895

Kim, E. N., Kim, M. Y., Lim, J. H., Kim, Y., Shin, S. J., Park, C. W., et al. (2018). The protective effect of resveratrol on vascular aging by modulation of the renin-angiotensin system. *Atherosclerosis* 270, 123–131. doi:10.1016/j.atherosclerosis.2018.01.043

Kim, J., Gupta, R., Blanco, L. P., Yang, S., Shteinfer-Kuzmine, A., Wang, K., et al. (2019). VDAC oligomers form mitochondrial pores to release mtDNA fragments and promote lupus-like disease. *Science* 366 (6472), 1531–1536. doi:10.1126/science.aav4011

Kirichenko, T. V., Markina, Y. V., Sukhorukov, V. N., Khotina, V. A., Wu, W. K., and Orekhov, A. N. (2020). A novel insight at atherogenesis: The role of microbiome. *Front. Cell Dev. Biol.* 8, 586189. doi:10.3389/fcell.2020.586189

Kleele, T., Rey, T., Winter, J., Zaganelli, S., Mahecic, D., Perreten Lambert, H., et al. (2021). Distinct fission signatures predict mitochondrial degradation or biogenesis. *Nature* 593 (7859), 435–439. doi:10.1038/s41586-021-03510-6

Ko, J., Kang, H. J., Kim, D. A., Kim, M. J., Ryu, E. S., Lee, S., et al. (2019). Uric acid induced the phenotype transition of vascular endothelial cells via induction of oxidative stress and glycocalyx shedding. *Faseb J.* 33 (12), 13334–13345. doi:10.1096/fj.201901148R

Koeth, R. A., Wang, Z., Levison, B. S., Buffa, J. A., Org, E., Sheehy, B. T., et al. (2013). Intestinal microbiota metabolism of L-carnitine, a nutrient in red meat, promotes atherosclerosis. *Nat. Med.* 19 (5), 576–585. doi:10.1038/nm.3145

Koren, O., Spor, A., Felin, J., Fåk, F., Stombaugh, J., Tremaroli, V., et al. (2011). Human oral, gut, and plaque microbiota in patients with atherosclerosis. *Proc. Natl. Acad. Sci. U. S. A.* 108 (1), 4592–4598. doi:10.1073/pnas.1011383107

Korytowski, W., Wawak, K., Pabisz, P., Schmitt, J. C., Chadwick, A. C., Sahoo, D., et al. (2015). Impairment of macrophage cholesterol efflux by cholesterol hydroperoxide trafficking: Implications for atherogenesis under oxidative stress. *Arterioscler. Thromb. Vasc. Biol.* 35 (10), 2104–2113. doi:10.1161/atvbaha.115.306210

Kubli, D. A., and Gustafsson, A. B. (2012). Mitochondria and mitophagy: The yin and yang of cell death control. *Circ. Res.* 111 (9), 1208–1221. doi:10.1161/circresaha.112.265819

Kubli, D. A., Zhang, X., Lee, Y., Hanna, R. A., Quinsay, M. N., Nguyen, C. K., et al. (2013). Parkin protein deficiency exacerbates cardiac injury and reduces survival following myocardial infarction. *J. Biol. Chem.* 288 (2), 915–926. doi:10.1074/jbc.M112.411363

Kuipers, F., Bloks, V. W., and Groen, A. K. (2014). Beyond intestinal soap-bile acids in metabolic control. *Nat. Rev. Endocrinol.* 10 (8), 488–498. doi:10.1038/nrendo.2014.60

Lampropoulou, V., Sergushichev, A., Bambouskova, M., Nair, S., Vincent, E. E., Loginicheva, E., et al. (2016). Itaconate links inhibition of succinate dehydrogenase with macrophage metabolic remodeling and regulation of inflammation. *Cell Metab.* 24 (1), 158–166. doi:10.1016/j.cmet.2016.06.004

Lawton, J. S., Tamis-Holland, J. E., Bangalore, S., Bates, E. R., Beckie, T. M., Bischoff, J. M., et al. (2022). 2021 ACC/AHA/SCAI guideline for coronary artery revascularization: Executive summary: A report of the American college of cardiology/American heart association joint committee on clinical practice guidelines. *Circulation* 145 (3), e4–e17. doi:10.1161/cir.0000000000001039

Le Roy, T., Moens de Hase, E., Van Hul, M., Paquot, A., Pelicaen, R., Régnier, M., et al. (2022). Dysosmobacter welbionis is a newly isolated human commensal bacterium preventing diet-induced obesity and metabolic disorders in mice. *Gut* 71 (3), 534–543. doi:10.1136/gutjnl-2020-323778

Li, C., Tan, Y., Wu, J., Ma, Q., Bai, S., Xia, Z., et al. (2020). Resveratrol improves bnip3-related mitophagy and attenuates high-fat-induced endothelial dysfunction. *Front. Cell Dev. Biol.* 8, 796. doi:10.3389/fcell.2020.00796

Li, J., Huynh, L., Cornwell, W. D., Tang, M. S., Simborio, H., Huang, J., et al. (2021). Electronic cigarettes induce mitochondrial DNA damage and trigger TLR9 (Toll-Like receptor 9)-mediated atherosclerosis. *Arterioscler. Thromb. Vasc. Biol.* 41 (2), 839–853. doi:10.1161/atvbaha.120.315556

Li, J., Jia, H., Cai, X., Zhong, H., Feng, Q., Sunagawa, S., et al. (2014). An integrated catalog of reference genes in the human gut microbiome. *Nat. Biotechnol.* 32 (8), 834–841. doi:10.1038/nbt.2942

Li, J., Zeng, Q., Xiong, Z., Xian, G., Liu, Z., Zhan, Q., et al. (2022). Trimethylamine N-oxide induces osteogenic responses in human aortic valve interstitial cells *in vitro* and aggravates aortic valve lesions in mice. *Cardiovasc Res.* 118 (8), 2018–2030. doi:10.1093/cvr/cvab243

Li, M., Zhou, W., Dang, Y., Li, C., Ji, G., and Zhang, L. (2020). Berberine compounds improves hyperglycemia via microbiome mediated colonic TGR5-GLP pathway in db/db mice. *Biomed. Pharmacother.* 132, 110953. doi:10.1016/j.biopha.2020.110953

Li, S., and Yang, G. (2015). Hydrogen sulfide maintains mitochondrial DNA replication via demethylation of TFAM. *Antioxid. Redox Signal* 23 (7), 630–642. doi:10.1089/ars.2014.6186

Li, X., Su, C., Jiang, Z., Yang, Y., Zhang, Y., Yang, M., et al. (2021). Berberine attenuates choline-induced atherosclerosis by inhibiting trimethylamine and trimethylamine-N-oxide production via manipulating the gut microbiome. *NPJ Biofilms Microbiomes* 7 (1), 36. doi:10.1038/s41522-021-00205-8

Li, Z., Li, Q., Wang, L., Li, C., Xu, M., Duan, Y., et al. (2021). Targeting mitochondria-inflammation circle by renal denervation reduces atheroprone endothelial phenotypes and atherosclerosis. *Redox Biol.* 47, 102156. doi:10.1016/j.redox.2021.102156

Lian N, N., Mao, X., Su, Y., Wang, Y., Wang, Y., Wang, Y., et al. (2022). Hydrogen-rich medium ameliorates lipopolysaccharides-induced mitochondrial fission and dysfunction in human umbilical vein endothelial cells (HUVECs) via up-regulating HO-1 expression. *Int. Immunopharmacol.* 110, 108936. doi:10.1016/j.intimp.2022.108936

Lian, W. S., Wang, F. S., Chen, Y. S., Tsai, M. H., Chao, H. R., Jahr, H., et al. (2022). Gut microbiota ecosystem governance of host inflammation, mitochondrial respiration and skeletal homeostasis. *Biomedicines* 10 (4), 860. doi:10.3390/biomedicines10040860

Liang, Y., Chu, P. H., Tian, L., Ho, K. F., Ip, M. S. M., and Mak, J. C. W. (2022). Targeting mitochondrial permeability transition pore ameliorates PM(2.5)-induced mitochondrial dysfunction in airway epithelial cells. *Environ. Pollut.* 295, 118720. doi:10.1016/j.envpol.2021.118720

Libiad, M., Vitvitsky, V., Bostelaar, T., Bak, D. W., Lee, H. J., Sakamoto, N., et al. (2019). Hydrogen sulfide perturbs mitochondrial bioenergetics and triggers metabolic reprogramming in colon cells. *J. Biol. Chem.* 294 (32), 12077–12090. doi:10.1074/jbc.RA119.009442

Lim, J. H., Woo, J. S., and Shin, Y. W. (2009). Cilostazol protects endothelial cells against lipopolysaccharide-induced apoptosis through ERK1/2- and P38 MAPK-dependent pathways. *Korean J. Intern Med.* 24 (2), 113–122. doi:10.3904/kjim.2009.24.2.113

Lim, S., Lee, S. Y., Seo, H. H., Ham, O., Lee, C., Park, J. H., et al. (2015). Regulation of mitochondrial morphology by positive feedback interaction between PKCδ and Drp1 in vascular smooth muscle cell. *J. Cell Biochem.* 116 (4), 648–660. doi:10.1002/jcb.25016

Lindskog Jonsson, A., Hållenius, F. F., Akrami, R., Johansson, E., Wester, P., Arnerlöv, C., et al. (2017). Bacterial profile in human atherosclerotic plaques. *Atherosclerosis* 263, 177–183. doi:10.1016/j.atherosclerosis.2017.06.016

Liu, H., You, L., Wu, J., Zhao, M., Guo, R., Zhang, H., et al. (2020). Berberine suppresses influenza virus-triggered NLRP3 inflammasome activation in macrophages by inducing mitophagy and decreasing mitochondrial ROS. *J. Leukoc. Biol.* 108 (1), 253–266. doi:10.1002/JLB.3MA0320-358RR

Liu, L., Gu, L., Ma, Q., Zhu, D., and Huang, X. (2013). Resveratrol attenuates hydrogen peroxide-induced apoptosis in human umbilical vein endothelial cells. *Eur. Rev. Med. Pharmacol. Sci.* 17 (1), 88–94.

Liu, L. L., Yan, L., Chen, Y. H., Zeng, G. H., Zhou, Y., Chen, H. P., et al. (2014). A role for diallyl trisulfide in mitochondrial antioxidative stress contributes to its protective effects against vascular endothelial impairment. *Eur. J. Pharmacol.* 725, 23–31. doi:10.1016/j.ejphar.2014.01.010

Liu, Q., Li, Y., Song, X., Wang, J., He, Z., Zhu, J., et al. (2020). Both gut microbiota and cytokines act to atherosclerosis in ApoE-/- mice. *Microb. Pathog.* 138, 103827. doi:10.1016/j.micpath.2019.103827

Liu, Q., Zhang, D., Hu, D., Zhou, X., and Zhou, Y. (2018). The role of mitochondria in NLRP3 inflammasome activation. *Mol. Immunol.* 103, 115–124. doi:10.1016/j.molimm.2018.09.010

Liu, Y., Chen, X., and Li, J. (2017). Resveratrol protects against oxidized low-density lipoprotein-induced human umbilical vein endothelial cell apoptosis via inhibition of mitochondrial-derived oxidative stress. *Mol. Med. Rep.* 15 (5), 2457–2464. doi:10.3892/mmr.2017.6304

Liu, Y., Liu, S., Zhao, Z., Song, X., Qu, H., and Liu, H. (2021). Phenylacetylglutamine is associated with the degree of coronary atherosclerotic severity assessed by coronary computed tomographic angiography in patients with suspected coronary artery disease. *Atherosclerosis* 333, 75–82. doi:10.1016/j.atherosclerosis.2021.08.029

Longchamp, A., Mirabella, T., Arduini, A., MacArthur, M. R., Das, A., Treviño-Villarreal, J. H., et al. (2018). Amino acid restriction triggers angiogenesis via GCN2/ATF4 regulation of VEGF and H(2)S production. *Cell* 173 (1), 117–129. e114. doi:10.1016/j.cell.2018.03.001

López-Salazar, V., Tapia, M. S., Tobón-Cornejo, S., Díaz, D., Alemán-Escondrillas, G., Granados-Portillo, O., et al. (2021). Consumption of soybean or olive oil at recommended concentrations increased the intestinal microbiota diversity and insulin sensitivity and prevented fatty liver compared to the effects of coconut oil. *J. Nutr. Biochem.* 94, 108751. doi:10.1016/j.jnutbio.2021.108751

Lopresti, A. L. (2018). The problem of curcumin and its bioavailability: Could its gastrointestinal influence contribute to its overall health-enhancing effects? *Adv. Nutr.* 9 (1), 41–50. doi:10.1093/advances/nmx011

Lu, Y., Wang, R. H., Guo, B. B., and Jia, Y. P. (2016). Quercetin inhibits angiotensin II induced apoptosis via mitochondrial pathway in human umbilical vein endothelial cells. *Eur. Rev. Med. Pharmacol. Sci.* 20 (8), 1609–1616.

Lv, Z., Shan, X., Tu, Q., Wang, J., Chen, J., and Yang, Y. (2021). Ginkgolide B treatment regulated intestinal flora to improve high-fat diet induced atherosclerosis in ApoE(-/-) mice. *Biomed. Pharmacother.* 134, 111100. doi:10.1016/j.biopha.2020.111100

Ma, J., Fu, Q., Wang, Z., Zhou, P., Qiao, S., Wang, B., et al. (2019). Sodium hydrosulfide mitigates dexamethasone-induced osteoblast dysfunction by interfering with mitochondrial function. *Biotechnol. Appl. Biochem.* 66 (4), 690–697. doi:10.1002/bab.1786

Ma, S., Chen, J., Feng, J., Zhang, R., Fan, M., Han, D., et al. (2018). Melatonin ameliorates the progression of atherosclerosis via mitophagy activation and NLRP3 inflammasome inhibition. *Oxid. Med. Cell Longev.* 2018, 9286458. doi:10.1155/2018/9286458

Ma, S. R., Tong, Q., Lin, Y., Pan, L. B., Fu, J., Peng, R., et al. (2022). Berberine treats atherosclerosis via a vitamine-like effect down-regulating Choline-TMA-TMAO production pathway in gut microbiota. *Signal Transduct. Target Ther.* 7 (1), 207. doi:10.1038/s41392-022-01027-6

Ma, Y., Huang, Z., Zhou, Z., He, X., Wang, Y., Meng, C., et al. (2018). A novel antioxidant Mito-Tempol inhibits ox-LDL-induced foam cell formation through restoration of autophagy flux. *Free Radic. Biol. Med.* 129, 463–472. doi:10.1016/j.freeradbiomed.2018.10.412

Mahmud, S. A., Qureshi, M. A., and Pellegrino, M. W. (2021). On the offense and defense: Mitochondrial recovery programs amidst targeted pathogenic assault. *FEBS J.* doi:10.1111/febs.16126

Maimaitijiang, A., Zhuang, X., Jiang, X., and Li, Y. (2016). Dynamin-related protein inhibitor downregulates reactive oxygen species levels to indirectly suppress high glucose-induced hyperproliferation of vascular smooth muscle cells. *Biochem. Biophys. Res. Commun.* 471 (4), 474–478. doi:10.1016/j.bbrc.2016.02.051

Makrecka-Kuka, M., Volska, K., Antone, U., Vilskersts, R., Grinberga, S., Bandere, D., et al. (2017). Trimethylamine N-oxide impairs pyruvate and fatty acid oxidation in cardiac mitochondria. *Toxicol. Lett.* 267, 32–38. doi:10.1016/j.toxlet.2016.12.017

McArthur, K., Whitehead, L. W., Heddleston, J. M., Li, L., Padman, B. S., Oorschot, V., et al. (2018). BAK/BAX macropores facilitate mitochondrial herniation and mtDNA efflux during apoptosis. *Science* 359 (6378), eaao6047. doi:10.1126/science.aao6047

McFadden, R. M., Larmonier, C. B., Shehab, K. W., Midura-Kiela, M., Ramalingam, R., Harrison, C. A., et al. (2015). The role of curcumin in modulating colonic microbiota

during colitis and colon cancer prevention. *Inflamm. Bowel Dis.* 21 (11), 2483–2494. doi:10.1097/mib.0000000000000522

Michael, D. R., Davies, T. S., Moss, J. W. E., Calvente, D. L., Ramji, D. P., Marchesi, J. R., et al. (2017). The anti-cholesterolaemic effect of a consortium of probiotics: An acute study in C57BL/6J mice. *Sci. Rep.* 7 (1), 2883. doi:10.1038/s41598-017-02889-5

Mikó, E., Vida, A., Kovács, T., Ujlaki, G., Trencsényi, G., Márton, J., et al. (2018). Lithocholic acid, a bacterial metabolite reduces breast cancer cell proliferation and aggressiveness. *Biochimica Biophysica Acta (BBA) - Bioenergetics* 1859 (9), 958–974. doi:10.1016/j.bbabio.2018.04.002

Misawa, T., Takahama, M., and Saitoh, T. (2017). "Mitochondria–endoplasmic reticulum contact sites mediate innate immune responses," in *Organelle contact sites: From molecular mechanism to disease*. Editors M. Tagaya and T. Simmen (Singapore: Springer Singapore), 187–197.

Módis, K., Bos, E. M., Calzia, E., van Goor, H., Coletta, C., Papapetropoulos, A., et al. (2014). Regulation of mitochondrial bioenergetic function by hydrogen sulfide. Part II. Pathophysiological and therapeutic aspects. *Br. J. Pharmacol.* 171 (8), 2123–2146. doi:10.1111/bph.12368

Mohammadi, A., Najar, A. G., Yaghoobi, M. M., Jahani, Y., and Vahabzadeh, Z. (2016). Trimethylamine-N-Oxide treatment induces changes in the ATP-binding cassette transporter A1 and scavenger receptor A1 in murine macrophage J774A.1 cells. *Inflammation* 39 (1), 393–404. doi:10.1007/s10753-015-0261-7

Mohanty, A., Tiwari-Pandey, R., and Pandey, N. R. (2019). Mitochondria: The indispensable players in innate immunity and guardians of the inflammatory response. *J. Cell Commun. Signal* 13 (3), 303–318. doi:10.1007/s12079-019-00507-9

Mollica, M. P., Mattace Raso, G., Cavaliere, G., Trinchese, G., De Filippo, C., Aceto, S., et al. (2017). Butyrate regulates liver mitochondrial function, efficiency, and dynamics in insulin-resistant obese mice. *Diabetes* 66 (5), 1405–1418. doi:10.2337/db16-0924

Murphy, B., Bhattacharya, R., and Mukherjee, P. (2019). Hydrogen sulfide signaling in mitochondria and disease. *Faseb J.* 33 (12), 13098–13125. doi:10.1096/fj.201901304R

Najjar, R. S., and Feresin, R. G. (2019). Plant-based diets in the reduction of body fat: Physiological effects and biochemical insights. *Nutrients* 11 (11), 2712. doi:10.3390/nu11112712

Nguyen, E. K., Koval, O. M., Noble, P., Broadhurst, K., Allamargot, C., Wu, M., et al. (2018). CaMKII (Ca(2+)/calmodulin-dependent kinase II) in mitochondria of smooth muscle cells controls mitochondrial mobility, migration, and neointima formation. *Arterioscler. Thromb. Vasc. Biol.* 38 (6), 1333–1345. doi:10.1161/atvbaha.118.310951

Nie, J., Zhang, L., Zhao, G., and Du, X. (2019). Quercetin reduces atherosclerotic lesions by altering the gut microbiota and reducing atherogenic lipid metabolites. *J. Appl. Microbiol.* 127 (6), 1824–1834. doi:10.1111/jam.14441

Oliveira, H. C. F., and Vercesi, A. E. (2020). Mitochondrial bioenergetics and redox dysfunctions in hypercholesterolemia and atherosclerosis. *Mol. Asp. Med.* 71, 100840. doi:10.1016/j.mam.2019.100840

Orekhov, A. N., Nikiforov, N. N., Ivanova, E. A., and Sobenin, I. A. (2020a). Possible role of mitochondrial DNA mutations in chronification of inflammation: Focus on atherosclerosis. *J. Clin. Med.* 9 (4), 978. doi:10.3390/jcm9040978

Orekhov, A. N., Poznyak, A. V., Sobenin, I. A., Nikifirov, N. N., and Ivanova, E. A. (2020b). Mitochondrion as a selective target for the treatment of atherosclerosis: Role of mitochondrial DNA mutations and defective mitophagy in the pathogenesis of atherosclerosis and chronic inflammation. *Curr. Neuropharmacol.* 18 (11), 1064–1075. doi:10.2174/1570159x17666191118125018

Panyod, S., Wu, W. K., Chen, P. C., Chong, K. V., Yang, Y. T., Chuang, H. L., et al. (2022). Atherosclerosis amelioration by allicin in raw garlic through gut microbiota and trimethylamine-N-oxide modulation. *NPJ Biofilms Microbiomes* 8 (1), 4. doi:10.1038/s41522-022-00266-3

Park, S., Juliana, C., Hong, S., Datta, P., Hwang, I., Fernandes-Alnemri, T., et al. (2013). The mitochondrial antiviral protein MAVS associates with NLRP3 and regulates its inflammasome activity. *J. Immunol.* 191 (8), 4358–4366. doi:10.4049/jimmunol.1301170

Paul, B. D., Snyder, S. H., and Kashfi, K. (2021). Effects of hydrogen sulfide on mitochondrial function and cellular bioenergetics. *Redox Biol.* 38, 101772. doi:10.1016/j.redox.2020.101772

Peace, C. G., and O'Neill, L. A. (2022). The role of itaconate in host defense and inflammation. *J. Clin. Invest.* 132 (2), e148548. doi:10.1172/jci148548

Peng, X., Chen, H., Li, Y., Huang, D., Huang, B., and Sun, D. (2020). Effects of NIX-mediated mitophagy on ox-LDL-induced macrophage pyroptosis in atherosclerosis. *Cell Biol. Int.* 44 (7), 1481–1490. doi:10.1002/cbin.11343

Peng, X., Zhang, C., Zhou, Z. M., Wang, K., Gao, J. W., Qian, Z. Y., et al. (2022). A20 attenuates pyroptosis and apoptosis in nucleus pulposus cells via promoting mitophagy and stabilizing mitochondrial dynamics. *Inflamm. Res.* 71 (5-6), 695–710. doi:10.1007/s00011-022-01570-6

Pham, P. T., Fukuda, D., Nishimoto, S., Kim-Kaneyama, J. R., Lei, X. F., Takahashi, Y., et al. (2021). STING, a cytosolic DNA sensor, plays a critical role in atherogenesis: A link between innate immunity and chronic inflammation caused by lifestyle-related diseases. *Eur. Heart J.* 42 (42), 4336–4348. doi:10.1093/eurheartj/ehab249

Picca, A., Guerra, F., Calvani, R., Romano, R., Coelho-Junior, H. J., Damiano, F. P., et al. (2022). Circulating mitochondrial DNA and inter-organelle contact sites in aging and associated conditions. *Cells* 11 (4), 675. doi:10.3390/cells11040675

Pollack, R. M., Barzilai, N., Anghel, V., Kulkarni, A. S., Golden, A., O'Broin, P., et al. (2017). Resveratrol improves vascular function and mitochondrial number but not glucose metabolism in older adults. *J. Gerontol. A Biol. Sci. Med. Sci.* 72 (12), 1703–1709. doi:10.1093/gerona/glx041

Pols, T. W., Nomura, M., Harach, T., Lo Sasso, G., Oosterveer, M. H., Thomas, C., et al. (2011). TGR5 activation inhibits atherosclerosis by reducing macrophage inflammation and lipid loading. *Cell Metab.* 14 (6), 747–757. doi:10.1016/j.cmet.2011.11.006

Primec, M., Klemenak, M., Di Gioia, D., Aloisio, I., Bozzi Cionci, N., Quagliariello, A., et al. (2019). Clinical intervention using Bifidobacterium strains in celiac disease children reveals novel microbial modulators of TNF-α and short-chain fatty acids. *Clin. Nutr.* 38 (3), 1373–1381. doi:10.1016/j.clnu.2018.06.931

Pu, Y., Zhang, H., Wang, P., Zhao, Y., Li, Q., Wei, X., et al. (2013). Dietary curcumin ameliorates aging-related cerebrovascular dysfunction through the AMPK/uncoupling protein 2 pathway. *Cell Physiol. Biochem.* 32 (5), 1167–1177. doi:10.1159/000354516

Puhm, F., Afonyushkin, T., Resch, U., Obermayer, G., Rohde, M., Penz, T., et al. (2019). Mitochondria are a subset of extracellular vesicles released by activated monocytes and induce type I IFN and TNF responses in endothelial cells. *Circ. Res.* 125 (1), 43–52. doi:10.1161/circresaha.118.314601

Pursnani, A., Massaro, J. M., D'Agostino, R. B., Sr., O'Donnell, C. J., and Hoffmann, U. (2017). Guideline-based statin eligibility, cancer events, and noncardiovascular mortality in the framingham heart study. *J. Clin. Oncol.* 35 (25), 2927–2933. doi:10.1200/jco.2016.71.3594

Qi, Y., Liu, W., Yan, X., Zhang, C., Zhang, C., Liu, L., et al. (2022). Tongxinluo may alleviate inflammation and improve the stability of atherosclerotic plaques by changing the intestinal flora. *Front. Pharmacol.* 13, 805266. doi:10.3389/fphar.2022.805266

Querio, G., Antoniotti, S., Geddo, F., Levi, R., and Gallo, M. P. (2022). Trimethylamine N-oxide does not impact viability, ROS production, and mitochondrial membrane potential of adult rat cardiomyocytes. *Int. J. Mol. Sci.* 23 (7), 3045. doi:10.3390/ijms20123045

Querio, G., Antoniotti, S., Levi, R., and Gallo, M. P. (2019). Trimethylamine N-oxide does not impact viability, ROS production, and mitochondrial membrane potential of adult rat cardiomyocytes. *Int. J. Mol. Sci.* 20 (12), 3045. doi:10.3390/ijms20123045

Ramachandran, R. P., Spiegel, C., Keren, Y., Danieli, T., Melamed-Book, N., Pal, R. R., et al. (2020). Mitochondrial targeting of the enteropathogenic *Escherichia coli* map triggers calcium mobilization, ADAM10-MAP kinase signaling, and host cell apoptosis. *mBio* 11 (5), 013977–e1420. doi:10.1128/mBio.01397-20

Rassow, J. (2011). *Helicobacter pylori* vacuolating toxin A and apoptosis. *Cell Commun. Signal* 9, 26. doi:10.1186/1478-811x-9-26

Robert, P., Nguyen, P. M. C., Richard, A., Grenier, C., Chevrollier, A., Munier, M., et al. (2021). Protective role of the mitochondrial fusion protein OPA1 in hypertension. *Faseb J.* 35 (7), e21678. doi:10.1096/fj.202000238RRR

Rodrigues, R. R., Gurung, M., Li, Z., García-Jaramillo, M., Greer, R., Gaulke, C., et al. (2021). Transkingdom interactions between Lactobacilli and hepatic mitochondria attenuate Western diet-induced diabetes. *Nat. Commun.* 12 (1), 101. doi:10.1038/s41467-020-20313-x

Roger, A. J., Muñoz-Gómez, S. A., and Kamikawa, R. (2017). The origin and diversification of mitochondria. *Curr. Biol.* 27 (21), R1177–r1192. doi:10.1016/j.cub.2017.09.015

Rong, Q., Han, B., Li, Y., Yin, H., Li, J., and Hou, Y. (2021). Berberine reduces lipid accumulation by promoting fatty acid oxidation in renal tubular epithelial cells of the diabetic kidney. *Front. Pharmacol.* 12, 729384. doi:10.3389/fphar.2021.729384

Ross, J. M., Coppotelli, G., Hoffer, B. J., and Olson, L. (2014). Maternally transmitted mitochondrial DNA mutations can reduce lifespan. *Sci. Rep.* 4, 6569. doi:10.1038/srep06569

Rossman, M. J., Santos-Parker, J. R., Steward, C. A. C., Bispham, N. Z., Cuevas, L. M., Rosenberg, H. L., et al. (2018). Chronic supplementation with a mitochondrial antioxidant (MitoQ) improves vascular function in healthy older adults. *Hypertension* 71 (6), 1056–1063. doi:10.1161/hypertensionaha.117.10787

Rossmann, M. P., Dubois, S. M., Agarwal, S., and Zon, L. I. (2021). Mitochondrial function in development and disease. *Dis. Model Mech.* 14 (6), dmm048912. doi:10.1242/dmm.048912

Salnikova, D., Orekhova, V., Grechko, A., Starodubova, A., Bezsonov, E., Popkova, T., et al. (2021). Mitochondrial dysfunction in vascular wall cells and its role in atherosclerosis. *Int. J. Mol. Sci.* 22 (16), 8990. doi:10.3390/ijms22168990

Sazonova, M. A., Sinyov, V. V., Barinova, V. A., Ryzhkova, A. I., Zhelankin, A. V., Postnov, A. Y., et al. (2015). Mosaicism of mitochondrial genetic variation in atherosclerotic lesions of the human aorta. *Biomed. Res. Int.* 2015, 825468. doi:10.1155/2015/825468

Sazonova, M. A., Sinyov, V. V., Ryzhkova, A. I., Galitsyna, E. V., Khasanova, Z. B., Postnov, A. Y., et al. (2017). Role of mitochondrial genome mutations in pathogenesis of carotid atherosclerosis. *Oxid. Med. Cell Longev.* 2017, 6934394. doi:10.1155/2017/6934394

Schellenberg, B., Wang, P., Keeble, J. A., Rodriguez-Enriquez, R., Walker, S., Owens, T. W., et al. (2013). Bax exists in a dynamic equilibrium between the cytosol and mitochondria to control apoptotic priming. *Mol. Cell* 49 (5), 959–971. doi:10.1016/j.molcel.2012.12.022

Schneider, J., Girreser, U., Havemeyer, A., Bittner, F., and Clement, B. (2018). Detoxification of trimethylamine N-oxide by the mitochondrial amidoxime reducing component mARC. *Chem. Res. Toxicol.* 31 (6), 447–453. doi:10.1021/acs.chemrestox.7b00329

Shames, S. R., Croxen, M. A., Deng, W., and Finlay, B. B. (2011). The type III system-secreted effector EspZ localizes to host mitochondria and interacts with the translocase of inner mitochondrial membrane 17b. *Infect. Immun.* 79 (12), 4784–4790. doi:10.1128/iai.05761-11

Shen, X., Carlström, M., Borniquel, S., Jädert, C., Kevil, C. G., and Lundberg, J. O. (2013). Microbial regulation of host hydrogen sulfide bioavailability and metabolism. *Free Radic. Biol. Med.* 60, 195–200. doi:10.1016/j.freeradbiomed.2013.02.024

Shi, R., Zhu, D., Wei, Z., Fu, N., Wang, C., Liu, L., et al. (2018). Baicalein attenuates monocrotaline-induced pulmonary arterial hypertension by inhibiting endothelial-to-mesenchymal transition. *Life Sci.* 207, 442–450. doi:10.1016/j.lfs.2018.06.033

Shi, X., Zhou, X., Chu, X., Wang, J., Xie, B., Ge, J., et al. (2019). Allicin improves metabolism in high-fat diet-induced obese mice by modulating the gut microbiota. *Nutrients* 11 (12), 2909. doi:10.3390/nu11122909

Shi, Y., Hu, J., Geng, J., Hu, T., Wang, B., Yan, W., et al. (2018). Berberine treatment reduces atherosclerosis by mediating gut microbiota in apoE-/- mice. *Biomed. Pharmacother.* 107, 1556–1563. doi:10.1016/j.biopha.2018.08.148

Song, Y., Xu, Y., Liu, Y., Gao, J., Feng, L., Zhang, Y., et al. (2021). Mitochondrial quality control in the maintenance of cardiovascular homeostasis: The roles and interregulation of UPS, mitochondrial dynamics and mitophagy. *Oxid. Med. Cell Longev.* 2021, 3960773. doi:10.1155/2021/3960773

Song, Y., Zhou, Y., and Zhou, X. (2020). The role of mitophagy in innate immune responses triggered by mitochondrial stress. *Cell Commun. Signal* 18 (1), 186. doi:10.1186/s12964-020-00659-x

Sprenger, H. G., MacVicar, T., Bahat, A., Fiedler, K. U., Hermans, S., Ehrentraut, D., et al. (2021). Cellular pyrimidine imbalance triggers mitochondrial DNA-dependent innate immunity. *Nat. Metab.* 3 (5), 636–650. doi:10.1038/s42255-021-00385-9

Springo, Z., Tarantini, S., Toth, P., Tucsek, Z., Koller, A., Sonntag, W. E., et al. (2015). Aging exacerbates pressure-induced mitochondrial oxidative stress in mouse cerebral arteries. *J. Gerontol. A Biol. Sci. Med. Sci.* 70 (11), 1355–1359. doi:10.1093/gerona/glu244

Stewart, J. B., and Chinnery, P. F. (2021). Extreme heterogeneity of human mitochondrial DNA from organelles to populations. *Nat. Rev. Genet.* 22 (2), 106–118. doi:10.1038/s41576-020-00284-x

Subramanian, N., Natarajan, K., Clatworthy, M. R., Wang, Z., and Germain, R. N. (2013). The adaptor MAVS promotes NLRP3 mitochondrial localization and inflammasome activation. *Cell* 153 (2), 348–361. doi:10.1016/j.cell.2013.02.054

Sukumaran, S. K., Fu, N. Y., Tin, C. B., Wan, K. F., Lee, S. S., and Yu, V. C. (2010). A soluble form of the pilus protein FimA targets the VDAC-hexokinase complex at mitochondria to suppress host cell apoptosis. *Mol. Cell* 37 (6), 768–783. doi:10.1016/j.molcel.2010.02.015

Sun, A., Wang, Y., Liu, J., Yu, X., Sun, Y., Yang, F., et al. (2016). Exogenous H2S modulates mitochondrial fusion-fission to inhibit vascular smooth muscle cell proliferation in a hyperglycemic state. *Cell Biosci.* 6, 36. doi:10.1186/s13578-016-0102-x

Sun, Y., Lu, F., Yu, X., Wang, B., Chen, J., Lu, F., et al. (2020). Exogenous H(2)S promoted USP8 sulfhydration to regulate mitophagy in the hearts of db/db mice. *Aging Dis.* 11 (2), 269–285. doi:10.14336/ad.2019.0524

Sung, M. M., Kim, T. T., Denou, E., Soltys, C. M., Hamza, S. M., Byrne, N. J., et al. (2017). Improved glucose homeostasis in obese mice treated with resveratrol is associated with alterations in the gut microbiome. *Diabetes* 66 (2), 418–425. doi:10.2337/db16-0680

Swiader, A., Nahapetyan, H., Faccini, J., D'Angelo, R., Mucher, E., Elbaz, M., et al. (2016). Mitophagy acts as a safeguard mechanism against human vascular smooth muscle cell apoptosis induced by atherogenic lipids. *Oncotarget* 7 (20), 28821–28835. doi:10.18632/oncotarget.8936

Tang, W. H., Wang, Z., Levison, B. S., Koeth, R. A., Britt, E. B., Fu, X., et al. (2013). Intestinal microbial metabolism of phosphatidylcholine and cardiovascular risk. *N. Engl. J. Med.* 368 (17), 1575–1584. doi:10.1056/NEJMoa1109400

Tang, X., Ma, S., Li, Y., Sun, Y., Zhang, K., Zhou, Q., et al. (2020). Evaluating the activity of sodium butyrate to prevent osteoporosis in rats by promoting osteal GSK-3β/nrf2 signaling and mitochondrial function. *J. Agric. Food Chem.* 68 (24), 6588–6603. doi:10.1021/acs.jafc.0c01820

Tian, L., Li, N., Li, K., Tan, Y., Han, J., Lin, B., et al. (2022). Ambient ozone exposure induces ROS related-mitophagy and pyroptosis via NLRP3 inflammasome activation in rat lung cells. *Ecotoxicol. Environ. Saf.* 240, 113663. doi:10.1016/j.ecoenv.2022.113663

Toksoy, A., Sennefelder, H., Adam, C., Hofmann, S., Trautmann, A., Goebeler, M., et al. (2017). Potent NLRP3 inflammasome activation by the HIV reverse transcriptase inhibitor abacavir. *J. Biol. Chem.* 292 (7), 2805–2814. doi:10.1074/jbc.M116.749473

Toral, M., Romero, M., Rodríguez-Nogales, A., Jiménez, R., Robles-Vera, I., Algieri, F., et al. (2018). Lactobacillus fermentum improves tacrolimus-induced hypertension by restoring vascular redox state and improving eNOS coupling. *Mol. Nutr. Food Res.* 62, e1800033. doi:10.1002/mnfr.201800033

Ungvari, Z., Labinskyy, N., Mukhopadhyay, P., Pinto, J. T., Bagi, Z., Ballabh, P., et al. (2009). Resveratrol attenuates mitochondrial oxidative stress in coronary arterial endothelial cells. *Am. J. Physiol. Heart Circ. Physiol.* 297 (5), H1876–H1881. doi:10.1152/ajpheart.00375.2009

Untereiner, A. A., Wang, R., Ju, Y., and Wu, L. (2016). Decreased gluconeogenesis in the absence of cystathionine gamma-lyase and the underlying mechanisms. *Antioxid. Redox Signal* 24 (3), 129–140. doi:10.1089/ars.2015.6369

Valente, W. J., Ericson, N. G., Long, A. S., White, P. A., Marchetti, F., and Bielas, J. H. (2016). Mitochondrial DNA exhibits resistance to induced point and deletion mutations. *Nucleic Acids Res.* 44 (18), 8513–8524. doi:10.1093/nar/gkw716

Vecoli, C., Borghini, A., Pulignani, S., Mercuri, A., Turchi, S., Carpeggiani, C., et al. (2018). Prognostic value of mitochondrial DNA(4977) deletion and mitochondrial DNA copy number in patients with stable coronary artery disease. *Atherosclerosis* 276, 91–97. doi:10.1016/j.atherosclerosis.2018.07.015

Vecoli, C., Borghini, A., Pulignani, S., Mercuri, A., Turchi, S., Picano, E., et al. (2019). Independent and combined effects of telomere shortening and mtDNA(4977) deletion on long-term outcomes of patients with coronary artery disease. *Int. J. Mol. Sci.* 20 (21), 5508. doi:10.3390/ijms20215508

Vendrov, A. E., Stevenson, M. D., Alahari, S., Pan, H., Wickline, S. A., Madamanchi, N. R., et al. (2017). Attenuated superoxide dismutase 2 activity induces atherosclerotic plaque instability during aging in hyperlipidemic mice. *J. Am. Heart Assoc.* 6 (11), e006775. doi:10.1161/jaha.117.006775

Verhaar, B. J. H., Prodan, A., Nieuwdorp, M., and Muller, M. (2020). Gut microbiota in hypertension and atherosclerosis: A review. *Nutrients* 12 (10), 2982. doi:10.3390/nu12102982

Vezza, T., Abad-Jiménez, Z., Marti-Cabrera, M., Rocha, M., and Víctor, V. M. (2020). Microbiota-mitochondria inter-talk: A potential therapeutic strategy in obesity and type 2 diabetes. *Antioxidants (Basel)* 9 (9), 848. doi:10.3390/antiox9090848

Videja, M., Vilskersts, R., Korzh, S., Cirule, H., Sevostjanovs, E., Dambrova, M., et al. (2020). Microbiota-derived metabolite trimethylamine N-oxide protects mitochondrial energy metabolism and cardiac functionality in a rat model of right ventricle heart failure. *Front. Cell Dev. Biol.* 8, 622741. doi:10.3389/fcell.2020.622741

Wan, Q., Liu, Z. Y., Yang, Y. P., and Liu, S. M. (2016). Effect of curcumin on inhibiting atherogenesis by down-regulating lipocalin-2 expression in apolipoprotein E knockout mice. *Biomed. Mater Eng.* 27 (6), 577–587. doi:10.3233/bme-161610

Wang, J., Ghosh, S. S., and Ghosh, S. (2017). Curcumin improves intestinal barrier function: Modulation of intracellular signaling, and organization of tight junctions. *Am. J. Physiol. Cell Physiol.* 312 (4), C438–c445. doi:10.1152/ajpcell.00235.2016

Wang, L., Tang, X. Q., Shi, Y., Li, H. M., Meng, Z. Y., Chen, H., et al. (2022). Tetrahydroberberrubine retards heart aging in mice by promoting PHB2-mediated mitophagy. *Acta Pharmacol. Sin*. doi:10.1038/s41401-022-00956-w

Wang, Y., Christopher, B. A., Wilson, K. A., Muoio, D., McGarrah, R. W., Brunengraber, H., et al. (2018). Propionate-induced changes in cardiac metabolism, notably CoA trapping, are not altered by l-carnitine. *Am. J. Physiol. Endocrinol. Metab.* 315 (4), E622–e633. doi:10.1152/ajpendo.00081.2018

Wang, Z., Klipfell, E., Bennett, B. J., Koeth, R., Levison, B. S., Dugar, B., et al. (2011). Gut flora metabolism of phosphatidylcholine promotes cardiovascular disease. *Nature* 472 (7341), 57–63. doi:10.1038/nature09922

Wang, Z., Wu, F., Zhou, Q., Qiu, Y., Zhang, J., Tu, Q., et al. (2022). Berberine improves vascular dysfunction by inhibiting trimethylamine-N-oxide via regulating the gut microbiota in angiotensin II-induced hypertensive mice. *Front. Microbiol.* 13, 814855. doi:10.3389/fmicb.2022.814855

Wei, T., Huang, G., Gao, J., Huang, C., Sun, M., Wu, J., et al. (2017). Sirtuin 3 deficiency accelerates hypertensive cardiac remodeling by impairing angiogenesis. *J. Am. Heart Assoc.* 6 (8), e006114. doi:10.1161/jaha.117.006114

Wellman, A. S., Metukuri, M. R., Kazgan, N., Xu, X., Xu, Q., Ren, N. S. X., et al. (2017). Intestinal epithelial sirtuin 1 regulates intestinal inflammation during aging in mice by altering the intestinal microbiota. *Gastroenterology* 153 (3), 772–786. doi:10.1053/j.gastro.2017.05.022

West, A. P., Brodsky, I. E., Rahner, C., Woo, D. K., Erdjument-Bromage, H., Tempst, P., et al. (2011). TLR signalling augments macrophage bactericidal activity through mitochondrial ROS. *Nature* 472 (7344), 476–480. doi:10.1038/nature09973

West, A. P., Khoury-Hanold, W., Staron, M., Tal, M. C., Pineda, C. M., Lang, S. M., et al. (2015). Mitochondrial DNA stress primes the antiviral innate immune response. *Nature* 520 (7548), 553–557. doi:10.1038/nature14156

Witkowski, M., Weeks, T. L., and Hazen, S. L. (2020). Gut microbiota and cardiovascular disease. *Circ. Res.* 127 (4), 553–570. doi:10.1161/circresaha.120.316242

Wu, D., Hu, Q., Liu, X., Pan, L., Xiong, Q., and Zhu, Y. Z. (2015). Hydrogen sulfide protects against apoptosis under oxidative stress through SIRT1 pathway in H9c2 cardiomyocytes. *Nitric Oxide* 46, 204–212. doi:10.1016/j.niox.2014.11.006

Wu, D. N., Guan, L., Jiang, Y. X., Ma, S. H., Sun, Y. N., Lei, H. T., et al. (2019). Microbiome and metabonomics study of quercetin for the treatment of atherosclerosis. *Cardiovasc Diagn Ther.* 9 (6), 545–560. doi:10.21037/cdt.2019.12.04

Wu, M., Yang, S., Wang, S., Cao, Y., Zhao, R., Li, X., et al. (2020). Effect of berberine on atherosclerosis and gut microbiota modulation and their correlation in high-fat diet-fed ApoE-/- mice. *Front. Pharmacol.* 11, 223. doi:10.3389/fphar.2020.00223

Wu, W., Xu, H., Wang, Z., Mao, Y., Yuan, L., Luo, W., et al. (2015). PINK1-Parkin-Mediated mitophagy protects mitochondrial integrity and prevents metabolic stress-induced endothelial injury. *PLoS One* 10 (7), e0132499. doi:10.1371/journal.pone.0132499

Xian, H., Watari, K., Sanchez-Lopez, E., Offenberger, J., Onyuru, J., Sampath, H., et al. (2022). Oxidized DNA fragments exit mitochondria via mPTP- and VDAC-dependent channels to activate NLRP3 inflammasome and interferon signaling. *Immunity* 55 (8), 1370–1385.e8. e1378. doi:10.1016/j.immuni.2022.06.007

Xie, T., Wang, C., Jin, Y., Meng, Q., Liu, Q., Wu, J., et al. (2020). CoenzymeQ10-Induced activation of AMPK-YAP-OPA1 pathway alleviates atherosclerosis by improving mitochondrial function, inhibiting oxidative stress and promoting energy metabolism. *Front. Pharmacol.* 11, 1034. doi:10.3389/fphar.2020.01034

Xu, A., Deng, F., Chen, Y., Kong, Y., Pan, L., Liao, Q., et al. (2020). NF-κB pathway activation during endothelial-to-mesenchymal transition in a rat model of doxorubicin-induced cardiotoxicity. *Biomed. Pharmacother.* 130, 110525. doi:10.1016/j.biopha.2020.110525

Xu, H., Pan, L. B., Yu, H., Han, P., Fu, J., Zhang, Z. W., et al. (2022). Gut microbiota-derived metabolites in inflammatory diseases based on targeted metabolomics. *Front. Pharmacol.* 13, 919181. doi:10.3389/fphar.2022.919181

Xu, L., Li, M., Yang, Y., Zhang, C., Xie, Z., Tang, J., et al. (2022). Salmonella induces the cGAS-STING-dependent type I interferon response in murine macrophages by triggering mtDNA release. *mBio* 13 (3), e0363221. doi:10.1128/mbio.03632-21

Xue, H., Chen, X., Yu, C., Deng, Y., Zhang, Y., Chen, S., et al. (2022). Gut microbially produced indole-3-propionic acid inhibits atherosclerosis by promoting reverse cholesterol transport and its deficiency is causally related to atherosclerotic cardiovascular disease. *Circ. Res.* 131 (5), 404–420. doi:10.1161/circresaha.122.321253

Yang, J., Zhou, X., Zeng, X., Hu, O., Yi, L., and Mi, M. (2019). Resveratrol attenuates oxidative injury in human umbilical vein endothelial cells through regulating mitochondrial fusion via TyrRS-PARP1 pathway. *Nutr. Metab. (Lond)* 16, 9. doi:10.1186/s12986-019-0338-7

Yang, L., Lin, X., Tang, H., Fan, Y., Zeng, S., Jia, L., et al. (2020). Mitochondrial DNA mutation exacerbates female reproductive aging via impairment of the NADH/NAD(+) redox. *Aging Cell* 19 (9), e13206. doi:10.1111/acel.13206

Yang, M., Zheng, J., Zong, X., Yang, X., Zhang, Y., Man, C., et al. (2021). Preventive effect and molecular mechanism of Lactobacillus rhamnosus JL1 on food-borne obesity in mice. *Nutrients* 13 (11), 3989. doi:10.3390/nu13113989

Yang, Y. N., Wang, Q. C., Xu, W., Yu, J., Zhang, H., and Wu, C. (2022). The berberine-enriched gut commensal Blautia producta ameliorates high-fat diet (HFD)-induced hyperlipidemia and stimulates liver LDLR expression. *Biomed. Pharmacother.* 155, 113749. doi:10.1016/j.biopha.2022.113749

Yao, S., Yuan, Y., Zhang, H., Meng, X., Jin, L., Yang, J., et al. (2020). Berberine attenuates the abnormal ectopic lipid deposition in skeletal muscle. *Free Radic. Biol. Med.* 159, 66–75. doi:10.1016/j.freeradbiomed.2020.07.028

Yaron, J. R., Gangaraju, S., Rao, M. Y., Kong, X., Zhang, L., Su, F., et al. (2015). K(+) regulates Ca(2+) to drive inflammasome signaling: Dynamic visualization of ion flux in live cells. *Cell Death Dis.* 6 (10), e1954. doi:10.1038/cddis.2015.277

Yin, Z., Burger, N., Kula-Alwar, D., Aksentijević, D., Bridges, H. R., Prag, H. A., et al. (2021). Structural basis for a complex I mutation that blocks pathological ROS production. *Nat. Commun.* 12 (1), 707. doi:10.1038/s41467-021-20942-w

Yoo, J. Y., Sniffen, S., McGill Percy, K. C., Pallaval, V. B., and Chidipi, B. (2022). Gut dysbiosis and immune system in atherosclerotic cardiovascular disease (ACVD). *Microorganisms* 10 (1), 108. doi:10.3390/microorganisms10010108

Yoshida, Y., Shimizu, I., Shimada, A., Nakahara, K., Yanagisawa, S., Kubo, M., et al. (2022). Brown adipose tissue dysfunction promotes heart failure via a trimethylamine N-oxide-dependent mechanism. *Sci. Rep.* 12 (1), 14883. doi:10.1038/s41598-022-19245-x

You, S., Qian, J., Wu, G., Qian, Y., Wang, Z., Chen, T., et al. (2019). Schizandrin B attenuates angiotensin II induced endothelial to mesenchymal transition in vascular endothelium by suppressing NF-κB activation. *Phytomedicine* 62, 152955. doi:10.1016/j.phymed.2019.152955

Yu, C. H., Davidson, S., Harapas, C. R., Hilton, J. B., Mlodzianoski, M. J., Laohamonthonkul, P., et al. (2020). TDP-43 triggers mitochondrial DNA release via mPTP to activate cGAS/STING in ALS. *Cell* 183 (3), 636–649. e618. doi:10.1016/j.cell.2020.09.020

Yu, E., Calvert, P. A., Mercer, J. R., Harrison, J., Baker, L., Figg, N. L., et al. (2013). Mitochondrial DNA damage can promote atherosclerosis independently of reactive oxygen species through effects on smooth muscle cells and monocytes and correlates with higher-risk plaques in humans. *Circulation* 128 (7), 702–712. doi:10.1161/circulationaha.113.002271

Yu, E. P., and Bennett, M. R. (2014). Mitochondrial DNA damage and atherosclerosis. *Trends Endocrinol. Metab.* 25 (9), 481–487. doi:10.1016/j.tem.2014.06.008

Yu, E. P. K., Reinhold, J., Yu, H., Starks, L., Uryga, A. K., Foote, K., et al. (2017). Mitochondrial respiration is reduced in atherosclerosis, promoting necrotic core formation and reducing relative fibrous cap thickness. *Arterioscler. Thromb. Vasc. Biol.* 37 (12), 2322–2332. doi:10.1161/atvbaha.117.310042

Yu, J., Nagasu, H., Murakami, T., Hoang, H., Broderick, L., Hoffman, H. M., et al. (2014). Inflammasome activation leads to Caspase-1-dependent mitochondrial damage and block of mitophagy. *Proc. Natl. Acad. Sci. U. S. A.* 111 (43), 15514–15519. doi:10.1073/pnas.1414859111

Yu, M., Alimujiang, M., Hu, L., Liu, F., Bao, Y., and Yin, J. (2021). Berberine alleviates lipid metabolism disorders via inhibition of mitochondrial complex I in gut and liver. *Int. J. Biol. Sci.* 17 (7), 1693–1707. doi:10.7150/ijbs.54604

Zaharuddin, L., Mokhtar, N. M., Muhammad Nawawi, K. N., and Raja Ali, R. A. (2019). A randomized double-blind placebo-controlled trial of probiotics in post-surgical colorectal cancer. *BMC Gastroenterol.* 19 (1), 131. doi:10.1186/s12876-019-1047-4

Zhai, T., Wang, P., Hu, X., and Zheng, L. (2022). Probiotics bring new hope for atherosclerosis prevention and treatment. *Oxid. Med. Cell Longev.* 2022, 3900835. doi:10.1155/2022/3900835

Zhang, C., He, X., Sheng, Y., Yang, C., Xu, J., Zheng, S., et al. (2020). Allicin-induced host-gut microbe interactions improves energy homeostasis. *Faseb J.* 34 (8), 10682–10698. doi:10.1096/fj.202001007R

Zhang, J., Ou, C., and Chen, M. (2022). Curcumin attenuates cadmium-induced atherosclerosis by regulating trimethylamine-N-oxide synthesis and macrophage polarization through remodeling the gut microbiota. *Ecotoxicol. Environ. Saf.* 244, 114057. doi:10.1016/j.ecoenv.2022.114057

Zhang, J. Z., Liu, Z., Liu, J., Ren, J. X., and Sun, T. S. (2014). Mitochondrial DNA induces inflammation and increases TLR9/NF-κB expression in lung tissue. *Int. J. Mol. Med.* 33 (4), 817–824. doi:10.3892/ijmm.2014.1650

Zhang, L., Zhou, G., Song, W., Tan, X., Guo, Y., Zhou, B., et al. (2012). Pterostilbene protects vascular endothelial cells against oxidized low-density lipoprotein-induced apoptosis *in vitro* and *in vivo*. *Apoptosis* 17 (1), 25–36. doi:10.1007/s10495-011-0653-6

Zhang, M., Pan, H., Xu, Y., Wang, X., Qiu, Z., and Jiang, L. (2017). Allicin decreases lipopolysaccharide-induced oxidative stress and inflammation in human umbilical vein endothelial cells through suppression of mitochondrial dysfunction and activation of Nrf2. *Cell Physiol. Biochem.* 41 (6), 2255–2267. doi:10.1159/000475640

Zhang, Q., Raoof, M., Chen, Y., Sumi, Y., Sursal, T., Junger, W., et al. (2010). Circulating mitochondrial DAMPs cause inflammatory responses to injury. *Nature* 464 (7285), 104–107. doi:10.1038/nature08780

Zhang, S. J., Li, Z. H., Zhang, Y. D., Chen, J., Li, Y., Wu, F. Q., et al. (2021). Ketone body 3-hydroxybutyrate ameliorates atherosclerosis via receptor gpr109a-mediated calcium influx. *Adv. Sci. (Weinh)* 8 (9), 2003410. doi:10.1002/advs.202003410

Zhang, X., Chen, W., Li, J., Qi, S., Hong, S., Wang, Y., et al. (2018). Involvement of mitochondrial fission in calcium sensing receptor-mediated vascular smooth muscle cells proliferation during hypertension. *Biochem. Biophys. Res. Commun.* 495 (1), 454–460. doi:10.1016/j.bbrc.2017.11.048

Zhang, Y., Guallar, E., Ashar, F. N., Longchamps, R. J., Castellani, C. A., Lane, J., et al. (2017). Association between mitochondrial DNA copy number and sudden cardiac death: Findings from the atherosclerosis risk in communities study (ARIC). *Eur. Heart J.* 38 (46), 3443–3448. doi:10.1093/eurheartj/ehx354

Zhang, Y., Wang, C., Jin, Y., Yang, Q., Meng, Q., Liu, Q., et al. (2018). Activating the PGC-1α/TERT pathway by catalpol ameliorates atherosclerosis via modulating ROS production, DNA damage, and telomere function: Implications on mitochondria and telomere link. *Oxid. Med. Cell Longev.* 2018, 2876350. doi:10.1155/2018/2876350

Zhang, Y., Zhang, J., and Duan, L. (2022). The role of microbiota-mitochondria crosstalk in pathogenesis and therapy of intestinal diseases. *Pharmacol. Res.* 186, 106530. doi:10.1016/j.phrs.2022.106530

Zhao, M., Liu, S., Wang, C., Wang, Y., Wan, M., Liu, F., et al. (2021). Mesenchymal stem cell-derived extracellular vesicles attenuate mitochondrial damage and inflammation by stabilizing mitochondrial DNA. *ACS Nano* 15 (1), 1519–1538. doi:10.1021/acsnano.0c08947

Zhao, T., Gu, J., Zhang, H., Wang, Z., Zhang, W., Zhao, Y., et al. (2020). Sodium butyrate-modulated mitochondrial function in high-insulin induced HepG2 cell dysfunction. *Oxid. Med. Cell Longev.* 2020, 1904609. doi:10.1155/2020/1904609

Zhao, Y., Guo, Y., Chen, Y., Liu, S., Wu, N., and Jia, D. (2020). Curculigoside attenuates myocardial ischemia-reperfusion injury by inhibiting the opening of the mitochondrial permeability transition pore. *Int. J. Mol. Med.* 45 (5), 1514–1524. doi:10.3892/ijmm.2020.4513

Zheng, M., Qiao, W., Cui, J., Liu, L., Liu, H., Wang, Z., et al. (2014). Hydrogen sulfide delays nicotinamide-induced premature senescence via upregulation of SIRT1 in human umbilical vein endothelial cells. *Mol. Cell Biochem.* 393 (1-2), 59–67. doi:10.1007/s11010-014-2046-y

Zhou, P., Zhao, X. N., Ma, Y. Y., Tang, T. J., Wang, S. S., Wang, L., et al. (2022). Virtual screening analysis of natural flavonoids as trimethylamine (TMA)-lyase inhibitors for coronary heart disease. *J. Food Biochem.* 46, e14376. doi:10.1111/jfbc.14376

Zhou, R., Yazdi, A. S., Menu, P., and Tschopp, J. (2011). A role for mitochondria in NLRP3 inflammasome activation. *Nature* 469 (7329), 221–225. doi:10.1038/nature09663

Zhou, X., Chen, M., Zeng, X., Yang, J., Deng, H., Yi, L., et al. (2014). Resveratrol regulates mitochondrial reactive oxygen species homeostasis through Sirt3 signaling pathway in human vascular endothelial cells. *Cell Death Dis.* 5 (12), e1576. doi:10.1038/cddis.2014.530

Zhou, Y., Little, P. J., Xu, S., and Kamato, D. (2021). Curcumin inhibits lysophosphatidic acid mediated MCP-1 expression via blocking ROCK signalling. *Molecules* 26 (8), 2320. doi:10.3390/molecules26082320

Zhu, L., Zhang, D., Zhu, H., Zhu, J., Weng, S., Dong, L., et al. (2018). Berberine treatment increases Akkermansia in the gut and improves high-fat diet-induced atherosclerosis in Apoe(-/-) mice. *Atherosclerosis* 268, 117–126. doi:10.1016/j.atherosclerosis.2017.11.023

Zhu, N., Li, J., Li, Y., Zhang, Y., Du, Q., Hao, P., et al. (2020). Berberine protects against simulated ischemia/reperfusion injury-induced H9C2 cardiomyocytes apoptosis *in vitro* and myocardial ischemia/reperfusion-induced apoptosis *in vivo* by regulating the mitophagy-mediated HIF-1α/BNIP3 pathway. *Front. Pharmacol.* 11, 367. doi:10.3389/fphar.2020.00367

Zhu, W., Yuan, Y., Liao, G., Li, L., Liu, J., Chen, Y., et al. (2018). Mesenchymal stem cells ameliorate hyperglycemia-induced endothelial injury through modulation of mitophagy. *Cell Death Dis.* 9 (8), 837. doi:10.1038/s41419-018-0861-x

Ziganshina, E. E., Sharifullina, D. M., Lozhkin, A. P., Khayrullin, R. N., Ignatyev, I. M., and Ziganshin, A. M. (2016). Bacterial communities associated with atherosclerotic plaques from Russian individuals with atherosclerosis. *PLoS One* 11 (10), e0164836. doi:10.1371/journal.pone.0164836

Zou, J., Zhang, S., Li, P., Zheng, X., and Feng, D. (2018). Supplementation with curcumin inhibits intestinal cholesterol absorption and prevents atherosclerosis in high-fat diet-fed apolipoprotein E knockout mice. *Nutr. Res.* 56, 32–40. doi:10.1016/j.nutres.2018.04.017

frontiers | Frontiers in Pharmacology

TYPE Review
PUBLISHED 20 January 2023
DOI 10.3389/fphar.2023.1083875

Check for updates

OPEN ACCESS

EDITED BY
Chen Huei Leo,
Singapore University of Technology and Design, Singapore

REVIEWED BY
Zhen Guo,
Washington University in St. Louis, United States
Zhaohua Cai,
Shanghai Jiao Tong University, China
Junping Zhang,
First Teaching Hospital of Tianjin University of Traditional Chinese Medicine, China
Xiaoyan Zhu,
The Affiliated Hospital of Qingdao University, China
Peizheng Yan,
Shandong University of Traditional Chinese Medicine, China

*CORRESPONDENCE
Shihan Wang,
wangshihan91@126.com

†These authors have contributed equally to this work and share first authorship

SPECIALTY SECTION
This article was submitted to Ethnopharmacology, a section of the journal Frontiers in Pharmacology

RECEIVED 29 October 2022
ACCEPTED 05 January 2023
PUBLISHED 20 January 2023

CITATION
Wu Q, Lv Q, Liu X, Ye X, Cao L, Wang M, Li J, Yang Y, Li L and Wang S (2023), Natural compounds from botanical drugs targeting mTOR signaling pathway as promising therapeutics for atherosclerosis: A review. *Front. Pharmacol.* 14:1083875. doi: 10.3389/fphar.2023.1083875

COPYRIGHT
© 2023 Wu, Lv, Liu, Ye, Cao, Wang, Li, Yang, Li and Wang. This is an open-access article distributed under the terms of the Creative Commons Attribution License (CC BY). The use, distribution or reproduction in other forums is permitted, provided the original author(s) and the copyright owner(s) are credited and that the original publication in this journal is cited, in accordance with accepted academic practice. No use, distribution or reproduction is permitted which does not comply with these terms.

Natural compounds from botanical drugs targeting mTOR signaling pathway as promising therapeutics for atherosclerosis: A review

Qian Wu[1†], Qianyu Lv[1†], Xiao'an Liu[2], Xuejiao Ye[1], Linlin Cao[1], Manshi Wang[3], Junjia Li[1], Yingtian Yang[1], Lanlan Li[1] and Shihan Wang[1*]

[1]Guang'anmen Hospital, Chinese Academy of Chinese Medical Sciences, Beijing, China, [2]Capital University of Medical, Beijing, China, [3]Beijing Xicheng District Guangwai Hospital, Beijing, China

Atherosclerosis (AS) is a chronic inflammatory disease that is a major cause of cardiovascular diseases (CVDs), including coronary artery disease, hypertension, myocardial infarction, and heart failure. Hence, the mechanisms of AS are still being explored. A growing compendium of evidence supports that the activity of the mechanistic/mammalian target of rapamycin (mTOR) is highly correlated with the risk of AS. The mTOR signaling pathway contributes to AS progression by regulating autophagy, cell senescence, immune response, and lipid metabolism. Various botanical drugs and their functional compounds have been found to exert anti- AS effects by modulating the activity of the mTOR signaling pathway. In this review, we summarize the pathogenesis of AS based on the mTOR signaling pathway from the aspects of immune response, autophagy, cell senescence, and lipid metabolism, and comb the recent advances in natural compounds from botanical drugs to inhibit the mTOR signaling pathway and delay AS development. This review will provide a new perspective on the mechanisms and precision treatments of AS.

KEYWORDS

mTOR, herbal medicine, rapamycin, autophagy, mechanism, cell senescence, atherosclerosis

1 Introduction

Atherosclerosis (AS) is a chronic inflammatory disease of blood vessels, which is the main pathologic basis of ischemic cardiovascular diseases, including most cases of myocardial infarction, stroke, and peripheral artery disease (Riggs et al., 2022; Simonetto et al., 2022). Hyperlipidemia, hypertension, and diabetes are major risk factors for AS and are associated with the development, progression, and rupture of atherosclerotic plaque initiation (Yang et al., 2022). Although the therapies for AS have been advanced in recent decades, atherosclerotic cardiovascular disease accounts for most of the mortality worldwide (Libby, 2021a). The pathogenesis underlying AS is complex. Although not fully understood, the occurrence of AS is mainly related to the deposition of inner membrane lipid, endothelial cell injury, adhesion of platelets and leukocytes, invasion and proliferation of smooth muscle cells and collagen fibers, and formation of foam cells (Figure 1) (Bhattacharya et al., 2022; Kim et al., 2022; Lu et al., 2022). Multiple cellular processes and signaling pathways are involved in these biological processes, and the mTOR signaling pathway is one of the regulatory ones (Kong et al., 2022).

The mammalian target of rapamycin (mTOR) is a serine/threonine protein kinase that is evolutionarily highly conserved and can mediate various cellular responses, such as cell growth,

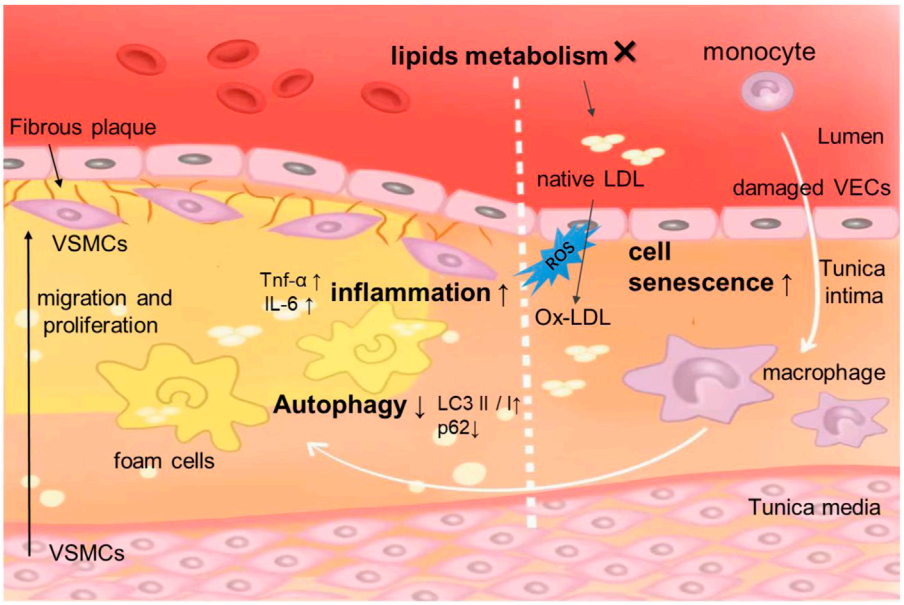

FIGURE 1
Schematic representation of the pathogenesis of AS. The damage of endothelial cells is the initial lesion of atherosclerosis. Endothelial cell damage that can be caused by disorders of lipid metabolism, monocytes/macrophages, foam cell formation release more inflammatory factors. VECs, VSMCs, macrophages are involved in the process of autophagy. In AS, cell senescence often occurs in VECs, VSMCs.

metabolism, motility, proliferation, and survival, protein synthesis, cell senescence, apoptosis, and autophagy (Laplante and Sabatini, 2012). Targeting mTOR signaling using specific pharmacological inhibitors may offer a therapeutic promise in inflammatory-associated diseases (Soltani et al., 2018). Recently, much attention has been focused on the potential role of the mTOR signaling pathway as a therapeutic target of atherosclerotic cardiovascular disease. Early studies have shown that the mTOR receptor inhibitor Everolimus firmly inhibits the development of AS in low-density lipoprotein receptor knockout ($LDLR^{-/-}$) mice, providing new insights into the mechanisms of AS (Mueller et al., 2008). Rapamycin is an agent that inhibits the activity of the mTOR signaling pathway. Considering that the current application of Rapamycin is limited by side effects, low biological availability, and lack of targeting, applications of several new technologies targeting atherosclerotic plaques, including 1 and 2, have also been observed in experimental animal models to reduce inflammation and lipid load and shrink plaques, further suggesting that reduced mTOR signaling pathway activity can be used to treat AS. Rapamycin is an inhibitor of the mTOR signaling pathway. By applying advanced technology that makes Rapamycin target atherosclerotic plaques in experimental animals, a reduction in inflammation and lipid load and a shrinking of plaques was also observed in animal models, further suggesting that reduced mTOR signaling pathway activity can promote atheroprotective changes in AS (Huang et al., 2022a; Cheraga et al., 2022; Guo et al., 2022).

For centuries, botanical drugs used in Traditional Chinese Medicine (TCM) have been widely practiced for the prevention and treatment of chronic heart disease. Botanical drugs have attracted widespread attention for their wide range of sources and multi-target effects (Zhi et al., 2023). Various natural agents derived from botanical drugs have been proven to have anti-AS effects (Wang et al., 2019; Penson and Banach, 2021). The current research targeting the mTOR signaling pathway by botanical drugs used in TCM provides new ideas for the treatment of AS (Poznyak et al., 2022). In recent years, an increasing number of studies have been conducted on the mTOR signaling pathway, and the relationship between mTOR and AS has been reviewed in terms of inhibition of inflammatory responses and suppressing the immune response (Cai et al., 2018). However, a review of preclinical evidence for TCM interventions targeting AS mTOR is lacking. Therefore, a comprehensive and systematic clarification of the molecular mechanisms by which natural agents target the mTOR signaling pathway is needed.

Based on the importance of the mTOR signaling pathway in AS, in this review, we first summarized our current understanding of the mTOR signaling pathway's role in AS from the aspects of immune response, autophagy, cell senescence, and lipid metabolism (Figure 2). Subsequently, we review the preclinical evidence of botanical drugs acting on the mTOR signaling pathway for the prevention and treatment of AS and related pathological processes.

2 mTOR signaling pathway participates in AS pathogenesis

The mTOR protein, a member of the phosphatidyl inositol 3-kinase (PI3K) related kinases (PIKKs), is a highly conserved serine/threonine protein kinase that catalyzes the transfer of phosphate to the hydroxyl group of the serine or threonine chains (Liu and Sabatini, 2020). Various proteins interact with mTOR to form two large protein complexes, named mammalian target of rapamycin complex 1 (mTORC1) and mammalian target of rapamycin complex 2 (mTORC2), the core complexes of the mTOR signaling pathway (Yang et al., 2013). More studies on AS currently focus on mTORC1 than mTORC2.

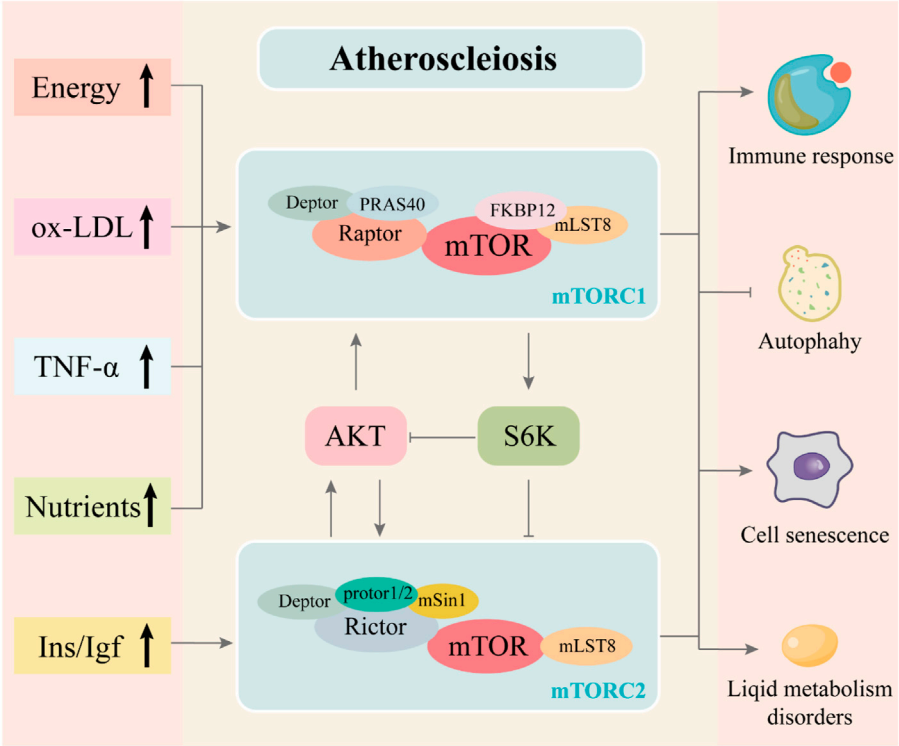

FIGURE 2
Association of mTOR signaling pathway with AS and the composition of the mTORC1 and mTORC2 complexes. The mTORC1 complex is composed of mTOR, Raptor, mLST8, PRAS40, Deptor and FKBP12. The mTORC2 complex is composed of mTOR, Rictor, mLST8, protor1/2, Deptor and mSin1. The mutual regulation is between mTORC1 and mTORC2. The development of atherosclerosis is often accompanied by abnormal lipid and energy metabolism and increased inflammatory response, which may activate the mTOR signaling pathway through complex mechanisms. These stimuli, as upstream signals of the mTOR signaling pathway, regulate the activity of the mTORC1 and mTORC2 complexes in the mTOR signaling pathway and influence downstream regulation, producing effects that promote immune response and cell senescence, disrupt lipid metabolism and inhibit autophagy, thereby exacerbating atherosclerosis.

mTORC1 is closely related to autophagy, lipolysis, protein synthesis, and other cell biological processes, which are sensitive to Rapamycin (Ben-Sahra and Manning, 2017). As one of the essential components of mTORC1, the regulatory protein associated with mTOR (Raptor) is a nutrient-sensitive polypeptide bound to mTOR, modulating the kinase activity of mTOR by forming the mTOR-Raptor association, in which the catalytic domain of mTOR phosphorylates substrates only upon binding to Raptor (Kim et al., 2002; Kim and Sabatini, 2004; Avruch et al., 2009). The substrates mainly contain S6 kinase (S6K) and eukaryotic translation initiation factor 4E-binding proteins 1(4E-BP1), which control cap-dependent translation initiation and elongation of mRNA (Ma and Blenis, 2009). Both mTORC1 and mTORC2 compounds contain Mammalian lethal with SEC13 protein 8 (mLST8), an indispensable protein subunit of the mTORC complex that interacts with the mTOR protein kinase domain to stabilize its active site (Saxton and Sabatini, 2017). Unlike Raptor in mTORC1, Rapamycin-insensitive companion of mTOR (Rictor) promotes mTOR substrate recruitment in mTORC2, similar to the effect of another vital component—serum-and glucocorticoid-induced protein kinase 1 (sin1) (Sarbassov et al., 2004; Chen and Sarbassov dos, 2011). Growth factors activate mTORC2; then, mTORC2 phosphorylates substrates, including some AGC-family kinases such as protein kinase B (AKT), serum-and glucocorticoid-induced protein kinase 1(SGK1), and protein kinases C (PKC), subsequently participates in cell survival, regulates ion transport, glucose metabolism, and other activities (Garcia-Martinez and Alessi, 2008; Viana et al., 2018). There is also a mutual regulatory mechanism between mTORC1 and mTORC2. AKT, as well as a negative modulation of the upstream activator of the inhibitory subunit in mTORC1, can be phosphorylated by mTORC2. Meanwhile, S6K, as a substrate of mTORC1, also acts upstream of mTORC2, and after Ins/IGF activation, S6K can inhibit the phosphorylation of IRS1, which in turn suppresses the activation of the PI3K-AKT signaling pathway in the upstream regulation of mTORC2 (Julien et al., 2010). The mTORC complex acts as a hub, coordinating upstream signaling and downstream effects. The mTOR signaling pathway can be activated by growth factors, insulin, ox-LDL, nutrients, and TNF-α, which are also stimuli closely related to the occurrence of AS.

AS is recognized as associated with immune disorders, but also involves a variety of mechanisms, including the death, autophagy, and senescence of vascular smooth muscle cells (VSMCs) and vascular endothelial cells (VECs), macrophage polarization, death, and autophagy, which are related to the function of mTOR signaling (Jia et al., 2007). The mTOR signaling pathway plays a complex role in the process of AS formation, plaque development, and stabilization. Although the specific mechanism of its intervention remains unclear, studies have shown that immune responses,

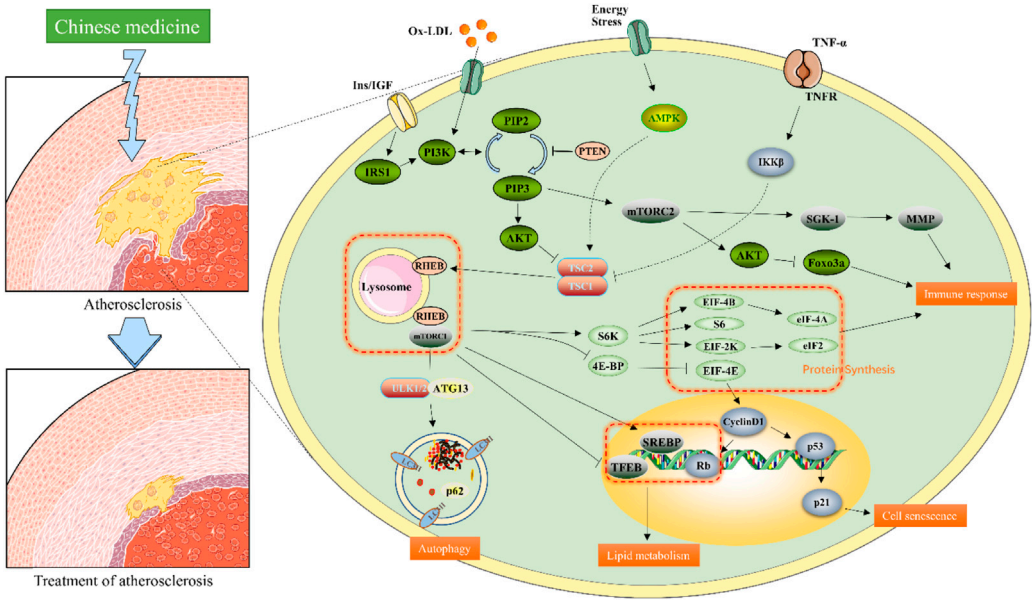

FIGURE 3
Molecular mechanism of the mTOR signaling pathway associated with AS. When the site of atherosclerosis occurs, TNF-α, lipid deposition, and increased nutrients activate the mTOR signaling pathway. These signal transductions converge on TSC1/2, which in turn inhibits Rheb activity. Rheb regulates mTORC1 activity by modulating conception. mTOR2 is mainly regulated by PI3K/AKT signaling pathway. mTORC1 and mTORC2 work together to regulate downstream proteins. The application of natural compounds from botanical drugs affects the activity of factors related to the mTOR signaling pathway in different ways, thereby increasing autophagy, inhibiting inflammation, delaying aging, and regulating lipid levels.

autophagy, regulation of lipid metabolism disorder, and cell senescence (in which the mTOR signaling pathway is involved) can crucially contribute to AS. Therefore, we will elaborate on the role of the mTOR signaling pathway in AS from the following four aspects; the specific mechanism is shown in Figure 3.

2.1 Immune response and mTOR signaling pathway in AS

The immune response is considered a vital component of AS, and the specific mechanism of immune response mediated by the mTOR signaling pathway in AS is complex (Kaldirim et al., 2022). Most studies have focused on drugs that can inhibit mTOR signaling pathway activation, particularly the mTORC1 complex, and the use of Rapamycin was found to significantly reduce the expression of inflammatory factors (Shrimali et al., 2013; Vitiello et al., 2015; Peng et al., 2018). Further study shows that the knockdown of PRAS40, an inhibitory subunit of the mTORC1 complex, promotes TNFα-induced the mTOR signaling pathway, proliferation, upregulation of inflammatory markers, and monocyte recruitment (Aspernig et al., 2019; Dai et al., 2019). The underlying molecular mechanisms are valuable but have not been completely elucidated. The endothelial dysfunction caused by abnormal lipid metabolism, diabetes, and many other factors is the initial stage of AS, which will lead to the adhesion of monocytes and monocyte-derived macrophages to the inner lining of the blood vessels and ingestion of deposited oxidized low-density lipoprotein (ox-LDL), forming foam cells (Hetherington and Totary-Jain, 2022; Scipione and Cybulsky, 2022). Previous studies have shown that ox-LDL upregulated the protein expression of p-mTOR, p-S6K1, p-4EBP1, and the mRNA expression levels of inflammatory cytokines, including interleukin 6 (IL-6), monocyte chemoattractant protein-1 (MCP-1), Toll-like receptor-4 (TLR-4), and tumor necrosis factor-alpha (TNF-α), in THP-1-derived macrophages (Liao et al., 2021). After applying everolimus to inhibit mTORC1, the macrophages in the vascular wall were selectively cleared (Verheye et al., 2007). Furthermore, TNF-α is one of the upstream activators of the mTOR signaling pathway (Gao et al., 2015), which further binds to TNFR on the cell membrane, activates IKKβ, and suppresses the tuberous sclerosis complex 1/2 (TSC1/2) following phosphorylation (Dan and Baldwin, 2008). TSC1/2 is a converging factor for several signaling pathways upstream of the mTOR signaling pathway, including those of PI3K/AKT, MAPK, and AMPK (Sarbassov et al., 2005; Yang et al., 2014; Holczer et al., 2019). TSC1/2 has been shown to regulate the polarization of M1/M2 macrophages (Fang et al., 2015). Notably, it inhibits Ras homolog enriched in the brain (Rheb) protein downstream (Menon et al., 2014). Rheb activates mTORC1 by allosterically realigning the active site residues, putting them into the right register for catalysis, further leading to downstream S6K activation and 4E-BP inhibition (Choo et al., 2008; Yang et al., 2017). Several studies have shown that S6K activation is associated with endothelial cell migration, angiogenesis, T cell activation, and nitric oxide synthase production, and drugs that inhibit the mTOR signaling pathway can protect endothelial cells by reducing S6K activity (Zheng et al., 2007; Habib et al., 2013; Hwang et al., 2015; Jiang et al., 2018; Medina-Jover et al., 2020; Arora et al., 2022).

In another study mTORC2 has also been revealed to be associated with immune responses in AS. Recent research has demonstrated that Rictor-deficient monocytes are unable to effectively move to the sites of inflammation and fully develop into macrophages, reducing the inflammatory response *in vivo* (Jangani et al., 2022). In mice with myeloid lineage-specific Rictor deletion, the survival rate of

TABLE 1 Summary of the effects of polyphenolic natural compounds on different models of AS.

Active ingredients	Source	Experimental model	Dose/concentration	Efficiency	Molecular targets	Signaling pathway	References
Quercetin	*Cuscuta chinensis Lam.; Morus alba L.*	vivo: HFD fed 8weeks male ApoE$^{-/-}$ mice; vitro: ox-LDL induced HAECs	vivo: 20mg/kg/d vitro: 3,1,0.3 mmol/L	Alleviate lipid deposition and atheroscle-rotic; alleviate cell senescence	Sirtuin↑ sIcam-1↓ IL-6↓ VCAM-1 ↓	//	Jiang et al. (2020)
Quercetin	//	HFD fed 12 weeks male ApoE−/− mice	12.5 mg/kg/d	Regulate blood lipid; Reduce inflammation; Induce autophagy	LC3 II/I↑	mTOR	Cao et al. (2019)
					p53↓		
					p21↓		
Resveratrol	*Morus alba L., Smilax glabra Roxb.*	6 weeks HFD fed male ApoE$^{-/-}$ mice	50 mg/kg/day	Regulate blood lipid;	MMP-9↓	PI3K/AKT/mTOR	Ji et al. (2022)
				Reduce inflammation	CD40L↓		
Resveratrol	//	Ox-LDL induced rabbit SMC	25 μM	Inhibit cell proliferation	//	PI3K/AKT/mTOR/ p70S6K	Brito et al. (2009)
Paeonol	*Paeonia × suffruticosa Andrews*	**Vivo:** 6 weeks male ApoE$^{-/-}$ mice fed by a high-cholesterol diet **vitro:** ox-LDL treated VSMCs	**Vivo:** 400, 200, and 100 mg/kg/d **vitro:** 15,30,60 μM	Inhibit cell proliferation; Induce autophagy	α-SMA↓	AMPK/mTOR	Wu et al. (2017)
					LC3II↑ p62↓		
					LC3II/actin↑		
Kaempferol	*Ardisia japonica (Thunb.) Blume*	HUVECs induced by ox-LDL	50,100,200 μM	Attenuate cell injury; Induce autophagy	LC3-II/I↑ p-mTOR↓	AMPK/mTOR/p70S6K	Che et al. (2017)
Curcumin	*Curcuma longa L.*	H_2O_2 induced EA.hy926 cell line	5,20 μM	Induce autophagy;	p-AKT↓	AKT/mTOR	Guo et al. (2016)
				Reduce oxidative stress	p-mTOR↓		
					LC3-II↑		
Curcumin	//	Ox-LDL-induced HUVECs	5 μM	Regulate blood lipid; Reduce inflammation; Reduce oxidative; stress; Induce autophagy	LC3-II↑	AMPK/mTOR/p70S6K	Zhao et al. (2021)
Nicotinate-Curcumin	//	Ox-LDL-induced THP-1 cell line	10 μM	Induce autophagy	LC3-II↑ p62↓	PI3K-AKT-mTOR	Gu et al. (2016)
Hydroxyl Acetylated Curcumin (Sonodynamic therapy)	//	Human THP-1 monocytes	5.0 μg/mL	Reduce lipid accumulation; Induce autophagy	Beclin1↑ LC3-II↑ p62↓	PI3K/AKT/mTOR	Zheng et al. (2016)
Chicoric acid	*Cichorium intybus L.*	Vivo: Sprague-Daw-ley rats with ligated left common carotid artery; vitro: PDGF-BB induced VSMCs	**vivo:** 50 mg/kg/d **vitro:** 10,50,100 μM	Inhibit cell proliferation and migration	p-mTOR↓ PCNA↓	mTOR/P70S6K	Lu et al. (2018)
					cyclin D1↓		
					p27↓		
6-Gingerol	*Zingiber officinale Roscoe*	Hydrogen- peroxide induced HUVECs	10, 20, 40 μM	Reduce oxidative stress; Induce autophagy	LC3-II↑	PI3K/AKT/mTOR	Wang et al. (2016a)
					Bcl-2↑		
					Beclin1↑ p-AKT↓		
					p-mTOR↓		

↑, upgrade; ↓, downgrade.

10.3389/fphar.2023.1083875

TABLE 2 Summary of effects of natural alkaloids on different AS models.

Active ingredients	Source	Experimental model	Dose/ concentration	Efficiency	Molecular targets	Signaling pathway	References
Berberine	*Coptis chinensis Franch.*	HFD fed 8-week-old male ApoE$^{-/-}$ mice	78,117,156 mg/kg	Regulate blood lipid; Induce autophagy	Beclin-1↓ p62↓ p-PI3K↑ p-mTOR↑ p-AKT↓	PI3K/AKT/ mTOR	Song and Chen, (2021)
Berberine	//	Murine cell line J774A incubated with ox-LDL	25,50 μM	Induce autophagy; Reduce inflammation	LC3 II/I↑ SQSTM1/p62↓	AMPK/mTOR	Fan et al. (2015)
Berberine (sonodynamic therapy)	//	Human THP-1 monocytes	30 μg/mL	Induce autophagy; Regulate cholesterol efflux	LC3-II/I↑ p62↓	PI3K/AKT/ mTOR	Kou et al. (2017)
Matrine	*Sophora flavescens Aiton*	AGE- induced HCSMCs	0,0.25,0.5,0.75 and 1.0mmol/L	Suppress fibrotic response	PI3K↓	PI3K/AKT/ mTOR/p70S6k	Ma et al. (2019)

↑, upgrade; ↓, downgrade.

monocytes/macrophages and mTORC2 activity were significantly decreased (Babaev et al., 2018). Furthermore, SGK-1, the downstream product of mTORC2, regulates metal ion transportation to control cell survival (Garcia-Martinez and Alessi, 2008). SGK1 plays a key role in vascular inflammation during AS due to its participation in the regulation of monocyte/macrophage migration and MMP-9 transcription through the regulation of nuclear factor-κB(NF-κB) (Yamamoto et al., 2022). MMP-9 is an independent predictor of atherosclerotic plaque instability in patients with stable coronary heart disease (Olejarz et al., 2020). Nf-κB-dependent upregulation of MMP-9 transcription levels and production triggers macrophage invasion and inflammation of the arterial wall, which promotes inflammation within the atherosclerotic plaque and subsequent progression of AS formation (Borst et al., 2015).

2.2 mTOR signaling pathway-associated autophagy and AS

Autophagy is an evolutionarily conserved subcellular process that degrades damaged protein aggregates in organelles and the cytoplasm (Wen et al., 2021). According to the different methods of cargo delivery to the lysosomal lumen, autophagy is divided into macroautophagy, microautophagy, and chaperone-mediated autophagy. The autophagy referred to here is macroautophagy (Liu et al., 2022). Autophagy plays a protective role in AS by degrading proteins and necrotic organelles to ensure cellular health and homeostasis (Henderson et al., 2021; Xu et al., 2021). Defective autophagy exacerbates cholesterol crystal-mediated hyperactivation of macrophage inflammatory vesicles and their pro-atherogenic IL-1β response (Razani et al., 2012). Research evidence shows that inhibitors of the mTOR pathway enhance the stability of atherosclerotic plaque by inducing autophagy (Ma et al., 2016). Lipophagy is a special type of autophagy, a process in which lysosomes degrade lipids, release fatty acids, and convert them to ATP (Shin, 2020). Prior research suggests that lipophagy degraded cytosolic lipid droplets, reduced the accumulation of intracellular free fatty acids (FFAs) and lipotoxicity, and promoted cholesterol efflux in foam cells. However, the specific mechanism of lipophagy in AS needs to be further studied (Liu et al., 2020; Robichaud et al., 2021; Zheng et al., 2021).

The mTOR signaling pathway regulates the upstream of autophagy in multiple cell types, including macrophages, VECs, and VSMCs. mTORC1 is a crucial regulator of autophagy with a negative regulatory effect through both direct and indirect approaches. mTORC1 directly phosphorylates unc-51-like kinase 1 (ULK1) and autophagy-related protein 13 (ATG13) (Kim et al., 2011). ULK1 is a homologue of yeast ATG1 that forms as a complex with ATG13, which can tightly regulate autophagy (Hosokawa et al., 2009; Jung et al., 2009). Meanwhile, mTOR indirectly inhibits autophagy by blocking lysosomal biogenesis by inhibiting the nuclear translocation of transcription factor EB (TFEB) (Martina et al., 2012; Napolitano et al., 2018). Defective autophagy releases more TNF-α, exacerbating further endothelial cell damage and increasing the expression of intercellular adhesion molecule 1 (ICAM-1), aggravating AS (Vion et al., 2017). Additionally, p62 is known as one of the specific substrates degraded by the autophagy-lysosomal pathway and its elevated levels often indicate autophagia dysfunction (Lippai and Low, 2014). Microtubule-associated protein 1 light chain 3 (LC-3) is located on the surface of the autophagosome membrane and participates in the formation of autophagosome, and LC3-II is a conjugated form of LC3 protein (Mizushima and Yoshimori, 2007). P62 and LC3-II (LC3II/LC3I ratio) are considered as the binding components of the core autophagy machinery and typical biomarkers associated with autophagic flux (Mizushima et al., 2010). As previously published studies describe, intracellular expression of p62 and LC3-II was significantly up- and downregulated, respectively, at sites of AS and frequently served as biomarkers of autophagy levels (Wang et al., 2016b; Zhang et al., 2018; Pattarabanjird et al., 2022; Sabbieti et al., 2022). This phenotypic alteration was also observed in ox-LDL-inhibited VSMCs *via* inhibiting the PI3K/AKT/mTOR signaling pathway (Qin et al., 2022). Several studies have also shown that increasing autophagy by activating the upstream PI3K/AKT pathway and inhibiting the activity of the mtor signaling pathway can attenuate ox-LDL-induced endothelial cell injury (Zhang et al., 2021a; Zhou et al., 2022b). Research in Dr. Babak Razani's lab showed that in macrophages, a high protein diet induces

TABLE 3 Summary of the effects of natural compounds of glycosides on different AS models.

Active ingredients	Source	Experimental model	Dose/concentration	Efficiency	Molecular targets	Signaling pathway	References
Polydatin	*Reynoutria japonica Houtt.*	HFD fed 8-week-old male ApoE$^{-/-}$ mice	50 mg/kg	Induce autophagy	LC3-I/II↑ p62↓	PI3K/AKT/mTOR	Xiong et al. (2021)
Ginsenoside Rg1	*Panax ginseng C.A.Mey.*	Murine Raw264.7 macrophages	20,50,100,200 μM	Induce autophagy	Bcl-2↑	AMPK/mTOR	Yang et al. (2018)
					Bax↓		
					LC3↑ p62/SQSMT1↑		
Geniposide combined with Notoginse-noside	*Gardenia jasminoides J.Ellis* and *Panax notoginseng (Burkill) F.H.Chen*	vivo: HFD fed 8 weeks-old male ApoE$^{-/-}$ mice vitro: H2O2 induced HUVECs	vivo: Geniposide 50 mg kg^{-1} + Notoginsenosid50 mg kg^{-1} vitro: Geniposide100 μM + Notoginseno-sid 100 μM	Alleviate cells damage; Induce autophagy; Reduce inflammation	NLRP3↑	AMPK/mTOR/Nrf2	Liu et al. (2021)
					caspase-1↑		
					VCAM-1↑		
Ophiopogonin D	*Ophiopogon japonicus (Thunb.) Ker Gawl.*	vivo: HFD fed 8-week-old male ApoE$^{-/-}$ mice vitro: LO_2 cells	vivo: 0.5 mg/kg/d vitro: 20,40,80 mM	Regulate blood lipid	p-mTOR↓	mTOR/SREBP1/ SCD1	Zhang et al. (2021b)
					SREBP1↓		
					SCD1↓		
Naringin	*Citrus × aurantium L.;*	TNF-α-induced VSMCs	10,15,25 mM	Inhibit cell invasion and migration	MMP-9↓	PI3K/AKT/mTOR/ p70S6K	Lee et al. (2009)
	Plantago lanceolata L.				NF-κB↓		
Verbascoside	*Plantago lanceolata L.;*	HFD fed male wistar rats	2 mg/kg	Regulate blood lipid; Reduce inflammation	MMP-9↓	AMPK/mTOR	Fan and Zhang, (2021)
	Forsythia suspensa (Thunb.) Vahl						

↑, upgrade; ↓, downgrade.

10.3389/fphar.2023.1083875

TABLE 4 Summary of the effects of other natural compounds on different AS models.

Active ingredients	Source	Experimental model	Dose/concentration	Efficiency	Molecular targets	Signaling pathway	References
Corylin	*Cullen corylifolium (L.) Medik.*	PDGF-BB induced VSMCs	20 μ M	Inhibite proliferation and migration in VSMCs	CDK4↓	mTOR/Drp1	Chen et al. (2020)
					CDK2↓		
					Cyclin D1↓		
					Cyclin E↓		
Morin	*Morus alba L.*;	Ox-LDL induced HUVECs	1,3,10,30 μmol/L	Attenuate cell injury; Induce autophagy	LC3↓ p62↑	AMPK/mTOR	Zhang et al. (2019)
					p-AMPK↑		
	Prunella vulgaris L.				p-mTOR↓		
Artemisinin	*Artemisia caruifolia var. caruifolia*	HFD fed 8weeks male ApoE$^{-/-}$ mice	50,100 mg/kg/d	Reduce inflammation; Induce autophagy	p62↓	AMPK/mTOR/ULK1	Cao et al. (2020)
					LC-3II↑		
Artemisinin and Procyanidins loaded multifunctional nanocomplexes	*Artemisia annua L.; Forsythia suspensa (Thunb.) Vahl*	vivo: HFD fed 6-week-old male ApoE$^{-/-}$ mice vitro: RAW264.7 stimulation with lipopolysaccharide	vivo: 0.9 mg/kg procyanidins +4.1 mg/kg artemisinin vitro: RAW264.7 stimulation with lipopolysaccharide	Inhibiting the formation of atheroscler-otic plaques; inhibitory inflammatory cytokines; romote cholesterol efflux and lipid influx	AMPK ↑	NF-κB/NLRP3; AMPK/mTOR	Zhou et al. (2022a)
					Beclin-1 ↑		
					LC3II/I↑		
					SR-BI↑		
					ABCA-1 ↑		
					ABCG-1 ↑		
Imperatorin	*Angelica dahurica (Hoffm.) Benth. & Hook.f. ex Franch. & Sav.*	Ox-LDL induced VSMCs	10,20,40 μM/L	Attenuate VSMCs migration, alleviate foam cell formation	p-PI3k↓	PI3K/AKT/mTOR	Li et al. (2020)
					p-AKT↓		
					p-mTOR↓		
Salvianolic acid B	*Salvia miltiorrhiza Bunge*	Cholesterol crystal-induced RAW264.7 cell line	100,150,200 μM	Attenuate cholesterol crystals; improve the autophagy	LC3-II↑ Beclin-1↑ p62↓	AKT/mTOR	Sun et al. (2021)
Salvianolic acid B	//	RAW264.7 cells	100,150,200 μM	Promote autophagy	p-AKT↓ p-mTOR↓	NF-κB/AKT/mTOR	Zou et al. (2022)
Salvianolic acid B	//	Hydrogen peroxide- induced HUVECs	5,10,20 μ g/ml	Promote autophagy	caspase-3↓	AMPK/mTOR	Gao et al. (2019)
					LC3-ll↑		
					Beclin-1↑ p62↓		
Zedoarondiol	*Curcuma aromatica Salisb.*	PDGF-BB induced VSMCs	5,10,20 μg/mL	Inhibit VSMCs proliferation	p53↑	AMPK/mTOR/p70S6K	Mao et al. (2016)
					p21↑		
Hydroxysafflor Yellow A (Sonodynamic Therapy)	*Carthamus tinctorius L.*	Human THP-1 monocytes	0.1,0.3,0.6,0.8,1mmol/L	Induce autophagy, inhibite inflammatory factors	LC3-II↓	PI3K/AKT/mTOR	Jiang et al. (2017)
					Beclin↓		
					p62↓		
Hypericin-mediated (sonodynamic Therapy)	*Sedum sarmentosum Bunge*	Human THP-1 monocytes	0.25 μg/mL	Activate autophagy	LC3-II/I↑	AMPK/AKT/mTOR	Li et al. (2016)
					Beclin↑		
					SQSTM1/p62↓ p-AMPK↑		

↑, upgrade; ↓, downgrade.

10.3389/fphar.2023.1083875

the activation of the leucine-mediated mTOR signaling pathway; mitochondrial autophagy is inhibited, exacerbating mitochondrial dysfunction and macrophage apoptosis, accelerating the progression of AS (Zhang et al., 2020). Interestingly, silencing of the RICTOR, the major subunit of mTORC2, increased LC3-II expression and decreased p62 protein levels in endothelial cells, suggesting that mTORC2 can also interfere with autophagic flux by a yet-to-be-fully elucidated mechanism (Bernard et al., 2014).

2.3 mTOR signaling pathway-mediated cell senescence in the pathogenesis of AS

Cell senescence is a state of indefinite cell cycle arrest implemented in response to sublethal stresses (Hwang et al., 2022). Current studies have found that dietary restriction (DR) without malnutrition is the most effective way to prevent cell senescence in humans, and *in vivo* experiments revealed that inhibition of mTORC1 activity in yeast, nematodes, flies, and mammals can lead to a longer lifespan (Vellai et al., 2003; Kapahi et al., 2004; Kaeberlein et al., 2005; Wu et al., 2013; Green et al., 2022). Excessive nutrient and lipid stimulation, the triggers of cellular senescence, activate the signaling pathways upstream of the mTOR signaling pathway, including those of PI3K/AKT, AMPK, and Rag-GATOR, resulting in increased mTORC1 activity, and then regulating the downstream cellular activities, such as protein synthesis and autophagy (Bent et al., 2016; Hesketh et al., 2020; Sadria and Layton, 2021). Existing studies suggest that the involvement of the mTOR pathway is central to cell senescence, mainly for the properties of mTOR inhibitors (e.g., Sirolimus and everolimus) available in humans. However, they are not primarily aimed at aging and have many side effects (primarily insulin resistance and immunosuppression) (Cruzado et al., 2016; Carosi et al., 2022).

AS is an age-related disorder, and the incidence of AS increases significantly with age. Age-related cell senescence is a key element in the pathogenesis of AS (Bjorkegren and Lusis, 2022). On the one hand, cell senescence blocks the cell cycle to G_1-G_2 phase and inhibits damaged cell proliferation, which has a protective effect in certain cases of cancer (Huang et al., 2022b). On the other hand, cell senescence also leads to hyperfunction in cells; studies have shown that the secretion of inflammatory factors in senescent cells is increased, and such pathological changes will aggravate the progression of AS (Bian et al., 2020; Xiang et al., 2022). Large VECs similar to senescent cells *in vitro* are often found on the surface of plaques, suggesting that vascular cells may undergo senescence *in vivo* (Minamino et al., 2002). Research has shown increased mTOR activity in senescent VSMCs induced by Adriamycin, and inhibiting the mTOR signaling pathway significantly decreased the expression of senescence markers (p53/p21/p16) (Sung et al., 2018). In addition, a decrease in the level of telomeric repeat-binding factor 2 (TRF2) in VSMCs derived from human plaques suggests the emergence of cell senescence and promotes endothelial dysfunction (Wang et al., 2015). Remarkably, in a murine model of AS, Rapamycin was used to enhance autophagy, and the mTORC1/ULK1/ATG13 signaling pathway was found to delay the senescence of mouse smooth muscle cells (Luo et al., 2017). Meanwhile, this study also revealed that inactivation of mTORC1 could inhibit p53 to suppress VSMC senescence. Subsequent studies elaborated upon the possible role of mTOR-p53-p21 signal cascades in cell senescence (Brooks and Gu, 2010; Huang et al., 2022b). However, whether this mechanism functions in AS, remains to be investigated.

2.4 Regulation of mTOR signaling pathway in AS lipid metabolism

It is well known that dyslipidemia is closely related to the occurrence and development of AS (Authors/Task Force et al., 2019). mTORC1 promotes fat storage by inhibiting lipolysis and promoting *de novo* lipogenesis, which may be related to the downstream of mTORC1/S6K signaling factors like sterol-regulatory element binding proteins (SREBPs), an important family of transcription factors that promotes lipogenesis and adipogenesis, and control lipid metabolism (Chakrabarti et al., 2010; Cheon and Cho, 2021). mTORC1 has been shown to regulate SREBP by controlling the nuclear import of phosphatidic acid phosphatase lipin 1 (Libby, 2021b). *In vivo* experiments reversed the inflammation-induced LDLr increase in $ApoE^{-/-}$ mice by the Rapamycin inhibitor and verified that increased mTORC1 activity upregulates SREBP-2-mediated cholesterol uptake through retinoblastoma tumor suppressor protein phosphorylation (Ma et al., 2013). By blocking mTOR expression using specific small interfering RNA (siRNA), it was observed that macrophage-derived foam cell formation was inhibited, accompanied by a reduction in lipid deposition (Wang et al., 2014). Meanwhile, mTORC1 can regulate lipolysis and adipose tissue thermogenesis by regulating the downstream GRB10 (Liu et al., 2014). Nevertheless, treatment of adipocytes with Rapamycin reduced insulin-stimulated TAG stores by about 50%, and the same trend was observed in RAPTOR knockout mice, which showed an increase in serum-free fatty acids, one of the reasons why mTOR inhibitor use often results in high triglyceride lipids (Soliman et al., 2010; Paolella et al., 2020). Hypertriglyceridemia is also a significant cause of AS, which has recently attracted more and more attention (Libby, 2021b). Therefore, modulation of mTORC1 activity in lipid regulation of AS is controversial, although most studies have demonstrated a significant inhibitory effect of mTOR inhibitors on plaque growth. Beyond this, it has also been shown that adipocyte-specific mTORC2 activity promotes adipogenesis, *de novo* lipogenesis, and controls insulin-stimulated glucose uptake, but direct evidence for these processes associated with AS is lacking (Tang et al., 2016; Szwed et al., 2021).

3 Natural compounds and anti-atherosclerosis

Many natural compounds extracted from botanical drugs have positive therapeutic effects on the occurrence and development of AS through various ways, such as promoting autophagy, regulating blood lipids, reducing inflammatory factors, alleviate cellular senescence, etc. (Xu et al., 2015; Rastogi et al., 2016; Lyu et al., 2022). In this paper, various natural compounds are divided into the following categories according to their chemical formulas: polyphenols, alkaloids, glycosides, and others, which are listed in Tables 1–Tables 4. The chemical composition is shown in Figure 4.

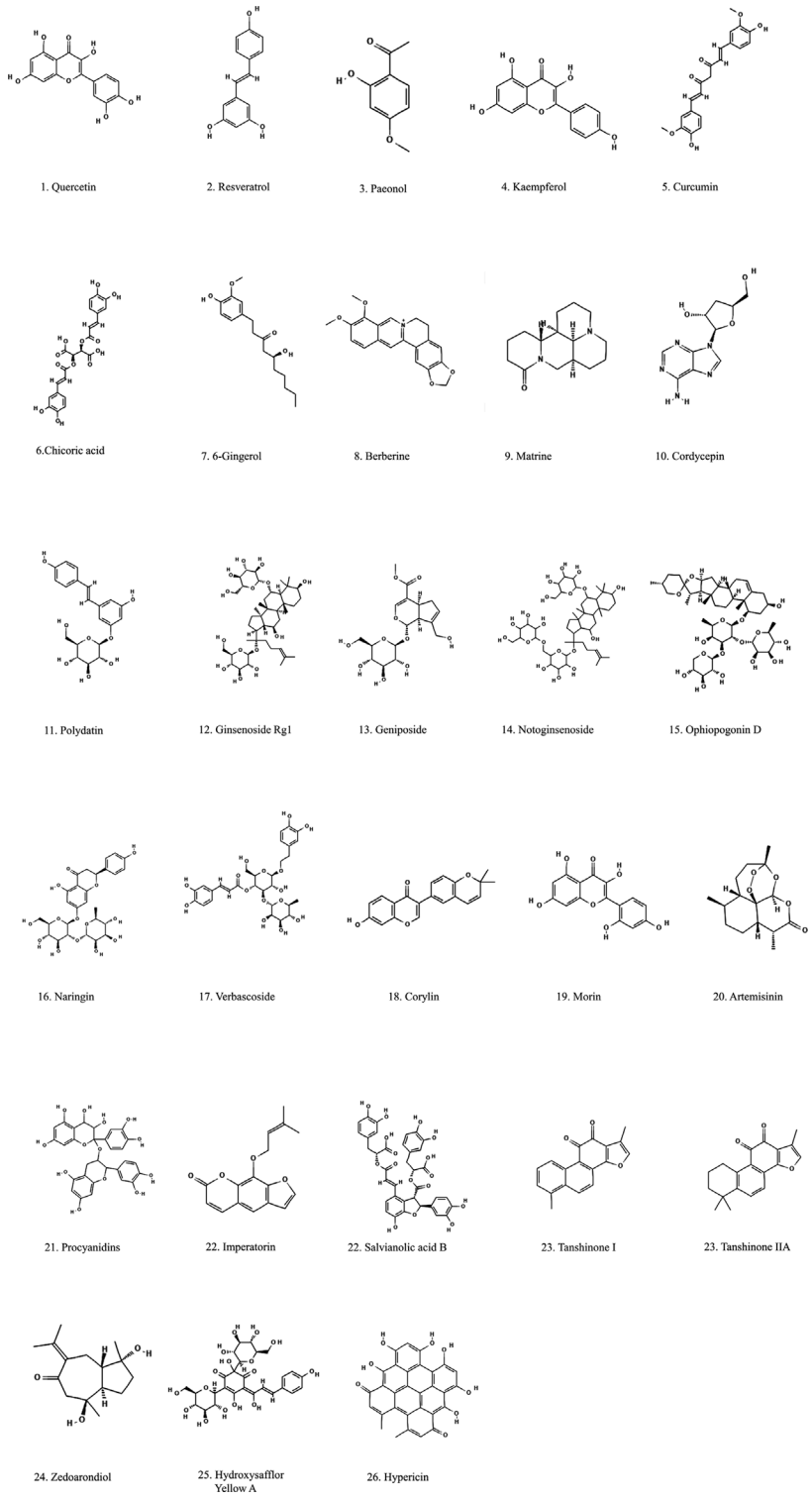

FIGURE 4
Structural formulation of natural compounds derived from botanical drugs with anti-atherogenic effects.

3.1 Polyphenols

As a kind of secondary metabolite, polyphenols are widely found in a variety of botanical drugs. Existing research on polyphenols mainly focuses on their anti-inflammatory, antioxidant, and anticancer effects (Cheng et al., 2017; Benvenuto et al., 2020). It is worth noting that some polyphenols, including resveratrol, paeonol, and curcumin, may display anti-AS properties by interacting with some cell receptors and/or gene expression regulators through mTOR and its related effectors due to their unique biological activity(Lu et al., 2018; Tian et al., 2019).

Quercetin is a flavonoid compound widely found in various vegetables, fruits, berries, and in many botanical drugs such as

Cuscuta chinensis Lam. and *Morus alba L.* It has a wide range of biological activities, including anti-inflammatory, anti-aging, antioxidant, etc. (Stewart et al., 2008; Kobori et al., 2016; Cui et al., 2022). Quercetin significantly reduced atherosclerotic plaque area, aortic lipid accumulation and serum inflammatory factor levels in mice (Sun et al., 2015; Ren et al., 2018; Jia et al., 2019). It has been observed that quercetin inhibits the development of atherosclerotic plaques in mice by activating the PI3K/AKT signaling pathway, which is also upstream of the mTOR signaling pathway (Lu et al., 2017). Also, quercetin could enhance autophagic flux and reduce lipid accumulation in the aortic roots of hfd-fed mice by inhibiting mTOR expression (Cao et al., 2019). Jiang et al. (2020) found that quercetin (20 mg/kg/d) gavage for 8 weeks could significantly inhibit AS in mice as well as increase the density of Sirt 1 in mice aorta, the changes of which are related to the decline of autophagy in the cell senescence. Although this study concluded by KEGG analysis stated that the mTOR signaling pathway is involved in the pharmacological mechanism of quercetin against ox-LDL, a rigorous experimental validation is lacking. Notably, some studies suggest that flavonoids represented by quercetin are prone to aggregation behavior and non-specific inhibition, which raises questions about the reliability of reports on the biological activity of polyphenols *in vitro* (Pohjala and Tammela, 2012; Sheridan and Spelman, 2022). It is also interesting to note that quercetin has been reported to have low solubility and poor bioavailability, which limits its applicability (Abdel-Tawab, 2021; Bertelli et al., 2021). Therefore, how to improve the bioavailability of these valuable compounds is also a promising topic to be explored in current and future studies (Sapino et al., 2015).

Resveratrol, a typical polyphenol compound, can be obtained from *Morus alba L*, *Smilax glabra Roxb.*, and other botanical drugs. Resveratrol has a variety of biological activities, and has been reported to protect the permeability of endothelial cells and maintain the integrity of the endothelial barrier, which has a protective effect against AS (Gurusinghe et al., 2017). Early studies found that the mTOR signaling pathway is activated by ox-LDL and is associated with VSMC proliferation; resveratrol inhibits DNA synthesis and proliferation of rabbit VSMCs by blocking ox-LDL-induced phosphorylation and activation of the PI3K/AKT/mTOR/p70S6K pathway (Brito et al., 2009). Ji et al. (2022) investigated the relationship between resveratrol and mTOR in umbilical vein endothelial cells (UVECs) in AS mice models. After intraperitoneal injections of resveratrol (50 mg/kg/day) for 5 weeks, resveratrol treatment significantly reduced the mRNA and protein expression levels of PI3K, AKT, and mTOR in UVEC, decreased serum inflammatory cytokine levels, and reduced the area of atherosclerotic lesions, but the relationship between these processes has not been demonstrated in the study.

Paeonol is the main active ingredient of *Paeonia × suffruticosa Andrews*, which has shown good anti-atherosclerotic effects in *in vitro* and *in vivo* experiments. Danserol could delay AS through processes such as inhibiting inflammation, regulating autophagy, promoting cholesterol efflux to inhibit foam cell production, and protecting vascular endothelial cells, which are processes closely related to the mTOR signaling pathway (Li et al., 2009; Li et al., 2015; Li et al., 2018; Liu et al., 2018). An investigation showed that high doses of salvianol (400 mg/Kg) had a good protective effect in mice with AS models. However, free drug plasma concentrations were not measured in this study to better understand the metabolism of the drug *in vivo*. Meanwhile, VSMC were treated *in vitro* using 30 μM dermatol, and the results showed that dermatol could activate autophagy and inhibit the proliferation of vascular smooth muscle cells by activating the AMPK/mTOR signaling pathway (Wu et al., 2017). In addition, research has shown that paeonol acts against premature senescence by modulating Sirtuin 1 pathway (Jamal et al., 2014). Although other studies have linked mTOR with Sirtuin 1 in the process of autophagy and senescence (Morselli et al., 2010; Liu et al., 2016), whether paeonol can regulate senescence through mTOR signaling still needs to be investigated.

Curcumin is a natural polyphenol, the most active ingredient of *Curcuma longa L*, which may be a potential multi-target therapeutic avenue for atherosclerotic diseases. Guo et al. (2016) conducted an *in vitro* experiment and found that compared to blank group and H_2O_2-treated (200 μmol/L) group, the expression level of LC3-II protein in curcumin-pretreated (5, 20 μmol/L) group was significantly increased, while the expression levels of p-AKT and p-mTOR were significantly decreased, suggesting AKT's involvement in curcumin-induced mTOR inhibition and autophagy to protect endothelial cells. Similarly, curcumin plays an important role in attenuating atherosclerotic endothelial cell injury by regulating the autophagy-related PI3K/AMPK/mTOR/p70S6K signaling pathway (Zhao et al., 2021). Curcumin promotes autophagy and reduces inflammation by promoting nuclear translocation in TFEB, one of the downstream factors of mTORC1 (Li et al., 2022). However, whether curcumin can regulate TFEB through mTOR still needs more specific studies. In addition, the current studies are using *in vitro* experiments to probe the pharmacological activity of curcumin targeting the mTOR signaling pathway, which is not always representative of the natural physiological environment and therefore may not provide an accurate prediction for *in vivo* botanical drugs.

Chicoric acid is a potent anti-atherosclerotic component that has been shown to have strong cardiovascular protective effects. Studies have shown that it alleviates endothelial dysfunction by attenuating ox-LDL (Tsai et al., 2017). Lu et al. (2018) conducted experiments to investigate the potential mechanism of chicoric acid in treating AS. They ligated the left carotid artery of rats for 8 weeks and found that 8 weeks of chicoric acid (50 mg/kg/d) gavage significantly inhibited carotid intimal hyperplasia and reduced the intima area of the injured carotid artery; western blot analysis showed that chrysotile acid decreased p-mTOR and p-P70S6K protein levels, suggesting its possible inhibition of the mTOR/P70S6K signaling pathway, which in turn hindered the VSMC phenotypic switching, proliferation, migration, and neointima formation and improving AS.

6-Gingerol is an important active component of *Zingiber officinale Roscoe* with anti-inflammatory and antioxidant abilities (Ballester et al., 2022). 6-gingerol reversed the significant reduction in oxidative stress-induced levels of LC3-II, Beclin1 (key protein for upregulation of autophagy), and Bcl-2 (key gene for inhibition of apoptosis) in HUVECs and decreased the expression of p-AKT and p-mTOR, demonstrating that 6-gingerol can induce autophagy through the AKT/mTOR pathway, avoid apoptosis, and protect vascular endothelial cell survival (Wang et al., 2016a). This experiment also provided research insights for further investigation of the possible mechanisms of the interaction between mTOR-mediated autophagy and apoptosis.

3.2 Alkaloids

Alkaloids are also a type of secondary metabolites, which are mainly derived from plants, but are also found in animals and fungi. Emerging evidence suggests that alkaloids have a wide range of biological activities (Mondal et al., 2019; Shang et al., 2020). Its mechanism includes the inhibition of cell proliferation, regulation of autophagy, and regulation of a variety of related genes and pathways. Therefore, the potential of alkaloids to inhibit AS is worth investigating.

Berberine, an isoquinoline alkaloid, widely exists in *Coptis chinensis Franch*. A recent study reported the potential mechanism of berberine in treating AS (Song and Chen, 2021). High-fat diet (HFD)-fed ApoE$^{-/-}$ mice were divided into a model group, positive drug group, and low (78 mg/kg), medium (117 mg/kg), and high dose (156 mg/kg) berberine groups. Interestingly, compared to the model group, all doses of berberine reduced AS plaque area and serum TC, TG, and LDL-C levels, while only high doseof berberine had an effect on HDL-C levels; middle and high doses had effects on the expressions of p-PI3K, p-mTOR, and p-AKT, suggesting that the biological effects of berberine in treating AS may be through the PI3K/AKT/mTOR signaling pathway. Another report (Fan et al., 2015) showed that berberine reduced ox-LDL-induced inflammation in a dose-and time-dependent manner and increased LC3II/LC3I and SQSTM1/p62 levels, indicating that berberine inhibited inflammation by upregulating autophagy; the activation of AMPK/mTOR signaling pathway stimulates autophagy in macrophages, and chloroquine could reduce these effects. Induction of ROS production and autophagy are important in regulating macrophage lipid deposition through lysosome/autophagosome-mediated degradation. Berberine-mediated sonodynamic therapy may become a new treatment option for AS, which promotes ROS production, induces cholesterol efflux, and induces autophagy in macrophages and foam cells through PI3K/AKT/mTOR signaling pathway inhibition (Kou et al., 2017).

Matrine is a tetracyclo-quinolizindine alkaloid, which can be extracted from *Sophora flavescens Aiton*. Advanced glycosylation end products (AGEs) are a group of substances existing in poorly controlled type 2 diabetes mellitus, which promote the fibrotic response of VSMCs and then aggravate AS through mTOR signaling pathway activation (de Vos et al., 2016). Matrine pretreatment reduced the expression of PI3K and the phosphorylation of mTOR in a concentration-dependent manner, as well as inhibited AGEs-induced fibrosis response in human coronary smooth muscle cells (HCSMCs) (Ma et al., 2019). The regulatory effect of matrine on mTOR provides a new idea for the treatment of type 2 diabetes-associated AS.

3.3 Glycosides

Glycosides are organic molecules whose therapeutic activities are manifested in many aspects. Some glycosides such as Polydatin, Astragaloside IV, and Ginsenoside Rg1, showed excellent anti-AS effects.

Polydatin has a wide range of pharmacological activities, and is a natural component extracted from *Reynoutria japonica Houtt*. Xiong and his colleagues (Xiong et al., 2021) observed high expression levels of PI3K (p-PI3K), AKT (p-AKT) and mTOR (p-mTOR) proteins in atherosclerotic plaques of ApoE$^{-/-}$ mice induced by a HFD. Polydatin intervention significantly reduced this effect and was accompanied by an elevated autophagic flux. The addition of 3-Methyladenine (3-MA) in the study inhibited autophagy and reversed the downregulation of p-mTOR by polydatin, suggesting that the mechanism of polydatin-mediated AS inhibition in the *in vivo* experiments may be by the regulation of autophagy through the mTOR signaling pathway.

Ginsenoside Rg1 is derived from *Panax ginseng* C.A. Mey and has cardiovascular protective and anti-inflammatory effects (Gao et al., 2020; Sarhene et al., 2021). Ginsenoside Rg1 ameliorates ox-LDL-induced apoptosis, senescence, and oxidative stress in HUVECs cells through the AMPK/SIRT3/p53 signaling pathway (Lyu et al., 2022). More experiments are needed to prove whether mTOR is involved in the anti-senescence effect of ginsenoside Rg1. Another study reported that ginsenoside Rg1, at the most effective dose of 50 uM, could inhibit ox-LDL-induced apoptosis of Raw264.7 macrophages by activating the AMPK/mTOR signaling pathway to upregulate autophagic flux, which is a protective factor in advanced AS, as excessive macrophage apoptosis increases atherosclerotic plaque instability (Yang et al., 2018). However, the relationship between mTOR-mediated autophagy and apoptosis in AS still requires new experimental evidence, as some studies also consider that autophagy and apoptosis are two different types of processes (Shan et al., 2021).

Ophiopogonin D is an effective compound isolated from botanical drugs *Ophiopogon japonicus (Thunb.) Ker Gawl.* Ophiopogonin D treatment can reduce blood lipid levels and alleviate mitochondrial damage and dysfunction in palmitic acid–stimulated mice(Li et al., 2021). Gavage of HDF-fed mice with Daidzein D (0.5 mg/kg/D) for 12 weeks significantly reduced lipid levels, mTOR and p-mTOR levels, SREBP1 and SCD1 levels, and aortic root plaques, suggesting that Daidzein D may decrease lipogenesis and alleviate AS by inhibiting phosphorylation of mTOR, and thus SREBP1 and SCD1 (Zhang et al., 2021b).

3.4 Others

Artemisinin is an endoperoxide sesquiterpene lactone mainly derived from *Artemisia caruifolia var. caruifolia*, which can be used as a potential therapeutic agent for AS. Cao et al. (2020) reported that artemisinin's (50,100 mg/kg) intragastolic administration for 8 weeks effectively reduced the formation of AS plaque in ApoE$^{-/-}$ mice and downregulated the levels of inflammatory factors such as MCP-1, IFN-γ, IL-6, and TNF-α. In addition, *in vitro* experiments showed that artemisinin (100 μM) promoted the autophagy of macrophages after ox-LDL treatment and inhibited the production of inflammatory cytokines, along with the upregulation of AMPK activation and the inhibition of phosphorylation of mTOR and ULK1. Another report showed that artemisinin and Procyanidins co-loaded nanocomplex can inhibit the RONS/NF-κB/NLRP3 pathway to reduce inflammation and inhibit lipid influx, and enhance the AMPK/mTOR pathway to regulate cholesterol efflux, thereby regulating lipid metabolism to attenuate atherosclerotic lesions (Zhou et al., 2022a).

Salvianolic acid B (Sal B) is a flavonoid compound, which is isolated from the botanical drug *Salvia miltiorrhiza Bunge*, it can inhibit the development of arterial plaque in ApoE$^{-/-}$ mice, reduce the production of ox-LDL in serum, and show significant anti-inflammatory effects (Yang et al., 2020). Sal B (200 μM) inhibited

the LPS + IFN-γ-activated AKT/mTOR pathway and enhanced autophagy, while insulin activation of the mTOR signaling pathway counteracted the inhibitory effect of Sal B on M1 macrophage polarization, suggesting that Sal B can inhibit M1 macrophage polarization and reduce the release of inflammatory factors through the mTOR signaling pathway, thus exerting an anti-atherogenic effect (Zou et al., 2022).

Tanshinone I and Tanshinone IIA are also important active substances extracted from *Salvia miltiorrhiza Bunge*. According to a recent report, tanshinone I significantly inhibited the activation of PI3K and the phosphorylation of mTOR, 70S6K, and S6 in a concentration-dependent manner, thereby inhibiting the proliferation of VSMCs and playing a protective role in AS (Wang et al., 2020b). Tanshinone IIA can phosphorylate endothelial oxide synthase (eNOS) by activating TGF-β/PI3K/AKT pathway, promote the product and release of endogenous nitric oxide, and protect vascular endothelial cells (Wang et al., 2020a). Tanshinone IIA can also down-regulate the activity of CD40 and MMP-2, downstream factors of mTOR, in HFD-induced AS rabbits for anti-inflammation, but whether this pathway is through mTOR has not been confirmed (Fang et al., 2008).

4 Conclusion and perspectives

The natural compounds derived from botanical drugs containing quercetin, resveratrol, and other botanical drugs have the characteristics of multi-target, multi-pathway collaboration, by which they perform anti-atherosclerotic effects through lipid-lowering, anti-inflammatory, slowing down the cell senescence, and autophagy-promoting mechanisms (Zhi et al., 2023). The mTOR signaling pathway plays an important role in the formation and development of AS. We summarized the effects of the mTOR signaling pathway from the immune response, autophagy, anti-aging, and regulation of lipid metabolism in atherogenesis, suggesting that mTOR signaling pathway inhibition may be a potential therapeutic target for AS. In current clinical studies, mTOR inhibitors are not applicable to the primary treatment of AS since they target the activity of the mTOR complex, which has a great impact on the cell cycle and causes disturbances in glucose and lipid metabolism, instead of being one of the risk factors for AS (Wang et al., 2022). On the contrary, numerous studies have shown that natural botanical drugs can effectively reduce lipid levels, while also inhibiting the mTOR signaling pathway, elevating autophagy and reducing immune response, indicating the advantages of TCM (Song et al., 2019; Zhou et al., 2022a).

Although a large body of preclinical evidence implicates the mTOR signaling pathway in the regulation of AS, there remain many limitations in the study of the effects and mechanisms of natural compounds that modulate the mTOR pathway in treating AS. The multi-targeted actions of TCM drugs may trigger additional effects upstream and downstream of the mTOR signaling pathway, generating some impacts other than anti-AS that were not all detectable throughout the experiments. Many studies have broadly attributed the regulatory effects of drugs on the mTOR signaling pathway to the regulation of protein synthesis by mTORC1. While this can be verified experimentally, whether it interferes with protein expression through other more complex molecular biological processes remains to be discovered. In the recent experimental studies on TCM, few have detected the expression levels of proteins in the mTORC1 and mTORC2 complexes other than the mTOR proteins, as well as these proteins playing a crucial role in the mTOR signaling pathway. In addition, existing studies are limited to the scope of animal or cellular experiments, and evidence based on the results of high-quality clinical studies is lacking, possibly due to the difficulty of extracting natural products from botanical drugs and their low bioavailability. The side effects of phytomedicines also need to be clarified before their possible clinical application. These limitations suggest additional directions for future fundamental research and clinical trials.

In conclusion, we have reviewed that the natural products of botanical drugs can slow down the progression of AS by inhibiting the mTOR signaling pathway. This work provides a theoretical basis and a reference for future research to further expand the mechanisms and applications of natural products of TCM. However, additional studies are needed to elucidate the specific mechanisms involved in order to achieve the ultimate goal of botanical drugs used in TCM for the prevention and treatment of AS.

Author contributions

QW and SW designed the study. YY, XY, MW, and LL collected literature data, created the tables and figures. QW and QL wrote the initial draft of the manuscript. XL, LC, and JL revised the manuscript. All authors contributed to the article and approved the final version of the manuscript.

Funding

This research is supported by the National Natural Science Foundation of China (81473465), Beijing Municipal Science & Technology Commission (Z191100006619025).

Conflict of interest

The authors declare that the research was conducted in the absence of any commercial or financial relationships that could be construed as a potential conflict of interest.

Publisher's note

All claims expressed in this article are solely those of the authors and do not necessarily represent those of their affiliated organizations, or those of the publisher, the editors and the reviewers. Any product that may be evaluated in this article, or claim that may be made by its manufacturer, is not guaranteed or endorsed by the publisher.

References

Arora, A., Kivela, A. M., Wang, L., Minkeviciene, R., Taskinen, J. H., Zhang, B., et al. (2022). Protrudin regulates FAK activation, endothelial cell migration and angiogenesis. *Cell Mol. Life Sci.* 79, 220. doi:10.1007/s00018-022-04251-z

Abdel-Tawab, M. (2021). Considerations to Be Taken When Carrying Out Medicinal Plant Research-What We Learn from an Insight into the IC50 Values, Bioavailability and Clinical Efficacy of Exemplary Anti-Inflammatory Herbal Components. *Pharmaceuticals (Basel)* 14 (5), 437. doi:10.3390/ph14050437

Aspernig, H., Heimbucher, T., Qi, W., Gangurde, D., Curic, S., Yan, Y., et al. (2019). Mitochondrial perturbations couple mTORC2 to autophagy in *C. elegans*. *Cell Rep.* 29, 1399–1409. doi:10.1016/j.celrep.2019.09.072

Authors/Task Force, M., Guidelines, E. S. C. C. F. P., and Societies, E. S. C. N. C. (2019). 2019 ESC/EAS guidelines for the management of dyslipidaemias: Lipid modification to reduce cardiovascular risk. *Atherosclerosis* 290, 140–205. doi:10.1016/j.atherosclerosis.2019.08.014

Avruch, J., Long, X., Lin, Y., Ortiz-Vega, S., Rapley, J., Papageorgiou, A., et al. (2009). Activation of mTORC1 in two steps: Rheb-GTP activation of catalytic function and increased binding of substrates to raptor. *Biochem. Soc. Trans.* 37, 223–226. doi:10.1042/BST0370223

Babaev, V. R., Huang, J., Ding, L., Zhang, Y., May, J. M., and Linton, M. F. (2018). Loss of rictor in monocyte/macrophages suppresses their proliferation and viability reducing atherosclerosis in LDLR null mice. *Front. Immunol.* 9, 215. doi:10.3389/fimmu.2018.00215

Ballester, P., Cerda, B., Arcusa, R., Marhuenda, J., Yamedjeu, K., and Zafrilla, P. (2022). Effect of ginger on inflammatory diseases. *Molecules* 27, 7223. doi:10.3390/molecules27217223

Ben-Sahra, I., and Manning, B. D. (2017). mTORC1 signaling and the metabolic control of cell growth. *Curr. Opin. Cell Biol.* 45, 72–82. doi:10.1016/j.ceb.2017.02.012

Bent, E. H., Gilbert, L. A., and Hemann, M. T. (2016). A senescence secretory switch mediated by PI3K/AKT/mTOR activation controls chemoprotective endothelial secretory responses. *Genes Dev.* 30, 1811–1821. doi:10.1101/gad.284851.116

Benvenuto, M., Albonici, L., Focaccetti, C., Ciuffa, S., Fazi, S., Cifaldi, L., et al. (2020). Polyphenol-mediated autophagy in cancer: Evidence of *in vitro* and *in vivo* studies. *Int. J. Mol. Sci.* 21, 6635. doi:10.3390/ijms21186635

Bertelli, A., Biagi, M., Corsini, M., Baini, G., Cappellucci, G., Miraldi, E., et al. (2021). Polyphenols: From Theory to Practice. *Foods* 10 (11), 2595. doi:10.3390/foods10112595

Bernard, M., Dieude, M., Yang, B., Hamelin, K., Underwood, K., and Hebert, M. J. (2014). Autophagy fosters myofibroblast differentiation through MTORC2 activation and downstream upregulation of CTGF. *Autophagy* 10, 2193–2207. doi:10.4161/15548627.2014.981786

Bhattacharya, P., Kanagasooriyan, R., and Subramanian, M. (2022). Tackling inflammation in atherosclerosis: Are we there yet and what lies beyond? *Curr. Opin. Pharmacol.* 66, 102283. doi:10.1016/j.coph.2022.102283

Bian, W., Jing, X., Yang, Z., Shi, Z., Chen, R., Xu, A., et al. (2020). Downregulation of LncRNA NORAD promotes Ox-LDL-induced vascular endothelial cell injury and atherosclerosis. *Aging (Albany NY)* 12, 6385–6400. doi:10.18632/aging.103034

Bjorkegren, J. L. M., and Lusis, A. J. (2022). Atherosclerosis: Recent developments. *Cell* 185, 1630–1645. doi:10.1016/j.cell.2022.04.004

Borst, O., Schaub, M., Walker, B., Schmid, E., Munzer, P., Voelkl, J., et al. (2015). Pivotal role of serum- and glucocorticoid-inducible kinase 1 in vascular inflammation and atherogenesis. *Arterioscler. Thromb. Vasc. Biol.* 35, 547–557. doi:10.1161/ATVBAHA.114.304454

Brito, P. M., Devillard, R., NèGRE-Salvayre, A., Almeida, L. M., Dinis, T. C., Salvayre, R., et al. (2009). Resveratrol inhibits the mTOR mitogenic signaling evoked by oxidized LDL in smooth muscle cells. *Atherosclerosis* 205, 126–134. doi:10.1016/j.atherosclerosis.2008.11.011

Brooks, C. L., and Gu, W. (2010). New insights into p53 activation. *Cell Res.* 20, 614–621. doi:10.1038/cr.2010.53

Cai, Z., He, Y., and Chen, Y. (2018). Role of mammalian target of rapamycin in atherosclerosis. *Curr. Mol. Med.* 18, 216–232. doi:10.2174/1566524018666180926163917

Cao, H., Jia, Q., Shen, D., Yan, L., Chen, C., and Xing, S. (2019). Quercetin has a protective effect on atherosclerosis via enhancement of autophagy in ApoE(-/-) mice. *Exp. Ther. Med.* 18, 2451–2458. doi:10.3892/etm.2019.7851

Cao, Q., Du, H., Fu, X., Duan, N., Liu, C., and Li, X. (2020). Artemisinin attenuated atherosclerosis in high-fat diet-fed ApoE-/- mice by promoting macrophage autophagy through the AMPK/mTOR/ULK1 pathway. *J. Cardiovasc Pharmacol.* 75, 321–332. doi:10.1097/FJC.0000000000000794

Carosi, J. M., Fourrier, C., Bensalem, J., and Sargeant, T. J. (2022). The mTOR-lysosome axis at the centre of ageing. *FEBS Open Bio* 12, 739–757. doi:10.1002/2211-5463.13347

Chakrabarti, P., English, T., Shi, J., Smas, C. M., and Kandror, K. V. (2010). Mammalian target of rapamycin complex 1 suppresses lipolysis, stimulates lipogenesis, and promotes fat storage. *Diabetes* 59, 775–781. doi:10.2337/db09-1602

Che, J., Liang, B., Zhang, Y., Wang, Y., Tang, J., and Shi, G. (2017). Kaempferol alleviates ox-LDL-induced apoptosis by up-regulation of autophagy via inhibiting PI3K/Akt/mTOR pathway in human endothelial cells. *Cardiovasc Pathol.* 31, 57–62. doi:10.1016/j.carpath.2017.08.001

Chen, C. C., Li, H. Y., Leu, Y. L., Chen, Y. J., Wang, C. J., and Wang, S. H. (2020). Corylin inhibits vascular cell inflammation, proliferation and migration and reduces atherosclerosis in ApoE-deficient mice. *Antioxidants (Basel)* 9, 275. doi:10.3390/antiox9040275

Chen, C. H., and Sarbassov Dos, D. (2011). The mTOR (mammalian target of rapamycin) kinase maintains integrity of mTOR complex 2. *J. Biol. Chem.* 286, 40386–40394. doi:10.1074/jbc.M111.282590

Cheng, Y. C., Sheen, J. M., Hu, W. L., and Hung, Y. C. (2017). Polyphenols and oxidative stress in atherosclerosis-related ischemic heart disease and stroke. *Oxid. Med. Cell Longev.* 2017, 8526438. doi:10.1155/2017/8526438

Cheon, S. Y., and Cho, K. (2021). Lipid metabolism, inflammation, and foam cell formation in health and metabolic disorders: Targeting mTORC1. *J. Mol. Med. Berl.* 99, 1497–1509. doi:10.1007/s00109-021-02117-8

Cheraga, N., Ye, Z., Xu, M. J., Zou, L., Sun, N. C., Hang, Y., et al. (2022). Targeted therapy of atherosclerosis by pH-sensitive hyaluronic acid nanoparticles co-delivering all-trans retinal and rapamycin. *Nanoscale* 14, 8709–8726. doi:10.1039/d1nr06514a

Choo, A. Y., Yoon, S. O., Kim, S. G., Roux, P. P., and Blenis, J. (2008). Rapamycin differentially inhibits S6Ks and 4E-BP1 to mediate cell-type-specific repression of mRNA translation. *Proc. Natl. Acad. Sci. U. S. A.* 105, 17414–17419. doi:10.1073/pnas.0809136105

Cruzado, J. M., Pascual, J., Sanchez-Fructuoso, A., Seron, D., Diaz, J. M., Rengel, M., et al. (2016). Controlled randomized study comparing the cardiovascular profile of everolimus with tacrolimus in renal transplantation. *Transpl. Int.* 29, 1317–1328. doi:10.1111/tri.12862

Cui, Z., Zhao, X., Amevor, F. K., Du, X., Wang, Y., Li, D., et al. (2022). Therapeutic application of quercetin in aging-related diseases: SIRT1 as a potential mechanism. *Front. Immunol.* 13, 943321. doi:10.3389/fimmu.2022.943321

Dai, J., Jiang, C., Chen, H., and Chai, Y. (2019). Rapamycin attenuates high glucose-induced inflammation through modulation of mTOR/NF-κB pathways in macrophages. *Front. Pharmacol.* 10, 1292. doi:10.3389/fphar.2019.01292

Dan, H. C., and Baldwin, A. S. (2008). Differential involvement of IkappaB kinases alpha and beta in cytokine- and insulin-induced mammalian target of rapamycin activation determined by Akt. *J. Immunol.* 180, 7582–7589. doi:10.4049/jimmunol.180.11.7582

De Vos, L. C., Lefrandt, J. D., Dullaart, R. P., Zeebregts, C. J., and Smit, A. J. (2016). Advanced glycation end products: An emerging biomarker for adverse outcome in patients with peripheral artery disease. *Atherosclerosis* 254, 291–299. doi:10.1016/j.atherosclerosis.2016.10.012

Fan, X., Wang, J., Hou, J., Lin, C., Bensoussan, A., Chang, D., et al. (2015). Berberine alleviates ox-LDL induced inflammatory factors by up-regulation of autophagy via AMPK/mTOR signaling pathway. *J. Transl. Med.* 13, 92. doi:10.1186/s12967-015-0450-z

Fan, Y., and Zhang, K. (2021). Verbascoside inhibits the progression of atherosclerosis in high fat diet induced atherosclerosis rat model. *J. Physiol. Pharmacol.* 72. doi:10.26402/jpp.2021.3.03

Fang, C., Yu, J., Luo, Y., Chen, S., Wang, W., Zhao, C., et al. (2015). Tsc1 is a critical regulator of macrophage survival and function. *Cell Physiol. Biochem.* 36, 1406–1418. doi:10.1159/000430306

Fang, Z. Y., Lin, R., Yuan, B. X., Yang, G. D., Liu, Y., and Zhang, H. (2008). Tanshinone IIA downregulates the CD40 expression and decreases MMP-2 activity on atherosclerosis induced by high fatty diet in rabbit. *J. Ethnopharmacol.* 115, 217–222. doi:10.1016/j.jep.2007.09.025

Gao, S., Li, S., Li, Q., Zhang, F., Sun, M., Wan, Z., et al. (2019). Protective effects of salvianolic acid B against hydrogen peroxide-induced apoptosis of human umbilical vein endothelial cells and underlying mechanisms. *Int. J. Mol. Med.* 44, 457–468. doi:10.3892/ijmm.2019.4227

Gao, S., Liu, W., Zhuo, X., Wang, L., Wang, G., Sun, T., et al. (2015). The activation of mTOR is required for monocyte pro-inflammatory response in patients with coronary artery disease. *Clin. Sci. (Lond)* 128, 517–526. doi:10.1042/CS20140427

Gao, Y., Li, J., Wang, J., Li, X., Li, J., Chu, S., et al. (2020). Ginsenoside Rg1 prevent and treat inflammatory diseases: A review. *Int. Immunopharmacol.* 87, 106805. doi:10.1016/j.intimp.2020.106805

Garcia-Martinez, J. M., and Alessi, D. R. (2008). mTOR complex 2 (mTORC2) controls hydrophobic motif phosphorylation and activation of serum- and glucocorticoid-induced protein kinase 1 (SGK1). *Biochem. J.* 416, 375–385. doi:10.1042/BJ20081668

Green, C. L., Lamming, D. W., and Fontana, L. (2022). Molecular mechanisms of dietary restriction promoting health and longevity. *Nat. Rev. Mol. Cell Biol.* 23, 56–73. doi:10.1038/s41580-021-00411-4

Gu, H. F., Li, H. Z., Tang, Y. L., Tang, X. Q., Zheng, X. L., and Liao, D. F. (2016). Nicotinate-curcumin impedes foam cell formation from THP-1 cells through restoring autophagy flux. *PLoS One* 11, e0154820. doi:10.1371/journal.pone.0154820

Guo, S., Long, M., Li, X., Zhu, S., Zhang, M., and Yang, Z. (2016). Curcumin activates autophagy and attenuates oxidative damage in EA.hy926 cells via the Akt/mTOR pathway. *Mol. Med. Rep.* 13, 2187–2193. doi:10.3892/mmr.2016.4796

Guo, Y., Qin, J., Zhao, Q., Yang, J., Wei, X., Huang, Y., et al. (2022). Plaque-targeted rapamycin spherical nucleic acids for synergistic atherosclerosis treatment. *Adv. Sci. (Weinh)* 9, e2105875. doi:10.1002/advs.202105875

Gurusinghe, S., Cox, A. G., Rahman, R., Chan, S. T., Muljadi, R., Singh, H., et al. (2017). Resveratrol mitigates trophoblast and endothelial dysfunction partly via activation of nuclear factor erythroid 2-related factor-2. *Placenta* 60, 74–85. doi:10.1016/j.placenta.2017.10.008

Habib, A., Karmali, V., Polavarapu, R., Akahori, H., Nakano, M., Yazdani, S., et al. (2013). Metformin impairs vascular endothelial recovery after stent placement in the setting of locally eluted mammalian target of rapamycin inhibitors via S6 kinase-dependent inhibition of cell proliferation. *J. Am. Coll. Cardiol.* 61, 971–980. doi:10.1016/j.jacc.2012.12.018

Henderson, J. M., Weber, C., and Santovito, D. (2021)., 10. Cells, 625. doi:10.3390/cells10030625Beyond self-recycling: Cell-specific role of autophagy in atherosclerosis*Cells*

Hesketh, G. G., Papazotos, F., Pawling, J., Rajendran, D., Knight, J. D. R., Martinez, S., et al. (2020). The GATOR-Rag GTPase pathway inhibits mTORC1 activation by lysosome-derived amino acids. *Science* 370, 351–356. doi:10.1126/science.aaz0863

Hetherington, I., and Totary-Jain, H. (2022). Anti-atherosclerotic therapies: Milestones, challenges, and emerging innovations. *Mol. Ther.* 30, 3106–3117. doi:10.1016/j.ymthe.2022.08.024

Holczer, M., Hajdu, B., Lorincz, T., Szarka, A., Banhegyi, G., and Kapuy, O. (2019). A double negative feedback loop between mTORC1 and AMPK kinases guarantees precise autophagy induction upon cellular stress. *Int. J. Mol. Sci.* 20, 5543. doi:10.3390/ijms20225543

Hosokawa, N., Hara, T., Kaizuka, T., Kishi, C., Takamura, A., Miura, Y., et al. (2009). Nutrient-dependent mTORC1 association with the ULK1-Atg13-FIP200 complex required for autophagy. *Mol. Biol. Cell* 20, 1981–1991. doi:10.1091/mbc.e08-12-1248

Huang, C., Huang, W., Zhang, L., Zhang, C., Zhou, C., Wei, W., et al. (2022a). Targeting peptide, fluorescent reagent modified magnetic liposomes coated with rapamycin target early atherosclerotic plaque and therapy. *Pharmaceutics* 14, 1083. doi:10.3390/pharmaceutics14051083

Huang, W., Hickson, L. J., Eirin, A., Kirkland, J. L., and Lerman, L. O. (2022b). Cellular senescence: The good, the bad and the unknown. *Nat. Rev. Nephrol.* 18, 611–627. doi:10.1038/s41581-022-00601-z

Hwang, H. J., Kim, N., Herman, A. B., Gorospe, M., and Lee, J. S. (2022). Factors and pathways modulating endothelial cell senescence in vascular aging. *Int. J. Mol. Sci.* 23, 10135. doi:10.3390/ijms231710135

Hwang, S., Lee, H. J., Kim, G., Won, K. J., Park, Y. S., and Jo, I. (2015). CCN1 acutely increases nitric oxide production via integrin αvβ3-Akt-S6K-phosphorylation of endothelial nitric oxide synthase at the serine 1177 signaling axis. *Free Radic. Biol. Med.* 89, 229–240. doi:10.1016/j.freeradbiomed.2015.08.005

Jamal, J., Mustafa, M. R., and Wong, P. F. (2014). Paeonol protects against premature senescence in endothelial cells by modulating Sirtuin 1 pathway. *J. Ethnopharmacol.* 154, 428–436. doi:10.1016/j.jep.2014.04.025

Jangani, M., Vuononvirta, J., Yamani, L., Ward, E., Capasso, M., Nadkarni, S., et al. (2022). Loss of mTORC2-induced metabolic reprogramming in monocytes uncouples migration and maturation from production of proinflammatory mediators. *J. Leukoc. Biol.* 111, 967–980. doi:10.1002/JLB.1A0920-588R

Ji, W., Sun, J., Hu, Z., and Sun, B. (2022). Resveratrol protects against atherosclerosis by downregulating the PI3K/AKT/mTOR signaling pathway in atherosclerosis model mice. *Exp. Ther. Med.* 23, 414. doi:10.3892/etm.2022.11341

Jia, G., Cheng, G., and Agrawal, D. K. (2007). Autophagy of vascular smooth muscle cells in atherosclerotic lesions. *Autophagy* 3, 63–64. doi:10.4161/auto.3427

Jia, Q., Cao, H., Shen, D., Li, S., Yan, L., Chen, C., et al. (2019). Quercetin protects against atherosclerosis by regulating the expression of PCSK9, CD36, PPARγ, LXRα and ABCA1. *Int. J. Mol. Med.* 44, 893–902. doi:10.3892/ijmm.2019.4263

Jiang, R. H., Xu, X. Q., Wu, C. J., Lu, S. S., Zu, Q. Q., Zhao, L. B., et al. (2018). The CD40/CD40L system regulates rat cerebral microvasculature after focal ischemia/reperfusion via the mTOR/S6K signaling pathway. *Neurol. Res.* 40, 717–723. doi:10.1080/01616412.2018.1473075

Jiang, Y. H., Jiang, L. Y., Wang, Y. C., Ma, D. F., and Li, X. (2020). Corrigendum: Quercetin attenuates atherosclerosis via modulating oxidized LDL-induced endothelial cellular senescence. *Front. Pharmacol.* 11, 772. doi:10.3389/fphar.2020.00772

Jiang, Y., Kou, J., Han, X., Li, X., Zhong, Z., Liu, Z., et al. (2017). ROS-dependent activation of autophagy through the PI3K/Akt/mTOR pathway is induced by hydroxysafflor yellow A-sonodynamic therapy in THP-1 macrophages. *Oxid. Med. Cell Longev.* 2017, 8519169. doi:10.1155/2017/8519169

Julien, L. A., Carriere, A., Moreau, J., and Roux, P. P. (2010). mTORC1-activated S6K1 phosphorylates Rictor on threonine 1135 and regulates mTORC2 signaling. *Mol. Cell Biol.* 30, 908–921. doi:10.1128/MCB.00601-09

Jung, C. H., Jun, C. B., Ro, S. H., Kim, Y. M., Otto, N. M., Cao, J., et al. (2009). ULK-Atg13-FIP200 complexes mediate mTOR signaling to the autophagy machinery. *Mol. Biol. Cell* 20, 1992–2003. doi:10.1091/mbc.e08-12-1249

Kaeberlein, M., Powers, R. W., 3R. D., Steffen, K. K., Westman, E. A., Hu, D., Dang, N., et al. (2005). Regulation of yeast replicative life span by TOR and Sch9 in response to nutrients. *Science* 310, 1193–1196. doi:10.1126/science.1115535

Kaldirim, M., Lang, A., Pfeiler, S., Fiegenbaum, P., Kelm, M., Bonner, F., et al. (2022). Modulation of mTOR signaling in cardiovascular disease to target acute and chronic inflammation. *Front. Cardiovasc Med.* 9, 907348. doi:10.3389/fcvm.2022.907348

Kapahi, P., Zid, B. M., Harper, T., Koslover, D., Sapin, V., and Benzer, S. (2004). Regulation of lifespan in Drosophila by modulation of genes in the TOR signaling pathway. *Curr. Biol.* 14, 885–890. doi:10.1016/j.cub.2004.03.059

Kim, D. H., and Sabatini, D. M. (2004). Raptor and mTOR: Subunits of a nutrient-sensitive complex. *Curr. Top. Microbiol. Immunol.* 279, 259–270. doi:10.1007/978-3-642-18930-2_15

Kim, D. H., Sarbassov, D. D., Ali, S. M., King, J. E., Latek, R. R., Erdjument-Bromage, H., et al. (2002). mTOR interacts with raptor to form a nutrient-sensitive complex that signals to the cell growth machinery. *Cell* 110, 163–175. doi:10.1016/s0092-8674(02)00808-5

Kim, J., Kundu, M., Viollet, B., and Guan, K. L. (2011). AMPK and mTOR regulate autophagy through direct phosphorylation of Ulk1. *Nat. Cell Biol.* 13, 132–141. doi:10.1038/ncb2152

Kim, K., Park, S. E., Park, J. S., and Choi, J. H. (2022). Characteristics of plaque lipid-associated macrophages and their possible roles in the pathogenesis of atherosclerosis. *Curr. Opin. Lipidol.* 33, 283–288. doi:10.1097/MOL.0000000000000842

Kobori, M., Takahashi, Y., Sakurai, M., Akimoto, Y., Tsushida, T., Oike, H., et al. (2016). Quercetin suppresses immune cell accumulation and improves mitochondrial gene expression in adipose tissue of diet-induced obese mice. *Mol. Nutr. Food Res.* 60, 300–312. doi:10.1002/mnfr.201500595

Kong, P., Cui, Z. Y., Huang, X. F., Zhang, D. D., Guo, R. J., and Han, M. (2022). Inflammation and atherosclerosis: Signaling pathways and therapeutic intervention. *Signal Transduct. Target Ther.* 7, 131. doi:10.1038/s41392-022-00955-7

Kou, J. Y., Li, Y., Zhong, Z. Y., Jiang, Y. Q., Li, X. S., Han, X. B., et al. (2017). Berberine-sonodynamic therapy induces autophagy and lipid unloading in macrophage. *Cell Death Dis.* 8, e2558. doi:10.1038/cddis.2016.354

Laplante, M., and Sabatini, D. M. (2012). mTOR signaling in growth control and disease. *Cell* 149, 274–293. doi:10.1016/j.cell.2012.03.017

Lee, E. J., Kim, D. I., Kim, W. J., and Moon, S. K. (2009). Naringin inhibits matrix metalloproteinase-9 expression and AKT phosphorylation in tumor necrosis factor-alpha-induced vascular smooth muscle cells. *Mol. Nutr. Food Res.* 53, 1582–1591. doi:10.1002/mnfr.200800210

Li, C., Yang, L., Wu, H., and Dai, M. (2018). Paeonol inhibits oxidized low-density lipoprotein-induced vascular endothelial cells autophagy by upregulating the expression of miRNA-30a. *Front. Pharmacol.* 9, 95. doi:10.3389/fphar.2018.00095

Li, H., Dai, M., and Jia, W. (2009). Paeonol attenuates high-fat-diet-induced atherosclerosis in rabbits by anti-inflammatory activity. *Planta Med.* 75, 7–11. doi:10.1055/s-0028-1088332

Li, W., Ji, L., Tian, J., Tang, W., Shan, X., Zhao, P., et al. (2021). Ophiopogonin D alleviates diabetic myocardial injuries by regulating mitochondrial dynamics. *J. Ethnopharmacol.* 271, 113853. doi:10.1016/j.jep.2021.113853

Li, W., Niu, X., Yu, J., Xiao, X., Zang, L., Zhao, J., et al. (2020). Imperatorin alleviates the abnormal proliferation, migration, and foaming of ox-LDL-induced VSMCs through regulating PI3K/Akt/mTOR signaling pathway. *J. Funct. foods* 70, 103982. doi:10.1016/j.jff.2020.103982

Li, X., Zhang, X., Zheng, L., Kou, J., Zhong, Z., Jiang, Y., et al. (2016). Author Correction: Hypericin-mediated sonodynamic therapy induces autophagy and decreases lipids in THP-1 macrophage by promoting ROS-dependent nuclear translocation of TFEB. *Cell Death Dis.* 7, 202. doi:10.1038/s41419-019-1321-y

Li, X., Zhou, Y., Yu, C., Yang, H., Zhang, C., Ye, Y., et al. (2015). Paeonol suppresses lipid accumulation in macrophages via upregulation of the ATP-binding cassette transporter A1 and downregulation of the cluster of differentiation 36. *Int. J. Oncol.* 46, 764–774. doi:10.3892/ijo.2014.2757

Li, X., Zhu, R., Jiang, H., Yin, Q., Gu, J., Chen, J., et al. (2022). Autophagy enhanced by curcumin ameliorates inflammation in atherogenesis via the TFEB-P300-BRD4 axis. *Acta Pharm. Sin. B* 12, 2280–2299. doi:10.1016/j.apsb.2021.12.014

Liao, M., Hu, F., Qiu, Z., Li, J., Huang, C., Xu, Y., et al. (2021). Pim-2 kinase inhibits inflammation by suppressing the mTORC1 pathway in atherosclerosis. *Aging (Albany NY)* 13, 22412–22431. doi:10.18632/aging.203547

Libby, P. (2021a). The changing landscape of atherosclerosis. *Nature* 592, 524–533. doi:10.1038/s41586-021-03392-8

Libby, P. (2021b). The changing nature of atherosclerosis: What we thought we knew, what we think we know, and what we have to learn. *Eur. Heart J.* 42, 4781–4782. doi:10.1093/eurheartj/ehab438

Lippai, M., and Low, P. (2014). The role of the selective adaptor p62 and ubiquitin-like proteins in autophagy. *Biomed. Res. Int.* 2014, 832704. doi:10.1155/2014/832704

Liu, G. Y., and Sabatini, D. M. (2020). mTOR at the nexus of nutrition, growth, ageing and disease. *Nat. Rev. Mol. Cell Biol.* 21, 183–203. doi:10.1038/s41580-019-0199-y

Liu, H. W., Wei, C. C., Chen, Y. J., Chen, Y. A., and Chang, S. J. (2016). Flavanol-rich lychee fruit extract alleviates diet-induced insulin resistance via suppressing mTOR/SREBP-1 mediated lipogenesis in liver and restoring insulin signaling in skeletal muscle. *Mol. Nutr. Food Res.* 60, 2288–2296. doi:10.1002/mnfr.201501064

Liu, M., Bai, J., He, S., Villarreal, R., Hu, D., Zhang, C., et al. (2014). Grb10 promotes lipolysis and thermogenesis by phosphorylation-dependent feedback inhibition of mTORC1. *Cell Metab.* 19, 967–980. doi:10.1016/j.cmet.2014.03.018

Liu, Q., Wang, Y. M., and Gu, H. F. (2020). Lipophagy in atherosclerosis. *Clin. Chim. Acta* 511, 208–214. doi:10.1016/j.cca.2020.10.025

Liu, T., Jin, Q., Ren, F., Yang, L., Mao, H., Ma, F., et al. (2022). Potential therapeutic effects of natural compounds targeting autophagy to alleviate podocyte injury in glomerular diseases. *Biomed. Pharmacother.* 155, 113670. doi:10.1016/j.biopha.2022.113670

Liu, X., Xu, Y., Cheng, S., Zhou, X., Zhou, F., He, P., et al. (2021). Geniposide combined with notoginsenoside R1 attenuates inflammation and apoptosis in atherosclerosis via the AMPK/mTOR/Nrf2 signaling pathway. *Front. Pharmacol.* 12, 687394. doi:10.3389/fphar.2021.687394

Liu, Y., Li, C., Wu, H., Xie, X., Sun, Y., and Dai, M. (2018). Paeonol attenuated inflammatory response of endothelial cells via stimulating monocytes-derived exosomal MicroRNA-223. *Front. Pharmacol.* 9, 1105. doi:10.3389/fphar.2018.01105

Lu, Q. B., Wan, M. Y., Wang, P. Y., Zhang, C. X., Xu, D. Y., Liao, X., et al. (2018). Chicoric acid prevents PDGF-BB-induced VSMC dedifferentiation, proliferation and migration by suppressing ROS/NFκB/mTOR/P70S6K signaling cascade. *Redox Biol.* 14, 656–668. doi:10.1016/j.redox.2017.11.012

Lu, X. L., Zhao, C. H., Yao, X. L., and Zhang, H. (2017). Quercetin attenuates high fructose feeding-induced atherosclerosis by suppressing inflammation and apoptosis via ROS-regulated PI3K/AKT signaling pathway. *Biomed. Pharmacother.* 85, 658–671. doi:10.1016/j.biopha.2016.11.077

Lu, Y., Cui, X., Zhang, L., Wang, X., Xu, Y., Qin, Z., et al. (2022). The functional role of lipoproteins in atherosclerosis: Novel directions for diagnosis and targeting therapy. *Aging Dis.* 13, 491–520. doi:10.14336/AD.2021.0929

Luo, Z., Xu, W., Ma, S., Qiao, H., Gao, L., Zhang, R., et al. (2017). Moderate autophagy inhibits vascular smooth muscle cell senescence to stabilize progressed atherosclerotic plaque via the mTORC1/ULK1/ATG13 signal pathway. *Oxid. Med. Cell Longev.* 2017, 3018190. doi:10.1155/2017/3018190

Lyu, T. J., Zhang, Z. X., Chen, J., and Liu, Z. J. (2022). Ginsenoside Rg1 ameliorates apoptosis, senescence and oxidative stress in ox-LDL-induced vascular endothelial cells via the AMPK/SIRT3/p53 signaling pathway. *Exp. Ther. Med.* 24, 545. doi:10.3892/etm.2022.11482

Ma, K. L., Liu, J., Wang, C. X., Ni, J., Zhang, Y., Wu, Y., et al. (2013). Increased mTORC1 activity contributes to atherosclerosis in apolipoprotein E knockout mice and in vascular smooth muscle cells. *Int. J. Cardiol.* 168, 5450–5453. doi:10.1016/j.ijcard.2013.03.152

Ma, M., Song, L., Yan, H., Liu, M., Zhang, L., Ma, Y., et al. (2016). Low dose tunicamycin enhances atherosclerotic plaque stability by inducing autophagy. *Biochem. Pharmacol.* 100, 51–60. doi:10.1016/j.bcp.2015.11.020

Ma, W., Xu, J., Zhang, Y., Zhang, H., Zhang, Z., Zhou, L., et al. (2019). Matrine pretreatment suppresses AGEs- induced HCSMCs fibrotic responses by regulating Poldip2/mTOR pathway. *Eur. J. Pharmacol.* 865, 172746. doi:10.1016/j.ejphar.2019.172746

Ma, X. M., and Blenis, J. (2009). Molecular mechanisms of mTOR-mediated translational control. *Nat. Rev. Mol. Cell Biol.* 10, 307–318. doi:10.1038/nrm2672

Mao, H., Tao, T., Song, D., Liu, M., Wang, X., Liu, X., et al. (2016). Zedoarondiol inhibits platelet-derived growth factor-induced vascular smooth muscle cells proliferation via regulating AMP-activated protein kinase signaling pathway. *Cell Physiol. Biochem.* 40, 1506–1520. doi:10.1159/000453201

Martina, J. A., Chen, Y., Gucek, M., and Puertollano, R. (2012). MTORC1 functions as a transcriptional regulator of autophagy by preventing nuclear transport of TFEB. *Autophagy* 8, 903–914. doi:10.4161/auto.19653

Medina-Jover, F., Gendrau-Sanclemente, N., and Vinals, F. (2020). SGK1 is a signalling hub that controls protein synthesis and proliferation in endothelial cells. *FEBS Lett.* 594, 3200–3215. doi:10.1002/1873-3468.13901

Menon, S., Dibble, C. C., Talbott, G., Hoxhaj, G., Valvezan, A. J., Takahashi, H., et al. (2014). Spatial control of the TSC complex integrates insulin and nutrient regulation of mTORC1 at the lysosome. *Cell* 156, 771–785. doi:10.1016/j.cell.2013.11.049

Minamino, T., Miyauchi, H., Yoshida, T., Ishida, Y., Yoshida, H., and Komuro, I. (2002). Endothelial cell senescence in human atherosclerosis: Role of telomere in endothelial dysfunction. *Circulation* 105, 1541–1544. doi:10.1161/01.cir.0000013836.85741.17

Mizushima, N., and Yoshimori, T. (2007). How to interpret LC3 immunoblotting. *Autophagy* 3, 542–545. doi:10.4161/auto.4600

Mizushima, N., Yoshimori, T., and Levine, B. (2010). Methods in mammalian autophagy research. *Cell* 140, 313–326. doi:10.1016/j.cell.2010.01.028

Mondal, A., Gandhi, A., Fimognari, C., Atanasov, A. G., and Bishayee, A. (2019). Alkaloids for cancer prevention and therapy: Current progress and future perspectives. *Eur. J. Pharmacol.* 858, 172472. doi:10.1016/j.ejphar.2019.172472

Morselli, E., Maiuri, M. C., Markaki, M., Megalou, E., Pasparaki, A., Palikaras, K., et al. (2010). The life span-prolonging effect of sirtuin-1 is mediated by autophagy. *Autophagy* 6, 186–188. doi:10.4161/auto.6.1.10817

Mueller, M. A., Beutner, F., Teupser, D., Ceglarek, U., and Thiery, J. (2008). Prevention of atherosclerosis by the mTOR inhibitor everolimus in LDLR-/- mice despite severe hypercholesterolemia. *Atherosclerosis* 198, 39–48. doi:10.1016/j.atherosclerosis.2007.09.019

Napolitano, G., Esposito, A., Choi, H., Matarese, M., Benedetti, V., Di Malta, C., et al. (2018). mTOR-dependent phosphorylation controls TFEB nuclear export. *Nat. Commun.* 9, 3312. doi:10.1038/s41467-018-05862-6

Olejarz, W., Lacheta, D., and Kubiak-Tomaszewska, G. (2020). Matrix metalloproteinases as biomarkers of atherosclerotic plaque instability. *Int. J. Mol. Sci.* 21, 3946. doi:10.3390/ijms21113946

Paolella, L. M., Mukherjee, S., Tran, C. M., Bellaver, B., Hugo, M., Luongo, T. S., et al. (2020). mTORC1 restrains adipocyte lipolysis to prevent systemic hyperlipidemia. *Mol. Metab.* 32, 136–147. doi:10.1016/j.molmet.2019.12.003

Pattarabanjird, T., Marshall, M., Upadhye, A., Srikakulapu, P., Garmey, J. C., Haider, A., et al. (2022). B-1b cells possess unique bHLH-driven P62-dependent self-renewal and atheroprotection. *Circ. Res.* 130, 981–993. doi:10.1161/CIRCRESAHA.121.320436

Peng, S., Xu, L. W., Che, X. Y., Xiao, Q. Q., Pu, J., Shao, Q., et al. (2018). Atorvastatin inhibits inflammatory response, attenuates lipid deposition, and improves the stability of vulnerable atherosclerotic plaques by modulating autophagy. *Front. Pharmacol.* 9, 438. doi:10.3389/fphar.2018.00438

Penson, P. E., and Banach, M. (2021). Natural compounds as anti-atherogenic agents: Clinical evidence for improved cardiovascular outcomes. *Atherosclerosis* 316, 58–65. doi:10.1016/j.atherosclerosis.2020.11.015

Poznyak, A. V., Sukhorukov, V. N., Zhuravlev, A., Orekhov, N. A., Kalmykov, V., and Orekhov, A. N. (2022). Modulating mTOR signaling as a promising therapeutic strategy for atherosclerosis. *Int. J. Mol. Sci.* 23, 1153. doi:10.3390/ijms23031153

Pohjala, L., and Tammela, P. (2012). Aggregating behavior of phenolic compounds–a source of false bioassay results?. *Molecules* 17 (9), 10774–10790. doi:10.3390/molecules170910774

Qin, X., He, W., Yang, R., Liu, L., Zhang, Y., Li, L., et al. (2022). Inhibition of Connexin 43 reverses ox-LDL-mediated inhibition of autophagy in VSMC by inhibiting the PI3K/Akt/mTOR signaling pathway. *PeerJ* 10, e12969. doi:10.7717/peerj.12969

Rastogi, S., Pandey, M. M., and Rawat, A. K. (2016). Traditional herbs: A remedy for cardiovascular disorders. *Phytomedicine* 23, 1082–1089. doi:10.1016/j.phymed.2015.10.012

Razani, B., Feng, C., Coleman, T., Emanuel, R., Wen, H., Hwang, S., et al. (2012). Autophagy links inflammasomes to atherosclerotic progression. *Cell Metab.* 15, 534–544. doi:10.1016/j.cmet.2012.02.011

Ren, K., Jiang, T., and Zhao, G. J. (2018). Quercetin induces the selective uptake of HDL-cholesterol via promoting SR-BI expression and the activation of the PPARγ/LXRα pathway. *Food Funct.* 9, 624–635. doi:10.1039/c7fo01107e

Riggs, K. A., Joshi, P. H., Khera, A., Otvos, J. D., Greenland, P., Ayers, C. R., et al. (2022). GlycA, hsCRP differentially associated with MI, ischemic stroke: In the dallas heart study and multi-ethnic study of atherosclerosis: GlycA, hsCRP differentially associated MI, stroke. *Am. J. Prev. Cardiol.* 12, 100373. doi:10.1016/j.ajpc.2022.100373

Robichaud, S., Fairman, G., Vijithakumar, V., Mak, E., Cook, D. P., Pelletier, A. R., et al. (2021). Identification of novel lipid droplet factors that regulate lipophagy and cholesterol efflux in macrophage foam cells. *Autophagy* 17, 3671–3689. doi:10.1080/15548627.2021.1886839

Sabbieti, M. G., Marchegiani, A., Sufianov, A. A., Gabai, V. L., Shneider, A., and Agas, D. (2022). P62/SQSTM1 beyond autophagy: Physiological role and therapeutic applications in laboratory and domestic animals. *Life (Basel)* 12, 539. doi:10.3390/life12040539

Sadria, M., and Layton, A. T. (2021). Interactions among mTORC, AMPK and SIRT: A computational model for cell energy balance and metabolism. *Cell Commun. Signal* 19, 57. doi:10.1186/s12964-021-00706-1

Sarbassov, D. D., Ali, S. M., Kim, D. H., Guertin, D. A., Latek, R. R., Erdjument-Bromage, H., et al. (2004). Rictor, a novel binding partner of mTOR, defines a rapamycin-insensitive and raptor-independent pathway that regulates the cytoskeleton. *Curr. Biol.* 14, 1296–1302. doi:10.1016/j.cub.2004.06.054

Sarbassov, D. D., Ali, S. M., and Sabatini, D. M. (2005). Growing roles for the mTOR pathway. *Curr. Opin. Cell Biol.* 17, 596–603. doi:10.1016/j.ceb.2005.09.009

Sarhene, M., Ni, J. Y., Duncan, E. S., Liu, Z., Li, S., Zhang, J., et al. (2021). Ginsenosides for cardiovascular diseases; update on pre-clinical and clinical evidence, pharmacological effects and the mechanisms of action. *Pharmacol. Res.* 166, 105481. doi:10.1016/j.phrs.2021.105481

Sasaki, T., Maier, B., Bartke, A., and Scrable, H. (2006). Progressive loss of SIRT1 with cell cycle withdrawal. *Aging Cell* 5, 413–422. doi:10.1111/j.1474-9726.2006.00235.x

Sapino, S., Ugazio, E., Gastaldi, L., Miletto, I., Berlier, G., Zonari, D., et al. (2015). Mesoporous silica as topical nanocarriers for quercetin: characterization and in vitro studies. *Eur J Pharm Biopharm.* 89, 116–125. doi:10.1016/j.ejpb.2014.11.022

Saxton, R. A., and Sabatini, D. M. (2017). mTOR signaling in growth, metabolism, and disease. *Cell* 168, 960–976. doi:10.1016/j.cell.2017.02.004

Scipione, C. A., and Cybulsky, M. I. (2022). Early atherogenesis: New insights from new approaches. *Curr. Opin. Lipidol.* 33, 271–276. doi:10.1097/MOL.0000000000000843

Shan, R., Liu, N., Yan, Y., and Liu, B. (2021). Apoptosis, autophagy and atherosclerosis: Relationships and the role of Hsp27. *Pharmacol. Res.* 166, 105169. doi:10.1016/j.phrs.2020.105169

Shang, X. F., Yang, C. J., Morris-Natschke, S. L., Li, J. C., Yin, X. D., Liu, Y. Q., et al. (2020). Biologically active isoquinoline alkaloids covering 2014-2018. *Med. Res. Rev.* 40, 2212–2289. doi:10.1002/med.21703

Shin, D. W. (2020). Lipophagy: Molecular mechanisms and implications in metabolic disorders. *Mol. Cells* 43, 686–693. doi:10.14348/molcells.2020.0046

Sheridan, R., and Spelman, K. (2022). Polyphenolic promiscuity, inflammation-coupled selectivity: Whether PAINs filters mask an antiviral asset. *Front Pharmacol.* 13, 909945. doi:10.3389/fphar.2022.909945

Shrimali, D., Shanmugam, M. K., Kumar, A. P., Zhang, J., Tan, B. K., Ahn, K. S., et al. (2013). Targeted abrogation of diverse signal transduction cascades by emodin for the treatment of inflammatory disorders and cancer. *Cancer Lett.* 341, 139–149. doi:10.1016/j.canlet.2013.08.023

Simonetto, C., Heier, M., Peters, A., Kaiser, J. C., and Rospleszcz, S. (2022). From atherosclerosis to myocardial infarction: A process-oriented model investigating the role of risk factors. *Am. J. Epidemiol.* 191, 1766–1775. doi:10.1093/aje/kwac038

Soliman, G. A., Acosta-Jaquez, H. A., and Fingar, D. C. (2010). mTORC1 inhibition via rapamycin promotes triacylglycerol lipolysis and release of free fatty acids in 3T3-L1 adipocytes. *Lipids* 45, 1089–1100. doi:10.1007/s11745-010-3488-y

Soltani, A., Bahreyni, A., Boroumand, N., Roshan, M. K., Khazaei, M., Ryzhikov, M., et al. (2018). Therapeutic potency of mTOR signaling pharmacological inhibitors in the treatment of proinflammatory diseases, current status, and perspectives. *J. Cell Physiol.* 233, 4783–4790. doi:10.1002/jcp.26276

Song, S. B., Jang, S. Y., Kang, H. T., Wei, B., Jeoun, U. W., Yoon, G. S., et al. (2017). Modulation of mitochondrial membrane potential and ROS generation by nicotinamide in a manner independent of SIRT1 and mitophagy. *Mol. Cells* 40, 503–514. doi:10.14348/molcells.2017.0081

Song, T., and Chen, W. D. (2021). Berberine inhibited carotid atherosclerosis through PI3K/AKTmTOR signaling pathway. *Bioengineered* 12, 8135–8146. doi:10.1080/21655979.2021.1987130

Song, Z., Wei, D., Chen, Y., Chen, L., Bian, Y., Shen, Y., et al. (2019). Association of astragaloside IV-inhibited autophagy and mineralization in vascular smooth muscle cells with lncRNA H19 and DUSP5-mediated ERK signaling. *Toxicol. Appl. Pharmacol.* 364, 45–54. doi:10.1016/j.taap.2018.12.002

Stewart, L. K., Soileau, J. L., Ribnicky, D., Wang, Z. Q., Raskin, I., Poulev, A., et al. (2008). Quercetin transiently increases energy expenditure but persistently decreases circulating markers of inflammation in C57BL/6J mice fed a high-fat diet. *Metabolism* 57, S39–S46. doi:10.1016/j.metabol.2008.03.003

Sun, L., Li, E., Wang, F., Wang, T., Qin, Z., Niu, S., et al. (2015). Quercetin increases macrophage cholesterol efflux to inhibit foam cell formation through activating PPARγ-ABCA1 pathway. *Int. J. Clin. Exp. Pathol.* 8, 10854–10860.

Sun, M., Ye, Y., Huang, Y., Yin, W., Yu, Z., and Wang, S. (2021). Salvianolic acid B improves autophagic dysfunction and decreases the apoptosis of cholesterol crystal-induced macrophages via inhibiting the Akt/mTOR signaling pathway. *Mol. Med. Rep.* 24, 763. doi:10.3892/mmr.2021.12403

Sung, J. Y., Lee, K. Y., Kim, J. R., and Choi, H. C. (2018). Interaction between mTOR pathway inhibition and autophagy induction attenuates adriamycin-induced vascular smooth muscle cell senescence through decreased expressions of p53/p21/p16. *Exp. Gerontol.* 109, 51–58. doi:10.1016/j.exger.2017.08.001

Szwed, A., Kim, E., and Jacinto, E. (2021). Regulation and metabolic functions of mTORC1 and mTORC2. *Physiol. Rev.* 101, 1371–1426. doi:10.1152/physrev.00026.2020

Tang, Y., Wallace, M., Sanchez-Gurmaches, J., Hsiao, W. Y., Li, H., Lee, P. L., et al. (2016). Adipose tissue mTORC2 regulates ChREBP-driven de novo lipogenesis and hepatic glucose metabolism. *Nat. Commun.* 7, 11365. doi:10.1038/ncomms11365

Tian, J., Popal, M. S., Liu, Y., Gao, R., Lyu, S., Chen, K., et al. (2019). Erratum to "ginkgo biloba leaf extract attenuates atherosclerosis in streptozotocin-induced diabetic ApoE-/- mice by inhibiting endoplasmic reticulum stress via restoration of autophagy through the mTOR signaling pathway". *Oxid. Med. Cell Longev.* 2019, 3084083. doi:10.1155/2019/3084083

Tsai, K. L., Kao, C. L., Hung, C. H., Cheng, Y. H., Lin, H. C., and Chu, P. M. (2017). Chicoric acid is a potent anti-atherosclerotic ingredient by anti-oxidant action and anti-inflammation capacity. *Oncotarget* 8, 29600–29612. doi:10.18632/oncotarget.16768

Vellai, T., Takacs-Vellai, K., Zhang, Y., Kovacs, A. L., Orosz, L., and Muller, F. (2003). Genetics: Influence of TOR kinase on lifespan in *C. elegans*. *Nature* 426, 620. doi:10.1038/426620a

Verheye, S., Martinet, W., Kockx, M. M., Knaapen, M. W., Salu, K., Timmermans, J. P., et al. (2007). Selective clearance of macrophages in atherosclerotic plaques by autophagy. *J. Am. Coll. Cardiol.* 49, 706–715. doi:10.1016/j.jacc.2006.09.047

Viana, S. D., Reis, F., and Alves, R. (2018). Therapeutic use of mTOR inhibitors in renal diseases: Advances, drawbacks, and challenges. *Oxid. Med. Cell Longev.* 2018, 3693625. doi:10.1155/2018/3693625

Vion, A. C., Kheloufi, M., Hammoutene, A., Poisson, J., Lasselin, J., Devue, C., et al. (2017). Autophagy is required for endothelial cell alignment and atheroprotection under physiological blood flow. *Proc. Natl. Acad. Sci. U. S. A.* 114, E8675–E8684. doi:10.1073/pnas.1702223114

Vitiello, D., Neagoe, P. E., Sirois, M. G., and White, M. (2015). Effect of everolimus on the immunomodulation of the human neutrophil inflammatory response and activation. *Cell Mol. Immunol.* 12, 40–52. doi:10.1038/cmi.2014.24

Wang, D., Yang, Y., Lei, Y., Tzvetkov, N. T., Liu, X., Yeung, A. W. K., et al. (2019). Targeting foam cell formation in atherosclerosis: Therapeutic potential of natural products. *Pharmacol. Rev.* 71, 596–670. doi:10.1124/pr.118.017178

Wang, J., He, X., Chen, W., Zhang, N., Guo, J., Liu, J., et al. (2020a). Tanshinone IIA protects mice against atherosclerotic injury by activating the TGF-β/PI3K/Akt/eNOS pathway. *Coron. Artery Dis.* 31, 385–392. doi:10.1097/MCA.0000000000000835

Wang, J., Uryga, A. K., Reinhold, J., Figg, N., Baker, L., Finigan, A., et al. (2015). Vascular smooth muscle cell senescence promotes atherosclerosis and features of plaque vulnerability. *Circulation* 132, 1909–1919. doi:10.1161/CIRCULATIONAHA.115.016457

Wang, N., Zhang, X., Ma, Z., Niu, J., Ma, S., Wenjie, W., et al. (2020b). Combination of tanshinone IIA and astragaloside IV attenuate atherosclerotic plaque vulnerability in ApoE(-/-) mice by activating PI3K/AKT signaling and suppressing TRL4/NF-κB signaling. *Biomed. Pharmacother.* 123, 109729. doi:10.1016/j.biopha.2019.109729

Wang, S., Sun, X., Jiang, L., Liu, X., Chen, M., Yao, X., et al. (2016a). 6-Gingerol induces autophagy to protect HUVECs survival from apoptosis. *Chem. Biol. Interact.* 256, 249–256. doi:10.1016/j.cbi.2016.07.020

Wang, T., Zhang, L., Hu, J., Duan, Y., Zhang, M., Lin, J., et al. (2016b). Mst1 participates in the atherosclerosis progression through macrophage autophagy inhibition and macrophage apoptosis enhancement. *J. Mol. Cell Cardiol.* 98, 108–116. doi:10.1016/j.yjmcc.2016.08.002

Wang, W., Wang, Z., Zhao, Y., Wang, X., Li, H., and Zhang, Y. (2022). Analysis of serum lipid parameters predicting lipid metabolic disorders in TSC-AML patients with treatment of mTOR inhibitors. *J. Clin. Pharm. Ther.* 47, 979–985. doi:10.1111/jcpt.13631

Wang, X., Li, L., Niu, X., Dang, X., Li, P., Qu, L., et al. (2014). mTOR enhances foam cell formation by suppressing the autophagy pathway. *DNA Cell Biol.* 33, 198–204. doi:10.1089/dna.2013.2164

Wen, X., Yang, Y., and Klionsky, D. J. (2021). Moments in autophagy and disease: Past and present. *Mol. Asp. Med.* 82, 100966. doi:10.1016/j.mam.2021.100966

Wu, H., Song, A., Hu, W., and Dai, M. (2017). The anti-atherosclerotic effect of paeonol against vascular smooth muscle cell proliferation by up-regulation of autophagy via the AMPK/mTOR signaling pathway. *Front. Pharmacol.* 8, 948. doi:10.3389/fphar.2017.00948

Wu, J. J., Liu, J., Chen, E. B., Wang, J. J., Cao, L., Narayan, N., et al. (2013). Increased mammalian lifespan and a segmental and tissue-specific slowing of aging after genetic reduction of mTOR expression. *Cell Rep.* 4, 913–920. doi:10.1016/j.celrep.2013.07.030

Xiang, Q., Tian, F., Xu, J., Du, X., Zhang, S., and Liu, L. (2022). New insight into dyslipidemia-induced cellular senescence in atherosclerosis. *Biol. Rev. Camb Philos. Soc.* 97, 1844–1867. doi:10.1111/brv.12866

Xiong, Q., Yan, Z., Liang, J., Yuan, J., Chen, X., Zhou, L., et al. (2021). Polydatin alleviates high-fat diet induced atherosclerosis in apolipoprotein E-deficient mice by autophagic restoration. *Phytomedicine* 81, 153301. doi:10.1016/j.phymed.2020.153301

Xu, J., Kitada, M., Ogura, Y., and Koya, D. (2021). Relationship between autophagy and metabolic syndrome characteristics in the pathogenesis of atherosclerosis. *Front. Cell Dev. Biol.* 9, 641852. doi:10.3389/fcell.2021.641852

Xu, S., Zhong, A., Bu, X., Ma, H., Li, W., Xu, X., et al. (2015). Salvianolic acid B inhibits platelets-mediated inflammatory response in vascular endothelial cells. *Thromb. Res.* 135, 137–145. doi:10.1016/j.thromres.2014.10.034

Yamamoto, H., Yoshida, N., and Kihara, S. (2022). Esaxerenone blocks vascular endothelial inflammation through SGK1. *J. Cardiovasc Pharmacol.* 80, 583–591. doi:10.1097/FJC.0000000000001316

Yang, H., Jiang, X., Li, B., Yang, H. J., Miller, M., Yang, A., et al. (2017). Mechanisms of mTORC1 activation by RHEB and inhibition by PRAS40. *Nature* 552, 368–373. doi:10.1038/nature25023

Yang, H., Rudge, D. G., Koos, J. D., Vaidialingam, B., Yang, H. J., and Pavletich, N. P. (2013). mTOR kinase structure, mechanism and regulation. *Nature* 497, 217–223. doi:10.1038/nature12122

Yang, H., Wang, X., Zhang, Y., Liu, H., Liao, J., Shao, K., et al. (2014). Modulation of TSC-mTOR signaling on immune cells in immunity and autoimmunity. *J. Cell Physiol.* 229, 17–26. doi:10.1002/jcp.24426

Yang, M., Lu, Y., Piao, W., and Jin, H. (2022). Profiles of metabolic genes in *Uncaria rhynchophylla* and characterization of the critical enzyme involved in the biosynthesis of bioactive compounds-(iso)Rhynchophylline. *Biomolecules* 12, 1790. doi:10.3390/biom12121790

Yang, P., Ling, L., Sun, W., Yang, J., Zhang, L., Chang, G., et al. (2018). Ginsenoside Rg1 inhibits apoptosis by increasing autophagy via the AMPK/mTOR signaling in serum deprivation macrophages. *Acta Biochim. Biophys. Sin. (Shanghai)* 50, 144–155. doi:10.1093/abbs/gmx136

Yang, Y., Pei, K., Zhang, Q., Wang, D., Feng, H., Du, Z., et al. (2020). Salvianolic acid B ameliorates atherosclerosis via inhibiting YAP/TAZ/JNK signaling pathway in endothelial cells and pericytes. *Biochim. Biophys. Acta Mol. Cell Biol. Lipids* 1865, 158779. doi:10.1016/j.bbalip.2020.158779

Zhang, G., He, C., Wu, Q., Xu, G., Kuang, M., Wang, T., et al. (2021a). Impaired autophagy induced by oxLDL/β2GPI/anti-β2GPI complex through PI3K/AKT/mTOR and eNOS signaling pathways contributes to endothelial cell dysfunction. *Oxid. Med. Cell Longev.* 2021, 6662225. doi:10.1155/2021/6662225

Zhang, J. X., Qu, X. L., Chu, P., Xie, D. J., Zhu, L. L., Chao, Y. L., et al. (2018). Low shear stress induces vascular eNOS uncoupling via autophagy-mediated eNOS phosphorylation. *Biochim. Biophys. Acta Mol. Cell Res.* 1865, 709–720. doi:10.1016/j.bbamcr.2018.02.005

Zhang, X., Han, X., Zhang, P., Zhou, T., Chen, Y., Jin, J., et al. (2019). Morin attenuates oxidized low-density lipoprotein-mediated injury by inducing autophagy via activating AMPK signalling in HUVECs. *Clin. Exp. Pharmacol. Physiol.* 46, 1053–1060. doi:10.1111/1440-1681.13160

Zhang, X., Sergin, I., Evans, T. D., Jeong, S. J., Rodriguez-Velez, A., Kapoor, D., et al. (2020). High-protein diets increase cardiovascular risk by activating macrophage mTOR to suppress mitophagy. *Nat. Metab.* 2, 110–125. doi:10.1038/s42255-019-0162-4

Zhang, Y. X., Qu, S. S., Zhang, L. H., Gu, Y. Y., Chen, Y. H., Huang, Z. Y., et al. (2021b). The role of ophiopogonin D in atherosclerosis: Impact on lipid metabolism and gut microbiota. *Am. J. Chin. Med.* 49, 1449–1471. doi:10.1142/S0192415X21500683

Zhao, L., Luo, R., Yu, H., Li, S., Yu, Q., Wang, W., et al. (2021). Curcumin protects human umbilical vein endothelial cells against high oxidized low density lipoprotein-

induced lipotoxicity and modulates autophagy. *Iran. J. Basic Med. Sci.* 24, 1734–1742. doi:10.22038/IJBMS.2021.59969.13297

Zheng, L., Li, Y., Li, X., Kou, J., Zhong, Z., Jiang, Y., et al. (2016). Combination of hydroxyl acetylated curcumin and ultrasound induces macrophage autophagy with anti-apoptotic and anti-lipid aggregation effects. *Cell Physiol. Biochem.* 39, 1746–1760. doi:10.1159/000447875

Zheng, S., Du, Y., Ye, Q., Zha, K., and Feng, J. (2021). Atorvastatin enhances foam cell lipophagy and promotes cholesterol efflux through the AMP-activated protein kinase/mammalian target of rapamycin pathway. *J. Cardiovasc Pharmacol.* 77, 508–518. doi:10.1097/FJC.0000000000000942

Zheng, Y., Collins, S. L., Lutz, M. A., Allen, A. N., Kole, T. P., Zarek, P. E., et al. (2007). A role for mammalian target of rapamycin in regulating T cell activation versus anergy. *J. Immunol.* 178, 2163–2170. doi:10.4049/jimmunol.178.4.2163

Zhi, W., Liu, Y., Wang, X., and Zhang, H. (2023). Recent advances of traditional Chinese medicine for the prevention and treatment of atherosclerosis. *J. Ethnopharmacol.* 301, 115749. doi:10.1016/j.jep.2022.115749

Zhou, H., You, P., Liu, H., Fan, J., Tong, C., Yang, A., et al. (2022a). Artemisinin and Procyanidins loaded multifunctional nanocomplexes alleviate atherosclerosis via simultaneously modulating lipid influx and cholesterol efflux. *J. Control Release* 341, 828–843. doi:10.1016/j.jconrel.2021.12.021

Zhou, Y. H., Tang, Y. Z., Guo, L. Y., Zheng, L. L., Zhang, D., Yang, C. Y., et al. (2022b). Overexpression of sFlt-1 represses ox-LDL-induced injury of HUVECs by activating autophagy via PI3K/AKT/mTOR pathway. *Microvasc. Res.* 139, 104252. doi:10.1016/j.mvr.2021.104252

Zou, T., Gao, S., Yu, Z., Zhang, F., Yao, L., Xu, M., et al. (2022). Salvianolic acid B inhibits RAW264.7 cell polarization towards the M1 phenotype by inhibiting NF-κB and Akt/mTOR pathway activation. *Sci. Rep.* 12, 13857. doi:10.1038/s41598-022-18246-0

Glossary

3-MA 3-Methyladenine
4E-BP1 4E-binding proteins 1
AGE advanced glycation end product
AS Atherosclerosis
ATG13 autophagy-related protein 13
CVD cardiovascular disease
CRP C-reactive protein
DR dietary restriction
eNOS endothelial oxide synthase
FFA fatty acids
HDL-C high-density lipoprotein cholesterol
HFD high-fat diet
HCSMCs human coronary smooth muscle cells
HUVECs human umbilical vein endothelial cells
LC-3 microtubule-associated protein 1 light chain 3
LDL-C low density lipoprotein cholesterol
ICAM-1 intercellular adhesion molecule 1
IFN-γ Interferon-γ
IL-1β interleukin-1β
IL-6 interleukin 6
LDLR−/− low-density lipoprotein receptor knockout
mTOR mechanistic/mammalian target of rapamycin
mTORC1 mammalian target of rapamycin complex 1
MCP-1 monocyte chemoattractant protein-1
mTORC2 mammalian target of rapamycin complex 2
NF-κB nuclear factor-κB
ox-LDL oxidized low-density lipoprotein
p70S6K 70-kDa ribosomal protein S6 kinase
PBS phosphate buffer saline
PI3K phosphatidyl inositol 3-kinase
PIKKs phosphatidyl inositol 3-kinase related kinases
PKC protein kinases C
Raptor regulatory protein associated with mTOR
Rheb Ras homolog enriched in the brain
Rictor rapamycin-insensitive companion of mTOR
S6K S6 kinase
Sal B Salvianolic acid B
SCD1 stearoyl-CoA desaturase-1
SGK1 serum-and glucocorticoid-induced protein kinase 1
sin1 serum-and glucocorticoid-induced protein kinase 1
siRNA small interfering RNA
SMCs smooth muscle cells
SREBPs sterol-regulatory element binding proteins
TC total cholesterol
TG triglyceride
TCM Traditional Chinese Medicine
TFEB transcription factor EB
TLR-4 Toll-like receptor-4
TNF-α tumor necrosis factor-alpha
TRF2 telomeric repeat-binding factor 2
TSC1/2 tuberous sclerosis complex 1/2
ULK1 unc-51-like kinase 1
UVECs umbilical vein endothelial cells
VSMCs vascular smooth muscle cells
VECs vascular endothelial cells

frontiers | Frontiers in Pharmacology

TYPE Systematic Review
PUBLISHED 09 March 2023
DOI 10.3389/fphar.2023.1111459

Check for updates

OPEN ACCESS

EDITED BY
Yu-Qing Zhang,
McMaster University, Canada

REVIEWED BY
Altaf S. Darvesh,
Northeast Ohio Medical University, United States
Jing Xie,
Army Medical University, China

*CORRESPONDENCE
Yan Li,
15801434320@163.com
Xian Wang,
wx650515@163.com

†These authors have contributed equally to this work and share first authorship

SPECIALTY SECTION
This article was submitted to Ethnopharmacology, a section of the journal Frontiers in Pharmacology

RECEIVED 29 November 2022
ACCEPTED 28 February 2023
PUBLISHED 09 March 2023

CITATION
Li T, Jin J, Pu F, Bai Y, Chen Y, Li Y and Wang X (2023), Cardioprotective effects of curcumin against myocardial I/R injury: A systematic review and meta-analysis of preclinical and clinical studies. *Front. Pharmacol.* 14:1111459. doi: 10.3389/fphar.2023.1111459

COPYRIGHT
© 2023 Li, Jin, Pu, Bai, Chen, Li and Wang. This is an open-access article distributed under the terms of the Creative Commons Attribution License (CC BY). The use, distribution or reproduction in other forums is permitted, provided the original author(s) and the copyright owner(s) are credited and that the original publication in this journal is cited, in accordance with accepted academic practice. No use, distribution or reproduction is permitted which does not comply with these terms.

Cardioprotective effects of curcumin against myocardial I/R injury: A systematic review and meta-analysis of preclinical and clinical studies

Tianli Li[1,2†], Jialin Jin[1†], Fenglan Pu[3†], Ying Bai[4], Yajun Chen[1], Yan Li[5*] and Xian Wang[1*]

[1]Department of Cardiology, Dongzhimen Hospital, Beijing University of Chinese Medicine, Beijing, China, [2]National Integrated Traditional and Western Medicine Center for Cardiovascular Disease, China-Japan Friendship Hospital, Beijing, China, [3]Center for Evidence Based Chinese Medicine, Beijing University of Chinese Medicine, Beijing, China, [4]Department of Traditional Chinese Medicine, Peking Union Medical College Hospital, Beijing, China, [5]Department of Cardiology, Dongfang Hospital, Beijing University of Chinese Medicine, Beijing, China

Objective: Myocardial ischemia-reperfusion (I/R) injury is a complex clinical problem that often leads to further myocardial injury. Curcumin is the main component of turmeric, which has been proved to have many cardioprotective effects. However, the cardioprotective potential of curcumin remains unclear. The present systematic review and meta-analysis aimed to evaluate the clinical and preclinical (animal model) evidence regarding the effect of curcumin on myocardial I/R injury.

Methods: Eight databases and three register systems were searched from inception to 1 November 2022. Data extraction, study quality assessment, data analyses were carried out strictly. Then a fixed or random-effects model was applied to analyze the outcomes. SYRCLE's-RoB tool and RoB-2 tool was used to assess the methodological quality of the included studies. RevMan 5.4 software and stata 15.1 software were used for statistical analysis.

Results: 24 animal studies, with a total of 503 animals, and four human studies, with a total of 435 patients, were included in this study. The meta-analysis of animal studies demonstrated that compared with the control group, curcumin significantly reduced myocardial infarction size ($p < 0.00001$), and improved the cardiac function indexes (LVEF, LVFS, LVEDd, and LVESd) ($p < 0.01$). In addition, the indexes of myocardial injury markers, myocardial oxidation, myocardial apoptosis, inflammation, and other mechanism indicators also showed the beneficial effect of curcumin ($p < 0.05$). In terms of clinical studies, curcumin reduced the incidence of cardiac dysfunction, myocardial infarction in the hospital and MACE in the short term, which might be related to its anti-inflammatory and anti-oxidative property. Dose-response meta-analysis predicted, 200 mg/kg/d bodyweight was the optimal dose of curcumin in the range of 10–200 mg/kg/d, which was safe and non-toxic according to the existing publications.

Conclusion: Our study is the first meta-analysis that includes both preclinical and clinical researches. We suggested that curcumin might play a cardioprotective role in acute myocardial infarction in animal studies, mainly through anti-oxidative, anti-inflammatory, anti-apoptosis, and anti-fibrosis effects. In

addition, from the clinical studies, we found that curcumin might need a longer course of treatment and a larger dose to protect the myocardium, and its efficacy is mainly reflected on reducing the incidence of myocardial infarction and MACE. Our finding provides some meaningful advice for the further research.

KEYWORDS

curcumin, myocardial ischemia-reperfusion injury (MIRI), systematic review and meta-analysis, pre-clinical evidence, clinical evidence

1 Introduction

Cardiovascular disease (CVD), especially acute myocardial infarction (AMI), has become one of the main risk factors threatening human health (Mozaffarian et al., 2015). Thrombolytic, percutaneous coronary intervention (PCI), and coronary artery bypass grafting (CABG) are currently effective strategies to limit infarct size and reduce mortality in clinical practice (Ribas et al., 2017). However, there is growing evidence indicating that myocardial ischemia/reperfusion (I/R) injury is an inevitable pathological change in the process of reperfusion after revascularization (Heusch and Gersh, 2017). In addition, it will lead to myocardial dysfunction, structural damage, and myocardial electrical activity disorder, which further aggravates myocardial necrosis, severe complications such as arrhythmia, decreased ventricular function, and even sudden death (Grech et al., 1995). The mechanism is not yet fully understood, but research showed that it might be related to inflammation, oxidative stress, mitochondrial membrane permeability transition pore, cell apoptosis, et al. (Hausenloy and Yellon, 2013). Therefore, seeking novel myocardial protection strategies to ameliorate myocardial I/R injury and preserve normal heart function after revascularization is still of high priority.

Turmeric is a commonly used herb as a traditional medicine in Asian countries (China, Japan, Korea, et al.). According to the records of ancient Chinese medical books, turmeric is capable of relieving pain through promoting qi and blood circulation. Therefore, it is frequently used in the treatment of chest tightness, chest pain, shoulder and back pain, dysmenorrhea, et al. Curcumin (chemical structure shown in Figure 1) is the main component of turmeric and has a variety of biological activities, especially in the cardiovascular system (Ghosh et al., 2010). Curcumin has been proved to have anti-oxidative, anti-inflammatory, and anti-apoptosis properties, and it has been observed in experiments that curcumin inhibits myocardial fibrosis (Gorabi et al., 2020) and ventricular remodeling after acute infarction (Yao et al., 2004) and prevents the progression of heart failure after myocardial infarction (Saeidinia et al., 2018). Therefore, curcumin may be a potential cardioprotective candidate to ameliorate myocardial I/R injury.

However, the efficacy and mechanisms of curcumin on myocardial I/R injury have not been systematically reviewed in animal models. Moreover, some clinical trials (Offermanns et al., 1994; Srivastava et al., 1995; Peng and Qian, 2014; Hirsch et al., 2017) showed the contradictory results. In this study, we aim to review and analyze the animal and clinical research to find out whether curcumin has the potential for clinical application and suggested how such primary studies need to be improved.

2 Methods

2.1 Search strategies and study selection

Eight databases, including Pubmed, EMBASE, The Cochrane Library, Web of Science, China National Knowledge Infrastructure (CNKI), Wanfang database, China Science and Technology Journal Database (VIP), and China Biology Medicine disc (CBM), were searched systematically from inception to 1 November 2022. Moreover, references of eligible studies were also manually searched to identify additional eligible studies. The search language was restricted to English and Chinese, and the search strategy was as follows. The detailed search strategies in eight databases and retrieved results were provided in Supplementary Material.

2.2 Eligibility criteria

Inclusion criteria were as follows: 1) The I/R experimental model were established by ligating the left coronary artery (LCA) such as left anterior descending (LAD) or other proper methods, or ischemic heart disease patients receiving PCI or CABG in the hospital; 2) The treatment group (animal studies and human studies) received any dose of curcumin as monotherapy, and the control group received the same amount of non-functional fluid (normal saline) or no treatment at all; 3) The primary outcome of animal studies were myocardial infarction (MI) size and echocardiogram indicators. The secondary outcomes of animal studies were biomarkers of myocardial injury and mechanisms of curcumin in the treatment of myocardial I/R injury; 4) The human studies were RCT study. Exclusion criteria were set as follows: 1) not a myocardial I/R model or patients who beyond the relevant clinical diagnostic criteria; 2) combined with other drugs; 3) no control group; 4) duplicate publication; 5) not an animal model or not RCT study (e.g., case reports, reviews, non-RCT clinical trials and cell experiments).

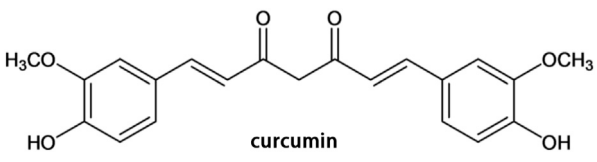

FIGURE 1
Chemical structure of curcumin.

2.3 Data extraction

Two independent reviewers (Fenglan Pu, Ying Bai) extracted the following details from the included studies: 1) first author name and year of publication; 2) Specific information about the animals and patients in each study, including species, number, sex, and body weight; 3) Myocardial I/R model and the anesthetic method used to prepare the model; 4) Information about curcumin treatment, including dose, method of administration, course of treatment; as well as corresponding information in the control group; 5) The mean and standard deviation (SD) of the results. Suppose there were many different time point results, only the last time point results would be recorded. Since some of the data is only presented in graphical format, we tried to contact the authors for detailed information. If we did not receive any response, the digital ruler software would be used to measure the value of the graph.

2.4 Risk of bias in individual studies

The quality of the included animal studies was assessed using Systematic Review Center for Laboratory Animal Experimentation (SYRCLE) risk of bias (RoB) tool 10-item scale (Hooijmans et al., 2014) as follows (A) sequence generation; (B) baseline characteristics; (C) allocation concealment; (D) random housing; (E) blinding investigators; (F) random outcome assessment; (G) blinding outcome assessor; (H) incomplete outcome data; (I) selective outcome reporting; (J) other sources of bias. Give one point to each item.

The quality of the included human studies was assessed using RoB-2 tool (Sterne et al., 2019) as follows: Randomization process; Assignment to intervention; Adhering to intervention; Missing outcome data; Measurement of outcome; Selection of the reported result; RoB-2 overall score. Two reviewers (Jialin Jin and Fenglan Pu) assessed the study quality independently. The divergences were resolved through negotiation or in consultation with the corresponding author (Yan Li and Xian Wang).

2.5 Data synthesis

The problem of curcumin divided into different dose subgroups in the original study was handled following the strategy recommended by Cochrane Handbook for Systematic Reviews of Interventions (CHSRI) (Cumpston et al., 2019). We merged the different dose subgroups in each original study into one treatment group, and the following was the merge formula for continuous variable (Zhou et al., 2020):

$$\text{Sample size } N_1 + N_2 + \cdots + N_k$$

$$\text{Mean } \frac{N_1M_1 + N_2M_2 + \cdots + N_kM_k}{N_1 + N_2 + \cdots + N_k}$$

$$\text{SD } \sqrt{\frac{(N_1 - 1)SD_1^2 + (N_2 - 1)SD_2^2 + \cdots + (N_k - 1)SD_K^2}{N_1 + N_2 + \cdots + N_k - k}}$$

2.6 Statistical analysis

RevMan software (version 5.4) was used for statistical analysis. Heterogeneity was determined by the Q-statistical test ($p < 0.05$ was considered statistically significant) and I^2-statistical test. According to the Cochrane handbook on heterogeneity analysis, I^2 value ranges from 0% to 40% means heterogeneity might not be important; 30%–60% may represent moderate heterogeneity; 50%–90% may represent substantial heterogeneity; 75%–100% means considerable heterogeneity. A fixed-effects model was adopted if $I^2 < 50\%$; otherwise, a random-effects model would be applied. All outcomes were continuous variables, so we used weighted mean difference (WMD) with 95% confidence intervals (CIs) to present, for outcomes reported in various measurement methods or different scales of measurement, we calculated with a standard mean difference (SMD). $p < 0.05$ was considered statistically significant.

2.7 Subgroup analysis and meta-regression

We preset four subgroups: 1) method of model establishment, 2) administration method, 3) genus of animals, 4) intervention moment. We conducted a subgroup analysis on the primary outcomes to evaluate the impact of variables and to explore the source of heterogeneity. A meta-regression analysis was further performed using Stata 15.1 software once the heterogeneity in the study was significant ($I^2 > 50\%$) and the preset subgroups failed to find the source of heterogeneity.

2.8 Sensitivity analysis

Sensitivity analysis should be performed on the outcomes whose heterogeneities were considerable. The purpose of the sensitivity analysis was not only to indirectly find the source of heterogeneity, but also to assess the stability and reliability of the merged results.

2.9 Publication bias

Publication bias was detected by a funnel plot combined with Egger's regression test on primary outcomes. The funnel plot was produced using RevMan 5.4 software, and Egger's regression test was completed using Stata 15.1 software.

2.10 Dose-response meta-analysis

The relationship between the standard dosage of curcumin and the ratio of means (RR = $means_{experimental}/means_{control}$) was modeled using STATA 15.1 software. According to the characteristics of point distribution, linear, exponential, logarithmic, quadratic, and cubic regression equations can be selected to try to fit. The generalized least squares method (GLS) was used to calculate each of the parameters while R^2 represents the degree of fitting (R^2 closer to one indicates a better fit of the prediction model).

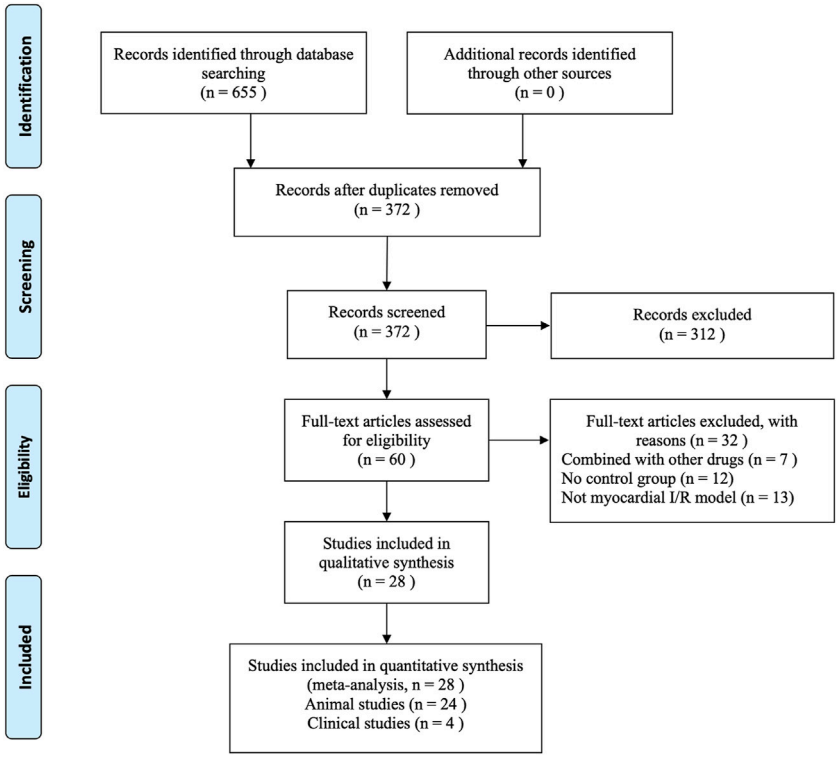

FIGURE 2
Flow chart of the process of study selection.

3 Results

3.1 Study selection

A total of 655 articles were retrieved from the eight databases. After the removal of duplicates using Endnote X9 software, 372 articles were screened through reading titles and abstracts by two reviewers individually (Jialin Jin and Fenglan Pu). Then the same two reviewers (Jialin Jin and Fenglan Pu) individually perused the remaining 60 full-texts, and finally 24 animal studies (Yeh et al., 2005; Ali et al., 2009; Gonzalez-Salazar et al., 2011; Duan et al., 2012; Jeong et al., 2012; Kim et al., 2012; Wang et al., 2012; Broskova et al., 2013; Wang et al., 2014; Yao and Jiang, 2014; Hardy et al., 2015; Chen et al., 2016; Liu et al., 2017a; Deng et al., 2018; Wang et al., 2018) published from 2005 to 2020 and four human studies (Wongcharoen et al., 2011; Wongcharoen et al., 2012; Aslanabadi et al., 2019; Phrommintikul et al., 2019) published from 2011 to 2019 were included in our systematic review and meta-analysis. During the selection process, any divergence was resolved by Ying Bai. Figure 2 describes the flow chart for inclusion in the study.

3.2 Characteristics of included studies

3.2.1 Animal studies

Twenty studies (Sato et al., 2000; Yeh et al., 2005; Kim et al., 2008; Ali et al., 2009; Gonzalez-Salazar et al., 2011; Duan et al., 2012; Jeong et al., 2012; Kim et al., 2012; Wang et al., 2012; Yang et al., 2013a; Broskova et al., 2013; Leong et al., 2013; Wang et al., 2014; Hardy et al., 2015; Chen et al., 2016; Liu et al., 2017a; Liu et al., 2017b; Deng et al., 2018; Wang et al., 2018; Jo et al., 2020) were published in English, and four studies (Cheng et al., 2005; Wu, 2011; Yao and Jiang, 2014; Gu et al., 2016) were published in Chinese. Sixteen studies (Sato et al., 2000; Cheng et al., 2005; Kim et al., 2008; Wu, 2011; Duan et al., 2012; Jeong et al., 2012; Kim et al., 2012; Wang et al., 2012; Leong et al., 2013; Wang et al., 2014; Liu et al., 2017a; Liu et al., 2017b; Wang et al., 2018; Jo et al., 2020) used Sprague-Dawley (SD) rats, five studies (Ali et al., 2009; Gonzalez-Salazar et al., 2011; Broskova et al., 2013; Hardy et al., 2015; Chen et al., 2016) used Wistar rats, two studies (Gu et al., 2016; Deng et al., 2018) used C57BL/6 mice, and one study (Yeh et al., 2005) used New Zealand white rabbits. Twenty studies (Cheng et al., 2005; Yeh et al., 2005; Kim et al., 2008; Ali et al., 2009; Gonzalez-Salazar et al., 2011; Wu, 2011; Duan et al., 2012; Jeong et al., 2012; Kim et al., 2012; Wang et al., 2012; Yang et al., 2013a; Broskova et al., 2013; Wang et al., 2014; Yao and Jiang, 2014; Hardy et al., 2015; Chen et al., 2016; Gu et al., 2016; Deng et al., 2018; Wang et al., 2018; Jo et al., 2020) used male animals, and the remaining four studies (Sato et al., 2000; Leong et al., 2013; Liu et al., 2017a; Liu et al., 2017b) did not clarify gender. Twelve studies (Sato et al., 2000; Cheng et al., 2005; Yeh et al., 2005; Gonzalez-Salazar et al., 2011; Wu, 2011; Duan et al., 2012; Jeong et al., 2012; Yang et al., 2013a; Leong et al., 2013; Yao and Jiang, 2014; Gu et al., 2016; Wang et al., 2018) used pentobarbital sodium for anesthetic, six studies (Kim et al., 2008; Kim et al., 2012; Wang et al., 2012; Wang et al., 2014; Liu et al., 2017b; Deng et al., 2018) used ketamine combined with xylazine,

TABLE 1 Basic characteristics of the 24 included animal studies.

Study ID	Country	Species (sex, n = experimental/ control group)	Weight	Model (method)	Anesthetic	Treatment group (method to curcumin)	Control group	Duration	Outcomes	*p*-Value
Ali, M. S.2009	India	Albino Wistar rats (male, n = 12/6)	200–250 g	Block LAD for 30min then reperfuse for 4 h	Thiopentone sodium (30 mg/kg)	Curcumin (5/10 mg/kg) dissolved in 80% DMSO and given as an i.p. Injection	0.2 mL of 80% DMSO and given as an i.p. Injection	10 min before reperfusion	1.ALT	1.$p < 0.05$
									2.AST	2.$p < 0.001$
									3.Catalase	3.$p < 0.05$
									4.GSH	4.$p < 0.001$
									5.MDA	5.$p < 0.05$
Brosková.Z.2013	Slovak Republic	Wistar rats (male, n = 6/12)	360–400 g	Turn off pumpig system for 30min then reflow 30min using Langendorff technique	Diethylether	Curcumin dissolved in DMSO at a concentration of 1*10–5 mol/L then reperfused for 30 min	DMSO reperfused for 30 min	30 min during reperfusion	1.VPB	1.$p < 0.05$
									2.VTP	2.$p < 0.05$
									3.VFP	3.$p < 0.05$
Chen, X. L. 2016	China	albino Wistar strain rats (male, n = 3/3)	160–180 g	Block coronary artery for 45min then reperfuse	5% chloral hydrate solution	Curcumin (50 mg/kg bwt) oral	Saline oral	15 days before ischemia	1.Cat	1.$p < 0.05$
									2.Caspase-3 protein	2.$p < 0.05$
									3.Cell viability%	3.$p < 0.05$
									4.CKMB	4.$p < 0.05$
									5.IA/LV	5.$p < 0.05$
									6.ISR%	6.$p < 0.05$
									7.MA	7.$p < 0.05$
									8.MDA	8.$p < 0.05$
									9.SOD activity	9.$p < 0.05$
Cheng, H.2005	China	Sprague-Dawley rats (male, 60/20)	270 ± 20 g	Block LAD for 60 min then reflow for 60 min	Pentobarbital sodium (30 mg/kg, 3%)	Intraperitoneal injection curcumin (10/20/40 mg/kg)	Intraperitoneal injection saline 5 min	5 min earlier before ischemia	1.AR/LV	1.$p < 0.05$
									2.CK	2.$p < 0.05$
									3.GSH Px	3.$p < 0.05$
									4.IR/AR	4.$p < 0.05$
									5.IR/LV	5.$p < 0.05$
									6.LDH	6.$p < 0.05$
									7.MDA	7.$p < 0.05$
									8.SOD	8.$p < 0.05$

(Continued on following page)

10.3389/fphar.2023.1111459

TABLE 1 (*Continued*) Basic characteristics of the 24 included animal studies.

Study ID	Country	Species (sex, n = experimental/ control group)	Weight	Model (method)	Anesthetic	Treatment group (method to curcumin)	Control group	Duration	Outcomes	*p*-Value
Deng Y.2018	China	C57BL/6 mice (male, n = 10/10)	20–25 g	Block LCA for 30 min then reperfuse for 4 h	Ketamine (100 mg/kg) and xylazine (5 mg/kg)	25ul,1 wt% curcumin solution into ischemia region with a 30-gauge needle	25ul,1 wt% normal saline into ischemia region with a 30-gauge needle	During reperfusion	1. Apoptosis	1.$p < 0.01$
									2.AR/LV	2.$p < 0.05$
									3.IR/AR	3.$p < 0.05$
									4.LVEF	4.$p > 0.05$
									5.LVFS	5.$p > 0.05$
									6.Bcl-2	6.$p < 0.05$
Duan, W.2012	China	Sprague-Dawley rats (male, n = 8/8)	220–250 g	Turn off pumpig system for 60 min then reflow 60 min using Langendorff technique	Pentobarbital sodium (50 mg/kg)	Perfused with KHB containing 1-lM curcumin	Perfused with KHB	During reperfusion for 10 min	1.Apoptosis	1.$p < 0.05$
									2.Bcl-2	2.$p < 0.05$
									3.DP/dtmax	3.$p < 0.05$
									4.HR	4.$p < 0.05$
									5.IR/LV	5.$p < 0.05$
									6.LDH	6.$p < 0.05$
									7.LVDP	7.$p < 0.05$
									8.p-STAT3	8.$p < 0.05$
González-Salazar, A.2011	Mexico	Wistar rats (male, n = 6/6)	270–300 g	Turn off pumpig system for 30min then reflow 60min using Langendorff technique	Pentobarbital sodium (60 mg/kg)	Curcumin (200 mg/kg) dissolved in carboxymethylcellulose 0.05% oral	Carboxymethylcellulose 0.05% oral	7 days before ischemia	1.GSH	1.$p < 0.05$
									2.SOD	2.$p < 0.05$
									3.CAT	3.$p < 0.05$
									4.OC	4.$p < 0.05$
Gu, H.P.2016	Chinese	C57BL/6 mice (male, n = 10/10)	18–22 g	Block LAD for 30 min then reflow for 4 h	Pentobarbital sodium (50 mg/kg)	By intraperitoneal injection of curcumin (100 mg/kg) 30 min	By intraperitoneal injection of saline 30 min	Before ischemia	1.IR/LV	1.$p < 0.001$
									2.cTnT	2.$p < 0.001$
									3.NF-κB protein	3.$p < 0.001$
									4.TNF-α protein	4.$p < 0.001$

(Continued on following page)

10.3389/fphar.2023.1111459

TABLE 1 (*Continued*) Basic characteristics of the 24 included animal studies.

Study ID	Country	Species (sex, n = experimental/ control group)	Weight	Model (method)	Anesthetic	Treatment group (method to curcumin)	Control group	Duration	Outcomes	*p*-Value
Hardy, N.2015	Australian	Wistar rats (male, n = 5/4)	NM	Turn off pumpig system for 30min then reflow 60min using Langendorff technique	NM	Curcumin (0.177 mg/mL) and nanoparticle (1 mg/mL) were pumped through the column at the flow rate of 1.5 mL/min with a run time of 10 min for 3 times	Nanoparticle (1 mg/mL) was pumped through the column at the flow rate of 1.5 mL/min with a run time of 10 min for 3 times	After reperfusion	1.CK	1.$p < 0.05$
									2.LDH	2.$p < 0.05$
									3.GGR	3.$p < 0.05$
Jeong, C.W.2012	Korea	Sprague-Dawley rats (male, n = 7/7)	250–300 g	Block LAD for 30 min then reflow for 120 min	Pentobarbital sodium (60 mg/kg)	Curcumin (100 mg/kg/day) oral	Saline oral	20 min before ischemia	1.AR/LV	1.$p < 0.05$
									2.HR	2.$p < 0.05$
									3.MAP	3.$p < 0.05$
									4.p-AKT	4.$p < 0.05$
Jo, W.2020	South Korea	Sprague-Dawley rats (male, 5/5)	285.33 ± 5.0 g	Block LAD for 30 min then reflow	Alfaxalone (50 mg/kg) and xylazine (5 mg/kg)	Curcumin gavage (25 mg/kg/d)	Vehicle (10% dimethyl sulfoxide and 90% polyethylene glycol) gavage	5 days before ischemia	1. IR/LV	1.$p < 0.01$
									2.LVEF	2.$p < 0.05$
									3.LVFS	3.$p < 0.05$
									4.LVDd	4.$p > 0.05$
									5.LVSd	5.$p > 0.05$
									6.SV	6.$p > 0.05$
									7.Fibrosis/LV	7.$p < 0.05$
Kim, Y.S.2008	Korea	Sprague-Dawley rats (male, n = 10/10)	190–210 g	Block LAD for 30 min then reflow for 24 h	Ketamine (1 mL/kg) and xylazine (10 mg/kg)	By intragastric gavage of curcumin (80 mg/kg/d)	By intragastric gavage of saline	7 days before ischemia	1.Fibrosis/LV	1.$p < 0.05$
									2.NOAC	2.$p < 0.05$
									3.LVDd	3.$p > 0.05$
									4.LVSd	4.*P*0.05
									5.LVFS	5.$p < 0.05$
									6.MPO	6.$p < 0.05$
									7.MDA	7.$p < 0.05$
Kim, Y.S.2012	Korea	Sprague-Dawley rats (male, n = 6/8)	200–230 g	Block LAD for 30 min then reflow for 2 weeks	Ketamine (50 mg/kg) and xylazine (5 mg/kg)	Curcumin (300 mg/kg/day) dissolved in distilled water oral	Distilled water oral	7 days befor ischemia and 14 days during reperfusion	1.Fibrosis/LV	1.$p < 0.05$
									2.LVFS	2.$p < 0.05$
									3.LVEF	3.$p < 0.05$
									4.LVDd	4.$p < 0.05$

(Continued on following page)

10.3389/fphar.2023.1111459

TABLE 1 (*Continued*) Basic characteristics of the 24 included animal studies.

Study ID	Country	Species (sex, n = experimental/ control group)	Weight	Model (method)	Anesthetic	Treatment group (method to curcumin)	Control group	Duration	Outcomes	*p*-Value
									5.LVSd	5.$p < 0.05$
									6.Max dp/dt	6.$p < 0.05$
									7.Min dp/dt"	7.$p < 0.05$
Leong, P.K.2013	China (Hong Kong)	Sprague-Dawley rats (NM, n = 5/5)	250–300 g	Turn off pumpig system for 40 min then reflow 20 min	Phenobarbtial sodium	Intragastrically administered curcumin (0.825 μmol/kg/day, 0.5 mL per rat)	Intragastrically administered vehicle (0.5 mL olive oil)	15 consecutive days before ischemia	1.AU	1.$p > 0.05$
									2.Initial GSH	2.$p > 0.05$
									3.LDH	3.$p < 0.05$
Liu, H.2017	China	Sprague-Dawley rats male (NM, n = 30/10)	200–250 g	Block LAD for 60 min then reflow for 180 min	Ketamine (90 mg/kg) and xylazine (10 mg/kg)	Curcumin (10/20/30 mg/kg/ day)oral	Saline oral	15 days before ischemia	1.IR/LV	1.$p < 0.01$
									2.Caspase-3	2.$p < 0.01$
									3.CAT	3.$p < 0.01$
									4.CK-MB	4.$p < 0.01$
									5.GPx	5.$p < 0.01$
									6.GR	6.$p < 0.01$
									7.LDH	7.$p < 0.01$
									8.MDA	8.$p < 0.01$
									9.SOD	9.$p < 0.01$
Liu, K.2017	China	Sprague-Dawley rats (NM, n = 6/6)	250–300 g	Turn off pumpig system for 30 min then reflow 30 min using Langendorff technique	Chloral hydrate (350 mg/kg)	Curcumin (0.5 mg/kg) myocardial perfusion	Krebs-Henseleit (K-H) solution perfusion	30 min after reperfusion	1.CF	1.$p < 0.01$
									2.CK	2.$p < 0.01$
									3.IR/LV	3.$p < 0.01$
									4.LDH	4.$p < 0.01$
									5.MC	5.$p < 0.01$
									6.STE	6.$p < 0.01$
									7.TNF-α protein	7.$p < 0.01$
Sato, M.2000	US	Sprague-Dawley rats (NM, n = 7/7)	about 300 g	Turn off pumpig system for 30 min then reflow 120 min using Langendorff technique	Pentobarbital sodium (80 mg/kg)	Curcumin (100 μM) myocardial perfusion	Krebs-Henseleit bicarbonate (KHB) solution perfusion	15 min before ischemia	1.IR/LV	1.$p < 0.05$
									2.CF	2.$p < 0.05$
									3.dP/dtmax	3.$p < 0.05$
									4.HR	4.$p < 0.05$

(Continued on following page)

10.3389/fphar.2023.1111459

TABLE 1 (*Continued*) Basic characteristics of the 24 included animal studies.

Study ID	Country	Species (sex, n = experimental/ control group)	Weight	Model (method)	Anesthetic	Treatment group (method to curcumin)	Control group	Duration	Outcomes	*p*-Value
									5.JNK1 protein	5.$p < 0.05$
									6.MAPK	6.$p < 0.05$
									7.p-JNK1	7.$p < 0.05$
Wang, N.P.2012	US	Sprague-Dawley rats (male, n = 8/8)	400–450 g	Block LCA for 45min then reflow for 42 days	Ketamine (90 mg/kg) and zylaxine (10 mg/kg)	Curcumin (150 mg/kg/day) oral	Saline oral	42 days during reperfusion	1. AR/LV	1.$p < 0.05$
									2.Fibrosis/LV	2.$p < 0.05$
									3.LVDd	3.$p>0.05$
									4.LVEF	4.$p < 0.05$
									5.LVFS	5.$p < 0.05$
									6.MDA	6.$p < 0.05$
									7.SV	7.$p < 0.05$
									8.MMP-9	8.$p < 0.05$
Wang N *p*.2014	US	Sprague-Dawley rats (male, n = 8/8)	400–450 g	Block LCA for 30min then reflow for 180min	Ketamine (90 mg/kg) and zylaxine (10 mg/kg)	Curcumin (50 mg/kg/day) oral	Saline oral	5 days before ischemia	1.AR/LV	1.$p < 0.05$
									2.IL-6 protein	2.$p < 0.05$
									3.IR/LV	3.$p < 0.05$
									4.MPO	4.$p < 0.05$
									5.TNF-α protein	5.$p < 0.05$
Wang, R.2021	China	Sprague-Dawley rats (male, n = 6/6)	250–300 g	45 min of ischemia followed by 120 min of reperfusion by using a modi-fied Langendorff technique	Pentobarbital sodium (50 mg/kg)	Curcumin (1 μM) myocardial perfusion	Saline oral	before ischemia	1.IR/AR	1.$p < 0.01$
									2.GSH px	2.$p < 0.01$
									3.LDH	3.$p < 0.01$
									4.MDA	4.$p < 0.01$
									5.SOD	5.$p < 0.01$
Wu,C.H.2011	China	Sprague-Dawley rats (male, 30/10)	200–250 g	Block LAD for 60 min then reflow for 30 min	Pentobarbital sodium (50 mg/kg, 1%)	Transduodenal injection curcumin (10/20/40 mg/kg)	Intravenous injection nothing	30 min earlier before reperfution	1.AST	1.$p < 0.05$
									2.IR/LV	2.$p < 0.05$
									3.LDH	3.$p < 0.05$
									4.LDH1	4.$p < 0.05$
									5.MDA	5.$p < 0.05$
									6.SOD	6.$p < 0.05$

(Continued on following page)

10.3389/fphar.2023.1111459

TABLE 1 (*Continued*) Basic characteristics of the 24 included animal studies.

Study ID	Country	Species (sex, n = experimental/ control group)	Weight	Model (method)	Anesthetic	Treatment group (method to curcumin)	Control group	Duration	Outcomes	*p*-Value
Yang, Y.2013	the U.S.	Sprague-Dawley rats (male, n = 24/8)	220–250 g	Block LAD for 45 min then reflow for 60 min	Pentobarbital sodium (50 mg/kg)	Curcumin (0.25/0.5/1 μM) oral	Saline oral	10 days before ischemia	1.Apoptosis index	1.$p < 0.01$
									2.IR/AR	2.$p < 0.01$
									3.LDH	3.$p < 0.01$
									4.LVDP	4.$p < 0.01$
									5.SIRT1 protein	5.$p < 0.01$
Yao,B.H.2014	China	Sprague-Dawley rats (male, 12/12)	200–250 g	Block LAD for 30 min then reflow for 360 min	Pentobarbital sodium (30 mg/kg, 3%)	Intravenous injection curcumin (20 mg/kg)	Intravenous injection nothing	1 min earlier before reperfution	1.CK	1.$p < 0.05$
									2.LDH	2.$p < 0.05$
									3.Max dp/dt	3.$p < 0.05$
									4.MDA	4.$p < 0.05$
									5.SOD	5.$p < 0.05$
Yeh, C. H. 2005	China (Taiwan)	New Zealand white rabbits (male, n = 20/10)	2.5–3.5 kg	Turn off pumpig system for 1 h then reflow 4 h using Langendorff technique	Pentobarbital sodium (30 mg/kg)	Curcumin (7/70 mmol/kg) injection	Saline injection	2 h before cardiopulmonary bypass	1. IL-6 mRNA	1. $p < 0.05$
									2.MCP-1 mRNA	2.$p < 0.05$
									3.NF-κB protein	3.$p < 0.05$
									4.TNF-α mRNA	4.$p < 0.05$
									5. MMP-2	5. $p < 0.05$
									6. MMP-9	6. $p < 0.05$

AKT, protein kinase B; AR/LV, area in risk/left ventricle; AU, area under the curve; Bcl-2 B-cell lymphoma/Leukemia-2; CF, cardiac flow; CK/CK-MB, creatine kinase; cTnT cardiac troponin T; DMSO, imethyl sulfoxide; dP/dtmax (min), the maximum (minimum) rate of pressure changing the ventricle: GGR GSH/GSSG, ratio; GR, glutathione reductas; GSH, Px glutathione peroxidase; HR, heart rate; IR/AR, infarction region/area in risk; IR/LV, infarction region/left ventricle; ISR, ischemic region; LAC, the left coronaryarter; LDH, lactate dehydrogenase; LVDd, left ventricular end diastolic diameter; LVDP, left ventricular peak developing pressure; LVEF, left ventricular ejection fraction; LVFS, left ventricular fraction shortening; LVSd, left ventricular end systolic diameter; MA, myocardial apoptosis; MAP, mean arterial pressure; MAPK, p38 mitogen-activated protein kinase; MC, myocardial contractility; MDA, malondialdehyde; MIS, myocardial infarction size; MPO, myeloperoxidase; NF-κB, nuclear factor kappa B; NM, no mention; NOAC, the number of apoptosis cells; OC, oxygen consumption; p-JNK1 phosphorylated c-Jun NH2-terminal kinase; PLVN, percentage left ventricle necrosis; SIRT1 sirtuin1; SMA, superior mesenteric artery; SOD, superoxide dismutase; STE ST-segment elevation; SV, stroke volume; VF, ventricular fibrillation; VPB, ventricular premature beats; VT, ventricular tachycardia.

10.3389/fphar.2023.1111459

TABLE 2 Basic characteristics of the four included human studies.

Study ID	Country	Male/female	Number of experimental group	Number of control group	Treatment group (method to curcumin)	Control group	Duration	Time of following-up	Outcomes	*p*-Value
Arintaya Phrommintikul. 2019	Thailand	69/31	50	50	Curcumin treatment: curcumin nanomicelle 4 g per day P.O for 1 day before PCI and 1day post PCI Conventional treatment: Not mention	Conventional treatment: Not mention	2 days	48 h after PCI	1.hs-TnT after PCI	1.p = 0.912
									2.hs-CRP after PCI	2.p = 0.873
Naser Aslanabadi. 2019	Iran	66/44	55	55	Curcumin treatment: curcumin nanomicelle 480 mg P.O at 1–2 h before PCI Conventional treatment: aspirin 325 mg and clopidogrel 300 mg orally plus weight-adjusted intravenous heparin with a target activated clotting time 250–350 s	Pretreatment: aspirin 325 mg and clopidogrel 300 mg orally plus weight-adjusted intravenous heparin with a target activated clotting time 250–350 s	once	8 and 24 h after PCI	1.CK-MB 8 h after PCI	1.p = 0.24
									2.CK-MB 24 h after PCI	2.p = 0.37
									3.cTnI 8 h after PCI	3.p = 1.0
									4.cTnI 24 h after PCI	4.p = 0.35
Wanwarang Wongcharoen. 2012	Thailand	69/52	61	60	Curcumin treatment: curcumin nanomicelle 4 g per day P.O for 3 days before CABG and 5 days post CABG Conventional treatment: Not mention	Conventional treatment: Not mention	8 days	30 days after CABG	1.CRP 3 days after CABG	1.p = 0.031
									2.CRP 5 days after CABG	2.p > 0.05
									3.MDA 5 days after CABG	3.p < 0.001
									4. Incidence of in-hospital MI	4.p = 0.028
									5. Incidence of left ventricular dysfunction	5.p = 0.021
									6.NT-proBNP	6.0.015
W. Wongcharoen. 2011	Thailand	Not mention	52	52	Curcumin treatment: curcumin nanomicelle 4 g per day P.O for 3 days before CABG and 7 days post CABG Conventional treatment: Not mention	Conventional treatment: Not mention	10 days	30 days after CABG	1. Incidence of in-hospital MI	1.p < 0.05
									2. Incidence of MACE	2.p < 0.05
									3.CK-MB after CABG	3.p < 0.05

CABG, coronary artery bypass grafting; CK-MB, creatine kinase; MB, form; cTnI, cardiac troponin; hs-CRP, high-sensitive cardiac troponin T; hs-TnT, high-sensitive cardiac troponin T; MACE, major adverse cardiovascular events; MDA, malonaldehyde; MI, myocardium infarction; P.O, peros; PCI, percutaneous coronary intervention.

10.3389/fphar.2023.1111459

two studies (Chen et al., 2016; Liu et al., 2017a) used chloral hydrate, one study (Broskova et al., 2013) used diethylether, one study (Ali et al., 2009) used thiopentone sodium, one study (Jo et al., 2020) used Alfaxalone combined with xylazine, and the remaining one (Hardy et al., 2015) did not specify the anaesthetic. 15 myocardial I/R models (Cheng et al., 2005; Kim et al., 2008; Ali et al., 2009; Wu, 2011; Jeong et al., 2012; Kim et al., 2012; Wang et al., 2012; Yang et al., 2013a; Wang et al., 2014; Yao and Jiang, 2014; Chen et al., 2016; Gu et al., 2016; Liu et al., 2017b; Deng et al., 2018; Jo et al., 2020) were produced by ligation of the coronary artery, the rest were produced by turning off and then turning on the Langendorff heart perfusion system which is supposed to pump blood to the heart. The outcomes mentioned were presented as follows: myocardial infarction size, left ventricular ejection fractions (LVEF), left ventricular fraction shortening (LVFS), left ventricular end diastolic dimension (LVDd), left ventricular end systolic dimension (LVSd), lactate dehydrogenase (LDH), creatine kinase (CK), CK-MB, superoxide dismutase (SOD), catalase (CAT), glutathione (GSH), malondialdehyde (MDA), myeloperoxidase (MPO), nuclear factor kappa B (NF-κB), tumor necrosis factor alpha (TNF-a), cardiac fibrosis area. The detailed characteristics of the included studies are shown in Table 1.

3.2.2 Human studies

All human studies (Wongcharoen et al., 2011; Wongcharoen et al., 2012; Aslanabadi et al., 2019; Phrommintikul et al., 2019) are English literature studies, mainly distributed in Iran and Thailand. All 435 patients included in the study were ischemic heart disease patients who needed PCI or CABG treatment, and were randomly divided into curcumin treatment group and conventional treatment group. The clinical characteristics are summarized in Table 2.

3.3 Study quality

3.3.1 Animal studies

We evaluated the quality of all included studies. The score of study quality ranged from two to six with a total of ten points. One study (Hardy et al., 2015) got two points, eight studies (Cheng et al., 2005; Yeh et al., 2005; Ali et al., 2009; Yang et al., 2013a; Leong et al., 2013; Chen et al., 2016; Gu et al., 2016; Deng et al., 2018) got three points, four studies (Sato et al., 2000; Duan et al., 2012; Liu et al., 2017a; Wang et al., 2018) got four points, five studies (Kim et al., 2008; Gonzalez-Salazar et al., 2011; Broskova et al., 2013; Liu et al., 2017b; Jo et al., 2020) got five points, and the remaining 6 (Wu, 2011; Jeong et al., 2012; Kim et al., 2012; Wang et al., 2012; Wang et al., 2014; Yao and Jiang, 2014) got six points. All studies reported random allocation of animals, but only 1 (Gu et al., 2016) of them reported the process of random sequence generation. Five studies (Yeh et al., 2005; Yang et al., 2013a; Leong et al., 2013; Hardy et al., 2015; Gu et al., 2016) did not fully report on how to balance baseline characteristics. Twelve studies (Sato et al., 2000; Cheng et al., 2005; Yeh et al., 2005; Ali et al., 2009; Duan et al., 2012; Yang et al., 2013a; Leong et al., 2013; Hardy et al., 2015; Chen et al., 2016; Gu et al., 2016; Liu et al., 2017a; Deng et al., 2018) did not report allocation concealment. Eight studied (Sato et al., 2000; Wu, 2011; Kim et al., 2012; Wang et al., 2012; Broskova et al., 2013; Wang et al., 2014; Yao and Jiang, 2014; Liu et al., 2017a) reported randomization of animal placement. No studies reported the implementation of blind methods for caregivers or experimental researchers. Thirteen studies (Yeh et al., 2005; Kim et al., 2008; Gonzalez-Salazar et al., 2011; Wu, 2011; Jeong et al., 2012; Kim et al., 2012; Wang et al., 2012; Yang et al., 2013a; Leong et al., 2013; Wang et al., 2014; Yao and Jiang, 2014; Liu et al., 2017b; Jo et al., 2020) used a random outcome assessment. Only one study (Duan et al., 2012) mentioned the blinding outcome assessor, while the others did not blind the assessors. No study reported incomplete data. Only one study (Jeong et al., 2012) had the study protocol, which showed no selective outcome reporting occurred, while the others remained unclear. All studies had no other sources of bias. The overall methodological quality of the included animal studies is shown in Table 3.

3.3.2 Human studies

RoB-2 tool was used to evaluate the methodological quality (deviation risk) of the four included human studies. Two of the studies were judged as low risk, while the other two were judged as some concerns. The details are shown in Table 4.

3.4 Data analysis of animal studies

3.4.1 Myocardial infarction size

Myocardial infarction (MI) size was calculated by infarct area/left ventricular area. A meta-analysis of 16 animal studies demonstrated that curcumin significantly decreased MI size compared with the control group (n = 246, WMD = −17.91%, 95% CI (−22.24%, −13.59%), $p < 0.00001$, $I^2 = 97\%$) (Figure 3). Because of the obvious heterogeneity in the included animal studies, we performed a sensitivity analysis. After removing the animal studies one by one, we failed to determine the source of heterogeneity, but the sensitivity analysis indicated that the outcome was steady.

3.4.1.1 Dose-response meta-analysis of curcumin

According to previous studies, different doses of curcumin could affect the efficacy (Yang et al., 2013a; Liu et al., 2017b), which might be one of the main reasons for the high outcome heterogeneity. Therefore, we performed a dose-response meta-analysis of animal studies (Jeong et al., 2012; Wang et al., 2012; Yang et al., 2013a; Wang et al., 2014; Chen et al., 2016; Liu et al., 2017b; Jo et al., 2020) in which curcumin was administered orally. Firstly, RR was recalculated and defined as the ratio of means ($means_{experimental}/means_{control}$). Then, scatter plot was drawn for curcumin dose and RR (Supplementary Figure S1). Through image analysis, the point distribution showed a non-linear relationship. We hypothesized that a non-linear relationship might be applicable to the relationship between dose and the protective effect of curcumin. Non-linear regression was conducted according to the quadratic regression method of meta-analysis (Orsini et al., 2012). with the increase of curcumin dosage, the protective effect of curcumin on myocardial I/R was firstly enhanced, then weakened and then strengthened (Figure 4). In our model, 200 mg/kg BW per day was the optimal dose of curcumin (when dosage ranges from 10 to 200 mg/kg BW per day) and had the best predictive protective effect, and the prediction relationship can be expressed as $LnRR = -1*10^{-6}\ x^3 + 0.0003\ x^2 - 0.0205\ x - 0.2386$, $R^2 = 0.638$.

TABLE 3 Methodological quality of included animal studies (SYRCLE tool).

Study ID	A	B	C	D	E	F	G	H	I	J	Scores
Ali, M. S. 2009	0	1	0	0	0	0	0	1	0	1	3
Brosková, Z. 2013	0	1	1	1	0	0	0	1	0	1	5
Chen, X. L. 2016	0	1	0	0	0	0	0	1	0	1	3
Cheng, H. 2005	0	1	0	0	0	0	0	1	0	1	3
Deng, Y. 2018	0	1	0	0	0	0	0	1	0	1	3
Duan, W. 2012	0	1	0	0	0	0	1	1	0	1	4
González-Salazar, A. 2011	0	1	1	0	0	1	0	1	0	1	5
Gu, H. P. 2016	1	0	0	0	0	0	0	1	0	1	3
Hardy, N. 2015	0	0	0	0	0	0	0	1	0	1	2
Jeong, C. W. 2012	0	1	1	0	0	1	0	1	1	1	6
Jo, W. 2020	0	1	1	0	0	1	0	1	0	1	5
Kim, Y. S. 2008	0	1	1	0	0	1	0	1	0	1	5
Kim, Y. S. 2012	0	1	1	1	0	1	0	1	0	1	6
Leong, P. K. 2013	0	0	0	0	0	1	0	1	0	1	3
Liu, H. 2017	0	1	1	0	0	1	0	1	0	1	5
Liu, K. 2017	0	1	0	1	0	0	0	1	0	1	4
Sato, M. 2000	0	1	0	1	0	0	0	1	0	1	4
Wang N. P. 2014	0	1	1	1	0	1	0	1	0	1	6
Wang, N. P. 2012	0	1	1	1	0	1	0	1	0	1	6
Wang, R. 2021	0	1	1	0	0	0	0	1	0	1	4
Wu, C. H. 2011	0	1	1	1	0	1	0	1	0	1	6
Yang, Y. 2013	0	0	0	0	0	1	0	1	0	1	3
Yao, B. H. 2014	0	1	1	1	0	1	0	1	0	1	6
Yeh, C. H. 2005	0	0	0	0	0	1	0	1	0	1	3

A, sequence generation; B, baseline characteristics; C, allocation concealment; D, random housing; E, blinding investigators; F, random outcome assessment; G, blinding outcome assessor; H, incomplete outcome data; I, selective outcome reporting; J, other sources of bias.

TABLE 4 Methodological quality of included human studies (RoB-2 tool).

Study ID	Randomization process	Assignment to intervention	Adhering to intervention	Missing outcome data	Measurement of outcome	Selection of the reported result	RoB-2 overall score
Arintaya Phrommintikul. 2019	Low risk	Low risk	Low risk	Low risk	Low risk	Low risk	Low risk
Naser Aslanabadi. 2019	Low risk	Some concerns	Low risk	Some concerns	Low risk	Some concerns	Some concerns
Wanwarang Wongcharoen. 2012	Low risk	Low risk	Low risk	Low risk	Low risk	Low risk	Low risk
Wanwarang Wongcharoen. 2011	Some concerns	Low risk	Low risk	Low risk	Low risk	Some concerns	Some concerns

TABLE 5 Meta-regression analysis of potential sources of animal studies heterogeneity.

Heterogeneity factor	Coefficient	SE	t	*p*-value	95% CI (lower limit, upper limit)
region	4.255238	2.975009	1.43	0.196	−2.77954, 11.29002
year of publication	3.702559	4.491461	0.82	0.437	−6.91806, 14.32318
whether thestudy set the dose subgroup	4.001104	5.08711	0.79	0.457	−8.027999, 16.03021
in vivo or *in vitro* experiments	−0.779716	5.795373	−0.13	0.897	−14.4836, 12.92416
myocardial ischemia duration	1.391345	2.765627	0.50	0.630	−5.148324, 7.931014
times of administration	0.21975	5.388646	0.04	0.969	−12.52237, 12.961873
animal sample size	2.58827	5.942484	0.44	0.676	−11.46347, 16.64001
publication language	3.311636	7.378133	0.45	0.667	−14.13488, 20.75815
Cutoff value	−35.80981	21.23304	−1.69	0.136	−86.01798, 14.39835

SE, standard error; CI, confidence interval.

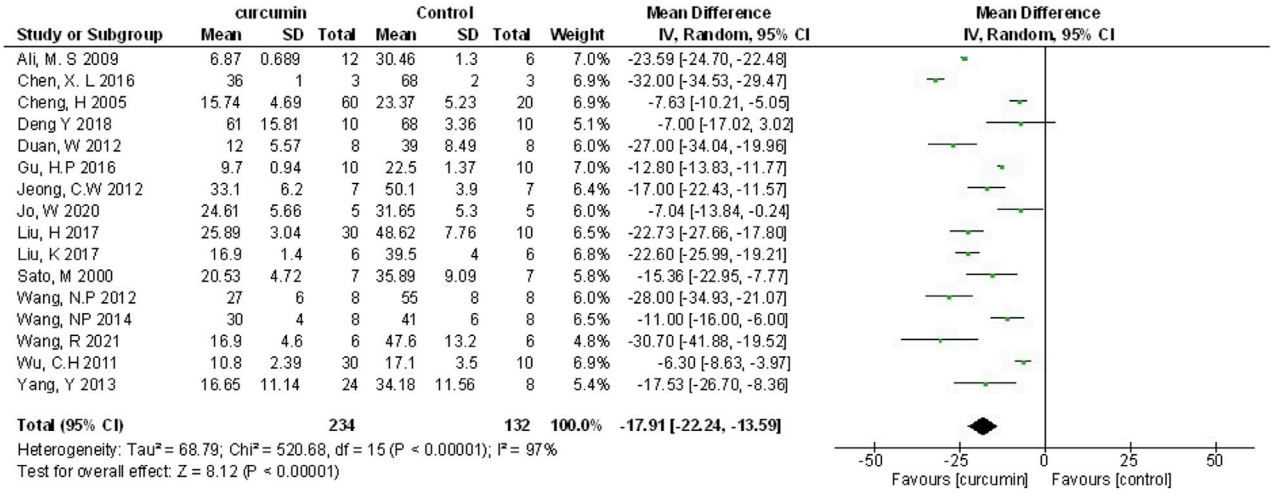

FIGURE 3
The meta-analysis results of the effect of curcumin on MI size.

3.4.2 Cardiac function

Left ventricular ejection fraction (LVEF), left ventricular fraction shortening (LVFS), left ventricular end-diastolic dimension (LVDD), left ventricular end-systolic dimension (LVSD) were examined to demonstrate improvement in cardiac function induced by curcumin. A total of four animal studies (Kim et al., 2012; Wang et al., 2012; Deng et al., 2018; Jo et al., 2020) reported the protective effects of curcumin on LVEF compared to the control group (n = 52, WMD = 10.29%, 95% CI (5.09%, −15.48%), p = 0.0001, I2 = 0%) (Figure 4A). Results from five animal studies (Kim et al., 2008; Kim et al., 2012; Wang et al., 2012; Deng et al., 2018; Jo et al., 2020) showed curcumin could increase LVFS compared to the control group (n = 72, WMD = 6.39%, 95% CI (4.27%, 8.50%), p < 0.00001, I2 = 47%) (Figure 4B). Results from three animal studies (Kim et al., 2008; Kim et al., 2012; Jo et al., 2020) showed curcumin could decrease LVDD compared to the control group (n = 44, WMD = −0.43, 95% CI (−0.74, −0.11), p = 0.008, I2 = 35%) (Figure 4C). Results from three animal studies (Kim et al., 2008; Kim et al., 2012; Jo et al., 2020) showed curcumin could decrease LVSD compared to the control group (n = 44, WMD = −1.05, 95% CI (−1.52, −0.59), p < 0.0001, I2 = 0%) (Figure 4D).

3.4.3 Myocardial injury marker

Compared with the control group, meta-analysis of three animal studies (Cheng et al., 2005; Chen et al., 2016; Liu et al., 2017b) showed curcumin can reduce CK-MB (n = 126, WMD = −37.19, 95% CI (−72.22, −2.16), p = 0.04, I2 = 98%) (Figure 5A). A meta-analysis of 10 animal studies (Cheng et al., 2005; Yeh et al., 2005; Duan et al., 2012; Yang et al., 2013a; Leong et al., 2013; Yao and Jiang, 2014; Hardy et al., 2015; Liu et al., 2017a; Liu et al., 2017b; Wang et al., 2018) showed curcumin can reduce LDH (n = 275, SMD = −4.29, 95% CI (−6.01, −2.58), p < 0.00001, I2 = 93%) (Figure 5B). Through removing the animal studies one by one, the sensitivity analysis indicated that the outcome was steady. The

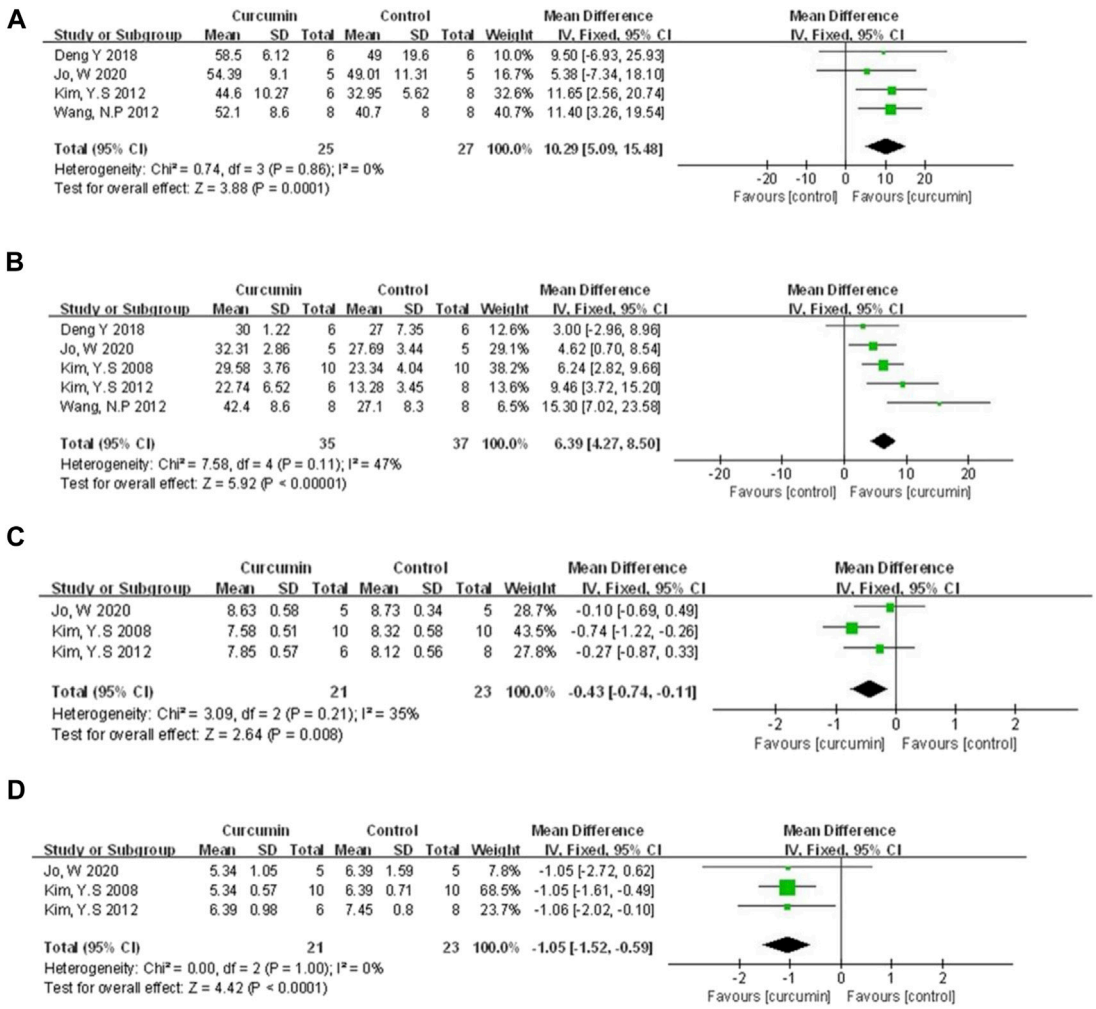

FIGURE 4
(A) The meta-analysis results of the effect of curcumin on LVEF **(B)** The meta-analysis results of the effect of curcumin on LVFS. **(C)** The meta-analysis results of the effect of curcumin on LVDd. **(D)** The meta-analysis results of the effect of curcumin on LVSd.

pooled results of two animal studies (Hardy et al., 2015; Liu et al., 2017a) on CK did not show difference between curcumin and control group (n = 21, WMD = −10.93, 95% CI (−28.62, 6.76), p = 0.23, I2 = 99%) (Figure 5C). Moreover, compared with the control group, one study (Gu et al., 2016) showed curcumin can decrease cTnT ($p < 0.05$), and another one (Kim et al., 2008) showed curcumin can decrease MPO ($p < 0.05$).

3.4.4 Cardioprotective mechanisms

The cardioprotective protective mechanisms involved in our study included cardiomyocyte inflammation, oxidation, apoptosis, myocardial fibrosis, and et al. A meta-analysis of four animal studies (Cheng et al., 2005; Gonzalez-Salazar et al., 2011; Yao and Jiang, 2014; Liu et al., 2017b) showed that curcumin had a significant effect on increasing SOD expression compared with the control group (n = 156, SMD = 4.47, 95% CI (1.17, 7.78), p = 0.008, I2 = 95%) (Figure 6A). A meta-analysis of three animal studies (Ali et al., 2009; Gonzalez-Salazar et al., 2011; Liu et al., 2017b) showed that curcumin had a significant effect on increasing CAT expression compared with the control group (n = 70, SMD = 4.70, 95% CI (1.48, 7.92), p = 0.004, I2 = 89%) (Figure 6B). Three animal studies (Cheng et al., 2005; Ali et al., 2009; Gonzalez-Salazar et al., 2011) showed that curcumin could increase GSH expression compared with the control group (n = 110, SMD = 3.66, 95% CI (0.43, 6.89), p = 0.03, I2 = 90%) (Figure 6C). A meta-analysis of seven animal studies (Cheng et al., 2005; Kim et al., 2008; Ali et al., 2009; Wang et al., 2012; Yao and Jiang, 2014; Chen et al., 2016; Liu et al., 2017b) showed that curcumin has a significant effect on reducing MDA expression compared with the control group (n = 190, SMD = −4.66, 95% CI (−7.00, −2.31), $p < 0.0001$, I2 = 91%) (Figure 6D). A meta-analysis of two animal studies (Yeh et al., 2005; Gu et al., 2016) indicated that curcumin can suppress the expression of NF-κB protein compared with the control group (n = 40, SMD = −5.82, 95% CI (−9.43, −2.22), p = 0.002, I2 = 79%) (Figure 6E). Results from four animal studies (Yeh et al., 2005; Wang et al., 2014; Gu et al., 2016; Liu et al., 2017a) showed curcumin could decrease TNF-α protein compared to the control group (n = 78, SMD = −4.05, 95% CI (−6.74, −1.37), p = 0.003, I2 = 89%) (Figure 6F). Results from four

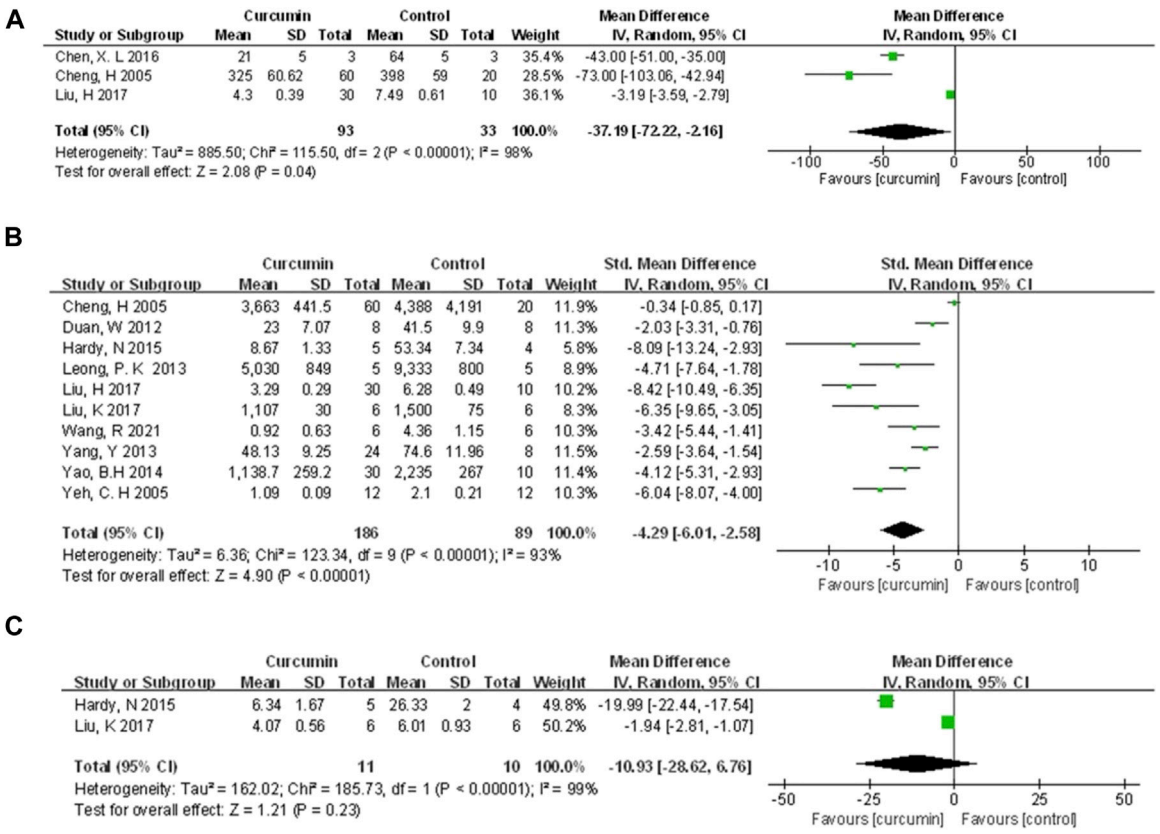

FIGURE 5
The meta-analysis results of the effect of curcumin on **(A)** CK-MB **(B)** LDH, and **(C)** CK.

animal studies (Kim et al., 2008; Kim et al., 2012; Wang et al., 2012; Jo et al., 2020) showed curcumin could decrease the area of fibrosis compared to the control group (n = 58, SMD = −2.40, 95% CI (−4.47, −0.33), p = 0.02, I2 = 87%) (Figure 6G).

Because of the small number of animal studies (<3 studies), other mechanism indicators reflecting the cardioprotective function of curcumin only are described as follows. Unless otherwise specified, these reports indicated positive effects of the curcumin group on the mechanism of anti-myocardial I/R injury (p-value indicates comparison with the control group). These indicators included Bcl-2 (Duan et al., 2012; Deng et al., 2018) ($p < 0.05$), Caspase-3 (Chen et al., 2016; Liu et al., 2017b) ($p < 0.05$ or $p < 0.01$), MMP-9 (Yeh et al., 2005; Wang et al., 2012) ($p < 0.05$), MPO (Kim et al., 2008; Wang et al., 2014) ($p < 0.05$), IL-6 mRNA (Yeh et al., 2005; Wang et al., 2014) ($p < 0.05$). The included animal studies also reported the regulation of curcumin on other proteins. However, because the frequency of occurrence was <2, they would not be described in detail (All reported indicators can be found in Table 1).

3.4.5 Subgroup analysis and meta-regression

We performed the subgroup analysis on primary outcomes according to preset subgroups. The LVEF, LVFS, LVDD, LVSD in the primary outcome indicators were not included in the subgroup analysis because of not enough animal studies, so we only carried out the subgroup analysis on MI size. Analysis of the three preset subgroups (method of model establishment, administration method, and genus of experimental animals) indicated outcomes that were consistent with the overall rusults ($p < 0.05$) (Figures 7–9). Some outcomes of the subgroup analysis by intervention moment (before ischemia/between ischemia and reperfusion/during reperfusion) were inconsistent with the overall results (Figure 10). The subgroup analyzed for before ischemia group and during reperfusion group were consistent with the overall results ($p < 0.05$), while the outcome of between ischemia and reperfusion group was inconsistent with the overall results ($p > 0.05$). Moreover, I2 did not decrease, suggesting that the preset subgroups did not explain the source of heterogeneity of MI size.

To further explore the source of heterogeneity, we conducted a meta-regression analysis. Eight characteristics were selected for meta-regression, including: 1) Region (US, China, India, or South Korea), 2) year of publication (2000–2016, 2017–2021), 3) whether the original study set the dose subgroup, 4) In vivo or ex-vivo experiments, 5) myocardial ischemia duration (30min, 45min or 60min), 6) times of administration (single-dose or multiple-dose), 7) No. of sample size (<20 or ≥20), 8) publication language (English or Chinese). However, meta-regression analysis (Table 5) did not reveal a significant impact of the covariates above, which indicated none of the above characteristics was the source of heterogeneity between animal studies.

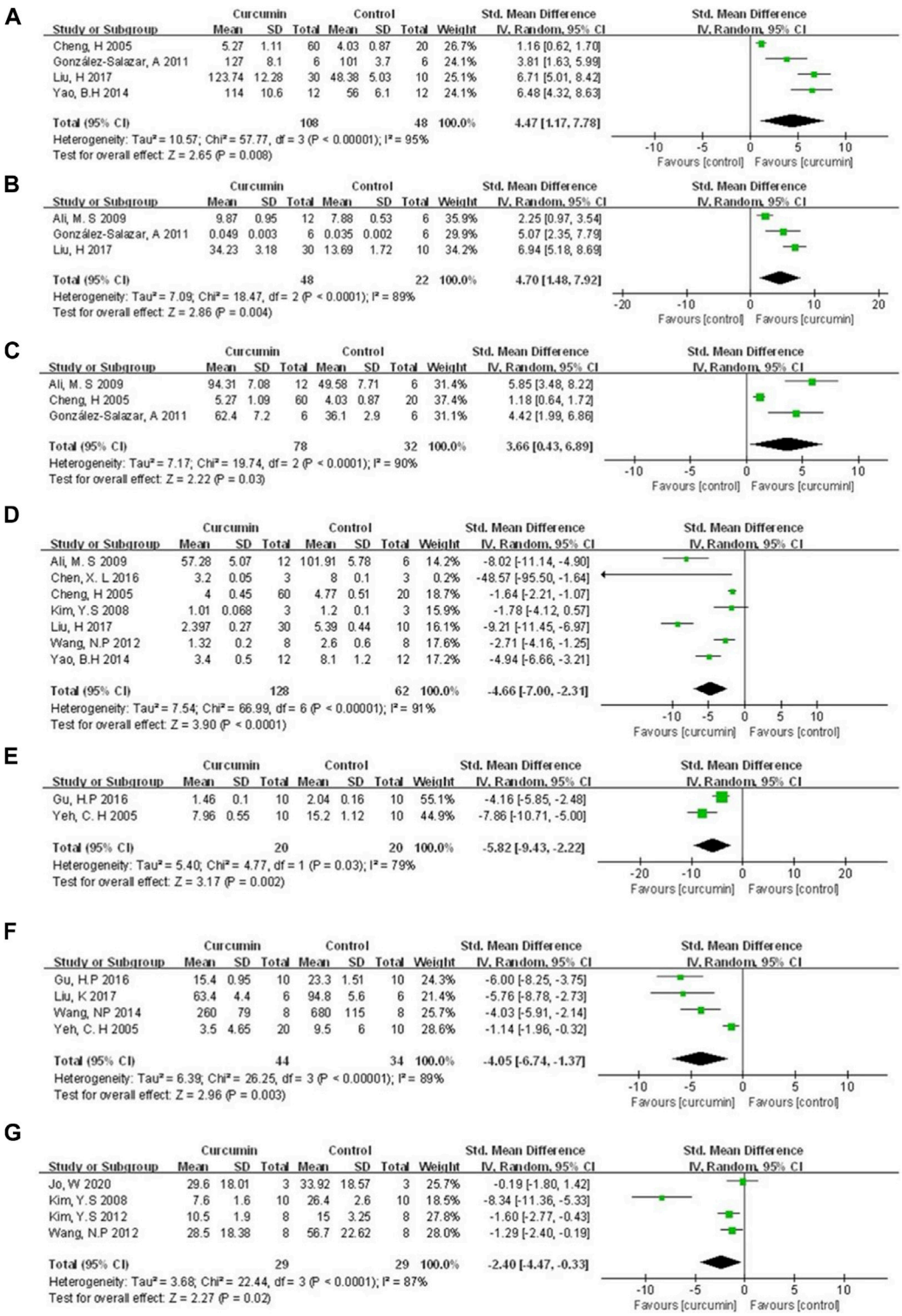

FIGURE 6
The meta-analysis results of the effect of curcumin on **(A)** SOD **(B)** CAT **(C)** GSH **(D)** MDA **(E)** NF-κB protein **(F)** TNF-α protein, and **(G)** Fibrosis/LV%.

3.4.5 Publication bias

A funnel plot was adopted to assess the publication bias regarding myocardial infarction size (Figure 11). Furthermore, we used Egger's regression test to check out the asymmetry of the graph, and the results indicated no publication bias in this study (p = 0.92 > 0.05).

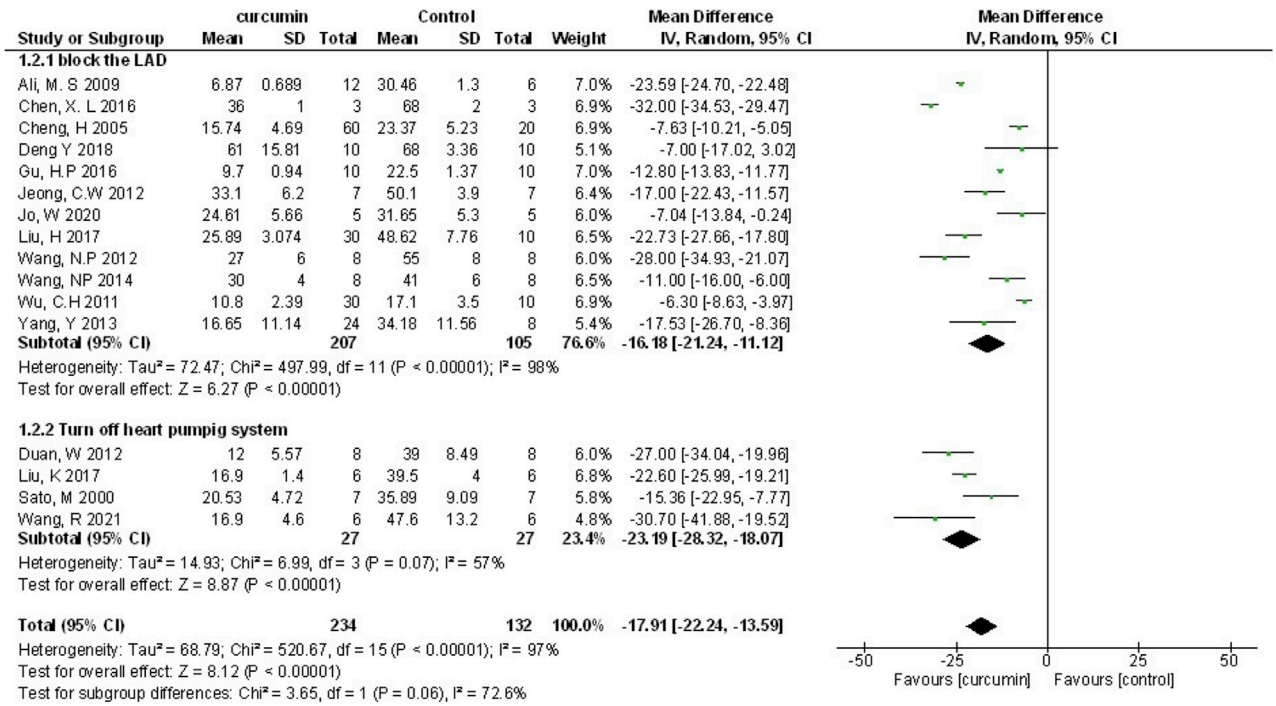

FIGURE 7
The subgroup analysis (method of model establishment) of curcumin on MI size.

3.5 Systematic analysis of human studies

3.5.1 Methods and characteristics of curcumin treatment

Oral curcumin nanomicelle was used in four human studies. Two studies (Aslanabadi et al., 2019; Phrommintikul et al., 2019) used a shorter course of treatment (1–2 days), with a total amount of 0.48g–8 g of curcumin. The other two studies (Wongcharoen et al., 2011; Wongcharoen et al., 2012) used a longer course of treatment (8–10 days), with a total amount of 32g–40 g of curcumin. All the curcumin treatment groups in the study were combined with conventional treatment, and only one study described the conventional treatment protocol in detail.

3.5.2 Biomarkers of myocardial injury

cTnI, cTnT and CK-MB have been used clinically for a long time to evaluate the myocardial injury in patients. Three studies (Wongcharoen et al., 2011; Aslanabadi et al., 2019; Phrommintikul et al., 2019) detected serum biomarkers of myocardial injury after revascularization, of which two (Aslanabadi et al., 2019; Phrommintikul et al., 2019) showed no statistically significant difference between curcumin treatment group and control group, hs TnT (201 ± 547 vs 187 ± 703.9 ng/L, p = 0.912), cTnI (180 ± 190 vs 220 ± 190 ng/L, p = 0.35), CK-MB (21.8 ± 5.4 vs 23.1 ± 8.5 U/L, p = 0.37). One study (Wongcharoen et al., 2011) showed that curcumin had a therapeutic effect in reducing CK-MB after revascularization (43 ± 18 vs 58 ± 44 ng/mL, p = 0.02).

3.5.3 Biomarkers of inflammation and oxidative stress injury

Serum CRP and MDA were used to evaluate the degree of inflammation and oxidative stress injury. The results of study (Phrommintikul et al., 2019) showed that there was no statistically significant difference in CRP reduction between the curcumin group and the control group (7.2 ± 18.8 vs 6.6 ± 17.5 mg/dL, p = 0.87), but the results of study (Wongcharoen et al., 2012) showed that compared with the control group, the curcumin group could reduce CRP (161.8 ± 54.1 vs 128.6 ± 60.5 mg/dL, p = 0.031) and MDA (0.8 ± 1.4 vs 5.7 ± 1.5 mmol/mL, p = 0.001).

3.5.4 Cardiac function, incidence of in-hospital MI and MACE within 30 days after revascularization

For patients with ischemic heart disease, in-hospital MI and MACE after revascularization are the most important clinical outcome, and cardiac function is the most important factor affecting the above outcome. The study (Wongcharoen et al., 2012) showed that compared with the control group, the curcumin group could reduce the incidence of left ventricular dysfunction, LVEF<40% (3.3% vs 25.9% p = 0.021), and NT-proBNP (1822.1 ± 2,102.9 vs 2,542.2 ± 2,631.2 pg/mL, p = 0.015). The results of two studies (Wongcharoen et al., 2011; Wongcharoen et al., 2012) showed that the incidence of in-hospital MI in the curcumin group was significantly lower than that in the control group. The study (Wongcharoen et al., 2011) showed that compared with the control group, the incidence of MACE within 30 days after revascularization in the curcumin group was lower (13.5% vs. 34.6%, p = 0.02).

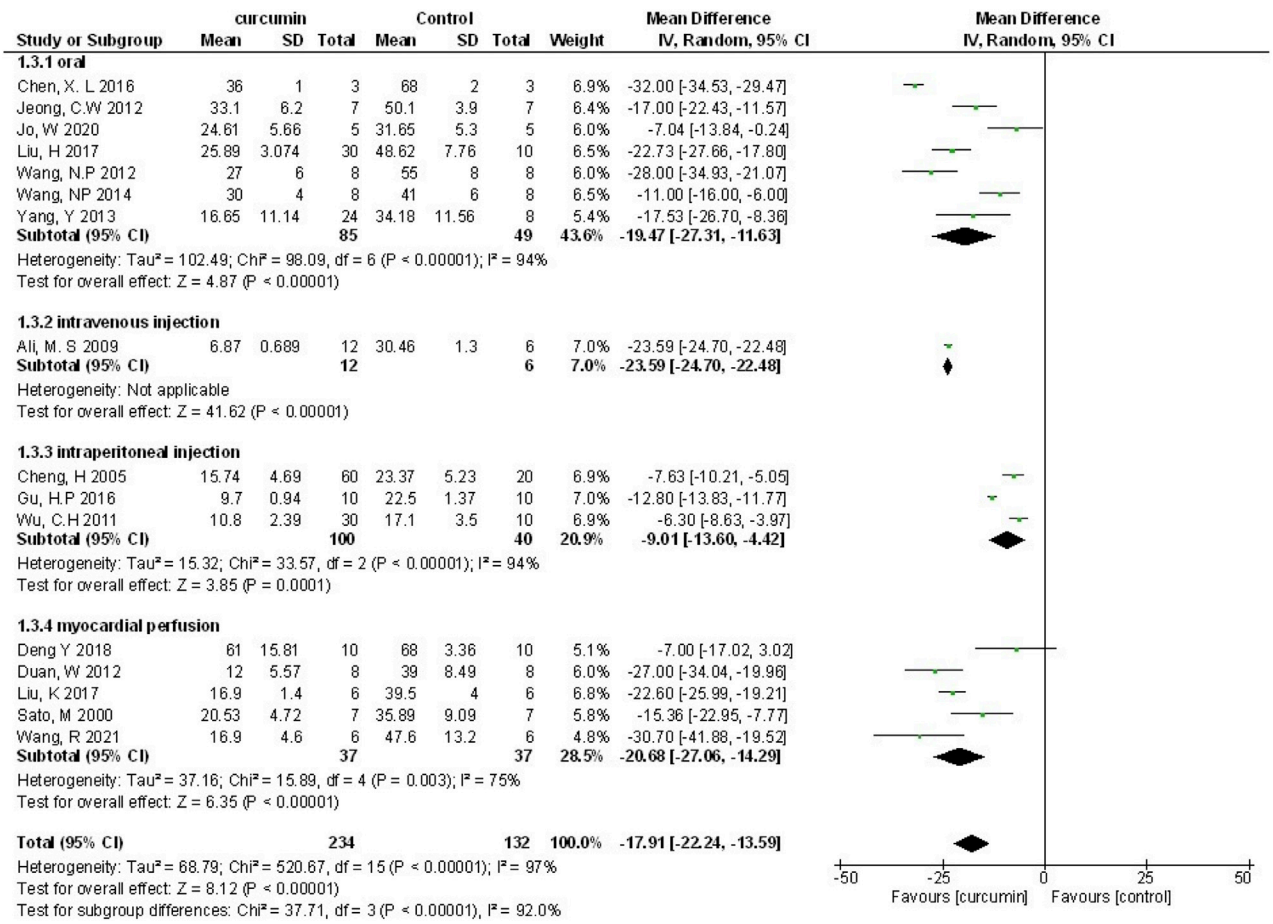

FIGURE 8
The subgroup analysis (administration method) of curcumin on MI size.

4 Discussion

4.1 Contradiction between human studies and animal studies

This is the first systematic review and meta-analysis consisting of preclinical and clinical evidence to investigate the cardioprotective effects of curcumin on myocardial I/R injury. Twenty-four studies with 503 animals and four human studies with 435 patients were included, and the overall methodological quality of the included studies was moderate. The results of animal studies meta-analysis suggested that curcumin might diminish myocardial infarction size, improve heart function, suppress biomarkers concentration for myocardial infarction, as well as ameliorate cardiomyocyte inflammation, oxidation, apoptosis, and myocardial fibrosis in animal studies.

Meta-analysis of animal studies shown the clinically potential of curcumin in the treatment of myocardial I/R injury. Interestingly, some of results of human studies showed different opinions. The results of two studies (Aslanabadi et al., 2019; Phrommintikul et al., 2019) showed that there was no statistically significance between curcumin group and control group in serum myocardial injury biomarkers (hscTnT, cTnI, CK-MB) after PCI or CABG. However, we found that in N. Aslanabadi et al.'s study (Aslanabadi et al., 2019), the incidence of CK-MB rising above the normal value during PCI in curcumin group was 50% less than that in control group. In addition, the decrease of serum CK-MB in patients in curcumin group 24 h after PCI were more notable than that in the control group (2.6 ± 8.7 vs 0.29 ± 8.8 U/L, $p = 0.75$). Although $p > 0.05$, both indicators showed descending trend. Besides, it should be noted that the protocol of curcumin treatment in these two studies (Aslanabadi et al., 2019; Phrommintikul et al., 2019) was only 0.48 g P.O. before PCI and 4 g P.O. before and after PCI. This short course of treatment may affect the statistical significance of the results. Furthermore, the other two studies (Wongcharoen et al., 2011; Wongcharoen et al., 2012) adopted a longer course of treatment, a larger total amount of drugs, and a longer follow-up time. The results of the two latter studies showed that curcumin might has cardioprotection in term of anti-inflammation, cardiac function, incidence of in-hospital myocardial infarction and MACE within 30 days after CABG or PCI. The reason why human studies showed drastic difference

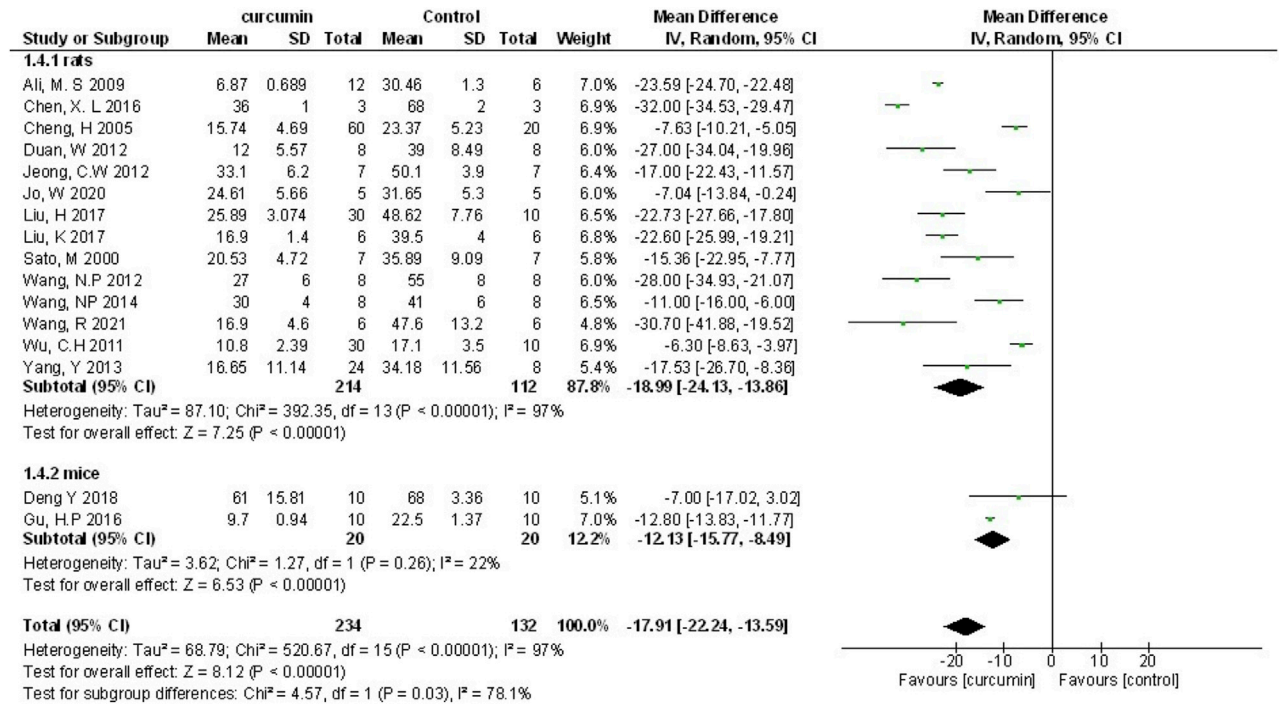

FIGURE 9
The subgroup analysis (genus of experimental animals) of curcumin on MI size.

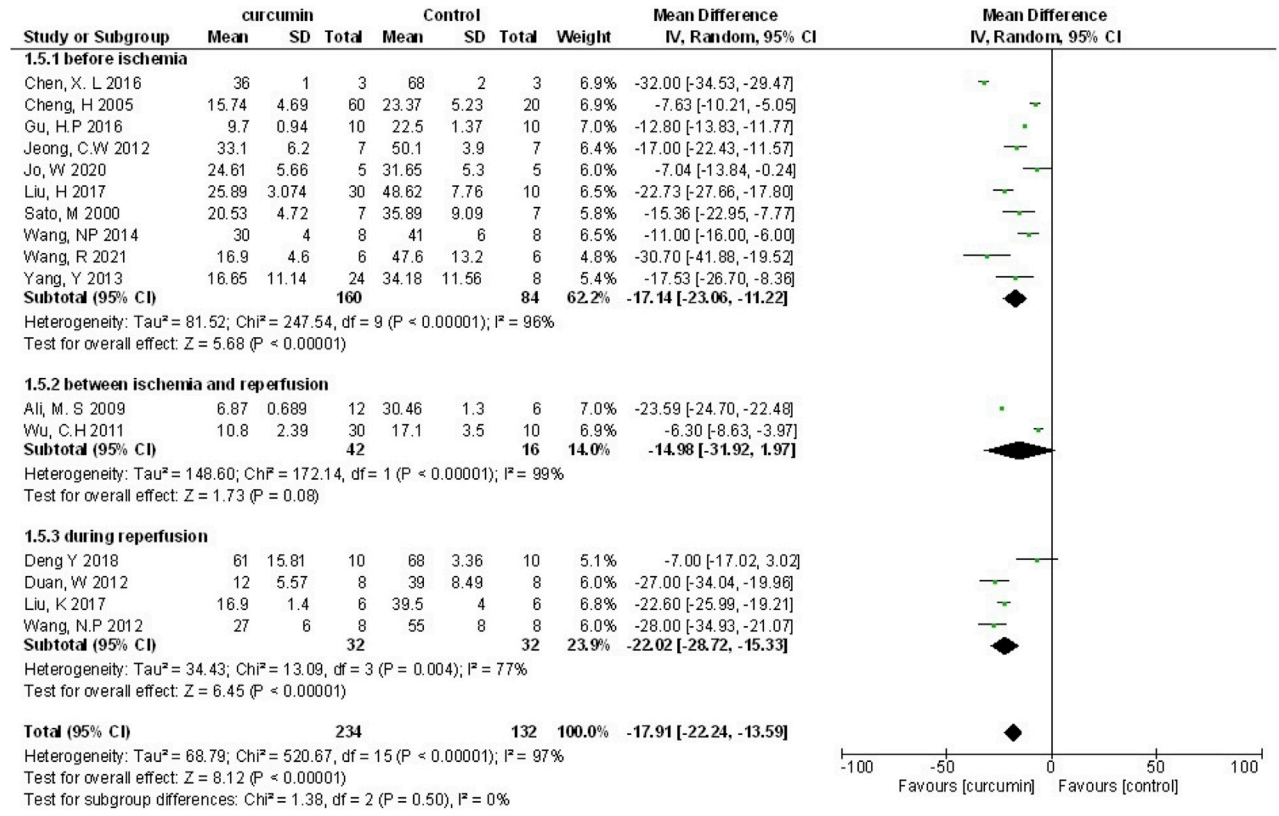

FIGURE 10
The subgroup analysis (intervention moment) of curcumin on MI size.

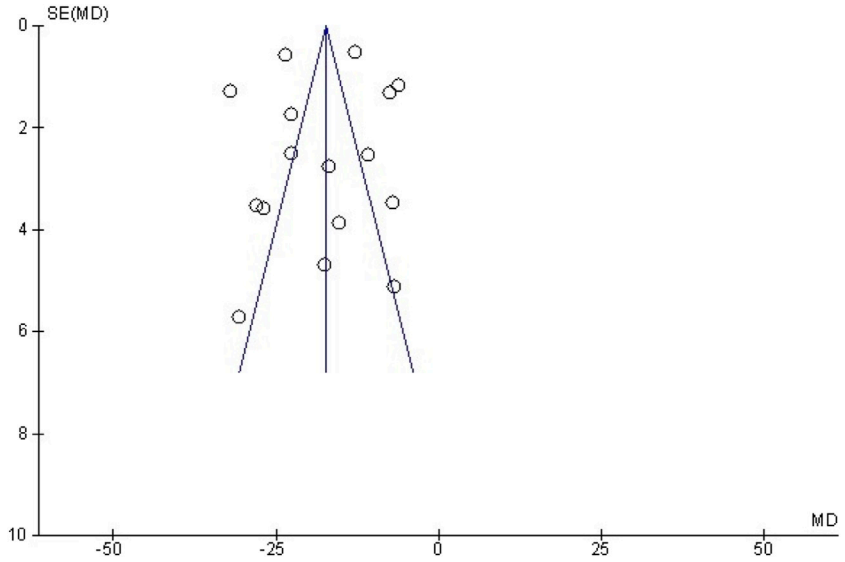

FIGURE 11
Funnel plot detailing publication bias in animal studies reporting the effect of curcumin on MI size.

might be relative to the dosage of curcumin and duration of treatment.

4.2 Safety and dose-response of curcumin

According to the existing research results, we found that poor resorption of curcumin was one of the reasons why curcumin was limited clinically. For example, volunteers took a large dose of curcumin 12 g a day in human pharmacokinetic trials. However, the blood concentration was too low to be detected, indicating that its bioavailability was low (Peng and Qian, 2014). Therefore, it is meaningful to find the relationship between the dosage and effectiveness within the safe dosage range of curcumin. First, we conducted a dose-response meta-analysis of animal studies in which curcumin was administered orally. In our model (animal studies), 200 mg/kg BW per day was the optimal dose of curcumin (when dosage ranges from 10 to 200 mg/kg BW per day) and had the best predictive protective effect. This analysis result is consistent with another curcumin dose response analysis result (Lin et al., 2020).

According to other curcumin toxicity studies, 200 mg/kg BW per day is acceptable. Many animal studies reported that significant toxicity, pathological effects, genotoxicity and death were not observed when the maximum intake dose of curcumin reached 5,000 mg/kg BW per day within 14 consecutive days (Wahlström and Blennow, 1978; Perkins et al., 2002; Aggarwal et al., 2016; Damarla et al., 2018). In human studies, when treated with purified nano curcumin, the most remarkable side effects observed include gastrointestinal flatulence (Hanai et al., 2006) and changes in liver function (Na et al., 2013; Zingg et al., 2017). Overall, based on the current research results, curcumin will be safe when it reaches the concentration we predicted.

4.3 Potential mechanisms of curcumin in myocardial I/R injury

Myocardial I/R injury is associated with various pathophysiological processes, such as calcium overload, generation of oxygen free radicals, endothelial dysfunction, inflammatory response, mitochondrial dysfunction, myocardial cell apoptosis, and autophagy (Kloner et al., 1989; Hausenloy and Yellon, 2003; Yellon and Hausenloy, 2007; Oerlemans et al., 2013; Merz et al., 2019). Considerable evidence indicates that curcumin exerts cardioprotective effects in myocardial I/R injury through multiple molecular mechanisms. Multiple molecular mechanisms might be involved in the underlying protective mechanisms of curcumin against myocardial injury, and a better understanding of these protective mechanisms will provide better insight into curcumin (Figure 12).

4.3.1 Anti-oxidant effect

Oxidative stress plays an essential role in myocardial I/R injury. Reducing oxidative stress is one of the strategies for dealing with I/R injury. The antioxidant activity of curcumin is mainly reflected by scavenging various reactive oxygen species (Broskova et al., 2013). Curcumin could regulate mitochondrial dysfunction after I/R through activating the silent Information regulator 1 (SIRT1) signal, up-regulating Bcl-2, and down-regulating Bax (Mokhtari-Zaer et al., 2018). Some studies also showed a direct antioxidant effect of curcumin, including increasing mitochondrial SOD activity and decreasing the generation of mitochondrial hydrogen peroxide and MDA (Yang et al., 2013a).

4.3.2 Anti-inflammatory effect

Inflammation is usually an active defense mechanism, but excessive inflammation will exacerbate myocardial reperfusion

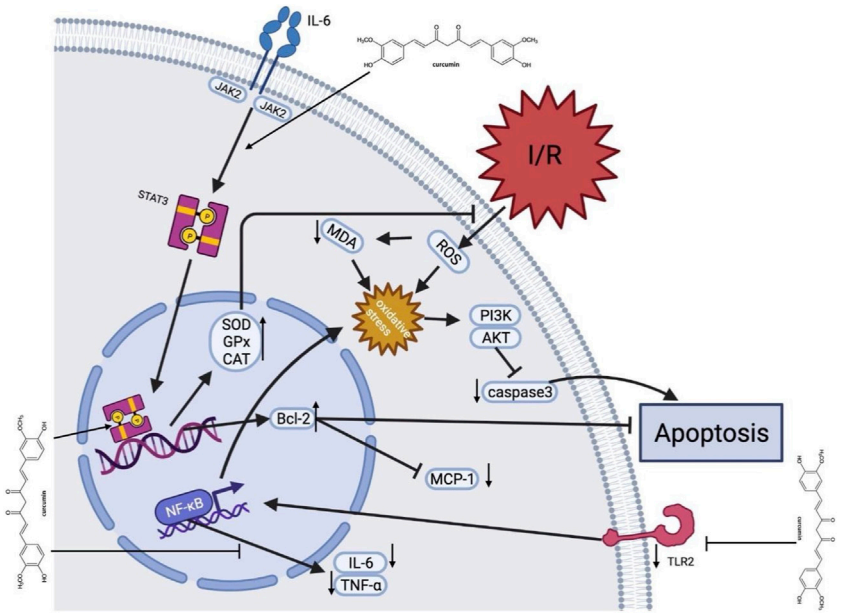

FIGURE 12
A schematic representation of cardioprotective mechanisms of curcumin for myocardial ischemia/reperfusion injury. After I/R occurs, curcumin inhibits cell apoptosis by activating JAK2/STAT3 pathway and relieving oxidative stress, with upregulated SOD, GPx and CAT expression, decrease of ROS production, and upregulated Bcl-2. In addition, curcumin inhibits the TLR2 and NF-κB pathways on the cell membrane surface *via* downregulation of TNF-α and IL-6. Moreover, curcumin suppresses caspase-3 expression to inhibit apoptosis. AKT, protein kinase B; Bcl-2, B-cell lymphona-2; CAT, catalase; GPx, Glutathione Peroxidase; I/R, ischemia/reperfusion; IL-6, interleukin-6; JAK2, Janus kinase two; McP-1, Monocyte chemotactic protein one; MDA, malondialdehyde; MPO, myeloperoxidase; PI3K, Phosphatidylinositide 3-kinases; ROS, Reactive oxygen species; Superoxide dismutase; STAT3, signal and activator of transcription three; TLR2, Toll-like receptor two; TNF-α, tumor necrosis factor α.

injury. Studies have shown that curcumin exerts anti-inflammatory effects by regulating NF-κB signaling pathway, an essential proinflammatory signaling pathway involved in cardiac injury (Fiorillo et al., 2008). It was shown that curcumin pretreatment over a week reduced TLR2 and MCP1 expression in cardiomyocytes, macrophage infiltration (CD68) and cardiac fibrosis (Kim et al., 2012). In addition, curcumin could inhibit the expression of early growth response 1 (EGR-1) in ischemic myocardial cells through lowering the levels of TNF-α and IL-6 (Wang et al., 2012). This might suggest that curcumin has a potent anti-inflammatory effect and could protect the cardiomyocytes through modulating the expression or activity of proinflammatory cytokines.

4.3.3 Anti-apoptosis effect

Apoptosis is a physiological phenomenon in most circumstances. However, excessive apoptosis under pathological conditions lead to unnecessary cell death. Due to myocardial I/R, STAT3 upregulates the expression of Bcl-2, Bcl-xl, and other genes, which have been shown to reduce cell death and lessen adverse cardiac remodeling after myocardial infarction (Yang et al., 2013b). We found that activation of Janus kinase signal sensor and transcriptional activator (JAK2-STAT3) signal pathway, upregulation of Bcl-2 and downregulation of caspase-3 could be the mechanisms of curcumin in relieving myocardial I/R injury (Duan et al., 2012).

4.3.4 Regulating autophagy effect

Autophagy is functional at low baseline levels in myocardium, removing unnecessary proteins and damaged organelles as a self-protective mechanism (Klionsky et al., 2021). Dysregulated or excessive autophagy could induce cell death (Zhao et al., 2021). A few studies indicated that curcumin might protect mouse cardiomyocytes from oxidative stress by stimulating autophagy (Rainey et al., 2020; Gu et al., 2021; Lin et al., 2021). Other studies claimed that curcumin protects myocardial I/R via downregulating elevated autophagy (Huang et al., 2015; Ma et al., 2021). This suggests that curcumin might be a potential bidirectional regulatory agent in myocardial I/R, either inhibiting excessive autophagy or promoting autophagy. In general, curcumin exerts cardioprotective effect through regulating autophagy.

4.4 Implications

Our study found that the animal myocardial IR model is not completely consistent with the characteristics of the clinical patients, and this is because that myocardial ischemia-reperfusion injury (MIR) is often accompanied by a variety of conditions, such as aging, hypertension, diabetes, etc. Therefore, more complex animal models such as aging animal models, should be used to study the pharmacological effects and mechanisms of curcumin in future researches.

The rationality and standardization of in vivo researches directly affect the further transformation from pre-clinical studies to clinical applications. According to SYRCLE 2.0 tool, the methodology quality of included animal studies is moderate. Therefore, when designing experimental protocols, researchers should strictly follow the animal experiment guidelines, such as random allocation, blinding investigators, random outcome assessment, etc., and record this information in the paper.

Many animal studies have shown that curcumin has acceptable security, and no significant toxicity was observed even when rats or mice were given a high dose (5 g/kg BW per day). According to the dose-response model of animal studies, the cardioprotective effect of curcumin may be stronger with the further increase of the dosage. Further, researchers developed a Polylactic-co-glycolic acid (PLGA) and Plga-polyethylene (PEG) (Plga-peg) nanoparticle containing curcumin, and it was observed that the nanoparticles increased the mean half-life of curcumin in about 6 h, enhanced the maximum blood concentration of curcumin by 7.4 times, and improved the bioavailability of curcumin by 55.4 times compared with curcumin aqueous suspension (Khalil et al., 2013). Therefore, we suggest that higher doses of curcumin (more than 200 mg/kg BW per day) and nanoparticle containing curcumin could be explored in future studies to determine the best effective dose.

Conducting more clinical trials should be encouraged because animal experiments have shown excellent effectiveness. In the existing clinical trials, the results showed that curcumin significantly reduced the incidence of MACE in patients after PCI or CABG in the short term. In addition, curcumin is widely consumed as a food material in Southeast Asia, and a large number of studies supported its high biological safety.

In clinical research, researchers should not only focus on the incidence of MACE events caused by MIR in the short term after PCI or CABG, but also focus on the incidence of MACE and cardiac function within 1 year after discharge by increasing follow-up time.

Patients with myocardial injury and reperfusion often need to take antiplatelet drugs. Some studies claimed that curcumin plays an antiplatelet role by inhibiting platelet aggregation (Srivastava et al., 1995; Hirsch et al., 2017), inhibiting cyclooxygenase activity, and blocking calcium channels (Offermanns et al., 1994). However, there is no study explaining the relationship between curcumin and other antiplatelet drugs in vivo experiments.

4.5 Limitations

First of all, we only retrieved English and Chinese studies, which may lead to selection bias. Secondly, positive results are no doubt more likely to be published, so the dominance of positive studies may lead to an overestimation of the efficacy of curcumin, although the funnel plot and Egger's regression test did not show significant publication bias. Thirdly, the overall quality of the animal studies was moderate, ranging from two to six points out of 10, for example, many animal studies ignored the need for randomization. In addition, myocardial infarction usually occurs in patients with cardiovascular risk factors, such as aging, diabetes, hypertension, and hyperlipidemia (Blankstein et al., 2012). However, no animal model with comorbidities was set in the included studies, so their results may be inconsistent with the complexity of the real medical environment.

5 Conclusion

Our study is the first study that includes both preclinical and clinical evidence in terms of curcumin in treatment of MIR, and our results suggest that curcumin might play a cardioprotective role in acute myocardial infarction, mainly through its anti-oxidative, anti-inflammatory, anti-apoptosis, and anti-fibrosis effects. In addition, we found that curcumin might need a longer course of treatment and a larger dosage to exert cardioprotection in the clinical studies, and its efficacy is mainly reflected in reducing the incidence of myocardial infarction and MACE in short term. Finally, our study summarized the main defects of the existing research and suggested how such primary studies need to be improved.

Data availability statement

The original contributions presented in the study are included in the article/Supplementary Material, further inquiries can be directed to the corresponding authors.

Author contributions

TL, JJ, and FP: study conception, design and writing. FP, YB, and YC: extraction, and analysis of data. YL and XW: final approval and overall responsibility for this published work. All authors contributed to the article and approved the submitted version.

Funding

This work was supported by the National Natural Science Foundation of China (Grant Nos. 8177140333, 81973622), key project of Beijing University of Chinese Medicine (Grant Nos. 2020-JYB-ZDGG-113).

Conflict of interest

The authors declare that the research was conducted in the absence of any commercial or financial relationships that could be construed as a potential conflict of interest.

Publisher's note

All claims expressed in this article are solely those of the authors and do not necessarily represent those of their affiliated organizations, or those of the publisher, the editors and the reviewers. Any product that may be evaluated in this article, or claim that may be made by its manufacturer, is not guaranteed or endorsed by the publisher.

Supplementary material

The Supplementary Material for this article can be found online at: https://www.frontiersin.org/articles/10.3389/fphar.2023.1111459/full#supplementary-material

SUPPLEMENTARY FIGURE S1

Non-linear dose-response relationship between Napierian logarithm of RR and the intake of curcumin. The black lines are regression curves of Ln RR for different curcumin doses. The red line represents the optimal effect. Dots represent each of the studies. RR: ratio of means, equal to meansexperimental/meanscontrol.

References

Aggarwal, M. L., Chacko, K. M., and Kuruvilla, B. T. (2016). Systematic and comprehensive investigation of the toxicity of curcuminoid-essential oil complex: A bioavailable turmeric formulation. *Mol. Med. Rep.* 13, 592–604. doi:10.3892/mmr.2015.4579

Ali, M. S., Mudagal, M. P., and Goli, D. (2009). Cardioprotective effect of tetrahydrocurcumin and rutin on lipid peroxides and antioxidants in experimentally induced myocardial infarction in rats. *Pharmazie* 64, 132–136.

Aslanabadi, N., Entezari-Maleki, T., Rezaee, H., Jafarzadeh, H. R., and Vahedpour, R. (2019). Curcumin for the prevention of myocardial injury following elective percutaneous coronary intervention; a pilot randomized clinical trial. *Eur. J. Pharmacol.* 858, 172471. doi:10.1016/j.ejphar.2019.172471

Blankstein, R., Ahmed, W., Bamberg, F., Rogers, I. S., Schlett, C. L., Nasir, K., et al. (2012). Comparison of exercise treadmill testing with cardiac computed tomography angiography among patients presenting to the emergency room with chest pain: The rule out myocardial infarction using computer-assisted tomography (ROMICAT) study. *Circ. Cardiovasc Imaging* 5, 233–242. doi:10.1161/CIRCIMAGING.111.969568

Broskova, Z., Drabikova, K., Sotnikova, R., Fialova, S., and Knezl, V. (2013). Effect of plant polyphenols on ischemia-reperfusion injury of the isolated rat heart and vessels. *Phytother. Res.* 27, 1018–1022. doi:10.1002/ptr.4825

Chen, X. L., Liu, X. R., Fang, Y. X., and Xu, L. (2016). Cardioprotective role of curcumin in myocardial ischemia-reperfusion of male albino rats. *Int. J. Clin. Exp. Med.* 9.

Cheng, H., Liu, W., and Ai, X. (2005). Protective effect of curcumin on myocardial ischemia reperfusion injury in rats. *Zhong Yao Cai* 28, 920–922.

Cumpston, M., Li, T., Page, M. J., Chandler, J., Welch, V. A., Higgins, J. P., et al. (2019). Updated guidance for trusted systematic reviews: A new edition of the Cochrane handbook for systematic reviews of interventions. *Cochrane Database Syst. Rev.* 10, ED000142. doi:10.1002/14651858.ED000142

Damarla, S. R., Komma, R., Bhatnagar, U., Rajesh, N., and Mulla, S. M. A. (2018). An evaluation of the genotoxicity and subchronic oral toxicity of synthetic curcumin. *J. Toxicol.* 2018, 6872753. doi:10.1155/2018/6872753

Deng, Y., Chen, G., Ye, M., He, Y., Li, Z., Wang, X., et al. (2018). Bifunctional supramolecular hydrogel alleviates myocardial ischemia/reperfusion injury by inhibiting autophagy and apoptosis. *J. Biomed. Nanotechnol.* 14, 1458–1470. doi:10.1166/jbn.2018.2582

Duan, W., Yang, Y., Yan, J., Yu, S., Liu, J., Zhou, J., et al. (2012). The effects of curcumin post-treatment against myocardial ischemia and reperfusion by activation of the JAK2/STAT3 signaling pathway. *Basic Res. Cardiol.* 107, 263. doi:10.1007/s00395-012-0263-7

Fiorillo, C., Becatti, M., Pensalfini, A., Cecchi, C., Lanzilao, L., Donzelli, G., et al. (2008). Curcumin protects cardiac cells against ischemia-reperfusion injury: Effects on oxidative stress, NF-kappaB, and JNK pathways. *Free Radic. Biol. Med.* 45, 839–846. doi:10.1016/j.freeradbiomed.2008.06.013

Ghosh, S. S., Salloum, F. N., Abbate, A., Krieg, R., Sica, D. A., Gehr, T. W., et al. (2010). Curcumin prevents cardiac remodeling secondary to chronic renal failure through deactivation of hypertrophic signaling in rats. *Am. J. Physiol. Heart Circ. Physiol.* 299, H975–H984. doi:10.1152/ajpheart.00154.2010

Gonzalez-Salazar, A., Molina-Jijon, E., Correa, F., Zarco-Marquez, G., Calderon-Oliver, M., Tapia, E., et al. (2011). Curcumin protects from cardiac reperfusion damage by attenuation of oxidant stress and mitochondrial dysfunction. *Cardiovasc Toxicol.* 11, 357–364. doi:10.1007/s12012-011-9128-9

Gorabi, A. M., Hajighasemi, S., Kiaie, N., Rosano, G. M. C., Sathyapalan, T., Al-Rasadi, K., et al. (2020). Anti-fibrotic effects of curcumin and some of its analogues in the heart. *Heart Fail Rev.* 25, 731–743. doi:10.1007/s10741-019-09854-6

Grech, E. D., Jackson, M. J., and Ramsdale, D. R. (1995). Reperfusion injury after acute myocardial infarction. *BMJ* 310, 477–478. doi:10.1136/bmj.310.6978.477

Gu, H. P., Wu, M. Y., and Guo, X. H. (2016). Protective effect of curcumin on myocardial ischemia-reperfusion injury in mice and its correlation with Toll-like receptor 4/nuclear factor -κB signaling pathway. *Chin. J. Biol.* 29, 932–935.

Gu, Y., Xia, H., Chen, X., and Li, J. (2021). Curcumin nanoparticles attenuate lipotoxic injury in cardiomyocytes through autophagy and endoplasmic reticulum stress signaling pathways. *Front. Pharmacol.* 12, 571482. doi:10.3389/fphar.2021.571482

Hanai, H., Iida, T., Takeuchi, K., Watanabe, F., Maruyama, Y., Andoh, A., et al. (2006). Curcumin maintenance therapy for ulcerative colitis: Randomized, multicenter, double-blind, placebo-controlled trial. *Clin. Gastroenterology Hepatology Official Clin. Pract. J. Am. Gastroenterological Assoc.* 4, 1502–1506. doi:10.1016/j.cgh.2006.08.008

Hardy, N., Viola, H. M., Johnstone, V. P., Clemons, T. D., Cserne Szappanos, H., Singh, R., et al. (2015). Nanoparticle-mediated dual delivery of an antioxidant and a peptide against the L-Type Ca2+ channel enables simultaneous reduction of cardiac ischemia-reperfusion injury. *ACS Nano* 9, 279–289. doi:10.1021/nn5061404

Hausenloy, D. J., and Yellon, D. M. (2013). Myocardial ischemia-reperfusion injury: A neglected therapeutic target. *J. Clin. Invest.* 123, 92–100. doi:10.1172/JCI62874

Hausenloy, D. J., and Yellon, D. M. (2003). The mitochondrial permeability transition pore: Its fundamental role in mediating cell death during ischaemia and reperfusion. *J. Mol. Cell Cardiol.* 35, 339–341. doi:10.1016/s0022-2828(03)00043-9

Heusch, G., and Gersh, B. J. (2017). The pathophysiology of acute myocardial infarction and strategies of protection beyond reperfusion: A continual challenge. *Eur. Heart J.* 38, 774–784. doi:10.1093/eurheartj/ehw224

Hirsch, G. E., Viecili, P. R. N., de Almeida, A. S., Nascimento, S., Porto, F. G., Otero, J., et al. (2017). Natural products with antiplatelet action. *Curr. Pharm. Des.* 23, 1228–1246. doi:10.2174/1381612823666161123151611

Hooijmans, C. R., Rovers, M. M., de Vries, R. B., Leenaars, M., Ritskes-Hoitinga, M., and Langendam, M. W. (2014). SYRCLE's risk of bias tool for animal studies. *BMC Med. Res. Methodol.* 14, 43. doi:10.1186/1471-2288-14-43

Huang, Z., Ye, B., Dai, Z., Wu, X., Lu, Z., Shan, P., et al. (2015). Curcumin inhibits autophagy and apoptosis in hypoxia/reoxygenation-induced myocytes. *Mol. Med. Rep.* 11, 4678–4684. doi:10.3892/mmr.2015.3322

Jeong, C. W., Yoo, K. Y., Lee, S. H., Jeong, H. J., Lee, C. S., and Kim, S. J. (2012). Curcumin protects against regional myocardial ischemia/reperfusion injury through activation of RISK/GSK-3β and inhibition of p38 MAPK and JNK. *J. Cardiovasc Pharmacol. Ther.* 17, 387–394. doi:10.1177/1074248412438102

Jo, W., Min, B. S., Yang, H. Y., Park, N. H., Kang, K. K., Lee, S., et al. (2020). Sappanone A prevents left ventricular dysfunction in a rat myocardial ischemia reperfusion injury model. *Int. J. Mol. Sci.* 21, 6935. doi:10.3390/ijms21186935

Khalil, N. M., do Nascimento, T. C. F., Casa, D. M., Dalmolin, L. F., de Mattos, A. C., Hoss, I., et al. (2013). Pharmacokinetics of curcumin-loaded PLGA and PLGA-PEG blend nanoparticles after oral administration in rats. *Colloids Surfaces. B, Biointerfaces* 101, 353–360. doi:10.1016/j.colsurfb.2012.06.024

Kim, Y. S., Kwon, J. S., Cho, Y. K., Jeong, M. H., Cho, J. G., Park, J. C., et al. (2012). Curcumin reduces the cardiac ischemia-reperfusion injury: Involvement of the toll-like receptor 2 in cardiomyocytes. *J. Nutr. Biochem.* 23, 1514–1523. doi:10.1016/j.jnutbio.2011.10.004

Kim, Y. S., Park, H. J., Joo, S. Y., Hong, M. H., Kim, K. H., Hong, Y. J., et al. (2008). The protective effect of curcumin on myocardial ischemia-reperfusion injury. *Korean Circ. J.* 38, 353. doi:10.4070/kcj.2008.38.7.353

Klionsky, D. J., Petroni, G., Amaravadi, R. K., Baehrecke, E. H., Ballabio, A., Boya, P., et al. (2021). Autophagy in major human diseases. *EMBO J.* 40, e108863. doi:10.15252/embj.2021108863

Kloner, R. A., Przyklenk, K., and Whittaker, P. (1989). Deleterious effects of oxygen radicals in ischemia/reperfusion. Resolved and unresolved issues. *Circulation* 80, 1115–1127. doi:10.1161/01.cir.80.5.1115

Leong, P. K., Chen, N., and Ko, K. M. (2013). Schisandrin B enhances hepatic/myocardial glutathione regeneration capacity and protects against oxidant injury in rat livers and hearts. *Open Nutraceuticals J.* 6, 124–128. doi:10.2174/1876396001306010124

Lin, K., Chen, H., Chen, X., Qian, J., Huang, S., and Huang, W. (2020). Efficacy of curcumin on aortic atherosclerosis: A systematic review and meta-analysis in mouse studies and insights into possible mechanisms. *Oxidative Med. Cell. Longev.* 2020, 1520747. doi:10.1155/2020/1520747

Lin, Z., Liu, H., Yang, C., Zheng, H., Zhang, Y., Su, W., et al. (2021). Curcumin mediates autophagy and apoptosis in granulosa cells: A study of integrated network pharmacology and molecular docking to elucidate toxicological mechanisms. *Drug Chem. Toxicol.* 45, 2411–2423. doi:10.1080/01480545.2021.1956941

Liu, H., Wang, C., Qiao, Z., and Xu, Y. (2017). Protective effect of curcumin against myocardium injury in ischemia reperfusion rats. *Pharm. Biol.* 55, 1144–1148. doi:10.1080/13880209.2016.1214741

Liu, K., Chen, H., You, Q. S., Ye, Q., Wang, F., Wang, S., et al. (2017). Curcumin attenuates myocardial ischemia-reperfusion injury. *Oncotarget* 8, 112051–112059. doi:10.18632/oncotarget.23002

Ma, B., Guan, G., Lv, Q., and Yang, L. (2021). Curcumin ameliorates palmitic acid-induced saos-2 cell apoptosis via inhibiting oxidative stress and autophagy. *Evid. Based Complement. Altern. Med.* 2021, 5563660. doi:10.1155/2021/5563660

Merz, S. F., Korste, S., Bornemann, L., Michel, L., Stock, P., Squire, A., et al. (2019). Contemporaneous 3D characterization of acute and chronic myocardial I/R injury and response. *Nat. Commun.* 10, 2312. doi:10.1038/s41467-019-10338-2

Mokhtari-Zaer, A., Marefati, N., Atkin, S. L., Butler, A. E., and Sahebkar, A. (2018). The protective role of curcumin in myocardial ischemia-reperfusion injury. *J. Cell Physiol.* 234, 214–222. doi:10.1002/jcp.26848

Mozaffarian, D., Benjamin, E. J., Go, A. S., Arnett, D. K., Blaha, M. J., Cushman, M., et al. (2015). Heart disease and stroke statistics--2015 update: A report from the American heart association. *Circulation* 131, e29–e322. doi:10.1161/CIR.0000000000000152

Na, L.-X., Li, Y., Pan, H.-Z., Zhou, X.-L., Sun, D.-J., Meng, M., et al. (2013). Curcuminoids exert glucose-lowering effect in type 2 diabetes by decreasing serum free fatty acids: A double-blind, placebo-controlled trial. *Mol. Nutr. Food Res.* 57, 1569–1577. doi:10.1002/mnfr.201200131

Oerlemans, M. I., Koudstaal, S., Chamuleau, S. A., de Kleijn, D. P., Doevendans, P. A., and Sluijter, J. P. (2013). Targeting cell death in the reperfused heart: Pharmacological approaches for cardioprotection. *Int. J. Cardiol.* 165, 410–422. doi:10.1016/j.ijcard.2012.03.055

Offermanns, S., Laugwitz, K. L., Spicher, K., and Schultz, G. (1994). G proteins of the G12 family are activated via thromboxane A2 and thrombin receptors in human platelets. *Proc. Natl. Acad. Sci. U. S. A.* 91, 504–508. doi:10.1073/pnas.91.2.504

Orsini, N., Li, R., Wolk, A., Khudyakov, P., and Spiegelman, D. (2012). Meta-analysis for linear and nonlinear dose-response relations: Examples, an evaluation of approximations, and software. *Am. J. Epidemiol.* 175, 66–73. doi:10.1093/aje/kwr265

Peng, J. R., and Qian, Z. Y. (2014). Drug delivery systems for overcoming the bioavailability of curcumin: Not only the nanoparticle matters. *Nanomedicine (Lond)* 9, 747–750. doi:10.2217/nnm.14.21

Perkins, S., Verschoyle, R. D., Hill, K., Parveen, I., Threadgill, M. D., Sharma, R. A., et al. (2002). Chemopreventive efficacy and pharmacokinetics of curcumin in the min/+ mouse, a model of familial adenomatous polyposis. *Cancer Epidemiol. Biomarkers Prev.* 11, 535–540.

Phrommintikul, A., Chanchai, R., and Wongcharoen, W. (2019). Effects of curcuminoids on myocardial injury after percutaneous coronary intervention. *J. Med. Food* 22, 680–684. doi:10.1089/jmf.2018.4321

Rainey, N. E., Moustapha, A., and Petit, P. X. (2020). Curcumin, a multifaceted hormetic agent, mediates an intricate crosstalk between mitochondrial turnover, autophagy, and apoptosis. *Oxid. Med. Cell Longev.* 2020, 3656419. doi:10.1155/2020/3656419

Ribas, N., Garcia-Garcia, C., Merono, O., Recasens, L., Perez-Fernandez, S., Bazan, V., et al. (2017). Secondary prevention strategies after an acute ST-segment elevation myocardial infarction in the AMI code era: Beyond myocardial mechanical reperfusion. *BMC Cardiovasc Disord.* 17, 54. doi:10.1186/s12872-017-0493-6

Saeidinia, A., Keihanian, F., Butler, A. E., Bagheri, R. K., Atkin, S. L., and Sahebkar, A. (2018). Curcumin in heart failure: A choice for complementary therapy? *Pharmacol. Res.* 131, 112–119. doi:10.1016/j.phrs.2018.03.009

Sato, M., Cordis, G. A., Maulik, N., and Das, D. K. (2000). SAPKs regulation of ischemic preconditioning. *Am. J. Physiol. Heart Circ. Physiol.* 279, H901–H907. doi:10.1152/ajpheart.2000.279.3.H901

Srivastava, K. C., Bordia, A., and Verma, S. K. (1995). Curcumin, a major component of food spice turmeric (Curcuma longa) inhibits aggregation and alters eicosanoid metabolism in human blood platelets. *Prostagl. Leukot. Essent. Fat. Acids* 52, 223–227. doi:10.1016/0952-3278(95)90040-3

Sterne, J. A. C., Savović, J., Page, M. J., Elbers, R. G., Blencowe, N. S., Boutron, I., et al. (2019). RoB 2: A revised tool for assessing risk of bias in randomised trials. *BMJ Clin. Res. ed.)* 366, l4898. doi:10.1136/bmj.l4898

Wahlström, B., and Blennow, G. (1978). A study on the fate of curcumin in the rat. *Acta Pharmacol. Toxicol.* 43, 86–92. doi:10.1111/j.1600-0773.1978.tb02240.x

Wang, N. P., Pang, X. F., Zhang, L. H., Tootle, S., Harmouche, S., and Zhao, Z. Q. (2014). Attenuation of inflammatory response and reduction in infarct size by postconditioning are associated with downregulation of early growth response 1 during reperfusion in rat heart. *Shock* 41, 346–354. doi:10.1097/SHK.0000000000000112

Wang, N. P., Wang, Z. F., Tootle, S., Philip, T., and Zhao, Z. Q. (2012). Curcumin promotes cardiac repair and ameliorates cardiac dysfunction following myocardial infarction. *Br. J. Pharmacol.* 167, 1550–1562. doi:10.1111/j.1476-5381.2012.02109.x

Wang, R., Zhang, J. Y., Zhang, M., Zhai, M. G., Di, S. Y., Han, Q. H., et al. (2018). Curcumin attenuates IR-induced myocardial injury by activating SIRT3. *Eur. Rev. Med. Pharmacol. Sci.* 22, 1150–1160. doi:10.26355/eurrev_201802_14404

Wongcharoen, W., Jai-Aue, S., Phrommintikul, A., Nawarawong, W., Woragidpoonpol, S., Tepsuwan, T., et al. (2011). Curcuminoids prevent myocardial infarction after coronary artery bypass grafting. *Eur. heart J.* 32, 77-78. doi:10.1093/eurheartj/ehr322

Wongcharoen, W., Jai-Aue, S., Phrommintikul, A., Nawarawong, W., Woragidpoonpol, S., Tepsuwan, T., et al. (2012). Effects of curcuminoids on frequency of acute myocardial infarction after coronary artery bypass grafting. *Am. J. Cardiol.* 110, 40–44. doi:10.1016/j.amjcard.2012.02.043

Wu, C. H. (2011). Protective effect of curcumin on myocardial ischemia-reperfusion injury in rats. *Chongqing Med.* 40, 25–26.

Yang, Y., Duan, W., Jin, Z., Yi, W., Yan, J., Zhang, S., et al. (2013). JAK2/STAT3 activation by melatonin attenuates the mitochondrial oxidative damage induced by myocardial ischemia/reperfusion injury. *J. Pineal Res.* 55, 275–286. doi:10.1111/jpi.12070

Yang, Y., Duan, W., Lin, Y., Yi, W., Liang, Z., Yan, J., et al. (2013). SIRT1 activation by curcumin pretreatment attenuates mitochondrial oxidative damage induced by myocardial ischemia reperfusion injury. *Free Radic. Biol. Med.* 65, 667–679. doi:10.1016/j.freeradbiomed.2013.07.007

Yao, B. H., and Jiang, W. H. (2014). Curcumin post-treatment has a protective effect on myocardial ischemia/reperfusion injury through heme oxygenase-1. *Chin. J. Arteriosclerosis* 22, 685–689.

Yao, Q. H., Wang, D. Q., Cui, C. C., Yuan, Z. Y., Chen, S. B., Yao, X. W., et al. (2004). Curcumin ameliorates left ventricular function in rabbits with pressure overload: Inhibition of the remodeling of the left ventricular collagen network associated with suppression of myocardial tumor necrosis factor-alpha and matrix metalloproteinase-2 expression. *Biol. Pharm. Bull.* 27, 198–202. doi:10.1248/bpb.27.198

Yeh, C. H., Lin, Y. M., Wu, Y. C., and Lin, P. J. (2005). Inhibition of NF-kappa B activation can attenuate ischemia/reperfusion-induced contractility impairment via decreasing cardiomyocytic proinflammatory gene up-regulation and matrix metalloproteinase expression. *J. Cardiovasc Pharmacol.* 45, 301–309. doi:10.1097/01.fjc.0000155385.41479.b3

Yellon, D. M., and Hausenloy, D. J. (2007). Myocardial reperfusion injury. *N. Engl. J. Med.* 357, 1121–1135. doi:10.1056/NEJMra071667

Zhao, Y. G., Codogno, P., and Zhang, H. (2021). Machinery, regulation and pathophysiological implications of autophagosome maturation. *Nat. Rev. Mol. Cell Biol.* 22, 733–750. doi:10.1038/s41580-021-00392-4

Zhou, X. T., Zou, J. J., Ao, C., Gong, D. Y., Chen, X., and Ma, Y. R. (2020). Renal protective effects of astragaloside IV, in diabetes mellitus kidney damage animal models: A systematic review, meta-analysis. *Pharmacol. Res.* 160, 105192. doi:10.1016/j.phrs.2020.105192

Zingg, J.-M., Hasan, S. T., Nakagawa, K., Canepa, E., Ricciarelli, R., Villacorta, L., et al. (2017). Modulation of cAMP levels by high-fat diet and curcumin and regulatory effects on CD36/FAT scavenger receptor/fatty acids transporter gene expression. *BioFactors Oxf. Engl.* 43, 42–53. doi:10.1002/biof.1307

Glossary

AMI acute myocardial infarction

AST aspartate aminotransferase

BW bodyweight

CABG coronary artery bypass grafting

CAT catalase

CK creatine kinase

CK-MB creatine kinase, MB form

CVD cardiovascular disease

cTnI cardiac troponin I

GR glutathione reductase

GPx glutathione peroxidase

GST glutathione S-transferase

GSH glutathione

hs-CRP high-sensitive cardiac troponin T

hs-TnT high-sensitive cardiac troponin T

I/R Ischemia-reperfusion

IL-6 interleukin-6

LDH lactate dehydrogenase

LVEF Left ventricular ejection fraction

LVFS left ventricular fraction shortening

LVEDd left ventricular end-diastolic diameter

LVESd left ventricular end-systolic diameter

MACE major adverse cardiovascular events

MDA malonaldehyde

MI myocardium infarction

MPO myeloperoxidase

MDA malondialdehyde

NF-κB nuclear factor kappa-B

PO peros

PCI percutaneous coronary intervention

SOD superoxide dismutase

TNF-α tumor necrosis factor alpha.

frontiers | Frontiers in Pharmacology

TYPE Original Research
PUBLISHED 05 April 2023
DOI 10.3389/fphar.2023.1074837

Check for updates

OPEN ACCESS

EDITED BY
Jian Zhang,
Tianjin Medical University, China

REVIEWED BY
Wen Wang,
Xuanwu Hospital, Capital Medical University, China
Leigang Jin,
The University of Hong Kong, Hong Kong SAR, China

*CORRESPONDENCE
Xinlong Chen,
13886801380@163.com
Xinwen Min,
minxinwen@163.com
Jun Chen,
chenjun0121@hbmu.edu.cn

†These authors have contributed equally to this work

SPECIALTY SECTION
This article was submitted to Ethnopharmacology, a section of the journal Frontiers in Pharmacology

RECEIVED 20 October 2022
ACCEPTED 27 March 2023
PUBLISHED 05 April 2023

CITATION
Yu S, Qian H, Tian D, Yang M, Li D, Xu H, Chen J, Yang J, Hao X, Liu Z, Zhong J, Yang H, Chen X, Min X and Chen J (2023), Linggui Zhugan Decoction activates the SIRT1-AMPK-PGC1α signaling pathway to improve mitochondrial and oxidative damage in rats with chronic heart failure caused by myocardial infarction. *Front. Pharmacol.* 14:1074837. doi: 10.3389/fphar.2023.1074837

COPYRIGHT
© 2023 Yu, Qian, Tian, Yang, Li, Xu, Chen, Yang, Hao, Liu, Zhong, Yang, Chen, Min and Chen. This is an open-access article distributed under the terms of the Creative Commons Attribution License (CC BY). The use, distribution or reproduction in other forums is permitted, provided the original author(s) and the copyright owner(s) are credited and that the original publication in this journal is cited, in accordance with accepted academic practice. No use, distribution or reproduction is permitted which does not comply with these terms.

Linggui Zhugan Decoction activates the SIRT1-AMPK-PGC1α signaling pathway to improve mitochondrial and oxidative damage in rats with chronic heart failure caused by myocardial infarction

Siyi Yu[1,2†], Hang Qian[1†], Dawei Tian[1†], Mingming Yang[1], Dongfeng Li[1], Hao Xu[1], Jishun Chen[1], Jingning Yang[3], Xincai Hao[4], Zhixin Liu[5], Jixin Zhong[6], Handong Yang[1], Xinlong Chen[7]*, Xinwen Min[1]* and Jun Chen[1,3,4,5]*

[1] Sinopharm Dongfeng General Hospital (Hubei Clinical Research Center of Hypertension), Hubei University of Medicine, Shiyan, Hubei, China, [2]Jiujiang No. 1 People's Hospital, Affiliated Jiujiang Hospital of Nanchang University, Jiujiang, Jiangxi, China, [3]Department of Immunology, School of Basic Medicine, Hubei University of Medicine, Shiyan, Hubei, China, [4]Hubei Key Laboratory of Wudang Local Chinese Medicine Research (Hubei University of Medicine), Shiyan, Hubei, China, [5]Institute of Virology, Hubei University of Medicine, Shiyan, Hubei, China, [6]Department of Rheumatology and Immunology, Tongji Hospital, Huazhong University of Science and Technology, Wuhan, Hubei, China, [7]Yunxi Hospital of Chinese Medicine, Shiyan, Hubei, China

Objective: To investigate the effects of Linggui Zhugan Decoction on mitochondrial and oxidative damage in rats with chronic heart failure after myocardial infarction and the related mechanisms.

Methods: Chronic heart failure after myocardial infarction was established by coronary artery ligation. Heart failure rats were randomly divided into three groups: Model group (n = 11), Linggui Zhugan Decoction group (n = 12), and captopril group (n = 11). Rats whose coronary arteries were only threaded and not ligated were sham group (n = 11). Cardiac function, superoxide dismutase (SOD), malondialdehyde (MDA) contents, soluble growth-stimulating expression factor (ST2), and N-terminal B-type brain natriuretic peptide precursor (NTproBNP) levels were analyzed after treatment. Moreover, the level of mitochondrial membrane potential was detected by JC-1 staining, the ultrastructural of myocardial mitochondria were observed by transmission electron microscopy. The related signal pathway of silent information regulator factor 2-related enzyme 1 (SIRT1), adenylate activated protein kinase (AMPK), phosphorylated adenylate activated protein kinase (p-AMPK), and peroxisome proliferator-activated receptor γ coactivator 1α (PGC-1α) is an important pathway to regulate mitochondrial energy metabolism, and to initiate mitochondrial biogenesis. The expression level was detected by Western blot and reverse transcription to explore the mechanism of the decoction.

Results: Compared with the model rats, Linggui Zhugan Decoction significantly improved cardiac function ($p < 0.05$), reduced MDA production ($p < 0.01$),

increased SOD activity ($p < 0.05$), reduced ST-2($p < 0.01$), and NT-proBNP($p < 0.05$) levels, increased mitochondrial membrane potential, and improved mitochondria function. In addition, Linggui Zhugan Decoction upregulated the expression of SIRT1, p-AMPK, PGC-1α protein, and mRNA in cardiac myocytes.

Conclusion: Linggui Zhugan Decoction can improve the cardiac function of heart failure rats by enhancing myocardial antioxidant capacity and protecting the mitochondrial function, the mechanism is related to activating SIRT1/AMPK/PGC-1α signaling pathway.

KEYWORDS

mitochondria, heart failure, myocardial infarction, animal experiments, traditional Chinese medicine

1 Introduction

Chronic heart failure (CHF) is a complex clinical syndrome and an end-stage cardiovascular disease. Although great progress has been achieved in understating the pathophysiology of the disease, the global incidence and mortality rates of CHF remain high. The main reason for this is an increase in the aging population. HF still represents a severe public health burden and has a huge impact on healthcare costs (Savarese and Lund, 2017). According to statistics, it has been estimated that the prevalence of heart failure in the United States will increase by 25% by 2030, while the treatment expenditure for heart failure will increase by two times (Tayal et al., 2017). Thus, searching for new drugs is crucial for improving prognosis and improving long-term survival in patients with heart failure.

CHF formation is regulated by a complex pathophysiological process (Braunwald, 2013). The energy metabolism disorder is one of the most important reasons for CHF (Lopaschuk et al., 2021). The existing research results (Bertero and Maack, 2018) have shown that myocardial energy metabolism disorders can induce heart failure, which further aggravates energy metabolism disorders. It has been suggested that mitochondria dysfunction has an important role in the occurrence and development of heart failure. Silent mating type information regulation 2 homolog 1 (SIRT1) is a histone deacetylase dependent on nicotinamide adenine dinucleotide, which can deacetylate many proteins and has a vital role in oxidative stress (Lee et al., 2018). Peroxisomeproliferator-activated receptor? coactivator-1α (PGC-1α) is the deacetylation substrate of SIRT1, and the stimulation of SIRT1 can promote the activation of PGC-1α and, in turn, inhibit oxidative stress damage (Gurd, 2011). Moreover, adenosine activated protein kinase (AMPK), known as "cell energy receptor," is the key molecule of biological energy metabolism regulation; it can improve mitochondrial dysfunction through PGC-1α and enhance AMPK activity, promoting cell survival (Herzig and Shaw, 2018). Thus, it is believed that SIRT1/AMPK/PGC-1α signaling pathway has a major role in the defense against oxidative stress and mitochondrial dysfunction.

Over recent years, research on traditional Chinese medicine has been rapidly increasing. Chinese medicine has the characteristics of multi-site synergy, offering anti-oxidative stress, anti-inflammation properties, improving ventricular remodeling, reducing myocardial fibrosis, and promoting angiogenesis (Xu et al., 2005; Wang et al., 2013; Cao et al., 2015; Zheng et al., 2019; Bu et al., 2020). Linggui Zhugan Decoction, derived from Synopsis of Golden Chamber by Zhang Zhongjing and composed of Fuling [the dry fungus nucleus of *Poria cocos* (Schw.) Wolf], Guizhi [the dry twigs of Neolitsea cassia (L.) Kosterm. (Lauraceae)], Baizhu [the dry rhizome of Atractylodes macrocephala Koidz. (Asteraceae)], and Gancao [the dry root and rhizome of Glycyrrhiza glabra L. (Fabaceae)], is a classical Chinese prescription often used as a complementary treatment to conventional western medicine for heart failure (Fu et al., 2010). The common research on Linggui Zhugan Decoction is limited to reducing myocardial oxygen consumption, such as slowing down heart rate and lowering blood pressure. Whether this decoction can treat heart failure by increasing oxygen supply has not been studied. In this study, we examined the effect and protective mechanism of Linggui Zhugan Decoction on cardiac function in CHF rats through mitochondria, which could provide a new theoretical basis and therapeutic target for the prevention and treatment of heart failure with Linggui Zhugan Decoction.

2 Materials and methods

2.1 Animals

Sixty SPF male SD rats, aged 6 weeks, weighing 210 ± 10 g, were provided by Beijing Weitong Lihua Experimental Animal Technology Co., Ltd (experimental animal certificate No. SCXK (Beijing) 2016-0006). All the animals were housed in a specific-pathogen-free (SPF) environment with a temperature of 25°C ± 2°C, relative humidity of 55%-70%, and a light/dark cycle of 12/12 h. All animal studies (including the rats euthanasia procedure) were done in compliance with the regulations and guidelines of Hubei University of Medicine institutional animal care and conducted according to the AAALAC and the IACUC guidelines (approval number: Dong (Fu) No.2020-Shi 035 of Hubei University of Medicine).

2.2 Medicines

Fuling (batch number: 200901), Guizhi (batch number: 200701), Baizhu (batch number: 201101), and Gancao (batch number: 201101), according to the ratio of 4:3:3:2, purchased from the outpatient pharmacy of Dongfeng General Hospital of Traditional Chinese Medicine, identified by Hubei Qiangkang Herbal Pieces Co., Ltd.; strain identification conforms to the

standard of traditional Chinese medicine. Add 10 times the volume of distilled water to soak the Chinese herbal pieces for 30 min. Then boil 3 times, mix the obtained 3 times filtrate, filter through gauze, rotate and concentrate to prepare a liquid containing 1 g/mL crude drug, which was stored in a refrigerator at 4°C. Captopril (purchased at TargetMol, lot number T1462). In order to ensure the quality and stability of the decoction, the four chemical constituents in the prepared Linggui Zhugan Decoction, including Pachymic acid (from Fuling), Cinnamic acid (from Guizhi), Atractylenolide III (from Baizhu) and Glycyrrhizic acid (from Gancao), were determined by HPLC. In addition, we also preliminarily measured the blood concentrations of these four chemical components in rats after Linggui Zhugan Decoction intervention for 1 h.

2.3 Reagents and instruments

Cinnamic acid (140-10-3), Glycyrrhizic acid (1,405-86-3), Atractylenolide III (73030-71-4), Pachymic acid (29070-92 -6), all purchased from Beijing Zhongke Quality Inspection Biological Co., Ltd. MDA and SOD kits were purchased from Nanjing Jiancheng Bioengineering Institute, with batch number A003-2 and A001-3, respectively; NT-proBNP kit was acquired from Immunoway (product number KE1761), and ST2 kit was purchased from Abcam (product number ab255716). p-AMPK antibody was obtained from Cell Signaling, (Batch No. 2,535); AMPK antibody was bought from Immunoway (Batch No. YT0216); SIRT1 antibody was purchased from Santa Cruz (Batch No. sc-74465); PGC-1α antibody was obtained from Abcam company (product number ab191838); GAPDH antibody was purchased from antGene (product number ANT325); Isoflurane was purchased from RWD Biotechnology Co., Ltd. (Batch No. R510-22); Pentobarbital sodium was purchased from MERCK(Product No. Y0002194).

EClassical 3,100 high performance liquid chromatograph (Elite, China); SupersilODS25um high performance liquid chromatography column (Elite, China); Small animal anesthesia machine (RWD, China); Vevo2100 ultra-high-resolution small animal color Doppler ultrasound real-time imaging system (Visual Sonics, Canada); MQX-200 microplate reader (Bio TEK INC, United States); Transmission electron microscope (Hitachi, Japan); U-0080D ultraviolet spectrophotometer (Hitachi, Japan); UPV INC gel imaging system (Gene company); MF43 microscope (Mingmei Radio and Television Technology, Guangzhou) were also used in this study.

2.4 Model preparation

After 7 days of adaptive feeding, 60 rats were randomly divided into sham operation group (13 rats) and model group (47 rats). Chronic heart failure after myocardial infarction was established by ligation of the left coronary artery. Briefly, rats were fasted for 12 h before the operation and were only allowed to drink water. Then 40 mg/kg pentobarbital sodium intraperitoneal injection anesthesia was applied, and rats were placed in a supine position and given fixed tracheal intubation, mechanical ventilation (respiratory rate 70-90 times/min, respiratory ratio 1:2). After precardiac skin disinfection, the left third to fourth intercostal space thoracotomy was performed to expose the heart. The left coronary artery was ligated with a 5–0 suture needle at 1–1.5 mm below the left atrial appendage and pulmonary cone (the sham operation group was only sutured without ligation), and after the thoracic cavity was closed. Next, the chest wall was hierarchically sutured, and the ventilator was closed. Consequently, rats were placed on the insulation blanket and then returned to the cage after restoring spontaneous breathing and waking up.

Each rat received an intraperitoneal injection of 400,000 U penicillin for three consecutive days to prevent infection. The ischemia and whitening of myocardial tissue at the lower end of the ligation line were immediately observed after ligation, and the ST segment of lead II ECG was significantly elevated as a sign of successful ligation (there was no above performance in the sham operation group after the ligation). After 1 week of routine feeding, the feed was halved, and the rats were forced to swim once a day until the chronic heart failure model was successfully established.

2.5 Grouping and processing

At the fourth week after the operation, if the rats gradually showed decreased activity, loss of appetite, loss of weight, accelerated respiratory heartbeat, cyanosis at the bottom of the paw, and left ventricular ejection fraction (LVEF %) < 45% by ultrasonic cardiogram, the heart failure model was considered to be successfully established (Zhang et al., 2013). During the modeling process, 10 rats died (including 2 rats with sham operation), 5 rats were excluded, and 34 rats with successful heart failure were randomly divided into three groups: Model group (n = 11), Linggui Zhugan Decoction group (n = 12) and captopril group (n = 11). Linggui Zhugan Decoction group and captopril group were treated with Linggui Zhugan Decoction group (5.4 g/(kg d) (crude herbs))and captopril group (6.75 mg/(kg d)), respectively, according to the clinical daily dose of 70 kg body weight, and converted dose based on human and animal body surface area. We also refer to the doses of other related experiments. Chen et al. (2022) designed experiments, using a low dose of 4.29 g/kg and a high dose of 8.58 g/kg of Lingguizhugan decoction to treat heart failure mice prepared by aortic coarctation; Wang et al. used 6.6 g/kg (crude herbs) LGSGT to treat adriamycin-induced heart failure mouse model (Wang et al., 2020). The sham operation group and the model group were given intragastric administration of an equal amount of distilled water. Rats in each group were given intragastric administration at the fifth week after the operation, once a day, for a total of 6 weeks. During the experiment, one rat in the sham operation group, two rats in the model group, two in the Chinese medicine group, and one in the western medicine group died. Captopril is an angiotensin converting enzyme inhibitor (ACEI), which is currently widely used as a guideline-recommended first-line drug for the treatment of heart failure (McDonagh et al., 2021). Previous studies have shown that ACEI can help maintain cardiac energy balance (Schultheiss et al., 1990). Captopril has also been shown to improve myocardial energy metabolism by maintaining mitochondrial function, restoring mitochondrial oxygen consumption and reducing cardiac preload (Sanbe et al., 1995;

Kojic et al., 2011). Therefore, captopril-intervened heart failure rats were set as the positive control in this experiment.

2.6 Detection indicator

2.6.1 HPLC

Using acetonitrile (A)-0.2% phosphoric acid aqueous solution (B) as the mobile phase gradient elution, the elution gradient is as follows: 0–10 min, 30%–50%A; 10–20 min, 50%–70%A; 20–25 min, 70%–82%A; 25–50 min, keep 82%A. The flow rate is 1.0 mL/min, the detection wavelength is 237 nm, the column temperature is 30°C.

2.6.2 General state observation

The body weight of the rats was measured, and the mental state, activity, color of skin, skin gloss, loss of hair, and eating were evaluated.

2.6.3 Echocardiography

Rates were first anesthetized with isoflurane inhalation (induction 4% 2 L/min, maintenance 2% 1.5 L/min), keeping the heart rate of rats at 300–400 times per minute, then fixed on table. M-mode echocardiography was then obtained by placing the M-type sampling line perpendicular to the ventricular septum and left posterior ventricular wall at the level of rat papillary muscle (at the maximum left ventricular diameter). The left ventricular ejection fraction (LVEF%), the left ventricular fraction shortening (LVFS%), the left ventricular end-diastolic diameter (LVIDd), and the left ventricular internal dimension systole (LVIDs) were continuously measured for five cardiac cycles, after which the average values were calculated. The relevant calculation formula is as follows:

$$LV\ vol\,(d,s) = \left(\frac{7.0}{2.4 + LVID;\,(d,s)}\right) \times LVID;\,(d,s)^3$$

$$LVEF\% = 100 \times \left(\frac{LV\ vol;d - LV\ vod,s}{LV\ vol,d}\right)$$

$$LVFS\% = 100 \times \left(\frac{LVID;d - LVID,s}{LVID,d}\right)$$

2.6.4 Exhaustive swimming time

Before anesthesia, 10% of the lead weight of the rat was tied to the tail of the rat. Then, the rats were placed in a water tank with a water depth of 50 cm and a water temperature of 30°C for an exhaustive swimming experiment. The standard of exhaustive swimming was that the head of the rats did not float to the water surface for 20 s after submerging, and the exhaustive time of the rats was recorded.

2.6.5 Serum levels of NT-proBNP, ST-2, SOD, and MDA detection

After the rats were sacrificed by intravenous injection of 150 mg/kg pentobarbital sodium, take 5 mL of rat abdominal aorta blood and centrifugate at 4°C 3000 r/min for 15 min, and the serum was stored at-80°C. The contents of MDA, SOD, NT-proBNP, and ST-2 in serum were detected according to the kit instructions. NT-proBNP and ST-2 were detected by ELISA, SOD by WST-1, MDA by thiobarbituric acid (TBA).

2.6.6 Holistic quality index (HW/BW)

The heart was quickly removed. Hearts were then placed in 10% KCL, washed with PBS, after which the aorta was cleared, and the heart weight (HW) and the mass heart index were calculated by heart weight (HW)/body weight (BW).

2.6.7 Mitochondria JC-1 staining

After the heart was collected, 1 mm^3 of the apical myocardium was cut. Then, the mitochondria were extracted according to the instructions of the mitochondrial kit, and the mito solution was used to resuspend the mitochondrial precipitation (Yang et al., 2018; Wei et al., 2020). The operation was performed following the mitochondrial membrane potential test kit (JC-1). When the mitochondrial membrane potential is high, JC-1 can be seen in the mitochondrial matrix and form a polymer to produce red fluorescence; if the mitochondrial membrane potential is low, this is not observed. JC-1 was a monomer at this time to produce green fluorescence. The relative proportion of red and green fluorescence was used to measure the proportion of mitochondrial depolarization.

2.6.8 Pathological section making and staining

After abdominal aorta blood collection, the chest was opened, the pericardial was cut, and the appendages were removed. The heart was repeatedly washed with ice saline solution until the solution became clear and bright, and the water was sucked into 4% neutral formaldehyde solution by filter paper. After ethanol dehydration and paraffin embedding, hearts were placed in a continuous slice machine. After dewaxing and treating with xylene, HE staining and Masson staining was performed. Finally, a light microscope was used for observation. Myocardial tissue collagen volume fraction (CVF = collagen area/total area) was performed on Masson-stained images using Image J image analysis software.

2.6.9 Electron microscope

The heart tissue of rats was cut into about 1–2 mm^3 pellets and fixed with 2.5% glutaraldehyde for more than 2 h. After dehydration and embedding, the samples were placed overnight in a 37°C oven, then placed in a 45°C oven for 12 h, and finally placed in a 60°C oven for 48 h. The tissue slicer was used to cut the 60 nm ultra-thin section, and the samples were stained with acetate-lead citrate. The samples were photographed by transmission electron microscope.

2.6.10 Western blot

The myocardial tissue proteins of rats were taken and lysed with protein lysate. The total proteins were extracted. Then, electrophoresis, membrane transfer, and blocking were successively performed. Samples were then incubated with primary antibody at 4°C overnight and secondary antibody for 1 h to detect the protein expression levels of Sirt1, AMPK, p-AMPK, PGC-1α, NRF1, and TFAM, in the myocardium. After ECL coloration, the images were analyzed by ImageJ software.

2.6.11 Reverse transcription-polymerase chain reaction (RT-PCR)

The collected myocardial tissue was ground with Trizol solution. The total RNA of myocardial tissue was isolated and extracted in accordance with the operating instructions of the Trizol reagent. After

TABLE 1 Primer sequences used for the RT-PCR.

Gene symbol	Primer sequence (5′–3′)
PGC-1α	Forward:CGGTGGATGAAGACGGATTGCC
	Reverse:ATTGTAGCTGAGCTGAGTGTTGGC
Sirt1	Forward:GCTCGCCTTGCTGTGGACTTC
	Reverse:GTGACACAGAGATGGCTGGAACTG
NRF1	Forward:AGATGCTAATGGCCCAGATG
	Reverse:AGCTCTGCCTGGTTGTTTGT
TFAM	Forward:GCTCGCCTTGCTGTGGACTTC
	Reverse:GTGACACAGAGATGGCTGGAACTG
β-actin	Forward:TGTCACCAACTGGGACGATA
	Reverse:GGGGTGTTGAAGGTCTCAAA

synthesizing the first-strand cDNA, the levels of Sirt1, PGC-1α, NRF1, and TFAM were detected by RT-PCR. The primer sequence was synthesized by the Shanghai Shenggong Biological Company. The specific sequence is as follows (Table 1). The reaction conditions were: Pre-denaturation: 94°C 5 min; pCR reaction: 94°C 30 s, 58°C 30 s, 72°C 30 s; annealing at 72°C for 3 min and 40 cycles. Then, the amplification curve and the melting curve were confirmed, and the expression levels of each gene were evaluated by $2^{-\triangle\triangle CT}$ method.

2.7 Statistical analysis

SPSS 22.0 software was used to analyze the data. The measurement data were expressed as mean ± standard deviation. One-way ANOVA was used to compare the normal distribution data between groups, and the LSD method was used to compare the data between groups. Non-normal distribution data were used to compare the differences between groups by a non-parametric test. A $p < 0.05$ indicated that the difference was statistically significant.

3 Results

3.1 Contents of four active ingredients in Linggui Zhugan Decoction

According to the peak area, it was calculated that the Linggui Zhugan Decoction contains 18.68 ug/mL pachymic acid, 153.49 ug/mL cinnamic acid, 67.47 ug/mL atractylenolide III and 621.34 ug/mL glycyrrhizic acid. It can be seen that glycyrrhizic acid is the most abundant component in Linggui Zhugan Decoction. The four components in the rat serum were measured 1 h after administration, the serum contained 12.55 ug/mL cinnamic acid, 2.90 ug/mL atractylenolide III, and 27.07 ug/mL glycyrrhizic acid. Pachymic acid may be difficult to detect due to insufficient HPLC sensitivity or low concentrations (Figure 1).

3.2 Linggui Zhugan Decoction inhibits myocardial remodeling and improves cardiac function in rats with heart failure caused by myocardial infarction

As shown in Figure 2A, HE staining showed that the myocardial cells in the sham operation group with intact myocardial fibers and no degeneration or necrosis were structurally regular and neatly arranged. The cardiomyocytes in the model group had different morphological sizes and loose cell arrangements. Some myocardial fibers showed disorganization, and necrosis with infiltration of inflammatory cells was seen in myocardial fibers and interstitium. The degree of myocardial structural damage in the Linggui Zhugan Decoction group and captopril group was significantly improved compared to the model group, and the myocardial fibers were neatly arranged. Masson staining showed that the sham operation group had almost no or only a small amount of collagen fibrous tissue and was evenly distributed. In the model group, a large number of flaky fibrous tissues, severe myocardial fibrosis. Compared with the model group, the collagen fibers in the infarct area and the infarct edge area in the Lingguizhugan decoction group and the captopril group were significantly reduced, and the myocardial cells were arranged more closely. As shown in Figure 2B, quantitative comparison using collagen volume fraction showed that the CVF of the model group was significantly increased compared with that of the sham-operated group ($p < 0.001$). Compared with the model group, the degree of myocardial fibrosis in the captopril group and Linggui Zhugan decoction group was significantly reduced ($p < 0.01$).

As shown in Figure 2D, the HW/BW ratio of whole heart weight index in the model group was significantly higher than that in the sham operation group, and the difference was statistically significant ($p < 0.05$). Compared with the model group, the HW/BW ratio of Linggui Zhugan Decoction group and captopril group decreased ($p < 0.05$), and there was no difference between the two groups ($p > 0.05$). This data indicated that Linggui Zhugan Decoction might affect the heart structure, which was also consistent with the result of Wang L. et al. (2020). This data was further verified by echocardiography performed in rats. As shown in Figures 3A–D, after 6 weeks of drug administration, the LVEF% and LVFS% in the model group were significantly lower than those in the sham operation group, and the LVIDd and LVIDs were significantly increased ($p < 0.01$ or $p < 0.001$). Compared with the model group, the LVEF% and LVFS% in the Linggui Zhugan Decoction group and the captopril group were obviously increased, while the LVIDd and LVIDs were apparently decreased (both $p < 0.05$). In the model group, the ventricular systolic and diastolic functions were damaged, and the cardiac function significantly decreased. After treatment with Linggui Zhugan Decoction or captopril, the volume of the ventricular cavity increased, the ventricular remodeling was delayed, and the cardiac function was improved. Moreover, the results of the two-drug regimens showed that LVIDs in the Linggui Zhugan Decoction group were significantly decreased ($p < 0.05$), and there was no significant difference in other ultrasonic indexes. These results indicated that the Linggui Zhugan Decoction group was better than captopril in improving the systolic function of rats, but there was no obvious difference in the effects of the two treatments on cardiac function.

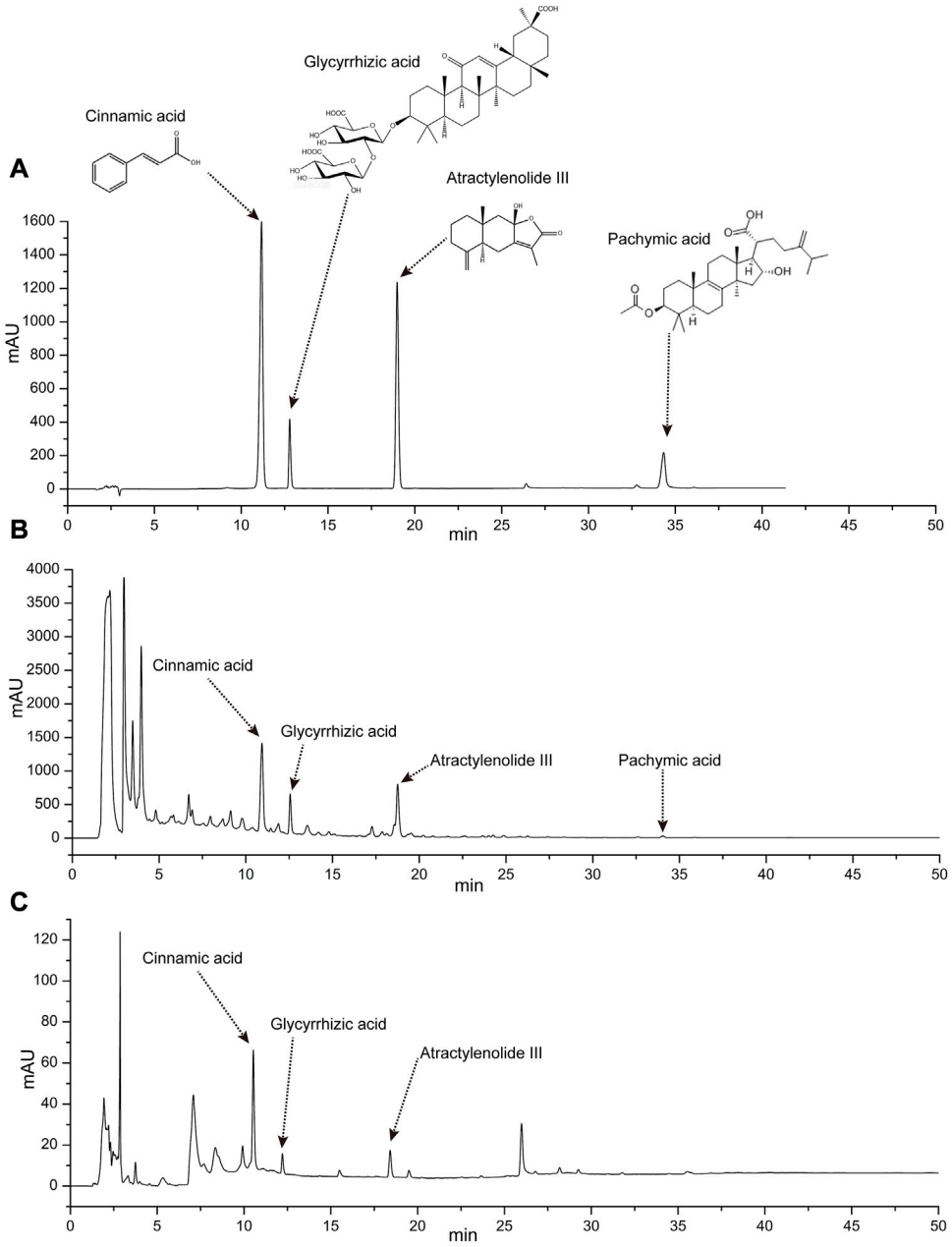

FIGURE 1
Determination of four chemical constituents of cinnamic acid, glycyrrhizic acid, atractylenolide III, and pachymic acid by HPLC. **(A)** High performance liquid chromatogram of the four chemical composition standards. **(B)** High performance liquid chromatogram of Linggui Zhugan Decoction. **(C)** High performance liquid chromatogram of rat serum after 1 h gavage of Linggui Zhugan decoction.

3.3 Linggui Zhugan Decoction improves the general state and exercises tolerance of rats with chronic heart failure after myocardial infarction

The sham operation group showed a good mental state, fair activity, smooth and bright hair color, and less struggle. The hair color of rats in the model was dark, while in some, fur was erect and messy. In the early morning, rats engaged in fierce fights accompanied by bites. With the extension of administration time, the fighting gradually eased, the rats became more docile and less irritable, and the overall difference among the groups was no longer obvious.

Cardiac failure can lead to decreased exercise tolerance, which is also a crucial indicator to evaluate the prognosis of heart failure (Passantino et al., 2006). In this study, we used the exhaustive swimming method to examine exercise tolerance. We found that compared with the sham operation group, the exhaustive swimming time of rats in the model group was shortened ($p < 0.05$). Contrary, in the Linggui Zhugan Decoction group and the captopril group, exhaustive swimming time was significantly higher than that in the model group ($p < 0.05$), while

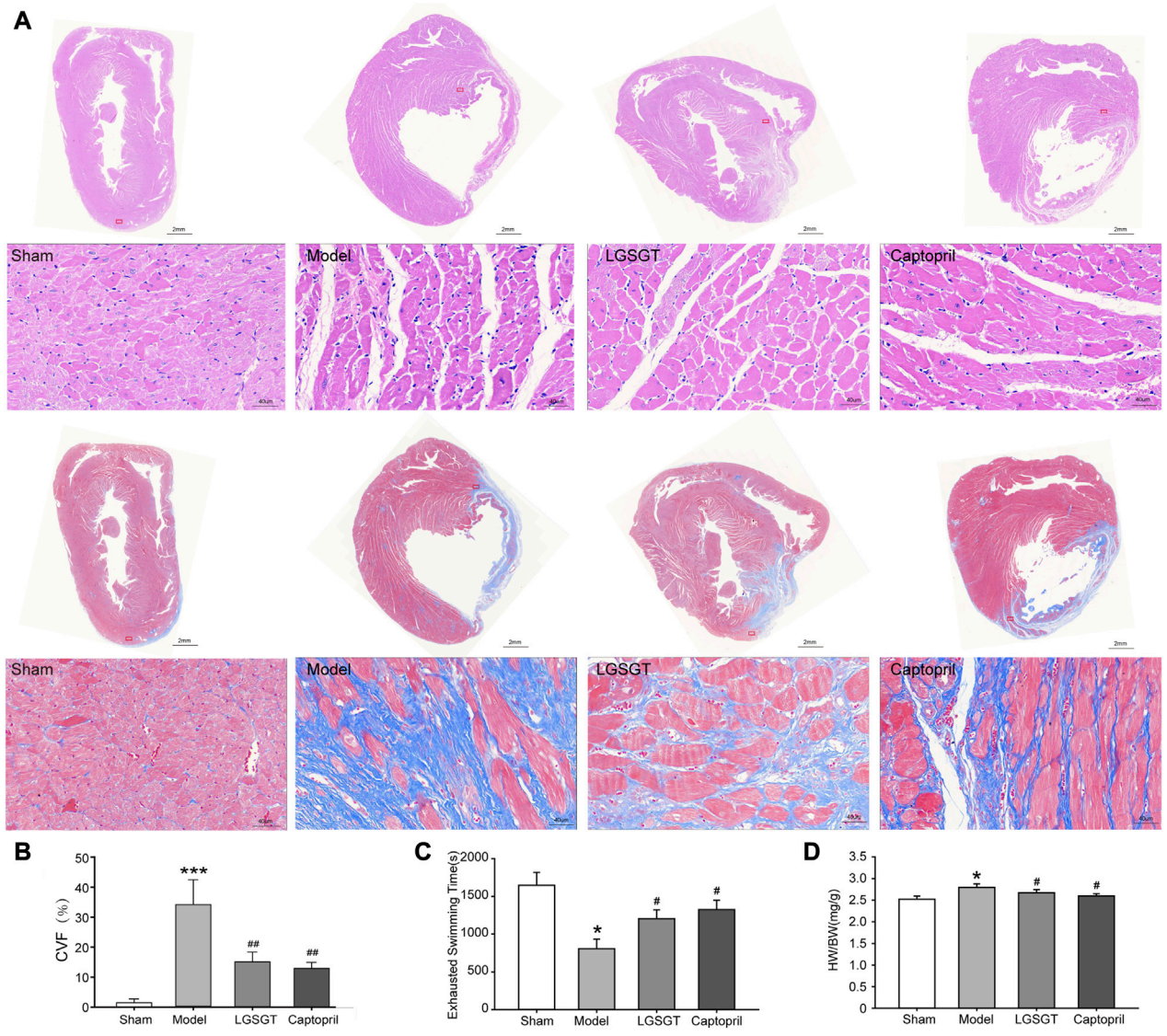

FIGURE 2
Linggui Zhugan Decoction protects the myocardium from myocardial injury and increases exercise tolerance in rats with chronic heart failure after myocardial infarction. **(A)** HE staining and Masson staining of myocardial tissue in each group. **(B)** The collagen volume fraction in each group (n = 6). **(C)** Exhaustive swimming method to evaluate exercise tolerance in rats with heart failure (n = 8). **(D)** The heart weight index in each group (heart weight/body weight). Asterisks indicate significant difference as compared with the sham group (n = 8). *p < 0.05 vs. sham group; $^{\#}p$ < 0.05 vs. model group.

there was no difference between the Linggui Zhugan Decoction group and the captopril group (Figure 2C), which indicates that both Linggui Zhugan Decoction and captopril can increase the exercise tolerance of rats with heart failure.

3.4 Linggui Zhugan Decoction reduces the level of heart failure markers in rats with heart failure caused by myocardial infarction

NT-proBNP and sST2 are independent risk factors for heart failure, which have predictive value for the prognosis of heart failure (Pan et al., 2020). In addition, both NT-proBNP and sST2 effect resisting ventricular remodeling (McCarthy and Januzzi, 2018; Daubert et al., 2019). As shown in Figure 4A, we found the serum NT-proBNP level of the model group was significantly increased compared with the sham operation group (p < 0.05). Moreover, a significant decrease of the serum NT-proBNP levels was found in the Linggui Zhugan Decoction group and captopril group compared to the model group (p < 0.05); there was no significant difference between the Linggui Zhugan Decoction group and captopril group (p > 0.05).

As shown in Figure 4B, Similar data were observed for serum ST-2. The ST-2 content in the model group was significantly higher than that in the sham operation group (p < 0.001), while the quantification analysis of Serum ST-2 contents within the Linggui

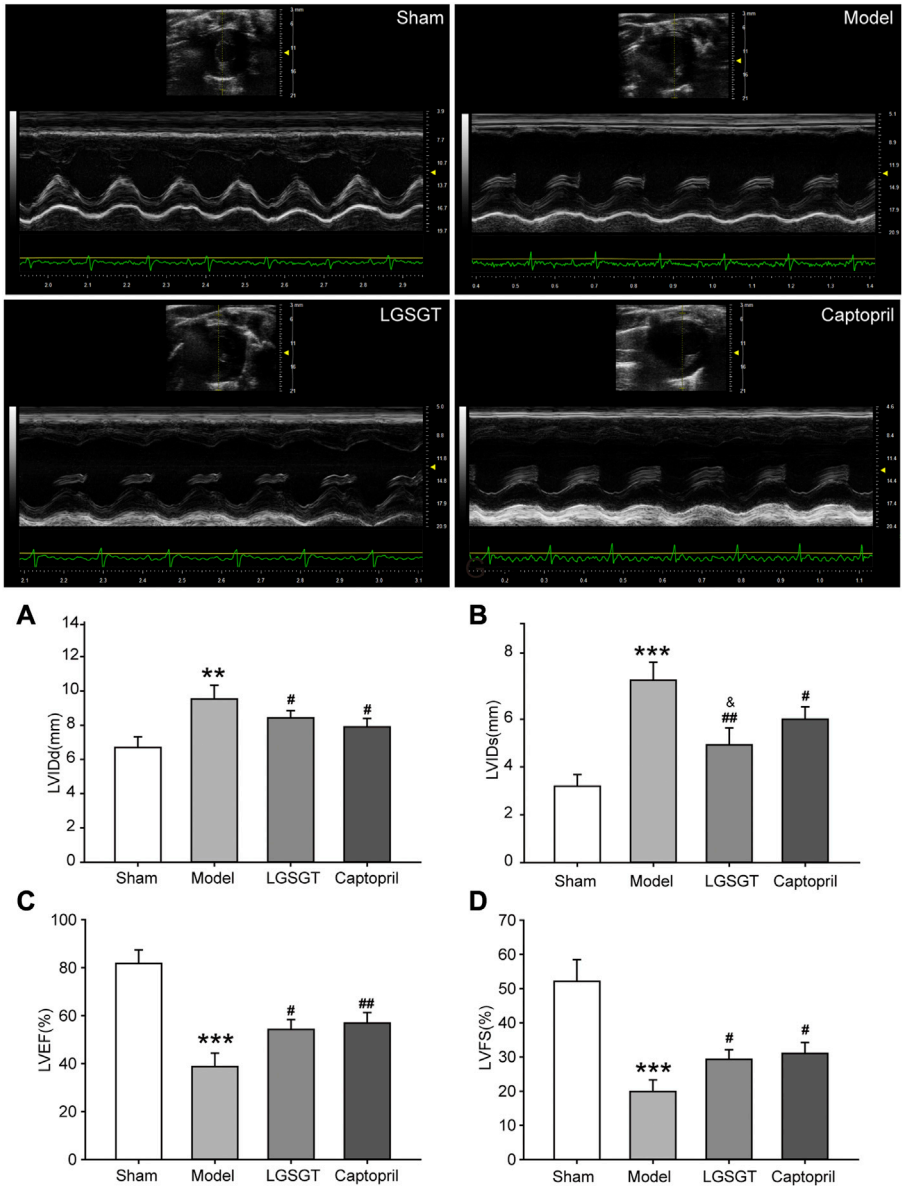

FIGURE 3
Linggui Zhugan Decoction improves cardiac function in rats with chronic heart failure after myocardial infarction. Ventricular structure and ejection fraction in rats with heart failure measured by echocardiography ($n = 9$) **(A–D)**. $^{*}p < 0.05$ vs. sham group; $^{**}p < 0.01$ vs. sham group; $^{***}p < 0.001$ vs. sham group; $^{\#}p < 0.05$ vs. model group; $^{\#\#}p < 0.01$ vs. model group; $^{\#\#\#}p < 0.001$ vs. model group.

Zhugan Decoction group and captopril group demonstrated a significant decrease compared to the model group ($p < 0.01$); there was no significant difference between Linggui Zhugan Decoction group and captopril group ($p > 0.05$). To sum up, our data showed that Linggui Zhugan Decoction could delay myocardial remodeling and improve cardiac function.

3.5 Linggui Zhugan decoction reduces mitochondrial injury

As shown in Figure 5, TEM was used to assess the structure of mitochondria. In the sham operation group, the cell membrane of myocardial cells was intact; besides, the myocardial fibers with intact sarcomere were neatly arranged, the transverse stripes were clear, and there were many mitochondria between the muscle fibers. Ultrastructural analysis with mitochondria showed that the control group had healthy mitochondria with normal and clear cristae structures. Meanwhile, the internal ridges were clear and closely arranged, and no swelling or vacuoles were found. In contrast, the myocardial structure of model group rats was destroyed, the arrangement of myocardial fibers was loose, disordered, irregular, and even possibly broken. Moreover, the sarcomere was incomplete, transverse striations were not clear, mitochondrial internal cristae were disorderly arranged, the membrane structure was damaged, mitochondria were denatured

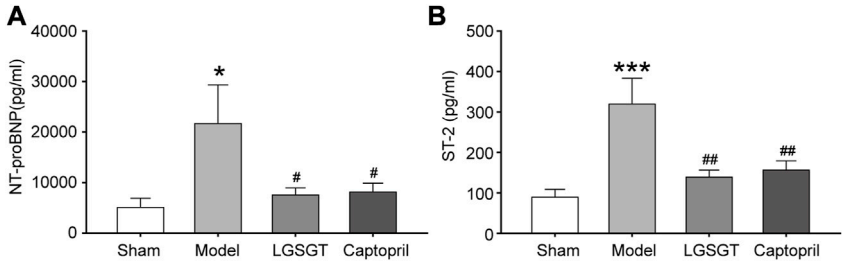

FIGURE 4
Linggui Zhugan Decoction reduces the level of myocardial markers (NT-proBNP and sST2) in rats with chronic heart failure after myocardial infarction. The levels of biomarker NT-proBNP and sST2 in rats with heart failure detected by ELISA ($n = 7$) **(A, B)**. *$p < 0.05$ vs. sham group; **$p < 0.01$ vs. sham group; ***$p < 0.001$ vs. sham group; $^{\#}p < 0.05$ vs. model group; $^{\#\#}p < 0.01$ vs. model group; $^{\#\#\#}p < 0.001$ vs. model group.

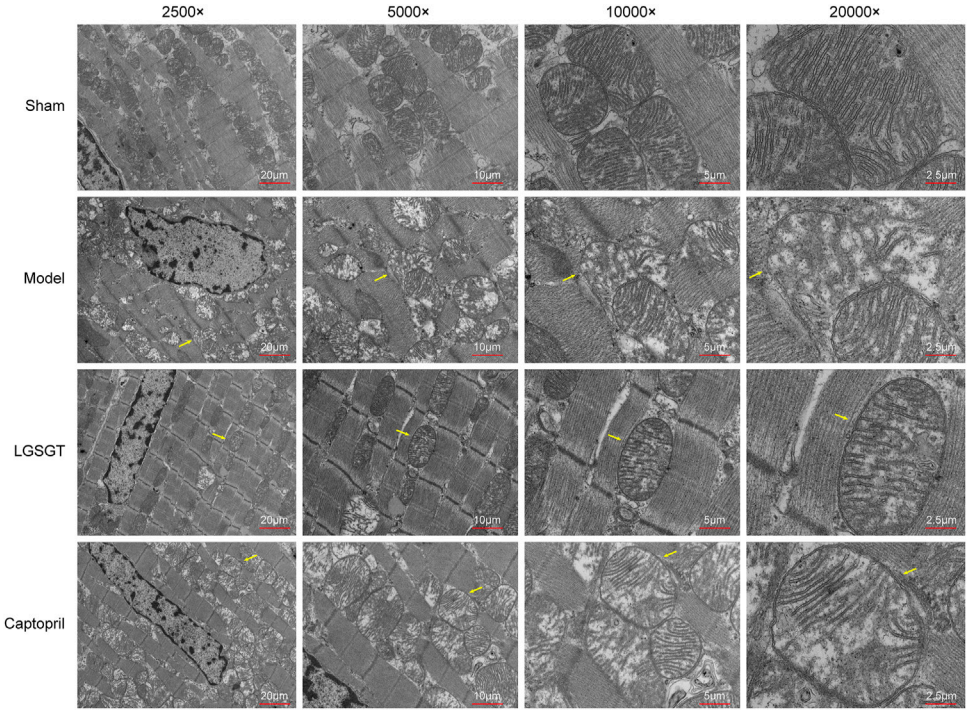

FIGURE 5
Linggui Zhugan Decoction protects the mitochondria of myocardial cells in rats with heart failure. Observe the differences in the ultrastructure of myocardial cells and mitochondria under the electron microscope.

and swollen, and the outer membrane was incomplete, with vague fusion. Compared to the model group, Linggui Zhugan Decoction or captopril markedly increased integrity in the pathological state of mitochondria (mitochondria of the myocardium were neatly arranged). Transverse stripes of the myocardium with regular sarcomere were slightly blurred, the degree of mitochondrial crista expansion and crista disorder was reduced, and the degree of membrane clarity was increased. This data suggests that Linggui Zhugan Decoction can improve the damage of mitochondrial structure to a certain extent.

Mitochondrial membrane potential is an electrochemical gradient necessary to maintain the structure and function of mitochondria, which can reflect the functional state of mitochondria and is also an indicator of early myocardial cell apoptosis (Daubert et al., 2019). As shown in Figures 6A, B, we performed mitochondrial staining with JC-1 and found a significant decrease in the membrane potential of myocardial mitochondria in the model group compared to the sham operation group ($p < 0.001$). However, after the intervention of Linggui Zhugan Decoction or captopril intragastrically, the mitochondrial membrane potential in the myocardial tissue of rats in the Linggui Zhugan Decoction group was significantly increased ($p < 0.01$), while that in the captopril group was slightly increased, but the difference was not statistically significant ($p > 0.05$). Therefore, this indicates that Linggui Zhugan Decoction can stabilize myocardial mitochondrial membrane potential in failure.

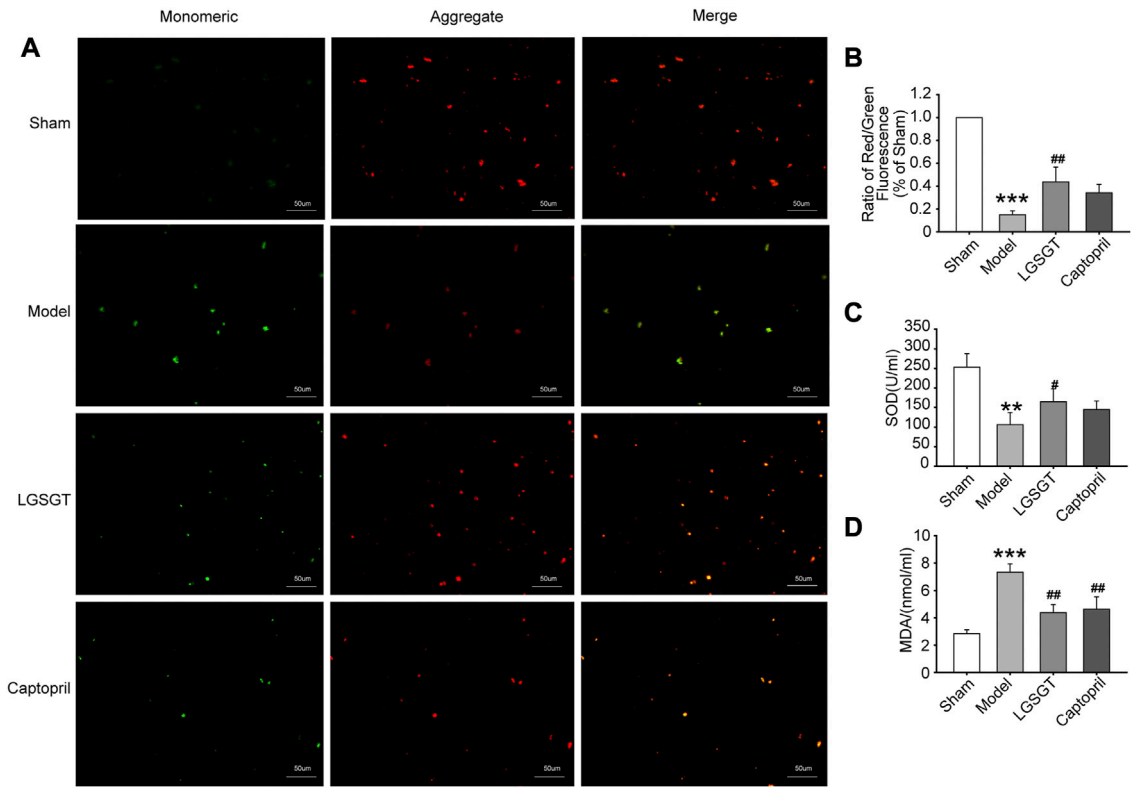

FIGURE 6
Linggui Zhugan Decoction antagonizes the oxidative stress in rats with heart failure and reduces the mitochondrial damage in myocardial cells. **(A, B)** JC-1 staining was used to observe the effect of Linggui Zhugan Decoction on mitochondrial membrane potential levels (n = 5). **(C, D)** ELISA was used to test the effect of Linggui Zhugan Decoction on serum oxidative stress indicators in rats with heart failure (n = 7). *p < 0.05 vs. sham group; **p < 0.01 vs. sham group; ***p < 0.001 vs. sham group; $^{\#}p$ < 0.05 vs. model group; $^{\#\#}p$ < 0.01 vs. model group; $^{\#\#\#}p$ < 0.001 vs. model group.

3.6 Linggui Zhugan Decoction alleviates oxidative stress injury in rats with heart failure caused by myocardial infarction

Oxidative stress-induced cardiomyocyte apoptosis is a major cause of heart failure (Zhou et al., 2018), and high levels of oxidative stress markers may reflect the severity of heart failure (Ayoub et al., 2017). As shown in Figures 6C, D, the serum SOD activity was significantly reduced in the model group compared to the sham group (p < 0.01). Contrary, SOD activity increased in the Linggui Zhugan Decoction compared to the model group (p < 0.05), while there was no difference between the captopril group and model group (p > 0.05). Quantification analysis also revealed a distinct increase of the serum MDA content of rats in the model group compared to the sham operation group (p < 0.001), while the MDA content in the Linggui Zhugan Decoction group and captopril group was significantly lower than that in the model group (p < 0.01). This data suggests that the Linggui Zhugan Decoction group could resist myocardial oxidative damage in rats.

3.7 Linggui Zhugan Decoction exerts the protective effect of mitochondria in rats with heart failure by activating the SIRT1-AMPK-PGC1α pathway

As shown in Figures 7A, B, SIRT1 and PGC-1α mRNA levels in the model group were observably lower than those in the sham operation group, and the differences were statistically significant (p < 0.01). Further, compared with the model group, the levels of SIRT1 and PGC-1α mRNA in the Linggui Zhugan Decoction group were increased (p < 0.05 or p < 0.01). Although the level of the captopril group was higher than that of the model group, the difference was not statistically significant (p > 0.05).

In addition, as shown in Figures 7C, D, compared with the model group, the mRNA levels of NRF1 and TFAM in the Linggui Zhugan Decoction group significantly increased (p < 0.05). NRF1 and TFAM were the important signaling molecules affecting mitochondrial biogenesis downstream of PGC-1α, indicating that Linggui Zhugan Decoction could increase mitochondrial biogenesis.

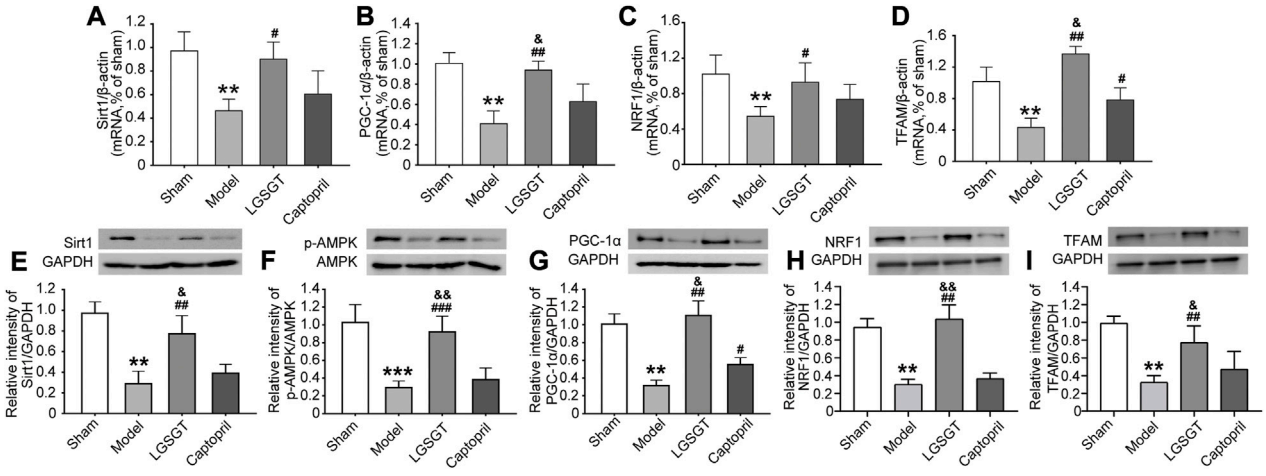

FIGURE 7
Linggui Zhugan Decoction played a protective role through the SIRT1-AMPK-PGC-1α pathway. **(A–D)** RT-PCR was used to detect the expression levels of the SIRT1-AMPK-PGC-1α pathway and downstream NRF1 and TFAMmRNA in the myocardial tissue of rats with heart failure after treatment with Linggui Zhugan Decoction (n = 6). **(E–I)** Western blot was used to detect the expressions of SIRT1, p-AMPK, PGC-1α, NRF1, and TFAM proteins in the myocardial tissue of rats with heart failure after treatment with Linggui Zhugan Decoction (n = 3). *p < 0.05 vs. sham group; **p < 0.01 vs. sham group; ***p < 0.001 vs. sham group; $^{\#}p$ < 0.05 vs. model group; $^{\#\#}p$ < 0.01 vs. model group; $^{\#\#\#}p$ < 0.001 vs. model group; $^{\&}p$ < 0.05 vs. captopril group; $^{\&\&}p$ < 0.01 vs. captopril group.

As shown in Figures 7E–I, compared with the sham operation group, the expression of SIRT1, p-AMPK, PGC-1α, NRF1 and TFAM protein in the model group was relatively decreased (p < 0.01). After the intervention of Linggui Zhugan Decoction, the relative expression of SIRT1, p-AMPK, PGC-1α, NRF1 and TFAM protein was significantly higher compared with the model group (p < 0.01), while the relative expression of the p-AMPK protein was higher; yet, the relative expression of AMPK protein did not change, and the difference of p-AMPK/AMPK protein was statistically significant (p < 0.05). The SIRT1, p-AMPK/AMPK, NRF1 and TFAM protein levels in captopril-treated rats were similar to those in the model group, but the level of PGC-1α protein was increased (p < 0.05).

All of these results indicate that Linggui Zhugan Decoction promotes the activation of AMPK signals in the myocardial tissue of rats with heart failure.

4 Discussion

Ischemic cardiomyopathy is one of the common causes of chronic heart failure. Oxidative stress injury associated with decreased ATP production, active oxygen accumulation, and mitochondrial dysfunction has an important role in the occurrence and development of ischemic cardiomyopathy (Akhmedov et al., 2015). The heart is a high-function, high-energy consumption, low-energy storage organ. Failing heart is also sometimes described as an “engine out of fuel” (Neubauer, 2007).

Mitochondria are key organelles in the cell that produce energy. The normal energy metabolism of the myocardium is the material basis for maintaining the stability of the cardiac environment and cardiac systolic and diastolic function of the heart, while the metabolism crisis generated by mitochondria has been associated with myocardial ischemia (Di Lisa et al., 1998). During this condition, metabolites such as reactive oxygen and Ca^{2+} are accumulated in cardiomyocytes in large amounts, resulting in changes in intracellular mitochondrial structure, enhanced activity and function decline of respiratory chain enzymes, decreased energy metabolism and increased oxidative stress, changes in ion concentration gradient inside and outside the mitochondrial membrane, destruction of mitochondrial inner membrane permeability, and unbalance of the mitochondrial energy metabolism process. The opening of mitochondrial membrane conversion pores promotes apoptosis and myocardial remodeling, all of which cause damage to the blood pumping function of the heart, aggravate the load for the maintenance of normal physiological function of the heart, and finally lead to heart failure (Brown et al., 2017). A large number of studies have confirmed that mitochondrial dysfunction and myocardial cell damage caused by oxidative stress are closely related to heart failure (Hsu et al., 2016; Ayoub et al., 2017). In this research, we constructed the rat model of chronic heart failure after myocardial infarction by coronary artery ligation and found that compared with the sham operation group, the rats with heart failure had the poor general condition and lower exercise tolerance, as well as increased levels of heart failure markers ST-2 and NT-proBNP, increased ventricular volume, and decreased ejection fraction. In addition, the serum ROS level and MDA content of rats in the model group also increased, and the cardiomyocytes were in a state of oxidative damage. The pathology and electron microscopy showed that rats with heart failure cardiomyocytes had different morphologies and a disordered arrangement with damaged structure. All this data suggested that rats with heart failure caused by ischemic cardiomyopathy might suffer from oxidative stress, which would induce mitochondrial damage and dysfunction, thus damaging the

cardiomyocytes, and, in turn, leading to ventricular remodeling and reducing cardiac function.

Previous studies on the molecular mechanism of Linggui Zhugan Decoction in treating heart failure mainly focused on delaying myocardial remodeling, participating in heart rate regulation, controlling blood pressure, regulating vascular activity, improving glucose metabolism and lipid metabolism (Zhou and Huang, 2020). Over recent years, more and more attention has been paid to the research on the effect of Chinese herbal medicine on improving mitochondrial function. For example, it has been found that Pachymic acid can affect ferroptosis induced by renal ischemia-reperfusion injury in mice, improve mitochondrial outer membrane rupture and internal cristae damage, stabilize mitochondrial ultrastructure, and resist acute kidney injury, which may be related to the activation of NRF2 and the upregulation of the expression of downstream ferroptosis-related proteins GPX4, SLC7A11 and HO-1 (Jiang et al., 2021). Wang et al. (2019) reported that Atractylodes Lactone III acts as an antioxidant by activating the oxidative stress-mediated PI3K/AKT/mTOR pathway, attenuating mitochondrial damage, reducing the accumulation of autophagosomes (AP) and autolysosomes (ALs) in muscle, to resist muscle atrophy. Atractylodes macrocephala Koidz may treat chronic gastritis by improving energy metabolism and regulating inflammatory response (Yang et al., 2019). Gualouguizhi granules can inhibit oxidative damage induced by ischemia-reperfusion in rat brain tissue by activating Nrf2/ARE signaling pathway (Zhang et al., 2018). Glycyrrhizin can protect liver mitochondria from oxidative damage in metabolic syndrome model rats by attenuating mitochondrial oxidative stress and aconitase degradation, improving the activities of electron transport chain-related enzymes (Sil and Chakraborti, 2016). Therefore, we hypothesized that Linggui Zhugan Decoction could treat heart failure by improving mitochondrial function.

In this study, we found that Linggui Zhugan Decoction can improve myocardial cell necrosis of rats with heart failure, improve myocardial fibrosis and alleviate hypertrophy of myocardial cells. At the same time, the levels of heart failure markers and serum ROS and MDA levels were all decreased, and the oxidative stress state was controlled. The mitochondrial function and structure of myocardial cells were normalized, and cardiac function was improved. These results indicate that Linggui Zhugan Decoction can recover mitochondrial membrane potential, reduce mitochondrial damage and myocardial cell oxidative damage, against myocardial fibrosis, and increase the ejection fraction in rats with heart failure.

SIRT1, AMPK, and PGC-1α constitute an energy-sensing system, which has an important role in regulating mitochondrial function. When the ratio of AMP/ATP in cells is increased, the *a* group of Thr172 in AMPK is activated by phosphorylation. p-AMPK can act on a variety of downstream substrates, inhibit the consumption of ATP, and initiate the pathway to generate ATP to maintain the body's energy metabolism balance, increase the content of intracellular NAD+, and then make NAD + -dependent SIRT1 depleted. Activation and exert its corresponding biological effect (Askin et al., 2020). Disturbance of SIRT1/PGC-1α deacetylation pathway can enhance oxidative stress and promote mitochondrial dysfunction (Wang et al., 2019). Many previous drug studies have confirmed that the SIRT1-AMPK-PGC-1α pathway is the keyway for Chinese herbal medicine to exert its role. Wu et al. (2018) found that icariin could protect mitochondria's structural and functional integrity by regulating the expression of SIRT1 and reducing the apoptosis induced by MI/R. When the SIRT1 gene was knocked down, or an inhibitor of SIRT1 was administered, the protective effect of icariin could be reversed. Moreover, another study found that naringenin promotes mitochondrial production and relieves mitochondrial oxidative stress by activating AMPK-PGC-1α, thus having a role in resisting MI/R injury (Yu et al., 2019). Melatonin can promote AMPK phosphorylation and upregulation of PGC-1α expression, enhance mitochondria's oxidative metabolism function, and reduce myocardial apoptosis caused by MI/R (Yu et al., 2017). Moreover, the cardioprotective effects of naringenin and melatonin were significantly reduced when AMPK expression was interfered with, or AMPK inhibitor (Compound C) was administered. Therefore, in order to further explore the possible molecular mechanism of Linggui Zhugan Decoction in the treatment of heart failure from the perspective of mitochondria, we detected the key protein molecules and their mRNA levels. The results showed that the AMPK phosphorylation level of rats with chronic heart failure caused by ischemic heart disease after the intervention of Linggui Zhugan Decoction increased, while the protein and mRNA levels of SIRT1 and PGC-1α were significantly increased. This indicated that Linggui Zhugan Decoction could activate the SIRT1/AMPK/PGC-1α pathway to protect mitochondria and resist oxidative stress in myocardial cells.

PGC-1α is a key factor in regulating mitochondrial biosynthesis (Sharma et al., 2013). PGC-1α activates NRF-1 and NRF-2 and increases the transcription of several mitochondrial DNA genes, thus participating in the process of the respiratory chain, which is especially more significant in the cardiovascular system (Whitaker et al., 2016). Cardiovascular cells such as myocardium and vascular endothelium regulate mitochondrial production through the PGC-1α signaling pathway, thereby maintaining and repairing the cell structure and function. Similarly, in this experiment, we found that Linggui Zhugan Decoction increased the expression of NRF1 and TFAM mRNA and protein downstream of PGC-1α and increased mtDNA content in rats with heart compared with the model group. We also found that, although captopril could repair mitochondrial damage in myocardial cells of rats with heart failure, it did not affect the protein and mRNA levels of SIRT1, p-AMPK, and PGC-1α. Previous studies have confirmed the protective effect of captopril on myocardial cells (Mujkosová et al., 2010). A previous study suggested that captopril has a protective role by improving energy metabolism (Gvozdjáková et al., 1999) and weakening apoptosis (Lin et al., 2013). Yet, there is insufficient evidence supporting that captopril can affect the SIRT1-AMPK-PGC-1α pathway.

In conclusion, our *in vivo* findings showed that the SIRT1-AMPK-PGC-1α signaling pathway was inhibited during heart failure, which is consistent with previous studies. Furthermore, the results showed that Linggui Zhugan Decoction could activate the SIRT1-AMPK-PGC-1α signaling pathway, restore mitochondrial membrane potential, reduce the degree of mitochondrial damage and oxidative damage, promote

mitochondrial biogenesis, and improve cardiac function. These results indicated that SIRT1-AMPK-PGC-1α is the key signaling pathway mediating the protection of Linggui Zhugan Decoction on the mitochondrial function in rats with heart failure.

Although this experiment verified the protective effect of Linggui Zhugan Decoction on myocardial mitochondrial function in rats with heart failure, reasonable treatment-related dose ranges and dose-response relationship cannot be clearly defined due to the lack of positive drug multiple-dose comparisons in the experimental design. Furthermore, the effects of Linggui Zhugan Decoction on mitochondrial oxygen consumption and oxidative phosphorylation, and which effective compounds in decoction have an effect on mitochondria, need to be further explored.

Data availability statement

The original contributions presented in the study are included in the article/Supplementary Material, further inquiries can be directed to the corresponding authors.

Ethics statement

The animal study was reviewed and approved by Ethics Committee of Hubei University of Medicine.

Author contributions

JC and XM conceived the project, designed the study, and revised the manuscript. SY, HQ and DT were responsible for design and collected the clinical data, analyzed data and wrote the paper. MY, DL, HX, JSC, JY, XH, ZL, JZ, and HY contributed to data analysis and revision. All the authors read, critically revised, and agreed to be accountable for the content of manuscript.

Funding

This work was supported by the National Natural Science Foundation of China (81400288, 81573244), Hubei Provincial Natural Science Foundation (2022CFB453), Foundation of Health Commission of Hubei (WJ2021M061, WJ2019F071), the Natural Science Foundation of the Bureau of Science and Technology of Shiyan City (Grant No. 21Y71, 19Y89), the Faculty Development Grants from Hubei University of Medicine (2018QDJZR04), and Hubei Key Laboratory of Wudang Local Chinese Medicine Research (Hubei University of Medicine) (Grant No. WDCM2022007), and the Advantages discipline Group (Medicine) Project in Higher Education of Hubei Province (2021–2025) (Grant No. 2022XKQT4).

Conflict of interest

The authors declare that the research was conducted in the absence of any commercial or financial relationships that could be construed as a potential conflict of interest.

Publisher's note

All claims expressed in this article are solely those of the authors and do not necessarily represent those of their affiliated organizations, or those of the publisher, the editors and the reviewers. Any product that may be evaluated in this article, or claim that may be made by its manufacturer, is not guaranteed or endorsed by the publisher.

Supplementary material

The Supplementary Material for this article can be found online at: https://www.frontiersin.org/articles/10.3389/fphar.2023.1074837/full#supplementary-material

References

Akhmedov, A. T., Rybin, V., and Marín-García, J. (2015). Mitochondrial oxidative metabolism and uncoupling proteins in the failing heart. *Heart Fail Rev.* 20 (2), 227–249. doi:10.1007/s10741-014-9457-4

Askin, L., Tibilli, H., Tanriverdi, O., and Turkmen, S. (2020). The relationship between coronary artery disease and SIRT1 protein. *North Clin. Istanb* 7 (6), 631–635. doi:10.14744/nci.2020.31391

Ayoub, K. F., Pothineni, N. V. K., Rutland, J., Ding, Z., and Mehta, J. L. (2017). Immunity, inflammation, and oxidative stress in heart failure: Emerging molecular targets. *Cardiovasc Drugs Ther.* 31 (5-6), 593–608. doi:10.1007/s10557-017-6752-z

Bertero, E., and Maack, C. (2018). Metabolic remodelling in heart failure. *Nat. Rev. Cardiol.* 15 (8), 457–470. doi:10.1038/s41569-018-0044-6

Braunwald, E. (2013). Research advances in heart failure: A compendium. *Circ. Res.* 113 (6), 633–645. doi:10.1161/circresaha.113.302254

Brown, D. A., Perry, J. B., Allen, M. E., Sabbah, H. N., Stauffer, B. L., Shaikh, S. R., et al. (2017). Expert consensus document: Mitochondrial function as a therapeutic target in heart failure. *Nat. Rev. Cardiol.* 14 (4), 238–250. doi:10.1038/nrcardio.2016.203

Bu, L., Dai, O., Zhou, F., Liu, F., Chen, J. F., Peng, C., et al. (2020). Traditional Chinese medicine formulas, extracts, and compounds promote angiogenesis. *Biomed. Pharmacother.* 132, 110855. doi:10.1016/j.biopha.2020.110855

Cao, J., Tsenovoy, P. L., Thompson, E. A., Falck, J. R., Touchon, R., Sodhi, K., et al. (2015). Agonists of epoxyeicosatrienoic acids reduce infarct size and ameliorate cardiac dysfunction via activation of HO-1 and Wnt1 canonical pathway. *Prostagl. Other Lipid Mediat* 116-117, 76–86. doi:10.1016/j.prostaglandins.2015.01.002

Chen, Y., Li, L., Hu, C., Zhao, X., Zhang, P., Chang, Y., et al. (2022). Lingguizhugan decoction dynamically regulates MAPKs and AKT signaling pathways to retrogress the pathological progression of cardiac hypertrophy to heart failure. *Phytomedicine* 98, 153951. doi:10.1016/j.phymed.2022.153951

Daubert, M. A., Adams, K., Yow, E., Barnhart, H. X., Douglas, P. S., Rimmer, S., et al. (2019). NT-proBNP goal achievement is associated with significant reverse remodeling and improved clinical outcomes in HFrEF. *JACC Heart Fail* 7 (2), 158–168. doi:10.1016/j.jchf.2018.10.014

Di Lisa, F., Menabò, R., Canton, M., and Petronilli, V. (1998). The role of mitochondria in the salvage and the injury of the ischemic myocardium. *Biochim. Biophys. Acta* 1366 (1-2), 69–78. doi:10.1016/s0005-2728(98)00121-2

Fu, S., Zhang, J., Gao, X., Xia, Y., Ferrelli, R., Fauci, A., et al. (2010). Clinical practice of traditional Chinese medicines for chronic heart failure. *Heart Asia* 2 (1), 24–27. doi:10.1136/ha.2009.001123

Gurd, B. J. (2011). Deacetylation of PGC-1α by SIRT1: Importance for skeletal muscle function and exercise-induced mitochondrial biogenesis. *Appl. Physiol. Nutr. Metab.* 36 (5), 589–597. doi:10.1139/h11-070

Gvozdjáková, A., Simko, F., Kucharská, J., Braunová, Z., Psenek, P., and Kyselovic, J. (1999). Captopril increased mitochondrial coenzyme Q10 level, improved respiratory chain function and energy production in the left ventricle in rabbits with smoke mitochondrial cardiomyopathy. *Biofactors* 10 (1), 61–65. doi:10.1002/biof.5520100107

Herzig, S., and Shaw, R. J. (2018). Ampk: Guardian of metabolism and mitochondrial homeostasis. *Nat. Rev. Mol. Cell. Biol.* 19 (2), 121–135. doi:10.1038/nrm.2017.95

Hsu, Y. R., Yogasundaram, H., Parajuli, N., Valtuille, L., Sergi, C., and Oudit, G. Y. (2016). MELAS syndrome and cardiomyopathy: Linking mitochondrial function to heart failure pathogenesis. *Heart Fail Rev.* 21 (1), 103–116. doi:10.1007/s10741-015-9524-5

Jiang, G. P., Liao, Y. J., Huang, L. L., Zeng, X. J., and Liao, X. H. (2021). Effects and molecular mechanism of pachymic acid on ferroptosis in renal ischemia reperfusion injury. *Mol. Med. Rep.* 23 (1), 63. doi:10.3892/mmr.2020.11704

Kojic, Z., Gopcevic, K., Marinkovic, D., and Tasic, G. (2011). Effect of captopril on serum lipid levels and cardiac mitochondrial oxygen consumption in experimentally-induced hypercholesterolemia in rabbits. *Physiol. Res.* 60, S177–S184. doi:10.33549/physiolres.932177

Lee, I. C., Ho, X. Y., George, S. E., Goh, C. W., Sundaram, J. R., Pang, K. K. L., et al. (2018). Oxidative stress promotes SIRT1 recruitment to the GADD34/PP1α complex to activate its deacetylase function. *Cell. Death Differ.* 25 (2), 255–267. doi:10.1038/cdd.2017.152

Lin, P. P., Hsieh, Y. M., Kuo, W. W., Lin, Y. M., Yeh, Y. L., Lin, C. C., et al. (2013). Probiotic-fermented purple sweet potato yogurt activates compensatory IGF-IR/PI3K/Akt survival pathways and attenuates cardiac apoptosis in the hearts of spontaneously hypertensive rats. *Int. J. Mol. Med.* 32 (6), 1319–1328. doi:10.3892/ijmm.2013.1524

Lopaschuk, G. D., Karwi, Q. G., Tian, R., Wende, A. R., and Abel, E. D. (2021). Cardiac energy metabolism in heart failure. *Circ. Res.* 128 (10), 1487–1513. doi:10.1161/circresaha.121.318241

McCarthy, C. P., and Januzzi, J. L., Jr. (2018). Soluble ST2 in heart failure. *Heart Fail Clin.* 14 (1), 41–48. doi:10.1016/j.hfc.2017.08.005

McDonagh, T. A., Metra, M., Adamo, M., Gardner, R. S., Baumbach, A., Böhm, M., et al. (2021). 2021 ESC Guidelines for the diagnosis and treatment of acute and chronic heart failure. *Eur. Heart J.* 42 (36), 3599–3726. doi:10.1093/eurheartj/ehab368

Mujkosová, J., Ulicná, O., Waczulíková, I., Vlkovicová, J., Vancová, O., Ferko, M., et al. (2010). Mitochondrial function in heart and kidney of spontaneously hypertensive rats: Influence of captopril treatment. *Gen. Physiol. Biophys.* 29 (2), 203–207. doi:10.4149/gpb_2010_02_203

Neubauer, S. (2007). The failing heart--an engine out of fuel. *N. Engl. J. Med.* 356 (11), 1140–1151. doi:10.1056/NEJMra063052

Pan, W., Yang, D., Yu, P., and Yu, H. (2020). Comparison of predictive value of NT-proBNP, sST2 and MMPs in heart failure patients with different ejection fractions. *BMC Cardiovasc Disord.* 20 (1), 208. doi:10.1186/s12872-020-01493-2

Passantino, A., Lagioia, R., Mastropasqua, F., and Scrutinio, D. (2006). Short-term change in distance walked in 6 min is an indicator of outcome in patients with chronic heart failure in clinical practice. *J. Am. Coll. Cardiol.* 48 (1), 99–105. doi:10.1016/j.jacc.2006.02.061

Sanbe, A., Tanonaka, K., Kobayasi, R., and Takeo, S. (1995). Effects of long-term therapy with ACE inhibitors, captopril, enalapril and trandolapril, on myocardial energy metabolism in rats with heart failure following myocardial infarction. *J. Mol. Cell. Cardiol.* 27 (10), 2209–2222. doi:10.1016/s0022-2828(95)91551-6

Savarese, G., and Lund, L. H. (2017). Global public health burden of heart failure. *Card. Fail Rev.* 3 (1), 7–11. doi:10.15420/cfr.2016:25:2

Schultheiss, H. P., Ullrich, G., Schindler, M., Schulze, K., and Strauer, B. E. (1990). The effect of ACE inhibition on myocardial energy metabolism. *Eur. Heart J.* 11, 116–122. doi:10.1093/eurheartj/11.suppl_b.116

Sharma, D. R., Sunkaria, A., Wani, W. Y., Sharma, R. K., Kandimalla, R. J., Bal, A., et al. (2013). Aluminium induced oxidative stress results in decreased mitochondrial biogenesis via modulation of PGC-1α expression. *Toxicol. Appl. Pharmacol.* 273 (2), 365–380. doi:10.1016/j.taap.2013.09.012

Sil, R., and Chakraborti, A. S. (2016). Oxidative inactivation of liver mitochondria in high fructose diet-induced metabolic syndrome in rats: Effect of glycyrrhizin treatment. *Phytother. Res.* 30 (9), 1503–1512. doi:10.1002/ptr.5654

Tayal, U., Prasad, S., and Cook, S. A. (2017). Genetics and genomics of dilated cardiomyopathy and systolic heart failure. *Genome Med.* 9 (1), 20. doi:10.1186/s13073-017-0410-8

Wang, J., Dong, Z. H., Gui, M. T., Yao, L., Li, J. H., Zhou, X. J., et al. (2019a). HuoXue QianYang QuTan Recipe attenuates left ventricular hypertrophy in obese hypertensive rats by improving mitochondrial function through SIRT1/PGC-1α deacetylation pathway. *Biosci. Rep.* 39 (12). doi:10.1042/bsr20192909

Wang, L., Shi, H., Huang, J. L., Xu, S., and Liu, P. P. (2020a). Linggui zhugan decoction inhibits ventricular remodeling after acute myocardial infarction in mice by suppressing TGF-β(1)/smad signaling pathway. *Chin. J. Integr. Med.* 26 (5), 345–352. doi:10.1007/s11655-018-3024-0

Wang, M., Hu, R., Wang, Y., Liu, L., You, H., Zhang, J., et al. (2019b). Atractylenolide III attenuates muscle wasting in chronic kidney disease via the oxidative stress-mediated PI3K/AKT/mTOR pathway. *Oxid. Med. Cell. Longev.* 2019, 1875471. doi:10.1155/2019/1875471

Wang, Q., Kuang, H., Su, Y., Sun, Y., Feng, J., Guo, R., et al. (2013). Naturally derived anti-inflammatory compounds from Chinese medicinal plants. *J. Ethnopharmacol.* 146 (1), 9–39. doi:10.1016/j.jep.2012.12.013

Wang, X., Gao, Y., Tian, Y., Liu, X., Zhang, G., Wang, Q., et al. (2020b). Integrative serum metabolomics and network analysis on mechanisms exploration of Ling-Gui-Zhu-Gan Decoction on doxorubicin-induced heart failure mice. *J. Ethnopharmacol.* 250, 112397. doi:10.1016/j.jep.2019.112397

Wei, L. Y., Zhang, P. J., Hu, Y. N., Zhao, W. S., Liu, X. T., Wang, X. F., et al. (2020). HOE-642 improves the protection of hypothermia on neuronal mitochondria after cardiac arrest in rats. *Am. J. Transl. Res.* 12 (5), 2181–2191.

Whitaker, R. M., Corum, D., Beeson, C. C., and Schnellmann, R. G. (2016). Mitochondrial biogenesis as a pharmacological target: A new approach to acute and chronic diseases. *Annu. Rev. Pharmacol. Toxicol.* 56, 229–249. doi:10.1146/annurev-pharmtox-010715-103155

Wu, B., Feng, J. Y., Yu, L. M., Wang, Y. C., Chen, Y. Q., Wei, Y., et al. (2018). Icariin protects cardiomyocytes against ischaemia/reperfusion injury by attenuating sirtuin 1-dependent mitochondrial oxidative damage. *Br. J. Pharmacol.* 175 (21), 4137–4153. doi:10.1111/bph.14457

Xu, X. B., Pang, J. J., Cao, J. M., Ni, C., Xu, R. K., Peng, X. Z., et al. (2005). GH-releasing peptides improve cardiac dysfunction and cachexia and suppress stress-related hormones and cardiomyocyte apoptosis in rats with heart failure. *Am. J. Physiol. Heart Circ. Physiol.* 289 (4), H1643–H1651. doi:10.1152/ajpheart.01042.2004

Yang, S., Zhang, J., Yan, Y., Yang, M., Li, C., Li, J., et al. (2019). Network pharmacology-based strategy to investigate the pharmacologic mechanisms of Atractylodes macrocephala Koidz. For the treatment of chronic gastritis. *Front. Pharmacol.* 10, 1629. doi:10.3389/fphar.2019.01629

Yang, X. Y., Yan, X. J., Yang, D. P., Zhou, J. K., Song, J., and Yang, D. W. (2018). Rapamycin attenuates mitochondrial injury and renal tubular cell apoptosis in experimental contrast-induced acute kidney injury in rats. *Biosci. Rep.* 38 (6), 876. doi:10.1042/BSR20180876

Yu, L., Gong, B., Duan, W., Fan, C., Zhang, J., Li, Z., et al. (2017). Melatonin ameliorates myocardial ischemia/reperfusion injury in type 1 diabetic rats by preserving mitochondrial function: Role of AMPK-PGC-1α-SIRT3 signaling. *Sci. Rep.* 7, 41337. doi:10.1038/srep41337

Yu, L. M., Dong, X., Xue, X. D., Zhang, J., Li, Z., Wu, H. J., et al. (2019). Naringenin improves mitochondrial function and reduces cardiac damage following ischemia-reperfusion injury: The role of the AMPK-SIRT3 signaling pathway. *Food Funct.* 10 (5), 2752–2765. doi:10.1039/c9fo00001a

Zhang, Y., Fan, L., Li, H., Wang, X., Xu, W., Chu, K., et al. (2018). Gualou Guizhi granule protects against oxidative injury by activating Nrf2/ARE pathway in rats and PC12 cells. *Neurochem. Res.* 43 (5), 1003–1009. doi:10.1007/s11064-018-2507-x

Zhang, Y. N., Feng, W. W., Chen, G. Y., and Ma, M. X. (2013). Establishment and evaluation of ISO induced heart failure rat model. *J Harbin Med. Univ.* 47 (05), 410–413.

Zheng, Y., Dai, Y., Liu, W., Wang, N., Cai, Y., Wang, S., et al. (2019). Astragaloside IV enhances taxol chemosensitivity of breast cancer via caveolin-1-targeting oxidant damage. *J. Cell. Physiol.* 234 (4), 4277–4290. doi:10.1002/jcp.27196

Zhou, H., Sun, Y., Zhang, L., Kang, W., Li, N., and Li, Y. (2018). The RhoA/ROCK pathway mediates high glucose-induced cardiomyocyte apoptosis via oxidative stress, JNK, and p38MAPK pathways. *Diabetes Metab. Res. Rev.* 34 (6), e3022. doi:10.1002/dmrr.3022

Zhou, P., and Huang, J. L. (2020). Prediction of material foundation of Ling-Gui-Zhu-Gan decoction for chronic heart failure based on molecular docking. *Pak J. Pharm. Sci.* 33 (4), 1459–1464.

frontiers | Frontiers in Pharmacology

TYPE Systematic Review
PUBLISHED 07 April 2023
DOI 10.3389/fphar.2023.1074400

Check for updates

OPEN ACCESS

EDITED BY
Kuo Gao,
Beijing University of Chinese Medicine, China

REVIEWED BY
Shihua Shi,
The First Affiliated Hospital of Chengdu University of Traditional Chinese Medicine, China
Fengwen Yang,
Tianjin University of Traditional Chinese Medicine, China
Wentai Pang,
Tianjin University of Traditional Chinese Medicine, China
Xiao Ma,
Chengdu University of Traditional Chinese Medicine, China

*CORRESPONDENCE
Yanming Xie,
ktzu2018@163.com

†These authors have contributed equally to this work and share first authorship

SPECIALTY SECTION
This article was submitted to Ethnopharmacology, a section of the journal Frontiers in Pharmacology

RECEIVED 19 October 2022
ACCEPTED 24 March 2023
PUBLISHED 07 April 2023

CITATION
Xi J, Wei R, Cui X, Liu Y and Xie Y (2023), The efficacy and safety of Xueshuantong (lyophilized) for injection in the treatment of unstable angina pectoris: A systematic review and meta-analysis.
Front. Pharmacol. 14:1074400.
doi: 10.3389/fphar.2023.1074400

COPYRIGHT
© 2023 Xi, Wei, Cui, Liu and Xie. This is an open-access article distributed under the terms of the Creative Commons Attribution License (CC BY). The use, distribution or reproduction in other forums is permitted, provided the original author(s) and the copyright owner(s) are credited and that the original publication in this journal is cited, in accordance with accepted academic practice. No use, distribution or reproduction is permitted which does not comply with these terms.

The efficacy and safety of Xueshuantong (lyophilized) for injection in the treatment of unstable angina pectoris: A systematic review and meta-analysis

Junyu Xi†, Ruili Wei†, Xin Cui†, Yi Liu and Yanming Xie*

Institute of Basic Research in Clinical Medicine, China Academy of Chinese Medical Sciences, Beijing, China

Objective: Xueshuantong (lyophilized) for injection (XST) is an effective botanical drug for treating unstable angina pectoris (UAP). However, a meta-analysis of XST combined with conventional treatment (CT) against UAP has not been conducted. Therefore, this study aimed to investigate the effectiveness and safety of XST combined with CT for UAP patients compared to CT alone.

Methods: Randomized controlled trials (RCT) of XST in UAP patients were retrieved from the Cochrane Library, PubMed, Web of Science, EMBASE, CNKI, VIP, Wanfang, and Chinese Biological Medicine Database databases. A meta-analysis was performed using Revman 5.4 and Stata 16.0, and the quality of the included literature was evaluated based on the Cochrane risk-of-bias 2.0 (RoB2.0) tool. The aggregate 95% confidence intervals (CIs), mean difference (MD), and relative risk (RR) estimates were calculated. A GRADE assessment was performed using GRADEprofiler 3.6, and trial sequent analysis was performed using TSA 0.9.

Results: Thirty-four studies involving 3,518 patients were included in the analysis. The combination of CT with XST improved the comprehensive clinical efficacy (RR = 1.22, 95% CI: 1.18–1.26, $p < 0.00001$) and ECG improvement (RR = 1.24, 95% CI: 1.18–1.31, $p < 0.00001$). The frequency of angina attacks was lower (MD = −0.73, 95% CI: −0.92 to −0.55, $p < 0.00001$), and the duration was shorter (MD = −1.08, 95% CI: −1.44 to −0.72, $p < 0.00001$) in the group that received CT combined with XST compared to the one without XST. Total cholesterol levels (MD = −1.30, 95% CI: −1.83 to −0.78, $p < 0.00001$) and triglyceride levels (MD = −0.76, 95% CI: −0.93 to −0.59, $p < 0.00001$) were lower in patients who received CT in combination with XST than those who received CT alone. CT

Abbreviations: ACS, Acute Coronary Syndrome; AE, Adverse Event; cAMP, cyclic Adenosine Monophosphate; CBM, Chinese Biological Medicine Database; CI, Confidence Intervals; CNKI, China National Knowledge Infrastructure; CT, Conventional Treatment; CPM, Chinese Patent Medicine; ECG, Electrocardiograph; HDL, High-density Lipoprotein; ICAM, Intercellular Adhesion Molecule; LDL, Low-density Lipoprotein; MD, Mean Difference; RCT, Randomized Controlled Trials; RR, Relative Risk; RRR, Relative Risk Reduction; RIS, Required Information Size; SR, Sarcoplasmic Reticulum; TSA, Trial Sequential Analysis; TXA2, Thromboxane A2; UAP, Unstable Angina Pectoris; VCAM-1, Vascular Cell Adhesion Molecule-1; VIP, VIP Chinese Sci-tech Periodical Database; XST, Xueshuantong (lyophilized) for injection; 5-HT, 5-hydroxytryptamine.

combined with XST reduced whole blood viscosity (MD = −0.72, 95% CI = −0.99 to −0.44, $p < 0.00001$) and plasma viscosity (MD = −0.24, 95% CI: −0.46 to −0.03, $p = 0.03$). There was no statistically significant difference in the incidence of cardiovascular events or adverse events among patients treated with the combination of XST and CT compared to CT alone. The GRADE assessment indicated that the composite quality of the evidence was low. The trial sequent analysis showed an adequate sample size and stable findings for the clinical efficacy of CT combined with XST for unstable angina.

Conclusion: The present systematic review and meta-analysis conditionally indicate that XST combined with CT improved the clinical outcomes of patients with unstable angina more than CT alone with a better safety profile. However, the results need further validation due to limitations in the quality of the included studies.

Systematic Review Registration: https://www.crd.york.ac.uk/PROSPERO/, identifier CRD42022357395.

KEYWORDS

Xueshuantong for injection, unstable angina pectoris, meta-analysis, trial sequential analysis, GRADE

1 Introduction

Unstable angina pectoris (UAP) is integral to acute coronary syndrome (ACS). An epidemiological investigation in China reported that 122 of 100,000 people had coronary heart disease, imposing a huge burden on families and society (Summary of Chinese Cardiovascular Health and Disease report 2019, 2020). As a non-ST segment-elevated acute coronary syndrome, UAP can develop into acute myocardial infarction and is the leading cause of death in patients with coronary heart disease. The main UAP treatments in modern medicine include anti-myocardial ischemia, antiplatelet, anticoagulation and statin medications, and revascularization (Guidelines for diagnosis and treatment of non-ST segment elevation acute coronary syndrome 2016, 2017). However, the long-term use of these drugs produces side effects and drug resistance, affecting treatment efficacy. Chinese medicine has been used in clinical practice for over 3,000 years (Jia et al., 2017; Zhang et al., 2017). Chinese patent medicine (CPM) refers to drugs prepared from various botanical drugs through unique methods and specific combinations. Modern evidence-based evaluation methods and basic research evidence have confirmed that CPM is advantageous and safe for treating UAP and is widely used for treating UAP. Chinese botanical drug injections are fast-acting and have better bioavailability than general CPM (Li et al., 2022).

Xueshuantong (lyophilized) for injection (XST) is a standardized botanical drug in the *Pharmacopoeia of the People's Republic of China*. It is listed in the 2018 National List of Essential Medicines as one of the most popular Chinese botanical drug injections for activating blood circulation and resolving blood stasis. *Panax notoginseng* saponins were isolated from the root and rhizome of *Panax notoginseng* (Burk.) F. H. Chen [Araliaceae; Notoginseng Radix], is the primary active component of XST (Shen et al., 2017). *Panax notoginseng* is a well-known botanical drug. It has the ability to invigorate blood, remove blood stasis, reduce swelling and relieve pain. Pharmaceutical manufacturer obtained 250 g of total saponins of *panax notoginseng*, and an appropriate amount of water was added for injection to dissolve it, followed by activated carbon. After homogenizing and filtering, water was injected into the specified volume. Then, 20% sodium citrate solution was added to adjust the pH value to 5.5–7.0, followed by filtering, filling, and freeze drying, to obtain XST. There are five main components of PNS: ginsenoside R1, ginsenoside Rg1, ginsenoside Rd, ginsenoside Re, ginsenoside Rb1. Previous studies confirmed that *Panax ginseng* total saponin could correct intracellular calcium ion ($Ca2^{+}$) overload in cardiomyocytes by increasing the calcium pump activity on the sarcoplasmic reticulum (SR) membrane of cardiomyocytes, thereby increasing left ventricular myocardial energy (Feng and Jiang, 1998). Animal experiments established that *Panax ginseng* total saponin could inhibit nuclear factor (NF)-κB activation in neutrophils and reduce intercellular adhesion molecule (ICAM)-1 expression and neutrophil infiltration. Thus, it improves myocardial microcirculation, narrowing the infarct range of myocardial ischemia and effectively counteracting T-wave elevations due to acute myocardial ischemia (Tang et al., 2002; Li and Wang, 2016). The literature search yielded a previous meta-analysis of XST in treating UAP (Gao et al., 2019), but with certain limitations. The study did not consider long-term outcomes, such as the incidence of adverse cardiovascular events. The level of evidence was not evaluated, and the findings were not updated with the results of clinical trials conducted in recent years. Simultaneously, various dosage forms of XST were analyzed without any quality evaluation or sample size estimation. The current analysis used only studies of high-purity XST freeze-dried powder for the test sequential analysis to explore the stability of the study conclusions. GRADE was also used to evaluate the evidence quality, hoping to provide physicians with an accurate and objective reference on XST.

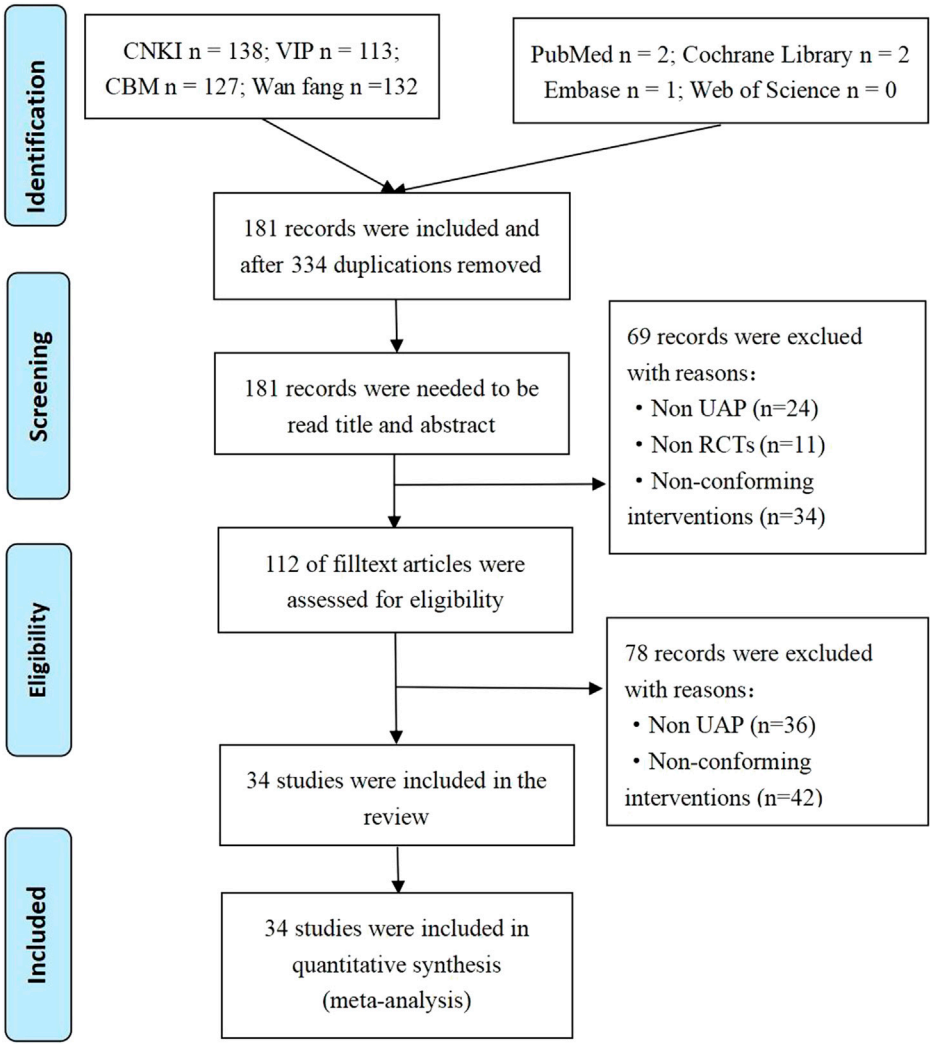

FIGURE 1
Flowchart of article selection process.

2 Methods

This meta-analysis was conducted and reported according to the PRISMA 2020 statement (Page et al., 2021) (Supplementary Material S1). The study protocol was registered with PROSPERO (registration number: CRD42022357395).

2.1 Eligibility criteria

2.1.1 Type of study

Randomized controlled trials (RCTs) were included, and the subjects met the diagnostic criteria of unstable angina pectoris (Chinese Medical Association, 2007).

2.1.2 Type of intervention

The test group was treated with XST, or XST was added to the control group. The control group was treated with routine medications (vasodilators, anticoagulants, antihypertensive drugs, and statins) (Chinese Medical Association, 2007) or other drugs.

2.1.3 Types of outcomes

The main index used to evaluate the effectiveness of this study was the comprehensive clinical efficacy, which referred to the sum of the percentage of patients whose curative effects were "significantly effective" and "effective" (FDA, 2007). Among them, a significant effect indicated that the number of angina pectoris events was reduced by more than 80%, and more than two grades improved the UAP grade. "Effective" suggested that the number of angina pectoris events decreased by 50% to more than 80%, and the UAP grade was improved by more than 1. The secondary outcomes were ECG improvement, the number of angina attacks, angina duration, blood lipid levels, and blood rheology assessments. ECG improvement was either the return of the ECG to normal, ST segment recovery >0.05 mV or the shallowing amplitude of the inverted T wave of the main lead is greater than 25% of the original

10.3389/fphar.2023.1074400

TABLE 1 Data analysis of included studies.

Study	Sample size			Gender (T/C)	Age/(year) (T/C)	Interventions		Duration/day	Outcomes
	T	C	Total			C	T		
Luan and Sun. (2005)	30	30	60	T: 19/11	63	CTs	CTs + XST 500 mg	15	①②
				C: 16/14					
Zeng (2007)	40	40	80	T: 28/12	T: 58.6	CTs	CTs + XST 500 mg	15	①⑤
				C: 27/13	C: 59.1				
Xie and Yan. (2008)	46	45	91	T: 46/36	T: 54.2 ± 9.0	CTs	CTs + XST 450 mg	7	①②⑤⑦
				C: 45/35	C: 54.1 ± 9.2				
Du (2009)	29	31	60	T: 15/15	T: 62	CTs	CTs + XST 400 mg	10	①②⑦⑧
				C: 16/14	C: 60				
Liang (2010)	60	60	120	66/54	54	CTs	CTs + XST 500 mg	21	① ②
Pan (2010)	98	98	196	T: 51/47	T: 62.3 ± 7.6	CTs	CTs + XST 500 mg	12	①
				C: 52/46	C: 61.4 ± 8.1				
Wang (2010)	58	56	114	T: 37/21	T: 63.4 ± 8.7	CTs	CTs + XST 500 mg	14	①
				C: 30/26	C: 64.1 ± 9.2				
Liang and Wu. (2011)	30	30	60	T: 18/12	T: 57.8 ± 10.4	CTs	CTs + XST 500 mg	10	①
				C: 16/14	C: 58.1 ± 10.9				
Ou (2011)	45	45	90	T: 29/16	T: 57.5 ± 6.1	CTs	CTs + XST 500 mg	14	①②
				C: 32/13	C: 56.3 ± 55.6				
Qi and Dong. (2011)	200	200	400	T: 110/90	T: 67.40 ± 10.21	CTs	CTs + XST 400 mg	14	①②
				C: 112/88	C: 66.93 ± 10.21				
Sun et al., 2011	48	48	96	55/41	54	CTs	CTs + XST 400 mg	14	①⑦
Zhang 2011	36	35	71	46/25	64	CTs	CTs + XST 450 mg	14	①②
Zhe (2011)	15	15	30	T: 15/10	UK	CTs	CTs + XST 500 mg	15	①②
				C: 15/10					
Zheng (2011)	40	40	80	T: 17/23	66.98 ± 12.12	CTs	CTs + XST 120 mg	14	①
				C: 19/21					
Chen et al. (2012)	40	40	80	T: 18/22	T: 54	CTs	CTs + XST 500 mg	14	①②⑥
				C: 17/23	C: 56				
Ju and Dong. (2012)	55	55	110	72/38	58	CTs	CTs + XST 500 mg	12	①
Wang et al. (2012)	30	30	60	UK	UK	CTs	CTs + XST 500 mg	14	①②④③
Ming (2013)	47	46	93	T: 28/19	T: 62.8 ± 5.9	CTs	CTs + XST 500 mg	21	①
				C: 28/18	C: 62.1 ± 3.9				
Pan et al. (2013)	30	30	60	UK	UK	CTs	CTs + XST 350 mg	—	①⑦
Li (2014)	30	30	60	T: 20/10	T: 62.5 ± 4.7	CTs	CTs + XST 400 mg	14	①②③ ④⑦⑧
				C: 21/9	C: 68.1 ± 4.8				
Luo (2014)	75	75	150	T: 40/35	T: 60.5 ± 10.7	CTs	CTs + XST 500 mg	14	①③⑦
				C: 39/36	C: 61.3 ± 10.5				
Tan (2014)	30	30	60	39/21	55.4 ± 7.5	CTs	CTs + XST 500 mg	14	①②

(Continued on following page)

TABLE 1 (*Continued*) Data analysis of included studies.

Study	Sample size			Gender (T/C)	Age/(year) (T/C)	Interventions		Duration/day	Outcomes
	T	C	Total			C	T		
Wang et al. (2014)	52	52	104	T: 25/25	T: 57.6 ± 4.6	CTs	CTs + XST 500 mg	14	①②
				C: 26/24	C: 55.9 ± 5.4				
Yan and Yu. (2014)	45	45	90	T: 25/20	T: 55.9 ± 6.3	CTs	CTs + XST 500 mg	14	①②⑦
				C: 26/19	C: 56.0 ± 6.1				
Chen (2015)	26	26	52	UK	61.2 ± 4.3	CTs	CTs + XST 300 mg	10	①
Dong and Yu. (2015)	60	60	120	T: 31/29	T: 62.9 ± 4.1	CTs	CTs + XST 450 mg	14	⑤⑥
				C: 36/24	C: 65.7 ± 4.5				
Guan et al. (2015)	54	54	108	T: 39/15	T: 53.26 ± 3.49	CTs	CTs + XST 400 mg	15	①⑤⑥
				C: 45/9	C: 56.91 ± 4.60				
Feldavus (2016)	130	130	260	T: 76/54	T: 53.7	CTs	CTs + XST	7	①⑥
				C: 69/61	C: 52.5				
Fei et al. (2016)	72	72	144	T: 52/20	T: 61 ± 3	CTs	CTs + XST 400 mg	15	①⑥
				C: 47/25	C: 60.6 ± 2.9				
Wang et al. (2014)	38	29	67	42/35	60.0 ± 5.2	CTs	CTs + XST 500 mg	12	①②⑦
Zhong et al. (2016)	25	25	50	28/22	45–70	CTs	CTs + XST 250 mg	14	①②
Huang (2017)	48	48	96	53/43	65.3 ± 5.9	CTs	CTs + XST 450 mg	14	①
Wang and Wei. (2018)	60	60	120	T: 29/31	T: 58.3 ± 7.1	CTs	CTs + XST 500 mg	14	①②
				C: 32/28	C: 57.2 ± 7.3				
Zang (2020)	43	43	86	T: 28/15	T: 54.65 ± 3.24	CTs	CTs + XST 250 mg	14	①②③
				C: 25/18	C: 57.65 ± 6.23				④⑥⑦

T, treatment group; C, control group; XST, Xueshuantong injection; CTs, Conventional treatments: vasodilators, anticoagulants, antihypertensive drugs, statins; UK, unknown; ①: Overall response rate; ②: Effectiveness in ECG; ③: Duration of angina pectoris; ④: Frequency of angina pectoris; ⑤: Hemorheology level; ⑥: Blood lipid level; ⑦: Adverse events; ⑧: Adverse cardiovascular events.

or a change in the T wave from flat to upright. The primary outcome index used to evaluate safety was the incidence of adverse reactions, and the secondary outcome index was the incidence of adverse cardiovascular events.

2.2 Retrieval strategy

We searched PubMed, Embase, Web of Science, Cochrane Library, China National Knowledge Infrastructure (CNKI), VIP Chinese Sci-tech Periodical Database (VIP), Chinese Biological Medicine Database (CBM), and the Chinese Wan Fang Database (Wan fang) from the inception of the database to October 2022. The retrieval strategies for each database are depicted in Supplementary Material S2.

2.3 Selection of research studies

The study selection process followed the PRISMA statement guidelines (Page et al., 2021). JX and XC independently screened the literature with predefined study selection criteria. The literature retrieved by subject terms was first imported into NoteExpress software for weight-checking, followed by a preliminary screening based on the titles of the publications. Afterward, the abstracts were read to exclude literature that did not meet the inclusion criteria. Finally, the full text of the studies was used to finalize inclusion in the current study. Disagreements were resolved by discussing with a third party. The data extraction table was created using Excel. The extracted data mainly included the first author, year of publication, the baseline characteristics of the study population, interventions (including dose and duration of treatment), and outcome indicators.

2.4 Methodological quality evaluation

Two investigators independently evaluated the methodological quality of the studies from relevant specialties, and a third party was consulted to resolve any disagreement. The quality of the included literature was assessed using the Cochrane risk-of-bias 2.0 (RoB2.0) tool (Liu et al., 2019). It focuses on randomization process,

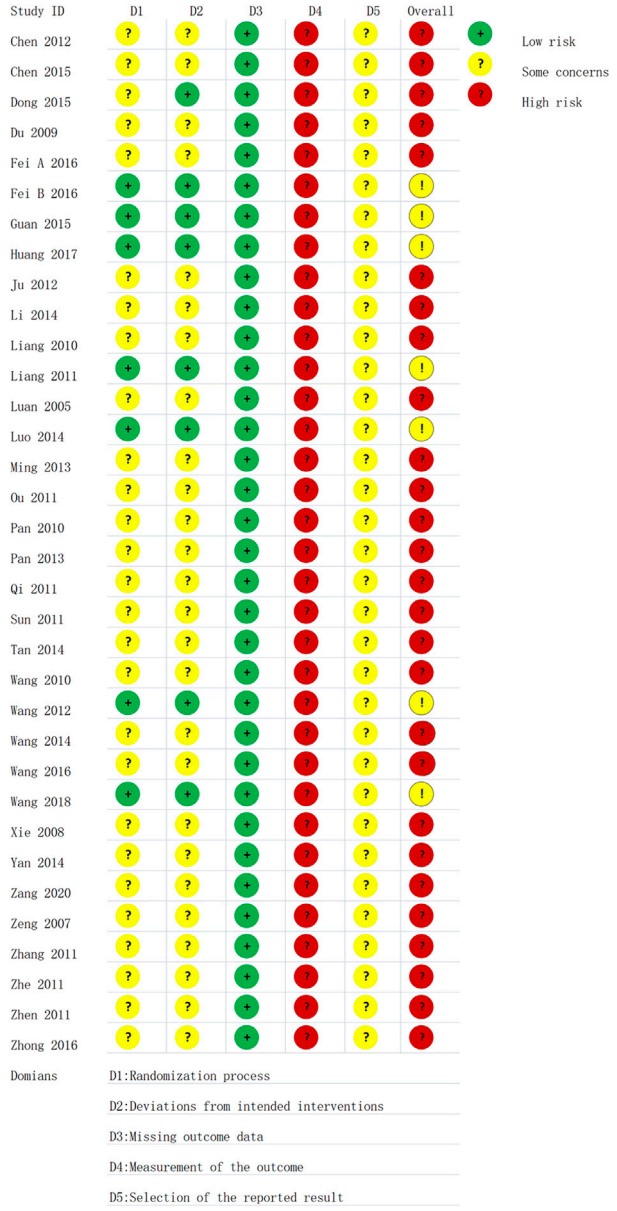

FIGURE 2
Risk of bias in each trial according to the Cochrane Ro B2 tool.

deviations from intended interventions, missing outcome data, measurement of the outcome, and selection of the reported result. Five aspects were evaluated, and the included studies were judged as having a low or high risk of bias, or some concerns.

2.5 Statistical analysis

Data analysis was performed using Revman 5.3 statistical software provided by the International Cochrane Collaboration. Mean difference (MD) (continuous variable) and relative risk (RR) (dichotomous variable) were selected as effect sizes, and 95% confidence intervals (CI) were utilized to express interval estimates. When the heterogeneity among the studies was small ($p \geq 0.1$, $I^2 \leq 50\%$), the fixed-effects model was selected for analysis. The reason was analyzed when the heterogeneity of each study was significant. If it was caused by clinical factors or research methods, subgroup or sensitivity analysis was performed. If the heterogeneity was still significant after analysis ($p < 0.1$, $I^2 > 50\%$), the random-effects model was selected for analysis. When more than 10 articles were included in the outcome index, a funnel chart was made using Stata.16.0 to analyze whether the studies had publication bias. TSA0.9 was used to sequentially analyze comprehensive clinical efficacy to evaluate whether the sample size of this meta-analysis was sufficient and whether there were false-positive results.

2.6 Assessment of evidence quality

JLX and RLW independently assessed the evidence quality according to previous rating standards (Balshem et al., 2011; Guyatt et al., 2011). The quality of the evidence included in the results was classified as high, medium, low, or very low. RCTs were initially classified as having high-quality evidence. The quality of each outcome was further graded according to five factors: deviation risk, inconsistency, indirectness, inaccuracy, and publication deviation. GRADEpro 3.6.1 software was utilized for data analysis and synthesis.

3 Results

3.1 Literature screening process

We systematically searched the databases and obtained 515 potentially related original studies. Of them, 334 duplicate studies were deleted, and the titles and abstracts of the remaining 181 articles were examined. Sixty-nine studies were deleted since they did not meet the eligibility criteria. Of these, 11 did not meet the inclusion criteria for the type of research, 34 did not meet the intervention criteria, and 24 were non-UAP studies. After further screening the full text of the studies, 78 articles were excluded since the study or intervention measures did not meet the inclusion criteria. Finally, a total of 34 original studies were included in the meta-analysis. The PRISMA flow chart study selection is represented in Figure 1.

3.2 Research and participant characteristics

The 34 included studies were all Chinese literature (Luan and Sun, 2005; Zeng, 2007; Xie and Yan, 2008; Du, 2009; Liang, 2010; Pan, 2010; Wang, 2010; Liang and Wu, 2011; Ou, 2011; Qi and Dong, 2011; Sun et al., 2011; Zhang, 2011; Zhe, 2011; Zheng, 2011; Chen et al., 2012; Ju and Dong, 2012; Wang et al., 2012; Ming, 2013; Pan et al., 2013; Li, 2014; Luo, 2014; Tan, 2014; Wang et al., 2014; Yan and Yu, 2014; Chen, 2015; Dong and Yu, 2015; Guan et al., 2015; Fei et al., 2016; Feldavus and Sarchen, 2016; Wang, 2016; Zhong et al., 2016; Huang, 2017; Wang and Wei, 2018; Zang, 2020). The total sample size included 3,518 subjects, 1,765 in the experimental group and 1,753 in

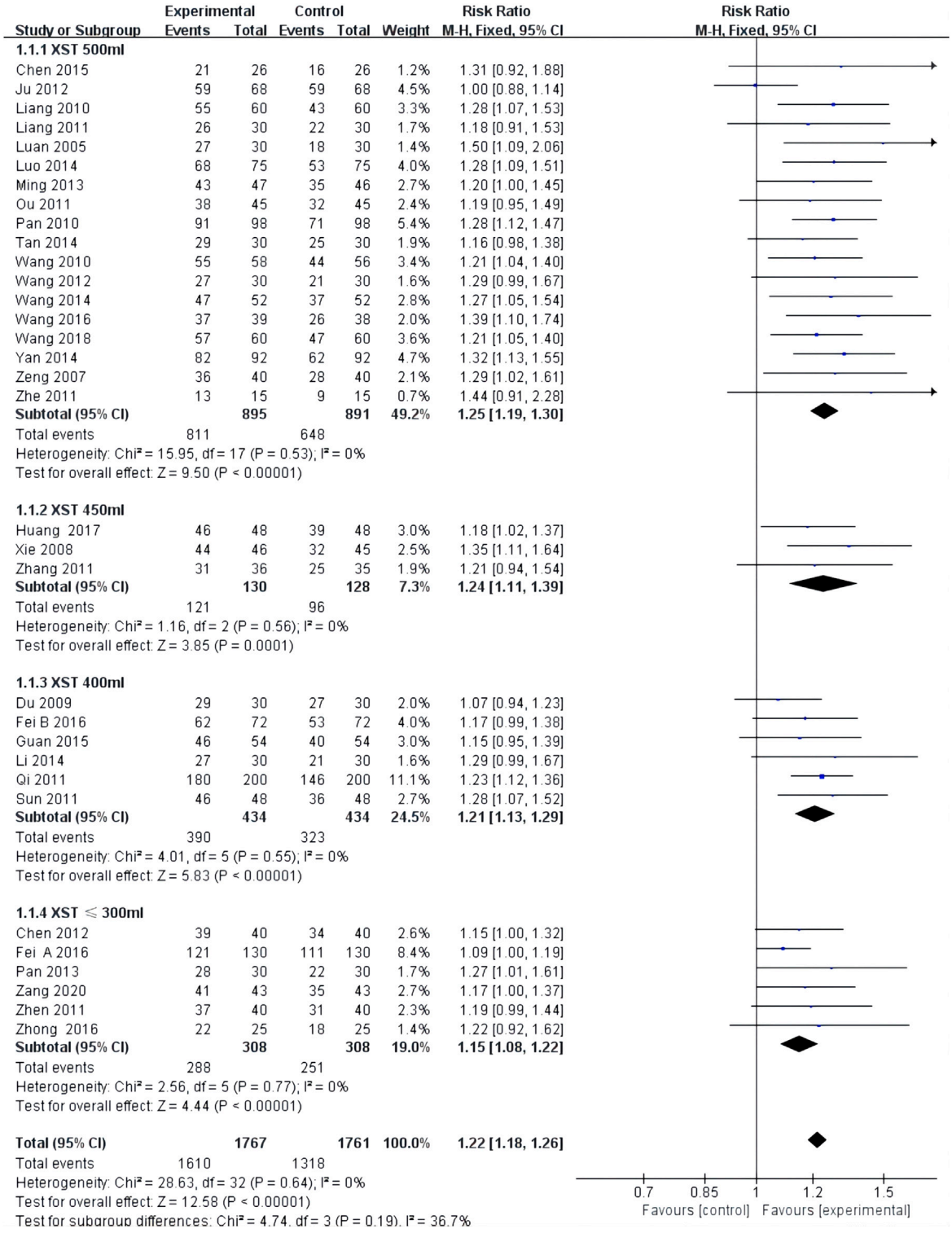

FIGURE 3
Forest plot of clinical comprehensive efficacy.

the control group. The maximum sample size of the trial group was 200, and the minimum sample size was 15. In the control group, the maximum sample size was 200, and the minimum sample size was 15. The shortest intervention period was 7 days while the longest was 21 and 14 days were the main ones (11/42, 52.94.19%). The mean age of the participants ranged from 45 to 79.1 years, as shown in Table 1.

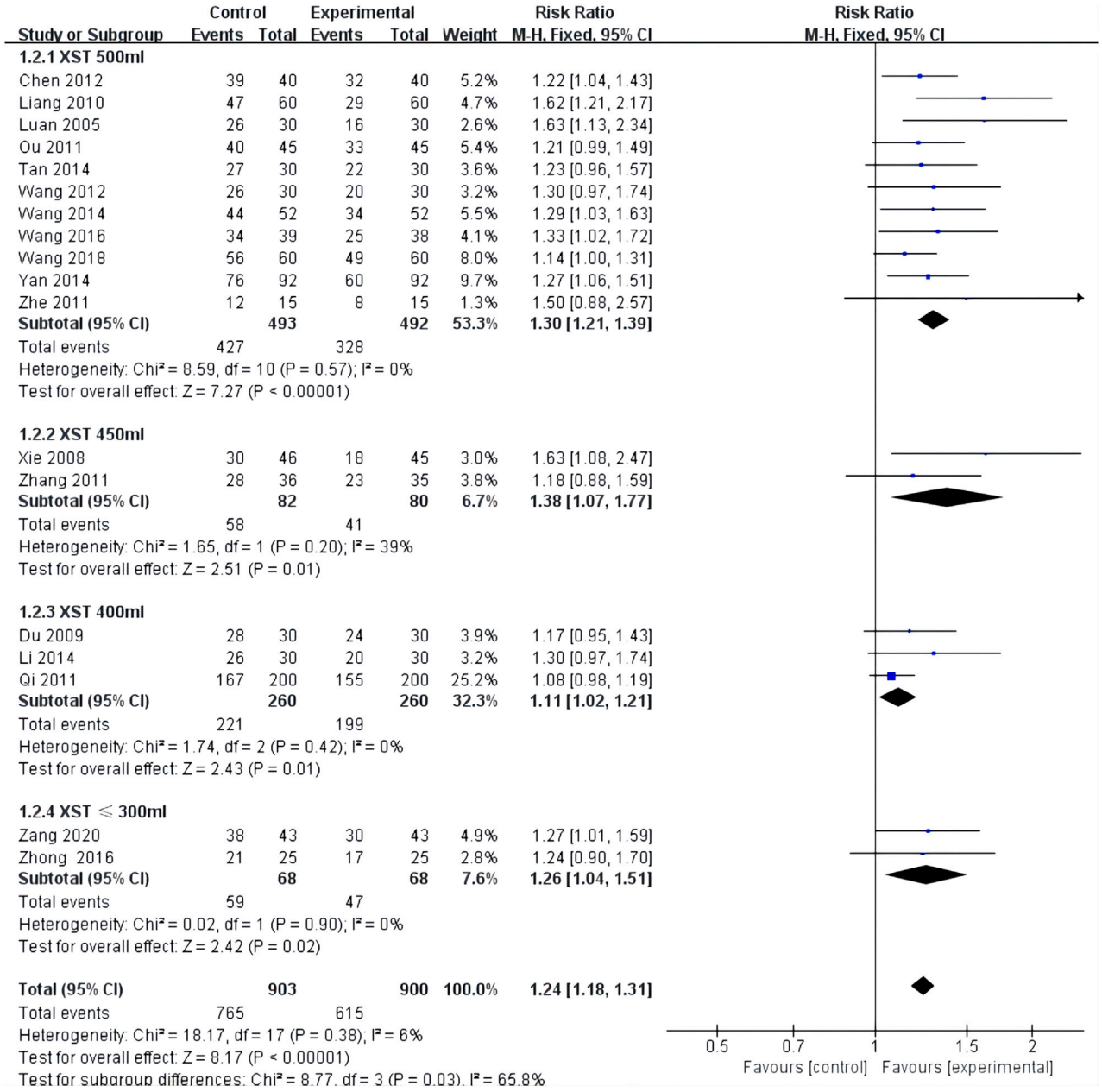

FIGURE 4
Forest plot of ECG Improvement.

3.3 Methodological quality

All included studies were RCTs, seven of which reported specific randomization methods, particularly the random number table method. The others only mentioned randomization. One study said that patients provided written informed consent. Sample size estimates and protocol concealment for all studies were not adequately reported. The presence of other biases was unclear in all of the studies. The risk of bias assessment is shown in Figure 2.

3.4 Meta-analysis

3.4.1 Primary efficacy outcome

3.4.1.1 Comprehensive clinical efficacy

Comprehensive clinical efficacy was reported in 33 studies with low heterogeneity among the studies (I^2 = 0.0%, p = 0.64) and was merged with a fixed-effects model. In a subgroup analysis based on XST dosage, the comprehensive clinical efficacy of the combination of CT and 500 mL of XST (RR = 1.25, 95% CI: 1.19–1.30, p < 0.00001; Figure 3), 450 ml of XST (RR = 1.24, 95% CI: 1.11–1.39, p =

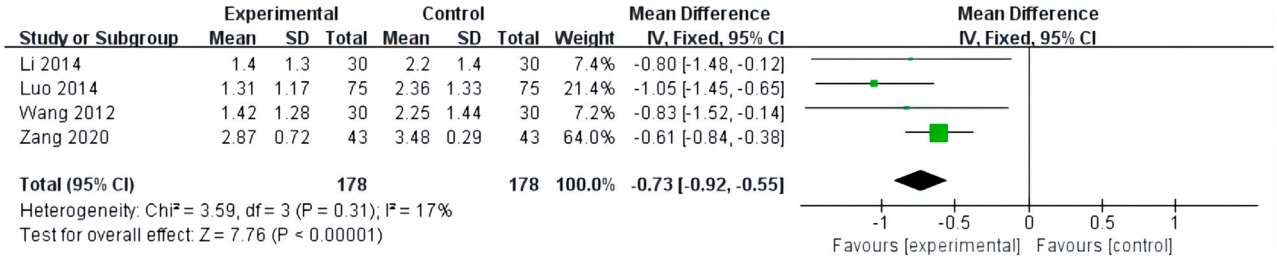

FIGURE 5
Forest plot of frequency of Duration of angina pectoris.

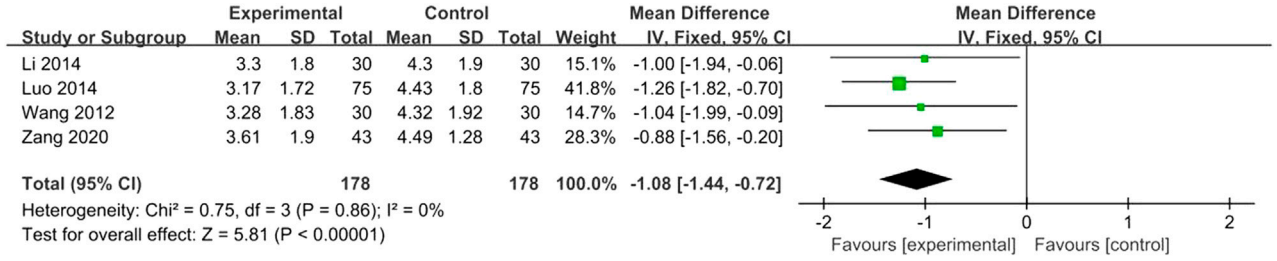

FIGURE 6
Forest plot of duration of angina pectoris.

0.0001; Figure 3), 400 ml of XST (RR = 1.21, 95% CI: 1.13–1.29, $p < 0.00001$; Figure 3), and less than 300 ml (RR = 1.15, 95% CI: 1.08–1.22, $p < 0.00001$; Figure 3) was significantly different from the control group.

3.4.2 Secondary efficacy outcomes

3.4.2.1 ECG improvement

ECG improvement was reported in 18 studies with low heterogeneity among the studies ($I^2 = 0.0\%$, $p = 0.54$) and was merged with a fixed-effects model. In a subgroup analysis based on the dose of XST, the ECG improvement by the combination of CT with 500 mL of XST (RR = 1.30, 95% CI: 1.21–1.39, $p < 0.00001$; Figure 4), 450 mL of XST (RR = 1.38, 95% CI: 1.07–1.77, $p = 0.01$; Figure 4), 400 ml of XST (RR = 1.11, 95% CI: 1.02–1.21, $p = 0.01$; Figure 4), or less than 300 ml (RR = 1.26, 95% CI: 1.04–1.51, $p = 0.02$; Figure 4) was significantly different from the control group.

3.4.2.2 Frequency of angina attacks

The frequency of angina attacks was reported in four studies with low heterogeneity ($I^2 = 17\%$, $p = 0.31$) and was analyzed using a fixed-effects model. The combination of XST and CT decreased the frequency of angina attacks (*MD* = −0.73, 95% *CI:* −0.92 to −0.55, $p < 0.00001$; Figure 5).

3.4.2.3 Duration of angina pectoris

The duration of angina was reported in four studies with low heterogeneity ($I^2 = 0\%$, $p = 0.86$) and was analyzed using a fixed-effects model. The combined use of XST and CT reduced the duration of angina pectoris (*MD* = −1.08, 95% *CI*: −1.44 to −0.72, $p < 0.00001$; Figure 6).

3.4.2.4 Hemorheology levels

Five studies reported total cholesterol and triglyceride levels, and four reported high-density lipoprotein (HDL) and low-density lipoprotein (LDL) levels. There was high heterogeneity among the studies ($I^2 = 99\%$, $p < 0.00001$; $I^2 = 100\%$, $p < 0.00001$; $I^2 = 79\%$, $p = 0.003$; $I^2 = 100\%$, $p < 0.00001$), and the random-effects model was utilized for analysis. The results indicated that XST combined with CT decreased total cholesterol (*MD* = −1.30, 95% *CI:*−1.83 to −0.78, $p < 0.00001$; Figure 7A) and triglyceride levels (*MD* = −0.76, 95% CI: −0.93 to −0.59, $p < 0.00001$; Figure 7B) and increased HDL levels (*MD* = 0.17, 95% *CI* = 0.00 to 0.33, $p = 0.05$; Figure 7C). However, there was no significant difference in LDL levels in patients treated with XST combined with CT compared to CT alone (*MD* = −0.68, 95% *CI*: −1.87 to 0.51, $p = 0.26$; Figure 7D). The greater heterogeneity in the analyses could be due to significant differences in basal lipid levels in the patients included in the studies and differences in XST doses and CT used in the included studies. In addition, the forest plot showed that in terms of total cholesterol and triglycerides, Fei A and Zang studies are more homogenous, and Fei B et al. and Guan et al. studies are more homogenous. This may be because CTs in the studies by Fei A et al. and Zang et al. were very similar, with a

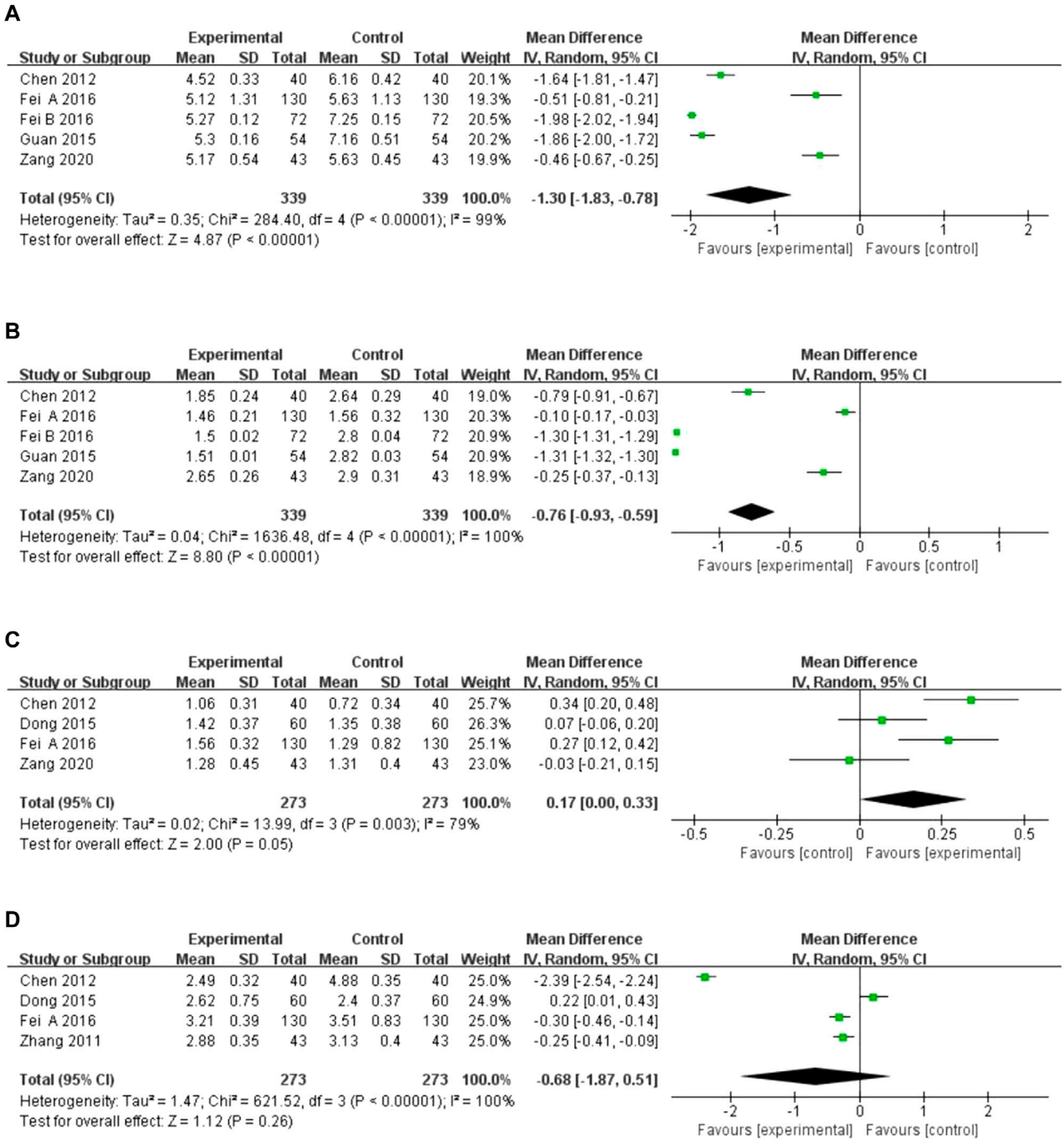

FIGURE 7
Forest plot of hemorheology leve. **(A)** Total cholesterol. **(B)** Triglyceride levels. **(C)** High-density lipoprotein. **(D)** Low-density lipoprotein.

similar average age of the patients. In contrast, the CTs used in the studies by Fei B et al. and Guan et al. were similar.

3.4.2.5 Blood lipid levels

Four studies reported the level of blood lipid levels assessed by different indicators. There was high heterogeneity among the studies, and the random-effects model was used for the analysis (I^2 = 72%, p = 0.03; I^2 = 80%, p = 0.006; I^2 = 87%, p = 0.0006; I^2 = 99%, p < 0.00001). The results showed that XST combined with CT decreased whole blood viscosity at a high shear rate (*MD* = −0.60, 95% *CI*: −0.83 to −0.37, p < 0.00001; Figure 8A), whole blood viscosity at a low shear rate (*MD* = −0.94, 95% *CI*: −1.69 to −0.19, p = 0.01; Figure 8A), and plasma viscosity (*MD* = −0.24, 95% *CI*: −0.46 to −0.03, p = 0.03; Figure 8B). However, no significant difference in the decreases in fibrinogen levels was observed between the patients who received CT combined with XST and those who received CT alone

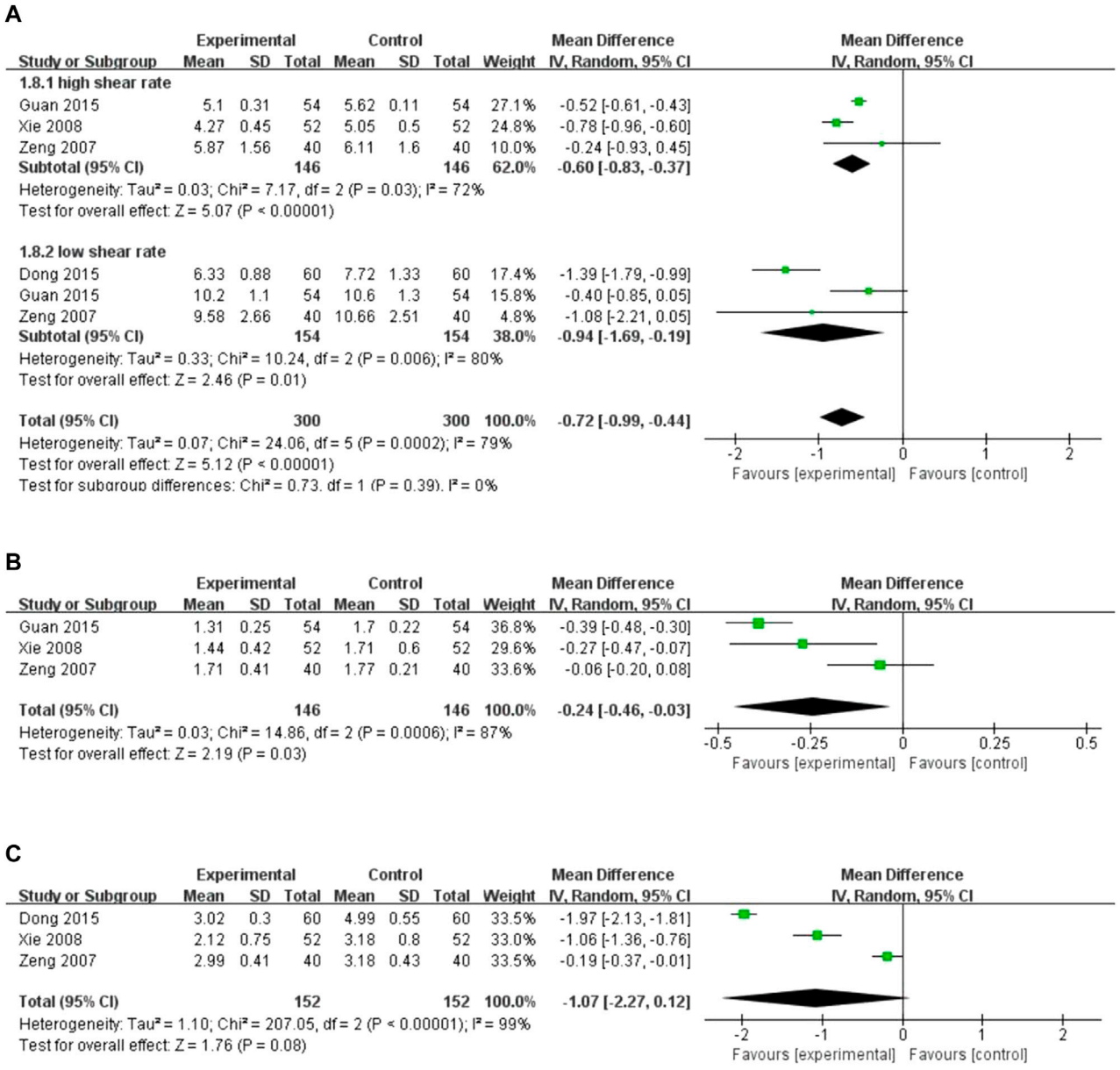

FIGURE 8
Forest plot of blood lipids level. **(A)** Whole blood viscosity. **(B)** Plasma viscosity. **(C)** Fibrinogen levels.

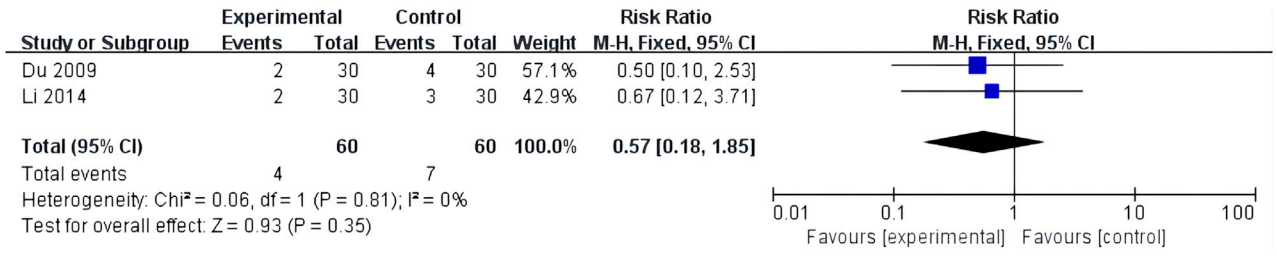

FIGURE 9
Forest plot of sdverse Cardiovascular Events.

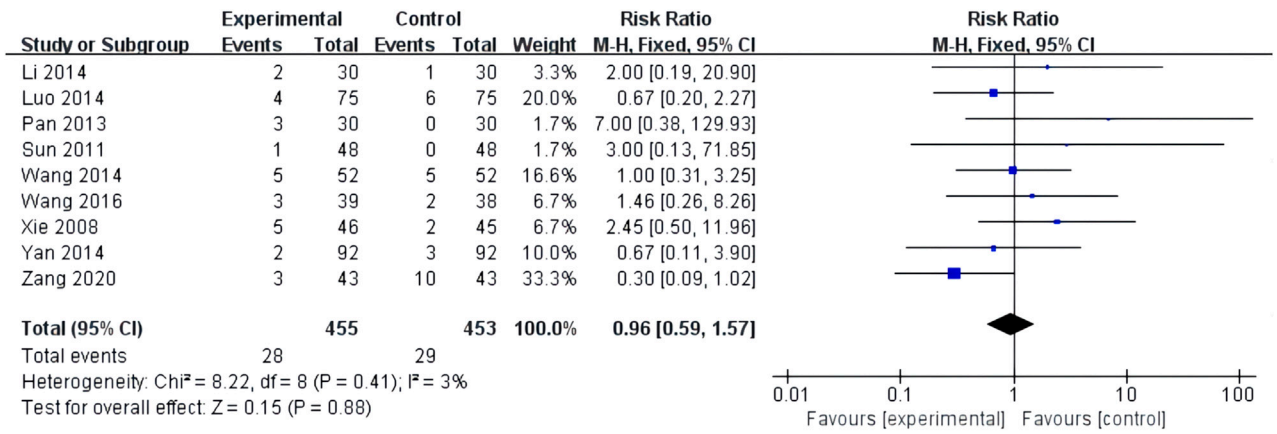

FIGURE 10
Forest plot of adverse events.

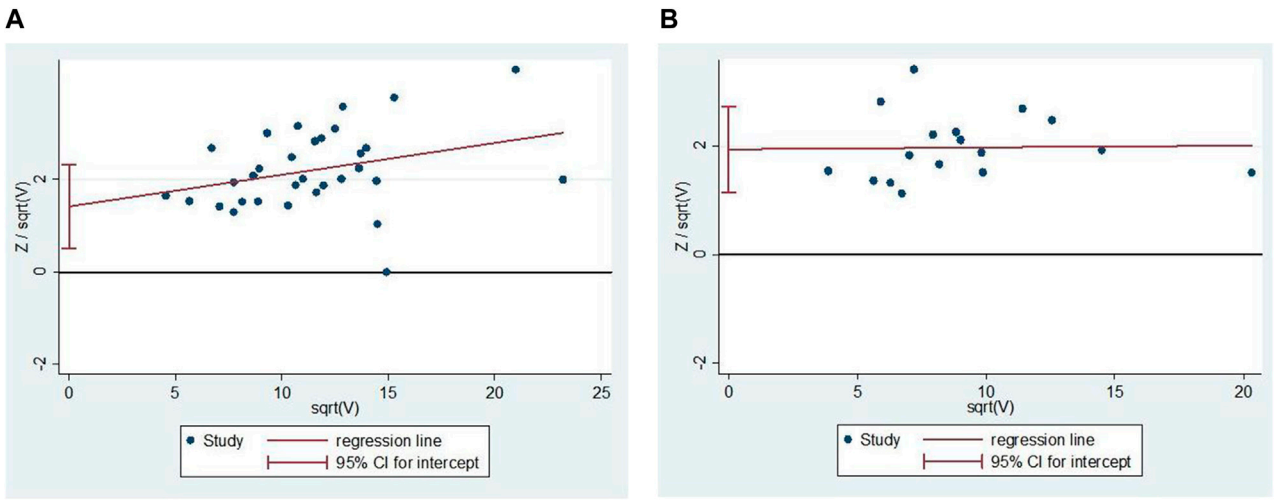

FIGURE 11
Publication bias. **(A)** The Harbord's test on comprehensive clinical efficacy. **(B)** The Harbord's test on ECG improvement.

(*MD* = −1.07, 95% *CI*: −2.27 to 0.12, $p = 0.08$; Figure 8C). Sensitivity analysis was conducted to explore the sources of heterogeneity, but the sources could not be identified. Differences in dosage, duration, and CT regimens among the four included studies could have been responsible for this heterogeneity. Therefore, these results were limited by substantial heterogeneity. More trials with good homogeneity are required to validate the results.

3.4.3 Primary safety outcome

3.4.3.1 Adverse cardiovascular events

Two studies reported adverse cardiovascular events, with low heterogeneity between the two studies ($I^2 = 0\%$, $p = 0.81$). The fixed-effects model analyzed the results. The results revealed no significant difference in cardiovascular events between patients treated with XST combined with CT and those treated with CT alone (*RR* = 0.57, 95% *CI* = 0.18–1.85, $p = 0.35$; Figure 9). The details are shown in Supplementary Material S3.

3.4.4 Secondary safety outcomes

3.4.4.1 Adverse events

Nine studies reported adverse events with low heterogeneity among the studies ($I^2 = 3\%$, $p = 0.41$). The random-effects model helped analyze the adverse reactions, with no significant difference between patients treated with the combination of XST and CT and those treated with CT alone (*RR* = 0.96, 95% *CI* = 0.59–1.57, $p = 0.88$; Figure 10). Our results revealed that gastrointestinal discomfort, tetter, allergy, and subcutaneous ecchymosis constitute the most frequently occurring AEs. These adverse reactions disappeared with

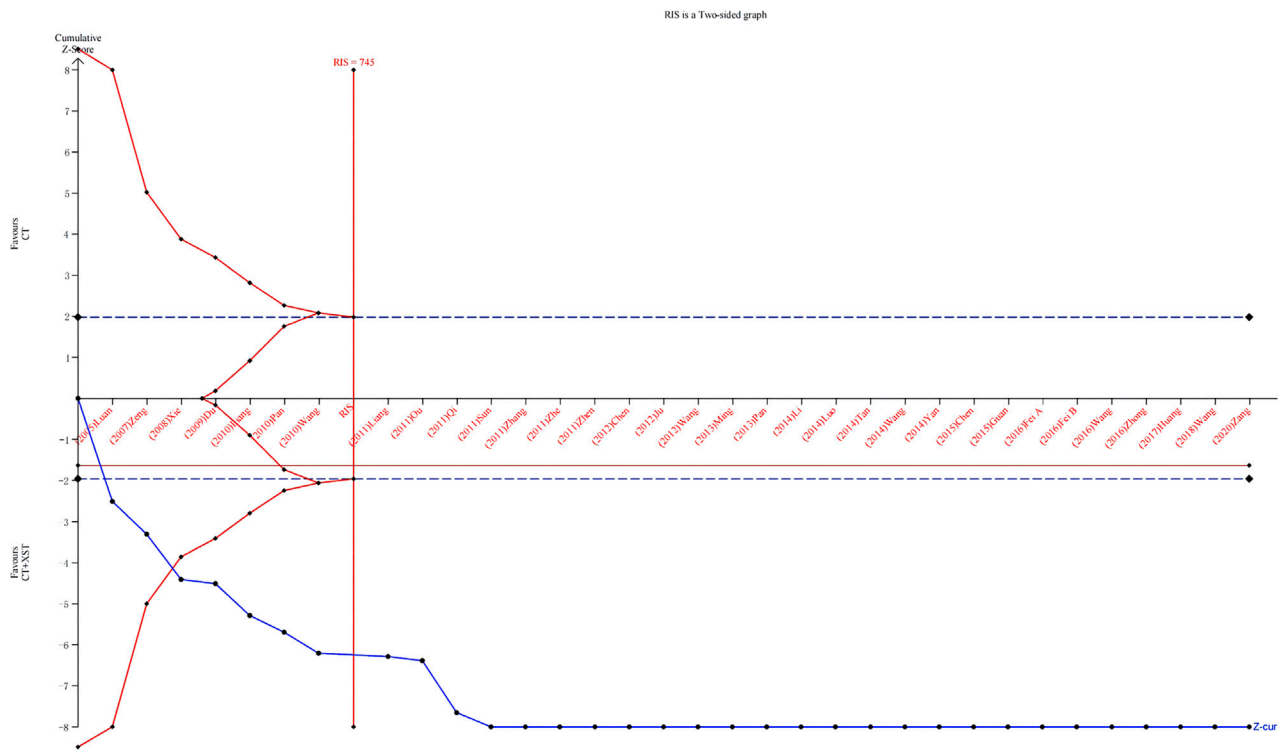

FIGURE 12
Trial sequential snalysis.

symptomatic management. No participants discontinued the study drug due to adverse events. The details are shown in Supplementary Material S4.

3.5 Publication bias

We analyzed the outcome indicators for more than 10 studies for publication bias. Since the heterogeneity was low, the Harbord test was adopted. The results showed publication bias for comprehensive clinical efficacy (p = 0.003; Figure 11A) and ECG improvement (p = 0.000; Figure 11B). There were multiple reasons for the biases, including the ease of publication, the retrieval of positive results, the small sample size of the included studies, and a small sample effect. All the included studies in the analysis were in Chinese, so there was language publication bias.

3.6 Trial sequential analysis

Thirty-three studies reporting comprehensive clinical efficacy were estimated by trial sequential analysis (TSA). Based on the results of related research and this meta-analysis, the class I error definition in this study was set to 0.05, and the statistical efficiency was 0.8. The relative risk reduction (RRR) was 15%, the relative incident rate in the control group was 76.8% (based on the meta-analysis results), and the information axis was set as the cumulative sample size. The TSA analysis showed that the cumulative Z value crossed the traditional boundary value curve (Z = 1.96) and the required information size (RIS) curve. Thus, the cumulative sample size achieved the expected value, the result was stable, and additional tests could not change the conclusion (Figure 12).

3.7 GRADE assessment

All outcome indicators were evaluated using the GRADE system. Due to the low risk of bias, accuracy, and heterogeneity, the certainty quality of the evidence was low or very low. An overview of the GRADE evidence is shown in Table 2. The following six reasons cause the serious risks of deviations and reported deviations: 1) No details on the randomization protocol were reported. 2) The implementation of blinding was not reported. 3) There was a lack of allocation concealment. 4) The heterogeneity between studies was high (p < 0.1, I^2 > 50%). 5) Evaluation of the data suggested publication bias, and an equivalent number of "negative" trials may not be included in this study. 6) The sample size included in the study is too small for imprecision. The results of the evidence quality evaluation of the above outcomes provide a reference basis for guiding clinical practice. More largesamples and high-quality RCTs are needed to improve the evidence of the effectiveness of XST in treating UAP.

TABLE 2 GRADE evidence profile.

Quality assessment							No of patients		Effect		Quality	Importance
No of studies	Design	Risk of bias	Inconsistency	Indirectness	Imprecision	Other considerations	SXT	Control	Relative (95% CI)	Absolute		
Comprehensive clinical efficacy												
33	Randomised trials	Serious[a,b,c]	No serious inconsistency	No serious indirectness	No serious imprecision	Reporting bias[d]	1610/1767 (91.1%)	1318/1761 (74.8%)	RR 1.22 (1.18–1.26)	165 more per 1000 (from 135 more to 195 more)	⊕⊕OO Low	Important
								73%		161 more per 1000 (from 131 more to 190 more)		
Electrocardiogram curative effect												
18	Randomised trials	Serious[a,b,c]	No serious inconsistency	No serious indirectness	No serious imprecision	Reporting bias[d]	765/903 (84.7%)	620/900 (68.9%)	RR 1.23 (1.17–1.29)	158 more per 1000 (from 117 more to 200 more)	⊕⊕OO Low	Important
								66.7%		153 more per 1000 (from 113 more to 193 more)		
Frequency of angina attacks (better indicated by lower values)												
4	Randomised trials	Serious[a,b,c]	No serious inconsistency	No serious indirectness	Serious[e]	None[d]	178	178	—	MD 0.73 lower (0.92–0.55 lower)	⊕⊕OO Low	Critical
TC (better indicated by lower values)												
5	Randomised trials	Serious[a,b,c]	Serious[f]	No serious indirectness	Serious[e]	None[d]	339	339	—	MD 1.3 lower (1.83–0.78 lower)	⊕OOO Very low	Important
TG (better indicated by lower values)												
5	Randomised trials	Serious[a,b,c]	Serious[f]	No serious indirectness	Serious[e]	None	339	339	—	MD 0.76 lower (0.93–0.59 lower)	⊕OOO Very low	Important
HDL-C (better indicated by lower values)												
4	Randomised trials	Serious[a,b,c]	Serious[f]	No serious indirectness	Serious[e]	None	273	273	—	MD 0.17 higher (0–0.33 higher)	⊕OOO Very low	Important
LDL-C (Better indicated by lower values)												
4	Randomised trials	Serious[a,b,c]	Serious[f]	No serious indirectness	Serious[e]	None	273	273	—	MD 0.86 lower (0.94–0.78 lower)	⊕OOO Very low	Important
Whole blood viscosity—high shear rate (better indicated by lower values)												
3	Randomised trials	Serious[a,b,c]	Serious[f]	No serious indirectness	Serious[e]	None	146	146	—	MD 0.6 lower (0.83–0.37 lower)	⊕OOO Very low	Important

(Continued on following page)

10.3389/fphar.2023.1074400

TABLE 2 (*Continued*) GRADE evidence profile.

Quality assessment							No of patients		Effect		Quality	Importance
No of studies	Design	Risk of bias	Inconsistency	Indirectness	Imprecision	Other considerations	SXT	Control	Relative (95% CI)	Absolute		
Whole blood viscosity—low shear rate (better indicated by lower values)												
3	Randomised trials	Serious[a,b,c]	Serious[f]	No serious indirectness	Serious[e]	None	154	154	—	MD 0.94 lower (1.69–0.19 lower)	⊕OOO Very low	Important
Plasma viscosity (better indicated by lower values)												
3	Randomised trials	Serious[a,b,c]	Serious[f]	No serious indirectness	Serious[e]	None	146	146	—	MD 0.24 lower (0.46–0.03 lower)	⊕OOO Very low	Important
Fibrinogen (better indicated by lower values)												
3	Randomised trials	Serious[a,b,c]	Serious[f]	No serious indirectness	Serious[e]	None	152	152	—	MD 1.07 lower (2.27 lower to 0.12 higher)	⊕OOO Very low	Important
Duration of angina (better indicated by lower values)												
4	Randomised trials	[a,b,c]	No serious inconsistency	No serious indirectness	Serious[e]	None	178	178	—	MD 1.08 lower (1.44–0.72 lower)		Critical
Adverse cardiovascular events												
2	Randomised trials	Serious[a,b,c]	No serious inconsistency	No serious indirectness	Serious[e]	None	6/ 60 (10%)	12/60 (20%)	—	200 fewer per 1000 (from 200 fewer to 200 fewer)	⊕⊕OO Low	Critical
								0%		-		
Adverse reactions												
8	Randomised trials	Serious[a,b,c]	No serious inconsistency	No serious indirectness	No serious imprecision	Strong association	25/ 425 (5.9%)	27/ 423 (6.4%)	—	64 fewer per 1000 (from 64 fewer to 64 fewer)		Important
								0%		—		

[a]No details of the random protocol were reported.
[b]Didn't report the implementation of blinding.
[c]Lack of allocation concealment.
[d]Evaluation of the data suggested publication bias, and there may be an equivalent number of "negative" trials didn't be included in this study.
[e]The sample size included in the study is too small to imprecision.
[f]The heterogeneity between studies is large ($p < 0.1$, $I^2 > 50\%$).

10.3389/fphar.2023.1074400

4 Discussion

Through systematic searching and screening, 34 RCTs were finally included in this meta-analysis to compare the efficacy and safety of XST combined with CT compared to CT alone for treating patients with UAP. We found that the combined use of XST and CT showed improved clinical efficacy in treating UAP by reducing the frequency and duration of angina pectoris. Moreover, it improves blood lipid levels and hemorheology parameter values, with no increases in adverse cardiovascular events or reactions.

A noticeable increase in blood viscosity can cause dyslipidemia, a significant risk factor for coronary atherosclerosis. Atherosclerosis causes coronary artery lumen stenosis or blockage, which leads to temporary myocardial blood supply insufficiency and the production of excess pyruvate, lactic acid, and polypeptides. These can stimulate cardiac autonomic ganglions and eventually cause angina pectoralis symptoms, including precordial pain, chest tightness, and palpitations (Qian et al., 2018; Sincer I et al., 2018; Chen and Wang, 2019). The results of a Chinese cohort study (n = 20,954, age 35–64 years) with a 20-year follow-up revealed (Zhang et al., 2018) that low-density lipoprotein cholesterol (LDL-C) levels (from <1.0 mmol/L to ≥4.1 mmol/L) were significantly and positively associated with the risk of coronary heart disease. The lower LDL-C levels were associated with a lower risk of coronary heart disease over the next 20 years and *vice versa*. Based on the results of this meta-analysis, combined treatment with XST and CT could reduce total cholesterol, triglyceride levels, and whole blood viscosity and increase HDL levels compared to CT alone. Qin et al., (2013) found that XST reduced total cholesterol, triglyceride, and LDL-C levels; increased HDL-C levels, and decreased the degree of aortic intimal lesions in atherosclerotic rabbits. The core drug in XST is *Panax notoginseng*, a typical traditional Chinese medicine used to promote blood circulation and remove blood stasis. Some studies (Han et al., 2017) found that *Panax notoginseng* saponins could inhibit platelet adhesion to the injured endothelial cell surface by inhibiting the expression of vascular cell adhesion molecule-1 (VCAM-1) and the secretion of thromboxane A2 (TXA2) by vascular endothelial cells. *Panax notoginseng* saponins also inhibited the expression of VCAM-1 and the release of thromboxane B2 to inhibit platelet activation and play a role in the prevention and treatment of thrombosis. Another study (Wang, 2020) found that *Panax notoginseng* inhibited thromboxane A2 production by increasing cyclic adenosine monophosphate (cAMP) levels in platelets. Additionally, it inhibited calcium ion and 5-hydroxytryptamine (5-HT) release to inhibit thrombus formation. Acute myocardial ischemia is a direct cause of UAP. Wu et al. (Wu et al., 2015) found that XST could reduce the extent of myocardial infarction, lower serum lactate dehydrogenase, creatine kinase, and creatine kinase isoenzyme levels, promote thrombus lysis, inhibit platelet aggregation, and thus, alleviate myocardial ischemic injury in myocardial ischemia model rats.

The safety indicators for this study were the incidence of adverse cardiovascular events and the incidence of adverse reactions. The incidence of adverse cardiovascular events was studied in 120 patients and experienced by 10% (6/60) of the patients treated with XST plus CT and 20% (12/60) of those treated with CT only. The results showed no statistical difference in the safety of XST combined with CT versus CT alone, indicating that XST combined with CT is safe. The incidence of adverse reactions was studied in 848 patients and was observed in 5.8% (25/425) of the patients treated with XST plus CT. Moreover, the incidence of adverse reactions in patients treated with CT alone was 6.3% (27/423). The main adverse reactions were skin pruritus, rash, subcutaneous ecchymosis, and gastrointestinal reactions. The allergic reactions resolved after taking antihistamines, and the gastrointestinal reactions resolved after slowing the infusion speed. There was no statistical difference in the incidence of adverse reactions between the test and control groups, which indicated that adding XST to CT would not increase the incidence of adverse reactions.

However, this study had some limitations. Most articles did not report the severity of angina pectoris, leading to potential heterogeneity. Several included studies did not report specific randomization methods or allocation blinding. It was also unclear whether randomization or blinding methods were implemented, which may have led to implementation and measurement biases. Blinding can objectively evaluate therapeutic effects, and the quality of the blinding method will directly affect the accuracy of the research results. Therefore, future RCT test designs should refer to the items in the Cochrane Collaboration Network's risk of bias tool. Moreover, attention should be paid to implementing randomization and blinding methods in designing trials and their execution. The sample size in the included studies was generally small. Only two studies had a sample size of more than 200 cases, and 22 had fewer than 100 cases. The therapeutic index of a study with a smaller sample size may be unstable. The asymmetrical distribution of the funnel chart indicated publication bias, and the subjective biases of the researchers may have exaggerated the therapeutic effect of UAP in the trial group. XST is a drug in *China's National Catalog of Essential Medicines*, and most of the subjects were Chinese, which may have led to ethnic and geographical biases.

Therefore, the following recommendations were made: 1) The relevant RCT should classify UAP into specific types, including initial angina pectoris, worsening exertional angina pectoris, resting angina pectoris, etc., to ensure targeted conclusions. Simultaneously, the classification of angina pectoris and its course should also be fully and comprehensively reported based on the CONSORT statement (David Moher et al., 2011). This can help identify the source of heterogeneity among studies, carry out subgroup analysis, and analyze the best timing and application of XST. 2) The specific medication category, usage, and dosage of CT must be reported in the primary studies for repeating the procedure. 3) Long-term follow-up after the trials are also necessary, especially for end-point events and safety outcomes. 4) Comprehensive clinical efficacy and ECG Improvement have been reported across most of the original literature. These two indicators are widely used, but the evaluation is difficult to quantify. However, there are few reports on quantifiable indicators, such as the Frequency of Angina Attacks and Duration of Angina Pectoris. Therefore, future research should focus on measurable indicators.

5 Conclusion

The available literature data and systematic evaluation methods demonstrated that XST combined with CT improved the therapeutic effect of UPA, relieved angina symptoms, and improved hemorheology parameter values compared to CT alone. No serious adverse effects were observed in this study, and the addition of XST to CT is conditionally recommended. However, a more rigorous RCT should be designed and completed before the widespread use of XST combined with CT is recommended.

Data availability statement

The original contributions presented in the study are included in the article/Supplementary Material, further inquiries can be directed to the corresponding author.

Author contributions

JX and YX conceived the idea of this study. JX and XC extracted the data. RW and YL performed the quality evaluation and sample size estimation of the data. JX wrote the manuscript. RW and XC revised the manuscript, and YL and YX interpreted the data based on their expertise. All authors contributed to the article and approved the submitted version.

Funding

This study was supported by the National Key Research and Development Program of China (2018YFC1707400).

Conflict of interest

The authors declare that the research was conducted in the absence of any commercial or financial relationships that could be construed as a potential conflict of interest.

Publisher's note

All claims expressed in this article are solely those of the authors and do not necessarily represent those of their affiliated organizations, or those of the publisher, the editors and the reviewers. Any product that may be evaluated in this article, or claim that may be made by its manufacturer, is not guaranteed or endorsed by the publisher.

Supplementary material

The Supplementary Material for this article can be found online at: https://www.frontiersin.org/articles/10.3389/fphar.2023.1074400/full#supplementary-material

References

Balshem, H., Helfand, M., Schünemann, H. J., Oxman, A. D., Kunz, R., Brozek, J., et al. (2011). GRADE guidelines: 3. Rating the quality of evidence. *J. Clin.Epidemiol.* 64, 401–406. doi:10.1016/j.jclinepi.2010.07.015

Chen, J. H., and Wang, J. L. (2019). Effect of ginseng and Taohong Siwu decoction on cardiac function and blood lipids in patients with angina pectoris of coronary heart disease. *China Med. Her.* 16 (24), 135–138.

Chen, T. N., Ge, C. J., Yang, J., and Sun, G. (2012). Clinical observation of Xueshuantong injection in the treatment of unstable angina pectoris. *Mod. Med. Health* 28 (19), 2909–2910.

Chen, Z. (2015). Clinical analysis of Xueshuantong in the treatment of coronary heart disease and angina pectoris in the elderly. *World's latest Med. Inf. Abstr.* 15 (55), 94.

Chinese Medical Association Cardiology Branch, editorial Board of Chinese Journal of Cardiovascular Diseases (2007). Guidelines for diagnosis and treatment of unstable angina pectoris and non-St segment elevation myocardial infarction. *Chin. J. Cardiovasc. Dis.* 35(4), 295–304.

Dong, Y., and Yu, Rui. (2015). Effect of Xueshuantong injection on blood biochemical indexes in patients with unstable angina pectoris. *J. Cardiovasc. Cerebrovasc. Dis. Integr. traditional Chin. West. Med.* 13 (01), 93–94.

Du, Z. A. (2009). Analysis of the efficacy of low molecular weight heparin combined with Xueshuantong in the treatment of 60 cases of unstable angina pectoris. *Clin. Med.* 29 (05), 99–100.

FDA (2007). *Guidance for industry clinical trial endpoints for the approval of cancer drugs and biologics*. May: Food Drug Admin. Available at: http://www.fda.gov/downloads/drugs/guidancecomplianceregulatoryinformation/guidances/ucm071590.pdf.

Fei, H. J., Liu, P., and Xiao, Y. l. (2016). The clinical efficacy of Xueshuantong injection in the treatment of patients with unstable angina. *China Pharmacoeconomics* 11 (09), 58–60.

Feldavus Sarchen (2016). Clinical observation of Atto vastatin combined with Xueshuantong in the treatment of unstable angina pectoris. *China Mod. Med.* 10 (05), 123–124. doi:10.14164/j.cnki.cn11-5581/r.2016.05.098

Feng, P. F., and Jiang, H. F. (1998). The effect of panax notoginseng saponins on Ca~(2+) in SHR myocardial cells and the activity of calcium pump on sarcoplasmic reticulum. *China J. Traditional Chin. Med.* (03), 45–47+65.

Gao, Y., Lv, J., Xie, Y. M., and Sun, M. H. (2019). Systematic evaluation on the efficacy and safety of Xueshuantong (freeze-dried powder) injection in the randomized controlled trial of unstable angina pectoris of coronary heart disease/Meta analysis. *Chin. J. Traditional Chin. Med.* 44 (20), 4366–4378. doi:10.19540/j.cnki.cjcmm.20190724.501

Guan, H. W., Fang, J., and Wang, C. Y. (2015). Effect of Xueshuantong injection on blood pressure, HR and cardiac function in patients with angina pectoris. *Electron. J. Transl. Med.* 2 (09), 75–78.

Guidelines for diagnosis and treatment of non-ST segment elevation acute coronary syndrome 2016 (2017). *Chronicles Cardiovasc. Dis.* 45 (05), 359–376.

Guyatt, G. H., Oxman, A. D., Sultan, S., Glasziou, P., Akl, E. A., Alonso-Coello, P., et al. (2011). GRADE guidelines: 9.Rating up the quality of evidence. *J. Clin. Epidemiol.* 64, 1311–1316. doi:10.1016/j.jclinepi.2011.06.004

Han, S. X., Chen, Y., Zhang, Q., Han, B., Ge, Y. M., Xiang, Y. H., et al. (2017). Study on the molecular pharmacological mechanism of Xueshuantong capsule against platelet adhesion under flow condition. *Chin. J. traditional Chin. Med.* 42 (02), 341–346. doi:10.19540/j.cnki.cjcmm.20161222.014

Huang, T. H. (2017). Clinical observation of Xueshuantong injection in the treatment of unstable angina pectoris. *World's latest Med. Inf. Abstr.* 17 (91), 94. doi:10.19613/j.cnki.1671-3141.2017.91.074

Jia, M. Q., Xiong, Y. J., Xue, Y., Wang, Y., and Yan, C. (2017). Using UPLC-MS/MS for characterization of active components in extracts of yupingfeng and application to a comparative pharmacokinetic study in rat plasma after oral administration. *Molecules* 22, 810. doi:10.3390/molecules22050810

Ju, M. Y., and Dong, J. (2012). Clinical observation on 110 cases of unstable angina pectoris treated with Xueshuantong (freeze-dried powder). *Chin. community physician (medical Major.* 14 (27), 36.

Li, H., Ma, S. H., Wang, Lan., Tian, B., and Sheng, J. F. (2022). Current situation and consideration of safety and aseptic guarantee system of traditional Chinese medicine injection. *Propr. Chin. Med.* 44 (09), 2939–2943.

Li, N. N. (2014). Clinical efficacy of Xueshuantong in the treatment of unstable angina pectoris. *J. Pract. Cardiac, Cerebrovasc. Pulm. Vasc. Dis.* 22 (12), 15–18.

Li, Y. H., and ang Wang, X. M. (2016). On the pharmacological effects of Panax notoginseng on blood system. Chinese Modern Drug use. *Jing* 10 (08), 253–254. doi:10.14164/j.cnki.cn11-5581/r.2016.08.201

Liang, Y. C., and Wu, Rong. (2011). Clinical observation on 30 cases of unstable angina pectoris treated with Xueshuantong injection. *Chin. J. Pract. Chin. West. Med.* (7).

Liang, Z. L. (2010). Clinical observation of Xueshuantong combined with nitroglycerin in the treatment of unstable angina pectoris. *Chin. Pract. Med.* 5 (11), 154–155. doi:10.14163/j.cnki

Liu, K., Sun, D. Q., Liao, X., and Zhang, L. (2019). Interpretation of the risk of bias assessment tool for randomized controlled trials, rev. 2.0. 2016:8565907. *Chin. J. Evid. Based Cardiovasc Med.* 11 (03), 284–291. doi:10.3969/j.issn.1674-4055.2019.03.05

Luan, Y. D., and Sun, L. (2005). Clinical observation on 60 cases of unstable angina pectoris treated with Xueshuantong. *Heilongjiang Med. Sci.* 29 (6), 438.

Luo, J. E. (2014). Efficacy and safety of Xueshuantong injection in the treatment of unstable angina pectoris. *J. Pract. Cardiac, Cerebrovasc. Pulm. Vasc. Dis.* 22 (09), 11–12.

Ming, L. (2013). Clinical observation of nitroglycerin combined with Xueshuantong in the treatment of 93 cases of unstable angina pectoris. *Chin. Foreign Health Abstr.* 10 (8), 64–65. doi:10.3969/j.issn.1672-5085.2013.08.055

Moher, David, Hopewell, S., Schulz, K. F., Montori, V., Gotzsche, P. C., Devereaux, P. J., et al. (2011). CONSORT 2010 explanation and elaboration: Updated guidelines for reporting parallel group randomised trials. *Int. J. Surg.* 10 (1), 28–55. doi:10.1016/j.ijsu.2011.10.001

Ou, E. X. (2011). Effect of Xueshuantong injection on platelet activation in patients with angina pectoris of coronary atherosclerotic heart disease. *Hebei Tradit. Chin. Med.* 33(06), 902–906.

Page, M. J., McKenzie, J. E., Bossuyt, P. M., Boutron, I., Hoffmann, T. C., Mulrow, C. D., et al. (2021). The PRISMA 2020 statement: An updated guideline for reporting systematic reviews. *Int. J. Surg.* 88, 105906. doi:10.1016/jijsu/2021/105906

Pan, G. Z. (2010). Clinical observation of Xueshuantong combined with nitroglycerin in the treatment of 98 cases of unstable angina pectoris. *Chin. Med. refers South* 8 (23), 55–56. doi:10.15912/j.cnki.gocm.2010.23.056

Pan, X. L., Wang, J., and Tang, Dan. (2013). Clinical observation of Xueshuantong in treating 30 cases of unstable angina pectoris of coronary heart disease. *Chin. Minkang Med.* 25 (01), 81–82.

Qi, H., and Dong, Y. W. (2011). Observation on the efficacy of Xueshuantong powder acupuncture in the treatment of unstable angina pectoris. *Chin. J. Clin. Electron. Ed.* 5 (19), 5801–5803.

Qian, H., Chen, J., Xu, H., Luo, Z., and Xiao, C. (2018). Red cell distribution width in coronary heart disease: Prediction of restenosis and its relationship with inflammatory markers and lipids: Prediction of restenosis and itsrelationship with inflammatory markers and lipids. *Postgrad. Med. J.* 94 (1115), 489–494. doi:10.1136/postgradmedj-2018-135806

Qin, Y. N., Liu, H. G., Lu, S. H., Zhang, H. L., Wen, L., Chen, M., et al. (2013). Comparison of preventive effects of Panax notoginseng saponins enteric-coated pellets and Panax notoginseng saponins on atherosclerosis in rabbits. *Chin. J. Exp. Pharm. J. Pharm.* 19 (12), 261–264.

Sincer, I., Aktas, G., Gunes, Y., Mansiroglu, A. K., and Cosgun, M. (2018). Association of mean platelet volume and red blood cell distribution width with coronary collateral development in stable coronary artery disease. *Postepy Kardiol. Interwencyjnej* 14 (4), 263–269. doi:10.5114/aic.2018.78329

Summary of Chinese Cardiovascular Health and Disease report 2019 (2020). *China J. Circulation* 35 (09), 833–854.

Sun, Z. H., Dong, P. F., Sun, D. W., Zhao, L. Y., and Zhang, C. Y. (2011). 48 cases of unstable angina pectoris were treated with Xueshuantong injection. *Harbin Med.* 31 (05), 345.

Tan, J. (2014). Effect of Xueshuantong injection on angina pectoris of coronary heart disease and its effect on platelet activation function. *J. Clin. Ration. Drug use* 7 (16), 42–43. doi:10.15887/j.cnki.13-1389/r.2014.16.007

Tang, X. D., Jiang, J. Q., Jiang, D. C., Yan, C. W., Liu, B. Y., and Gu, D. Y. (2002). Effects of Panax notoginseng saponins on activation and adhesion of neutrophil nuclear factor-κ B during myocardial ischemia-reperfusion. *China Pharmacol. Bull.* 18 (05), 556–560.

Wang, F. B. (2010). Clinical observation of Xueshuantong combined with nitroglycerin in the treatment of 58 cases of unstable angina pectoris. *Chin. Med. refers South* 8 (32), 79–80. doi:10.15912/j.cnki.gocm.2010.32.120

Wang, H. J. (2016). Clinical observation of Xueshuantong freeze-dried powder in the treatment of unstable angina pectoris. *Electron. J. Cardiovasc. Dis. Integr. traditional Chin. West. Med.* 4 (15), 67+70. doi:10.16282/j.cnki.cn11-9336/r.2016.15.046

Wang, L., Gao, Y., and Yuan, Q. C. (2014). Clinical observation of Xueshuantong (lyophilized) in the treatment of unstable angina pectoris. *Jilin Med.* 35 (04), 689–690.

Wang, T. R., and Wei, M. (2018). Effect of Xueshuantong injection on serum IL-6 and MMP-2 in patients with unstable angina pectoris. *China Med. Her.* 15 (15), 127–130.

Wang, Wei, Zhang, Y. D., and He, Xin. (2012). Clinical observation of Xueshuantong in the treatment of unstable angina pectoris. *Chin. Med. Eng. Program* 20 (09), 14–15.

Wang, X. Q. (2020). Research progress on pharmacological effects of panax notoginseng on blood system. *Shanxi Med. J.* 49 (10), 1231–1233.

Wu, T., Zhang, S. F., Dong, S. F., Wu, J. Y., Jia, Z. L., Zhang, S. W., et al. (2015). Effect of Xueshuantong capsule on acute myocardial ischemia and antithrombosis. *Chin. J. Comp. Med.* 25(12), 10–25.

Xie, P. D., and Yan, X. X. (2008). Observation on the efficacy of two methods in the treatment of unstable angina pectoris. *Chin. Trop. Med.* 8 (12), 2174–2175.

Yan, H., and Yu, Z. J. (2014). Efficacy of Xueshuantong in the treatment of unstable angina pectoris. *Contemp. Med.* 20 (14), 124–125.

Zang, C. X. (2020). Clinical study of Xueshuantong injection combined with rosuvastatin in the treatment of unstable angina pectoris. *Mod. Med. Clin.* 35(03), 487–491.

Zeng, L. F. (2007). Clinical observation on 40 cases of unstable angina pectoris treated with Xueshuantong. *World J. Integr. traditional Chin. West. Med.* 2(10), 594,595.

Zhang, Q. G. (2011). Clinical observation of Xueshuantong in the treatment of unstable angina pectoris of coronary heart disease. *Mod. Med. Health* 27 (19), 2960–2961.

Zhang, R. Z., Yu, S. J., Bai, H., and Ning, K. (2017). TCM-Mesh: The database and analytical system for network pharmacology analysis for TCM preparations. *Sci. Rep.* 7, 2821. doi:10.1038/s41598-017-03039-7

Zhang, X., Liu, J., Wang, M., Qi, Y., Sun, J., Liu, J., et al. (2018). Twenty-year epidemiologic study on LDL-C levels in relation to the risks of atherosclerotic event, hemorrhagic stroke, and cancer death among young and middle-aged population in China. *J. Clin. Lipidol.* 12 (5), 1179–1189 e4. doi:10.1016/j.jacl.2018.06.011

Zhe, Y. (2011). Observation on the efficacy of Xueshuantong injection in the treatment of angina pectoris coronary heart disease. *Misc. Rec. Clin. Ration. Drug use* 4 (23), 18–19. doi:10.15887/j.cnki.13-1389/r.2011.23.078

Zheng, D. W. (2011). Clinical observation of Xueshuantong in the treatment of unstable angina pectoris. *Clin. Res. traditional Chin. Med.* 3 (09), 28–29.

Zhong, F. P., Lu, X. W., Jian, Y. Y ., Zeng, Y. Z., and Chen, G. Y. (2016). Observation on the therapeutic effect of Xueshuantong injection on unstable angina pectoris. *Shenzhen J. Integr. traditional Chin. West. Med.* 26 (06), 14–16. doi:10.16458/j.cnki.1007-0893.2016.06.007

frontiers | Frontiers in Pharmacology

TYPE Original Research
PUBLISHED 10 May 2023
DOI 10.3389/fphar.2023.1104243

Check for updates

OPEN ACCESS

EDITED BY
Jian Zhang,
Tianjin Medical University, China

REVIEWED BY
Ding Zhao,
Hebei Medical University, China
Xiaoxu Zheng,
Georgia State University, United States

*CORRESPONDENCE
Jun He,
hejun673@163.com
Qilong Wang,
wangqilong_00@tjutcm.edu.cn

†These authors have contributed equally to this work and share first authorship

RECEIVED 21 November 2022
ACCEPTED 10 April 2023
PUBLISHED 10 May 2023

CITATION
Li S, Zhan J, Wang Y, Oduro PK, Owusu FB, Zhang J, Leng L, Li R, Wei S, He J and Wang Q (2023), Suxiao Jiuxin Pill attenuates acute myocardial ischemia via regulation of coronary artery tone. *Front. Pharmacol.* 14:1104243. doi: 10.3389/fphar.2023.1104243

COPYRIGHT
© 2023 Li, Zhan, Wang, Oduro, Owusu, Zhang, Leng, Li, Wei, He and Wang. This is an open-access article distributed under the terms of the Creative Commons Attribution License (CC BY). The use, distribution or reproduction in other forums is permitted, provided the original author(s) and the copyright owner(s) are credited and that the original publication in this journal is cited, in accordance with accepted academic practice. No use, distribution or reproduction is permitted which does not comply with these terms.

Suxiao Jiuxin Pill attenuates acute myocardial ischemia via regulation of coronary artery tone

Sa Li[1†], Jiaguo Zhan[1†], Yucheng Wang[1†], Patrick Kwabena Oduro[1], Felix Boahen Owusu[1], Jiale Zhang[1], Ling Leng[1,2], Ruiqiao Li[1,2], Shujie Wei[1], Jun He[1,2]* and Qilong Wang[1,2,3,4]*

[1]Institute of Traditional Chinese Medicine, Tianjin University of Traditional Chinese Medicine, Tianjin, China, [2]State Key Laboratory of Component-Based Chinese Medicine, Ministry of Education, Tianjin, China, [3]Haihe Laboratory of Modern Chinese Medicine, Tianjin, China, [4]Endocrinology Department, Fourth Teaching Hospital of Tianjin University of Traditional Chinese Medicine, Tianjin, China

Suxiao Jiuxin Pill (SJP) is a well-known traditional Chinese medicine drug used to manage heart diseases. This study aimed at determining the pharmacological effects of SJP in acute myocardial infarction (AMI), and the molecular pathways its active compounds target to induce coronary artery vasorelaxation. Using the AMI rat model, SJP improved cardiac function and elevated ST segment. LC-MS and GC-MS detected twenty-eight non-volatile compounds and eleven volatile compounds in sera from SJP-treated rats. Network pharmacology analysis revealed eNOS and PTGS2 as the key drug targets. Indeed, SJP induced coronary artery relaxation via activation of the eNOS-NO pathway. Several of SJP's main compounds, like senkyunolide A, scopoletin, and borneol, caused concentration-dependent coronary artery relaxation. Senkyunolide A and scopoletin increased eNOS and Akt phosphorylation in human umbilical vein endothelial cells (HUVECs). Molecular docking and surface plasmon resonance (SPR) revealed an interaction between senkyunolide A/scopoletin and Akt. Vasodilation caused by senkyunolide A and scopoletin was inhibited by uprosertib (Akt inhibitor) and eNOS/sGC/PKG axis inhibitors. This suggests that senkyunolide A and scopoletin relax coronary arteries through the Akt-eNOS-NO pathway. In addition, borneol induced endothelium-independent vasorelaxation of the coronary artery. The K_v channel inhibitor 4-AP, K_{Ca2+} inhibitor TEA, and K_{ir} inhibitor $BaCl_2$ significantly inhibited the vasorelaxant effect of borneol in the coronary artery. In conclusion, the results show that Suxiao Jiuxin Pill protects the heart against acute myocardial infarction.

KEYWORDS

Suxiao Jiuxin Pill, senkyunolide a, scopoletin, borneol, vasorelaxation, acute myocardial infarction

Abbreviations: 4-AP, 4-Aminopyridine; Ach, Acetylcholine chloride; Akt, Protein kinase B; AMI, Acute myocardial infarction; DMSO, Dimethyl sulfoxide; ECG, Electrocardiogram; EF, Ejection fraction; eNOS, Endothelial nitric oxide synthase; ESI-MS, Electrospray ionization mass spectrometry; FS, Fractional shortening; GC-MS, Gas chromatography-mass spectrometry; Gli, Glibenclamide; HUVEC, Human umbilical vein endothelial cells; INDO, Indomethacin; KCl, Potassium chloride; L-NAME, N^G-nitro-L-arginine methyl ester; LC-MS, Liquid chromatography-mass spectrometry; LVID, left ventricular internal dimension diastole; MB, Methylene blue; NO, Nitric oxide; ODQ, 1H- [1,2,4] oxadiazolo [4,2-a] quinoxalin-1-one; PGI_2, Prostacyclin; SJP, Suxiao Jiuxin Pill; SPR:Surfac, e plasmon resonance; TEA, Tetraethylammonium; U46619, 9, 11-Didexy-11α, 9α-epoxymethanoprostaglandin F2α.

1 Introduction

Acute myocardial ischemia (AMI) occurs due to an inadequate supply of oxygen to the myocardium due to narrowed coronary arteries. AMI causes angina, ischemic left ventricular dysfunction, arrhythmias, and myocardial necrosis. Vascular tone regulation is a complex multistep process (Jiang et al., 2015). The vascular endothelium is the innermost structure covering the lining of arteries, capillaries, and veins (Krüger-Genge et al., 2019). Endothelial cells contribute to the regulation of vascular tone by synthesizing and secreting prostacyclin (PGI_2), nitric oxide (NO), and other endothelium-derived relaxation factors (Godo and Shimokawa, 2017). These relaxation factors maintain the balance of the intravascular environment and form the basis for treating coronary artery diseases. In clinical practice, vasodilators, such as nitrates and calcium channel blockers, are used to treat angina and acute coronary syndrome.

Suxiao Jiuxin Pill (SJP) is a well-known medicine in China used in the treatment of coronary heart diseases like angina pectoris, acute coronary syndrome, *etc*. SJP reduces the occurrence of angina attacks and helps alleviate stable and unstable angina symptoms (Duan et al., 2008). In patients with coronary heart disease, SJP improves electrocardiogram (ECG), lowers blood cholesterol, and regulates blood lipid profiles (Ren, L. et al., 2018). Pharmacological studies demonstrate that long-term administration of SJP protects against mitochondrial damage and alters damage-related gene expression in myocardial ischemic injury (Ruan et al., 2017), enhancing atherosclerotic plaque stability (Zhang, J. et al., 2014). Also, short-term administration of SJP could improve blood flow, reduce myocardial ischemia, and protects dogs from angina ischemia (Lu, Z. et al., 2015). In addition, SJP relaxes the human aorta in an endothelium-dependent manner (Bai et al., 2014).

SJP is composed of two components; *Ligusticum chuanxiong* Hort. and *Borneolum syntheticum*. The main chemical constituents are phthalides (e.g., senkyunolide A), phenolic acids (e.g., ferulic acid), alkaloids (e.g., ligustrazine), and borneol (Lei et al., 2018). Borneol exhibits cardioprotective effects by inhibiting apoptosis and reducing Ca^{2+} concentration (Liu, S. et al., 2021). Literature suggests that borneol relaxes the rat aorta in a dose-dependent manner, and K_{ATP} participates in its vasodilatory effect (Santos et al., 2019). Senkyunolide A, tetramethylpyrazine, ligustilide, and ferulic acid in *ligusticum chuanxiong* Hort. also show vasorelaxant effects (Shan Au et al., 2003; Cao et al., 2006; Chan et al., 2007; Zhou et al., 2017).

To understand the cardioprotective role of SJP, it is essential to have evidence of the pharmacological effects *in-vivo* and the molecular signaling pathways targeted by SJP and its active compounds. In this study, a biologically relevant AMI model and coronary artery vasorelaxation assays was used to elucidate the bioactive effects of SJP and identify the main bioactive compounds of SJP that stimulate the vasodilatory signaling pathways that protect against AMI.

2 Methods and materials

2.1 Chemicals and drugs

Suxiao Jiuxin Pill, *Ligusticum chuanxiong* Hort. [Apiaceae, Chuanxiong Rhizoma] extract and *Bornolum syntheticum* were provided by the Tianjin Darentang Group Co., Ltd., the sixth TCM factory (Tianjin, China). Voucher specimens were deposited in the Institute of Traditional Chinese Medicine, Tianjin University of Traditional Chinese Medicine. Scopoletin, senkyunolide H/I/A, sedanolide, ligustilide, angelicide, isochlorogenic acid C, vanillin, tetramethylpyrazine, isochlorogenic acid B, ferulic acid, caffeic acid, isochlorogenicacid A, cryptochlorogenic acid, protocatechuic acid, vanillic acid, neochlorogenic acid, succinic acid, chlorogenic acid, and isoborneol, (Z)-3-butylidenephthalide were purchased from Yuanye Bio-technology Co. Ltd. (Shanghai, China). Acetylcholine chloride (Ach), 9,11-dideoxy-11α, 9α-epoxy-methanoprostaglandin $F_{2\alpha}$ (U46619), N^G-nitro-L-arginine methyl ester (L-NAME), indomethacin (INDO), methylene blue (MB), glibenclamide [Gli, ATP-sensitive K^+ channels (K_{ATP}) inhibitor], 4-aminopyridine [4-AP, voltage-dependent K^+ channels (K_V) inhibitor], tetraethylammonium [TEA, Ca^{2+}-activated K^+ channels (K_{Ca2+}) inhibitor], $BaCl_2$ [inward rectifier K+ channels (K_{ir})inhibitor], diltiazem (L-type calcium channel inhibitor), and dimethyl sulfoxide (DMSO) were purchased from Sigma-Aldrich (St. Louis, MO). HPLC grade acetonitrile was obtained from Fisher Scientific (Fair Lawn, NJ, USA). Potassium chloride (KCl) was bought from Guang Fu Technology Development Co. Ltd. (Tianjin, China). Uprosertib and 1H- [1,2,4] oxadiazolo [4,2-α] quinoxalin-1-one (ODQ) were acquired from MedChemExpress Co. Ltd. (Shanghai, China). All the chemicals were of analytical grade.

2.2 Animal treatment

Male Sprague-Dawley rats (200–250°g), 8–10°weeks old were purchased from SPF Biotechnology Company Ltd. (Beijing, China). All animals were kept in the Animal Center of Tianjin University of Traditional Chinese Medicine under standard conditions of 24°C–27°C, 60–70% relative humidity, and a 12 h light-dark cycle. All animals were fed a regular chow diet and water *ad libitum*. The Tianjin University of Traditional Chinese Medicine Institutional Animal Use and Care Committee approved all experimental procedures in this study with the following approval: No. TCM-LAEC2020079.

The rat AMI model was established by LAD ligation surgery (Li, J. et al., 2021). Rats were randomly divided into 5 groups: Sham, AMI model, SJP-IG group (54 mg/kg, intragastric gavage), SJP-IP group (54 mg/kg, intraperitoneal injection), and nitroglycerin group (0.0071 mg/kg, intragastric gavage). The SJP and nitroglycerin doses are the human equivalent doses calculated based on body surface area. SJP and nitroglycerin were administered immediately after ligation. Rats in both the sham and AMI groups received the same volume of saline.

2.3 Echocardiography

Transthoracic echocardiography was performed using an ultrasound system (Vinno, Suzhou, China) with a 22 MHz transducer at 5, 10, and 20 min after SJP and nitroglycerin treatment. The left ventricular internal dimension diastole (LVIDd), left ventricular internal dimension systole (LVIDs), left ventricular ejection fraction (EF), and fractional shortening (FS) were obtained with the heart rate controlled between 400 and 450 bpm. Three consecutive cardiac cycles were averaged to measure cardiac function.

2.4 Electrocardiogram (ECG)

SD rats were anesthetized and kept in the supine position. Needle electrodes were inserted subcutaneously according to lead II (right front leg, left hind leg, and left front leg) per the ECG protocol. ECG was recorded using PowerLab connected to BioAmp and analyzed by LabChart 8 software (AD instrument, Australia). The ECG signal was continuously monitored before ligation and for 20 min after drug administration. Changes in ECG patterns (ST segment) were analyzed.

2.5 Identification of chemical constituents in rat serum from SJP

2.5.1 Sample preparation

Six SD rats were randomly divided into two groups after 7 days of acclimatization: the liquid chromatography-mass spectrometry (LC-MS) group (n = 3) and the gas chromatography-mass spectrometry (GC-MS) group (n = 3). Then, blood samples (300 μL) were collected (using heparinized centrifuge tubes) from the fossa orbitalis at pre-dose and 5 and 15 min after orally administered SJP at a 54 mg/kg dose. Blood samples were centrifuged immediately at 6000 g for 10 min at 4 °C, and the supernatants were transferred into a clean centrifuge tube. Each 100 μL sample was added to 500 μL of acetonitrile (LC-MS group) or 150 μL of n-hexane (GC-MS group) for protein precipitation and component extraction. The mixtures were centrifuged at 15,000 g for 10 min at 4 °C after being vortexed for 3 min. The GC-MS group obtained supernatants were stored at 4 °C before analysis. The LC-MS group obtained supernatants were transferred to clean 1.5 mL centrifuge tubes, followed by evaporation under a milt nitrogen stream. The obtained residues were individually redissolved in 100 μL of acetonitrile and centrifuged at 15,000 g for 10 min at 4 °C after being vortexed for 3 min. A volume of 10 μL of individual supernatants were then injected for analysis.

2.5.2 LC-MS conditions for identification of non-volatile compounds in serum

Agilent 1290 and Q-TOF 6520 equipped with an X-select HSS T3 column (2.1 × 100 mm, 3.5 μm) were used to separate and detect non-volatile serum compounds after oral administration of SJP. The solvent system consisted of 0.1% formic acid aqueous solution A) and acetonitrile B). Electrospray Ionization Mass Spectrometry (ESI-MS) was set to both positive and negative ionization modes. The mass parameters were set as follows: capillary temperature, 350 °C; auxiliary gas rate, 11 L/h; spray voltage, 135 V; normalized collision energy, 40 V; and mass range, 150–1500 m/*z*.

2.5.3 GC-MS analysis for identification of volatile compounds in serum

Detection of the volatile compounds of SJP in serum was performed on a Shimadzu GC-MS 2010 solution (Shimadzu, Japan) equipped with a DB-17 column (30 m × 0.25 mm × 0.25 μm). Helium was used as the carrier gas at a 1.4 mL/min flow rate. The ion source and interface temperatures were set at 230 °C and 250 °C respectively.

2.6 Network pharmacology analysis

Gene targets of 14 identified serum compounds were summarized from TCMSP (https://old.tcmspe.com/tcmsp.php), BATMAN-TCM (http://bionet.ncpsb.org.cn/batman-tcm/index.php), and Swiss Target Prediction (http://www.swisstargetprediction.ch/). AMI-associated targets were retrieved from OMIM (https://omim.org/), GeneCards (https://www.genecards.org/), and CTD (http://ctdbase.org/). Cytoscape 3.7.2 and DAVID (https://david.ncifcrf.gov/) were used to filter key targets and search for key compounds and pathways. The compounds-targets-pathway network was visualized through Sankey Tools (https://www.zxgj.cn/g/sankey).

2.7 Coronary arterial ring preparation and vascular reactivity assessment

The fresh heart was removed from SD rats and immediately immersed in a petri dish containing a K-H solution composed of NaCl 118 mmol/L, KCl 4.7 mmol/L, $NaHCO_3$ 25 mmol/L, KH_2PO_4 1.2 mmol/L, $MgSO_4$ 1.2 mmol/L, $CaCl_2$ 1.3 mmol/L, and D-glucose 10 mmol/L. The rat coronary arteries were carefully separated and cut into 2 mm rings. The coronary artery from one rat was cut into 2 segments for each sample measurement. The arterial ring was suspended in an organ bath of wire myograph (DMT A/S, Model 630MA, Denmark) containing K-H solution with an aerating mixture of 95% O_2 and 5% CO_2 at 37 °C.

After equilibration, arterial rings were constricted with U46619 (100 nmol/L) to the maximal contraction, and endothelial integrity was evaluated using cumulative concentrations of Ach (10-9–10–5 mol/L). The endothelium was considered intact when the relaxation rate was more than 80%. Endothelium-denuded rings were obtained by rubbing the inner surface of the artery several times with rat whiskers. Finally, the cumulative concentration-response curve for the SJP and its components was investigated. The EC_{50} and R_{max} (maximal vasorelaxation) values were then calculated.

2.8 Cell culture and western blotting analysis

Human umbilical vein endothelial cells (HUVECs) were purchased from AllCells Biotech Co., Ltd. (Shanghai, China). The cells were cultured in an Endothelial Cell Complete Culture Medium (Procell, Wuhan, China) containing 10% FBS and 1% penicillin/streptomycin at 37 °C in a humidified atmosphere of 5% CO_2 and

95% air. The cells within 3-8 passages were used in the following experiments. The cells were serum-starved for 6 h, then treated with senkyunolide A or scopoletin for 15 min. Western blot analysis was performed using anti-eNOS (1:1000), anti-p-eNOS (1:1000, Ser1177), anti-Akt (1:1000), anti-p-Akt (1:1000, Thr308), and anti-GAPDH antibodies (1:1000) (CST, MA, USA).

2.9 Molecular docking

The X-ray 3D crystal structure of the human Akt1 pleckstrin homology (PH) domain, PDB ID: 1H10 (Thomas et al., 2002), was downloaded from the protein data bank repository (http://www.rcsb.org/). The 3D chemical structure of senkyunolide A, or scopoletin, was obtained from the PubChem database. The X-ray crystal protein preparation and the molecular docking were done using Discovery Studio Client (2019) and Autodock Vina, as described in our previous study (Fang et al., 2022), and the results were visualized with PyMOL.

2.10 Surface plasmon resonance (SPR) analysis

To evaluate the binding affinity of senkyunolide A or scopoletin to Akt, an SPR assay was performed using the Biacore T200 (Cytiva Corp., MA, USA). The recombinant human Akt1 protein (Biotechne, Shanghai, China) was immobilized on an S CM5 sensor chip using standard amine-coupling chemistry. A serial dilution of the senkyunolide A (62.5, 125, 250, 500, and 1000 μmol/L) or scopoletin (5, 10, 20, 40, and 80 μmol/L) in running buffer was injected over the human Akt1 protein (1775-KS-010, Bio-Techne). With Biacore T200 evaluation software (Cytiva), the data fit into a 1:1 steady binding model to calculate the binding affinity KD.

2.11 Statistical analysis

SPSS version 21.0 for Windows (SPSS Inc., Chicago, IL, USA) was used for statistical analysis. All values are given as means ± standard error of the mean (S.E.M). Statistical significance was analyzed using one-way or two-way analysis of variance, followed by the Bonferroni *post hoc* analysis, and $p < 0.05$ was considered to be statistically significant.

3 Results

3.1 SJP improves cardiac function and ECG in AMI rats

To assess the therapeutic effect of SJP on angina, AMI was induced in rats by LAD ligation, after which cardiac function was examined. In the rat AMI model, EF and FS were significantly reduced, with an increase in LVIDs and LVIDd values after LAD ligation. SJP treatment (54 mg/kg) significantly reduced EF, FS, and LVID values 5–20 min after intraperitoneal injection and 10–20 min after intragastric gavage administration. Nitroglycerin, as a positive control, exhibited a similar effect on cardiac function (Figure 1A–E). The ST segment elevation in ECG was observed in the AMI model group, compared with sham control rats. However, SJP treatment significantly reduced the ST segment elevation caused by LAD ligation (Figures 1F,G).

3.2 Identification of chemical components in serum from SJP-treated rat

To identify the active ingredients of SJP, LC-MS, and GC-MS analysis were performed on serum from SJP-treated rats and Agilent Masshunter Qualitative Analysis was used to determine the identities of the various circulating compounds. The base peak chromatogram of the non-volatile compounds for the positive and negative ion modes is shown in Figure 2A. By comparing their retention time, mass-to-charge ratio, and secondary mass spectrum to their respective standard chemical compounds and previous phytochemical investigation reports, a total of 28 compounds were identified (Table 1). In addition, a total of 11 volatile circulating compounds were detected when standard chemical compounds were compared to the NIST database. The GC-MS TIC traces chromatogram is shown in Figure 2B and Table 2 lists the GC-MS profiling of the volatile circulating compounds.

3.3 Network pharmacology analysis for SJP targets on AMI

Network pharmacology was used to identify potential pharmacological targets of SJP in the treatment of AMI. A total of 14 compounds found in the serum of SJP-treated rats were mapped to databases of cellular drug targets, and a total of 20 genes, and 15 pathways were identified as a result. To better understand the differential relationship between SJP and AMI, a PPI network was constructed, which identified PTGS2, CASP3, MMP9, and NOS3 genes as the leading targets (Figure 2C). In addition to understanding the cellular connection between SJP and AMI, a pathway enrichment analysis was conducted on the key targets. The cellular pathways through which SJP may exert its beneficial therapeutic effect were identified as lipid and atherosclerosis, fluid shear stress, atherosclerosis, and AGE-RAGE signaling (Figures 2D,E). It was also uncovered that ferulic acid and senkyunolide A were all closely associated with the top two cellular drug targets, PTGS2 and NOS3 (Figure 2F). These findings, combined with the previous observations indicate that PTGS2 and NOS3 play a direct role in the regulation of endothelial function and vascular tone, reveal that SJP improves AMI by regulating artery relaxation.

3.4 Evaluation of the vasorelaxant effect of SJP on coronary artery

A test was conducted to ascertain whether SJP could dilate coronary artery rings. Results revealed that SJP has a concentration-dependent vasodilatory effect on the endothelium-intact coronary artery rings (EC_{50} = 136.1 μg/mL; R_{max} = 80.72 ± 10.27%). Nitroglycerin, as a positive control, relaxed the coronary artery with an EC_{50} of 22.1 μg/mL (Figures 3A–C).

In line with the network pharmacology findings, investigations into whether the NOS3 inhibitor L-NAME or PTGS2 inhibitor

10.3389/fphar.2023.1104243

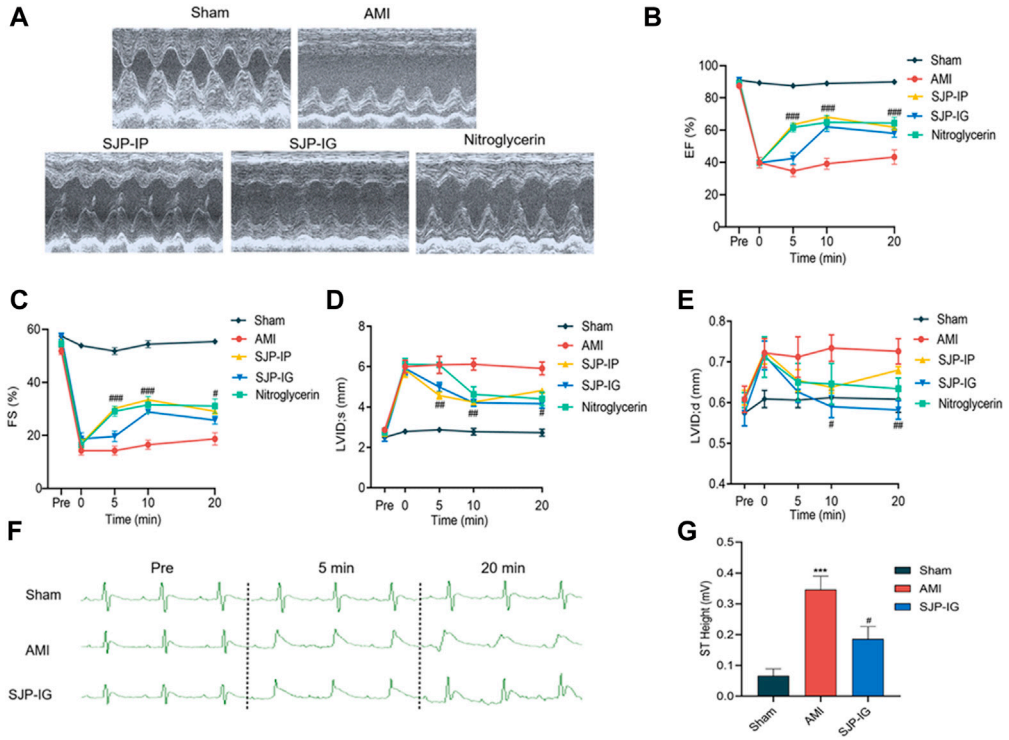

FIGURE 1
Evaluation of cardiac function and ECG in AMI rats treated with SJP. The rat AMI model was established by LAD ligation surgery. AMI rats were treated with SJP (54 mg/kg) by intragastric gavage (SJP-IG), intraperitoneal injection (SJP-IP), or nitroglycerin (0.0071 mg/kg) after LAD ligation. **(A)** Representative ultrasonic image of sham, AMI, SJP-IP, SJP-IG, and nitroglycerin group. AMI rat was administered with the drug for 20 min **(B–E)** Echocardiographic evaluation of cardiac function. Ejection fraction (EF), fractional shortening (FS), the left ventricular internal end-systole diameter (LVID, s), and the left ventricular internal end-diastolic diameter (LVID,d) were measured at 0, 5, 10, and 20 min of drugs administration. **(F)** Representative ECG images of sham, AMI, and SJP-IG group. **(G)** ST segment height in sham, AMI, and SJP-IG groups. N = 5; $^{***}p < 0.001$ vs. sham group; $^{\#}p < 0.05$, $^{\#\#}p < 0.01$, $^{\#\#\#}p < 0.001$ vs. AMI group.

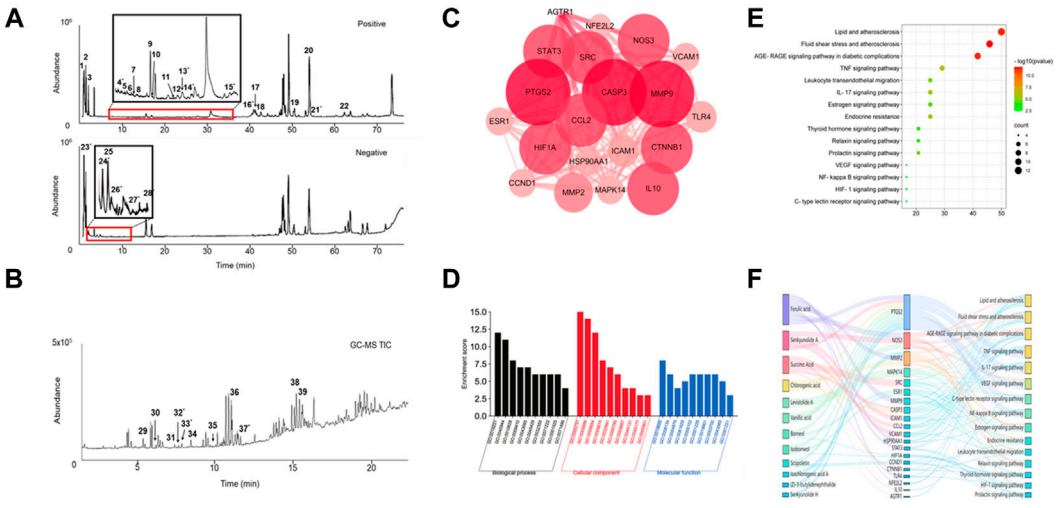

FIGURE 2
Chemical compounds found in serum and network pharmacology analysis. **(A)** The total ion current (TIC) chromatogram in both positive and negative modes for serum from SJP-treated rats. **(B)** The TIC chromatogram of GC-MS for serum from SJP-treated rats. **(C)** The PPI network of 20 intersection gene targets. **(D)** GO analysis. Enriched biological processes, cellular components, and molecular functions. **(E)** KEGG pathway analysis. A bubble diagram of differentially expressed genes. **(F)** The components-target-pathway interaction network of SJP improved AMI.

TABLE 1 Identification of non-volatile metabolites in rat plasma after Suxiao Jiuxin Pill treatment by LC-MS in positive and negative ion mode.

No.	RT time	m/z	Ion mode	Formula	Compound name	ppm	ms/ms
1	0.94	144.1009	$[M + H]^+$	$C_7H_{13}O_2N$	Stachydrine	-7.41	84.0803
2	0.94	116.0694	$[M + H]^+$	$C_5H_9NO_2$	L-Proline	-9.56	70.0655
3	1.27	132.1007	$[M + H]^+$	$C_6H_{13}NO_2$	L-Isoleucine	-9.43	86.0964
4[a]	7.62	193.0497	$[M + H]^+$	$C_{10}H_8O_4$	Scopoletin	1.24	178.0345, 137.0690
5	8.98	227.1260	$[M + H]^+$	$C_{12}H_{18}O_4$	Senkyunolide J	-8.80	153.0535
6	10.32	207.1011	$[M + H]^+$	$C_{12}H_{14}O_3$	Butylidene phthalide	-8.79	161.0551, 189.0879
7	11.05	229.0814	$[M + Na]^+$	$C_{12}H_{14}O_3$	Senkyunolide F	-8.79	161.1055
8	13.26	227.1267	$[M + H]^+$	$C_{12}H_{18}O_4$	Senkyunolide N	-6.66	209.1125
9	15.86	163.0392	$[M + H]^+$	$C_9H_6O_3$	7-Hydroxycoumarine	1.37	107.0435
10	15.93	205.0854	$[M + H]^+$	$C_{12}H_{12}O_3$	7-Hydroxy-3-butylphthalide	-6.80	187.0755
11	22.51	229.0814	$[M + Na]^+$	$C_{12}H_{14}O_3$	(Z)-3-Butylidene-4-hydroxyphthalide	-8.79	189.0884, 161.0965
12	22.78	209.1157	$[M + H]^+$	$C_{12}H_{16}O_3$	Senkyunolide K	-5.62	191.1041, 153.0527
13[a]	24.12	247.0938	$[M + Na]^+$	$C_{12}H_{16}O_4$	Senkyunolide I	-2.85	207.1077
14[a]	25.25	247.0936	$[M + Na]^+$	$C_{12}H_{16}O_4$	Senkyunolide H	-3.06	207.1135
15[a]	36.91	193.1197	$[M + H]^+$	$C_{12}H_{16}O_2$	Senkyunolide A	1.03	175.1031, 147.1072, 137.0527
16[a]	40.25	191.1058	$[M + H]^+$	$C_{12}H_{14}O_2$	3-Butylphthalide	-8.95	173.0779, 145.1045
17	43.61	195.1363	$[M + H]^+$	$C_{12}H_{18}O_2$	Neocnidilide	-7.17	167.0143, 157.0126, 140.9554
18	43.70	191.1075	$[M + H]^+$	$C_{12}H_{14}O_2$	(Z)-Ligustilide	2.61	149.1282, 145.1045
19	52.04	383.2226	$[M + H]^+$	$C_{24}H_{30}O_4$	Senkyunolide P	1.93	191.1080
20	53.86	279.1579	$[M + H]^+$	$C_{16}H_{22}O_4$	Senkyunolide Q	-4.92	191.1017
21[a]	55.53	381.2045	$[M + H]^+$	$C_{24}H_{28}O_4$	Levistolide A	-4.71	335.2108, 191.1020
22	63.24	281.2463	$[M + H]^+$	$C_{18}H_{32}O_2$	Linoleic acid	-4.56	245.2246, 97.1001
23[a]	1.39	117.0191	$[M-H]^-$	$C_4H_6O_4$	Succinic acid	-1.14	72.9920
24[a]	4.22	353.0982	$[M-H]^-$	$C_{16}H_{18}O_9$	Chlorogenic acid	-7.92	136.9158, 130.9671, 96.9604
25	4.49	197.0475	$[M-H]^-$	$C_9H_{10}O_5$	Danshensu	4.68	135.0520
26[a]	5.02	167.0398	$[M-H]^-$	$C_8H_8O_4$	Vanillic acid	-4.19	112.9856, 104.9537
27[a]	8.27	193.0557	$[M-H]^-$	$C_{10}H_{10}O_4$	Ferulic acid	6.73	178.0365, 134.0368
28[a]	10.28	515.1181	$[M-H]^-$	$C_{25}H_{24}O_{12}$	Isochlorogenic acid A	4.85	353.0878, 191.0513

[a]Compounds identified by comparison with reference standards.

INDO could prevent SJP-induced coronary artery relaxation revealed that the relaxation effect of SJP was significantly suppressed by L-NAME treatment (R_{max} dropped from 80.72% to 65.96%) but not by INDO (Figures 3D,E), indicating that SJP modulates the eNOS-NO pathway to induce vasorelaxation.

3.5 Evaluation of vasorelaxant components of SJP

Extracts of the two active ingredients in SJP (*Ligusticum chuanxiong* Hort. and *Borneolum syntheticum*) had potent vasodilatory effects on the endothelium-intact coronary artery rings (Figure 3F). The findings inform that the active compound(s) of SJP is responsible for SJP's vasorelaxation action. It was therefore tested to determine whether the compounds identified in the serum of SJP-treated mice, as well as other chemical compounds isolated from SJP (Lei et al., 2018; Li, S. L. et al., 2003; Liang et al., 2005), could respond to constricted coronary arteries in the vasoreactivity assay. All the compounds tested exhibited concentration-dependent vasodilation effects on coronary artery rings (Table 3). Scopoletin, sedanolide, butylphthalide, senkyunolide A, and borneol particularly had potent relaxation effects.

10.3389/fphar.2023.1104243

TABLE 2 GC-MS TIC parameters on the identified volatile metabolites in plasma from rats treated with Suxiao Jiuxin Pill.

No.	RT (min)	Formula	Molecular weight (m/z)	Identification	SI	Retention index	Ratio (%)
29	6.785	$C_{10}H_{22}$	142.282	3-Ethyl-3-methyl heptane	92	931	0.48
30	7.588	$C_{13}H_{28}$	184.361	3,8-Dimethylundecane	94	1185	0.80
31	8.473	$C_{10}H_{16}O$	152.233	(±)-Camphor	93	1121	0.23
32[a]	8.690	$C_{10}H_{18}O$	154.249	Isoborneol	93	1138	0.17
33[a]	8.855	$C_{10}H_{18}O$	154.249	Borneol	94	1088	0.31
34	9.344	$C_{12}H_{26}$	170.335	Dodecane	96	1214	0.50
35	10.764	$C_{18}H_{38}$	254.494	Octadecane	93	1810	0.71
36	11.364	$C_{12}H_{26}O$	186.334	2-Butyl-1-octanol	88	1393	2.85
37[a]	12.170	$C_{12}H_{12}O_2$	188.223	(Z)-3-Butylidenephthalide	87	1655	0.22
38	14.931	$C_{22}H_{46}$	310.601	Docosane	81	2208	0.39
39	15.321	$C_{13}H_{28}O$	200.361	Isotridecanol	86	1492	2.63

[a]Compounds identified by comparison with reference standards.

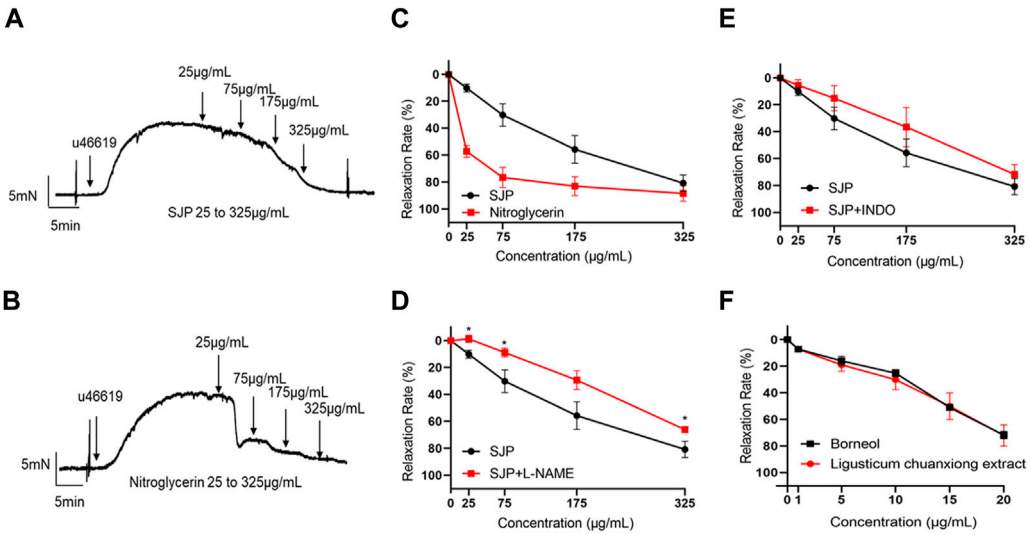

FIGURE 3
The vasorelaxant effect of SJP on coronary artery rings. **(A–B)** The representative tracing of a rat coronary artery treated with SJP **(A)** and nitroglycerin **(B)**. **(C)** The vasodilatory effects of SJP and nitroglycerin on rat coronary artery. **(D–E)** Relaxation curve of SJP on coronary arteries pre-contracted with U46619 in the presence of L-NAME (100 μmol/L) or INDO (10 μmol/L). **(F)** Vasorelaxation effects of *ligusticum chuanxiong* extract and borneol on U46619-induced vascular constriction in endothelium-intact rat coronary artery rings. N = 6, $*p < 0.05$ vs. no L-NAME treatment.

3.6 Vasorelaxation action mechanisms of senkyunolide a and scopoletin

Senkyunolide A, a chemical constituent of *Ligusticum chuanxiong* Hort., was found to relax isolated rat aortas (Chan et al., 2007). In line with the previous finding, this study also shows that senkyunolide A (1 mmol/L) significantly relaxes constricted endothelium-intact coronary artery rings with a R_{max} of 101.77%. However, in the endothelium-denuded coronary artery rings, senkyunolide A R_{max} value decreased to 64.43% (Figures 4A,B). Senkyunolide A relaxation curve and R_{max} value were significantly reduced in coronary artery rings pretreated with L-NAME but not INDO (Figures 4C,D). Furthermore, in the presence of sGC inhibitor ODQ or cGMP inhibitor MB, the relaxation curve and Rmax of senkyunolide A were significantly reduced compared to the control (Figures 4E,F), indicating that senkyunolide A promotes endothelial-dependent vasorelaxation mainly via the eNOS-NO-sGC-cGMP pathway. Coronary arteries are mainly through endothelium-dependent and non-endothelium-dependent dilation. This study revealed that eNOS, sGC, and cGMP inhibitors have limited effect. Senkyunolide A may also play a role in vasodilating through other pathways. Scopoletin, like senkyunolide A, had a potent endothelium-dependent vasorelaxant effect. The R_{max} of scopoletin in endothelium-intact

TABLE 3 Relaxation responses induced by the compounds of Suxiao Jiuxin Pill.

Chemical compound	Relaxation (%)					EC_{50} (μmol/L)
	0.1	1	10	100	1000 (μmol/L)	
Scopoletin	9.88 ± 0.89	48.26 ± 6.84**	75.00 ± 9.69**	91.03 ± 4.68**	96.58 ± 2.76**	1.51
Sedanolide	13.68 ± 1.69*	23.24 ± 3.63**	32.45 ± 6.88*	60.87 ± 11.51**	81.73 ± 17.26**	33.67
Butylphthalide	6.37 ± 6.11	11.2 ± 6.30	28.24 ± 14.28	62.59 ± 9.48**	97.51 ± 6.27**	37.42
Senkyunolide A	6.12 ± 1.4	14.84 ± 6.19	27.31 ± 6.05*	60.37 ± 13.94*	101.78 ± 8.03**	37.82
Ligustilide	5.02 ± 2.99	14.32 ± 3.15	23.07 ± 6.78	50.75 ± 8.01**	89.66 ± 1.82**	67.97
Borneol	7.45 ± 0.65	20.52 ± 7.37	27.39 ± 9.55	48.19 ± 17.46*	83.63 ± 7.00**	119.7
Senkyunolide H	5.28 ± 0.01	17.27 ± 13.25	25.44 ± 13.48	34.65 ± 11.60	73.82 ± 9.47**	174.1
Angelicide	4.99 ± 2.11	16.23 ± 1.22**	27.16 ± 5.35*	42.76 ± 13.45	63.34 ± 12.09**	207.1
Isochlorogenic acid C	3.35 ± 3.69	8.74 ± 1.75	13.23 ± 3.05	21.69 ± 8.21	73.41 ± 14.53**	339.8
Vanillin	3.06 ± 2.00	6.24 ± 4.43	14.83 ± 2.90	22.36 ± 3.28	64.60 ± 5.85**	455.3
Tetramethylpyrazine	3.84 ± 2.77	7.18 ± 2.65	11.33 ± 3.37	19.68 ± 6.00	60.82 ± 10.88**	576.9
Isochlorogenic acid B	3.36 ± 1.54	11.33 ± 9.36	19.37 ± 17.40	22.45 ± 18.93	59.64 ± 15.43*	625.6
Ferulic acid	5.20 ± 2.87	10.93 ± 4.6	17.55 ± 8.13	22.39 ± 6.07	47.72 ± 13.62	>1000
Caffeic acid	6.94 ± 2.83	11.25 ± 7.15	14.30 ± 8.15	21.24 ± 9.73	46.30 ± 9.39*	>1000
Isochlorogenicacid A	6.84 ± 2.73	9.88 ± 1.75	12.04 ± 2.24	25.78 ± 12.43	39.31 ± 14.26	>1000
Cryptochlorogenic acid	9.00 ± 4.21	16.22 ± 5.81	22.30 ± 7.14	28.26 ± 10.89	36.69 ± 15.30	>1000
Protocatechuic acid	6.67 ± 3.83	10.97 ± 6.07	15.38 ± 10.74	23.35 ± 9.90	32.53 ± 6.60	>1000
Vanillic acid	2.88 ± 7.10	9.12 ± 9.84	11.57 ± 15.02	17.75 ± 16.48	29.79 ± 13.03	>1000
Neochlorogenic acid	0.76 ± 1.80	4.24 ± 0.25	10.08 ± 3.89	15.74 ± 7.73	25.86 ± 9.46	>1000
Senkyunolide I	1.79 ± 4.37	5.56 ± 4.10	9.39 ± 5.40	18.22 ± 5.60	23.27 ± 7.67	>1000
Succinic acid	3.41 ± 2.65	6.19 ± 2.92	11.35 ± 4.01	13.33 ± 8.39	22.50 ± 10.24	>1000
Chlorogenic acid	7.38 ± 2.12	14.97 ± 6.15	20.57 ± 4.39	24.96 ± 5.53	22.27 ± 6.72	>1000
Acetylcholine	3.98 ± 4.74	14.82 ± 13.29	97.02 ± 5.54**			2.16

N = 6, *$p < 0.05$, **$p < 0.01$ vs. DMSO.

coronary arteries dropped from 96.58% to 75.98% in endothelium-denuded coronary arteries (Figures 5A,B). Scopoletin relaxation curves decreased significantly in the presence of L-NAME and INDO compared to the control (Figures 5C,D). Furthermore, in the presence of ODQ and MB, the relaxation curves for scopoletin were significantly reduced (Figures 5E,F). These findings indicate that scopoletin induces endothelial-dependent relaxation via both the NO and PGI2 pathways.

3.7 Vasorelaxation of senkyunolide a and scopoletin via akt-eNOS-NO pathway

The Akt kinase is needed to control the phosphorylation of eNOS and, in turn, NO production (Huang et al., 2020). Thus, the Akt-eNOS-NO endothelium-dependent pathway was studied to determine how senkyunolide A and scopoletin induce endothelium-dependent vasorelaxation. In HUVECs, senkyunolide A or scopoletin treatment increased Akt phosphorylation at Thr308 and eNOS phosphorylation at Ser1177 (Figure 6A–B, Supplementary Figure S1). Following that, *in silico* molecular docking was used to ascertain whether senkyunolide A or scopoletin could bind to critical regulatory sites on Akt, thereby promoting its phosphorylation.

For PDK1 or mTOR2 to phosphorylate Akt, the pleckstrin homology (PH) of Akt must first bind to the lipid second messengers PI (3,4,5) P3 and PI (3,4) P2 (Truebestein et al., 2021). Senkyunolide A and scopoletin both exhibited a strong binding affinity for the Akt1 PH domain (PDB ID: 1H10), with the former having a binding energy of -4.8 kcal/mol and the latter having a binding energy of -5.3 kcal/mol. Additionally, protein-ligand interaction analyses showed that senkyunolide A forms three hydrogen bonds with GLU17, ILE19, and ARG23, while scopoletin forms six hydrogen bonds with LYS14, GLU17, TYR18, ILE19, ARG23, and ASN53 (Figures 6C,D). This indicates that senkyunolide A and scopoletin may exert a

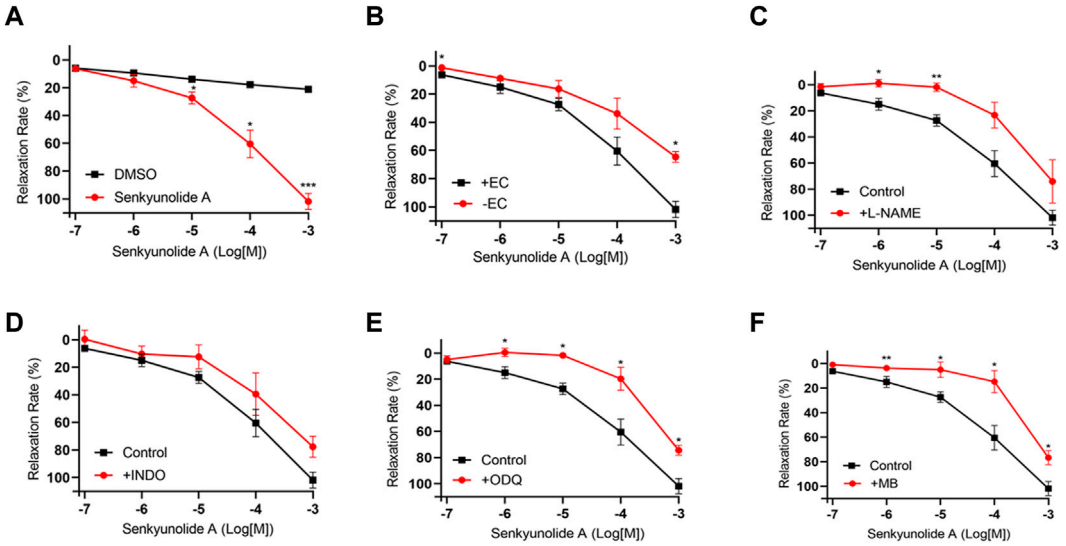

FIGURE 4
Endothelium-dependent mechanism of the vasodilation action of senkyunolide **(A)** **(A)** Relaxation curve of senkyunolide **(A)** **(B)** Relaxation curve of senkyunolide A on endothelium-intact (+EC) and endothelium-denuded (-EC) coronary artery rings. **(C–F)** Relaxation curve of senkyunolide A on coronary artery ring pretreatment with eNOS inhibitor L-NAME (100 μmol/L), COX inhibitor INDO (10 μmol/L), sGC inhibitor ODQ (10 μmol/L), or cGMP inhibitor methylene blue (MB) (10 μmol/L) in endothelium-intact artery rings. Arteries were pre-constricted with U46619. N = 6, $*p < 0.05$, $**p < 0.01$, $***p < 0.001$ vs. control.

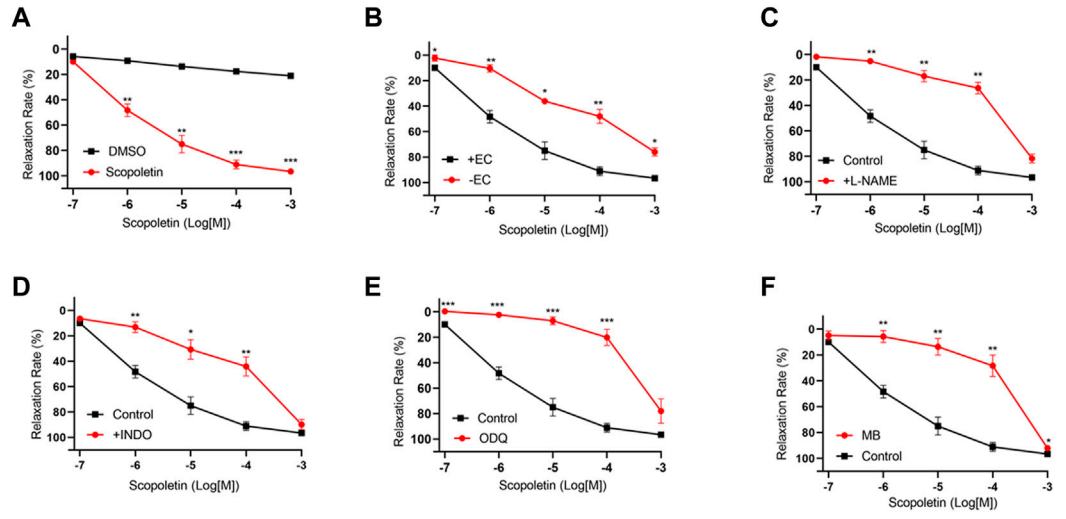

FIGURE 5
Endothelium-dependent mechanism of the vasorelaxation action of scopoletin. **(A)** Relaxation curve of scopoletin. **(B)** Relaxation curve of scopoletin on endothelium-intact (+EC) and endothelium-denuded (-EC) coronary artery rings. **(C–F)** Relaxation curve of scopoletin on coronary artery ring pretreatment with L-NAME (100 μmol/L), INDO (10 μmol/L), ODQ (10 μmol/L), or MB (10 μmol/L) in endothelium-intact artery rings. Arteries were pre-constricted with U46619. N = 6, $*p < 0.05$, $**p < 0.01$, $***p < 0.001$ vs. control.

regulatory activity on Akt phosphorylation through their interaction with key binding site residues in the PH domain. The SPR biophysical assay was carried out with recombinant Akt protein to investigate the direct interaction between senkyunolide A/scopoletin and Akt. The SPR assay consistently demonstrated that senkyunolide A or scopoletin interacts with Akt in a dose-dependent manner (Figures 6E,F). The value of the equilibrium dissociation constant (*KD*) for scopoletin was determined to be 11.09 μmol/L, while the value for senkyunolide A was 752 μmol/L.

Uprosertib, an inhibitor of Akt, decreased the expression of p-eNOS in HUVECs that had been treated with senkyunolide A and

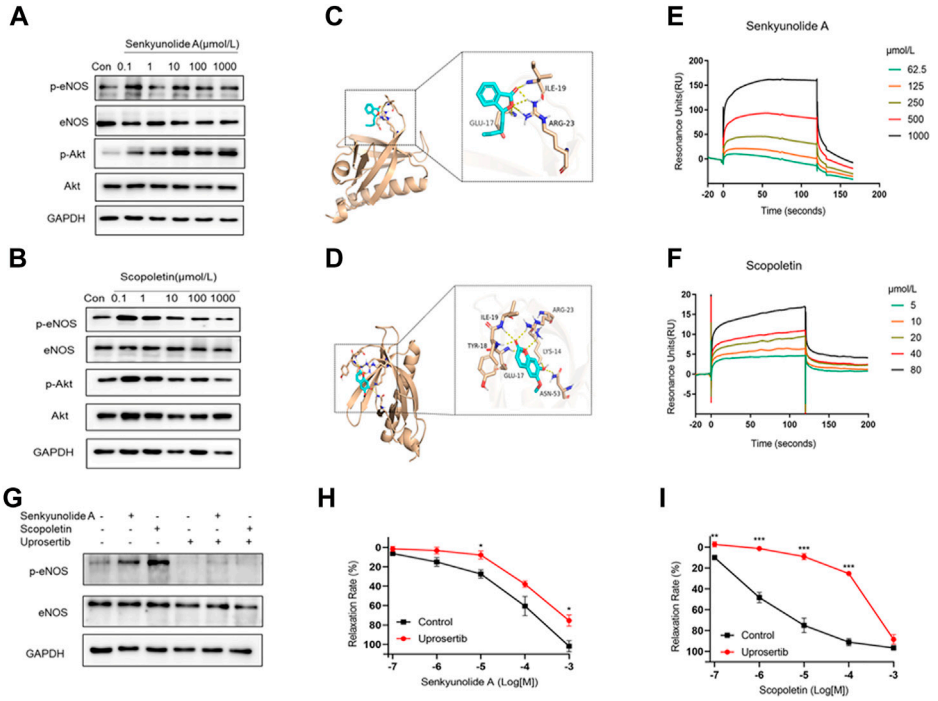

FIGURE 6
Senkyunolide A and scopoletin induced vasodilation via the Akt-eNOS pathway. **(A–B)** Western blot analysis of p-eNOS, eNOS, p-Akt, and Akt in HUVECs treatment with the indicated concentration of senkyunolide A **(A)** or scopoletin **(B)**. **(C–D)** Prediction of senkyunolide A **(C)** and scopoletin **(D)** binding with Akt by *in silico* molecular docking. **(E–F)** The real-time interactions between senkyunolide A **(E)** or scopoletin **(F)** and Akt were determined by SPR kinetic assay. **(G)** HUVECs were treated with the Akt inhibitor uprosertib (10 μmol/L) for 30 min before exposure to senkyunolide A or scopoletin (100 μmol/L). The regulation effect of senkyunolide A or scopoletin on p-eNOS was measured by Western blot analysis. **(H–I)** The cumulative concentration-response curve of senkyunolide A **(H)** or scopoletin **(I)** in endothelium-intact rings in the presence of uprosertib. N = 3, $*p < 0.05$, $**p < 0.01$, $***p < 0.001$ vs. control.

scopoletin (Figure 6G, Supplementary Figure S2). Consistently, in *ex-vivo*, coronary artery rings pretreated with 10 μmol/L of uprosertib, the relaxation curves of senkyunolide A and scopoletin were significantly decreased compared to the negative control (Figures 6H,I), indicating that senkyunolide A and scopoletin trigger endothelium-dependent vasodilation via the activation of the Akt-eNOS-NO signaling pathway.

3.8 Vasorelaxation action mechanisms of borneol

The EC_{50} value for borneol-induced concentration-dependent coronary artery ring relaxation was 119.7 μmol/L, and the R_{max} value was 83.63% (Table 3). However, the R_{max} value did not decrease in endothelium-deficient coronary arteries, which shows that the vasorelaxation action of borneol was caused by pathways that do not depend on endothelium (Figures 7A,B). The vasorelaxation effect of borneol was blocked in the presence of potassium channel inhibitors like $BaCl_2$, TEA, or 4-AP (Figures 7C–E). However, the vasodilation activity of borneol was unaffected by the K_{ATP} inhibitor glibenclamide or the L-type calcium channel inhibitor diltiazem (Figures 7F,G), indicating that borneol likely stimulates the opening of K_{ir}, K_{Ca2+}, and K_v channels in vascular smooth muscle cells to induce vasorelaxation.

4 Discussion

This study reveals the anti-angina pectoris and vasorelaxant effects of Suxiao Jiuxian Pill and clarifies the molecular mechanism of its bioactive constituents. This study reveals that Suxiao Jiuxin Pill alleviates acute myocardial infarction. Senkynolide A, scopoletin, and borneol are Suxiao Jiuxin Pill's bioactive compounds responsible for coronary artery relaxing actions. Senkynolide A and scopoletin relax coronary arteries by activating the endothelium-dependent Akt-eNOS-NO pathway. Borneol also relaxes coronary artery rings by activating K_{ir}, K_{Ca2+}, and K_v channels in endothelium vascular smooth muscle cells. These findings demonstrate that Suxiao Jiuxin Pill's anti-AMI effects are primarily mediated via coronary artery relaxation. Furthermore, the active compounds responsible for vasodilation are senkynolide A, scopoletin, and borneol.

Suxiao Jiuxin Pill is a well-known medicine used traditionally in China for the treatment of coronary heart diseases such as angina and acute coronary syndrome (Ren, L. et al., 2018). Sublingual administration of the Suxiao Jiuxin Pill provides rapid relief from angina (Duan et al., 2008). Suxiao Jiuxin Pill improves cardiac function after 5 min of intraperitoneal injection to mimic sublingual administration, which is faster than oral administration. Similarly, Lu *et al.* found that 30 min of duodenum infusion with the Suxiao Jiuxin Pill could attenuate

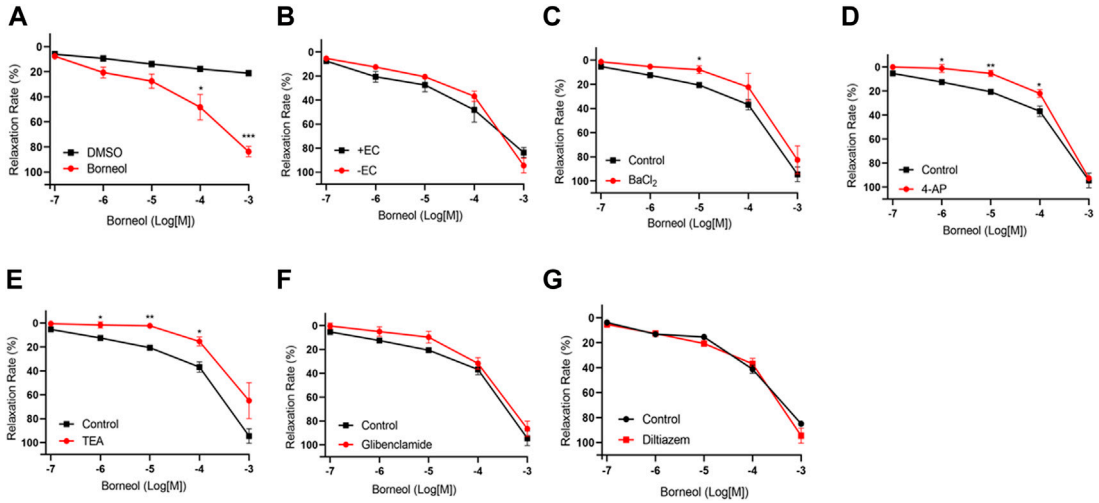

FIGURE 7
Endothelium-independent mechanism of the vasorelaxation action of borneol. **(A)** Relaxation curve of borneol. **(B)** Relaxation curve of borneol on coronary artery rings with or without endothelium. **(C–G)** Relaxation curve of borneol on endothelium-denuded coronary artery pretreatment with BaCl2 **(C)**, 4-AP **(D)**, TEA **(E)**, glibenclamide **(F)**, or diltiazem **(G)**. N = 6, $*p < 0.05$, $**p < 0.01$ vs. control.

myocardial ischemia, elevate the ST segment, and enhance serum SOD activity in MI dogs (Lu, Z. et al., 2015). These findings indicate that the Suxiao Jiuxin Pill possesses anti-anginal properties.

Coronary heart disease is caused by narrowed and blocked coronary arteries, which deprive the cardiac muscle of oxygen and nutrients (Du et al., 2021). Using LC-MS and GC-MS, 39 non-volatile and volatile compounds were identified in the sera of Suxiao Jiuxin Pill-treated rats. Network pharmacology analysis identified NOS3 and PTGS2 as core acute myocardial ischemia targets. NOS3 and PTGS2 proteins regulate vasodilation by inducing endothelial NO and PGI2 production. For this reason, it was hypothesized that Suxiao Jiuxin Pill's action on alleviating AMI might partially be due to its ability to induce endothelium-dependent vasorelaxation. Suxiao Jiuxin Pill did induce concentration-dependent vasorelaxant effects on coronary artery rings, with an EC_{50} value of 136.1 ug/mL. He *et al.* found that the Suxiao Jiuxin Pill relaxes the U46619-contracted human internal mammary artery with an EC_{50} of 645.65 ug/ml (Bai et al., 2014). L-NAME treatment prevented Suxiao Jiuxin Pill-induced vasorelaxation in both the coronary and internal mammary arteries. These findings corroborate the NOS3 pathway predicted by network pharmacology and show that the Suxiao Jiuxin Pill induced coronary arteries in a manner dependent on the endothelium.

In this study, 22 compounds from both the botanical material of Suxiao Jiuxin Pill as well as the sera of Suxiao Jiuxin Pill-treated mice were used to identify bioactive compounds responsible for the vasorelaxation effects of Suxiao Jiuxin Pill (Lei et al., 2018). The potential of these compounds to elicit vasorelaxation responses in coronary arteries with intact or denuded endothelium varied. A strong vasodilation response was induced by scopoletin, borneol, and four phthalides: sedanolide, butylphthalide, senkyunolide A, and ligustilide. Recent studies have shown that ligustilide (Chan et al., 2007), borneol (Silva-Filho et al., 2012), and the combination of senkyunolide A and liqustilide (Lei et al., 2018) have vasodilation activity on the aorta and mesenteric artery. This lends credence to the hypothesis that the vasorelaxant effect of Suxiao Jiuxin Pill may be attributed to the presence of these chemical compounds.

Senkyunolide A is a *ligusticum wallichii*-derived phthalide (Lei et al., 2018; Liu, J. L. et al., 2014). Some studies have emphasized the role of senkyunolide A in vasorelaxation. This study reveals that senkyunolide A causes vasorelaxation via an endothelium-dependent pathway. The two essential pathways that regulate endothelium-dependent vasorelaxation are NO/sGC/cGMP and PGI_2/AC/cAMP (Cohen, 1995). Results from this study show that L-NAME, methylene blue, or ODQ, which are all well-known inhibitors of the NO/sGC/cGMP pathway, inhibited senkyunolide A-induced vasorelaxation. INDO did not affect the relaxations induced by senkynolide A, suggesting that the endothelium-dependent relaxation induced by senkynolide A involves the NO-mediated vasodilatory pathway. Regulation of smooth muscle membrane potential through alteration in K channel activity is a major mechanism of vasodilation and vasoconstriction under both physiological and pathophysiological conditions (Li, X. et al., 2011). The diastolic mechanism of senkyunolide A for ion channels is unknown and needs to be further studied.

Many kinases stimulate the phosphorylation of eNOS at Ser1177 and NO production (Lee et al., 2018). These kinases include Akt, PKA, AMPK, PKG, and CaMKII. In this study, senkyunolide A led to an elevated phosphorylation of Akt-T308 and subsequently eNOS. Moreover, uprosertib, an Akt inhibitor, inhibited both Akt phosphorylation and endothelium-dependent relaxation, demonstrating that senkyunolide A induced vascular tone changes in rat-isolated coronary arteries via the endothelium

Akt-eNOS-NO pathway. Senkyunolide A and ligustilide from Suxiao Jiuxin Pill showed Ca^{2+}-inhibitory activity by activating CaMKII in VSMCs and causing thoracic aortic relaxation (Lu, Y. et al., 2022). These results suggest that senkyunolide A causes vasorelaxation by increasing CaMKII activity in VSMCs and activating the Akt/eNOS/NO pathway in endothelial cells. Scopoletin is a coumarin derivative isolated from *Liqusticum* chuanxiong Hort. (Ren, D. C. et al., 2007), *Liqusticum* jeholense Nakai et Kitagawa (Zhang, J. L. et al., 1996), and other plants. Scopoletin possesses various pharmacological properties including vasorelaxation, anti-angiogenesis, and anti-inflammation (Pan et al., 2011). In this study, scopoletin-mediated relaxation was inhibited by both L-NAME and INDO, indicating that scopoletin endothelium-dependent relaxation occurs via the NO and PGI_2 pathways. Scopoletin, like senkyunolide A, stimulates vasorelaxation by activating the Akt-eNOS-NO pathway.

Molecular docking is a molecular bioinformatics technique for predicting the binding mode and the intermolecular interactions between ligands and their target receptor or protein. The pleckstrin homology (PH) domain of Akt is critical in the phosphorylation process of Akt (Truebestein et al., 2021). Both senkyunolide A and scopoletin exhibited high binding affinities for the Akt1 PH domain. Senkyunolide A forms hydrogen bonds with amino acid residues Glu17, ILE19, and ARG23, whiles scopoletin forms hydrogen bonds with amino acid residues LYS14, GLU17, TYR18, ILE19, ARG23, and ASN53. Biophysical characterization study further confirmed the molecular interaction between senkyunolide A or scopoletin and Akt.

The conclusion that scopoletin does not induce endothelium-independent vasorelaxation is inconsistent with the findings of some earlier studies. For instance, a previous study found that scopoletin induces vasorelaxation of the rat thoracic aorta via the blockage of intracellular Ca^{2+} mobilization from noradrenaline-sensitive stores (Oliveira et al., 2001) or inhibits Ca^{2+} release from the sarcoplasmic reticulum (Iizuka et al., 2007). Moreover, EC_{50} values for the vasorelaxation activities of scopoletin in arteries appear distinct. In the rat coronary artery, the EC_{50} value was 1.51 μmol/L, while in the rat mesenteric artery, the EC_{50} value was 112 μmol/L. Also, in rat aortic rings, the EC_{50} value was 180–335 μmol/L. This suggests that scopoletin has tissue-specific sensitivity effects, and it is extremely treatment-sensitive to the coronary artery. Thus, scopoletin might be a potent drug candidate for the treatment of myocardial ischemia.

Borneol is another compound found in Suxiao Jiuxin Pill. Findings from this study indicate that borneol induces vasorelaxation activity via endothelium-independent pathways. Endothelium-independent vasodilation is achieved mainly by antagonizing or activating various ion channels on the VSMCs membrane, such as the K^+ channel and Ca^{2+} channel. In VSMCs, four distinct types of K^+ channels have been identified: K_{Ca2+}, K_V, K_{ATP}, and K_{ir} (Dogan et al., 2019). Modulating K^+ channel opening results in VSMCs membrane hyperpolarization and voltage-gated calcium channel closure, which inhibits Ca^{2+} influx and subsequent vasodilation (Yao et al., 2016). Indeed, pretreatment with $BaCl_2$, TEA, or 4-AP, but not Glibenclamide, reduced borneol's vasorelaxation effect, demonstrating that borneol's vasodilation is primarily triggered by the opening of K_v, $K_{Ca2+,}$ and K_{ir} channels. This result is consistent with a previous study that found that (-)-borneol induces an endothelium-independent vasorelaxant effect by a reduction in Ca^{2+} influx and activation of K_v, $K_{Ca2+,}$ and K_{ir} (Silva-Filho et al., 2012). In contrast, (-)-borneol relaxed rat aortic rings via NO and PGI_2-mediated endothelium-dependent vasorelaxation and directly impacted VSMCs via K_{ATP} channels (Santos et al., 2019). Thus, the mechanism of action of (-)-borneol-induced vasodilation is complicated and requires further investigation.

Overall, Suxiao Jiuxin Pill improves cardiac function in acute myocardial ischemia and causes vasorelaxation of the coronary artery. In addition, it was revealed that scopoletin, phthalides, and borneol are the primary bioactive compounds of Suxiao Jiuxin Pill that contribute to its vasodilatory effects. Vasorelaxation induced by senkyunolide A and scopoletin is through the endothelium-dependent Akt-eNOS-NO pathway. Borneol triggers vasodilation in VSMCs by opening potassium channels.

Data availability statement

The datasets presented in this study can be found in online repositories. The names of the repository/repositories and accession number(s) can be found in the article/Supplementary Material.

Ethics statement

The animal study was reviewed and approved by The Tianjin University of Traditional Chinese Medicine, Institutional Animal Use and Care Committee. Written informed consent was obtained from the owners for the participation of their animals in this study.

Author contributions

SL performed the *in vitro* and *ex vivo* experiments and wrote the manuscript. JZ performed the animal experiments. YW and SW performed the UPLC/Q-TOF-MS, GC-MS, and network pharmacology analysis. PK Oduro, Felix Boahen Owusu, LL, and RL wrote the manuscript. JZ performed molecular docking. JH and QW designed the research and supervised the study.

Funding

This study was supported by the National Key R&D Program of China (2022YFC3501800), The National Program for NSFC, China (81973624), the Science and Technology Program of Tianjin, China (21ZYJDJC00070), and the Innovation Team and Talents Cultivation Program of National Administration of the Traditional Chinese Medicine (ZYYCXTD-D-202002, ZYYCXTD-C-202203).

Conflict of interest

The authors declare that the research was conducted in the absence of any commercial or financial relationships that could be construed as a potential conflict of interest.

Publisher's note

All claims expressed in this article are solely those of the authors and do not necessarily represent those of their affiliated organizations, or those of the publisher, the editors and the reviewers. Any product that may be evaluated in this article, or claim that may be made by its manufacturer, is not guaranteed or endorsed by the publisher.

Supplementary material

The Supplementary Material for this article can be found online at: https://www.frontiersin.org/articles/10.3389/fphar.2023.1104243/full#supplementary-material

References

Bai, X. Y., Zhang, P., Yang, Q., Liu, X. C., Wang, J., Tong, Y. L., et al. (2014). Suxiao jiuxin pill induces potent relaxation and inhibition on contraction in human artery and the mechanism. *Evid. Based Complement. Altern. Med.*, 2014, 956924. doi:10.1155/2014/956924

Cao, Y. X., Zhang, W., He, J. Y., He, L. C., and Xu, C. B. (2006). Ligustilide induces vasodilatation via inhibiting voltage dependent calcium channel and receptor-mediated Ca2+ influx and release. *Vasc. Pharmacol.* 45 (3), 171–176. doi:10.1016/j.vph.2006.05.004

Chan, S. S., Cheng, T. Y., and Lin, G. (2007). Relaxation effects of ligustilide and senkyunolide A, two main constituents of Ligusticum chuanxiong, in rat isolated aorta. *J. Ethnopharmacol.* 111 (3), 677–680. doi:10.1016/j.jep.2006.12.018

Cohen, R. A. (1995). The role of nitric oxide and other endothelium-derived vasoactive substances in vascular disease. *Prog. Cardiovasc Dis.* 38 (2), 105–128. doi:10.1016/s0033-0620(05)80002-7

Dogan, M. F., Yildiz, O., Arslan, S. O., and Ulusoy, K. G. (2019). Potassium channels in vascular smooth muscle: A pathophysiological and pharmacological perspective. *Fundam. Clin. Pharmacol.* 33 (5), 504–523. doi:10.1111/fcp.12461

Du, Z., Shu, Z., Li, C., Song, X., Ma, X., Liao, L., et al. (2021). Baoyuan decoction alleviates myocardial infarction through the regulation of metabolic dysfunction and the mitochondria-dependent caspase-9/3 pathway. *Acupunct. Herb. Med.* 1 (1), 49–58. doi:10.1097/hm9.0000000000000003

Duan, X., Zhou, L., Wu, T., Liu, G., Qiao, J., Wei, J., et al. (2008). Chinese herbal medicine suxiao jiuxin wan for angina pectoris. *Cochrane Database Syst. Rev.* 2008 (1), Cd004473. doi:10.1002/14651858.CD004473.pub2

Fang, J., Li, R., Zhang, Y., Oduro, P. K., Li, S., Leng, L., et al. (2022). Aristolone in Nardostachys jatamansi DC. induces mesenteric vasodilation and ameliorates hypertension via activation of the K(ATP) channel and PDK1-Akt-eNOS pathway. *Phytomedicine* 104, 154257. doi:10.1016/j.phymed.2022.154257

Godo, S., and Shimokawa, H. (2017). Endothelial functions. *Arterioscler. Thromb. Vasc. Biol.* 37 (9), e108–e114. doi:10.1161/atvbaha.117.309813

Huang, C., Huang, W., Wang, R., and He, Y. (2020). Ulinastatin inhibits the proliferation, invasion and phenotypic switching of PDGF-BB-induced VSMCs via akt/eNOS/NO/cGMP signaling pathway. *Drug Des. Devel Ther.* 14, 5505–5514. doi:10.2147/dddt.S275488

Iizuka, T., Nagumo, S., Yotsumoto, H., Moriyama, H., and Nagai, M. (2007). Vasorelaxant effects of Acer nikoense extract and isolated coumarinolignans on rat aortic rings. *Biol. Pharm. Bull.* 30 (6), 1164–1166. doi:10.1248/bpb.30.1164

Jiang, M., Wan, F., Wang, F., and Wu, Q. (2015). Irisin relaxes mouse mesenteric arteries through endothelium-dependent and endothelium-independent mechanisms. *Biochem. Biophys. Res. Commun.* 468 (4), 832–836. doi:10.1016/j.bbrc.2015.11.040

Krüger-Genge, A., Blocki, A., Franke, R. P., and Jung, F. (2019). Vascular endothelial cell biology: An update. *Int. J. Mol. Sci.* 20 (18), 4411. doi:10.3390/ijms20184411

Lee, J. H., Parveen, A., Do, M. H., Lim, Y., Shim, S. H., and Kim, S. Y. (2018). Lespedeza cuneata protects the endothelial dysfunction via eNOS phosphorylation of PI3K/Akt signaling pathway in HUVECs. *Phytomedicine* 48, 1–9. doi:10.1016/j.phymed.2018.05.005

Lei, W., Ni, J., Xia, X., Jiang, M., and Bai, G. (2018). Searching for synergistic calcium antagonists and novel therapeutic regimens for coronary heart disease therapy from a Traditional Chinese Medicine, Suxiao Jiuxin Pill. *J. Chromatogr. B Anal. Technol. Biomed. Life Sci.* 1092, 220–227. doi:10.1016/j.jchromb.2018.06.015

Li, J., Ding, H., Li, Y., Zhou, H., Wang, W., Mei, Y., et al. (2021). Alarin alleviated cardiac fibrosis via attenuating oxidative stress in heart failure rats. *Amino Acids* 53 (7), 1079–1089. doi:10.1007/s00726-021-03005-8

Li, S. L., Chan, S. S., Lin, G., Ling, L., Yan, R., Chung, H. S., et al. (2003). Simultaneous analysis of seventeen chemical ingredients of Ligusticum chuanxiong by on-line high performance liquid chromatography-diode array detector-mass spectrometry. *Planta Med.* 69 (5), 445–451. doi:10.1055/s-2003-39709

Li, X., Hong, S., Li, P. L., and Zhang, Y. (2011). Docosahexanoic acid-induced coronary arterial dilation: Actions of 17S-hydroxy docosahexanoic acid on K+ channel activity. *J. Pharmacol. Exp. Ther.* 336 (3), 891–899. doi:10.1124/jpet.110.176461

Liang, M. J., He, L. C., and Yang, G. D. (2005). Screening, analysis and *in vitro* vasodilatation of effective components from Ligusticum Chuanxiong. *Life Sci.* 78 (2), 128–133. doi:10.1016/j.lfs.2005.04.038

Liu, J. L., Zheng, S. L., Fan, Q. J., Yuan, J. C., Yang, S. M., and Kong, F. L. (2014). Optimization of high-pressure ultrasonic-assisted simultaneous extraction of six major constituents from Ligusticum chuanxiong rhizome using response surface methodology. *Molecules* 19 (2), 1887–1911. doi:10.3390/molecules19021887

Liu, S., Long, Y., Yu, S., Zhang, D., Yang, Q., Ci, Z., et al. (2021). Borneol in cardio-cerebrovascular diseases: Pharmacological actions, mechanisms, and therapeutics. *Pharmacol. Res.* 169, 105627. doi:10.1016/j.phrs.2021.105627

Lu, Y., Ji, J., Chu, S., Shen, F., Yang, W., Lei, W., et al. (2022). CaMKII, that binds with ligustilide, as a potential drug target of Suxiao jiuxin pill, a traditional Chinese medicine to dilate thoracic aorta. *Clin. Transl. Med.* 12 (6), e907. doi:10.1002/ctm2.907

Lu, Z., Zhang, Y., Zhuang, P., Zhang, J., Zhou, H., Zhang, M., et al. (2015). Protective effect of Suxiao jiuxin pill, a traditional Chinese medicine, against acute myocardial ischemia in dogs. *BMC Complement. Altern. Med.* 15, 373. doi:10.1186/s12906-015-0908-9

Oliveira, E. J., Romero, M. A., Silva, M. S., Silva, B. A., and Medeiros, I. A. (2001). Intracellular calcium mobilization as a target for the spasmolytic action of scopoletin. *Planta Med.* 67 (7), 605–608. doi:10.1055/s-2001-17355

Pan, R., Gao, X., Lu, D., Xu, X., Xia, Y., and Dai, Y. (2011). Prevention of FGF-2-induced angiogenesis by scopoletin, a coumarin compound isolated from Erycibe obtusifolia Benth, and its mechanism of action. *Int. Immunopharmacol.* 11 (12), 2007–2016. doi:10.1016/j.intimp.2011.08.012

Ren, D. C., Yang, N. Y., Qian, S. H., Xie, N., Zhou, X. M., and Duan, J. A. (2007). Chemical study on aerial parts of Ligusticum chuanxiong. *Zhongguo Zhong Yao Za Zhi* 32 (14), 1418–1420.

Ren, L., Wang, J., Feng, L., Wang, S., and Li, J. (2018). Efficacy of suxiao jiuxin pill on coronary heart disease: A meta-analysis of randomized controlled trials. *Evid. Based Complement. Altern. Med.*, 2018, 9745804. doi:10.1155/2018/9745804

Ruan, X., Chen, T., Wang, X., and Li, Y. (2017). Suxiao Jiuxin Pill protects cardiomyocytes against mitochondrial injury and alters gene expression during ischemic injury. *Exp. Ther. Med.* 14 (4), 3523–3532. doi:10.3892/etm.2017.4964

Santos, S. E., Ribeiro, F., Menezes, P. M. N., Duarte-Filho, L. A. M., Quintans, J. S. S., Quintans-Junior, L. J., et al. (2019). New insights on relaxant effects of (-)-borneol monoterpene in rat aortic rings. *Fundam. Clin. Pharmacol.* 33 (2), 148–158. doi:10.1111/fcp.12417

Shan Au, A. L., Kwan, Y. W., Kwok, C. C., Zhang, R. Z., and He, G. W. (2003). Mechanisms responsible for the *in vitro* relaxation of ligustrazine on porcine left anterior descending coronary artery. *Eur. J. Pharmacol.* 468 (3), 199–207. doi:10.1016/s0014-2999(03)01691-1

Silva-Filho, J. C., Oliveira, N. N., Arcanjo, D. D., Quintans-Júnior, L. J., Cavalcanti, S. C., Santos, M. R., et al. (2012). Investigation of mechanisms involved in (-)-borneol-induced vasorelaxant response on rat thoracic aorta. *Basic Clin. Pharmacol. Toxicol.* 110 (2), 171–177. doi:10.1111/j.1742-7843.2011.00784.x

Thomas, C. C., Deak, M., Alessi, D. R., and van Aalten, D. M. (2002). High-resolution structure of the pleckstrin homology domain of protein kinase b/akt bound to

phosphatidylinositol (3,4,5)-trisphosphate. *Curr. Biol.* 12 (14), 1256–1262. doi:10.1016/s0960-9822(02)00972-7

Truebestein, L., Hornegger, H., Anrather, D., Hartl, M., Fleming, K. D., Stariha, J. T. B., et al. (2021). Structure of autoinhibited Akt1 reveals mechanism of PIP(3)-mediated activation. *Proc. Natl. Acad. Sci. U. S. A.* 118 (33), e2101496118. doi:10.1073/pnas.2101496118

Yao, Q., Huang, Y., Liu, A. D., Zhu, M., Liu, J., Yan, H., et al. (2016). The vasodilatory effect of sulfur dioxide via SGC/cGMP/PKG pathway in association with sulfhydryl-dependent dimerization. *Am. J. Physiol. Regul. Integr. Comp. Physiol.* 310 (11), R1073–R1080. doi:10.1152/ajpregu.00101.2015

Zhang, J. L., He, X. F., and Zhou, Z. H. (1996). HPLC determination of five constituents in plants of genus Ligusticum. *Yao Xue Xue Bao* 31 (8), 622–625.

Zhang, J., Zhuang, P., Lu, Z., Zhang, M., Zhang, T., Zhang, Y., et al. (2014). Suxiaojiuxin pill enhances atherosclerotic plaque stability by modulating the MMPs/TIMPs balance in ApoE-deficient mice. *J. Cardiovasc Pharmacol.* 64 (2), 120–126. doi:10.1097/fjc.0000000000000095

Zhou, Z. Y., Xu, J. Q., Zhao, W. R., Chen, X. L., Jin, Y., Tang, N., et al. (2017). Ferulic acid relaxed rat aortic, small mesenteric and coronary arteries by blocking voltage-gated calcium channel and calcium desensitization via dephosphorylation of ERK1/2 and MYPT1. *Eur. J. Pharmacol.* 815, 26–32. doi:10.1016/j.ejphar.2017.10.008

Frontiers in Pharmacology

Explores the interactions between chemicals and living beings

The most cited journal in its field, which advances access to pharmacological discoveries to prevent and treat human disease.

Discover the latest Research Topics

See more →

Frontiers

Avenue du Tribunal-Fédéral 34
1005 Lausanne, Switzerland
frontiersin.org

Contact us

+41 (0)21 510 17 00
frontiersin.org/about/contact